NK cell determinants of immunity to *Mycobacterium tuberculosis* in humans

Carly Young-Bailie

Thesis Presented for the Degree of

DOCTOR OF PHILOSOPHY

in the Department of Pathology

Faculty of Health Sciences

University of Cape Town

May 2023

Supervisor: Dr Virginie Rozot

Co-supervisor: Professor Thomas J. Scriba

Declaration

I, Carly Young-Bailie, hereby declare that the work on which this thesis is based is my original work (except where acknowledgements indicate otherwise) and that neither the whole work nor any part of it has been, is being, or is to be submitted for another degree in this or any other university. I empower the university to reproduce, for the purpose of research, either the whole or any portion of the contents in any manner whatsoever.

Signature: Signed by candidate

Date: May 2023

Summary

Natural killer (NK) cells are highly equipped killers of pathogen-infected and neoplastic cells. There has been an increased appreciation for NK cells as potentially important role players during the immune response to *Mycobacterium tuberculosis* infection and tuberculosis (TB) disease. However, our understanding of the precise role of NK cells in TB pathogenesis remains incomplete. To address this knowledge gap, this thesis set out to investigate NK cell determinants of immunity to *Mtb* in humans. The primary objective was to gain a better understanding of NK cell function and phenotype in the peripheral blood and human tissues, adding insights about various stages of the TB spectrum.

The first aim was to investigate NK cell functional changes occurring during progression to TB disease. Previous human studies in the TB field have highlighted differences in frequency and function of peripheral blood NK cells between TB and healthy controls. However, findings from different studies have been conflicting and none have provided a longitudinal analysis of NK cell function during progression to active TB disease. To address this gap, NK cell functions were investigated longitudinally with time to TB diagnosis in a cohort of adolescent progressors and controllers who were followed up for two years. Using mass cytometry, NK cell cytokine responses were measured in peripheral blood mononuclear cells (PBMC) stimulated with *Mtb* antigens. Results showed that NK cell cytokine responses were low at timepoints further from TB diagnosis, which steadily increased to significantly higher levels at timepoints closer to TB diagnosis in progressors relative to controllers. Further investigation revealed that increased NK cell functions during progression to TB disease were significantly associated with *Mtb*-specific interleukin (IL)-2 responses by CD4 T cells, possibly suggesting T cell-associated bystander activation of NK cells during progression to TB disease, which was investigated further.

NK cells rapidly respond to signalling by immune cells in the local microenvironment and their functions are modulated during inflammatory responses via bystander activation. Bystander NK activation in response to accessory cell cytokine secretion may be triggered through cytokine-receptor binding on the NK cell surface. However, the precise role of accessory cell cytokines during NK cell bystander activation and function (particularly cytotoxic potential) in the immune response during *Mtb* infection and TB disease remains unknown. Therefore, this study set out to further investigate NK cell cytokine production and cytotoxic potential in the context of T cell- and myeloid-associated accessory cytokines involved in NK cell bystander activation during inflammatory TB disease. To this end, a flow cytometry cytokine neutralization assay was designed to measure NK cell cytokine production and cytotoxic marker expression in PBMC stimulated with *Mtb* antigens from TB patients and healthy, *Mtb*-sensitized controls. Results showed that myeloid cytokine-mediated activation was important for NK cell IFN-γ responses to *Mtb* antigens, while the cytotoxic potential of NK cells in TB patients were dependent on T cell-associated IL-2 bystander activation. These data reveal the complex interplay between T cells, myeloid cells, and NK cell function in the context of *Mtb* infection and TB disease. Further investigation into NK cell activation and function may highlight new mechanistic targets for developing clinical interventions that possibly modulate NK cell activity for better *Mtb* clearance and favorable TB prognosis.

Despite extensive studies performed using peripheral blood, the TB field lacks a comprehensive understanding of phenotypic and functional characteristics of NK cells in human tissues, where the disease mostly manifests. To address this major knowledge gap, human NK cells were characterized in a cohort of TB patients who succumbed to disease, and controls who were apparently healthy but died from trauma. Using postmortem samples from peripheral blood, lung, hilar lymph nodes, bronchoalveolar lavage (BAL), and spleen, NK cell phenotypes and cytotoxic potential were characterized by mass cytometry. Results

showed that NK cells in the peripheral blood of TB patients displayed predominantly mature, activated phenotypes, expressing higher levels of cytotoxic molecules in TB than those from healthy controls. In contrast, NK cells in tissues, including lungs, hilar lymph nodes, BAL, and spleen were phenotypically immature and lacked expression of maturation markers and cytotoxic molecules. Immature NK cells with low cytotoxic potential were particularly enriched in the TB lung relative to controls. These findings indicate that NK cells in the tissues may be playing an immunoregulatory role to maintain homeostasis and prevent inflammation-induced tissue pathology. Further investigation into the functional capacity of immature lung NK cells that accumulate during TB disease may reveal mechanistic targets for clinical interventions.

Overall, this thesis delves into the complex phenotypic and functional characteristics of NK cells, offering insights into tissue immunology in the context of TB disease. The findings presented herein have relevance in immunopathogenesis and development of new interventions, such as vaccines.

Acknowledgements

To my supervisor, Virginie, thank you from the bottom of my heart for your guidance and support. I am most appreciative of your endless encouragement, and for always being the reassuring voice telling me “It’s going to be okay!”. Your supervision style afforded me the freedom to explore my potential and gain new skills, while always offering a pillar of support when I needed it. My co-supervisor, Tom, thank you for offering your guiding hand throughout. Along with Virginie, you have pushed me to my full potential and helped me grow as a young researcher. I could not have asked for better supervisors and mentors to walk beside me through this journey.

To the study participants, to those who passed, and to the loved ones of those who passed – your selfless contributions have been the cornerstone of this research. When the day comes for TB to no longer plague our lives, you will be remembered with honour.

To the entire SATVI team, I thank you for making this project possible through your continued hard work and dedication. It has been an absolute pleasure to work with the most encouraging and supportive group of people. You are all so valued and appreciated!

To Al Leslie at AHRI, thank you for selflessly offering me a lifeline when I needed it most. Your willingness to help was a light at the end of a tunnel that allowed me to begin building the foundations of my project. For this, I am endlessly grateful.

This project would not have been possible without Dr Stephen Cose, Gift and Marjorie at MRC/UVRI & LSHTM, Ugandan Research Unit. Thank you for your tireless efforts that made this project a reality. Together we have achieved a mammoth task and I cannot thank you enough for your hand in making this possible.

To Hasse, Desirée, Agano, and Miguel – At the risk of sounding overly dramatic, thank you for changing my life! You are the individuals who introduced me to the world of R and without your efforts, I could never have accomplished this work. I am eternally grateful for the role you’ve played in my career as young scientist.

To the IIDMM, SATVI and the NRF, thank you for making this opportunity a possibility for me. Thank you for providing me with the facilities and financial support to chase my dreams and make them a reality.

I would like to extend a special thanks to the examiners who so selflessly offered their valuable time to evaluate this work. I am truly grateful for your expert input, critique, and feedback.

To my friends that have become family, thank you for cheering me on from the sidelines and for being a source of strength, love, and encouragement through the highs and lows. Thank you for being the shoulders that I’ve leaned on, cried on and the shoulders that have carried me throughout this journey.

Sister, when I held your small body in my arms for the first time, I was overjoyed to have somebody to play with and boss around occasionally. At that point in life, my tiny mind could never have comprehended that my new playmate would grow up to become my life-long best friend. From the very beginning, you have been the one I’ve laughed with, cried with, and shared life’s challenges and adventures with. Jody, I could never have walked this journey without you by my side. Thank you for believing in me and being my biggest supporter.

Shane, thank you for being the calm in the chaotic storm that has been this PhD journey and everyday life. Thank you for showing me what it means to be kind, patient, resilient and brave. Our big dreams and wild ambitions are what keeps me putting one foot in front of the other. I know that whatever obstacles we face and whichever paths we decide to walk in life, we will do so together, with purpose in our step and fire in our hearts; *“'Cause we been high, darlin', we been low. And all of it's helped us grow. We belong here and we deserve to dream”.* – Xavier Rudd.

Mom and Dad, when I think back to memories of my childhood, I am overwhelmed with gratitude for the life you have given me. Life with you has been filled with an abundance of laughter and unconditional love. Mom, throughout my entire life, I have watched as you have conquered every challenge with courage and perseverance, while always putting the needs of others before your own. Thank you for teaching me, through example, how to be a powerful, strong, and selfless woman. Dad, you have shown me what it means to work tirelessly for the important things in life and make sacrifices for the ones you love. Dad, because of your endless love and adoration, I have walked through life believing that I am capable of achieving everything to my heart’s content. Mom and Dad, everything I do is done in love and with appreciation for you.

Jody, Shane, Mom, and Dad – for you.

"Start at the bottom. And work your way down."

- Brigham Young

Table of Contents

List of Abbreviations

Special characters and units of measurement

%	Percentage
°C	Degrees Celsius
α	Alpha
β	Beta
γ	Gamma
δ	Delta
Δ	Change (or difference)
cells/mL	Cells per milliliter
g/dL	Grams per deciliter
IU/mL	International units per milliliter
kDa	Kilodaltons
mg/mL	Milligram per milliliter
mL	Milliliter
mM	Millimolar
n	Sample number
nm	Nanometer
rpm	Revolutions per minute
w/v	Weight per volume
xg	Relative centrifugal force
µg	Microgram
µg/mL	Microgram per millilitre
µL	Microliter
µm	Micrometer

A

Ab	Antibody
ACS	Adolescent Cohort Study
ADCC	antibody-dependent cellular cytotoxicity
AHRI	African Health Research Institute
ALD	Autoimmune liver disease
ANOVA	Analysis of variance
APC	Antigen presenting cell
ARV	Antiretroviral

B

BAL	Bronchoalveolar lavage
BALT	Bronchus-associated lymphoid tissue
BCG	Bacillus Calmette Guérin
Bcl	B cell leukemia
BCR	B cell receptor
BD	Becton Dickinson
BMI	Body mass index
BSL	Biosafety level
BV	Brilliant violet

C

CAR	Chimeric antigen receptor
CCC	Concordance correlation coefficient
Cd	Cadmium
CD	Cluster of differentiation
CEF/HCMV	Cytomegalovirus, Epstein-Barr virus, influenza virus / human cytomegalovirus peptide pool
CFP-10	Culture filtrate protein-10
CI	Confidence interval
CLR	C-type lectin receptor
CMV	Cytomegalovirus
CO_2	Carbon dioxide
COMPASS	Combinatorial Polyfunctionality analysis of Antigen-Specific Subsets
COPD	Chronic obstructive pulmonary disease
COVID-19	Coronavirus Disease of 2019
CSV	Comma-separated values
CTL	Cytotoxic T lymphocyte
CyTOF	Cytometry by time-of-flight

D

DC	Dendritic cell
DMSO	Dimethyl sulfoxide
DNA	Deoxyribonucleic acid
DNAM	DNAX accessory molecule
DNase	Deoxyribonuclease
DR-TB	Drug resistant tuberculosis
DS-TB	Drug sensitive tuberculosis

DURT	Donor unrestricted T cell

E

EBV	Epstein-Barr virus
EDTA	Ethylenediaminetetraacetic acid
ELISPOT	Enzyme-linked immunospot
ER	Endoplasmic reticulum
ESAT-6	6kDa early secreted antigenic target
ESX-I	6kDa early secreted antigenic target (ESAT-6) secretion system-I

F

FACS	Fluorescence-activated cell sorting
FAUST	Full Annotation Using Shaped-constrained Trees
FBS	Fetal bovine serum
FCS	Flow cytometry standard
FDA	U.S. Food and Drug Administration
FS	Functionality score
FSC-A	Forward scatter area
FSC-H	Forward scatter height

G

GM-CSF	Granulocyte-macrophage colony-stimulating factor
GSH	Glutathione

H

HCMV	Human cytomegalovirus
HIV	Human immunodeficiency virus
HRP	Horse radish peroxidase

I

ICS	Intracellular cytokine staining
IFN	Interferon
Ig	Immunoglobulin
IGRA	Interferon-γ release assay
IIDMM	Institute of Infections Disease and Molecular Medicine
IL	Interleukin
IQR	Interquartile range
Ir	Iridium

ITIM	Immunoreceptor tyrosine-based inhibitory motif

K

KIR	Killer immunoglobulin-like receptor
KLRG	Killer cell lectin-like receptor G
KNN	K-Nearest Neighbours
KS	Kaposi's sarcoma

L

LAIR	Leukocyte-associated immunoglobulin (Ig)-like receptor
LIR	Leukocyte immunoglobulin (Ig)-like inhibitory receptor
LMIC	Low- and middle-income countries
Ln	Lanthanide
LTBI	Latent TB infection

M

MAIT	Mucosa-associated invariant T cell
MALT	Mucosal-associated lymphoid tissue
MCMV	Murine cytomegalovirus
MDR-TB	Multidrug resistant tuberculosis
MFI	Median fluorescence intensity
MGIT	Mycobacteria Growth Indicator Tube
MHC	Major histocompatibility complex
MNRH	Mulago National Referral Hospital
MPR	Mannose-6-phospahe receptor
MRC/UVRI	Medical Research Council/Uganda Virus Research Institute
& LSHTM	& London School of Hygiene & Tropical Medicine
MSI	Median staining intensity
Mtb	*Mycobacterium tuberculosis*
MTBC	*Mycobacterium tuberculosis* complex
MTOC	Microtubule organizing centre
MZ	Marginal zone

N

NAAT	Nucleic acid amplification test
NCAM	Neural cell adhesion molecule
NCR	Natural cytotoxicity receptor
NHP	Non-human primate

NK	Natural killer
$NK_{cytotoxic}$	Cytotoxic NK cell
$NK_{regulatory}$	Regulatory (cytokine-producing) NK cell
NKG2A	Natural killer group 2 member A
NKG2C	Natural killer group 2 member C
NKG2D	Natural killer group 2 member D
NLR	Nucleotide-binding and oligomerization domain (NOD)-like receptor
NO	Nitric oxide
NOD	Nucleotide-binding and oligomerization domain
NTM	Non-tuberculous mycobacteria

P

PAMPs	Pathogen-associated molecular patterns
PAR	Protease activated receptor
PBMC	Peripheral blood mononuclear cells
PBS	Phosphate buffered saline
PCC	Pearson correlation coefficient
Pen/strep	Penicillin-streptomycin
PET-CT	Positron emission tomography-computed tomography
PFA	Paraformaldehyde
PFS	Polyfunctionality score
PHA	Phytohemagglutinin
PI-9	Proteinase inhibitor-9
PLHIV	People living with HIV
PMA	Phorbol 12-myristate 13-acetate
PMI	Postmortem interval
PMT	Photomultiplier tube
PPD	Purified protein derivative
PRRs	patterns recognition receptors

Q

QC	Quality control
QFT	QuantiFERON

R

Rh	Rhodium
ROS	Reactive oxygen species
RPMI	Roswell Park Memorial Institute

S

SATVI	South African Tuberculosis Vaccine Initiative
SEB	Staphylococcal enterotoxin B
SLE	Systemic lupus erythematosus
SSC-A	Side scatter area

T

T1DM	Type 1 diabetes mellitus
TB	Tuberculosis
TBST	*Mtb* antigen-based skin test
TCEP	Tris (2-carboxyethyl) phosphine
TCR	T cell receptor
T_{FH}	Follicular helper T cell
Th	T helper cells
TIGIT	T cell immunoreceptor with immunoglobulin (Ig) and immunoreceptor tyrosine-based inhibitory motif (ITIM) domains
TLR	Toll-like receptor
TNF	Tumor necrosis factor
TPT	TB preventative therapy
T_{reg}	Regulatory T cell
tSNE	t-Distributed Stochastic Neighbor Embedding
TST	Tuberculin skin test

U

UCT	University of Cape Town
ULBP	UL16 binding protein
UNS	Unstimulated

W

WHO	World Health Organization

X

XDR-TB	Extensively drug resistant tuberculosis

List of Figures

List of Tables

List of Equations

Chapter 1: Introduction and Literature Review.

The White Rabbit put on his spectacles. "Where shall I begin, please your Majesty?" he asked. "Begin at the beginning," the King said gravely, "and go on till you come to the end: then stop."

- Lewis Carroll, *Alice in Wonderland*

1.1 Tuberculosis is a Global Health Threat

Mycobacterium tuberculosis (*Mtb*) is one of the main etiological agents of tuberculosis (TB) disease in humans, belonging to a group of genetically related TB-causing mycobacterium species of the *Mycobacterium tuberculosis* complex (MTBC). *Mtb* is characterized as an obligate, intracellular, aerobic, non-motile bacillus species. Despite widespread vaccination and various anti-*Mtb* drug regimens, TB remains one of the largest killers due to infectious disease worldwide, accounting for 10.6 million cases of TB disease and 1.6 million deaths (including 187 000 individuals living with human immunodeficiency virus – HIV infection) in 2021 alone, making TB the second leading infectious killer after Coronavirus Disease of 2019 (COVID-19) (WHO, 2022). For the most part, individuals who are infected with *Mtb* can contain the infection and do not progress to TB disease. This is based on the estimation that between only 5-15% of individuals who have been infected with *Mtb* will progress to active disease (Vynnycky & Fine, 1997a).

The Bacillus Calmette Guérin (BCG) vaccine was first used in humans in 1921 and is the only licenced TB vaccine administered to newborns. BCG is efficacious against severe and extrapulmonary forms of TB disease, with 50-80% efficacy in infants and children (Roy et al., 2014; Trunz et al., 2006). However, the duration of protection of BCG is estimated up to only ten years, after which a waning effect occurs over time (Abubakar et al., 2013). Although advantageous for protecting newborns and children, the variable and limited efficacy of BCG against TB disease in adolescents and adults poses a major problem since most cases of transmissible, pulmonary TB disease occur within post-infancy/-childhood age groups (Colditz et al., 1994; Mangtani et al., 2014).

Tuberculosis is a curable disease. However, there are several contributing factors to relapse (i.e., recurrence of the disease and/or the signs and symptoms following a period of improvement) and high prevalence and death rates of TB. These contributing factors include

missed diagnoses, low treatment compliance due to lengthy, toxic antibiotic regimens, and a rise in drug resistant (DR)-*Mtb* strains. According to the 2022 World Health Organization (WHO) Tuberculosis Global Report, it is estimated that only 61% of diagnosed TB cases received treatment in 2021. Of those receiving anti-TB treatment, 86% were cured (WHO, 2022). Despite cure, individuals remain at high risk of relapse or recurrence (Hermans et al., 2021).

Altogether, it may be said that TB is one of the oldest afflictions and infectious diseases known to mankind (Daniel, 2006), facing multifaceted management challenges while causing severe socio-economic burden, particularly in low- and middle-income countries (LMIC) and TB endemic regions.

1.1.1 Symptoms and diagnosis across the TB spectrum

Mtb is transmitted via inhalation of aerosolized, bacilli-containing droplets and primary infection occurs in mammalian respiratory systems, although *Mtb* may cause disease throughout the body. TB disease has diverse clinical manifestations and presents as a dynamic spectrum, ranging from asymptomatic *Mtb* infection to life-threatening disease (Barry et al., 2009; Drain et al., 2018; Esmail et al., 2014).

In healthy, asymptomatic individuals, a positive result from one or both of two tests are generally used to detect immunological sensitization to *Mtb* antigens namely, the tuberculin skin test (TST) or interferon (IFN)-γ release assay (IGRA). It is estimated that 23% of the global population is healthy, with immunological sensitization to *Mtb* (R. M. G. J. Houben & Dodd, 2016). The TST technique is performed by administering an intradermal injection of purified protein derivative (PPD), or one of three other antigen preparations developed for newer *Mtb* antigen-based skin tests (TBST), including C-Tb (Serum Institute of India, India), C-TST (formerly known as ESAT6-CFP10 test, Anhui Zhifei Longcom, China), and Diaskintest (Generium, Russian Federation). For individuals with cell-mediated immunity to

these antigens, a delayed-type hypersensitivity reaction typically occurs within 48-72 hours and interpretation of the test occurs by measuring the size of induration. However, one caveat to PPD-based TST includes cross-reactivity with BCG in cases of late (post-infancy) or repeated BCG vaccination and exposure to non-tuberculous mycobacteria (NTM) (Farhat et al., 2006). This PPD-associated cross-reactivity has been the rationale for developing alternative antigen preparations for new generation TBST. The use of IGRAs is also a workaround for potential cross-reactivities of traditional TST. The use of alternative antigens offers readouts of cell-mediated immune responses to antigens that are more specific to *Mtb* and not encoded within the genome of BCG and most NTMs (Andersen et al., 2000; Sørensen et al., 1995). The *in vitro,* blood-based IGRA quantifies the amount of IFN-γ released or the number of IFN-γ-expressing immune cells following stimulation with 6kDa early secreted antigenic target (ESAT-6) and culture filtrate protein 10 (CFP-10) for 16-24 hours. Two widely used IGRAs are approved by the U.S. Food and Drug Administration (FDA) and are commercially available: QuantiFERON-TB Gold Plus (QFT) and TSPOT-TB. Both tests have reduced sensitivity in immunocompromised individuals and neither test is able to differentiate between different states of the TB spectrum, nor distinguish between new and re-infections (Pai et al., 2014; Sester et al., 2011). At best, these tests indicate prior immunological sensitization (specifically, acquired immune responses with T cell priming and memory) to *Mtb* antigens (discussed further in Section 1.2.1) and are useful for identifying individuals who may be eligible for TB preventative therapy (TPT).

Active TB disease is characterized as a transmissible state, oftentimes presenting with symptoms (unless in cases of subclinical TB, discussed below). Symptoms may include coughing, haemoptysis (coughing up blood), loss of appetite, weight loss, malaise, fever, and/or night sweats. Diagnosis of TB disease is based on self-reported symptoms in combination with various diagnostic techniques. Four main technologies are used for diagnosing active TB: radiology, microscopy, culture and/or molecular test (WHO, 2013; Pai,

Behr, et al., 2016). Imaging/radiology techniques, including x-rays and positron emission tomography-computed tomography (PET-CT) scans, may indicate lung abnormalities characteristic to pulmonary disease. However, radiology techniques lack specificity and are often followed up with microbiological tests, such as microscopy, culture and molecular tests (Pande et al., 2015; Esmail et al., 2016). Microscopy includes qualitative microbiological tests to directly visualize acid-fast bacilli in sputum smears (Steingart, Henry, et al., 2006). Culture-based methods are used to detect live, actively replicating *Mtb* (Cruciani et al., 2004). Molecular tests enable identification of genomic signatures characteristic to *Mtb* (Boehme et al., 2010, 2011; Detjen et al., 2015; Steingart et al., 2014). However, microbiological tests also have drawbacks. More specifically, smear microscopy is fast and inexpensive, but has low sensitivity, especially in individuals co-infected with HIV (Steingart, Ng, et al., 2006). Culture-based methods remain the gold standard for laboratory confirmation of TB disease. However, the cost of culture-based methods is high and long duration of culturing may delay diagnosis. Molecular-based, nucleic acid amplification tests (NAATs) for TB diagnosis detects *Mtb*-specific DNA in a sputum sample, with added advantages of quick results and detection of drug-resistance (specifically rifampicin resistance). However, NAATs are costly and require highly specialized equipment. Additionally, NAATs cannot discriminate between DNA from viable or non-viable bacilli. Therefore, a positive NAAT result may arise due to persisting DNA from dead bacilli in those with prior, cured TB. Due to these limitations, considerable effort is being made to develop new diagnostics and improve current tools to allow for rapid, cost-effective, specific, and sensitive diagnosis of TB disease.

Also falling on the TB spectrum is incipient and subclinical TB. Incipient TB is characterized as a state of *Mtb* infection which is likely to progress to active TB disease in the absence of intervention, but an individual experiences no clinical symptoms, radiographic abnormalities of microbiologic evidence of active TB disease (Drain et al., 2018). In subclinical TB, patients

may by asymptomatic but have culture-positive disease, meaning that viable, actively replicating *Mtb* can be detected in their sputum and may therefore, transmit the organism to others (Dowdy et al., 2013; Drain et al., 2018; Frascella et al., 2021). Subclinical TB may also be identified by radiological abnormalities characteristic to pulmonary disease. In a 2021 review and analysis of data from TB prevalence population surveys, Frascella and colleagues estimated that approximately 50% of prevalent bacteriologically confirmed TB is subclinical (Frascella et al., 2021).

Individuals may advance or revert between different disease states along the TB spectrum, depending on host immunity and/or other risk factors including under- and mal-nourishment (Sinha et al., 2021), air pollution (Y. Liu et al., 2021), excessive alcohol consumption (Rehm et al., 2009), smoking (Bates et al., 2007) and co-morbidities such as HIV infection (Havlir et al., 2008) and type 2 diabetes mellitus (Jeon & Murray, 2008). Following establishment of *Mtb* infection, the spectrum of TB disease may progress via the following pathways: 1) asymptomatic infection (which is most common and can result in *Mtb* persistence or elimination), 2) rapid or 3) slow progression through incipient and subclinical TB to active, symptomatic TB disease, or 4) a period of cycling through incipient and subclinical states that may precede active, symptomatic disease or resolution of disease. Progression and reversion between different stages of the TB spectrum can be clinically subtle or completely undetectable, highlighting the exceptional complexity of this disease and the extraordinary level of coevolution and adaptation of *Mtb* to infect and survive in its human hosts.

Development of new specific and sensitive TB diagnostics is a major priority, specifically for identifying high-risk asymptomatic infection, incipient TB, subclinical TB and active, symptomatic (including drug-resistant) TB disease in individuals who cannot produce sputum. The gold standard for new diagnostic tools would be a low-cost, point-of-care technique that utilizes venous blood, urine, or other easily accessible sample/s. To this end, urine-based diagnostics are currently being investigated to detect *Mtb* antigens in people

living with HIV (PLHIV) and children (Nicol & Zar, 2020; Nicol et al., 2021; Peter et al., 2016). Novel diagnostics are currently under investigation and may be used to identify biomarker signatures such as antibodies, cytokines, volatile organic compounds, protein and enzymatic markers, and/or gene transcripts to infer various states of infection, risk of progression and/or antigen load (reviewed elsewhere by Pai et al., 2016; Guo et al., 2022; Yong et al., 2019; van Rensburg & Loxton, 2015). Ideally, new diagnostic tools would enable sensitive and specific diagnosis and distinguish between individuals across the TB spectrum from asymptomatic infection to incipient and subclinical TB, through to active symptomatic TB disease.

1.1.2 TB treatment

Once diagnosed, TB treatment is lengthy with the standard treatment for drug-sensitive TB comprised of a minimum six-month regimen which is split into two phases. Although not the only treatment option, Rifafour is the most typically used regimen comprising a fixed-dose combination of four anti-TB drugs. The first phase of treatment is the intensive phase with two months of rifampicin, isoniazid, pyrazinamide, and ethambutol treatment. Thereafter, the continuation phase is carried out for the remaining four months with isoniazid and rifampicin (reviewed by Pai et al., 2016). Although having a high success rate (approximately 86% under routine, adherent conditions) (WHO, 2022), the standard treatment regimen remains lengthily with high toxicity, which are contributing factors to poor patient compliance and the rise of DR-*Mtb* strains.

In cases of DR-TB disease, rapid diagnosis and timely initiation of an effective drug regimen are key to obtaining good treatment outcomes, minimizing transmission, and preventing further drug resistance. However, deciding on appropriate treatment is a complex task factoring in patient characteristics, disease presentation and drug susceptibility profile of the infecting *Mtb* strain (Dheda et al., 2014, 2016; Pai, Behr, et al., 2016). Multidrug resistant-

TB (MDR-TB) has been reported in virtually all countries, characterized as *Mtb* strains resistant to at least isoniazid and rifampicin. Extensively drug resistant-TB (XDR-TB) is characterized as being resistant to isoniazid, rifampicin, any fluoroquinolone, and any second-line injectable aminoglycoside (WHO, 2022). In some cases, resistance to all first-line TB drugs can occur. Reports of potentially totally drug-resistant *Mtb* strains have been documented, posing a terrifying public health risk (Dheda et al., 2014; Udwadia, 2012).

Besides the use of drug therapy for those with active TB disease, there has been increased uptake of TPT for individuals with evidence of *Mtb*-immunological sensitization by TST and/or IGRA positivity, who are considered high-risk. Examples of high-risk individuals who may benefit from TPT include known contacts of a person with active TB disease (including adults and children), PLHIV, individuals on anti-tumor necrosis factor (TNF) treatment, on dialysis with end-stage renal disease, taking immunosuppressive agents (such as those preparing for organ or haematological transplantation) or individuals with silicosis. The rationale for prioritizing TPT in these groups is due to their high risk of progressing to active TB disease, and studies have demonstrated a positive impact of TPT to significantly lower risk of progression to TB disease (Erkens et al., 2016; Mølhave & Wejse, 2020; Morán-Mendoza et al., 2010; Reichler et al., 2020). TPT treatment regimens recommended by the WHO include a weekly dose of isoniazid and rifapentine for 3 months (3HP), a daily dose of isoniazid and rifampicin for 3 months (3HR), a daily dose of isoniazid and rifapentine for 1 month (1HP), a daily dose of rifampicin for 4 months (4R), and a daily dose of isoniazid for 6 months (6H) or longer (WHO, 2022). Despite a promising outlook to lower risk of progression in high-risk groups, the practicality of TPT in low-resourced and high TB-burdened countries remains unaffordable due the high number of people with evidence of *Mtb*-sensitization, and may be counterproductive considering the high risk of reinfection, even after completing TPT (Churchyard et al., 2017; Mathema et al., 2017).

1.2 The Immune Response to *Mtb* Infection

1.2.1 Innate and adaptive immune systems

The central dogma surrounding immunology is based in two distinct counterparts, namely, the innate and adaptive immune systems. Innate immune responses are characterized as rapid and ever-present, being the first response to potential threats. A major characteristic of innate immunity is the ability of cells to recognise pathogen-associated molecular patterns (PAMPs) through germline-encoded pattern recognition receptors (PRRs), thereby enabling non-specific, yet prompt immune activation (K. Murphy & Weaver, 2016).

In contrast, the adaptive immune response is highly specific and can have long-lived memory capacity. The adaptive immune system is divided into two subsections according to the cell types and molecules mounting a response, including 1) cell-mediated immunity mediated by T cells, and 2) and humoral immunity mediated by B cells (Abbas et al., 2014; K. Murphy & Weaver, 2016). The main feature of adaptive cells includes their ability to undergo genetic recombination (somatic hypermutation) of genes encoding the T cell receptor (TCR) and B cell receptor (BCR), resulting in a large repertoire of clonal diversity. Upon activation, the adaptive immune response triggers clonal selection, proliferation, and expansion of antigen-specific effector cells and long-lived memory cells (Abbas et al., 2014; K. Murphy & Weaver, 2016). Although typically discussed as distinct systems, innate and adaptive responses are not mutually exclusive, but rather considered as flexible, interacting subsystems (Figure 1.1). Particularly in the context of infection and vaccination, the innate and adaptive immune systems experience bi-directional interactions, which is essential for immunity. In this sense, innate cells amplify and direct the adaptive response, while effector cells of the adaptive system activate innate cells (Clark & Kupper, 2005; Hoebe et al., 2004; Horowitz et al., 2010a). Essentially, each system provides information and assistance to the other.

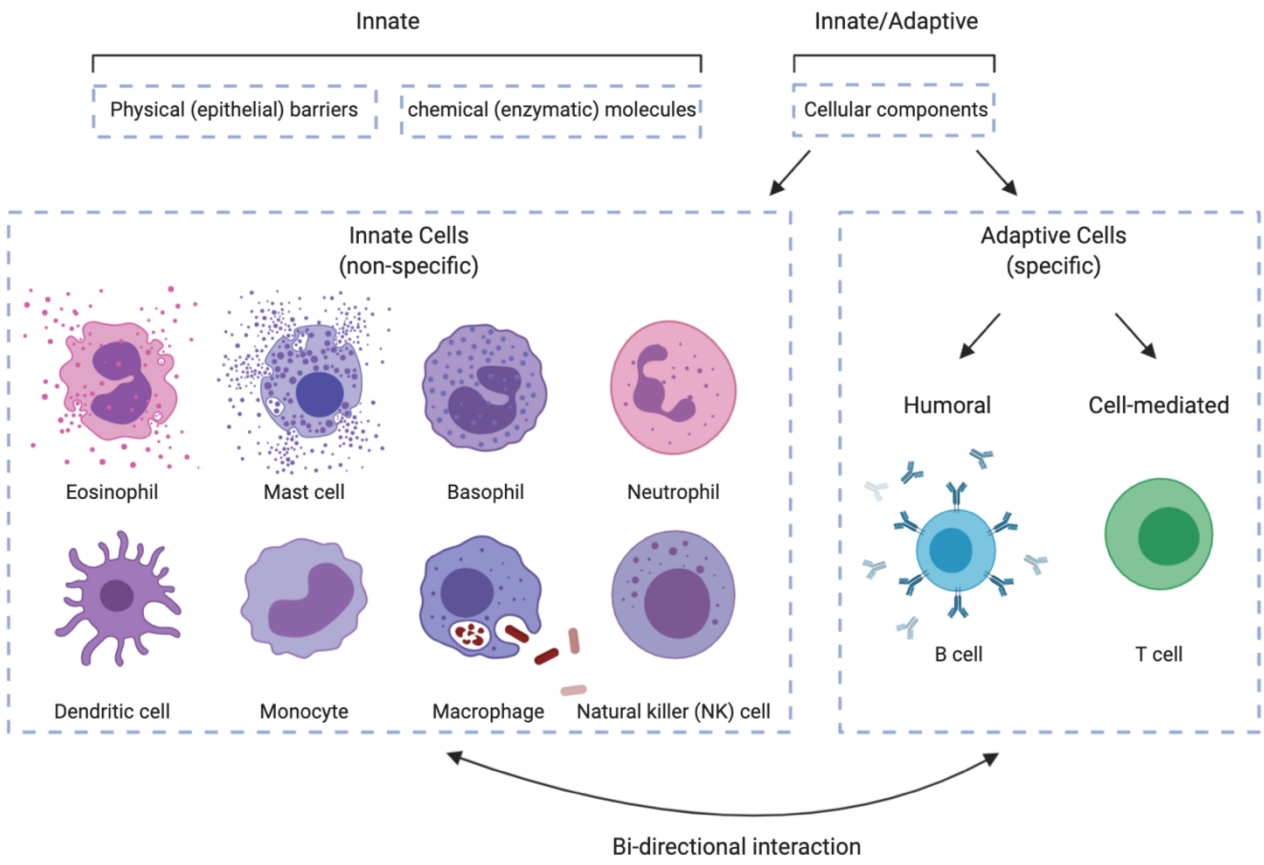

Figure 1.1: Innate and adaptive arms of the immune system are not mutually exclusive. Rather, these are flexible, interacting systems experiencing bi-directional interactions to elicit optimal immune responses. Innate physical barriers, chemical molecules and cellular components are considered the first line of defence of the immune system and are critical for amplifying and directing the adaptive response. Adaptive features of the immune system are long-lasting, highly specific and are necessary for efficient activation of innate cells.

Broadly speaking, the outcome of exposure to *Mtb* is either 1) elimination of *Mtb* by the immune system or 2) persistence of the pathogen. In the case of elimination, first-line innate responses and/or adaptive immune responses can eradicate *Mtb.* If *Mtb* elimination occurs solely due to innate immunity or by acquired immune responses without T cell priming or memory, an individual may not have a positive TST and/or IGRA response. On the other hand, some individuals may successfully eliminate/clear *Mtb* and retain a memory T cell response, in which case, positive TST and/or IGRA results are likely. If the pathogen is not eliminated, *Mtb* can persist in a quiescent state and these individuals are thought to develop positive TST and/or IGRA responses but experience no symptoms of active TB disease. Notably, patients with active TB disease may generate negative TST and/or IGRA due to

immune anergy resulting from the disease itself or immune suppression caused by comorbidities (such as HIV infection or malnutrition) (Barry et al., 2009; Esmail et al., 2014; Pai, Behr, et al., 2016). For a long time, positive TST and /or IGRA responses were thought to directly imply *Mtb* infection, where bacilli are not totally cleared by the immune system and persists in a quiescent state (also referred to as "latency"). Previously, the term for this state was dubbed "latent TB infection" (LTBI), which appears often in published literature. However, based on the information presented here, it is evident that the outcomes of immune responses to *Mtb* infection and clearance of the pathogen are more nuanced than the oversimplified TST/IGRA-LTBI dogma. Interpretation of positive TST and/or IGRA results imply, at best, prior immunological sensitization to *Mtb* antigens with T cell priming or memory. Therefore, from this point further, use of the terms "latency" and "LTBI" will be limited, and evidence of *Mtb* immunological sensitization will be reported directly as the assay outcome (i.e., $IGRA^+$ and/or TST^+).

The following Sections 1.2.2 and 1.2.3 provide a general overview of the innate and adaptive responses to *Mtb* infection, respectively. These sections are discussed in terms of the generalized (admittingly oversimplified) understanding of innate phagocytes and adaptive T cell responses, which have been underpinned as major role players in TB. Since the primary focus of this thesis includes natural killer (NK) cells, the intricacies of phagocyte and T cell responses are not detailed. Rather, a broad overview is provided to introduce the themes of immune activation upon *Mtb* infection. Later, in Section 1.4, the finer details of NK cell responses are discussed in the context of TB.

1.2.2 The innate response to *Mtb* infection

Upon inhalation of aerosolized bacilli-containing droplets into the airways, *Mtb* encounters alveolar macrophages (which are the dominant phagocytic subset of the lower respiratory tract) and other innate cells, such as monocytes, neutrophils, and dendritic cells (DCs).

Among these, macrophages and DCs are also classified as classical, phagocytic antigen presenting cells (APCs). The innate response is initiated by PRRs on the immune cell surface (such as toll-like receptors – TLRs, and C-type lectin receptors – CLRs) or intracellular receptors in cytosolic, phagosomal, or endosomal compartments of immune cells (such as nucleotide-binding and oligomerization domain (NOD)-like receptors – NLRs) binding *Mtb*-associated PAMPs (such as mycobacterial carbohydrates, glycolipids, glycoproteins, and lipoproteins). Via receptor-mediated phagocytosis, macrophages and DCs internalize *Mtb* and attempt to kill bacilli within the highly acidic, enzyme-rich phagolysosome. Despite this well-orchestrated innate phagocytosis pathway, *Mtb* has been shown to actively block fusion of the phagosome with the lysosome to prevent formation of the phagolysosome, thereby enabling bacterial survival (Russell, 2011; Zhai et al., 2019). In this way, the alveolar macrophage (in particular) can form a niche for *Mtb* replication. Additionally, the *Mtb* ESAT-6 secretion system-I (ESX-I secretion system) can disrupt the phagosomal membrane to release bacilli and bacterial products into the macrophage cytosol (D. Houben et al., 2012). Although phagocytosis is the main innate immunological response for containing and eliminating *Mtb,* other processes include autophagy (Deretic, 2014), apoptosis (Lam et al., 2017) and inflammasome maturation (J. Ma et al., 2021; Wawrocki & Druszczynska, 2017); the mechanisms of which have been extensively reviewed elsewhere and are not detailed in this thesis, as this falls beyond the scope of primary focus.

Upon recognition of *Mtb,* innate cells also secrete pro-inflammatory cytokines and chemokines into the local microenvironment to initiate recruitment and activation of more innate cells to the site of infection including, recruited macrophages, neutrophils, DCs and NK cells (Algood et al., 2005; A. M. Cooper et al., 2011). Following infection of innate cells in the airways, *Mtb* may gain access to the lung interstitium. It has been proposed that *Mtb* may access the parenchyma through direct infection of epithelial cells and/or transmigration of *Mtb*-infected macrophages across the epithelium. Besides assisting in mycobacterial

clearance, the immune cascade of recruiting immune cells to the site of infection may also generate a granuloma (Pai, Behr, et al., 2016).

The granuloma is often considered a canonical feature of TB disease, comprising a structured organization of cells, most often formed in the lung. Granulomas are also frequent in the lymphoid organs, such as lymph nodes and spleen, and other tissues including the liver. The center of the typical TB granuloma contains *Mtb*-infected macrophages or cell-free *Mtb,* and is surrounded by innate cells such as monocytes, neutrophils, and DCs. On the exterior is a lymphocytic cuff, comprised mainly of B cells and T cells (Kaufmann, 2001; Ndlovu & Marakalala, 2016; Ramakrishnan, 2012). Granulomas exhibit intra-host variability (P. L. Lin et al., 2014) and are highly heterogenous, being classified as caseous, necrotic, non-necrotizing or calcified (Ehlers & Schaible, 2012; Flynn et al., 2011; Pagán & Ramakrishnan, 2014).

The TB granuloma has been a longstanding research priority, illustrating dual functions during *Mtb* infection: from the perspective of the host, the granuloma may act as a safeguard to contain infection and prevent dissemination to the rest of the body. However, from a pathogen point of view, the granuloma may serve as a niche for persistence and survival. Sometimes, bacilli actively replicate within the granuloma and the granuloma may fail to contain the infection if bacterial burden becomes excessive, possibly resulting in *Mtb* dissemination (P. L. Lin et al., 2014).

1.2.3 The adaptive response to *Mtb* infection

Returning to early events following *Mtb* infection, if the innate response fails to eliminate *Mtb,* the adaptive immune system is required to improve bacterial killing by innate cells. With the establishment of infection, macrophages, inflammatory monocytes, and/or DCs are transported to the pulmonary lymph nodes for T cell priming. More specifically, DCs are the primary APCs responsible for linking innate and adaptive immune systems in the context of

Mtb infection. However, *Mtb* has been shown to actively delay T cell priming in the lymphoid tissues by interfering with immune cell (specifically DC) activation, maturation, and trafficking to the lung (Baena & Porcelli, 2009; C. H. Liu et al., 2017).

T cell priming in the lymph nodes requires three signals: 1) antigen presentation to the TCR, 2) co-stimulation to initiate T cell proliferation and effector functions, and 3) release of cytokines by APCs to direct polarization of T cells. Processed *Mtb* peptide antigens are expressed on the cell surface of APCs via the major histocompatibility complex (MHC)-II presentation pathway (K. Murphy & Weaver, 2016). CD4 T cells are the major subset which recognizes peptide antigens presented by MHC-II on APCs, resulting in a cascade of immune responses to initiate adaptive immunity and further amplify the innate response. The interaction of APC co-stimulatory molecules (CD70, CD80, CD86 and CD40) and their T cell ligands (CD27, CD28 and CD40L), induces a T cell signaling cascade to stimulate proliferation and effector functions. Finally, cytokines and chemokines released by APCs can further activate T cell transcription factors for T cell polarization into various T helper (Th) lineages including, Th1, Th2, Th9, Th17, Th22, regulatory T cells (T_{regs}) and follicular helper T cells (T_{FH}). The effector and functional profiles of these lineages have been reviewed elsewhere (Geginat et al., 2013; Kara et al., 2014; Zhu et al., 2010) and fall beyond the scope of this thesis.

1.2.4 *Mtb*-specific T cell responses for protective immunity

Generally, protection from TB disease is associated with a strong CD4 Th1 immune response (Caruso et al., 1999; Casanova et al., 2012; Getahun et al., 2010; Scanga et al., 2000; Walzl et al., 2011). Since vaccination is one of the most effective public health interventions against disease, the development of improved and effective TB vaccines has been a major research priority to reduce TB burden (Abu-Raddad et al., 2009; R. C. Harris et al., 2020). To this end, the central role of CD4 Th1-mediated protection has rationalized

most recent TB vaccine strategies which focussed on identifying immunodominant *Mtb* antigens, with the intent to induce a repertoire of *Mtb*-specific polyfunctional CD4 Th1 responses as the cornerstone for T cell-mediated protective immunity against TB disease. The first novel TB vaccine candidate, MVA85A, was shown to boost the Ag85A-specific component of BCG-induced responses to promote polyfunctional and durable memory CD4 Th1 cells (Scriba et al., 2011; M. Tameris et al., 2014). However, efficacy testing revealed no significant protection above that afforded by the newborn BCG vaccination (M. D. Tameris et al., 2013). Published results of the M72/AS01$_E$ candidate, showed that the vaccine provided protection against active TB disease in *Mtb*-infected adults for at least 3 years with an efficacy of roughly 50% (Tait et al., 2019). Interestingly, findings showed that the M72/AS01$_E$ vaccine induced durable T cell and humoral antibody responses (Tait et al., 2019), as well as antigen-dependent NK cell IFN-γ production for up to 6 months post-vaccination (Penn-Nicholson et al., 2015).

These bodies of evidence reinforce the hypothesis that CD4 Th1 responses do not act alone to protect against TB disease progression (Sakai et al., 2016). This has led to the idea that successful immune responses against *Mtb* infection are multifaceted and may not be interpreted on the oversimplified CD4 Th1 response paradigm. Rather, cytokines secreted by CD4 T cells are necessary for optimal activation of other cell subsets, which in turn, provide feedback signals to steer innate and adaptive immune responses towards protective or non-protective immunity. Through these complex bi-directional signalling interactions, other cell subsets also play a role in the regulation of host immune responses against *Mtb.* Recently, innate NK cells have moved to the forefront of interest, with growing evidence to support their important role in modulating the immune response to *Mtb* (Choreño Parra et al., 2017; Esin & Batoni, 2015). In the following sections, the emerging role of NK cell subsets are reviewed as potentially important role players during progression to TB disease.

1.3 Characterization of NK Cell Subsets

1.3.1 NK cell function and activation

In terms of function, NK cells are notorious for their ability to recognize and eliminate pathogen-infected and neoplastic cells. Once activated, NK cells respond by producing immunoregulatory cytokines (Paul & Lal, 2017), anti-microbial mediators (such as nitric oxide, α-defensins, and granulysin) and engage in cytotoxic activity to lyse infected cells (Choreño Parra et al., 2017; Esin & Batoni, 2015).

Most circulating NK cells are in a resting state and may be activated indirectly or classically. Indirect activation of NK cells occurs by microbial antigens binding PRRs on myeloid accessory cells to initiate a cascade of cytokine responses from nearby cells. Soluble factors in the milieu, such as IL-12 (Lehmann et al., 2001), IL-15 (Carson et al., 1994), IL-18 (Senju et al., 2018) and IFN-α (Ellis et al., 1989; Jewett & Bonavida, 1995; Tomescu et al., 2007, 2015) are produced by myeloid accessory cells and induce NK cell activation. IL-2 secreted by activated bystander T cells also induces NK cell activation (K. S. Wang et al., 1999). This process is referred to as “bystander activation”, also known as cytokine-mediated indirect activation, shown in Figure 1.2. (Caligiuri, 2008; Mandal & Viswanathan, 2015; Chalifour et al., 2004; Esin et al., 2004; Esin & Batoni, 2015).

Classical activation is governed by the fine balance of activation/inhibitory signals delivered to NK cells via surface receptors. Figure 1.3 illustrates common NK cell surface receptors grouped according to their activating or inhibitory classification. Inhibitory receptors on NK cells are mainly killer immunoglobulin-like receptors (KIR), CLRs (CD94-NKG2A), leukocyte Ig-like inhibitory receptor-1 (LIR-1) and leukocyte-associated Ig-like receptor-1 (LAIR-1) (Figure 1.3) (S. Kumar, 2018; Sivori et al., 2019a). Inhibitory receptors typically recognize self MHC-I and prevent NK cell activation. Inhibitory signals via MHC-I binding are important

for self-tolerance and homeostasis (Anfossi et al., 2006a; Kärre et al., 1986). When MHC-I is downregulated (as would occur in virus-infected or tumour cells to escape recognition), there is “missing self-recognition” and NK cells are activated to effect killing of the compromised target cells (Figure 1.2) (Kärre et al., 1986).

Activating receptors include CD16, natural killer group 2 member D (NKG2D) receptors and natural cytotoxicity receptors (NCR) (such as, NKp30, NKp44, NKp46) (Figure 1.3) (Cong & Wei, 2019; Islam et al., 2021; Vivier et al., 2011). NK cells also express co-activating receptors including NKp80, Ig-like receptors (2B4), or the DNAX accessory molecule-1 (DNAM-1) (Konjević et al., 2017; Paul & Lal, 2017). When the balance of signal delivered via activating signals outweighs the binding of ligands to inhibitory receptors, NK cells are activated. In humans, lysis of *Mtb*-infected monocytes by NK cells involves NKG2D and NKp46 activating receptors recognizing UL16 binding protein 1 (ULBP1) and vimentin, respectively (Vankayalapati et al., 2005). During pathological conditions, a cell may express stress-induced ligands for NK activating receptors (Bauer et al., 1999; Cerwenka et al., 2001; Cosman et al., 2001; Diefenbach et al., 2001), thereby eliciting an “induced self” NK cell response (Figure 1.2) (Horowitz et al., 2012; Newman & Riley, 2007). NK cells express between two and four inhibitory receptors with an array of activation receptors. Different NK cells may express these in different combinations, accounting for the large degree of heterogeneity observed within the NK population (Horowitz et al., 2013; Bauer et al., 1999; Malnati et al., 1993; Mandal & Viswanathan, 2015).

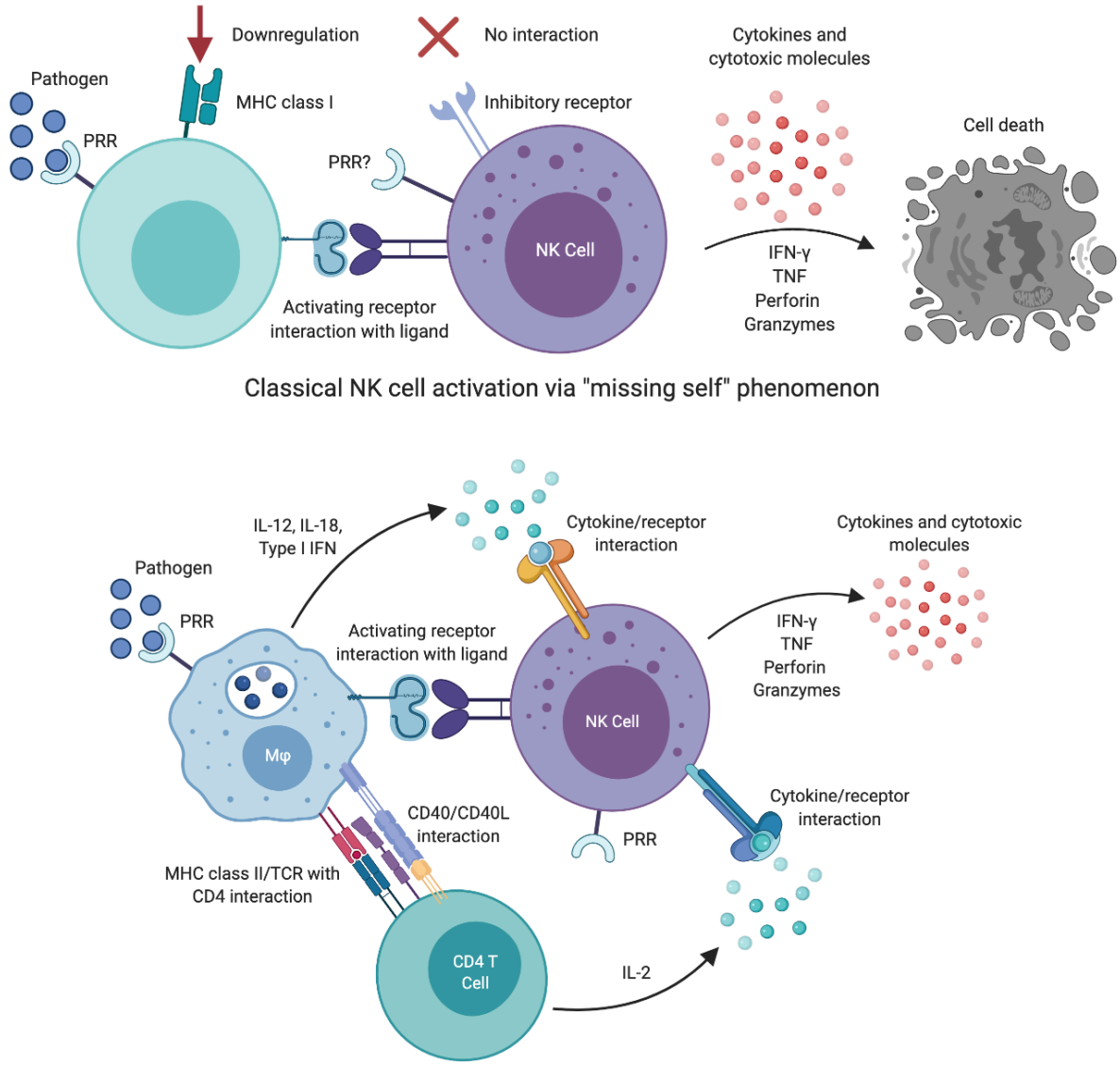

Figure 1.2: Classical and indirect activation of NK cells. Classical activation follows downregulation of MHC-I molecules on immune cells and no binding with NK cell inhibitory receptors occurs. This is known as the "missing self" phenomenon of NK cell activation. Stress-induced ligands on immune cells may also bind activating receptors on NK cells to result in "induced self" activation. Indirect NK cell activation occurs by accessory cells (such as antigen presenting cells and T cells) releasing soluble molecules into the milieu which bind to cytokine receptors on the NK cells to induce "bystander activation". NK cells themselves also express PRRs for direct recognition of PAMPs to induce activation. (Image adapted from Horowitz et al., 2012; Newman & Riley, 2007).

An interesting finding in NK cell biology suggests that NK cells themselves can express PRRs, such as members of the TLR family (Becker et al., 2003; Eriksson et al., 2006; Souza-Fonseca-Guimaraes, Parlato, Fitting, et al., 2012; Souza-Fonseca-Guimaraes, Parlato, Philippart, et al., 2012), intracellular receptors like NOD2 (Qiu et al., 2011), or members of the NCR family (Sivori et al., 2014). Thus, NK cells may also be activated by directly

recognizing PAMPs. For example, NK cells may directly recognize *Mtb* and become activated by TLR2 binding peptidoglycan and NKp44 binding unknown components of the *Mtb* cell wall (Esin et al., 2013b). BCG has also been found to directly stimulate purified NK cells from peripheral blood in healthy humans in the absence of accessory cells and cytokines (Batoni et al., 2005; Esin et al., 2004). These effects are not seen upon physical separation by a pore barrier, indicating direct interaction and activation of NK cells with BCG (Esin et al., 2004). Thus, direct sensing of microbial pathogens may represent a previously unappreciated mechanism of NK cell participation to the immune system's first line of defence.

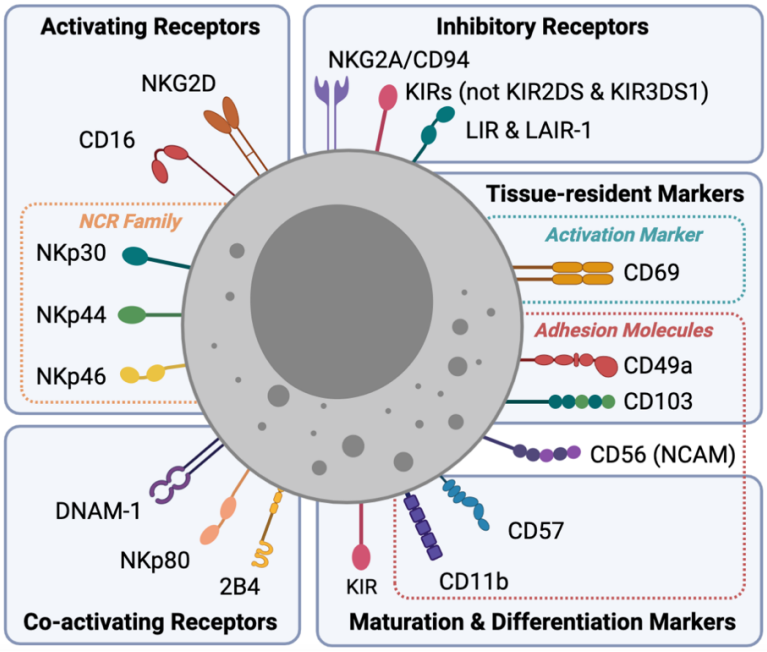

Figure 1.3: Phenotypic markers and surface receptors expressed by NK cells. Receptors may be divided into categories of activating, co-activating and inhibitory receptors. The archetypal marker for NK cells is CD56, also known as neural cell adhesion molecule (NCAM). Other markers expressed by NK cells include tissue-resident, maturation, and differentiation markers, some of which may be activation markers and/or adhesion molecules. NK cells may express these markers and receptors in different combinations, accounting for the large degree of heterogeneity within the NK cell population. (Image adapted from Cong & Wei, 2019; Islam et al., 2021; Vivier et al., 2011).

Cytotoxic activity of NK cells is mediated by several pathways. Firstly, NK cells may secrete cytotoxic molecules (such as perforin and granzymes) to induce apoptosis, during a process referred to as degranulation (Prager & Watzl, 2019; Smyth et al., 2005). Perforin released during degranulation is a membrane-disrupting protein that facilitates entry of granzymes into the target cell. Granzymes are a family of serine proteases that activate caspase molecules to induce apoptosis of infected or neoplastic cells (Martínez-Lostao et al., 2015;

Pardo et al., 2002; Topham & Hewitt, 2009). For degranulation to occur, an immunological synapse is formed between NK cells and the target cell. The actin cytoskeleton of the NK cell is reorganized and polarization of the microtubule organizing centre (MTOC) occurs. A secretory lysosome is formed towards the lytic synapse and is docked at the plasma membrane of the NK cell. The secretory lysosome is then fused with the plasma membrane of the target cell, releasing cytotoxic molecules (i.e., perforin and granzymes) to induce apoptosis (Paul & Lal, 2017).

Secondly, caspase-dependent apoptosis may occur by death receptors (Fas/CD95) on a target cell binding with the NK cell equivalent ligands (FasL, TRAIL) (Prager & Watzl, 2019; Smyth et al., 2005). Thirdly, NK cells expressing CD40L may bind CD40 on APCs. This leads to upregulation of co-stimulatory molecules, CD80 and CD86, on the surface of APCs and the production of nitric oxide (NO) (Carbone et al., 1997; Suttles & Stout, 2009). There have also been reports of glutathione (GSH) influencing NK cell cytotoxic function (Allen et al., 2015). Indeed, Allen and colleagues found that low levels of intracellular GSH decreases NK cytotoxic function, while increased GSH inhibits intracellular *Mtb* within human monocyte-derived macrophages (Allen et al., 2015).

Another mechanism of NK cell-mediated killing includes antibody-dependent cellular cytotoxicity (ADCC) (Nigro et al., 2019). A subset of cytotoxic NK cells is known to express the low-affinity Fc receptor of IgG (FcγRIII), also known as CD16. Via CD16, NK cells actively bind and eliminate targets cells whose surface antigens have been bound by antibodies (Lanier, Ruitenberg, et al., 1988; W. Wang et al., 2015). In addition to cellular cytotoxicity, NK cells also play immunomodulatory roles by producing a range of cytokines including IFN-γ, TNF, IL-5, IL-10, IL-22 and granulocyte-macrophage colony-stimulating factor (GM-CSF) (Biron et al., 1999; P. Kumar et al., 2013; van den Bosch et al., 1995; Warren et al., 1995; Xu et al., 2014). To this end, soluble factors and cytokines secreted by NK cells can mediate

phagocyte effector mechanisms and killing of intracellular mycobacteria by macrophages (Allen et al., 2015; Choreño Parra et al., 2017).

1.3.2 NK cell subsets

NK cells represent approximately 10-15% of the total peripheral lymphocyte population. In humans, NK cells are traditionally identified phenotypically by the expression of CD56 (the archetypal marker of NK cells) and/or CD16, in combination with the lack of CD3 and CD19 expression (Lanier, Ruitenberg, et al., 1988; Lanier et al., 1989, 1991). The NK population is not homogenous, but rather represents a population of multiple subsets with distinct phenotypes, functional activity and tissue localization (Horowitz et al., 2013; Bauer et al., 1999; Malnati et al., 1993; Mandal & Viswanathan, 2015). The two most well-known subsets of human NK cells include $CD56^{dim}CD16^{bright}$ and $CD56^{bright}CD16^{dim}$, distinguished according to their immunophenotype, function and maturation status. Figure 1.4 describes the principal NK cell subsets in terms of their common phenotypic and functional characteristics.

The highly cytotoxic $CD56^{dim}CD16^{bright}$ ($NK_{cytotoxic}$) subset comprises approximately 90% of the total NK cell population in the peripheral blood with the capacity to secrete cytotoxic molecules to initiate apoptosis and/or induce ADCC. In contrast, the $CD56^{bright}CD16^{dim}$ ($NK_{regulatory}$) subset comprises approximately 10% of the total peripheral NK cell population. This NK cell subset is less cytotoxic and less mature relative to their $CD56^{dim}CD16^{bright}$ $NK_{cytotoxic}$ counterparts, and principally produces cytokines (such as, IFN-γ, TNF and IL-22) (Figure 1.4) (Béziat et al., 2011; Björkström, Riese, et al., 2010; Yu et al., 2010).

Unlike in the peripheral blood, $NK_{regulatory}$ $CD56^{bright}CD16^{dim}$ cells predominate in the liver and secondary lymphoid organs (Björkström et al., 2016; Marquardt et al., 2015; Sharkey et al., 2015). In healthy lung tissue, NK cells occur at a frequency of 5-20% of the total lymphocyte population, which is similar, if not slightly higher, than peripheral blood

(Marquardt et al., 2017b). Also, similarly to PBMC, approximately 80% of lung NK cells display a mature, $NK_{cytotoxic}$ $CD56^{dim}CD16^{bright}$ phenotype. The remaining ~20% of NK cells comprise the more immature $NK_{regulatory}$ $CD16^{dim}$ phenotype in healthy lung tissue (Björkström, Riese, et al., 2010; M. A. Cooper et al., 2001; Marquardt et al., 2017b; Y. Zhang et al., 2007).

NK cell subsets within the lung compartment differentially express tissue residency markers such as CD69, CD49a, CD103 (Figure 1.3) (Hervier et al., 2019a). The mature, terminally differentiated $NK_{cytotoxic}$ $CD56^{dim}CD16^{bright}$ phenotype (comprising ~80% of total lung NK cells) generally lack expression of tissue resident markers and are considered as "circulating" NK cells (Marquardt et al., 2017a). These circulating lung NK cells are hypofunctional, displaying poor cytotoxicity and ADCC activity against target cells, despite stimulation with phorbol 12-myristate 13-acetate (PMA)/ionomycin or IFN-α (G. E. Cooper et al., 2018; Marquardt et al., 2017b). The remaining 20% of lung NK cells expressing CD69, CD49a and/or CD103 are considered "tissue-resident" NK cells with a less mature phenotype (Hervier et al., 2019a). Interestingly, in comparison to their matched peripheral cells, $CD49a^{+}CD56^{bright}$ lung tissue-resident NK cells display higher capacity for degranulation and IFN-γ production upon interaction with virally infected autologous macrophages *in vitro* (G. E. Cooper et al., 2018). Overall, current evidence suggests that the predominant circulating lung NK cells are highly differentiated but hypofunctional, while tissue-resident lung NK cells are less mature, yet functionally competent.

As discussed in Section 1.2.1, adaptive immunity is characterized by genetic recombination of antigen receptors and vast clonal diversity. Upon antigen sensitization, the adaptive response undergoes clonal selection, proliferation, and expansion of antigen-specific effector cells that establish long-lived immunological memory once the antigen is cleared. For years, NK cells have been classified as an innate component, owing to their germ-line

encoded receptors and their perceived inability to adapt to repeated antigen exposure. Despite the lack of antigen-specific receptors derived from somatically rearranged genes, several lines of evidence suggest that NK cells are closely related to adaptive T cells and B cells (J. C. Sun et al., 2011; Lanier, 2005; Raulet, 2004; J. C. Sun & Lanier, 2009). Firstly, like T cells and B cells, NK cells develop from the common lymphoid precursor (Kondo et al., 1997) and require cytokines of the IL-2R common-γ-chain family (such as IL-15) for development, homeostasis, and survival (A. Ma et al., 2006). Like T cells and B cells in their early developmental stages, NK cells also undergo a process of selection for self-tolerance (Fernandez et al., 2005; Johansson et al., 2005; Kim et al., 2005b; Tripathy et al., 2008). Activated T cells and NK cells also express a range of shared surface receptors including CD25, CD43, CD44, CD69, CD122, CD62L and killer cell lectin-like receptor G1 (KLRG1) (M. A. Williams & Bevan, 2007; Yokoyama et al., 2004). In terms of functionality, NK cells and T cells are similar in their ability to produce IFN-γ and TNF following activation, and cytotoxic T lymphocytes (CTLs) are also related to NK cells through their shared ability to mediate cytotoxic killing of target cells via secretion of perforin and granzymes (M. A. Williams & Bevan, 2007; Yokoyama et al., 2004). Finally, immature T cells lacking the B cell leukaemia 11b (Bcl11b) transcription factor have been shown to dedifferentiate into NK-like precursor cells (Ikawa et al., 2010; L. Li et al., 2010; P. Li et al., 2010). Together, these observations suggest NK cell developmental and functional similarities that are closely related to adaptive immune cells. Therefore, it may not be totally surprising for NK cells to have “adaptive-like” features.

A less common adaptive-like feature of NK cells was first published in 2009 (J. C. Sun et al., 2009), which suggested the presence of a clonally expanded, memory-like subset of NK cells in a murine model that provided protection against lethal challenge with murine cytomegalovirus (MCMV). Following control of initial infection, the pool of expanded NK effector cells underwent a contraction phase to establish long-lived and self-renewing

memory-like NK cells that could be recovered several months following infection (J. C. Sun et al., 2009). Although more investigation is needed, there is accumulating evidence to suggest memory responses evoked in NK cells from experimental models in mice (Gillard et al., 2011; Majewska-Szczepanik et al., 2013; O'Leary et al., 2006), non-human primates (NHPs) (Reeves et al., 2015) and humans (Nikzad et al., 2019). In humans, memory-like NK cells have been studied extensively in the context of human cytomegalovirus (HCMV) seropositivity (Lopez-Verges, 2011). Most memory-like NK cells are thought to be derived from the expansion of adaptive $CD57^{+}NKG2C^{+}$ cells (Figure 1.4) (Béziat et al., 2012; Lopez-Vergès et al., 2011), which has been demonstrated in human peripheral blood. However, it remains to be shown whether NKG2C overexpression occurs in lung NK cells from healthy individuals and whether these memory-like features occur in the tissues (G. E. Cooper et al., 2018; Hervier et al., 2019a).

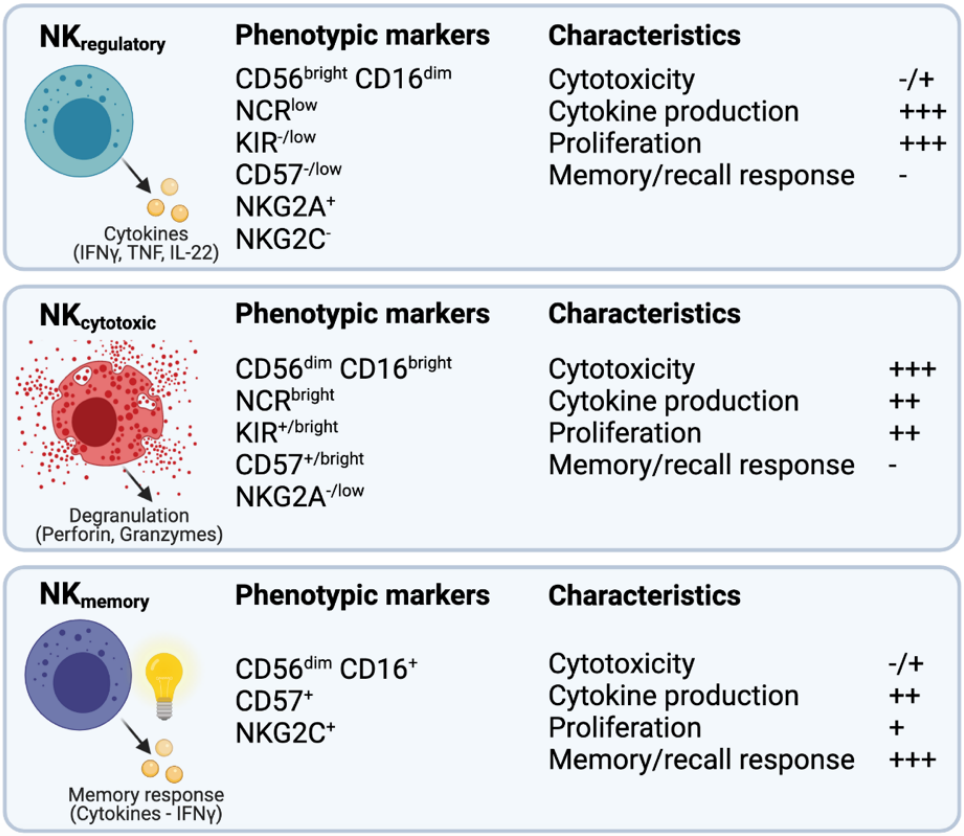

Figure 1.4: Phenotypic markers and functional characteristics of regulatory, cytotoxic and memory NK cell subsets. (Image adapted from Björkström et al., 2010; Cao et al., 2020; Poznanski & Ashkar, 2019).

Despite the widely used phenotypic definitions of NK cell subsets (shown in Figure 1.4), an interesting review by Poznanski and Ashkar summarizes evidence for instances where traditional phenotypic NK profiling confounds functional characteristics (Poznanski & Ashkar, 2019). In fact, there is a growing body of evidence to suggest that NK cells expressing the same phenotypic characteristics may have divergent functions, while those with similar functions may express a broad range of phenotypic markers (Lunemann et al., 2019; Poznanski et al., 2018; J. A. Wagner et al., 2017). As an alternative, it has been suggested that metabolism is integral to NK cell effector functions and may be used as a fingerprint to distinguish functional fates (Poznanski & Ashkar, 2019).

To summarize metabolism as a fingerprint of NK cell functionality, glucose-driven glycolysis and oxidative metabolism are associated with classical cytotoxic effector functions of mature $NK_{cytotoxic}$ cells (Assmann et al., 2017; Donnelly et al., 2014; Keating et al., 2016; Keppel et al., 2015; Loftus et al., 2018). In contrast, $NK_{regulatory}$ (cytokine-producing) NK cells are said to predominate under hypoxic and glycolysis-limiting conditions. Such conditions are also associated with long-lived memory NK cells that are marked by enhanced mitochondrial respiratory capacity and membrane potential, with decreased levels of reactive oxygen species (ROS) (Poznanski & Ashkar, 2019; Balsamo et al., 2013; Cong et al., 2018; Wolter et al., 2015; Zaiatz-Bittencourt et al., 2018). Potentially, markers of metabolic features could be used in conjunction with classic phenotypic profiling to identify NK cell fates. For example, cytometry or microscopy techniques could be used to assess functional mitochondrial measures (such as mitochondrial mass, membrane potential, ROS production and oxidative stress), in addition to expression and phosphorylation of metabolic regulators (such as mTOR, AMPK and their downstream targets). Although not being direct measurements of metabolic activity, assessing cell-surface receptors such as Glut1, CD71 and CD98 may reflect metabolic states in NK cells (Salzberger et al., 2018; Poznanski & Ashkar, 2019).

Much remains to be investigated to fully delineate and validate this paradigm. However, more comprehensive investigations of the interplay between NK cell phenotype and metabolism may provide a deeper understanding of the mechanisms governing the spectrum of NK cell function.

Having described the foundations of NK cell activation, function, and classification; the emerging role of NK cells are now discussed further in the context of the immune response against *Mtb* infection and TB disease.

1.4 The Emerging Role of NK cells in TB

1.4.1 The role of NK cells in lung diseases

Most NK biology studies have focussed on peripheral blood NK cells in humans, while relatively little is known about lung NK cells. However, recent topics considering tissue-resident NK cells and tissue microenvironments have provided evidence that NK cells are important participants in lung immune responses (Cong & Wei, 2019; Culley, 2009; Hervier et al., 2019a).

As an innate component, NK cells are rapid responders to invading pathogens and have the potential to clear infection promptly, particularly in instances of viral infection (Biron et al., 1989, 1999; Björkström et al., 2021; Brandstadter & Yang, 2011; Hammer et al., 2018; Orange, 2002). However, NK cells may also contribute to uncontrolled inflammation and pathological damage in certain circumstances. This is particularly true for autoimmune conditions including systemic lupus erythematosus (SLE) (Segerberg et al., 2019), type 1 diabetes mellitus (T1DM) (Berhani et al., 2019) and autoimmune liver disease (ALD) (Hudspeth et al., 2013). The role of NK cells in the development of autoimmune diseases stems from their ability to shape the adaptive response through secreted cytokines and/or chemokines, as well as their ability to cross-interact and influence other immune cell activity

(M. Liu et al., 2021). Therefore, NK cell hyperactivation or dysfunction may be associated with pathogenesis of various inflammatory-associated diseases.

The involvement of NK cells in various lung diseases, such as lung cancer, chronic obstructive pulmonary disease (COPD), asthma, and other respiratory infections has been discussed in a recent review by Cong and Wei (Cong & Wei, 2019). NK cells of the lung are thought to originate and develop in the bone marrow and then migrate to the lung, where the comprise approximately 10-20% of the lymphocytes in the parenchyma (Cong & Wei, 2019; Grégoire et al., 2007; Marquardt et al., 2017a). In the 2017 study by Marquardt and colleagues, human NK cells were isolated from macroscopically normal lung tissue taken as distal as possible from the tumour side of resected lung lobes in patients indicated for lobectomy (Marquardt et al., 2017a). The results from this investigation found that human lung NK cells are comprised mainly of the $NK_{cytotoxic}$ $CD56^{dim}CD16^{bright}$ subset, which are considered highly differentiated due to their KIR-expressing, $CD57^{+}NKG2A^{-}$ phenotype (Figure 1.4) (Marquardt et al., 2017a). Although highly differentiated in phenotype, these lung NK cells were shown to be functionally hyporesponsive to stimulation by target cells, relative to their peripheral blood counterparts, despite priming with IFN-α (Marquardt et al., 2017b). It is thought that the effects of suppressive/regulatory alveolar macrophages and soluble factors within fluid of the respiratory tract may contribute to the observed hypofunctional NK activity (Marquardt et al., 2017a; Robinson et al., 1984). It has been proposed that hypofunctional lung NK cells may contribute to pulmonary homeostasis and prevent inflammation-induced tissue pathology in response to the myriad of inhaled environmental and autologous antigens (Cong & Wei, 2019; Robinson et al., 1984). Although yet to be proven, perhaps hyporesponsive NK cells that maintain homeostasis in the lung may be a double-edged sword, contributing to an immunosuppressive microenvironment that favours disease progression in *Mtb*-infected individuals.

1.4.2 Evidence supporting the role of NK cells in TB disease

Several studies, predominantly based on animal models, have demonstrated that NK cells are involved in the response to *Mtb* infection. Earlier studies illustrated upregulated expression of CD69, IFN-γ and perforin by lung NK cells of *Mtb*-infected, immunocompetent mice, relative to uninfected controls. However, depleting NK cells did not appear to influence the course of infection (Junqueira-Kipnis et al., 2003a). Nevertheless, a more recent investigation in T cell deficient mice suggests NK cell-mediated defence against *Mtb* infection through IFN-γ production (Feng et al., 2006). All aspects considered, it must be noted that traditional inbred mouse strains infected with *Mtb* experience differences in disease pathology (such as the absence of caseating granulomas) compared to humans (Apt & Kramnik, 2009; Ordonez et al., 2016); although newer techniques of low-dose aerosol infection in outbred or collaborative-cross murine models have shown promise in the fields of screening new TB vaccines and drug candidates (Singh & Gupta, 2018; Apt & Kramnik, 2009; Cong & Wei, 2019; Orme, 1988). The common mouse model also lacks CD56 and KIR expression on NK cells, which have been found to be important in the context of human lung disease (Hayakawa et al., 2006). Furthermore, murine models do not express granulysin (or a homologue), which is a cytolytic molecule produced by CTLs and NK cells with particular importance as a mediator involved in *Mtb* killing (Krensky & Clayberger, 2005; Semple et al., 2010; Stenger et al., 1998). Therefore, studies reporting on the role of NK cells during TB disease in murine models may be informative, but not entirely translatable in the human context.

In human studies, peripheral blood NK cells respond to stimulation with *Mtb* or BCG by upregulating IFN-γ expression (Feinberg et al., 2004; Gerosa et al., 2002; Suliman et al., 2016). Indeed, a study by Bozzano and colleagues also illustrated that human NK cells isolated from healthy donors respond and exert effector functions when cultured with live

Mtb bacilli (Bozzano et al., 2009). This study also highlighted reduced frequencies of $CD56^{bright}$ NK cells amongst peripheral leukocytes, with reduced expression of activating receptors (namely, NKp30 and NKp46) and lesser functional capacity in TB patients relative to healthy controls (presumed uninfected).

In a 2018 publication by Chowdhury and colleagues, significantly increased frequencies of peripheral cytotoxic NK cells were observed in QFT^{+} adolescents relative to QFT^{-} controls (Chowdhury et al., 2018). In a longitudinal study of the South African Adolescent Cohort Study (ACS), peripheral NK cell frequencies were decreased in progressors 0-180 days before TB diagnosis, while no significant changes were observed in non-progressors during the two years of follow up (Chowdhury et al., 2018). In a different cohort of active TB patients, individuals who responded well to treatment had NK cell levels that increased significantly between baseline and end of treatment, while treatment non-responders did not have significant changes in their circulating NK cell frequencies between initiation and completion of treatment (Chowdhury et al., 2018). Interestingly, changes in peripheral NK cell frequencies inversely correlated with the extent of inflammation of the lung, indicated by glycolytic activity measured by PET-CT scans of TB patients at diagnosis and 4 weeks after treatment initiation (Chowdhury et al., 2018). This supports the notion that circulating NK cells can serve as surrogates of the immune response at the primary site of *Mtb* infection. Together, findings from Chowdhury and colleagues suggest that longitudinal measurements of peripheral NK cell frequencies may inform disease progression, therapeutic responses, and lung inflammation of active TB patients in South African cohorts.

In an independent study, a group of researchers suggested the CD3-CD7+GranzB+ subset of NK-like cells could be used as a TB biomarker to distinguish between active TB and $IGRA^{+}$ controls (Cai et al., 2020). More specifically, this study observed significant stepwise depletion of these NK-like cells along the TB spectrum from $IGRA^{-}$ controls (highest frequencies observed) through to $IGRA^{+}$ and active TB disease (lowest frequencies

observed). The CD3-CD7+GranzB+ subset was also shown to increase following successful anti-TB treatment (Cai et al., 2020). Finally, a whole blood transcriptomic study performed by our research group at SATVI, investigated South African adolescent participants of the ACS who progressed to TB disease and matched, *Mtb*-immunologically sensitized (QFT^+ and/or TST^+) controls who remained asymptomatic (non-progressors) over 2 years of follow-up. The results of this study indicate significantly decreased peripheral blood expression of genes in modules representing NK cell subsets in those who progressed to active disease compared to matched non-progressors (Scriba et al., 2017). Together, these findings indicate that perturbations in peripheral blood NK cells are associated with TB disease. However, it remains unclear whether these observations implicate the cause or reflect a consequence of TB disease.

More recently, a study by Harris and colleagues investigated NK cell phenotype and function in QFT^+ and QFT^- adults in Kenya (a TB endemic setting) and compared these findings to *Mtb*-immunologically naïve healthy controls in the United States (a non-TB endemic setting) (L. D. Harris et al., 2020). Findings showed that a distinct subset of $CD56^{dim}$ NK cells differentiated Kenyan and US groups. Within the Kenyan group, NK cells from QFT^+ participants showed significant downregulation of NKp44 and the inhibitory receptor TIGIT (T cell immunoreceptor with Ig and immunoreceptor tyrosine-based inhibitory motif (ITIM) domains) relative to QFT^- participants. Furthermore, participants from TB endemic Kenya had $CD56^{dim}$ phenotypic profiles of diminished NK cell activation, degranulation, and cytokine production in response to *Mtb* antigens relative to *Mtb*-naïve US healthy controls. Thus, the authors postulate that phenotypic and functional profiles of NK cells are modified in TB endemic settings (L. D. Harris et al., 2020).

Current evidence suggests that changes do occur in the peripheral NK cell compartment during progression to TB disease. However, much remains to be uncovered regarding the precise role and/or reasoning. It is well documented that chronic infection and inflammatory

diseases (including TB) alter myelopoiesis and lymphopoiesis, in turn, resulting in changes to peripheral cellular compartments during disease (Baldridge et al., 2010, 2011; Naranbhai et al., 2014; Scriba et al., 2017). Therefore, the changes in the peripheral NK cell compartments observed during progression to TB disease may reflect a cause and/or consequence of disease progression, the specifics to which remain unknown. Studying such phenomena in humans to define the kinetic and role of these cellular changes during disease progression may identify early biomarkers of risk of TB disease and may inform novel immune interventions.

Moving towards the site of TB disease, an early study found enrichment of IFN-γ-producing $CD56^{bright}$ NK cells in the pleural fluid of TB patients. Further investigation revealed that enrichment of this subset was due to selective apoptosis of cytotoxic $CD56^{dim}CD16^{+}$ NK cells via soluble factors present within the pleural effusion fluid (Schierloh, Yokobori, et al., 2005). Within the lung itself, a study by Portevin and colleagues investigated lung lesions of TB patients using immunofluorescent microscopy and demonstrated that NK cells are recruited to the site of disease in TB patients and are prominent in granulomatous lesions (Portevin et al., 2012). Here, NK cells interact with infected cells and extracellular mycobacteria that are released following lysis of infected cells by specific CD8 T cells or NK cells. In this study, NK cells were found in close proximity to blood vessels, suggesting recent extravasation. Additionally, NK cells were found infiltrating the epithelioid macrophage layer of a well-cuffed granuloma where liquefaction was evident. Notably, signals for NK cells were rarely observed in unaffected airway tissues, while only few were evident in the surroundings of a calcified granuloma or within its sclerotic rim (Portevin et al., 2012). Collectively, these findings suggest that NK cells are recruited and play a dynamic role at the site of TB disease in humans. Importantly, these data were generated from MDR-TB patients for whom lung resections were indicated due to severe immunopathology. These findings may therefore not reflect what happens in more common drug-sensitive

(DS)-TB cases or those who have less severe TB disease. Additionally, these studies did not include healthy controls, such as those with and without evidence of immunological sensitization to *Mtb*. It may be said that in human studies, our understanding in the TB domain is largely hampered by the difficulty of sampling tissues from DS-TB patients and appropriate healthy controls, where tissue resections are not indicated. Therefore, the field requires more tissue immunology studies to gain a better understanding of the role of NK cells in TB immunopathogenesis.

In an NHP study characterizing the lung immune landscape, accumulation of $CD27^+$ NK cells were observed in the lungs of *Mtb*-infected, asymptomatic macaques. The same $CD27^+$ subset was also increased in the circulation of healthy, QFT^+ human participants compared to TB patients. These findings suggest that NK cells (particularly the CD27-expressing subset) may be associated with *Mtb* control (Esaulova et al., 2021). CD27 is considered a marker of memory/mature NK cells and these $CD27^+$ NK cells have been shown to expand and survive long-term to generate memory-like responses and promote vaccine-induced protective immunity against *Mtb* infection in mice (Venkatasubramanian et al., 2017). Moreover, the mouse $CD27^+$ NK subset appears to be more functionally reactive than their $CD27^-$ counterpart with respect to cytotoxicity, cytokine production and proliferation (Hayakawa & Smyth, 2006; Inngjerdingen et al., 2011). These findings suggest that lung $CD27^+$ NK cells may be a key feature of protection in the lung landscape during *Mtb* infection.

In addition to cytotoxicity, NK cells produce soluble mediators upon activation. These may include (among others), proinflammatory IFN-γ and TNF, and regulatory IL-5 and IL-10 cytokines. Although IL-22 production was previously believed to be mainly attributed to T cells, NK cells have also been identified as IL-22 expressing cells (H. Guo & Topham, 2010; Xu et al., 2014). The role of IL-22 is considered protective by stimulating epithelial cell

proliferation/regeneration, maintaining epithelial barrier integrity, activating the acute-phase response, and inducing production of antimicrobial peptides and immune mediators (Arshad et al., 2020; Dudakov et al., 2015; Zenewicz & Flavell, 2011). Together, these activities limit microbial replication and dissemination, which are necessary protective functions during *Mtb*-infection. In the context of TB patients, soluble IL-22 has been found to be predominant at the site of disease (Matthews et al., 2011). Liu and colleagues demonstrated a higher abundance of soluble IL-22 in pleural fluid, plasma, and culture supernatants of TB patients relative to *Mtb*-infected healthy controls (presumably classified as such based on positive IGRA and/or TST results, although the authors do not clarify). Further analysis revealed that IL-22 production was, in part, attributed to CD4 and CD8 T cells, although no other cell subsets were investigated in this study (Y. Liu et al., 2017). This begs the question of whether NK cells may too be contributing to the observed effects. In a study of bovine tuberculosis, IFN-γ and IL-22 gene expression was strongly upregulated, and blood gene expression signatures highlighted these markers as surrogates of protection in BCG-vaccinated cattle (Bhuju et al., 2012). NK cells expressing IFN-γ and IL-22 in response to cytokines and mycobacterial antigens were also found in pleural fluid of TB patients (Fu et al., 2016). Indeed, IL-22 production by NK cells has been associated with inhibited *Mtb* growth within macrophages of healthy individuals by enhancing phagolysosomal fusion (Dhiman et al., 2009). Thus, there is accumulating evidence to support the role of cytokine-producing NK cells in *Mtb* immunity.

Since the 2009 study by Sun and colleagues demonstrating memory-like responses by NK cells in the context of MCMV (J. C. Sun et al., 2009), NK cell “memory-like” responses have been investigated in the context of mycobacterial infection. However, results have been contradictory, highlighting the difficulty in studying the role of memory NK cells in human immunopathogenesis to *Mtb* infection. In the context of adaptive-like features, NK cells isolated from pleural fluid of TB patients express memory markers such as CD45RO and

produce IFN-γ and IL-22 upon BCG stimulation (Fu et al., 2016). Additionally, data produced at SATVI also illustrated elevated frequencies of IFN-γ-expressing NK cells up to one-year post-BCG re-vaccination in healthy, $IGRA^+$ individuals (Suliman et al., 2016). In a subsequent study by Rozot and colleagues at SATVI, NK cells were shown to comprise ~20% of the total IFN-γ-expressing population in BCG-restimulated blood (Rozot et al., 2020). An independent study illustrated that BCG vaccination was associated with increased pro-inflammatory NK cell responses to unrelated pathogens (Kleinnijenhuis et al., 2014a). Here, the findings suggest that BCG could "train" NK cells independently of antigen-specific CD4 T cells via bystander activation. Human vaccination with $M72/AS01_E$ was associated with increased frequencies of IFN-γ-producing NK cells in response to M72 peptide stimulation of peripheral blood mononuclear cells (PBMC). These NK cell responses positively correlated with frequencies of M72-specific, IL-2-producing CD4 T cells (Penn-Nicholson et al., 2015). However, murine models have provided contradictory results showing no enhanced secondary responses by NK cells following BCG vaccination. Taken together, these studies reiterate the need for more conclusive evidence to support the role of memory-like NK cells in TB, particularly in the human context.

1.5 Investigating Tissue Immunology in TB

Animal models have been of great value to the TB field, offering opportunities to perform tissue immunology studies to better understand TB pathogenesis. However, the field still lacks animal models that sufficiently reproduce the diversity and heterogeneity of TB disease seen in humans (as discussed in earlier sections). Perhaps genetically diverse animal models, such as the "humanized mouse" (Herndler-Brandstetter et al., 2017) may be a suitable option to capture the TB disease spectrum and investigate NK cells as the site of disease. Certainly, NHP models are more closely related to humans. With the rise in interest and necessity of such models, results from NHP studies in the context of TB have already

uncovered interesting findings. However, humanized mouse models and NHPs are very expensive, and the most important fact remains: no animal model can completely mimic immunology during human TB disease. Naturally, the gold standard of investigating the role of NK cells in TB would be directly within the tissues of human participants.

In a human context, the TB field has been dominated by investigations studying immune responses in the peripheral blood, mainly due to ease of accessibility, relatively low sampling cost, and most importantly, with little risk to the study participant. While studying peripheral blood is certainly important, circulating cells represent only a small compartment of immune cells in the body and does not necessarily reflect the immune composition and response in the tissues. Studying immune responses derived directly from the site of infection and disease may uncover valuable information to better understand TB immunopathology. However, human tissue immunology studies are lacking in the TB field, partly due to challenges faced in obtaining appropriate samples.

Obtaining samples directly from the tissues (where *Mtb* infection occurs) remains challenging in TB patients, even more so from their control groups (including healthy *Mtb*-immunologically sensitized and non-sensitized community controls), where medical procedures and advanced diagnostics are not indicated. In instances where site-of-disease studies have been performed, findings most often reflect more severe cases, such as drug-resistant forms of *Mtb* infection where procedural intervention was required, and these studies also lacked control groups (Portevin et al., 2012; Schierloh, Yokobori, et al., 2005). As a workaround, several TB immunology studies have investigated immune cells isolated from bronchoalveolar lavage (BAL) procedures, some of which have included healthy controls (recently reviewed by Herrera et al., 2022). BAL studies are advantageous since immune cells are sampled from the bronchial airways and alveolar spaces, which is near to the site of primary *Mtb* infection. However, the airways do not necessarily represent the lung parenchyma where *Mtb* infection is most often established in the tissues. Additionally,

sampling from the site of disease requires more advanced facilities, higher costs, and qualified medical staff. When performed in a research setting, sampling using more advanced medical procedures requires ethical deliberation to consider the risk versus benefit ratio for the research participants, particularly those who are not indicated for medical intervention or invasive diagnostics. Despite these challenges, the TB field is gravitating in the direction of site-of-disease studies as technologies advance and such sampling becomes more readily accessible, with emerging evidence to support value in clinical research and safety for research participants (Young et al., 2019; Collins et al., 2014; Thiel et al., 2021). An interesting avenue would be to perform longitudinal tissue immunology studies, although obtaining human lung tissue specimens at various timepoints would be impossible with current procedures and technologies. In this regard, sequential BAL sampling from research participants and/or an *in vitro* granuloma model may be useful to investigate the role of immune cells longitudinally (Elkington et al., 2019).

Adding further challenge to the field of human tissue immunology, samples derived from the lungs and airways of individuals are often black in colour and highly autofluorescent due to intracellular carbon build-up within cells (Young et al., 2019). Carbon from air pollution and smoke exposure is thought to be the source of intracellular carbon accumulation within resident innate phagocytic lung cell populations, presumably through the process of phagocytosis (Demling, 2008; Kulkarni et al., 2005; Phipps et al., 2010). Due to the autofluorescent nature of immune cells samples from the lungs and airrways, fluorescence-based flow cytometry techniques are often not suitable for acquiring immunophenotypic data in these samples. Therefore, fluorescence-independent techniques such as mass cytometry (or cytometry by time-of-flight – CyTOF) has given rise to a powerful tool that is fit-for-purpose to accommodate the need for immunophenotyping in autofluorescent samples.

Current interventions to curb the TB epidemic are insufficient to achieve the case reduction targets and eradication of the disease by 2050, as set out by the World Health Organization

(WHO, 2008). Overall, a better understanding of the protective immune responses to *Mtb* infection at the site of disease, uncovering the mechanisms by which *Mtb* manipulates the host, and identifying robust correlates of protection are needed to combat the TB pandemic. To achieve this, is imperative that TB researchers gain a more comprehensive understanding of immunopathogenesis of *Mtb* infection in human tissues.

1.6 Conclusions

Our quest to enhance control and ultimately end TB is still ongoing, and although great progress is being made each day, we are still far from our target. With rising evidence suggesting that other role players in TB are important for the fine balance of protection and pathogenesis, the field should think deeper and broaden its views. Perhaps the functionality of NK cells holds an important key to the puzzle. Certainly, with more interest growing in this sector, we are hopefully soon to find out.

1.7 Project Aims, Outlook and Impact

1.7.1 Aims and outlook

Our overall understanding of the precise role of NK cells during *Mtb* infection and TB disease is incomplete. Therefore, the overarching aim of this study is to gain a better understanding of NK cell determinants of immunity to *Mtb* in humans. The outlook of this thesis set out to address three main themes surrounding NK cell biology and function in the TB field.

Firstly, human studies in the TB field have highlighted differences in peripheral blood NK cells between TB and control cohorts. However, none have provided a longitudinal analysis of peripheral NK cell functions during progression to active TB disease. By addressing this knowledge gap, it may be possible to track changes that occur in the peripheral NK cell compartment, potentially highlighting features of TB progression and/or correlates of risk. Secondly, NK cells are rapid responders to immune signalling by accessory cells in the local microenvironment and their functions are modulated during inflammatory responses. However, the precise role of accessory cell cytokines on NK cell bystander activation and function (particularly cytotoxic potential) in the immune response during *Mtb* infection and TB disease remains unknown. Therefore, this study set out to further investigate NK cell cytokine production and cytotoxic potential in the context of T cell accessory cytokines involved in NK cell bystander activation during inflammatory TB disease. Finally, there is a major knowledge gap regarding NK cell tissue immunology during TB disease in humans. Therefore, this thesis performed phenotypic and functional characterization of NK cells within tissue specimens collected postmortem. In this way, NK cell biology could be studied in human tissues, enabling high-dimensional characterization and identification of key differences between TB cases and healthy controls which, to the best of our knowledge, has yet to be performed.

1.7.2 Objectives and hypotheses

I. Investigate proportions and functional changes of peripheral NK cells during the longitudinal transition from *Mtb* infection to active disease (Chapter 3).

   Hypotheses:

   a. Frequencies of peripheral blood NK cells are associated with longitudinal progression to active TB disease, decreasing upon time to diagnosis in progressors relative to controllers. Rationale: Published data from a transcriptomic study at SATVI suggests NK cells are depleted in progressors relative to controllers (Scriba et al., 2017).
   b. NK cell cytokine responses in PBMC stimulated with *Mtb* antigens are associated with progression, increasing with longitudinal time to TB diagnosis in progressors relative to controllers. Rationale: Active TB disease induces a cascade of inflammatory-associated immune responses, likely resulting in activation of NK cells and increased functional activity (Bozzano et al., 2009; Feinberg et al., 2004; Gerosa et al., 2002).
   c. NK cell cytokine responses in PBMC stimulated with *Mtb* antigens are positively associated with IL-2 production by T cells. Rationale: IL-2 produced by T cells in response to *Mtb* antigens and inflammatory-associated immune responses may initiate bystander activation and production of cytokines by NK cells (Horowitz et al., 2010b; Suliman et al., 2016).

II. Investigate NK cell functional alterations via bystander activation pathways in TB and healthy, *Mtb*-sensitized controls (Chapter 3, continued).

   Hypotheses:

   a. NK cell cytokine production and cytotoxic potential are higher in TB patients relative to healthy, *Mtb*-sensitized controls in PBMC stimulated with *Mtb* antigens.

Rationale: Active TB disease induces a cascade of inflammatory-associated immune responses, likely resulting in activation of NK cells and increased functional activity (Bozzano et al., 2009; Feinberg et al., 2004; Gerosa et al., 2002).

b. Myeloid (IL-12 and IL-18) and T cell (IL-2) cytokines are required for optimal activation of NK cells in PBMC stimulated with *Mtb* peptide antigens, and neutralization of these bystander-activating cytokines diminishes expression of cytokines (IFN-γ and TNF) and cytotoxic molecules (perforin and granzyme B) by peripheral NK cells. Rationale: Published data from a study at SATVI showed that IL-12, IL-18 and IL-2 were required to optimally activate NK cells in blood stimulated with BCG, and cytokine neutralization with αIL-2, αIL-12 and αIL-18 antibodies diminished BCG-specific NK cell IFN-γ responses (Suliman et al., 2016).

c. NK cell responses are suppressed more by blocking T cell-associated IL-2 than myeloid-associated IL-12/IL-18 when PBMC are stimulated with *Mtb* peptides. Rationale: T cells are the primary subset activated by peptide antigens *in vitro,* which in turn, activate NK cells via IL-2-mediated bystander activation.

d. NK cells exhibit subset-specific responsiveness to bystander cytokine activation and suppression of NK functional responses in PBMC stimulated with *Mtb* antigens upon blocking IL-2 is more pronounced in $CD56^{hi}$ NK cells than $CD56^{lo}$ cells. Rationale: $CD56^{hi}$ NK cells expresses higher affinity IL-2 receptors and are likely to experience greater changes to functional responses upon blocking compared to $CD56^{lo}$ NK cells (Becknell & Caligiuri, 2005; Carson et al., 1997; Fehniger et al., 2003).

e. Blocking-mediated suppression of NK cell cytokine and cytotoxic molecule expression is more pronounced in TB patients than healthy, *Mtb*-sensitized

controls. Rationale: Bystander activation is a potentially important pathway in NK cell functional responses during active TB disease.

III. Use a standardized SATVI in-house flow cytometry ICS assay as a secondary check for the TSPOT test as a classification tool for distinguishing between *Mtb* sensitized and non-sensitized healthy controls and evaluate the use of the *Mtb*-specific T cell ΔHLA-DR MFI biomarker to distinguish between TB and $TSPOT^{+}$ individuals in a cohort of individuals whose PBMC were sampled postmortem (Chapter 4).

Hypotheses:

a. T cell response magnitude to *Mtb* peptides in PBMC distinguishes between $TSPOT^{-}$ and $TSPOT^{+}$ in postmortem samples, with $TSPOT^{+}$ individuals expressing a significantly higher frequency of IFN-$\gamma^{+}TNF^{+}$ T cells than $TSPOT^{-}$ individuals in response to ESAT-6 and CFP-10 peptides. Rationale: A secondary check of TSPOT test which has not been validated for postmortem PBMC samples.

b. The *Mtb*-specific T cell ΔHLA-DR MFI biomarker distinguishes between TB and $TSPOT^{+}$ in postmortem PBMC, with TB patients having a significantly higher ΔHLA-DR MFI biomarker score relative to $TSPOT^{+}$ controls. Rationale: Published data from a study at SATVI described the *Mtb*-specific T cell ΔHLA-DR MFI biomarker that distinguished between TB and $IGRA^{+}$ participants in a living cohort (Mpande et al., 2021).

IV. Delineate bulk myeloid and lymphoid immune subsets, and characterize expression of cytotoxic molecules in cytotoxic lymphocytes of human tissues of the lung, hilar lymph node, BAL, spleen, and PBMC in TB patients and healthy controls (Chapter 4, continued).

Hypotheses:

a. There is an HIV-associated depletion of CD4 T cells in peripheral blood and tissues of HIV-infected relative to uninfected individuals. Rationale: HIV-associated depletion of CD4 T cell occurs in the peripheral blood and tissues of HIV-infected individuals (Brenchley et al., 2004; Kalsdorf et al., 2009).
b. Lymphocyte subsets, including T cells, NK cells and B cells, are depleted in the peripheral blood with enrichment of these subsets in the tissues in TB decedents relative to controls. Rationale: Immune cells are trafficked from the blood and homed in the tissues during *Mtb* infection (Junqueira-Kipnis et al., 2003b; Masopust & Schenkel, 2013; Portevin et al., 2012).
c. Expression of cytotoxic molecules and frequencies of cytotoxic molecule-expressing lymphocytes are enriched in the peripheral blood and tissues in TB decedents relative to controls. Rationale: TB disease induces a cascade of inflammatory-associated immune responses, likely resulting in activation of NK cells and increased cytotoxic potential (Chávez-Galán et al., 2019; Serbina et al., 2000; Nisha Rajeswari et al., 2006).

V. Characterize human NK cell phenotypes and expression of cytotoxic molecules across human tissue compartments (Chapter 5).

Hypotheses:

a. Tissue-resident NK cells are depleted in the peripheral blood and enriched in the tissues of TB decedents relative to controls. Rationale: Immune cells are trafficked from the blood and homed in the tissues during *Mtb* infection (Junqueira-Kipnis et al., 2003b; Masopust & Schenkel, 2013; Portevin et al., 2012).
b. NK cells in the peripheral blood and lung tissue are predominantly $CD16^{hi}$ cells (Björkström, Riese, et al., 2010; M. A. Cooper et al., 2001; Marquardt et al., 2017b;

Y. Zhang et al., 2007), while and NK cells in the secondary lymphoid organs are predominantly $CD56^{hi}CD16^{lo}$ cells (Björkström et al., 2016; Marquardt et al., 2015; Sharkey et al., 2015) lacking expression of tissue-resident markers.

c. Expression of cytotoxic markers is higher in peripheral blood NK cells than NK cells from tissues, and mature $CD16^{hi}$ NK cells express the highest levels of cytotoxic molecules relative to their phenotypically immature $CD56^{hi}CD16^{lo}$ counterparts. Rationale: NK cells in the tissues are immunoregulatory and hypo-cytotoxic relative to their peripheral blood counterparts (G. E. Cooper et al., 2018; Marquardt et al., 2017b).
d. In the peripheral blood and tissues of TB decedents, there is higher expression and frequencies of maturation-, activation-, and cytotoxic marker-expressing NK cells, and lower expression and frequencies of inhibiting receptor- and checkpoint protein-expressing NK cells relative to controls. Rationale: TB disease induces a cascade of inflammatory-associated immune responses, likely resulting in activation of NK cells and increased cytotoxic potential (Chávez-Galán et al., 2019; Serbina et al., 2000; Nisha Rajeswari et al., 2006).

1.7.3 Impact

There is a strong need to identify new methods, interventions, and targets for developing host-directed therapies and novel vaccine strategies against TB. Most previous efforts in the TB field have been focused on the *Mtb*-specific Th1 dogma as targets for such interventions. By studying NK cells, recently highlighted as important role players in the dynamic *Mtb*-host interaction, a better understanding of their role during TB progression and at the site of infection will hopefully reveal new opportunities to curb the TB epidemic.

Chapter 2: Methods and Materials.

"Though this be madness, yet there is method in't."

- William Shakespeare, *Hamlet*

2.1 Introduction

The experimental protocols and assays used in this thesis span multiple techniques that overlap between different objectives and chapters. To avoid redundancy and repetition, the broad methods and materials for the main techniques used in the presented work are described here. The finer details pertaining to specific cohorts, antigen-specific stimulations, and data analysis approaches for each objective are specified in each chapter, as appropriate. Statistical analyses performed are also described independently in respective chapters.

2.2 PBMC Isolation and Cryopreservation

The protocol for PBMC isolation and cryopreservation from living study participants in South African cohorts is described here. Notably, peripheral blood was also sampled from the postmortem Ugandan cohort, with minor differences in the PBMC isolation and cryopreservation protocols, further described in Section 2.3.1. From living South African study participants, peripheral blood was collected into heparinized blood tubes and processed for PBMC isolation within 2 hours of phlebotomy. Peripheral blood cells were separated by centrifugation using Ficoll-Paque density gradient medium (Histopaque-1077; Sigma Chemical Co.), according to manufacturer's recommendations. Briefly, heparinized whole blood was diluted in a 1:1 ratio with 1x phosphate buffered saline (PBS) (Phosphate Buffered Saline; Lonza) and layered on 15mL Ficoll-paque density gradient medium (Histopaque-1077; Sigma Chemical Co.). Layered blood was centrifuged (Eppendorf Centrifuge 5810) at 400xg for 25 minutes (acceleration off and break off). The mononuclear cell layer was removed, and cells were washed twice by centrifugation at 400xg for 10 minutes. Cells were counted and viability determined using the Trypan Blue exclusion method (Strober, 1997) (Trypan Blue Solution, 0.4%; Thermo Fisher Scientific Inc.). Isolated

PBMC were resuspended in complete medium (Roswell Park Memorial Institute – RPMI supplemented with 10% fetal bovine serum – FBS; RPMI 1640 with L-glutamine, Lonza; HyCloneTM Calf Serum, GE Healthcare-Healthcare-HyClone Laboratories, Inc.) to a final concentration of $20x10^6$ cells/mL before transferring 500µL of resuspended cells to cryopreservation vials. Thereafter, 500µL of a cold (4°C) solution containing 20% dimethyl sulfoxide (DMSO) (Dimethyl Sulfoxide; Sigma-Aldrich Co.) in FBS was added dropwise to cells. Cells were thus cryopreserved within a final volume of 1mL solution containing RPMI/FBS/DMSO in a 45:45:10 ratio. Cryopreservation vials containing single cell suspensions were transferred to a Mr. Frosty Freezing Container (Thermo Fisher Scientific Inc.) filled with isopropyl alcohol. The Mr. Frosty container was stored at -80°C overnight (no longer than three days) before transferring vials to liquid nitrogen for long term storage.

2.3 Postmortem Tissue Dissociation and Cell Isolation

Recruitment and autopsies of deceased individuals, sample collection, tissue dissociation and cell isolation of specimens obtained postmortem were performed by a collaborating research group led by Dr Stephen Cose based at the Medical Research Council/Uganda Virus Research Institute and London School of Hygiene & Tropical Medicine (MRC/UVRI & LSHTM) Uganda Research Unit. Decedents were identified via next of kin, who were approached by a trained counsellor for consent to include tissues from the deceased person. Recruitment and consenting were performed at the Mulago National Referral Hospital (MNRH), Uganda. Two weeks following initial consent, the next of kin were contacted again to reconfirm their agreement for the deceased to be included in the study. Autopsies were performed by a trained pathologist, who sampled tissue resections of lung, lymph nodes and spleen. Additionally, peripheral blood and BAL fluid were sampled postmortem. Following resection and sampling, specimens were transported in RPMI (supplemented with 20%

FBS) to the laboratory for tissue dissociation and cell isolation, according to the following protocols.

2.3.1 Peripheral blood

Peripheral blood samples obtained postmortem were collected into heparinized blood tubes and processed for PBMC isolation using standard density gradient centrifugation. Briefly, blood was diluted and manually layered onto Ficoll-Paque density gradient medium (Ficoll® Paque Plus; Merck). Layered blood was centrifuged at 1000rpm (Eppendorf Centrifuge 5810) for 22 minutes (acceleration off and breaks off) and the mononuclear cell layer ("buffy coat") was removed. Red blood cells remaining in the cell pellet were lysed using ACK lysis buffer (Thermo Fisher Scientific Inc.) and remaining PBMC were washed and counted using the automated TC20 counter (Biorad), before being cryopreserved. Single cell suspensions were cryopreserved by resuspending cells in DMSO and FBS in a 1:9 ratio and stored at -80°C for 16 hours before transferring to liquid nitrogen for long term storage.

2.3.2 Lung tissue

Cells were isolated from postmortem lung tissues by enzymatic digestion using collagenase medium (RPMI supplemented with 1mg/mL collagenase D, and 1g/ml DNase I), and physical dissociation using the GentleMACS Octo Dissociator (Milteyni Biotech). Briefly, lung tissue samples were cut into small pieces using fine scissors and forceps on a sterile petri dish, placed in gentleMACS C Tubes with the collagenase digestion medium, loaded on the GentleMACS and run on the lung program 1. Samples were then incubated at 37°C in a 5% CO_2 incubator for 25 minutes, followed by further digestion using lung program 2 on the GentleMACS instrument. Dissociated tissue was then filtered through a 70µm filter, followed by another filtration step using a smaller 40µm filter. Single cell suspensions were

centrifuged at 600xg for 5 minutes to obtain a cell pellet. Red blood cells remaining in the cell pellet were lysed using ACK lysis buffer (Thermo Fisher Scientific Inc.), resulting in a pure black cell pellet. Isolated lung cells were washed and counted before cryopreservation. As discussed in Chapter 1, Section 1.5, the black colour of cell pellets (isolated from lung, hilar lymph nodes and BAL) are thought to be a result of carbon residue accumulation in airway, lung and lung-draining cells (presumably in the phagocytic cell fraction) via inhalation of carbon-loaded particles due to air pollution and/or smoking (Kulkarni et al., 2005; Phipps et al., 2010; Demling, 2008; Young et al., 2019).

2.3.3 Hilar lymph nodes

Postmortem hilar lymph nodes were cleaned by teasing the lymph node tissue from surrounding fat using fine scissors and forceps, chopped into small pieces on a sterile petri dish, and mixed with complete medium (RPMI supplemented with 20% FBS). Resuspended cells were filtered through 70µm filter followed by an additional filtration step using a smaller 40µm filter. The cell suspension was centrifuged at 600xg for 5 minutes to obtain a black cell pellet. Red blood cells were lysed using ACK lysis buffer, and the resultant cell pellet was washed and counted before cryopreservation.

2.3.4 Spleen

Resected splenic tissue obtained postmortem was chopped into small pieces using fine scissors and forceps on a sterile petri dish and mixed with complete medium (RPMI supplemented with 20% FBS). The resultant mixture was filtered through a 70µm filter and centrifuged at 600xg for 5 minutes to obtain a cell pellet. The cell pellet was reconstituted with complete medium and layered manually onto Ficoll-Paque Plus medium. Splenic mononuclear cells were obtained by density gradient centrifugation (1000rpm, 22 minutes, acceleration off, break off). The mononuclear cell layer (“buffy coat”) was harvested and

washed to obtain a cell pellet. Red blood cells remaining in the pellet were lysed using ACK lysis buffer. Splenic mononuclear cells were then washed and counted before cryopreservation.

2.3.5 Bronchoalveolar lavage (BAL) fluid

BAL fluid obtained postmortem was filtered through 70µm filter, followed by a smaller 40µm filter before centrifugation at 600xg for 5 minutes to isolate BAL cells and obtain a cell pellet. Red blood cells were lysed using ACK lysis buffer. The resultant pellet was washed, and cells were counted prior to cryopreservation.

2.3.6 Tonsil tissue

Tonsil tissue from living individuals were obtained from research participants indicated for tonsillectomy. Tonsil specimens were collected and processed by a collaborating research group led by Dr Al Leslie at the African Health Research Institute (AHRI) based in Durban, South Africa. Briefly, tonsil tissue was chopped into small pieces on a sterile petri dish using fine scissors and forceps. Minced tissue was centrifuged at 2000rpm (Eppendorf Centrifuge 5810) for 5 minutes at room temperature and resuspended in warmed collagenase medium (RPMI supplemented with 0.5mg/mL collagenase D, and 40U/mL DNase I) and transferred to GentleMACS C Tubes to be homogenised using the GentleMACS program C C01. Samples were then incubated in a 37°C waterbath for 25 minutes. The GentleMACS homogenization procedure was repeated before filtering samples through a 70µm cell strainer and centrifuging at 2000rpm for 5 minutes at room temperature. Single cell suspensions of tonsil samples were layered onto Ficoll-Paque density gradient medium and centrifuged for 20 minutes at 2000rpm (acceleration off, break off). The mononuclear cell layer was removed and washed using complete medium (RPMI supplemented with 10%

FBS). Cells were filtered once more through a 70µm cell strainer before counting and cryopreservation.

2.4 TSPOT Assay on Postmortem PBMC

The TSPOT assay was performed on postmortem PBMC samples using the T-SPOT®.TB kit (TB.300, Oxford Immunotec) to quantify the number of *Mtb* antigen-specific activated effector T cells producing IFN-γ in response to ESAT-6 and CFP-10 peptides. This test utilizes the principles of enzyme-linked immunospot (ELISPOT) methodology to enumerate *Mtb*-sensitized T cells by capturing IFN-γ in the vicinity of T cells from which the cytokine was secreted. The TSPOT assay was performed by the collaborating research group at MRC/UVRI & LSHTM in Uganda using freshly isolated PBMC obtained postmortem, as per manufacturers recommendations with minor modifications.

Briefly, isolated PBMC were placed into microtiter wells where they are stimulated with 1) a phytohemagglutinin (PHA) positive control (a mitogenic stimulator to illustrate cell functionality), 2) nil (negative) control, and two separate panels of 3) ESAT-6 and 4) CFP-10 peptides. A total of $1x10^6$ PBMC were resuspended in complete medium (PRMI containing 20% FBS, as opposed to the AIM-V serum-free medium recommended by the manufacturer) and divided equally between the four conditions, so that ~$2.5x10^5$ cells were added to each microtiter well. Cells were then incubated in a 5% CO_2 incubator for 48 hours (as opposed to the 16-20 hours recommended by the manufacturer). Cells were washed and plates were developed according to manufacturer's recommendations. Spot-forming units were quantified using an ELISPOT reader (AID *i*Spot ELR08IFL; AID Autoimmun Diagnostika GmbH) and results were interpreted as per manufacturer's instructions. Samples were assayed in duplicate.

2.5 Flow Cytometry ICS and Data Acquisition

2.5.1 PBMC thawing, resting and stimulation

To perform intracellular cytokine staining (ICS) assays, cryopreserved PBMC were thawed, rested, and stimulated prior to staining. Briefly, cryopreserved PBMC were thawed and rested in complete medium (RPMI supplemented with 10% FBS and 100U/mL pen/strep; Penicillin-Streptomycin; Sigma-Aldrich Co.), for 2 hours at 37ºC in a humidified 5% CO_2 incubator. Cells were counted and viability determined using the Trypan Blue exclusion method. Cells then underwent stimulation with a series of selected antigens, according to the specific assay designs. Two flow cytometry ICS assays were designed to 1) quantify NK cell responses in a cytokine neutralization assay using PBMC stimulated with *Mtb* lysate and a peptide pool of secreted *Mtb* antigens (Chapter 3); and 2) quantify T cell responses to *Mtb* peptides including ESAT-6 and CFP-10 (Chapter 4). The details of specific antigen stimulations and assay designs are described in the respective chapters.

2.5.2 Antibody staining

For flow cytometry antibody staining and data acquisition, stimulated PBMC were stained with a panel of fluorochrome-labelled extracellular and intracellular antibodies. Details for each of the two flow cytometry antibody panels are described in their respective chapters. Both panels were previously designed and optimized by members at SATVI and are routinely used as in-house ICS panels. Despite different antibody panels, the same protocol for flow cytometry antibody staining was used consistently.

Briefly, stimulated cells were harvested by incubation with 1mL of 1x PBS supplemented with 2mM EDTA (Ethylenediaminetetraacetic acid, Sigma Chemical Co.) for 10 minutes at 4ºC and centrifuged at 2000rpm (Eppendorf Centrifuge 5810) for 5 minutes. A cocktail of

viability and surface markers were added to cells in a total staining volume of 100µL. Cells were stained for 30 minutes in the dark, on ice before washing twice with 1mL FACS Wash solution (1x PBS supplemented with 2% FBS and 0.4% 0.5M EDTA; Phosphate Buffered Saline, Lonza; HyCloneTM Calf Serum, GE Healthcare-Healthcare-HyClone Laboratories; 0.5M Ethylenediaminetetraacetic acid, Sigma Chemical Co.). Cells were then fixed and permeabilized with 300µL of fixation and permeabilization solution (BD Cytofix/Cytoperm, Becton, Dickinson and Co.) for 20 minutes on ice before washing twice with 1x permeabilization buffer (BD 10x Perm/Wash solution, Becton, Dickinson and Co.). A cocktail of intracellular cytokine markers was then added to cells in a total staining volume of 100µL and incubated for 30 minutes in the dark, on ice. Cells were washed twice with 1mL of 1x permeabilization buffer before adding 100µL of 1% paraformaldehyde (PFA, Kimix). Cells were washed once with 1mL 1x PBS at 2000rpm for 5 minutes and resuspended in 100µL 1x PBS for data acquisition.

2.5.3 Compensation controls and data acquisition

For data acquisition on the BD LSR II flow cytometer, the instrument was started, and photomultiplier tube (PMT) voltage settings were checked and optimized to monitor performance daily using a mixture of BD Sphero Fluorescent Particles (3.0-3.4µm, mid-range FL1 fluorescence; Becton, Dickinson and Co.) and Cyto-Cal Multifluor Beads (Applied Microspheres).

In addition to daily quality checks, freshly made single-stained compensations beads (Becton, Dickinson and Co.) were used to create a compensation matrix for each acquisition. Briefly, a pre-optimized volume of each antibody within the panel was added to 40µL of compensation beads comprising equal volumes of positive and negative beads. Beads were stained for 15 minutes at room temperature. For compensation controls of live/dead staining,

50µL of live PBMC (~5x10^5 cells) were killed by incubating with 50µL of 70% ethanol for 10 minutes at room temperature. Ethanol-killed cells were washed using 1mL FACS Wash solution and centrifuging at 2000rpm for 5 minutes. Dead cells were then added to 50µL of live cells (~5x10^5 cells) and stained with a pre-optimized titre of live-dead fixable near-IR dead cell stain (Thermo Fisher Scientific Inc.) and incubated for 20 minutes at room temperature. Following staining, compensation beads and live/dead cells were washed with 1mL FACS Wash solution and centrifuged for 5 minutes at 2000rpm. Supernatants were discarded and all compensation controls (beads and cells) were fixed using 1% PFA for 10 minutes at room temperature before washing with 1mL FACS Wash solution and centrifuged for 5 minutes at 2000rpm. Supernatants were discarded and compensation controls were kept refrigerated until samples were acquired later that day. Samples were run at low speed until all cells had been acquired using BD FACSDiva Software version 8.0.1 (Becton, Dickinson and Co.).

2.6 CyTOF Antibody Panel Design and Optimization

The 44-marker CyTOF antibody panel was conceptualized to perform phenotyping of NK and B cell subsets. However, B cell phenotyping analyses were not included in this thesis and will be performed as a future study. Only NK cell-specific markers within the panel were used for subsequent NK cell phenotyping (Chapter 5). For transparency, the full antibody panel is shown in Table 2.1 and optimizations are discussed within the full context of the panel design, which included both NK and B cells.

Table 2.1: CyTOF Antibody Panel.

Marker	Metal	Rationale	Clone	Antibody supplier
Extracellular (surface) markers				
CD45	89Y	Lymphocytes	HI30	Standard BioTools
CD3	*110Cd	T cells	UCHT1	BioLegend
CD4	*141Pr	T cells	RPA-T4	BioLegend
CD8a	*106Cd	T cells	RPA-T8	BioLegend
γδTCR	*151Eu	T cells	B1.1	BioLegend
CD7	*116Cd	T cells, NK cells	CD7-6B7	BioLegend
CD45RA	*160Gd	T cell memory	HI100	BioLegend
CD14	151Eu	Monocytes	M5E2	Standard BioTools
CD33	*112Cd	Myeloid cells	WM53	BioLegend
CD127	176Yb	Pan-ILC	A019D5	Standard BioTools
CD69	*165Ho	Activation marker	FN50	BioLegend
CD49a	*162Dy	Tissue-residency	TS2/7	BioLegend
CD103	*145Nd	Tissue-residency	Ber-ACT8	BioLegend
CCR6	*147Sm	Tissue-residency	G034E3	BioLegend
CXCR3	*113Cd	Tissue-residency	G025H7	BioLegend
HLA-DR	170Er	B cells, NK activation	L243	Standard BioTools
CD19	*164Dy	B cell lineage	HIB19	BioLegend
CD21	152Sm	B cell lineage	BL13	Standard BioTools
CD10	*173Yb	Immature B cells	HI10a	BioLegend
CD5	142Nd	Transitional B cells, B_{reg}	UCHT2	Standard BioTools
CD24	*161Dy	Transitional B cells	ML5	BioLegend
IgD	*171Yb	Naïve/non-class switched B cells	IA6-2	BioLegend
CD11c	159Tb	B cell memory	Bu15	Standard BioTools
CD27	*146Nd	NK and B cell maturation/memory	O323	BioLegend
CD38	167Er	Plasma cells, NK maturation	HIT2	Standard BioTools
CD138	*174Yb	Plasma cells	DL-101	BioLegend

* In-house conjugated antibodies using Maxpar Antibody Labeling Kits (Standard BioTools).
Cisplatin 194 was used as a live/dead marker.

Table 2.1 (continued): CyTOF Antibody Panel

Marker	Metal	Rationale	Clone	Antibody supplier
Extracellular (surface) markers				
CD56	149Sm	NK lineage	NCAM16.2	Standard BioTools
CD16	209Bi	NK maturation	3G8	Standard BioTools
CD57	172Yb	NK maturation	HCD57	Standard BioTools
CD11b	144Nd	NK maturation	ICRF44	Standard BioTools
NKp46	*163Dy	NK activating receptor	9E2	BioLegend
DNAM1	*155Gd	NK activating receptor	DX11	BD Biosciences
NKG2D	166Er	NK activating receptor	ON72	Standard BioTools
NKG2A	169Tm	NK inhibiting receptor	Z199	Standard BioTools
KIR	*156Gd	NK inhibiting receptor	DX27	BioLegend
PD1	*153Eu	Checkpoint protein	EH12.2H7	BioLegend
PDL1	*150Nd	Checkpoint protein	29E.2A3	BioLegend
TACTILE	*165Ho	Checkpoint protein	NK92.39	BioLegend
TIGIT	154Sm	Checkpoint protein	MBSA43	Standard BioTools
Fas-L	*148Nd	Cytotoxic mediator	NOK-1	BioLegend
Intracellular (functional) markers				
Perforin	175Lu	Cytotoxic molecule	B-D48	Standard BioTools
Granzyme B	*168Er	Cytotoxic molecule	GB11	BioLegend
Granzyme K	*158Gd	Cytotoxic molecule	GM26E7	BioLegend

* In-house conjugated antibodies using Maxpar Antibody Labeling Kits (Standard BioTools).
Cisplatin 194 was used as a live/dead marker.

2.6.1 Panel design

The CyTOF antibody panel was designed by me, Carly Young-Bailie, using the Standard BioTools online Panel Designer platform (https://pdv2.dvssciences.com). A selection of pre-defined markers and clones were manually assigned to metal tags to minimize signal overlap between co-expressed channels and background signals arising from common environmental contaminants, such as barium, also considering instrument sensitivity for

assigned channels and target antigen abundance. Although there is the minimal signal overlap that occurs between channels, mass cytometry is not totally devoid of spillover and three sources of signal interference occur. Firstly, metals that are used to label antibodies may not reach 100% purity due to limitations in the enrichment process. Secondly, plasma ionization of samples may cause oxidation of metals, resulting in spillover into +16 atomic mass channels (i.e., channels of 16 mass units above a given metal). Finally, abundance sensitivity spillover results in +1 atomic mass signal spillover due to imprecise detection that arises from asynchronous movement of ions upon acceleration towards the detector (Leipold et al., 2015; Nicholas et al., 2016; Takahashi et al., 2017). Fortunately, signal overlap in mass cytometry is minimal, measurable, and predictable. Using the panel designer platform, main lineage markers were allocated to metal targets that experienced little interference with one another, ensuring that clean lymphocyte and myeloid populations could be identified. To maximize the use of the remaining channels, markers for sub-classifying NK and B cell subsets were strategically allocated to allow overlap between channels that were, to the best of current knowledge, not co-expressed between NK and B cell lineages. For example, Figure 2.1a shows CD57, an NK-specific marker not co-expressed on B cells, that overlaps into three channels that were of interest for phenotyping B cells: CD10, IgD and CD138. This overlap was predicted using the Standard BioTools panel wheel and acquired data showed that CD57 staining spillover was observed in CD10, IgD and CD138 channels that were empty (i.e., cells were not stained with those antibodies). Figure 2.1a illustrates high staining intensity of CD57, shown as red phenotypic islands on the tSNE plot. The CD10, IgD and CD138 channels were stained above background levels, shown as green phenotypic islands corresponding to high CD57 staining, indicating signal overlap. Since CD10, IgD and CD138 were of interest for B cell phenotyping, the signal interference by CD57 was removed by gating out $CD57^{+}$ cells co-expressing the CD19 B cell lineage marker. The same logic was applied to all remaining markers in the panel.

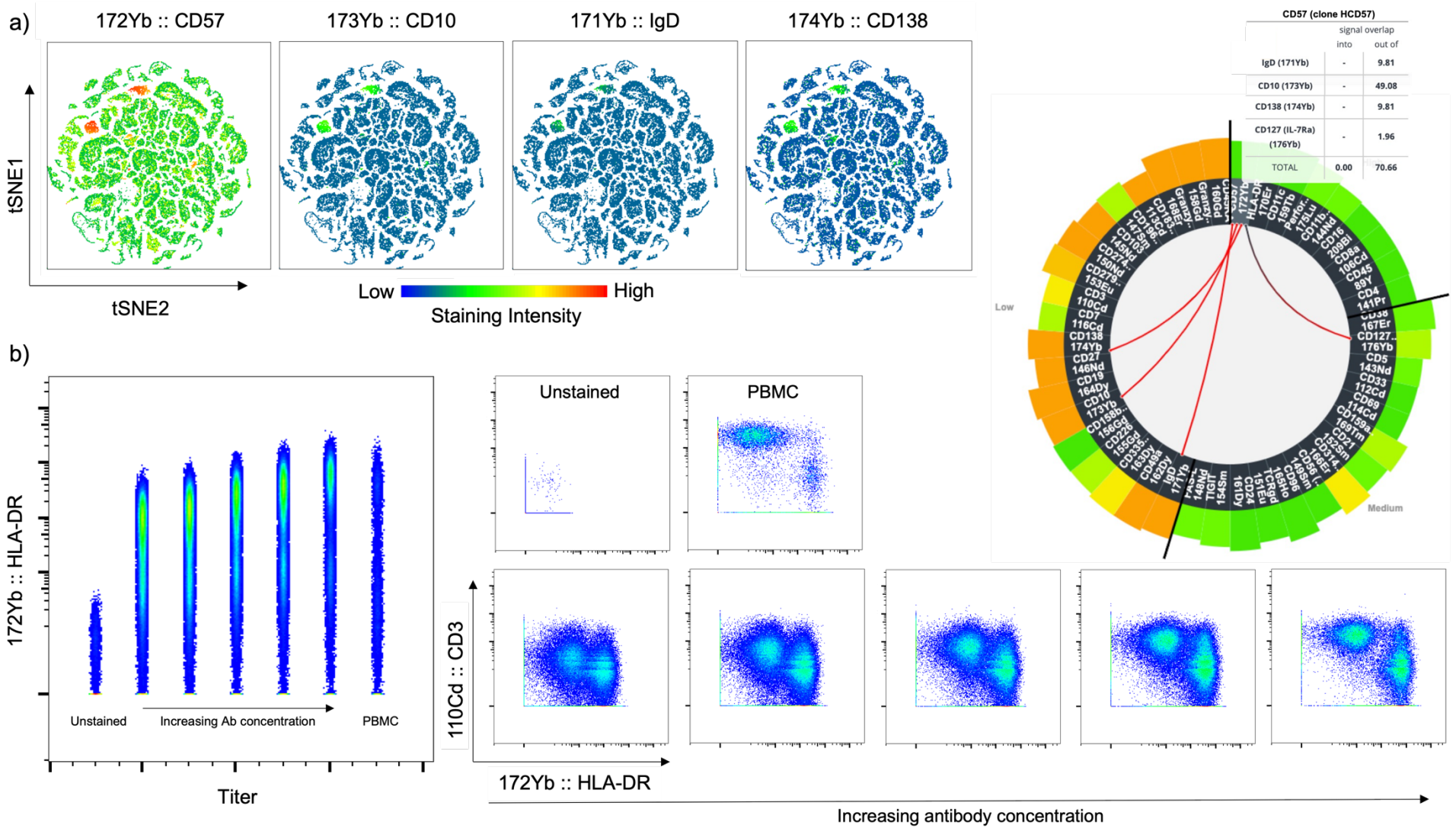

Figure 2.1: CyTOF signal spillover and titration optimization. a) Representative example of signal spillover of CD57 into empty channels of CD10, IgD and CD138. Spillover was predicted using the Standard BioTools Panel Designer wheel (right) and was shown in a dimensionality reduction analysis using tSNE (left). b) Flow plots of HLA-DR and CD3 titration data in tonsil tissue with antibody titres serially halved, beginning with the highest concentration of 5µg/mL (right). Optimal separation in tonsil tissue was observed at the highest titre. An unstained control was included, with PBMC stained at the highest titre (5µg/mL). Plot on the left shows HLA-DR expression for concatenated live cells at increasing antibody (Ab) concentrations.

2.6.2 Antibody titrations

To further optimize the panel, metal-conjugated antibodies were titrated. Titrations were performed by decreasing antibody concentrations for a fixed number of cells to determine the best signal-to-noise ratio for staining. Defining the best signal-to-noise ratio maximizes the signal detected while diminishing the inherent background noise within the instrument, non-specific binding of antibodies to low-affinity targets, as well as reduces detector saturation and signal spillover from different channels. Five antibody titration experiments were performed by using predicted signal overlap to group antibodies with no interference within a single titration assay. This approach allowed for multiple antibodies to be titrated at once. Briefly, markers were grouped in a single titration experiment if they had no signal overlap into or receiving from another channel (based on predicted isotope impurity), also excluding +1 atomic mass and -1 atomic mass channels (abundance sensitivity spillover), and +16 atomic mass channels (oxide formation). Titration experiments were performed by staining cells with five serial halving titers of antibody, beginning with a concentration of 5µg/mL. An unstained control was also included for each titration experiment. Tonsil tissue cells from living participants were used for titration experiments, courtesy of a donation from collaborators at AHRI, South Africa. Tonsil tissue was used for titrations as other tissue samples were limited in the postmortem cohort. A total of $2x10^6$ tonsil cells were stained for each titer (i.e., $12x10^6$ tonsil cells were required per participant, for each of the five titration experiments). PBMC from a living cohort were also included in each titration experiment, using only $2x10^6$ PBMC for one condition at the maximum titer (5µg/mL). Following titrations, postmortem tissues (lung, hilar lymph nodes, BAL, spleen, and PBMC) were stained with the optimized panel to test staining, for which all markers were staining optimally, requiring no further optimization.

Figure 2.1b shows an example of titration data for HLA-DR and CD3 that were titrated in the same experiment. Results showed that HLA-DR and CD3 had better separation with higher antibody titers. Therefore, the maximum concentration (5µg/mL) was chosen as the optimal titer for these markers. PBMC also showed good separation of markers at the highest titer. PBMC were only stained at the maximum concentration during titration experiments. Instances where a lower titer was chosen for tissues, PBMC were also reverted to the same titer. Following titrations, PBMC were stained using the full panel of tissue-titrated antibodies and was shown to have optimal separation of markers, requiring no further optimization.

2.7 In-house Conjugation of Metal-Labelled CyTOF Antibodies

Certain antibody targets within the designed CyTOF panel were not commercially available with the desired metal isotope tag. Therefore, unlabeled antibodies were conjugated to cadmium (Cd)- and lanthanide (Ln)-loaded polymers using Maxpar Antibody Labeling Kits (Standard BioTools), strictly according to manufacturer's recommendations.

2.7.1 Lanthanide labelling

Preload the polymer

For lanthanide labelling, polymers were preloaded with the lanthanide of interest by adding 50mM of lanthanide metal chloride solution (Maxpar Lanthanide Solution, Standard BioTools), to the resuspended polymer (Maxpar X8 Polymer, Standard BioTools), and incubating at 37°C for 40 minutes in a waterbath. To purify the lanthanide-loaded polymer, following incubation, 200µL L-Buffer (Maxpar L- Buffer, Standard BioTools) was added to a 3kDa filter, with 100µl of the metal-loaded polymer mixture and centrifuged at 12000xg for 25 minutes at room temperature. Washing was repeated by adding 400µL C-Buffer (Maxpar

C-Buffer, Standard BioTools) to the filter and centrifuged at 12000xg for 30 minutes at room temperature.

Partially reduce the antibody

To partially reduce the antibody, 100µg of the stock antibody was first washed with 400µL R-Buffer (Maxpar R-Buffer, Standard BioTools), and added to a 50kDa filter followed by centrifugation at 12000xg for 10 minutes at room temperature. For each antibody undergoing labelling, 100µL of 4mM tris (2-carboxyethyl) phosphine (TCEP)-R-Buffer was added to the antibody and incubated at 37°C for 30 minutes in a water bath. To purify the partially reduced antibodies, 300µL C-Buffer was added to the 50kDa filter to wash the antibody and centrifuged at 12000xg for 10 minutes at room temperature. The wash step was repeated by adding 400µL C-Buffer to the filter and centrifuging at 12000xg for 10 minutes at room temperature.

Antibody conjugation and quantification

The purified lanthanide-loaded polymer was resuspended in 60µL C-Buffer and transferred to the corresponding purified, partially reduced antibody in the 50kDa filter, followed by incubation at 37°C for 90 minutes in a waterbath. The metal-conjugated antibody was washed using 200µL W-Buffer (Maxpar W-Buffer, Standard BioTools) and centrifuged at 12000xg for 10 minutes at room temperature. The wash step was repeated another three times using 400µL W-Buffer. Following the final wash step, 80µL W-Buffer was added to the 50kDa filter to dilute the conjugate. The conjugate antibody was quantified by measuring absorbance at 280nm against a W-Buffer blank using a NanoDrop instrument (NanoDrop 2000 spectrophotometer, Thermo Fisher Scientific Inc.). Thereafter, W-Buffer was removed by centrifugation at 12000xg for 10 minutes at room temperature.

Antibody stabilization buffer (Antibody Stabilizer PBS, CANDOR Bioscience; supplemented with 0.05% (w/v) Sodium Azide, Sigma-Aldrich) was added to obtain a final concentration of 0.5mg/mL or that yielded a solution that contains at least 50% antibody stabilization buffer by volume. Half of the calculated antibody stabilizer volume was added to the 50kDa filter, carefully rinsing the walls of the filter. Labelled antibodies were recovered by inverting the 50kDa filter over a collection tube and centrifuging at 1000xg for 2 minutes at room temperature. The same process was repeated using the remaining volume of antibody stabilization buffer. The resulting lanthanide-labelled antibodies were stored at 4°C.

2.7.2 Cadmium labelling

For labelling antibodies with cadmium metals, the protocol is similar to the lanthanide antibody labelling kit, with minor differences according to manufacturer's recommendations.

Preload the polymer

To preload the polymer, the resuspended MCP9 polymer (Maxpar MCP9 Polymer, Standard BioTools) was preloaded with 50mM of cadmium nitrate metal solution (Maxpar Cadmium Solution, Standard BioTools) and incubated at 37°C for 60 minutes in a waterbath. The metal-loaded polymer was then added to a 3kDa filter unit and washed twice with L-Buffer and centrifugation at 12000xg for 25 minutes at room temperature each time. The polymer was washed once more using C-Buffer and centrifugation at 12000xg for 45 minutes at room temperature.

Partially reduce the antibody

Before partial reduction, 100µg of the stock antibody was added to a 50kDa filter and washed three times using 400µL R-Buffer (Maxpar R-Buffer, Standard BioTools), and

centrifuged at 12000xg for 10 minutes at room temperature. For each antibody undergoing labelling, 100µL of 4mM TCEP-R-Buffer was added to the antibody and incubated at 37°C for 30 minutes in a water bath. To purify the partially reduced antibody, C-Buffer was used to wash the 50kDa filter, centrifuging each time at 12000xg for 10 minutes at room temperature.

Antibody conjugation and quantification

The metal-loaded polymer was resuspended in C-Buffer and transferred to the partially reduced antibody in the 50kDa filter before incubating at 37°C for 90 minutes in a waterbath. Following conjugation, W-Buffer was added to the 50kDa filter, and the contents transferred to a 100kDa filter unit before centrifuging at 5000xg for 10 minutes. The conjugated antibody was then washed three more times using 400µL W-Buffer and centrifugation at 5000xg for 10 minutes at room temperature. As with lanthanide conjugation, the conjugated antibody was quantified using a NanoDrop instrument to measure absorbance at 280nm using W-Buffer as a blank. The W-Buffer was removed by centrifugation at 12000xg for 5 minutes.

Horse radish peroxidase (HRP)-Protector peroxidase stabilizer (CANDOR Bioscience) supplemented with ProClin 150 (1.5%, Sigma-Aldrich) was used as the medium for antibody storage. The solution was comprised of 45µL ProClin 150 per 50mL HRP-protector. The volume of antibody stabilization medium was calculated to obtain a final concentration of 0.5mg/mL conjugated antibody or that yielded a solution that contains at least 50% antibody stabilization buffer by volume. Half of the HRP-protector solution was added to the 100kDa filter and inverted over a collection tube and centrifuged at 1000xg for 2 minutes at room temperature. The same process was repeated using the other half of the calculated volume of HRP-protector solution. The resulting cadmium conjugated antibodies were stored at 4°C.

2.8 CyTOF Antibody Staining and Data Acquisition

2.8.1 Thawing and resting

Cryopreserved single cell suspensions were thawed and rested in complete medium (RPMI supplemented with 10% FBS, 100U/mL pen/strep and 6000U/mL DNase I) for 1-2 hours 37ºC in a humidified 5% CO_2 incubator (PBMC were rested for 2 hours, while tissue samples were rested for 1 hour). All postmortem tissue samples (lung, hilar lymph node, spleen, and BAL) were thawed and stained in the biosafety level (BSL)-3 facility of the Institute of Infectious Disease and Molecular Medicine (IIDMM), UCT. Postmortem PBMC and tonsils from the living cohort were thawed and stained at SATVI's BSL-2 laboratory.

2.8.2 Antibody staining

Following resting, cells were washed with complete medium and centrifuged at 1800rpm (Eppendorf Centrifuge 5810) for 10 minutes at room temperature before filtering through a 35µm filter to remove clumped cells and debris. Cells were counted and viability determined using the Trypan Blue exclusion method. To remove serum, 2-3x10^6 cells were washed by resuspending cells in 2mL PBS (Maxpar PBS, Standard BioTools) and centrifuged at 300xg for 5 minutes at room temperature. Cells were then stained with a final concentration of 0.5µM cisplatin (Maxpar Cell-ID Cisplatin 194Pt, Standard BioTools) for 5 minutes at room temperature before quenching staining with 2mL of cell staining buffer (Maxpar Cell Staining Buffer, Standard BioTools). The resulting cell suspension was washed twice using 1mL cell staining buffer and centrifugation at 300xg for 5 minutes at room temperature.

A cocktail of extracellular (surface) antibodies (Table 2.1) was added to cells in a total staining volume of 100µL. Cells were stained for 30 minutes at room temperature before washing twice with 1mL cell staining buffer and centrifugation at 300xg for 5 minutes at room

temperature. Cells were then fixed and permeabilized using 1x Fix I buffer (Maxpar 5x Fix I Buffer, Standard BioTools) and incubated at room temperature for 30 minutes before washing twice using 1mL Perm-S buffer (Maxpar Perm-S Buffer, Standard BioTools). A cocktail of antibodies for intracellular cytotoxic markers (Table 2.1) was added in a total staining volume of 100µL and incubated at room temperature for 30 minutes. Cells were washed twice more using 1mL of cell staining buffer and centrifugation at 800xg for 5 minutes at room temperature before fixation with 1.6% PFA for 10 minutes at room temperature. PFA was removed by centrifugation at 800xg for 5 minutes at room temperature, before staining DNA using an intercalating metal.

DNA staining was performed by incubating cells at 4°C overnight with a final concentration of 50nM iridium (Ir) intercalator 191/193 (Maxpar Cell-ID Intercalator-Ir, Standard BioTools) resuspended in fixation and permeabilization buffer (Maxpar Fix and Perm Buffer, Standard BioTools). A comprehensive list of all antibody targets in the panel, their corresponding isotope label, and cell types represented by the extracellular antibody lineage markers is included in Table 2.1.

2.8.3 Data acquisition

The following morning, cells were washed twice using 2mL MilliQ water and centrifugation at 800xg for 5 minutes before removal from the BSL-3 facility. EQ Four-Element Calibration Beads (Standard BioTools) were diluted 10-fold in MilliQ water. For data acquisition, the CyTOF2 instrument was started, plasma ignited, and left to warm up for 20 minutes before performing tuning using Tuning Solution (Standard BioTools), according to manufacturer's recommendations. Immediately prior to injection, cell pellets were diluted to 1-2mL (depending on the size of the cell pellet) using the 0.1x EQ four-element calibration beads and filtered through a 35µm cell strainer. Samples were kept on ice throughout acquisition.

2.9 CyTOF Data Analysis Approach

Calibration beads are standard in the mass cytometry workflow for the purpose of normalizing signal variance of the mass cytometer over time. In essence, normalization methods serve to correct for instrument sensitivity fluctuations occurring over the course of acquisition. All data acquired on the CyTOF2 instrument were normalized by diluting cell suspensions with 0.1x EQ four-element calibration beads immediately before injection of each sample for data acquisition. Following data acquisition, the raw FCS (flow cytometry standard) files were normalized using Normalizer v0.3 software (GitHub, Inc; https://github.com/nolanlab/bead-normalization/releases) which was run using MATLAB R2012a, implementing an algorithm to account for signal fluctuations of the instrument (Diggins et al., 2015; Finck et al., 2013).

Normalized data were imported into FlowJo v10.7.1 (BD Life Sciences) and gated according to the gating strategy described in Figure 2.2. In summary, each channel containing isotopes for the EQ four-element calibration beads (these being 175Lu, 165Ho, 151Eu, 153Eu and 140Ce) were plotted against DNA to gate on the non-bead, cellular population (standard practice, data not shown). The Cell-ID DNA intercalator is a cationic nucleic acid intercalator that contains natural-abundance 191Ir and 193Ir. Gating on event length and DNA were used to identify singlet events. The “event length” parameter in mass cytometry is generated based on the time taken for the contents of a vaporized ion cloud to reach the detector (Lai et al., 2017). As a crude estimate of cell size, event length was used with a DNA intercalating agent to identify cellular events. Thereafter, the two Ir channels were plotted against one another for singlet discrimination, since single cell events present as a double-positive population for 191Ir and 193Ir. Cisplatin was used as a marker for discriminating dead cells, since cisplatin readily enters dead/dying cells with compromised cellular membranes where it reacts non-specifically with protein nucleophiles to a greater extent than live cells.

Therefore, live, singlet lymphocytes were identified as being positive for DNA markers and CD45 (a lymphocyte marker), and low for cisplatin staining (Figure 2.2).

At the point of live, singlet lymphocyte gating, cells were exported as individual FCS files from FlowJo and imported into RStudio (R v4.2.1) for analysis of the myeloid and lymphoid immune subsets in human tissues (Chapter 4) using an algorithm named Full Annotation Using Shaped-constrained Trees (FAUST) (Greene et al., 2021). By combining novel algorithms for variable selection, clustering, cluster matching, and feature selection, FAUST has been shown to be a valuable machine-learning method to discover and annotate cell populations across cytometry experiments. The FAUST algorithm was chosen as a tool to cluster and label cell phenotypes as it is robust to batch effects, correctly identifies clusters, even when within-cluster marker expression is non-normally distributed, and provides semantic cluster labels (Greene et al., 2021).

Live, singlet lymphocytes also underwent further manual gating to identify NK cells, shown in Figure 2.2. NK cells were identified as $CD56^{lo/+/hi}$-expressing cells with CD57 co-expression at any level. This population of crude NK cells were cleaned by further gating to exclude other lineage markers not characteristic to NK cells to yield a final population of clean, bulk NK cells (defined as $CD56^{+}CD19^{-}CD33^{-}CD21^{-}CD14^{-}\gamma\delta TCR^{-}CD3^{-}IgD^{-}$). Clean, bulk populations of NK cells for each sample were then exported as single FCS files and imported into RStudio (R v4.2.1) for further sub-classification using phenotypic clustering by FAUST (Chapter 5).

Although beyond the scope of this thesis, B cells were also manually gated, and the frequencies obtained by manual gating were used to validate FAUST clustering results (discussed further in Chapter 4). B cells were identified as $CD19^{+}$ cells with IgD co-expression at any level, which also underwent cleaning of the crude B cell population to

remove lineage markers not characteristic to B cell expression. The final population of clean, bulk B cells were defined as $CD19^{+}CD33^{-}CD14^{-}\gamma\delta TCR^{-}CD3^{-}CD8a^{-}CD56^{-}CD57^{-}$.

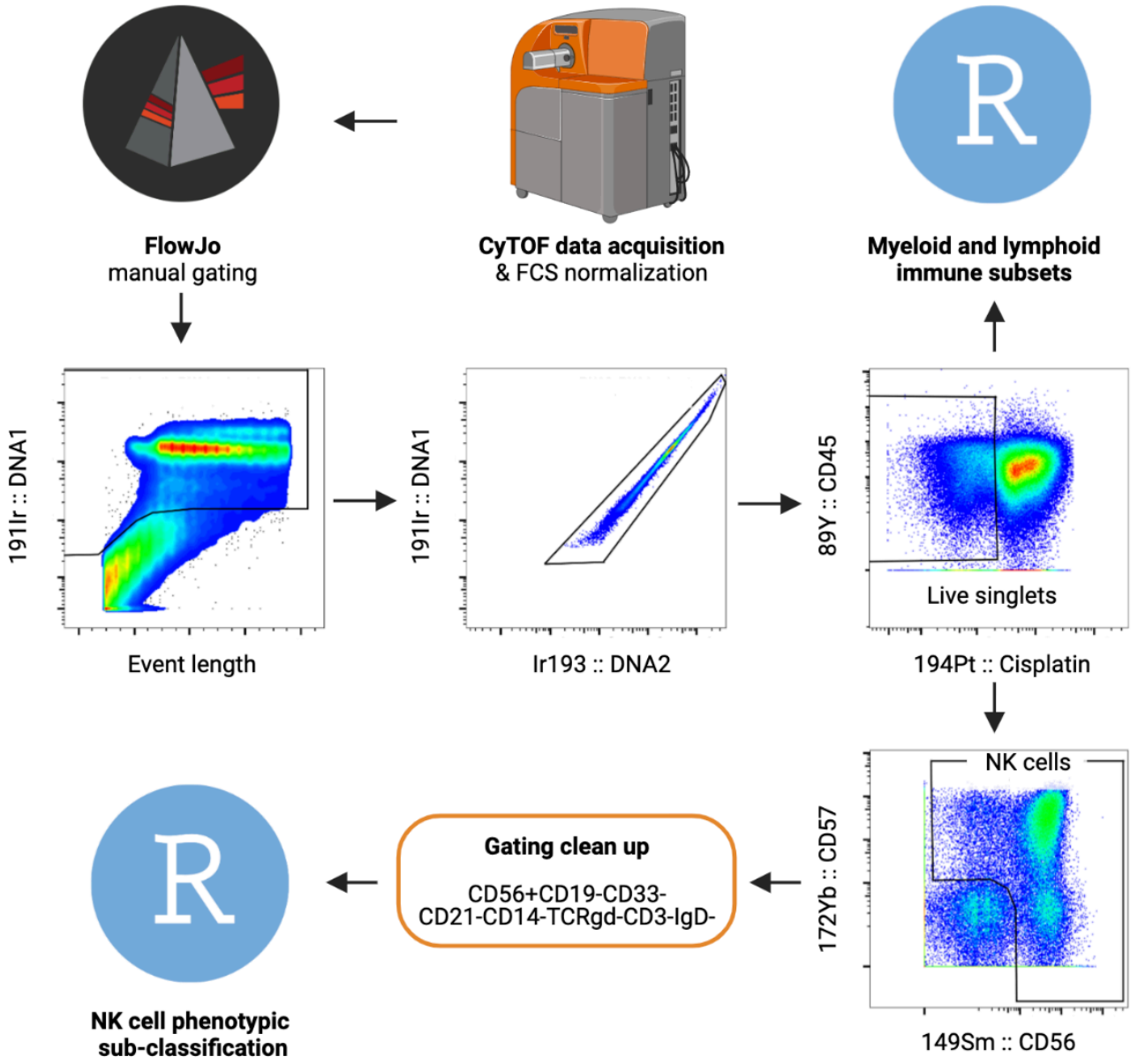

Figure 2.2: CyTOF data analysis workflow. Data from postmortem samples were acquired and raw FCS files exported from the CyTOF2 instrument were normalized using Normalizer v0.3 software (GitHub, Inc; https://github.com/nolanlab/bead-normalization/releases). Normalized FCS files were imported into FlowJo v10.7.1 (BD Life Sciences) to gate on total live singlet cells, phenotypically defined as $DNA1^{+}DNA2^{+}CD45^{+}cisplatin^{lo}$. Live singlets were exported from FlowJo as single FCS files and imported into RStudio for evaluation of the myeloid and lymphoid immune subsets in human tissues (Chapter 4). Total live singlets also underwent further gating to identify crude NK cells gated as $CD56^{lo/+/hi}$ cells. Bulk populations of NK cells underwent further manual gating to exclude lineage markers not characteristic to NK cells. The final population of clean, bulk NK cells were defined as $CD56^{+}CD19^{-}CD33^{-}CD21^{-}CD14^{-}\gamma\delta TCR^{-}CD3^{-}IgD^{-}$. Single FCS files of clean, bulk NK cells were exported from FlowJo and imported into RStudio to perform sub-classification of NK cells using phenotypic clustering by FAUST, detailed in Chapters 5.

Chapter 3: NK cell functional alterations via bystander activation pathways in TB and healthy, *Mycobacterium tuberculosis*-sensitized controls.

"There are no innocent bystanders."

- William S. Burroughs

3.1 Introduction

NK cells are considered important first-line responders to pathogen-infected and neoplastic cells by directly killing target cells and secreting immunoregulatory cytokines. Although NK cells have been a point of rising interest in recent years, our understanding of the role of NK cells in TB pathogenesis remains incomplete (Choreño Parra et al., 2017; Esin & Batoni, 2015).

It is well documented that chronic infection and inflammatory diseases (including TB) alter myelopoiesis and lymphopoiesis, resulting in changes to peripheral cellular compartments (Baldridge et al., 2010, 2011; Naranbhai et al., 2014; Scriba et al., 2017). A study by Chowdhury et al*.,* including SATVI co-authors, reported significantly decreased frequencies of peripheral blood NK cells in TB patients relative to $IGRA^{+}$ participants (Chowdhury et al., 2018). Additionally, results of a transcriptomic study at SATVI indicated downregulation of peripheral blood gene modules representing NK cell products in adolescents who progressed to active TB disease, compared to healthy controls with evidence of *Mtb* immunological sensitization (QFT^{+} and/or TST^{+}) in a South African cohort (Scriba et al., 2017). Therefore, published data in the field suggest that peripheral blood NK cells are depleted in TB patients relative to controls. However, none have provided longitudinal analyses of the peripheral NK cell compartment, particularly functional changes that occur during progression to active disease, which may highlight features of TB progression and/or correlates of risk.

In humans, NK cells represent a highly heterogenous population comprising several subsets that are phenotypically identified by co-expression of CD56 (the archetypal marker of NK cells) and/or CD16 (Lanier, Ruitenberg, et al., 1988; Lanier et al., 1989, 1991). Two main subsets of human NK cells have been largely studied including, $CD56^{dim}CD16^{bright}$ and

$CD56^{bright}CD16^{dim}$ cells. The $CD56^{dim}CD16^{bright}$ population also known as $NK_{cytotoxic}$ cells, which are considered the mature subset, comprising majority (~90%) of the peripheral NK cell population. $NK_{cytotoxic}$ cells initiate apoptosis of a target cell by secreting cytotoxic molecules and/or inducing ADCC. On the other end of the NK spectrum, $CD56^{bright}CD16^{dim}$ or $NK_{regulatory}$ cells encompass approximately 10% of the total peripheral NK population and primarily produce immunoregulatory cytokines (such as, IFN-γ, TNF and IL-22) (Béziat et al., 2011; Björkström, Riese, et al., 2010; Yu et al., 2010). More recently, with technological advances in the immunology field, a broad spectrum of human NK cell subset diversity has been uncovered and is becoming increasingly appreciated (Freud et al., 2017). To this end, several other NK subsets occur with intermediate levels of CD56 and/or CD16 phenotypic co-expression patterns. However, less is known about the developmental and functional characteristics of these subsets.

To exert functional and cytotoxic responses, NK cells are activated via classical or bystander pathways, as discussed in Chapter 1, Section 1.3.1. Briefly, classical or "missing-self" activation occurs when neoplastic or infected cells downregulate MHC-I molecules, causing killing of target cells through lack of NK inhibitory receptor engagement. Bystander NK activation can be triggered through cytokine-receptor binding on the cell surface. This involves nearby accessory cells secreting activating cytokines for which NK cells possess receptors (Caligiuri, 2008; Chalifour et al., 2004; Esin et al., 2004; Esin & Batoni, 2015; Mandal & Viswanathan, 2015). Previous studies have demonstrated that accessory cytokines, such as recombinant cytokines of rhIL-12, rhIL-18, and rhIL-2, induced robust IFN-γ cytokine responses by NK cells (Horowitz et al., 2010b; Suliman et al., 2016) and were required to optimally activated NK cells within blood stimulated with BCG in revaccinated South African adults (Suliman et al., 2016). Although BCG is a close relative of *Mtb,* it remains to be shown whether bystander activation via accessory cytokines is important for NK cell activation during the immune response to *Mtb*-specific antigens. Additionally, NK

cell bystander activation has been demonstrated in the context of NK cell cytokine responses. However, there is a knowledge gap concerning the role of bystander activation on NK cell cytotoxic potential during the immune response to *Mtb* infection and TB disease.

The overarching aims of the study presented in this chapter were to 1) investigate functional changes in peripheral blood NK cells that occur during progression to TB disease; and 2) determine how bystander activation influences NK cell function, including cytokine production and cytotoxic potential of several NK cell subsets, in the context of *Mtb* infection and TB disease.

To achieve the first aim, data from a longitudinal study was used to quantify NK cell functional responses in PBMC stimulated with *Mtb* antigens in a cohort of adolescents who progressed to TB disease and controllers who remained healthy during two years of follow-up. During TB disease, high *Mtb* antigen load activates immune cells and initiates the inflammatory response to aid in pathogen clearance. Since NK cell responses are largely mediated via bystander activation, it was hypothesized that NK cell function increased during progression to TB disease above *Mtb*-sensitized controllers, possibly as a feature of disease-associated inflammatory signals within the cytokine milieu.

To achieve the second aim, a cytokine neutralization assay was designed to evaluate NK cell function in the context of bystander activation during TB disease. To this end, *Mtb* peptide antigens were used to initiate bystander activation in PBMC (the proposed mechanisms are discussed in the following section), and NK cell functions were assessed by measuring cytokine production (IFN-γ-, TNF- and polyfunctional IFN-γ^+TNF$^+$-expressing NK cells) and cytotoxic potential (by quantifying perforin and granzyme B expression). It was hypothesized that blocking NK cell-activating cytokines (including myeloid-derived IL-12 and IL-18, and T cell-associated IL-2) would diminish NK cell responses in TB patients to a

greater degree than healthy, *Mtb*-sensitized controls, which may suggest an important role for bystander activation during TB disease. The rationale for this hypothesis is based on the concept of accessory cells in the inflammatory milieu being a primary driver of NK cell responses during active TB disease.

For the cytokine neutralization assay, isolated PBMC from TB patients and healthy, *Mtb*-immunologically sensitized controls were stimulated *in vitro* with a peptide pool of secreted *Mtb* antigens or whole *Mtb* lysate; in the presence or absence of neutralizing antibodies against myeloid cytokines, IL-12 and IL-18, or a T cell cytokine, IL-2. Notably, *Mtb* peptides and larger proteins cannot be directly recognized by NK cells, but these antigens do activate T cells and APCs, respectively. When PBMC are stimulated with *Mtb* peptides *in vitro,* peptides bind MHC-II molecules on APCs, allowing direct engagement with TCRs to activate T cells. In contrast to purified *Mtb* peptides, a lysate of whole *Mtb* contains a mixture of peptides and protein fragments. Therefore, *Mtb* lysate is most often used as a strong activator of T cells (since the lysate contains peptides) but can also activate myeloid cells with larger protein fragments. More specifically, larger protein components of *Mtb* lysate can bind PRRs on myeloid cells to initiate activation and secretion of NK-activating cytokines, such as IL-12 and IL-18. Upon binding of *Mtb* proteins on myeloid cell PRRs, proteins are phagocytosed, and the processed peptide antigens are then presented to T cells. Once T cells recognize their antigen and become activated, they secrete NK cell-activating cytokines, such as IL-2. Notably, other NK cell-activating cytokines also play a role in the bystander activation pathway, such as IL-15, IL-21 and type-I interferons (Zwirner & Domaica, 2010). However, for the designed assay presented in this chapter, blocking cytokines were limited to myeloid-associated IL-12 and IL-18 (as a combination) and T cell-associated IL-2. Since T cells are the primary subset for activation using *Mtb* peptides and lysate, it was hypothesized that NK cell responses are suppressed more by blocking T cell-

associated IL-2 than myeloid-associated IL-12/IL-18 when PBMC were stimulated with *Mtb* antigens.

NK cell subsets have distinct receptor expression patterns that play a role in cell signaling. In the context of bystander activation, cytokine receptors expressed on NK cells have the potential to shape NK cell activation and function. For example, human $CD56^{bright}$ NK cells express the high affinity IL-2 receptor, composed of the IL-2Rα chain (CD25), the IL-2Rβ chain (CD122), and the IL-2Rγc chain (CD132). In contrast, $CD56^{dim}$ NK cells only express the intermediate affinity IL-2 receptor, composed of the IL-2Rβ chain and the IL-2Rγc chain (Becknell & Caligiuri, 2005). Even within the $CD56^{bright}$ NK populations that expresses the high affinity IL-2 receptor, $CD56^{bright}CD16^{-}$ and $CD56^{bright}CD16^{dim}$ subsets have distinct functional and proliferative responses to IL-2 (Carson et al., 1997; Fehniger et al., 2003). Little is known regarding expression patterns of IL-12 and IL-18 receptors across NK populations and the differential responses of NK cell subsets upon ligand binding. Overall, current evidence suggests that NK cell subsets have distinct functional responses to activating cytokines (at least IL-2) produced by accessory cells in the milieu. It was therefore, hypothesized that blocking IL-2 would suppress functional responses to a greater degree in the $CD56^{bright/hi}$ subset than in $CD56^{dim/lo}$ NK cells. The rationale for this hypothesis is that NK cells expressing higher affinity receptors (e.g., $CD56^{bright/hi}$ NK cells) are likely to experience greater changes to functional responses upon binding and subsequent blocking of their ligands, relative to subsets with lower affinity receptors (such as $CD56^{dim/lo}$ NK cells).

Overall, the study presented in this chapter set out to investigate the complex interplay between T cells, myeloid cells, and NK cell function in the context of TB disease, with relevance in immunopathogenesis.

3.2 Methods and Materials

3.2.1 Study participants

ACS participants for CyTOF ICS

The Adolescent Cohort Study (ACS), including progressors and controllers was previously described (Zak et al., 2016; Scriba et al., 2017). Briefly, 6 363 adolescents within the Worcester region of the Western Cape, South Africa, were enrolled and followed up for two years. To be enrolled into the study, written informed assent was provided by adolescents, while parents or legal guardians provided written informed consent. Evidence of *Mtb* infection was measured either by a positive TST or QFT result. Of those with evidence of *Mtb* infection, 45 adolescents developed active TB disease within the two years of follow-up, diagnosed by positive sputum smear microscopy and/or Mycobacteria Growth Indicator Tube (MGIT) liquid culture. To exclude early asymptomatic disease at the time of assessment, participants were excluded from the progressor cohort if they developed TB within the first six months of enrollment (or the first TST- or QFT-positive result). Controllers were characterized as healthy participants with evidence of *Mtb* infection (i.e., TST^+ or QFT^+) who did not progress to active disease during the follow-up period. Progressors and controllers were matched for age, sex, ethnicity, school of attendance and prior history of TB disease. Participants were excluded if they were HIV^+ or become pregnant over the two-year of follow-up.

NK functional assay cohort

Ten adult TB patients and ten adult healthy controls were enrolled for this study. Participants with active pulmonary TB disease were diagnosed by positive sputum culture, positive smear microscopy and/or chest x-ray results characteristic to active TB disease. Blood was

collected from participants within the first 6 days of initiating anti-TB treatment. Participants were excluded if they were HIV^+ or were pregnant. Healthy community controls were recruited from the same community as TB patients, in the Worcester region of the Western Cape, South Africa, with high *Mtb* infection pressure. The QFT assay was used to indicate *Mtb*-immunological sensitization in healthy controls with a positive result.

3.2.2 CyTOF ICS and data acquisition

The CyTOF ICS assay was performed on PBMC from ACS participants in a study that was originally designed to investigate T cell responses to *Mtb* antigens and identify T cell correlates of risk (Rozot, et. al., manuscript in preparation). The study was designed, and protocols optimized by Dr Virginie Rozot (the primary supervisor of this thesis) and colleagues at SATVI. The mass cytometry panel also included markers to identify all major known leukocyte subsets present in normal human peripheral blood, including NK cells. As a sub-study, CyTOF data generated from the ACS T cell correlates of risk study was used in this chapter to investigate NK cells during progression to TB disease.

To summarize the protocol, cryopreserved PBMC were thawed and rested according to protocols outlined in Chapter 2, Section 2.5.1. Cells were left unstimulated or stimulated with antigens in the presence of αCD28 (anti-CD28, BD) and αCD49 (anti-CD49, BD). Stimulation conditions included 1) a peptide pool of secreted *Mtb* antigens (a mixture comprising 87 peptides at 1μg/mL each, JPT Peptide Technologies), 2) a peptide pool of non-secreted antigens (containing 24 peptides at 1μg/mL each, JPT Peptide Technologies), 3) live *Mtb* (*Mtb* triple-auxotroph strain derived from H37Rv through deletion of leucine, pantothenate and arginine synthesis pathways; donated by Bill Jacobs, Albert Einstein University and propagated by Digby Warner, UCT), and 4) a positive control of immunodominant Epstein-Barr virus and cytomegalovirus (EBV/CMV) antigens (a mixture

of EBV and CMV peptides at 1μg/mL each, JPT Peptide Technologies). Cells were stimulated for a total of 12 hours at 37°C, adding Brefeldin A (10μg/mL Golgi Plug, BD) at the 5-hour timepoint.

Following stimulation, cells from each of the five stimulation tubes for two participants were barcoded and pooled (i.e., total of ten samples barcoded and pooled to be stained in the same tube). Cells were barcoded with a combination of five metal-conjugated αCD45 antibodies (In113, In115, Pd108, Pt198, Bi209) in different combinations, such that each sub-sample were identifiable based on its unique barcode. The rhodium (Rh) 103 DNA intercalator was used for live/dead discrimination and total cells were stained with the Ir191/193 DNA intercalator. Following barcoding, cells were stained with a CyTOF antibody panel (Table 3.1), which was designed and optimized for the ACS T cell correlates of risk study. Once finalized, the panel was tested in a pilot cohort of 25 healthy, *Mtb*-sensitized donors and 25 TB patients to confirm successful performance. Data were acquired on the CyTOF2 instrument using the protocol outlines in Chapter 2, Section 2.8.3.

Table 3.1: CyTOF antibody panel for ACS T cell correlates of risk study.

Marker	Metal	Clone	Antibody supplier
Extracellular (surface) markers			
CCR6	141Pr	11A9	Fluidigm
CD11c	142Nd	0.6	In-house conjugation
CD127	143Nd	A-019D5	In-house conjugation
CD27	144Nd	O323	In-house conjugation
CD4	145Nd	RPA-T4	Fluidigm
CD20*	147Sm	2H7	Fluidigm
CD16*	148Nd	3G8	Fluidigm
CD26	149Sm	M-A261	In-house conjugation
HLA-DR	151Eu	G46-6	In-house conjugation
CD19*	152Sm	HIB19	In-house conjugation
TCR_{gd}	152Sm	11F2	Fluidigm
CCR4	153Eu	205410	Fluidigm
CD3*	154Sm	UCHT1	Fluidigm
CD161	159Tb	HP-3G10	Fluidigm
CD14*	160Gd	M5E2	Fluidigm
CD33*	161Dy	WM53	In-house conjugation
CD25	162Dy	M-A251	In-house conjugation
CXCR3	163Dy	G025H7	Fluidigm
CD7*	166Er	M-T701	In-house conjugation
CCR7	167Er	150503	In-house conjugation
IgD	168Er	IA6-2	In-house conjugation
CD8	168Er	SK1	Fluidigm
CD45Ra	169Tm	HI100	Fluidigm
CCR5	170Er	2D7/CCR5	In-house conjugation
CXCR5	171Yb	RF8B2	Fluidigm
Vα7.2	172Yb	3C10	In-house conjugation
PD1	173Yb	EH12.2H7	In-house conjugation
CD38	174Yb	HIT2	In-house conjugation
CD56*	176Lu	HCD56	Fluidigm
Intracellular (functional) markers			
MIP1β	155Gd	24006	In-house conjugation
IL-2	158Gd	MQ1-17H12	Fluidigm
IFN-γ *	165Ho	B27	Fluidigm
IL-22*	150Nd	22URTI	Fluidigm
IL-17A	164Dy	N49-653	Fluidigm
Perforin	175Lu	BD-48	Fluidigm
IL-6	156Gd	MQ2-13A5	Fluidigm
TNF*	146Nd	Mab11	Fluidigm

In-house conjugated antibodies using Maxpar Antibody Labeling Kits (Standard BioTools).
* Antibodies for identifying total NK cells (extracellular) and evaluating NK function (intracellular markers).

3.2.3 Flow cytometry ICS and data acquisition

As a follow-on to the NK cell sub-study of the ACS T cell correlates of risk dataset, a cytokine neutralization assay was designed to investigate NK cell functional alterations via bystander activation pathways during TB. This assay was designed and optimized by me, Carly Young-Bailie.

Peripheral blood was collected from research participants, and PBMC were isolated and cryopreserved within two hours of phlebotomy according to protocols outlined in Chapter 2, Section 2.2. Following resting and thawing (Chapter 2, Section 2.5.1), PBMC were stimulated using *Mtb* lysate (10μg/mL; BEI Resources) and a peptide pool of secreted *Mtb* proteins (1μg/mL each of 87 pooled peptides, JPT Peptide Technologies) and cytokine stimulation acted as positive controls using rhIL-2 (0.1μg/mL; Recombinant Human IL-2, carrier-free; BioLegend) or rhIL-12/18 (0.1μg/mL of each; Recombinant Human IL-12, p70, carrier-free; BioLegend; Recombinant Human IL-18, carrier-free; BioLegend). Unstimulated (UNS) cells were included as a negative control. At the beginning of stimulation, neutralizing antibodies (10μg/mL) or isotype-matched control antibodies (10μg/mL) were added to each stimulation condition. Neutralizing antibodies included αIL-12 in combination with αIL-18 (each at a concentration of 10μg/mL; Human IL-18/IL-1F4 Mab, clone 125-2H; R&D Systems; Human IL-12 p70 Mab, clone 24910; R&D Systems) or αIL-2 (Purified NA/LE Rat Anti-Human IL-2, clone MQ1-17H12; BD Pharmingen Inc.). Isotype controls for αIL-12/18 and αIL-2 included mouse IgG_1 (Mouse IgG1 Isotype Control, clone 11711; R&D Systems) and rat IgG_{2A} (Purified Rat IgG2a, κ Isotype Control, clone A110-2; BD Pharmingen Inc.), respectively.

One million PBMC were added to complete medium supplemented with the appropriate stimulant and neutralizing antibody or isotype control. Figure 3.1 shows a schematic diagram

describing the experimental layout of the cytokine neutralization assay. Cells were stimulated at 37°C in a humidified 5% CO_2 incubator for a total of 18 hours, adding Brefeldin A (5µg/mL; Brefeldin A; Sigma Chemical Co.) at 13 hours (i.e., 5 hours before the end of stimulation). Brefeldin A is a fungal metabolite that inhibits Golgi vesicle formation *in vivo* and *in vitro*, thus inhibiting protein trafficking by the membrane system to prevent secretion and enabling detection of cytokines using ICS and flow cytometry (Donaldson et al., 1991; Nebenführ et al., 2002; Orcl et al., 1991).

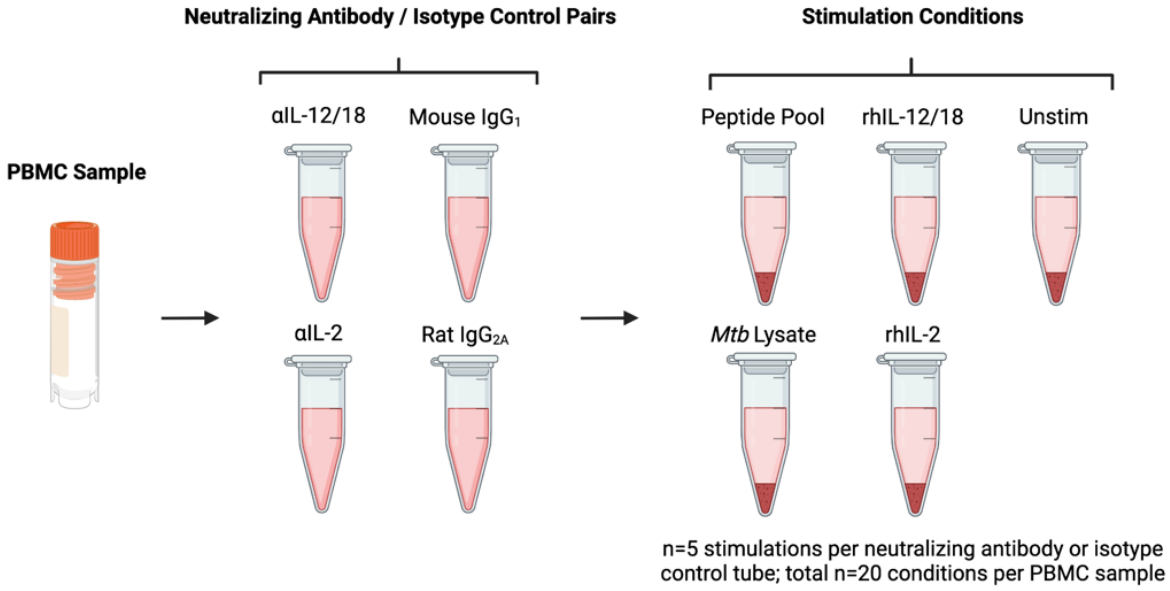

Figure 3.1: Schematic describing experimental layout of the cytokine neutralization assay.

Following stimulation, cells were stained with a panel of fluorochrome-labelled extracellular and intracellular antibodies using the flow cytometry ICS and data acquisition protocol described in Chapter 2, Section 2.5.2 and 2.5.3. Table 3.2 describes the flow cytometry ICS panel for investigating NK cell functional responses via bystander activation pathways in PBMC stimulated with *Mtb* antigens.

Table 3.2: Flow cytometry ICS antibody panel for measuring NK cell responses in PBMC stimulated with *Mtb* antigens and recombinant cytokines.

Marker	Fluorochrome/Dye	Rationale	Clone	Supplier
Extracellular (surface) markers				
Live/Dead	Fixable Near-IR Stain	Dead cell exclusion	N/A	ThermoFisher Scientific
CD3	BV786	T cells	UCHT1	BD Biosciences
CD56	BV570	NK cells	HCD56	BioLegend
CD16	AF488	NK cells/monocytes	3G8	BioLegend
CD14	PerCpeF710	Monocytes	61D3	Invitrogen
CD19	BV711	B cells	SJ25C1	BD Biosciences
CD33	BV605	Myeloid cells	P67.6	BioLegend
Intracellular (functional) markers				
IFN-γ	AF700	Function	B27	BD Biosciences
TNF	PE-Cy7	Function	Mab11	eBioscience
Granzyme B	BV510	Cytotoxicity	GB11	BD Biosciences
Perforin	BV421	Cytotoxicity	B-D48	BioLegend

3.2.4 Data analysis

CyTOF ICS data analysis

Methods for analysing the CyTOF ICS dataset in the ACS T cell correlates of risk study were designed and performed by Miguel Rodo, PhD candidate at SATVI, whose project involves development of new analytical and statistical pipelines for high dimensional datasets. Briefly, three batches of acquired data corresponding to six participant-timepoint combinations with five stimulations each, were removed due to unimodal expression of CD3, thereby rendering these samples unusable for discriminating between crucial lineage markers. Exclusion of these samples reduced the number of samples from 154 to 148 and excluded all samples from one controller (leaving 36 controllers in the dataset, rather than 37). Data were normalized using the reference bead method described in Chapter 2, Section 2.9 (Finck et

al., 2013). Bead data was removed from cell data using the CATALYST package in R (Chevrier et al., 2018). Live cells and singlets were manually gated based on double positive Ir (DNA) channels, which were lowly stained with the Rh103 (dead cell) exclusion marker. Deconvolution of barcoded sub-samples were performed using the method developed by Zunder and colleagues (Zunder et al., 2015). Further gating was performed to remove segments of data that exhibited within-run time effects that were not fully corrected for during bead normalization, using the flowCut package in R (Meskas et al., 2022). Samples that still contained cell doublet events and residual beads were manually gated further to ensure clean cell populations.

The FAUST algorithm was used to cluster and label cell phenotypes (Greene et al., 2021). NK cells were identified by the following phenotype: $CD3^{-}CD33^{-}CD7^{+}CD14^{-}CD20^{-}CD19^{-}$. Frequencies of FAUST-annotated NK cells were correlated with a subset of 60 samples (comprising randomly selected 6 progressors and 6 controllers, each with five stimulation conditions) that were manually gated by myself, Carly Young-Bailie, using FlowJo v10.7.1 software (gating strategy defined in Figure 3.2). FAUST-annotated frequencies were correlated against manual gating using concordance correlation coefficient (CCC) and Pearson correlation coefficient (PCC) scores.

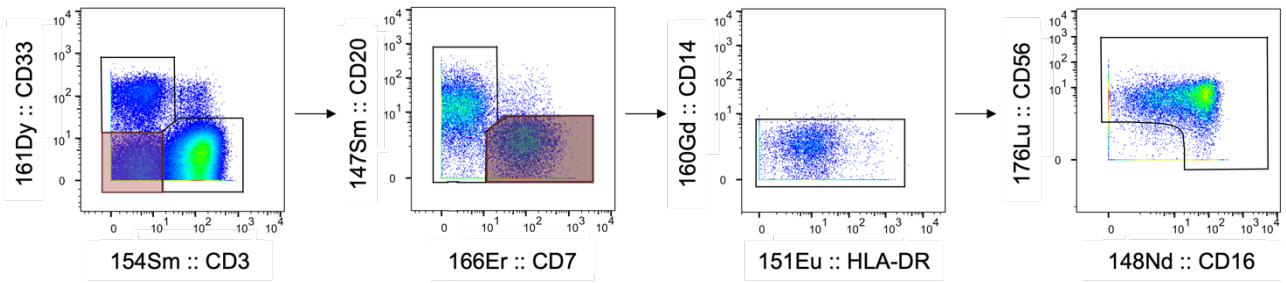

Figure 3.2: Manual gating strategy to identify NK cells in PBMC of ACS participants. Gating of NK cells using gold standard manual gating is shown for a representative PBMC sample. Normalization and debarcoding were performed on FCS files exported from CyTOF data acquisition, and live singlets were gated (not shown). NK cells were phenotypically identified as $CD33^{-}CD3^{-}CD20^{-}CD7^{+}CD14^{-}$, with a rainbow gate to identify total NK cells with CD56 and/or CD16 co-expression.

FAUST could not reliably identify cytokine-expressing cells due to low frequencies and unimodal distribution of cytokine data. Therefore, COMPASS (Combinatorial Polyfunctionality analysis of Antigen-Specific Subsets) was used to investigate *Mtb* antigen-specific NK cells (L. Lin et al., 2015). This approach uses a Bayesian hierarchical framework to model cell subsets and highlights those most likely to be antigen-specific, while regularizing small counts that may arise in high dimensional datasets. The COMPASS model provides a posterior probability of specificity for each cell subset and each sample, which is used to profile the immune response to a stimulus (L. Lin et al., 2015). Cytokine combinations with low response probability were excluded. Response probability and proportion analyses were also excluded if there was little variability.

To identify differential NK cell responses between progressors and controllers, a mixed-effects model was developed and implemented by Miguel Rodo (Rozot, et. al., manuscript in preparation). Briefly, the model allowed for testing three effects: the “progression effect” (to test if there was a progression effect and/or a time-to-TB effect), the “distal TB effect” (indicating an effect of progression far from TB diagnosis), and the “proximal TB effect” (indicating an effect of increasing proximity to TB diagnosis).

To determine if there was an association (i.e., a likely bystander relationship) between *Mtb*-specific T cells and *Mtb*-specific NK cell responses, frequencies of secreted *Mtb* peptide-specific cytokine-expressing NK cells were modelled against frequencies of secreted *Mtb* peptide-specific IL-2 expressing CD4 T cells. NK cell responses were summed over total cytokine-producing cells for IFN-γ, TNF and/or IL-22. T cell responses were frequencies of IL-2-expressing CD4 T cells. Response frequencies were background-subtracted counts of cytokine-positive cells. The data were modelled as a negative binomial distribution with random effects for participants and splines to allow for non-linear effects.

Flow cytometry cytokine neutralization assay data analysis

Methods for analysing the data from the flow cytometry cytokine neutralization assay were performed entirely by myself, Carly Young-Bailie. Flow cytometry data were exported in FCS format and imported into FlowJo v10.7.1 software for gating. Gating to identify NK cell subsets was performed according to the gating strategy outlined in Figure 3.3. Total NK cells were identified as singlet, live, $CD3^{-}CD33^{-}CD14^{-}CD19^{-}$ cells in combination with CD56 and/or CD16 expression (referred to as a "rainbow" gate). Five subsets of NK cells were characterized as either $CD56^{hi}CD16^{lo}$, $CD56^{int}CD16^{lo}$, $CD56^{hi}CD16^{int/hi}$, $CD56^{int}CD16^{int}$ or $CD56^{lo}CD16^{hi}$, delineated by CD56 and CD16 co-expression patterns (Figure 3.3). Frequencies and median fluorescence intensity (MFI) data were exported in CSV (comma-separated values) format and imported into R Studio (R v4.2.1) for statistical analysis and data visualization.

In studies analysing the induced cellular response to stimulation in terms of frequencies of cytokine-producing cells, it is common practice to perform "background subtraction". Background subtraction was achieved by subtracting the frequencies of cytokine-positive unstimulated cells (i.e., the "background" or basal value) from the frequencies of the induced cellular responses (i.e., the cytokine-producing responses in each stimulated conditions) (Equation 1a). Here, frequency refers to a normalized value reflecting the proportion of cells expressing a particular marker, reported as a percentage, relative to a parent population of cells. In some cases, background subtraction of cytokine-producing cell frequencies produces negative values, which is not truly a "negative response" due to uncertainty around zero for lowly-producing stimulated and unstimulated cell populations. Therefore, the distribution around zero was computed for each cell subset by calculating the 80% confidence interval (CI) for all negative values after background subtraction. The lower and upper bounds of the 80% CI were then applied as a threshold for positive values, and all

values less than this threshold. Therefore, all values falling within the distribution around zero threshold were set to zero.

In some cases, a precise frequency may be challenging to obtain for a given marker, since antibody staining may not yield a definable, bimodal distribution for gating. Instead, the distribution of a marker may spread across the spectrum of staining (fluorescence) intensity, making it difficult to gate cells appropriately. This is common for cytotoxic molecules such as perforin and granzyme B. Rather than analysing frequencies for such markers, a measure of MFI is used, which is a relative value reflecting the median level of marker expression within a cell population. To normalize for background expression of cytotoxic molecules (which are pre-formed and readily present even at basal level in NK cells), a fold-change of the MFI in stimulated cells was calculated above the unstimulated condition (Equation 1b). No distribution around zero threshold was calculated, as negative values were not obtained when performing fold-change background treatment for MFI.

a) %cytokine^{+}cells = %**stimulated** cytokine^{+}cells - %**unstimulated** cytokine^{+}cells

b) MFI cytotoxic molecule = $\frac{\text{MFI in } \textbf{stimulated} \text{ cells}}{\text{MFI in } \textbf{unstimulated} \text{ cells}}$

Equation 1: Mathematical procedures to determine a) frequencies of background-subtracted cytokine-producing cells, and b) induced expression (MFI) of cytotoxic molecules above the unstimulated control.

Reported frequencies and MFI values have been background-treated using the methods described in Equation 1, unless specified otherwise.

Statistical significance was determined by either one- or two-sided, paired, Wilcoxon non-parametric signed-rank tests for comparisons between responses in the same participant. Statistical significance to compare responses between cohorts (i.e., TB versus QFT^{+}) was determined by either one- or two-sided, unpaired, Mann-Whitney, non-parametric signed-

rank tests. One-sided tests were appropriate when differences between groups were rationalized by a specific, pre-hypothesized direction in response. Two sided tests were used to test if one variance was greater or less than another variance according to a hypothesis, with no pre-defined direction of the difference in response. The Kruskal-Wallis, paired, non-parametric analysis of variance (ANOVA) test was used to compare responses between five NK cell subsets within the same participant. The Holm-Bonferroni test was used to control for multiple comparisons (q-values).

For qualitative analysis using t-Distributed Stochastic Neighbor Embedding (tSNE), total NK cells from a single representative QFT^+ participant (n=1), stimulated with recombinant cytokines, with and without their corresponding neutralizing antibodies, were concatenated using sample-identifiable keywords using FlowJo (v10.7.1). Using the FlowJo tSNE plugin, NK cells were dimensionally reduced according to their relative expression of the following markers: IFN-γ, TNF, granzyme B, perforin, CD56 and CD16. Default iteration and perplexity values were used at 1000 and 30, respectively. The approximate (random projection forest – ANNOY) K-Nearest Neighbours (KNN) algorithm was used with the Barnes-Hut gradient algorithm, and the learning configuration was auto set to opt-SNE. Following dimensionality reduction, identifiable keywords were used to gate and separate individual sample conditions.

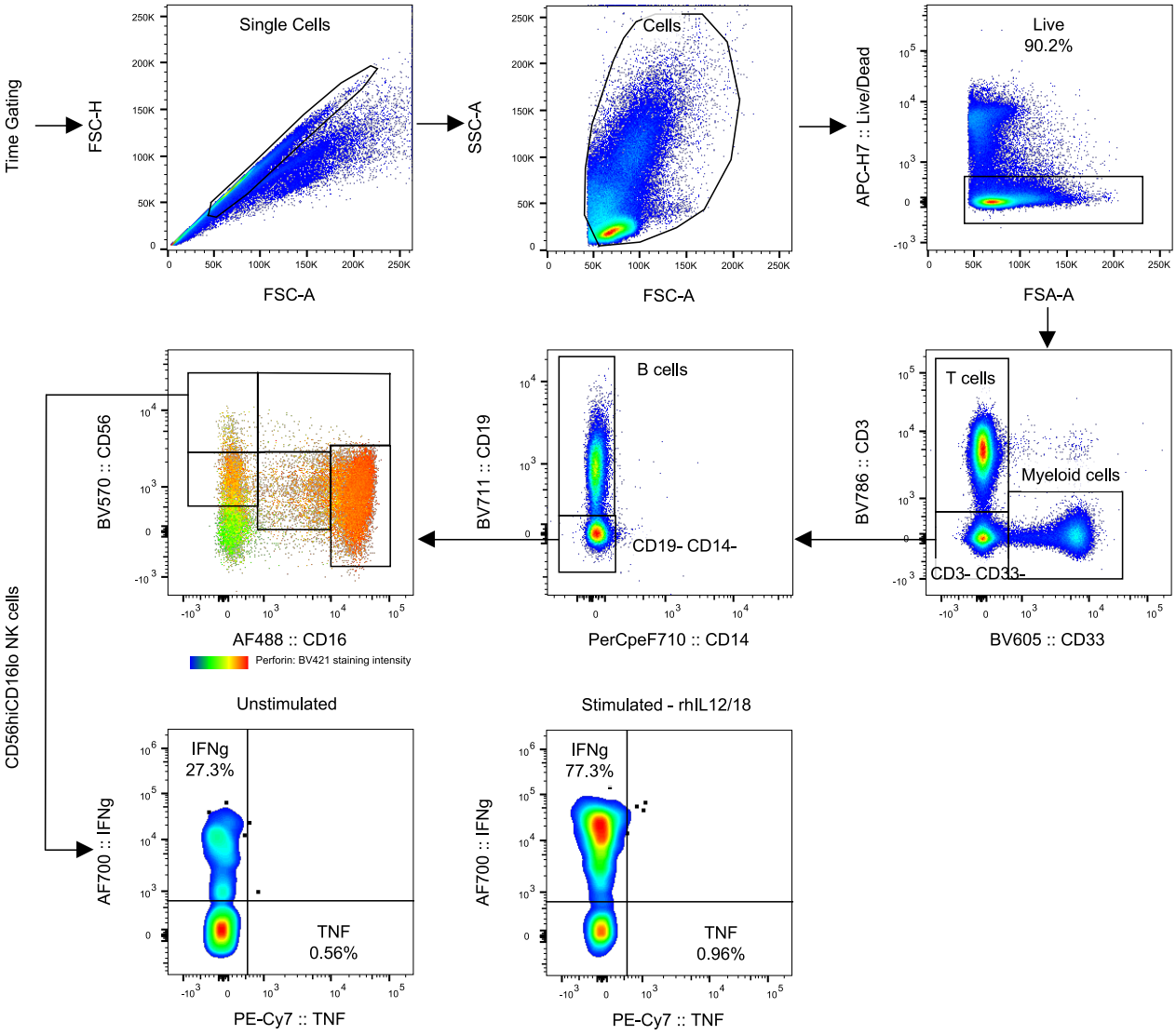

Figure 3.3: Flow chart describing the gating strategy to identify NK cell subsets within PBMC. Live cells were identified after gating on time (time vs each laser, not shown) and single cells (FSC-H vs FSC-A and SSC-A vs FSC-A). T cells (CD3), B cells (CD19) and myeloid cells (CD33 and CD14) were excluded before gating on NK cells, delineated by CD56 and CD16 co-expression patterns. The expression of perforin, a cytotoxic marker, aided gating decisions for the NK cell subsets. Five NK subsets were identified, including $CD56^{hi}CD16^{lo}$, $CD56^{int}CD16^{lo}$, $CD56^{hi}CD16^{int/hi}$, $CD56^{int}CD16^{int}$, $CD56^{lo/int}CD16^{hi}$ cells. Cytokine gating for IFN-γ and TNF is demonstrated on the $NK_{regulatory}$ $CD56^{hi}CD16^{lo}$ subset, showing unstimulated and rhIL-12/18 stimulated samples from a representative QFT^{+} participant.

3.3 Results

3.3.1 Participant characteristics

ACS participants for CyTOF ICS

Among the 6 363 adolescents enrolled, 45 progressors developed microbiologically proven, pulmonary TB during the study follow-up. Of the 45 progressors, 37 had PBMC samples available to be assayed by ICS. For each progressor, one matched controller with available PBMC samples were assayed by CyTOF ICS. Longitudinally collected PBMC at six-monthly intervals were available for most participants. Following data QC and filtering, data from 37 progressors and 36 controllers were analyzed, yielding a total sample size of 148 PBMC, collected between 1 and 897 days before TB diagnosis ("time to TB", for progressors). ACS participant characteristics were previously described (Zak et al., 2016; Scriba et al., 2017) and patient characteristics data for the ACS T cell correlates of risk study are currently being prepared for publication (Rozot, et al., manuscript in preparation).

Participants for NK Functional Assay

Ten patients with confirmed TB disease were HIV-uninfected, adult men and women between the ages of 19 and 46 years. Ten healthy community controls were *Mtb*-sensitized, HIV-uninfected, adult women between the ages of 23 and 48 years. Healthy controls had no household contacts with confirmed TB disease and no clinical evidence of active TB disease or other respiratory ailments. No other known medical conditions were detected. Study participant characteristics are detailed in Table 3.3.

Table 3.3: Study participant characteristics for investigating NK cell functional alterations via bystander activation pathways in TB and healthy, *Mtb*-sensitized controls.

Cohort Definition		TB	QFT^{+}
Total participants enrolled, n		10	10
Median age, years [range]		27 [19-46]	29 [23-48]
Sex: male, n (%)		5 (50%)	0 (0%)
Ethnicity, n (%)			
	Coloured	10 (100%)	6 (60%)
	Black	n.d.	4 (40%)
HIV status, n (%)			
	Positive	0 (0%)	0 (0%)
	Negative	10 (100%)	10 (100%)
QuantiFERON test: positive, n (%)		n.d.	10 (100%)
Previous episode of TB, n (%)		2 (20%)	0 (0%)
Culture, n (%)			
	Positive	2 (20%)	n.a.
	Negative[1]	1 (10%)	n.a.
	Not done/no result	7 (70%)	n.a.
Smear, n (%)			
	+++	3 (30%)	n.a.
	++	2 (20%)	n.a.
	+	3 (30%)	n.a.
	Negative[2]	2 (20%)	n.a.
Median treatment duration at sampling, days [range]		6 [3-6]	n.a.

[1] Participant with negative culture had a smear positive result.
[2] Both participants with negative smear results had chest x-ray results and clinical presentations characteristic to active TB disease, and one smear negative participant had a positive culture result.

3.3.2 *Mtb* peptide-specific NK cells are associated with progression to TB disease and correlate with T cell responses

To validate FAUST as a tool for automated gating and annotation of cell subsets, FAUST-identified NK cells were correlated with frequencies obtained by gold standard manual gating. Manual gating was performed on a subset of 60 ACS samples and the manual gating strategy for identifying NK cells was outlined in Figure 3.2. Correlation analyses revealed that FAUST-annotated NK cells (with the phenotypic definition $CD3^-CD33^-CD7^+CD14^-CD20^-CD19^-$) demonstrated good CCC and PCC scores against manual gating (Figure 3.4).

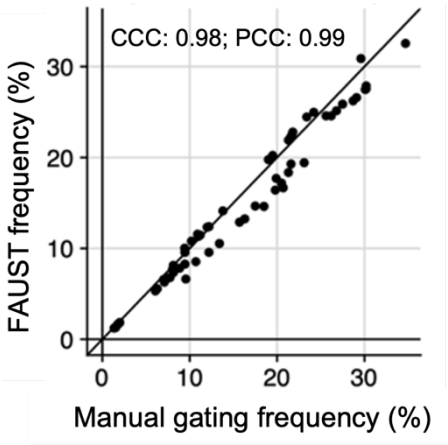

Figure 3.4: Frequency correlations of manually gated NK cells with FAUST-annotated NK cells. Frequencies of FAUST-identified NK cells ($CD3^-CD33^-CD7^+CD14^-CD20^-CD19^-$) correlate with manual phenotypic gating (gating strategy defined in Figure 3.2), demonstrating good concordance correlation coefficient (CCC) and Pearson correlation coefficient (PCC) values. Manual gating and correlation analysis was performed on a subset of 60 ACS samples.

Total NK cells were extracted from FAUST and COMPASS analysis was performed to obtain response probabilities, functionality scores (FS) and polyfunctionality scores (PFS) (Figure 3.5a). NK cells in stimulated PBMC had a high probability of response to secreted *Mtb* peptides, *Mtb* auxotroph and EBV/CMV peptides, particularly for single-positive IFN-γ^+ and double-positive IFN-γ^+TNF^+ responses. The highest scores were for secreted *Mtb* peptides, for which the FS was higher than PFS. The NK cell response probabilities to non-secreted

Mtb proteins were low and did not pass filtering steps for robust analysis and were therefore, not considered further.

COMPASS scores for antigen-specific NK cell responses were modelled against time to TB in progressors and controllers (Figure 3.5b). Results suggest that there was a significant progression effect ($p=5.63x10^{-3}$) for the FS of secreted *Mtb* peptide-specific NK cell responses. The distal TB effect was significantly lower in progressors than controllers at timepoints far from TB diagnosis ($p=4.89x10^{-3}$), but the FS for secreted *Mtb* peptide-specific NK cell responses increased with time-to-TB diagnosis, which was significantly higher in progressors than controllers at proximal timepoints to diagnosis ($p=3.95x10^{-3}$). Therefore, cytokine responses by NK cells in peripheral blood stimulated with secreted *Mtb* peptides were lower at timepoints far from diagnosis but increased significantly with time to diagnosis in those who progressed to TB, compared to those who controlled *Mtb* infection.

Typically, NK cells do not directly detect peptide antigens. Therefore, the finding that NK cell cytokine responses were induced by peptide antigens suggests a bystander activation mechanism through secretion of cytokines by accessory cells, such as activated T cells. This was supported by findings in the ACS dataset, that showed frequencies of secreted *Mtb* peptide-specific cytokine-expressing NK cells were significantly associated with frequencies of secreted *Mtb* peptide-specific IL-2 expressing CD4 T cells ($p=3.07x10^{-10}$, Figure 3.5c). Frequencies of total cytokine-expressing NK cells were summed over IL-22^{+}, TNF^{+}, and/or IFN-γ^{+} cells. This effect was *Mtb*-specific, as there was no significant association with EBV/CMV peptides ($p>0.05$, Figure 3.5c).

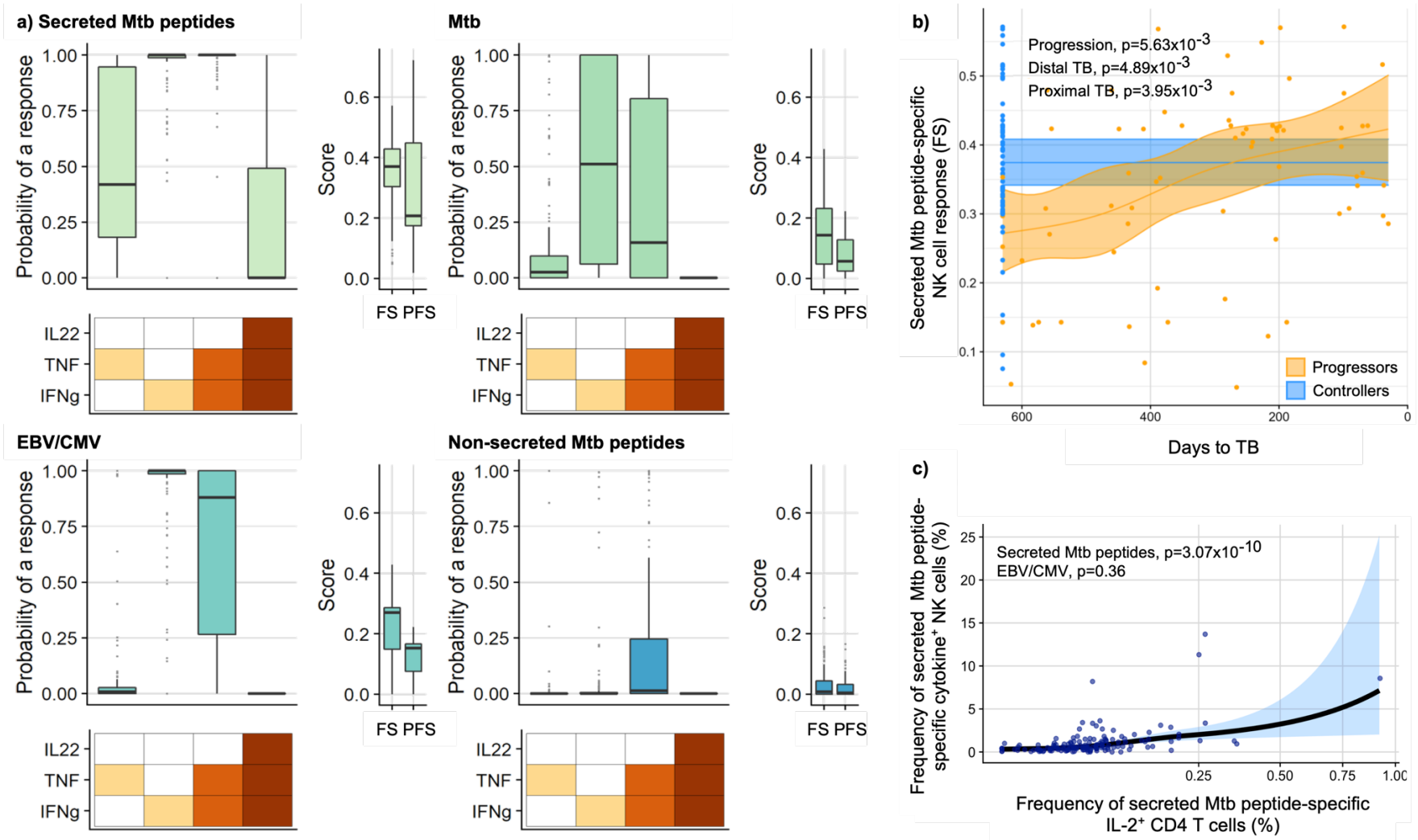

Figure 3.5: Antigen-specific NK cell cytokine responses in ACS progressors and controllers. a) COMPASS scores for NK cell cytokine responses in PBMC stimulated with secreted *Mtb* peptides, non-secreted *Mtb* peptides, live *Mtb* auxotroph and immunodominant EBV/CVM peptides (positive control). Plotted COMPASS results show probability of responses with different combinations of cytokines produced by NK cells (IL-22, TNF, and IFN-γ), and functionality scores (FS) and polyfunctionality scores (PFS). b) Secreted *Mtb* peptide-specific NK cell FS was modelled using Miguel Rodo's longitudinal mixed model to evaluate the progression effect and/or a time-to-TB effect in ACS progressors (orange) and controllers (blue). c) Frequencies of secreted *Mtb* peptide-specific cytokine-expressing NK cells (summed over IL-22$^+$, TNF$^+$, and/or IFN-γ^+ cells) modelled against frequencies of secreted *Mtb* peptide-specific IL-2-expressing CD4 T cells.

To further investigate NK cell functional alterations via bystander activation, a cytokine neutralization assay was designed and optimized to investigate NK cell cytokine production and cytotoxic potential in TB patients and healthy, *Mtb*-sensitized controls. These findings are discussed in the sections to follow.

3.3.3 Frequencies of peripheral NK cells are similar in TB patients and QFT^{+} controls

Based on findings from research at SATVI (Chowdhury et al., 2018; Scriba et al., 2017), it was hypothesized that NK cell frequencies were lower in TB patients relative to QFT^{+} controls (Figure 3.6).

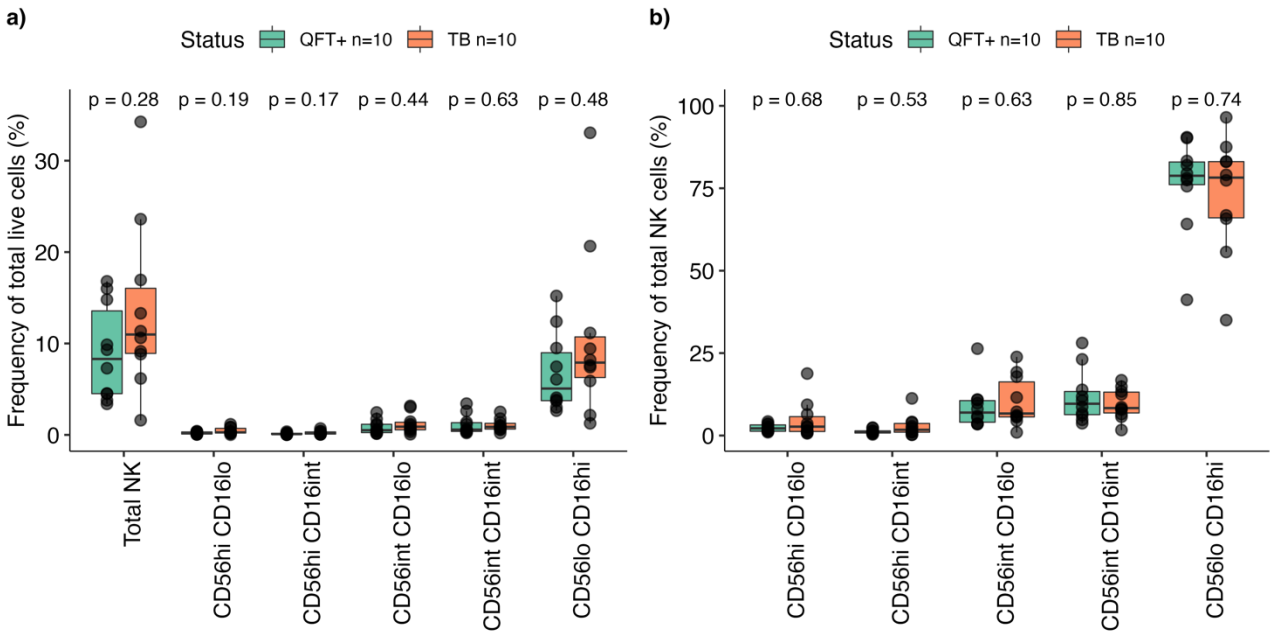

Figure 3.6: Frequencies of peripheral NK cells in TB and healthy, *Mtb*-sensitized controls. Frequencies of unstimulated NK cells shown as a proportion of a) total live cells, and b) total NK cells. Mann-Whitney, unpaired, non-parametric T-test was used to compare TB (n=10) vs QFT^{+} (n=10).

Consistent with published literature, the total NK population comprised ~10-15% of total live cells in the peripheral blood (Figure 3.6a). Within the total NK population, the CD56^{lo}CD16^{hi} subset was the most predominant subset, comprising ~85% of total NK cells (Figure 3.6b), as expected. No significant differences (p>0.05) were observed for frequencies of total NK

cells or NK subsets between TB patients and healthy, QFT^+ controls (Figure 3.6). Frequencies of total NK cells from the ACS dataset were also not associated with progression and no significant differences were observed between progressors and controllers within 2 years of follow-up (p=0.16, determined by Rodo's mixed effects longitudinal model, data not shown).

3.3.4 Cytokine neutralization assay optimization

To optimize the flow cytometry cytokine blocking assay, *in vitro* stimulation time was first investigated to determine how long PBMC needed to be stimulated to detect the highest cytokine response from NK cells. Two timepoints were investigated: 6 and 18 hours, with PHA as the positive control. The rationale for using PHA was due to its strong induction of T cells, which in turn, triggers NK cell activation. Since NK cell activation via the bystander pathway was the primary focus of this investigation, PHA was thought a suitable control. Results indicated that 6-hour stimulation induced low frequencies of cytokine-expressing NK cells, while 18-hour stimulation generated the highest frequencies of IFN-γ- and TNF-expressing NK and T cells (Figure 3.7a). Therefore, 18 hours was chosen as the stimulation timepoint.

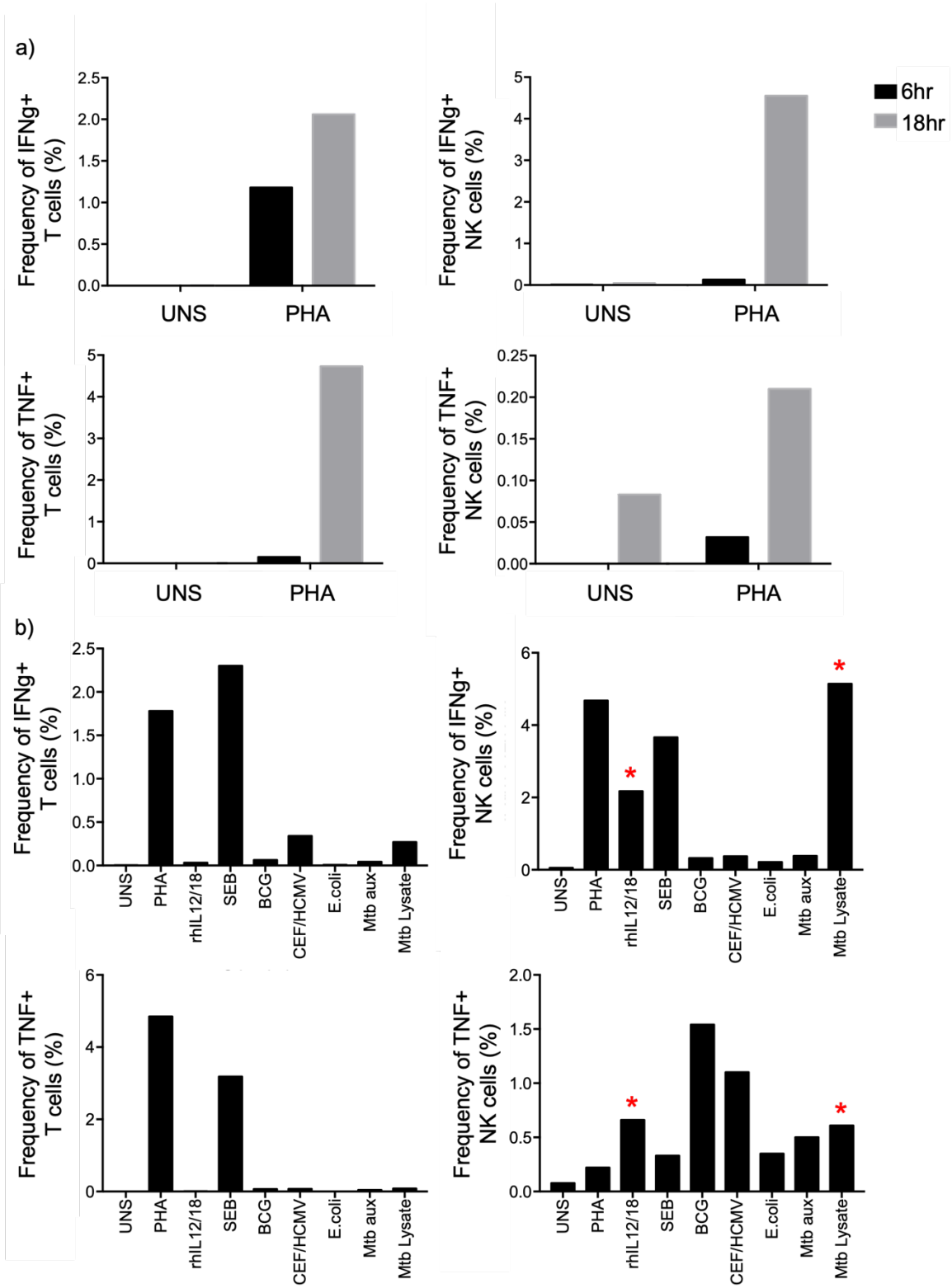

Figure 3.7: Bar graphs showing frequencies of IFN-γ- and TNF-expressing T cells and NK cells for optimizing PBMC stimulation times and antigens for PBMC stimulation. a) T cell and NK cell cytokine responses in PHA-stimulated PBMC, comparing 6-hour and 18-hour timepoints (n=1). b) T cell and NK cell cytokine responses in PBMC stimulated for 18 hours, comparing various stimulation conditions (n=1). Stimulation conditions generating the highest frequencies of IFN-γ- and TNF-expressing NK cells were used for further investigation (indicated by red asterisk *), to be compared with the peptide pool of secreted *Mtb* antigens in question. UNS = unstimulated; PHA = phytohaemagglutinin; hr = hours; rhIL12/18 = recombinant human IL-12 and IL-18; SEB = staphylococcal enterotoxin B; BCG = Bacillus Calmette-Guérin; CEF/HCMV = Cytomegalovirus, Epstein-Barr Virus, Influenza Virus/Human Cytomegalovirus peptide pool; E. coli = *Escherichia coli;* Mtb aux = *Mycobacterium tuberculosis* auxotroph.

The primary aim of the cytokine neutralization assay was to evaluate bystander-induced NK cell responses in PBMC stimulated with the peptide pool of secreted *Mtb* antigens that was associated with progression in the ACS dataset (Figure 3.5b) and associated with IL-2-producting T cells (Figure 3.5c). In addition to secreted *Mtb* peptides, other control antigens were tested for inclusion in the neutralization assay, including myeloid-derived recombinant human cytokines (rhIL12/18), viral peptides CEF/HCMV (a peptide pool comprising a mixture of peptides from cytomegalovirus, Epstein-Barr virus, influenza virus, and human cytomegalovirus), bacterial *Escherichia coli,* and staphylococcus enterotoxin B (SEB). Mycobacterial antigens were also investigated, including BCG (a close relative of *Mtb*), live *Mtb* auxotroph (also investigated in the ACS dataset), and whole *Mtb* lysate. Stimulation conditions for inclusion in the assay were chosen based on the ability of the antigens to induce TNF and IFN-γ responses by NK cells in stimulated PBMC. Therefore, *in vitro* stimulation of PBMC with rhIL-12/18 and *Mtb* lysate for 18 hours were selected as these antigens appeared to induce the highest balance of both TNF- and IFN-γ-producing NK cells (Figure 3.7).

The flow cytometry panel for the cytokine neutralization assay was previously designed and optimized by members at SATVI as a routinely used in-house ICS assay. However, CD33 and perforin antibodies were added as additional markers to this panel and therefore, required titration to determine optimal staining. Optimal antibody titers were determined using standard flow cytometry techniques of staining index (Equation 2) and separation dot plots (Figure 3.8a).

$$\text{Staining index} = (\text{MFI positive} - \text{MFI negative}) / (\text{standard deviation negative} \times 2)$$

Equation 2: Mathematical procedure to determine staining index of titrated antibodies in flow cytometry data. MFI = median fluorescence intensity.

Lastly, Brefeldin A is a standard reagent used to inhibit protein trafficking and detect intracellular cytokines by ICS. However, monensin (with a slightly different mode of action) is sometimes used in conjunction with brefeldin A to obtain optimal detection of intracellular cytokines. Briefly, monensin is an inhibitor of trans-Golgi function (Mollenhauer et al., 1990), while brefeldin A inhibits protein transport between the endoplasmic reticulum (ER) and the Golgi apparatus (Klausner et al., 1992). To test whether monensin should be used in conjunction with brefeldin A, PBMC were stimulated with rhIL-12/18, *Mtb* lysate and the peptide pool of secreted *Mtb* antigens for 18 hours in the presence of brefeldin A, with or without monensin. Results showed that there was no significant difference between background-subtracted frequencies of IFN-γ- and TNF-expressing NK cells, or perforin and granzyme B expression (fold-change MFI above unstimulated conditions) with and without monensin (Figure 3.8b). Therefore, monensin was not included in the assay.

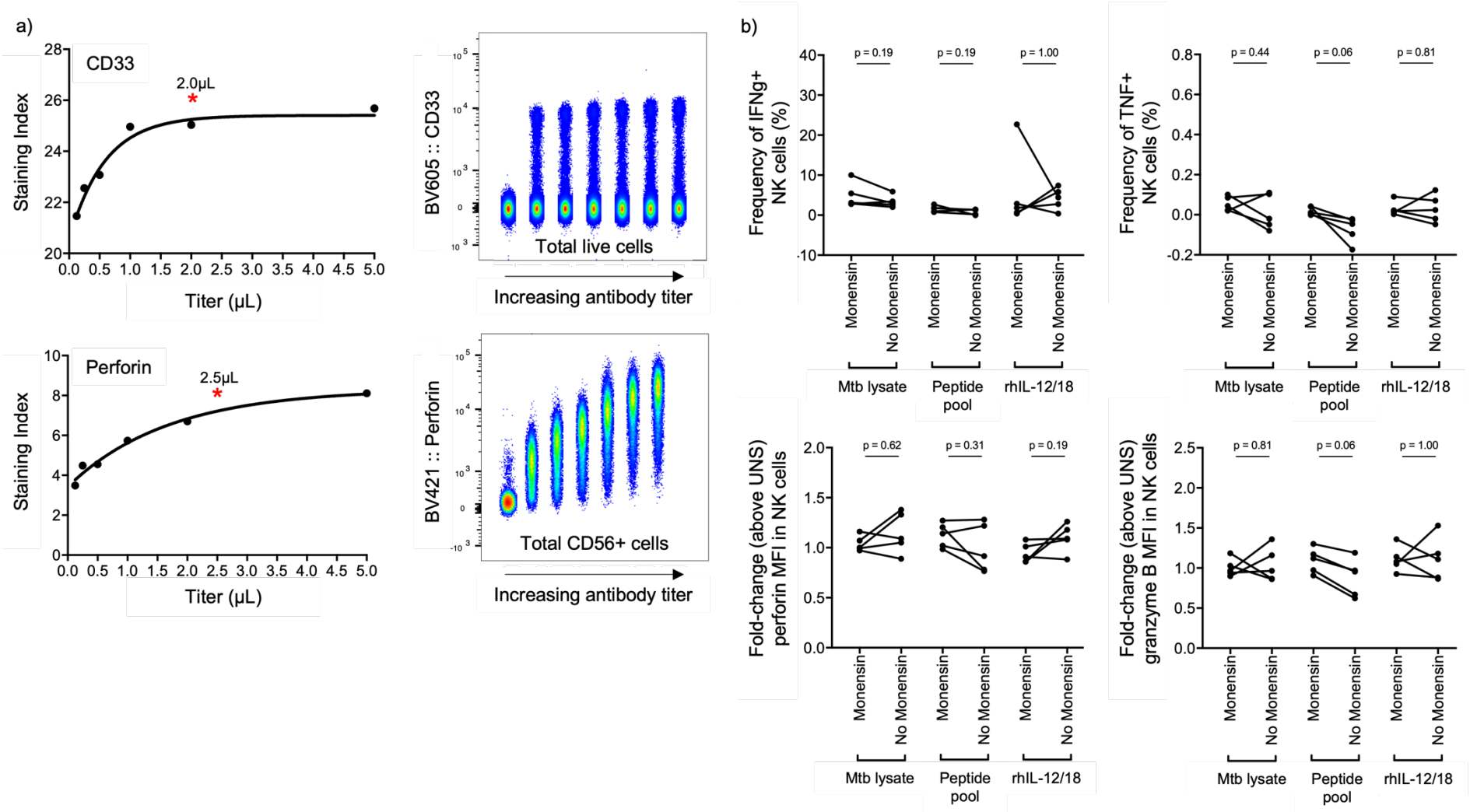

Figure 3.8: Flow cytometry antibody titrations and monensin investigation for optimized detection of NK cell responses. a) Staining index and scatter plots for titrated CD33 and perforin antibodies. Optimal titer for each antibody indicated by red asterisk (*). Titrations performed on unstimulated cells. CD33 staining shown on total live cells, and perforin staining shown for $CD56^{+}$ NK cells. b) Frequencies of IFN-γ- and TNF-expressing NK cells, and perforin and granzyme B expression in PBMC stimulated with rhIL-12/18, *Mtb* lysate and the secreted *Mtb* peptides for 18 hours in the presence of brefeldin A, with or without monensin (n=5). Frequencies of unstimulated controls were background subtracted from cytokine-producing cells. Perforin and granzyme B expression reported in terms of median fluorescence intensity (MFI), which were normalized by determining a fold-change value above the unstimulated control. Wilcoxon, paired, non-parametric T-test was used to compare conditions of monensin versus no monsenin.

3.3.5 Blocking myeloid or T cell cytokines inhibits NK cell IFN-γ responses in PBMC stimulated with *Mtb* antigens

Previous literature has shown that NK cells produce cytokines in response to recombinant cytokine stimulation (including rhIL-12, rhIL-18 and rhIL-2) and whole blood stimulated with BCG (a close relative of *Mtb*) (Horowitz et al., 2010b; Suliman et al., 2016). It was therefore hypothesized that PBMC stimulated with cytokines or *Mtb* antigens will increase IFN-γ and TNF production in $NK_{regulatory}$ ($CD56^{hi}CD16^{lo}$) cells above unstimulated cells (Figure 3.9). As hypothesized, *Mtb* antigens and cytokine stimulation in peripheral blood successfully induced IFN-γ-producing $NK_{regulatory}$ cells significantly above background levels ($p<0.05$ and $q<0.05$; Figure 3.9a). Although statistically significant, frequencies of TNF- and polyfunctional IFN-γ^{+}TNF^{+}-producing $NK_{regulatory}$ cells above background levels were slight (Figure 3.9b and c).

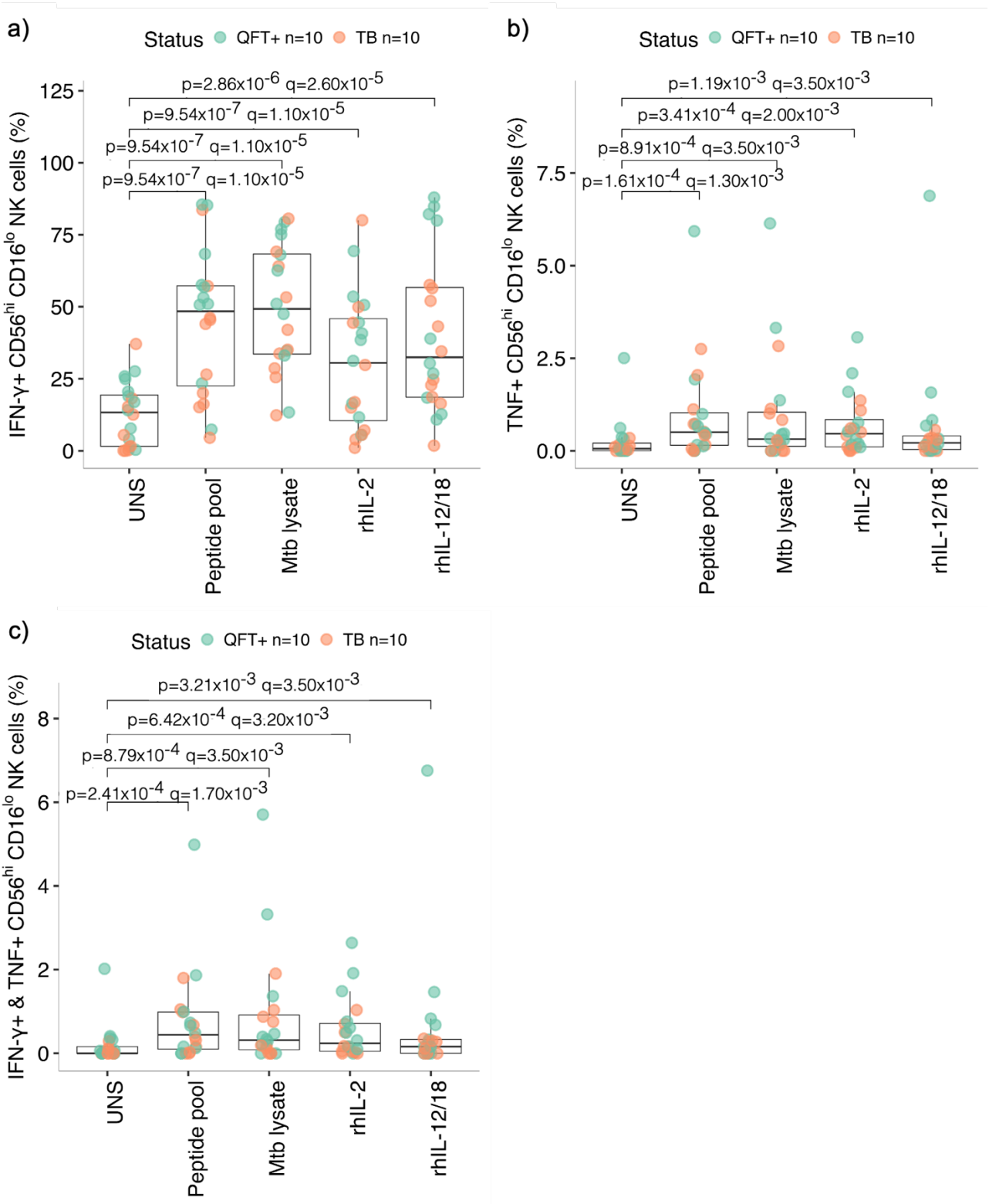

Figure 3.9: NK cell cytokine responses to recombinant cytokine stimulation and *Mtb* antigens. Increased frequencies of a) IFN-γ-, b) TNF- and c) polyfunctional IFN-γ^{+}TNF^{+}-producing $NK_{regulatory}$ $CD56^{hi}CD16^{lo}$ cells above background levels (unstimulated, UNS) upon stimulation (total n=20; TB n=10; QFT^{+} n=10). One-sided Wilcoxon, paired, non-parametric T-test was used to compare stimulation conditions with unstimulated control as the reference group. The Holm-Bonferroni test was used to correct for multiple comparisons (q-values).

Since *Mtb*-specific NK cell responses in PBMC of ACS participants were significantly higher at proximal timepoints to TB diagnosis in progressors relative to controllers (Figure 3.5b), it was hypothesized that NK cell cytokine responses would also be higher in recently diagnosed TB patients, relative to healthy *Mtb*-sensitized controls. The rationale for this hypothesis is that heightened immune cell function during TB disease likely occurs due to high antigen load and inflammatory signals in the host may induce bystander activation of NK cells. Contrary to the hypothesis, NK IFN-γ responses in PBMC stimulated with *Mtb* antigens were similar between TB patients and healthy controls (p>0.05; Figure 3.10). Frequencies of TNF- and polyfunctional IFN-γ^{+}TNF^{+}-producing NK cells were also investigated, with no significant findings (data not shown).

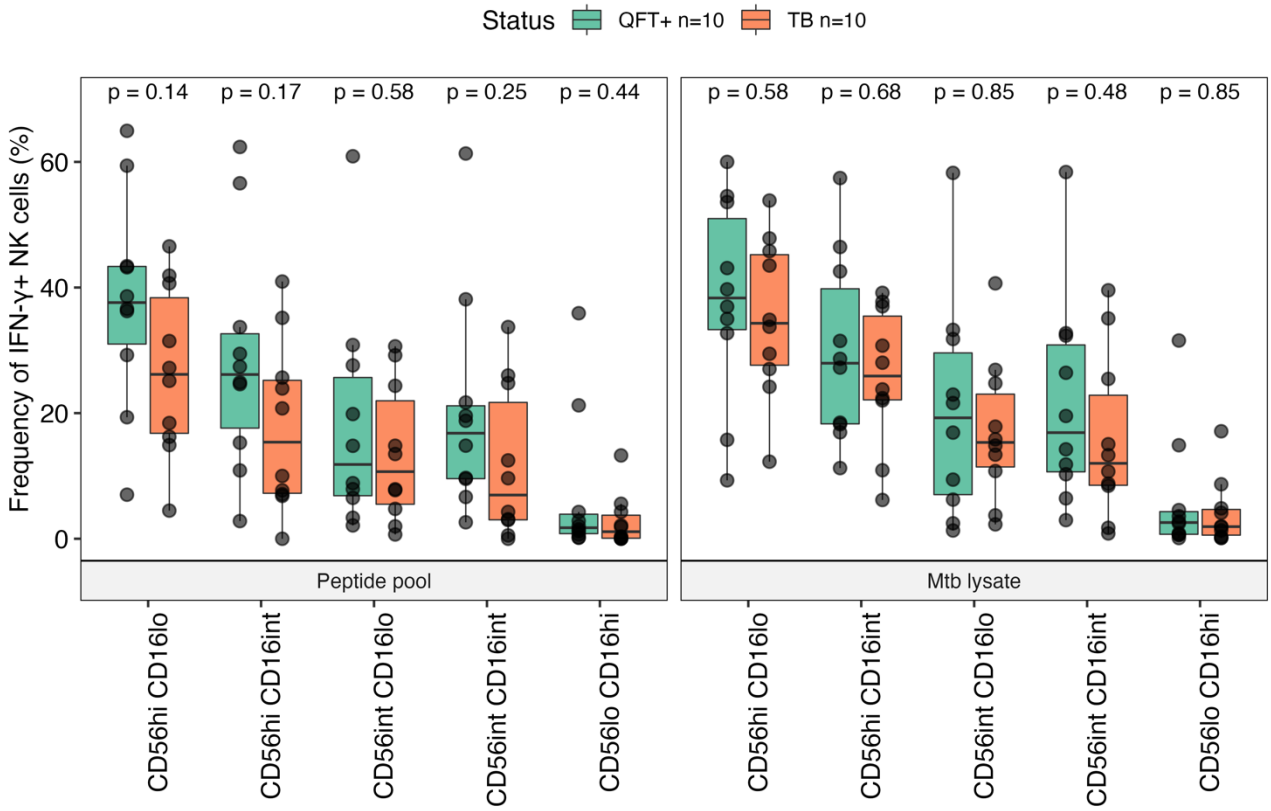

Figure 3.10: Frequencies of IFN-γ-producing NK cells in PBMC stimulated with *Mtb* antigens, comparing TB vs QFT^{+}. Mann-Whitney, unpaired, non-parametric T-test was used to compare TB (n=10) vs QFT^{+} (n=10). Frequencies of unstimulated controls were background subtracted from cytokine-producing cells.

To confirm that cytokine blocking resulted in lower IFN-γ production by NK cells, PBMC were stimulated with recombinant human cytokines in the presence of matched blocking antibodies. It was hypothesized that blocking with αIL-12/18 and αIL-2 would reduce NK IFN-γ responses to recombinant cytokines, rhIL-12/18 and rhIL-2, respectively in $NK_{regulatory}$ cells (Figure 3.11).

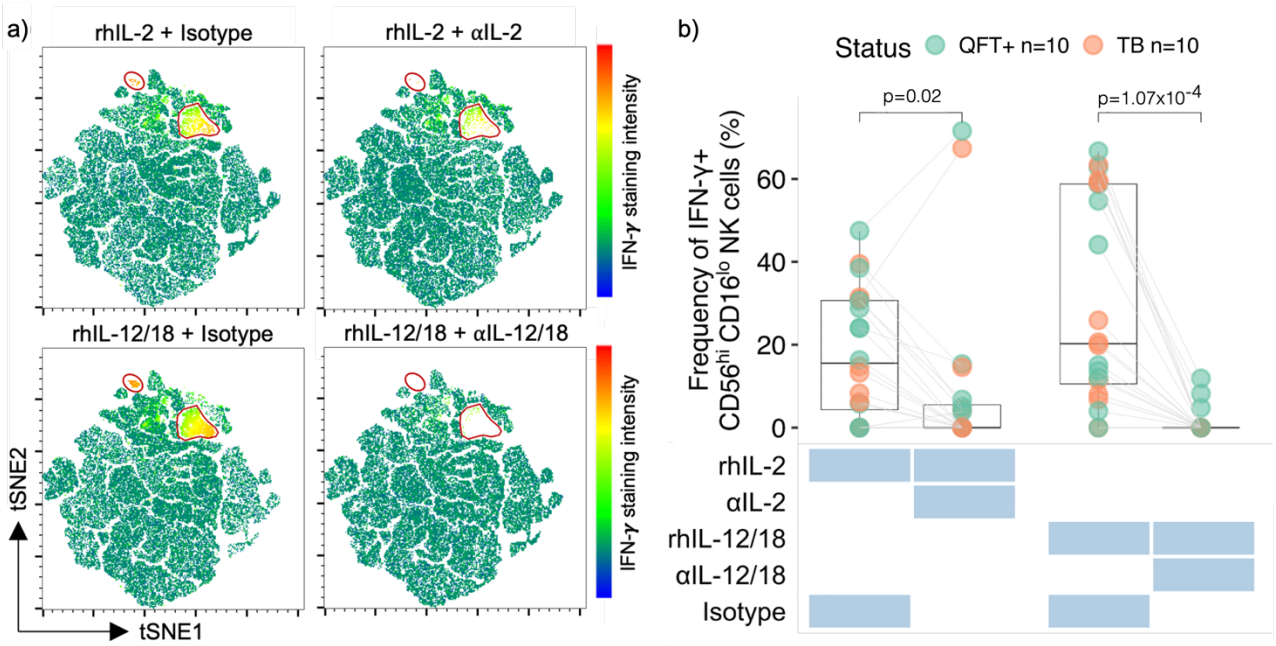

Figure 3.11: The effect of cytokine neutralization on NK cell IFN-γ responses in PBMC stimulated with recombinant human cytokines. a) tSNE map and b) frequencies of IFN-γ-expressing $NK_{regulatory}$ $CD56^{hi}CD16^{lo}$ cells in response to recombinant human cytokine stimulation (rhIL-2 and rhIL-12/18) with or without cytokine neutralizing antibodies (αIL-2 and αIL-12/18). One-sided Wilcoxon, paired, non-parametric T-test was used to compare isotype control (total n=20; TB n=10, QFT^+ n=10) vs blocking (total n=20; TB n=10, QFT^+ n=10) conditions (b). Frequencies of unstimulated controls were background subtracted from cytokine-producing cells. Phenotypic islands outlined in red on the tSNE map correspond to populations of IFN-γ-producing NK cells (a).

Dimensionality reduction by tSNE was performed on ~240 000 NK cells (no down-sampling performed) from a single representative donor to demonstrate blocking-induced reduction in NK cytokine production (Figure 3.11a). Populations of IFN-γ-producing NK cells were identified based on their relative staining (fluorescence) intensity of this marker (phenotypic islands outlined in red; Figure 3.11a). Treatment with neutralizing antibodies (rhIL-2 + αIL-2; and rhIL-12/18 + αIL-12/18) reduced the expression of IFN-γ compared to isotype

controls, detected by absence of the IFN-γ^+ phenotypic islands. Qualitative results of tSNE dimensionality reduction were confirmed by quantitative manual gating and statistical significance (Figure 3.11b). Together, these findings demonstrated a significant reduction in the IFN-γ response mediated by neutralizing antibodies, even in the presence of their matched recombinant cytokines. Therefore, the cytokine neutralization assay was considered successful.

Previous data has shown that recombinant cytokines (IL-12, IL-18 and IL-2) were required to optimally activate NK cells in blood stimulated with BCG, and cytokine neutralization with αIL-2, αIL-12 and αIL-18 antibodies diminished BCG-specific NK cell IFN-γ responses (Suliman et al., 2016). It was thus hypothesized that blocking with αIL-12/18 and αIL-2 antibodies will significantly decrease NK cytokine responses to *Mtb* antigens in terms of IFN-γ, TNF and polyfunctionality (Figure 3.12).

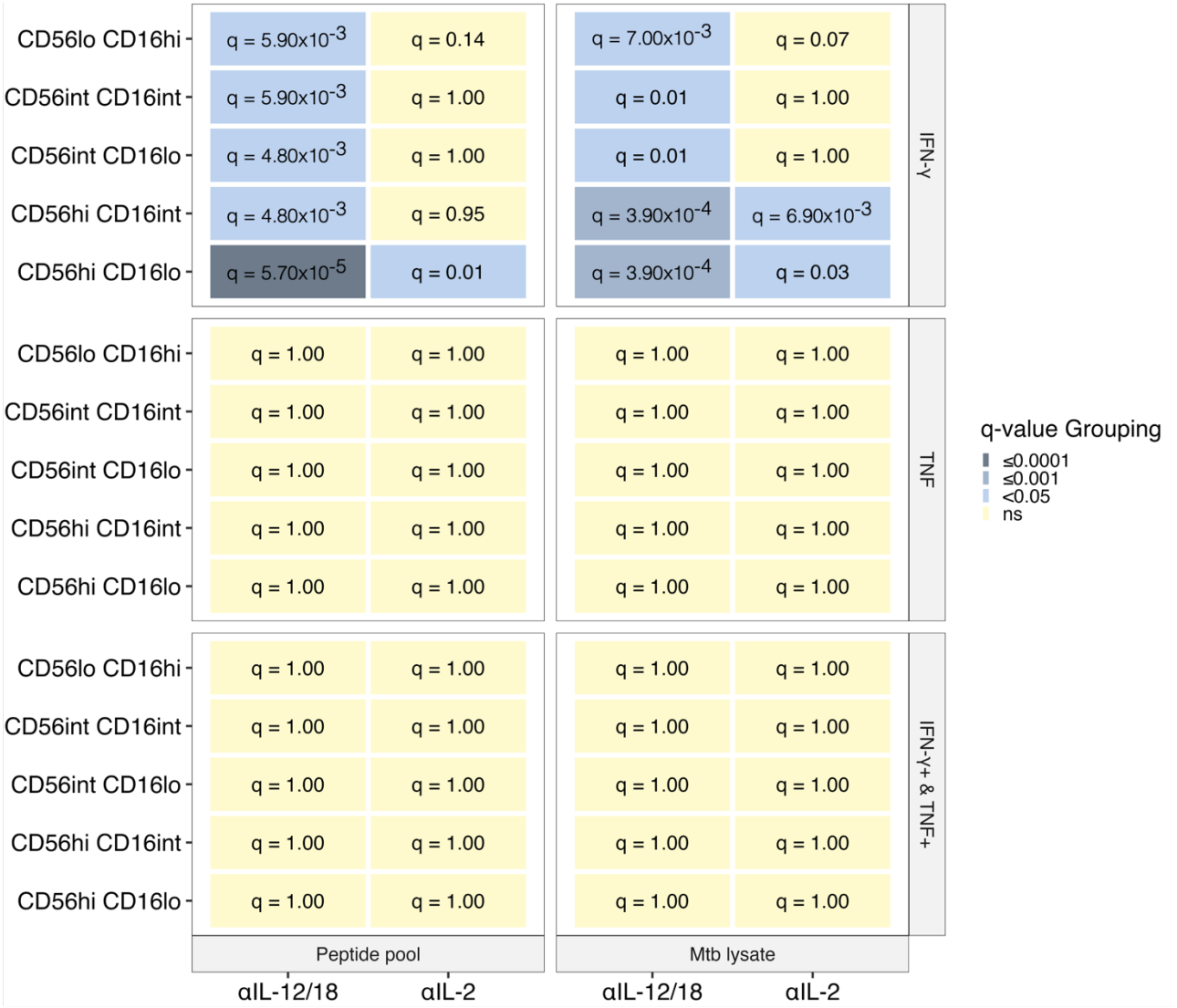

Figure 3.12: Heatmap summarising significance in reduction of NK cytokine responses upon blocking with αIL-12/18 and αIL-2 antibodies, relative to PBMC stimulation with *Mtb* antigens. One-sided Wilcoxon, paired, non-parametric T-test was used to compare isotype control vs blocking conditions (total n=20; TB n=10, QFT^+ n=10). The Holm-Bonferroni test was used to correct for multiple comparisons (q-values). Frequencies of unstimulated controls were background subtracted from cytokine-producing cells.

Neutralizing myeloid cytokines (IL-12 and IL-18) significantly reduced NK IFN-γ responses in PBMC stimulated with *Mtb* antigens (q<0.05) in all NK cell subsets (Figure 3.12). Blocking with T cell αIL-2 neutralizing antibodies significantly reduced the IFN-γ response to *Mtb* antigens in $CD56^{hi}CD16^{lo}$ cells (q<0.05), and the IFN-γ response to *Mtb* lysate in $CD56^{hi}CD16^{int}$ cells only (q<0.05). With regards to the single-positive TNF and polyfunctional ($IFN\text{-}\gamma^+TNF^+$) responses to blocking, there were no significant reductions

observed across NK cell subsets and conditions (q>0.05; Figure 3.12). Together, results suggest that myeloid IL-12/18 production upon *Mtb* antigen stimulation mediates IFN-γ responses in all NK cell subsets, while T cell IL-2 particularly mediates IFN-γ responses in the $CD56^{hi}CD16^{lo}$subset.

3.3.6 NK cell IFN-γ responses depend more on myeloid cytokines than T cell cytokines during bystander activation responses to *Mtb* antigens

To estimate the effect of cytokine-neutralisation on NK cell IFN-γ expression when PBMC were stimulated with *Mtb* antigens, the difference (or change) in response was calculated upon blocking. The magnitude of the blocking effect for an isotype control/neutralizing antibody pair was calculated using the relative change (Δ) in response by determining the difference in response upon blocking (i.e., Δ response = isotype – blocking; Figure 3.13). A higher Δ response therefore represents greater blocking-mediated suppression of NK function.

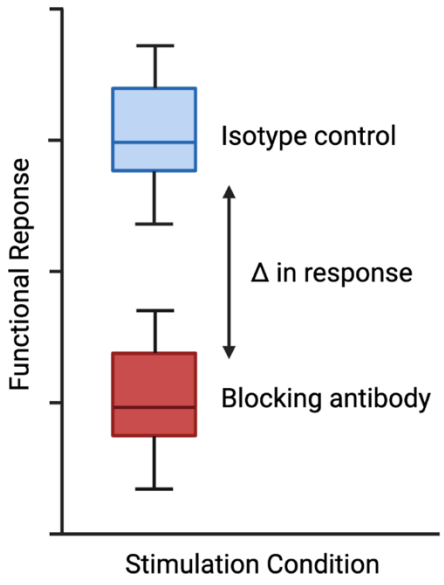

Figure 3.13: Graphical demonstration for calculating the magnitude of effect of cytokine neutralization. The relative change in response was calculated by subtracting response of a blocking condition from the isotype control under a given stimulation condition. Δ = change.

The difference (or change) in response was compared between αIL-12/18 and αIL-2 to determine which cytokine neutralization conditions resulted in a greater suppression of NK function. It was hypothesized that NK cell responses would be suppressed more by blocking T cell-associated IL-2 than myeloid-associated IL-12/IL-18 when PBMC were stimulated with *Mtb* lysate and *Mtb* peptides, in all NK cell subsets (Figure 3.14).

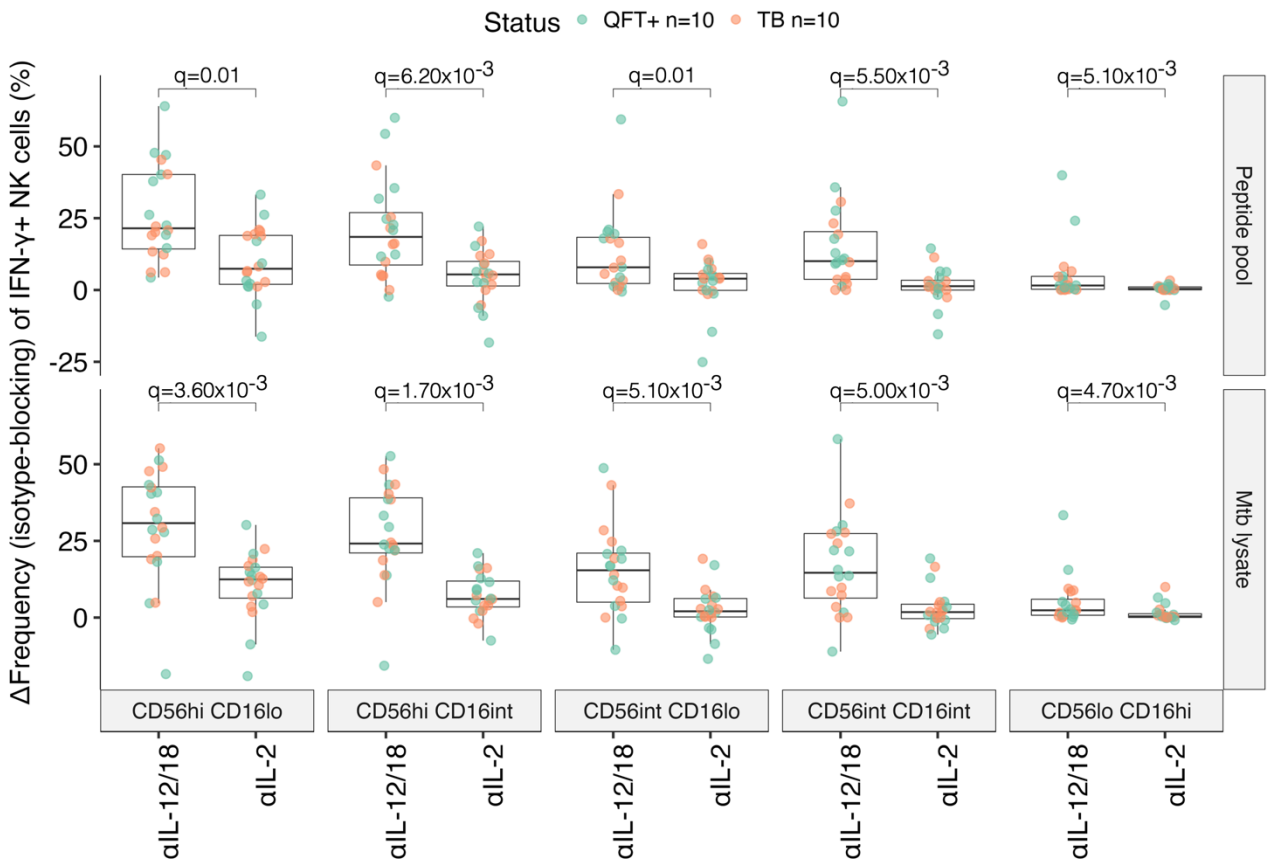

Figure 3.14: Change in frequency of *Mtb*-specific, IFN-γ-expressing NK cells upon blocking, comparing effects of neutralizing antibodies (αIL-2 vs αIL-12/18). Wilcoxon, paired, non-parametric T-test was used to compare blocking conditions (total n=20, TB n=10, QFT^{+} n=10). The Holm-Bonferroni test was used to correct for multiple comparisons (q-values). Frequencies of unstimulated controls were background subtracted from cytokine-producing cells.

For all NK cell subsets, inhibition of IFN-γ production was significantly more pronounced ($p<0.05$ and $q<0.05$) when blocking with αIL-12/18 compared to αIL-2 blocking (Figure 3.14). These findings were contrary to the hypothesis. Notably, blocking with αIL-12/18 and αIL-2 inhibited cytokine-dependent IFN-γ responses equally in TB patients and controls

(Figure 3.15), indicating no differences in the magnitude of blocking effects between cohorts. Additionally, diminished IFN-γ responses upon blocking were similar between *Mtb* stimulation conditions (Figure 3.16); thus, the outcome of blocking in terms of magnitude of response reduction, was the same for *Mtb* lysate versus *Mtb* peptide stimulation. Measures of TNF production and polyfunctionality (IFN-γ^{+}TNF^{+}) were also included in these analyses and no significant findings were observed (data not shown).

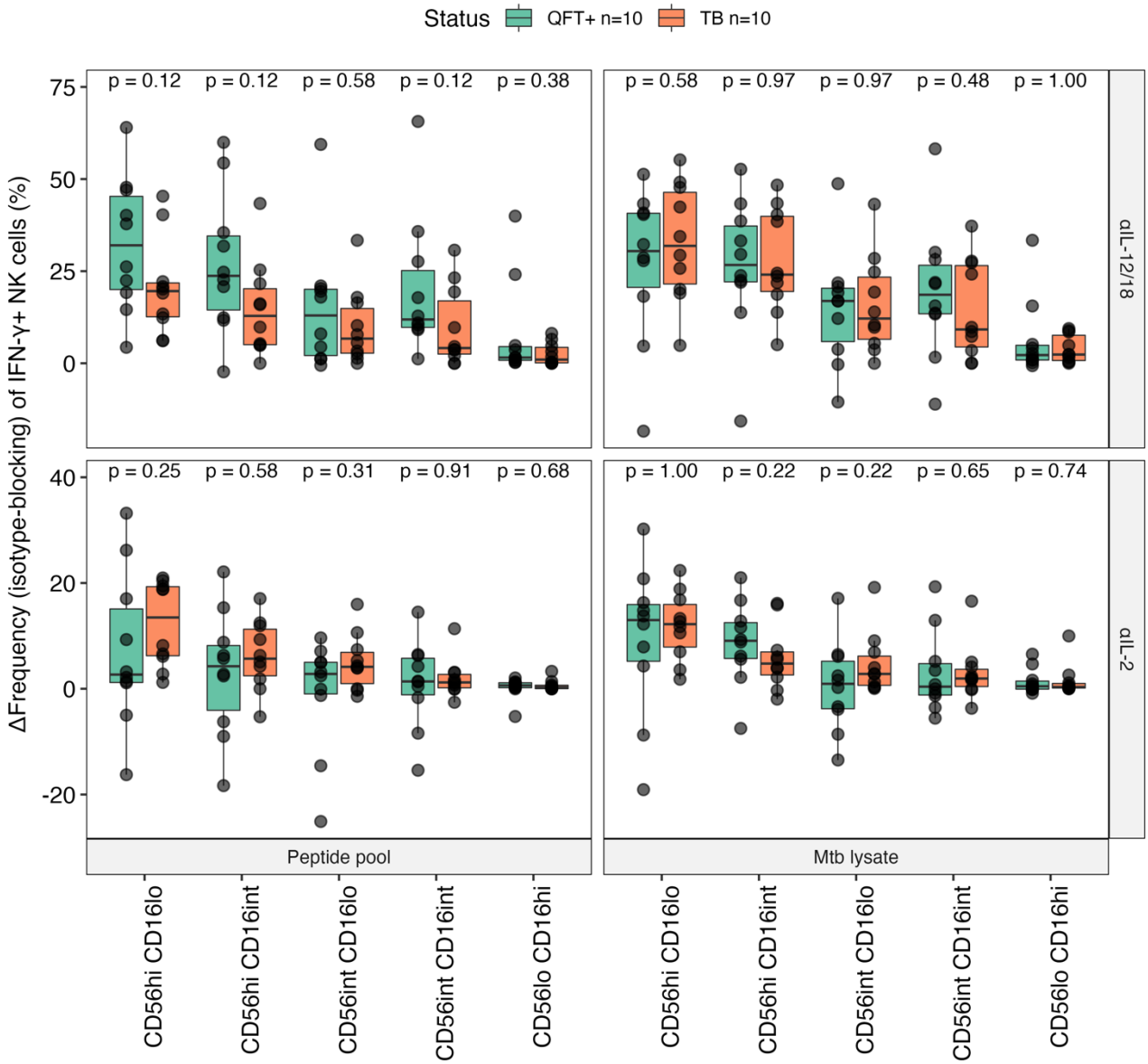

Figure 3.15: Blocking-mediated changes in frequencies of IFN-γ-expressing NK cells, comparing responses between TB and QFT^{+} participants. Mann-Whitney, unpaired, non-parametric T-test was used to compare TB (n=10) vs QFT^{+} (n=10). Frequencies of unstimulated controls were background subtracted from cytokine-producing cells.

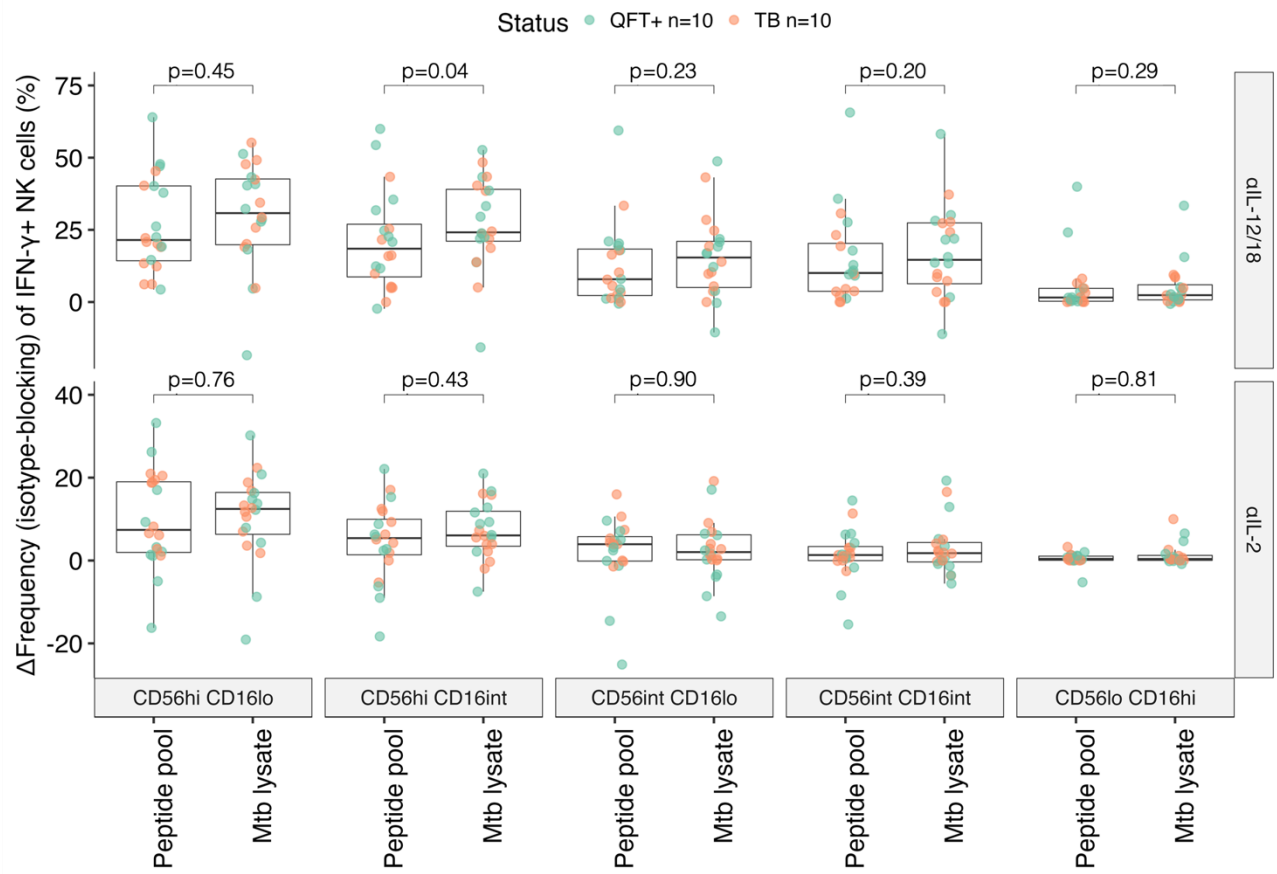

Figure 3.16: Change in frequency of IFN-γ-expressing cells upon blocking with neutralizing antibodies (αIL-2 and αIL-12/18), comparing responses between stimulation conditions with *Mtb* antigens. Wilcoxon, paired, non-parametric T-test was used to compare stimualtion conditions (total n=20, TB n=10, QFT^+ n=10). Frequencies of unstimulated controls were background subtracted from cytokine-producing cells.

3.3.7 Blocking-mediated inhibition of IFN-γ production affects NK cell subsets differently

NK cells are a highly heterogenous population, comprising multiple subsets with unique receptor expression profiles and responsiveness to stimuli. To demonstrate subset-specific responsiveness to bystander cytokine activation, the magnitude of suppressed NK cell responses upon blocking were compared between subsets. It was hypothesized that blocking IL-2 would suppress functional responses to a greater degree in the $CD56^{hi}$ subset than in $CD56^{lo}$ NK cells (Figure 3.17). The rationale for this hypothesis was based on $CD56^{hi}$ cells expressing higher affinity IL-2 receptors that are likely to experience greater changes to functional responses upon binding and subsequent blocking of their ligands.

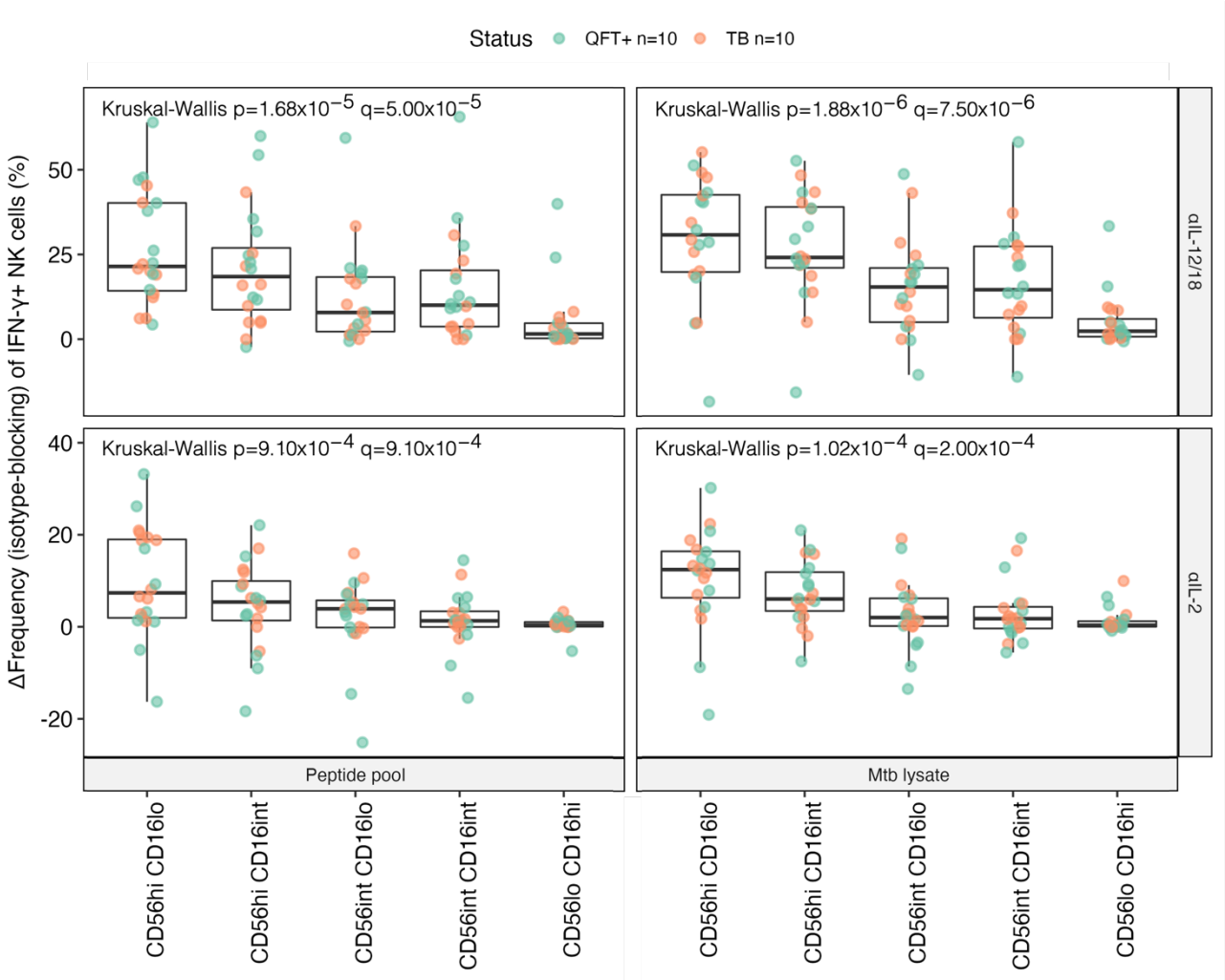

Figure 3.17: Change in frequency of IFN-γ-expressing NK cells upon blocking with neutralizing antibodies (αIL-2 and αIL-12/18), comparing responses between NK cell subsets. Kruskal-Wallis, paired, non-parametric analysis of variance (ANOVA) was used to compare NK cell subsets (total n=20, TB n=10, QFT^+ n=10). The Holm-Bonferroni test was used to correct for multiple comparisons. Frequencies of unstimulated controls were background subtracted from cytokine-producing cells.

Blocking-mediated suppression of IFN-γ production was significantly different between NK cell subsets ($q<0.05$, Figure 3.17), suggesting that changes in the cytokine milieu affect NK cell subsets differently. No significant changes were observed for measures of TNF production and polyfunctionality (IFN-γ^+TNF$^+$) ($p>0.05$ and $q>0.05$; data not shown). Overall, cytokine blocking diminished IFN-γ production greatly in $NK_{regulatory}$ cells, with the magnitude of these effects decreasing along the spectrum towards the $NK_{cytotoxic}$ subset.

3.3.8 NK cell cytotoxic potential is greater in TB patients than QFT^+ controls

In previous sections, the effects of *Mtb* antigen stimulation and cytokine blocking were investigated in terms of NK cell cytokine responses in TB patients and healthy controls. A major aim of this investigation was to evaluate the cytotoxic alterations via bystander activation pathways, which has not yet been investigated in the context of TB.

The presence of *Mtb* antigens and progression to active disease induces a cascade of immune responses resulting in activation of NK cells and heightened cytokine production (Figures 3.5 and 3.7) (Bozzano et al., 2009; Feinberg et al., 2004; Gerosa et al., 2002). Therefore, it was hypothesized that stimulation with *Mtb* antigens will also increase cytotoxic potential in $NK_{cytotoxic}$ cells (Figure 3.18). Notably, NK cells harbour pre-formed granules containing cytotoxic molecules that are released to kill target cells upon activation. However, stimulation and NK cell activation also induces upregulated expression of intracellular cytotoxic molecules (Grossman et al., 2004; Nogusa et al., 2012; Judge et al., 2020; Choi et al., 2019). Therefore, increased cytotoxic potential of NK cells in this assay was demonstrated as upregulated expression of intracellular perforin and granzyme B, since NK cells were activated to produce more cytotoxic molecules.

PBMC stimulation with secreted *Mtb* peptides resulted in a positive shift in cytotoxic marker expression (MFI) in NK cells above background levels (Figure 3.18a). Although the effect was slight, the results were statistically significant for *Mtb* lysate and peptide pool stimulation in $NK_{cytotoxic}$ cells above background levels ($p<0.05$ and $q<0.05$, Figure 3.18b and c). Cytokine stimulation with rhIL-2 also significantly increased perforin and granzyme B expression above the unstimulated condition ($p<0.05$) in $NK_{cytotoxic}$ cells. However, rhIL-12/18 did not significantly increase perforin or granzyme B MFI above background levels ($p>=0.05$, Figure 3.18). Overall, these data suggest that *Mtb* antigens and T cell-associated

IL-2 upregulated cytotoxic responses, but myeloid cytokines were not strong inducers of cytotoxic responses in $NK_{cytotoxic}$ cells.

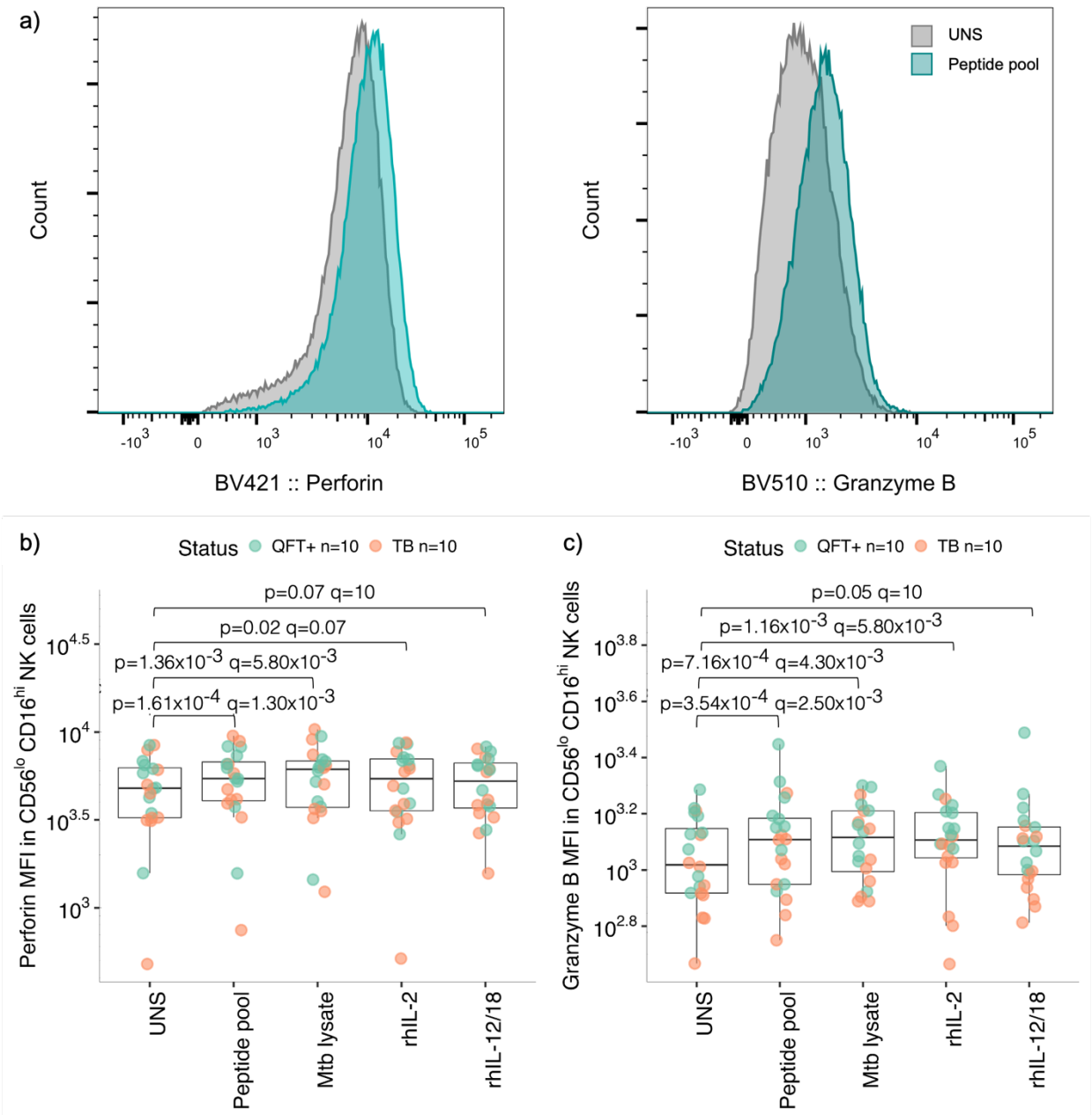

Figure 3.18: NK cell cytotoxic marker expression in in PBMC stimulated with *Mtb* antigens and recombinant cytokines. Increased expression of a) NK cell perforin (left) and granzyme B (right) in PBMC from a representative donor (n=1) stimulated with a peptide pool of secreted *Mtb* antigens (blue) relative to the unstimulated condition (UNS, grey). Increased expression of b) perforin and c) granzyme B in $NK_{cytotoxic}$ $CD56^{lo}CD16^{hi}$ cells above background levels. Cytotoxic molecule expression reported in terms of median staining intensity (MFI). Data on the y-axis were log10 transformed (b and c). One-sided Wilcoxon, paired, non-parametric T-test was used to compare stimulation conditions with unstimulated control as the reference group (total n=20; TB n=10, QFT^{+} n=10). The Holm-Bonferroni test was used to correct for multiple comparisons (q-values).

Differences in NK cell function between health and TB disease was evaluated in terms of cytokine production in Figures 3.5 and 3.8. However, it was also of interest to evaluate differences in NK cell cytotoxic potential (perforin and granzyme B expression) in PBMC stimulated with *Mtb* antigens, which were hypothesized to be higher in TB patients relative to QFT^+ controls (Figure 3.19). As previously discussed, the rationale for this hypothesis was based on the TB inflammatory milieu activating NK cells via bystander pathways.

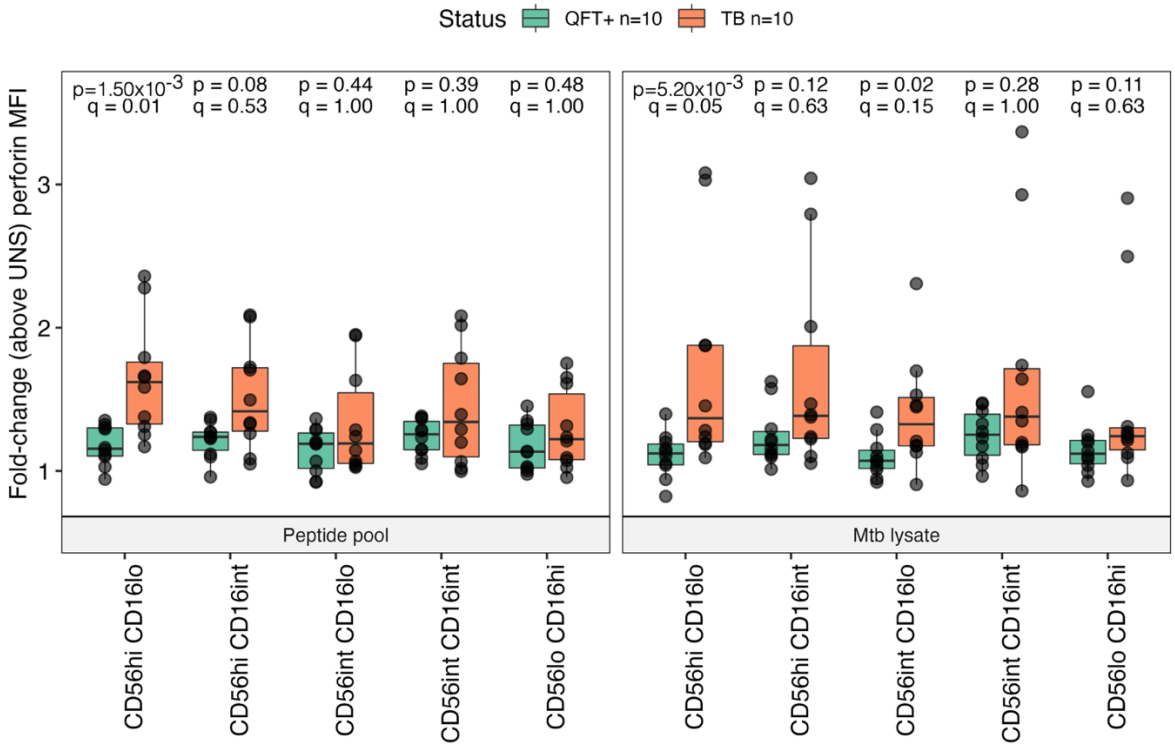

Figure 3.19: Fold-change perforin MFI in NK cells within PBMC stimulated with *Mtb* antigens, comparing TB vs QFT^+. Mann-Whitney, unpaired, non-parametric T-test was used to compare TB (n=10) vs QFT^+ (n=10). The Holm-Bonferroni test was used to correct for multiple comparisons (q-values). MFI values were normalized to account for background by determining a fold-change value above the unstimulated control. MFI = median fluorescence intensity.

Perforin expression in $NK_{regulatory}$ $CD56^{hi}CD16^{lo}$ cells was significantly higher in TB patients than healthy controls, in PBMC stimulated with secreted *Mtb* peptides ($p=1.5x10^{-3}$ and q=0.01) and *Mtb* lysate ($p=5.2x10^{-3}$ and q=0.03, Figure 3.19). Although not statistically significant (p>0.05 and q>0.05), perforin expression in remaining NK cell subsets appeared to be following the same trend. TB patients also tended towards higher granzyme B

expression compared to QFT^+ controls, although not of statistical significance ($p>0.05$ and $q>0.05$, Figure 3.20a). Importantly, these findings were specific to *Mtb* antigens, since significance were not observed when performing the same comparisons of cytotoxic molecule expression for recombinant cytokine data (rhIL-12/18 and rhIL-2, $p>0.05$ and $q>0.05$, Figure 3.20b). Together these results indicate that *Mtb*-specific NK cytotoxic potential, particularly perforin expression by $NK_{regulatory}$ cells, was higher in TB patients relative to healthy, *Mtb*-sensitized controls.

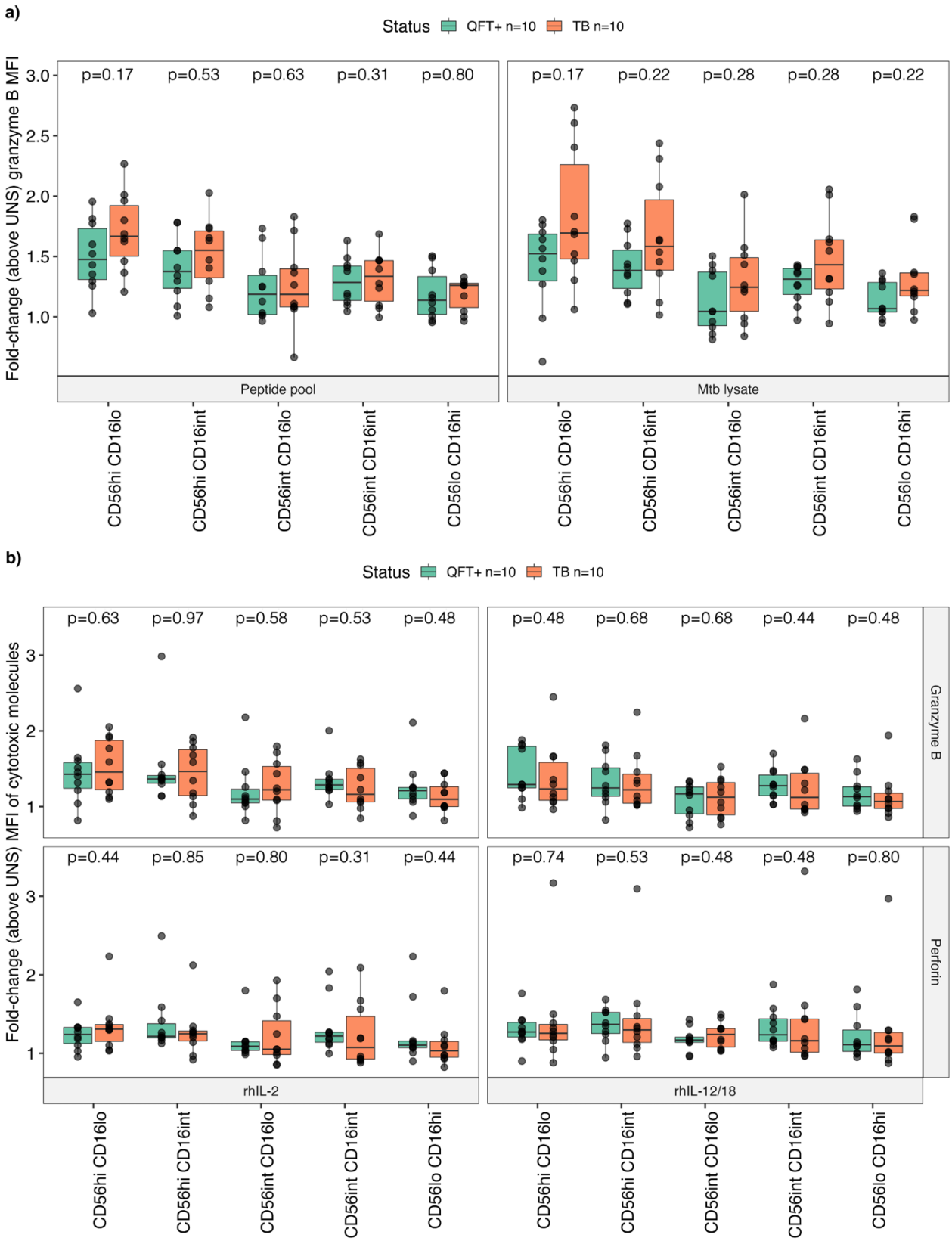

Figure 3.20: a) Granzyme B MFI in NK cells within PBMC stimulated with *Mtb* antigens, and b) MFI of cytotoxic molecules (perforin and granzyme B) in NK cells responding to control recombinant human cytokines, comparing TB vs QFT$^+$. Mann-Whitney, unpaired, non-parametric T-test was used to compare TB (n=10) vs QFT$^+$ (n=10). MFI values were normalized to account for background by determining a fold-change value above the unstimulated control. MFI = median fluorescence intensity.

3.3.9 αIL-2-mediated suppression of cytotoxic potential is more pronounced in TB patients compared to QFT$^+$ controls

Previously published data and results reported in Figures 3.6 and 3.7 showed that *Mtb*-specific IFN-γ expression by NK cells was dependent on cytokine activation. However, blocking with αIL-2 and αIL-12/18 did not significantly decrease the cytotoxic potential (perforin and granzyme B expression) in NK cells (Figure 3.21).

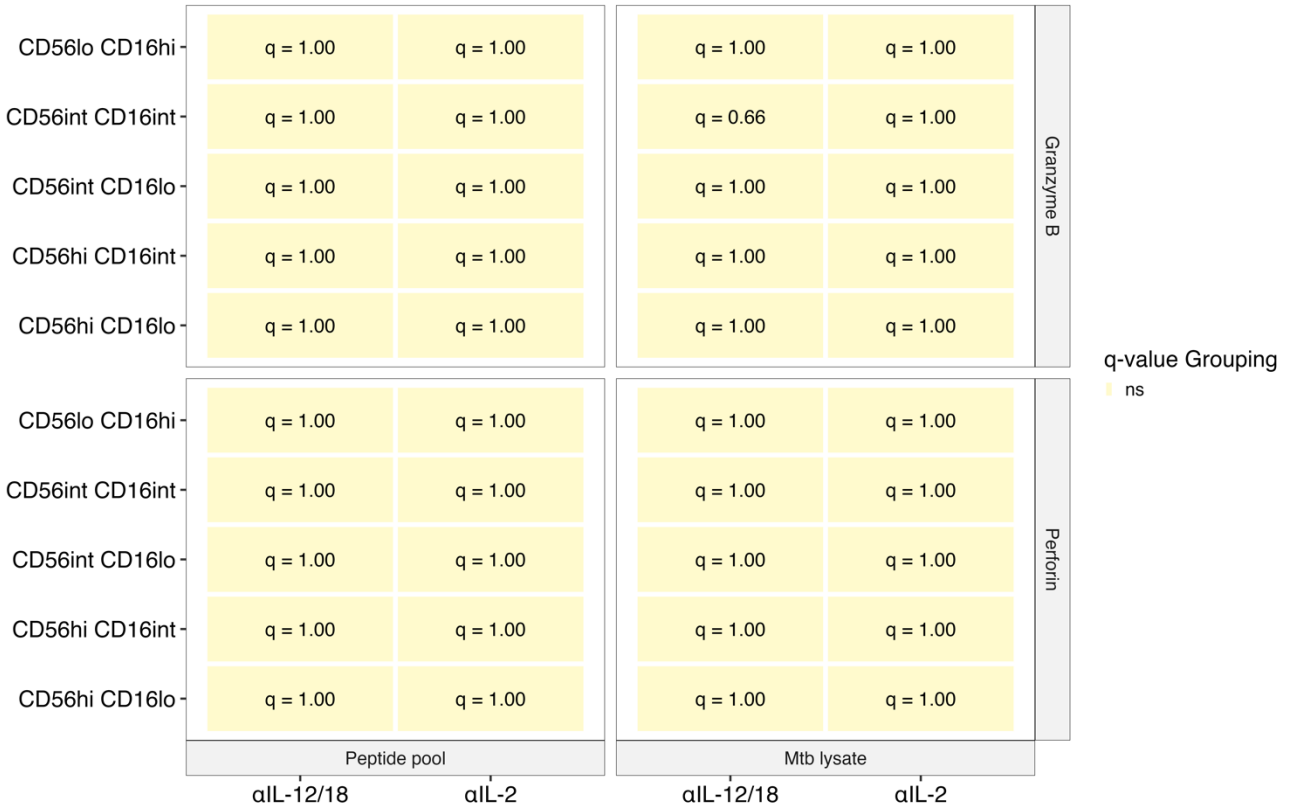

Figure 3.21: Heatmap summarising no significance in reduction of cytotoxic potential for NK cell subsets upon blocking with αIL-12/18 and αIL-2 neutralizing antibodies, relative to PBMC stimulation with *Mtb* antigens. Cytotoxic potential measured in terms of median fluorescence intensity (MFI) of perforin and granzyme B. One-sided Wilcoxon, paired, non-parametric T-test was used to compare isotype control vs blocking conditions (total n=20; TB n=10, QFT$^+$ n=10). The Holm-Bonferroni test was used to correct for multiple comparisons (q-values). MFI values were normalized to account for background by determining a fold-change value above the unstimulated controls.

The magnitude of blocking-induced decrease in cytotoxic potential (represented as a change in response; Figure 3.13) was then investigated in TB patients versus healthy controls (Figure 3.22).

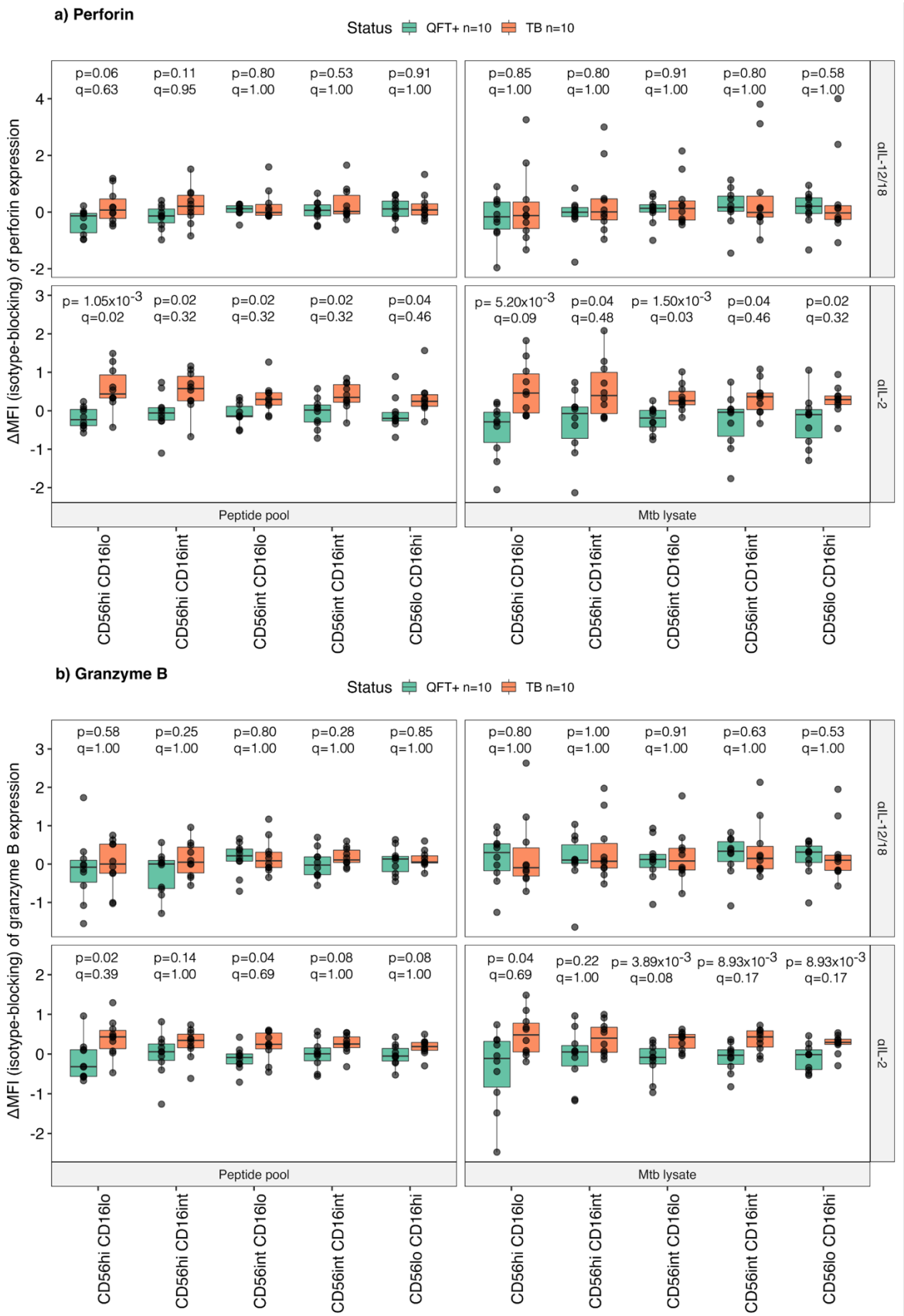

Figure 3.22: Blocking-mediated changes in expression of cytotoxic molecules by NK cells, comparing TB and QFT$^+$. The effect of cytokine neutralization on a) perforin and b) granzyme B expression by NK cells in PBMC stimulated with *Mtb* antigens. Expression reported in terms of median staining intensity (MFI). Mann-Whitney, unpaired, non-parametric T-test was used to compare TB (n=10) vs QFT$^+$ (n=10). The Holm-Bonferroni test was used to correct for multiple comparisons (q-values). MFI values were normalized to account for background by determining a fold-change value above the unstimulated control.

αIL-2-mediated suppression of perforin expression was significantly more pronounced in TB patients compared to QFT^+ controls ($p<0.05$) (Figure 3.22a), for all NK cell subsets in PBMC stimulated with *Mtb* antigens. However, when controlling for multiple comparisons (q-values), significance was not obtained for all but $NK_{regulatory}$ $CD56^{hi}CD16^{lo}$ cells responding to *Mtb* peptides ($q<0.05$), and $CD56^{int}CD16^{lo}$ cells responding to *Mtb* lysate only ($q<0.05$). Although significant for only some NK cell subsets, granzyme B expression appeared to be following the same trend of greater αIL-2-mediated suppression in TB patients relative to controls (Figure 3.22b). However, all findings were insignificant when accounting for multiple comparisons ($q>0.05$). No significant findings of the same effect were evident with αIL-12/18 neutralizing antibodies (Figure 3.22); and no significant observations or trends were observed when performing the same comparisons for stimulations with recombinant cytokine data (rhIL-12/18 and rhIL-2, $p>0.05$ and $q>0.05$, Figure 3.23), indicating that the findings were *Mtb*-specific. Overall, these data suggest an important role of T cell bystander activation in NK cytotoxic responses in TB.

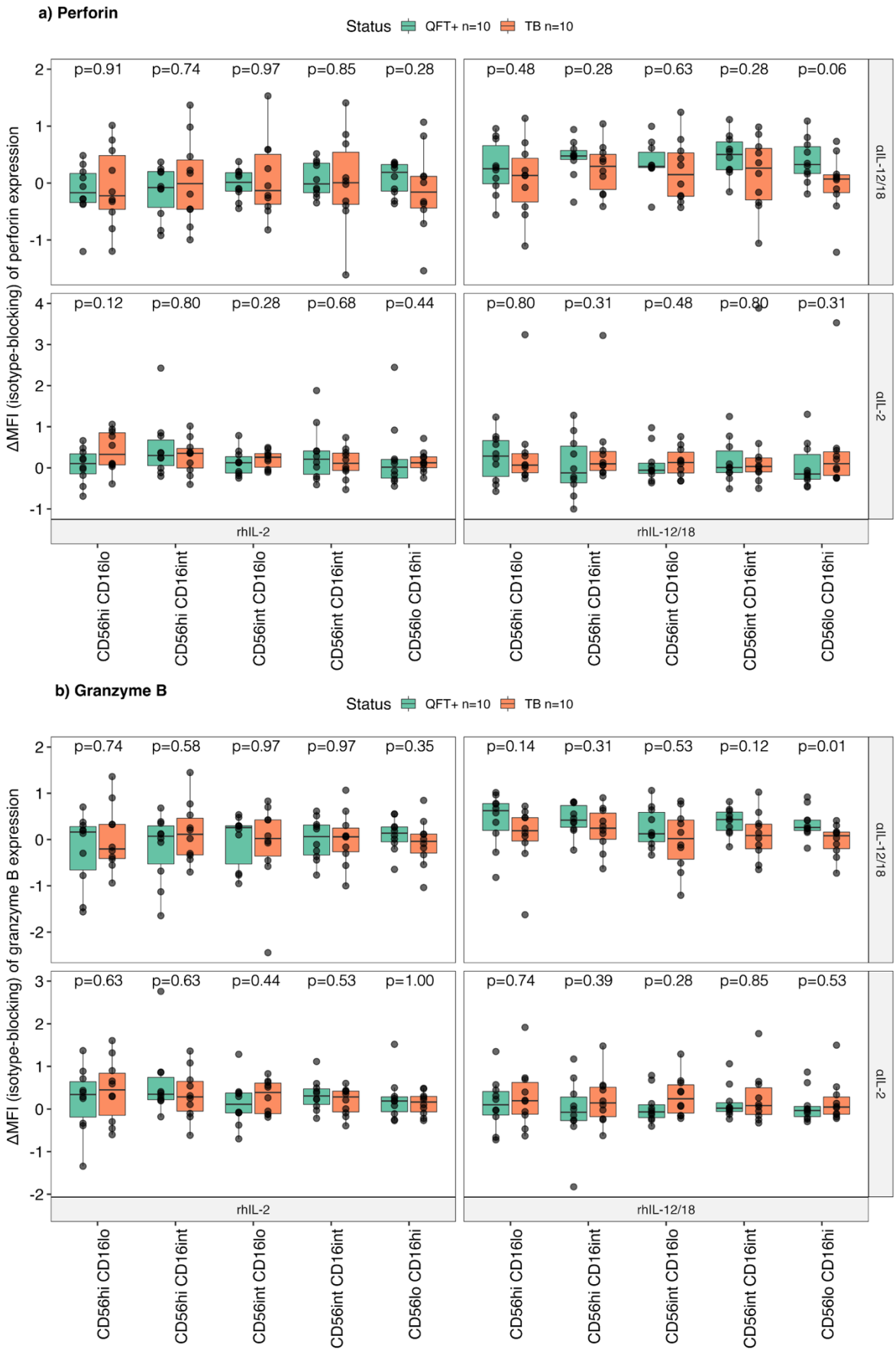

Figure 3.23: Blocking-mediated changes in MFI of a) perforin- and b) granzyme B-expressing NK cells, comparing responses to control recombinant human cytokines between TB and QFT$^+$ participants. Mann-Whitney, unpaired, non-parametric T-test was used to compare TB (n=10) vs QFT$^+$ (n=10). MFI values were normalized to account for background by determining a fold-change value above the unstimulated control. MFI = median staining intensity.

3.4 Discussion and Conclusions

The study presented in this chapter aimed to investigate NK cell functional changes during progression to TB disease; and determine how cytokine-mediated bystander activation of NK cell function differs between TB patients and healthy, *Mtb*-immunologically sensitized controls.

Published data have suggested that fewer NK cells circulate in TB patients compared to healthy, *Mtb*-sensitized controls (Chowdhury et al., 2018; Scriba et al., 2017). However, results presented in this thesis showed that frequencies of total peripheral NK cells and five NK cell subsets were not different between TB and QFT^+ participants. There were also no differences in circulating NK cell frequencies modelled longitudinally with time to TB diagnosis in the ACS dataset between controllers and progressors. Older publications have also shown no significant differences in peripheral NK cell numbers or relative proportions between TB patients and healthy control groups (Nirmala et al., 2001; Vankayalapati et al., 2002). In fact, total peripheral NK cells in TB patients presented in this chapter tended to occur in higher proportions compared to healthy controls, which was also observed by Schierloh and colleagues in 2005 (Schierloh, Alemán, et al., 2005). It remains plausible that the apparent trend reported in this thesis would have been confirmed as significant with a larger sample size. Despite the constraints of small sample size, conflicting results reported between studies may be also due to differences in patient demographics, inflammatory status of the host, or stage of disease between study cohorts. The inflammatory status of the host is known to regulate hematopoiesis and influence numbers of circulating lymphocytes, including NK cells (Baldridge et al., 2010, 2011; Naranbhai et al., 2014; Scriba et al., 2017). Additionally, the inflammatory status of the host is different between different stages of progression to TB disease (Scriba et al., 2017). A recent study by Li and colleagues in 2021 also showed significantly increased peripheral NK cells in patients with

cavitary TB relative to non-cavitary TB (S. Li et al., 2021), indicating that frequencies of peripheral NK cells may differ at different stages of disease.

An important control for this assay was to demonstrate inducible NK functional responses in PBMC stimulated with *Mtb* antigens and recombinant cytokine controls. Stimulation with recombinant cytokines (rhIL-2 and rhIL-12/18) and *Mtb* antigens (secreted peptides and lysate) significantly increased IFN-γ, TNF and polyfunctional (IFN-γ^{+}TNF^{+}) responses in $NK_{regulatory}$ cells above background levels, as expected. Cytotoxic molecules were also inducible above background levels in $NK_{cytotoxic}$ cells using *Mtb* antigens and T cell-associated IL-2 to stimulate PBMC. Although the positive shift in molecule expression was slight, the findings were statistically significant. However, myeloid IL-12 and IL-18 cytokines did not upregulate cytotoxic potential above the unstimulated condition. Interestingly, a study by Nirmala and colleagues found that IL-12 alone did not increase NK cell cytotoxicity in TB patients or healthy controls, yet IL-2 alone or in combination with IL-12 significantly increased NK cytotoxicity (measured in terms of NK lytic activity against U937 target cells), suggesting that T cell IL-2 was the necessary component for inducing NK cell cytotoxicity (Nirmala et al., 2001). The NK cell functionality assay presented in this chapter did not investigate the effects of IL-12 with IL-2. However, together with the data by Nirmala et al*.,* evidence suggests that cytotoxic NK responses are strongly responsive to T cell-derived cytokines but less so toward myeloid-associated cytokines, indicating an important role of T cells in NK cytotoxicity.

Studies have suggested that NK cell functionality may differ in health and TB disease. Bozzano and colleagues showed that peripheral NK cells from TB patients have reduced capacity to produce IFN-γ relative to healthy controls (Bozzano et al., 2009). Several studies have also shown reduced NK cell cytotoxicity in TB patients compared to healthy controls, measured as lytic activity against target cell lines (Restrepo et al., 1990; Nirmala et al., 2001;

Schierloh, Alemán, et al., 2005; Bozzano et al., 2009) and *Mtb*-infected monocytes (Vankayalapati et al., 2002). Low cytotoxic capacity in TB patients was associated with downregulation of costimulatory and adhesion molecules (Schierloh, Alemán, et al., 2005) and activating receptors, such as NKp46 and NKp30 (Vankayalapati et al., 2002; Bozzano et al., 2009). In contrast, two older publications reported significantly increased cytotoxic killing of target cells in TB patients compared to healthy controls (Yoneda et al., 1983; Morikawa et al., 1989). Despite conflicting directions of results, these published studies show that differences in NK cell function may reflect a cause or consequence of disease, the specifics to which could not be detangled. However, the data reported in this chapter provide some evidence towards altered NK cell function as a consequence of inflammatory disease, which is discussed further in the following section.

More specifically, the longitudinal modelling of the ACS progressors and controllers dataset indicated that NK cytokine responses were lower at distal timepoints but increased significantly with time to diagnosis in progressors compared to controllers. Upon further investigation, the frequencies of cytokine-expressing NK cells were significantly and positively associated with *Mtb*-specific CD4 T cell IL-2 production in the ACS dataset. In the cohort of adult TB patients, NK cell cytotoxic potential in PBMC stimulated with *Mtb* antigens were higher in TB patients than healthy controls, particularly perforin expression in the $NK_{regulatory}$ subset. Moreover, blocking T-cell IL-2 resulted decreased perforin expression that was significantly more pronounced in TB relative to controls (Figure 3.24). Together, these results indicate two main findings: 1) NK cytokine production and cytotoxic potential is higher during TB, relative to healthy, *Mtb*-sensitized individuals; and 2) T cell bystander cytokines play an important role by potentially driving NK cell cytotoxic responses during TB disease. It is most likely that *Mtb* antigen load increases with progression to active disease, thereby initiating an inflammatory milieu in the host, which in turn, activates NK cells via T cell bystander pathways.

Notably, higher cytotoxic potential in TB patients relative to healthy controls were reported for the $CD56^{bright}CD16^{dim}$ $NK_{regulatory}$ subset. However, $NK_{regulatory}$ cells are a minority subset, encompassing only ~10% of the total peripheral NK population and primarily produce immunoregulatory cytokines (such as, IFN-γ, TNF and IL-22) (Béziat et al., 2011; Björkström, Riese, et al., 2010; Yu et al., 2010). The $NK_{regulatory}$ subset is also considered immature, with relatively low cytotoxic potential compared to their $CD56^{dim}CD16^{bright}$ $NK_{cytotoxic}$ counterparts, which are regarded mature and differentiated. Therefore, it is possible that significantly higher perforin expression in $NK_{regulatory}$ cells of TB patients may be due to inflammation-induced upregulation of cytotoxic potential and activation of immature NK cells towards terminal differentiation, while differentiated $NK_{cytotoxic}$ cells remain at maximum cytotoxicity capacity in both cohorts.

It should also be noted that NK cell cytokine responses were significantly higher in adolescent progressors at proximal (i.e., closer) timepoints to TB diagnosis relative to controllers. Based on this finding, it was hypothesized that NK cell cytokine responses in the cohort of newly diagnosed adult TB patients would also be significantly higher than healthy, *Mtb*-sensitized controls, although results indicated no statistical differences. Firstly, the ACS dataset had more participants per cohort (37 progressors and 36 controllers), multiple timepoints per participant, and more statistical power, compared to the adult cohort with only ten TB patients and ten healthy controls. Additionally, ACS progressors and controllers were carefully matched by age, sex, ethnicity, and geographical region, while such precise pairing were not possible in the adult TB cohort. It should also be noted that NK cytokine responses in the ACS dataset were modelled using COMPASS functionality scores, while frequencies of cytokine-expressing NK cells were compared for the adult cohort. In the ACS dataset, frequencies of *Mtb*-specific IFN-γ-expressing NK cells were also modelled against time to TB, although results showed that there was also no significant association at proximal timepoints to diagnosis (data not shown). Therefore, the type of response reported (i.e.,

COMPASS functionality score versus frequencies) is a likely point of difference in reported results. Notably, COMPASS analysis was not performed for the cytokine neutralization dataset, as these analyses fell beyond the scope of the analysis plan, which was primarily focused on evaluating differences in the magnitude of cytokine blocking effects.

Myeloid-derived cytokines (IL-12/18) were necessary to induce IFN-γ responses by all NK subsets in PBMC stimulated with *Mtb* antigens (secreted peptides and lysate). However, T cell-derived IL-2 was only necessary to induce IFN-γ responses in the $CD56^{hi}CD16^{lo}$ subset. Additionally, blocking reduced cytokine-dependent IFN-γ responses to the same degree in TB patients and controls. Diminished NK IFN-γ production in PBMC stimulated with *Mtb* lysate and peptides was more pronounced when blocking with myeloid-derived αIL-12/18 than T cell-associated αIL-2. This is consistent with findings by Suliman and colleagues at SATVI (Suliman et al., 2016), who showed greater αIL-12/18-mediated inhibition of IFN-γ production by NK cells in blood stimulated with BCG than blocking with αIL-2, in revaccinated adults. The same study by Suliman and colleagues showed that stimulation with myeloid-derived rhIL-12/18 induced greater NK cell IFN-γ responses than rhIL-2 in the presence or absence of BCG (Suliman et al., 2016). It thus seems logical that cytokines inducing greater activation would correspond to greater inhibition upon blocking. However, due to the different nature of *in vitro* antigen processing mechanisms between live BCG (used in Suliman's study) and peptide pools, it was hypothesized that T cell cytokines were the major activators of NK cell responses to *Mtb* peptides. This was based on T cells as the primary responders to peptide pool stimulation, which bypasses the myeloid phagocytosis/antigen presentation pathway that BCG and other complex protein antigens would typically undergo (Figure 3.24). However, blocking myeloid cytokines resulted in greater inhibition of NK cell IFN-γ response compared to T cell cytokines in the presence of *Mtb* lysate and peptides.

A possible explanation includes T cells secreting myeloid-activating cytokines (IFN-γ and TNF) upon activation, which in turn leads to myeloid cells secreting NK-activating IL-12 and IL-18. The proportion and/or potency of myeloid-activating cytokines (IFN-γ and TNF) produced by peptide-activated T cells could outweigh the T-cell NK-activating cytokine (IL-2). In this way, blocking with αIL-2 may not have fully neutralized the T cell-associated activation of NK cells in response to *Mtb* peptides. Therefore, NK activation by *Mtb* peptides may occur via the T cell- to myeloid cell- to NK cell activation pathways, in addition to T cell- to NK cell activation (Figure 3.24). This highlights the immense complexity of the activation/inhibition mechanisms that ultimately modulate NK cell functionality under different pathological and/or homeostatic conditions. In this regard, the vast variability and plasticity of functional potential within the spectrum of NK cell subsets puts these cells in good stead as important responders to pathogenic threats.

This study also demonstrated cytokine blocking having a more pronounced effect on $NK_{regulatory}$ cell function by greatly reducing IFN-γ production, compared to NK subsets closer towards the differentiated $NK_{cytotoxic}$ end of the NK cell spectrum. These data point toward subset-specific responsiveness to cytokine activation, which is not surprising given the large heterogeneity of the global NK cell subset. It was also found that blocking IL-2 or IL-12/18 did not significantly reduce NK cytotoxic potential in PBMC stimulated with *Mtb* antigens. Interestingly, Vankayalapati and colleagues also showed that αIL-18 or αIFN-γ antibodies did not reduce NK lytic activity against *Mtb* infected monocytes, although αIL-12 and αIL-2 were not investigated in this study (Vankayalapati et al., 2002). Together, evidence may indicate that changes to the cytokine milieu does not significantly alter the cytotoxic potential in NK cells. However, data presented in this chapter showed that αIL-2-mediated suppression of cytotoxic marker expression was more pronounced in TB patients compared

to controls, suggesting an important role of T cell bystander activation in NK cytotoxicity in the context of TB.

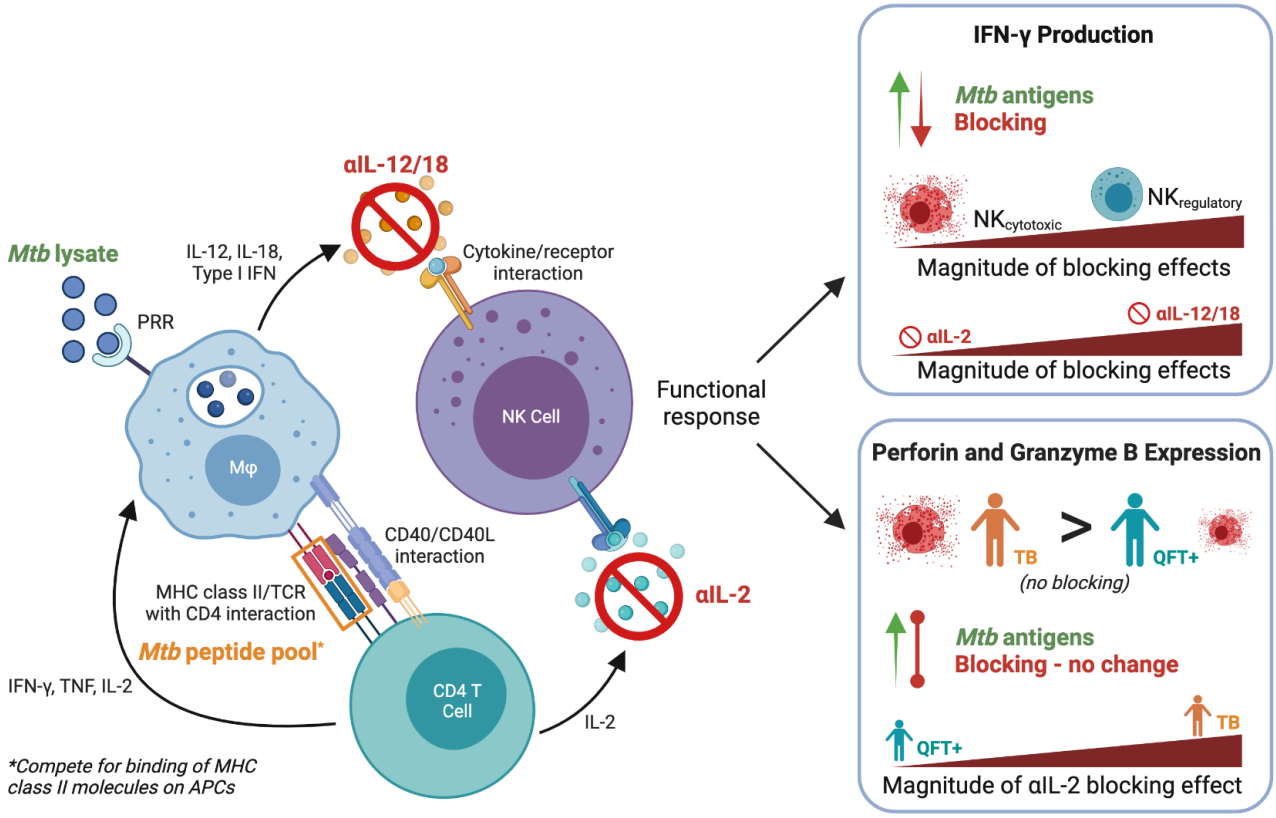

Figure 3.24: NK cell functional alterations via cytokine bystander activation pathways in TB and healthy, *Mtb*-sensitized controls. Larger protein fragments of *Mtb* lysate activates NK cells by binding to PRRs on the surface of myeloid cells, resulting in secretion of NK-activating cytokines (such as IL-12 and IL-18). Bound antigens on PRRs are phagocytosed and processed peptides are presented to T cells via MHC-II molecules. Interaction of TCRs with the MHC-II/peptide complex causes activation of T cells and cytokine secretion. *Mtb* peptide pools compete for direct binding of MHC-II molecules on APCs, thereby bypassing the myeloid phagocytosis/antigen processing pathway. In this way, T cells are directly activated to secrete IL-2 (an NK-activating cytokine), as well as IFN-γ and TNF (myeloid-activating cytokines). Activated myeloid cells, in turn, secrete NK-activating IL-12 and IL-18. The presence of *Mtb* lysate and peptides in PBMC increased IFN-γ and TNF production, as well as perforin and granzyme B expression in NK cells. Blocking myeloid and T cell cytokines diminished NK IFN-γ responses but did not change cytotoxic marker expression. The magnitude of cytokine blocking effects were greater in $NK_{regulatory}$ cells than the $NK_{cytotoxic}$ subset with regards to NK IFN-γ responses. Blocking-mediated reduction in NK IFN-γ responses in PBMC stimulated with *Mtb* lysate and peptides were more pronounced with αIL-12/18 blocking antibodies than αIL-2. There was increased cytotoxic marker expression in TB patients compared to healthy controls. Anti-IL-2-mediated reduction in cytotoxic responses were more pronounced in TB cases compared to controls, suggesting an important role of T cell bystander activation in NK cytotoxicity in the context of TB.

3.4.1 Limitations

The study presented in this chapter was subject to a few limitations. Firstly, there was a female bias in the healthy control cohort (10 out of 10 participants were female among QFT^+ participants, while 5 out of 10 participants were female in the TB cohort; Table 3.3). There is evidence to suggest that bidirectional communication occurs between the neuroendocrine and immune systems, such that steroid hormones have been shown to regulate immune cell proliferation and activity (Bouman et al., 2005; Klein & Flanagan, 2016). Particularly, progesterone (Arruvito et al., 2008) and estrogen (Hao et al., 2007) are known to reduce NK cell activity (Bouman et al., 2005). Several studies have demonstrated that males have increased frequencies of peripheral NK cells compared to females (Abdullah et al., 2012; Chng et al., 2004; Phan et al., 2017), with differing proliferative abilities (Abdullah et al., 2012) and receptor expression (Phan et al., 2017) observed between sexes. Notably, increased NK cells in males occurs in childhood/pre-puberty and post-puberty/adulthood phases of life (Lee et al., 1996), whereafter, females display increased NK cell frequencies at old age (Hirokawa et al., 2013; Klein & Flanagan, 2016), having a higher ratio of immature $CD56^{bright}$ to mature $CD56^{dim}$ NK cells and more robust cytokine and cytotoxic response compared to males (Al-Attar et al., 2016; Lutz et al., 2016). Altogether, these data suggest that sex and steroid hormones may influence NK cell frequency, maturation status and functional activity, and these influences may be informed by age and stage of life. Although no significant differences in NK cell frequencies were observed between cohorts, it remains possible that the functional data were skewed due to sex. Additionally, significant differences in cytotoxic capacity were observed between TB and healthy QFT^+ cohorts, which may indeed be influenced by the skewed sex distribution in these data. To evaluate the impact of sex on these observations, more datapoints including a more balanced male to female ratio are needed.

This study demonstrated NK cell functional alterations upon blocking T cell IL-2 and myeloid-associated IL-12/IL-18. However, other NK cell-activating cytokines, such as IL-15, IL-21 and type-I interferons, also play a role in the bystander activation pathway (Zwirner & Domaica, 2010). As a follow-up study, NK responses upon treatment with neutralizing antibodies against additional NK-activating cytokines (such as IL-15, IL-21 and IFN-α) could be investigated using the experimental design described in this chapter. Additionally, it would be of interest to quantify other features of NK cell activation, such as proliferation, and include a larger panel for detecting cytokines produced by activated NK cells, including GM-CSF, IL-10, IL-5, IL-13, and IL-22.

Cytotoxic responses in NK cells were measured as expression of cytotoxic molecules, perforin and granzyme B. In this assay, only cytotoxic potential is reported rather than cytotoxic activity, as this requires demonstration using a functional NK cell killing/lysis assay against target cells. Although perforin and granzyme B are both notorious potent cytotoxic proteins, it remains plausible that expression does not necessarily translate to killing activity. To elaborate more, it is known that perforin is stored in acidic secretory granules where it remains functionally inert prior to delivery to a target cell (Lopez et al., 2013), requiring post-translational modification for activation prior to secretion (House et al., 2017). In the case of granzyme B, regulation also occurs at a post-translational level that includes the synthesis of granzyme B as a pro-peptide (zymogen), requiring proteolytic cleavage for activation and tagging with a mannose-6-phospahe receptor (MPR) to target the protease to the acidic lytic granule (Griffiths & Isaaz, 1993). Furthermore, it is also known that granzyme B is released in active and inactive forms, suggesting that there may be an extracellular granzyme B activator for the zymogen form of the enzyme (Boivin et al., 2009; Prakash et al., 2009). Additionally, granzyme B inhibitors (such as proteinase inhibitor-9; PI-9) exist in various human tissues and at immune-privileged sites to regulate activity and minimize potential pathological granzyme B-mediated apoptosis (Bird et al., 1998; J. Sun et al., 1996).

Therefore, the killing capacity of cytotoxic proteins is dependent on mechanistic components of the secretory granule/exocytosis pathways and factors such as, post-translational modifications, pH and/or enzyme inhibitors. Additionally, the B-D48 perforin antibody clone detects perforin in multiple forms (late and newly synthesized forms), not only in the granule-associated conformation (Hersperger et al., 2008). Thus, upregulated perforin expression reflects increased production, although cytotoxic function of the proteins detected (which may be in an inactive state) could not be evaluated. Overall, the assay presented in this chapter demonstrated increased cytotoxic potential of NK cells as increased expression of perforin and granzyme B enzymes. However, it cannot be claimed for certain whether increased expression translates to enhanced cytotoxic activity *in vivo*.

Measuring NK-activating IL-2 production by T cells responding to *Mtb* antigens would have been useful to make comparisons with T cell production of myeloid-activating cytokines (IFN-γ and TNF). However, IL-2 was not included in the ICS flow cytometry panel. Naturally, detection of IL-2 would not have been possible under cytokine neutralization conditions (as expressed IL-2 would have been neutralized by αIL-2). However, detection of IL-2 production by T cells in the isotype control conditions may have supported the speculation of NK activation upon *Mtb* peptide stimulation occurring via the T cell- to myeloid cell- to NK cell activation pathways.

Finally, NK cell responses to *Mtb* antigens were investigated in the context of bystander activation via accessory cell cytokine secretion. However, evidence exists to suggest that NK cells may be activated by NK receptors (such as extracellular and intracellular PRRs) directly recognizing mycobacterial PAMPs (Batoni et al., 2005; Esin et al., 2004, 2013a). Thus, the role of NK receptors and their contributions towards NK cell activation by direct sensing of *Mtb* lysate or peptide constituents was not investigated in this study. Further to the point on NK receptors, subclassification of NK cells based on expression of various NK

activating and inhibitory receptors may have aided in identifying NK cell subsets. However, there were limitations to the number of available spectral channels on the flow cytometer used for this study, precluding the use of markers other than CD56 and CD16 to define NK cells. Certainly, technologies such as spectral flow cytometry or mass cytometry, which allow more markers to be detected per cell, would prove useful for designing large phenotyping panels to subclassify NK cells based on expression of the vast array of activating and inhibitory NK receptors that contribute towards the phenotypic heterogeneity observed under the total NK umbrella.

3.4.2 Conclusions

Despite several limitations, this study was successful in demonstrating NK cell functional responses that are dependent on cytokine-mediated bystander activation in TB and healthy, *Mtb*-sensitized controls. This study reveals the complex interplay between T cells, myeloid cells, and NK cell function in the context of *Mtb* infection and TB disease. Further investigation into NK cell activation and function (particularly in the tissues and at the site of disease) may highlight new mechanistic targets for developing clinical interventions that possibly modulate NK cell activity for better *Mtb* clearance and favorable TB prognosis.

Chapter 4: Myeloid and lymphoid immune subsets of postmortem tissues in TB and controls.

"Research is formalized curiosity. It is poking and prying with a purpose."

- Zora Neale Hurston

4.1 Introduction

To curb the TB epidemic, a better understanding of the immune response to *Mtb* infection and immunopathogenesis is needed. Since TB disease occurs in the tissues, performing studies using sampled organs holds potential to uncover immune mechanisms by which *Mtb* manipulates the host and identify correlates of immunopathogenesis or protective immunity to *Mtb*.

Although mouse and NHP models are commonly used to study tissues in the context of *Mtb* infection and TB disease, human tissue immunology studies remain the gold standard for investigating immune cell phenotypes and function during TB disease. However, performing tissue immunology studies in human organs is challenging and, in most instances, sampling control tissues from healthy, living participants is simply not feasible (as discussed in Chapter 1, Section 1.5). The study presented in this chapter proposes to address this gap by performing phenotypic characterization of immune populations from specimens collected during autopsy from recently deceased TB patients and those who were otherwise healthy but died due to trauma. Using this approach, differences in tissue-specific immune cell phenotypes, frequencies, and functional properties between disease and health could be identified, offering avenues for further investigation to uncover mechanistic targets for clinical intervention (such as new TB drugs, host-directed therapies, and vaccine design).

In this study, postmortem specimens were sampled from the lungs, BAL, lymph nodes, spleen, and blood (PBMC). Each tissue/compartment has unique and specific roles for maintaining homeostasis and have distinct cellular compositions, including immune subsets. As a brief overview, the lung is a vital organ that enables gaseous exchange and serves as an immune organ to protect the host against inhaled pathogens. The major immune cell populations of the lung include macrophages, granulocytes, epithelial cells, DCs, NK cells

and other ILCs, as well as T cell and B cell subsets (V. Kumar, 2020). Being a large organ, the lung is characterized into several components: 1) the upper respiratory tract, serving as a mucosal and glandular component, 2) peripheral airways without mucosal tissue, and 3) the parenchymal or alveolar interstitium enabling gaseous exchange. The peripheral airways on the luminal side remain in contact with bronchoalveolar cells, which comprise mostly alveolar macrophages (~80-90%), and the remaining 10% are lymphocytes (Heron et al., 2012; Stanzel, 2012). The macrophages that are present in the lung tissue interstitium are referred to as interstitial macrophages. There are also respiratory epithelial lymphocyte compartments which are lymphocytes residing in the respiratory tract epithelium over the epithelial membrane and between the epithelial cells, offering another immune component to protect the host from pulmonary infections (V. Kumar, 2020; Pabst & Tschernig, 1995). There are also respiratory lymphoid cells that form lymphoid follicles or aggregates (resembling Peyer's Patches in the intestine) within the bronchial walls, also referred to as bronchus-associated lymphoid tissue (BALT) containing T cells, B cells and DCs (Bienenstock, 1982; Pabst & Tschernig, 1995; Richmond et al., 1993). Overall, the pulmonary immune system is complex and separable into multiple different compartments that interact with one another.

The lymph nodes form a central hub of the immune system by providing an environment for efficient interaction between innate and adaptive immune cells. The hilar lymph nodes are located in the area where the bronchus enters the lung and serves to collect lymph from the pulmonary nodes and drain to the tracheobronchial nodes. When antigens are phagocytosed and processed by APCs (most often DCs), cells are trafficked within the lymphatic vessels towards the lymph nodes where APCs display antigens to lymphocytes to initiate clonal expansion of antigen-specific cells. The lymph node has a highly organized, sub-compartmentalized structure that creates separate areas for T and B cells to interact with their APCs and undergo clonal expansion. B cells home to the primary follicles to survey

follicular DCs. Once stimulated and actiavted, B cells proliferate within the follicles to form germinal centers that are then referred to as secondary follicles. Plasma cell precursors produced by B cell activation and proliferation migrate to the medullary cords where they mature and secrete antibodies directly into the lymph to be transported throughout the body. T cells home to the paracortex and interfollicular cortex to survey DCs where stimulated T cells proliferate but do not form distinctive structures like B cells in the germinal centers (Willard-Mack, 2006; Liao & Padera, 2013; K. Murphy & Weaver, 2016). The lymph nodes have been a particular point of rising interest in the TB field as they have been highlighted as a potential niche for *Mtb* persistence and/or *Mtb* killing in the NHP model (Ganchua et al., 2018, 2020; Flynn et al., 2015). Novel studies have set out to investigate lymph nodes as the central sites at which the battle against *Mtb* infection is won or lost in the host.

Tonsil tissues were included in this study as a control from living individuals. According to the current dogma, the cellular architecture of adenoids and tonsils resembles that of lymph nodes. However, the lack of afferent lymphatics predisposes the tonsils to direct interactions with environmental antigens. The tonsils also contain germinal centers in B cell follicles and extrafollicular T cell-enriched compartments (Arambula et al., 2021) and overall, comprised almost exclusively of B cells and T cells, primarily of the CD4 T cell subset (Boyaka et al., 2000).

The spleen is an important organ for iron metabolism and erythrocyte homeostasis, and acts as a filter for blood-borne pathogens and antigens. The spleen consists of organized regions known as red pulp and white pulp, which are separated by the marginal zone (MZ) interface. The red pulp serves to mostly filter blood and recycle iron from aging red blood cells. The white pulp is structurally similar to a lymph node, containing T cell and B cell zones to allow for initiation and regulation of innate and adaptive immune responses (Bronte & Pittet, 2013). The spleen contains various immune cell subsets including T cells, B cells, DCs and

macrophages with distinct localized functions. More specifically, macrophages within the red pulp are specialized to phagocytose aging red blood cells and regulate iron recycling and release, while macrophages localized to the MZ express PRRs to detect and phagocytose blood borne bacteria, viruses, and other pathogenic threats. The splenic MZ also contains B cells and DCs which also phagocytose passing antigens and migrate to the white pulp where they present antigens to other lymphocytes. B cells, CD4 T cells, CD8 T cells and DCs are located within the white pulp (Mebius & Kraal, 2005).

Cytotoxic immune cells play a role in controlling infections by secreting cytokines, chemokines and cytotoxins. Cytotoxic lymphocytes can be activated via several mechanisms such as 1) peptides presented by APCs, 2) via surface proteins that are expressed by stressed/infected/neoplastic cells, and/or 3) bystander activation via cytokines secreted by immune cells within the local microenvironment. Upon activation, cytotoxic immune cells may secrete cytotoxic molecules (such as perforin, granzymes, and granulysin) to induce apoptosis of infected cells, thus playing important roles in control of *Mtb* replication. The process by which cytotoxic lymphocytes secrete cytotoxic molecules to lyse target cells is known as degranulation (described in Chapter 1, Section 1.3.1). Cytotoxic molecules investigated in this postmortem tissue study included perforin, granzyme B and granzyme K. Perforin molecules perforate the target cell membrane, creating pores through which granzymes enter a target cell to cleave caspase molecules and induce apoptosis. In humans, five granzymes with differing substrate specificity have been identified (Lieberman, 2003; Trapani, 2001). Granzyme B is the hallmark molecule of cytotoxicity, expressing the most potent killing potential and acts by cleaving after aspartic acid residues (Bratke et al., 2005; Trapani, 2001). Granzyme K generally exhibits low cytotoxic potential relative to its granzyme B counterpart and has extracellular targets that are known to induce cytokine production and therefore play a role in immunoregulation (D. M. Cooper et al., 2011; Kaiserman et al., 2022; Sharma et al., 2016; Wensink et al., 2014). Granzyme K has trypsin-

like properties that cleaves basic residues (arginine and lysine) (Bouwman et al., 2021; Bratke et al., 2005; Wilharm et al., 1999).

Cytotoxic lymphocytes encompass NK cells and CTL subsets. The most widely recognized CTL includes CD8 T cells, although other T cell subsets have also been identified as cytotoxic mediators with growing interest in the TB field. These include NKT cells, CD4 T cells, and donor-unrestricted T cells (DURTs) including mucosa-associated invariant T cells (MAITs), CD1-restricted T cells, and T$\gamma\delta$ cells (Godfrey et al., 2015; Gutierrez-Arcelus et al., 2019). In this chapter, the following cytotoxic lymphocytes were investigated in postmortem tissues: NK cells, CD8 T cells, CD4 T cells, NKT-like cells, and T$\gamma\delta$ cells. Each of these cytotoxic immune cell subsets have unique hematopoietic origins, mechanism of activation, functional activity, and tissue localizations. A brief overview is provided for each in the following section.

Despite having similar haemopoietic origins, NK and T$\gamma\delta$ cells do not require antigens to be presented by MHC molecules on APCs to be activated (which are required by conventional T cell subsets) but are rather activated via innate receptors. NK cells are the most notorious cytotoxic lymphocyte, forming part of the innate immune system. Human NK cells constitute 5-15% of peripheral blood lymphocytes and are present in relative abundance in the bone marrow, liver, uterus, spleen, and lung, and to a lesser extent, NK cells can be found in the secondary lymphoid tissue, mucosal-associated lymphoid tissue (MALT), and thymus (Yu et al., 2013). The mechanisms of NK cell activation were discussed extensively in Chapter 1, Section 1.3.1. To briefly recap, NK cells are activated via the classical “missing self” phenomenon but can also be activated via the bystander activation pathway (which was demonstrated and investigated in Chapter 3). The growing interest in the role of NK cells during *Mtb* infection and TB disease is becoming increasingly appreciated (as discussed in Chapter 1, Section 1.4.2).

NKT cells co-express the TCR and NK cell surface receptors, which confers both adaptive and innate immune properties (Makino et al., 1995; Tupin et al., 2007). NKT cells arise from the thymus, complete maturation in the periphery, and are mainly found in the liver and spleen (Wu & Van Kaer, 2011). NKT cells recognize self and foreign lipids presented by the glycoprotein CD1d (Brigl & Brenner, 2004) and have been a growing point of interest in controlling *Mtb* infection (Ruibal et al., 2021). NKT cells have been shown to have activated phenotypes in TB patients relative to healthy controls (Montoya et al., 2008) and the number of NKT cells measured at TB diagnosis have been correlated with treatment response to anti-TB therapy (Veenstra et al., 2006), thereby having the potential to be a predictive correlate for TB.

T$\gamma\delta$ cells express unique T cell receptors composed of one γ-chain and one δ-chain. The T$\gamma\delta$ subset is rare in the secondary lymphoid organs, but is often found in peripheral tissues such as the epithelial and mucosal layers of the skin, intestine, and lung, where they serve as important first-line responders against infections (Ribot et al., 2021). Activation of T$\gamma\delta$ cells occurs largely via innate mechanisms and mainly recognize non-peptide antigens and metabolic intermediates (Meraviglia et al., 2011; Poccia et al., 1999). T$\gamma\delta$ cells have become a point of rising interest in the context of TB disease and have been shown to traffic to the airways early after *Mtb* challenge (reviewed by Bhatt et al., 2015). Several clinical studies have shown that T$\gamma\delta$ cells in TB patients harbor robust cytolytic and cytokine-producing capabilities (Ogongo et al., 2020; Ordway et al., 2005; Peng et al., 2008), and the expansion of this subset decreased with anti-TB therapy (Poccia et al., 1999). The cytolytic killing of intracellular and extracellular *Mtb* by T$\gamma\delta$ cells has been shown to occur via secretion of perforin and granulysin (Dieli et al., 2001), thus potentially playing a central role in pathogen control.

CD8 T cells are largely known as killer T cells which develop in the thymus and reside predominantly in secondary lymphoid organs. Upon engagement of the TCR with antigen presented via MHC-I molecules, CD8 T cell effector functions are initiated to help eliminate intracellular pathogens. Like NK cells, CD8 T cells kill target cells by expressing Fas-L (which binds Fas expressed on target cells to induce apoptosis) and by releasing pre-formed cytotoxic molecules (perforin and granzymes) that are stored in lytic granules to be released at the ready. *Mtb*-specific CD8 T cells have the ability to migrate to the lung post-infection (Kamath et al., 2004) and have been shown to lyse human *Mtb*-infected macrophages and inhibit intracellular persistence of *Mtb* bacilli (Cho et al., 2000).

CD4 T cells with cytotoxic activity have been characterized by their ability to secrete cytotoxic molecules (perforin and granzyme B) and kill target cells in an MHC-II restricted manner. Initially, cytotoxic CD4 T cells were thought to be an *in vitro* artifact arising due to long-term culturing. However, cytotoxic CD4 T cells have since been identified *in vivo* as important role players in inflammatory responses to pathogen-infected and neoplastic cells (Takeuchi & Saito, 2017). In the context of TB disease, CD4 T cells have been the most studied cell subset and have been underpinned as crucial role players in the protective response to *Mtb* infections. For the most part, the cytokine-producing capabilities of CD4 T cells have been widely appreciated and are important for maintaining other cell subsets, reducing cellular exhaustion, and improving control of *Mtb in vivo* (Y.-J. Lu et al., 2021; Serbina et al., 2001; C. M. Smith et al., 2004). Compared to the cytokine-producing role of CD4 T cells during *Mtb* infection, relatively little has been demonstrated regarding their cytotoxic capacities. In one early study, human CD4 T cells with mycobacterium-specific cytotoxic activity were shown to be enriched in the BAL and expended upon stimulation with PPD antigens (Tan et al., 1997). A later study by Bastian and colleagues in 2008 showed that peptides presented by *Mtb*-infected macrophages elicited cytolytic CD4 T cell

responses (by upregulating granulysin and perforin), altogether challenging the previous dogma that cytotoxic T cell activities were restricted to the CD8 subset (Bastian et al., 2008).

The overarching theme of this thesis was centered around NK cells. However, before delving into detailed NK-specific tissue immunology (detailed in Chapter 5), this chapter provides a comprehensive overview of bulk myeloid and lymphoid immune subsets of various tissues in TB patients and healthy controls and provides insights into the cytotoxic potential of cytotoxic immune cell subsets in human tissues.

4.2 Methods and Materials

4.2.1 Study participants

Living participant validation cohort

Living participants for the PBMC flow cytometry ICS validation included the following cohorts from the 2021 study by Mpande and colleagues at SATVI (Mpande et al., 2021): the “Test Cohorts” of persistent QFT^+ individuals (n=25) from the Adolescent Cohort Study (ACS) and adult TB patients (n=25). For the persistent QFT^+ cohort, healthy adolescents between the ages of 12 and 18 years were enrolled from the Worcester region of the Western Cape, South Africa. Individuals were excluded is they were pregnant, infected with HIV, or had any acute or chronic medical conditions resulting in hospitalization within 6 months prior to enrollment. To be enrolled into the study, written informed assent was provided by adolescents, while parents or legal guardians provided written informed consent. PBMC were sampled from blood collected at six-monthly intervals during two years of follow-up. Persistent QFT^+ adolescents were defined as participants who were otherwise healthy and had four positive QFT tests consecutively, 6 months apart over 1.5 years (with at least two QFT positive results >0.7IU/mL).

Adult TB patients were recruited from the Worcester region of the Western Cape, South Africa. Participants were included if they were 18 years or older and recently diagnosed with pulmonary TB by positive Xpert MTB/RIF (Cepheid). TB patients were excluded if they were HIV co-infected, anaemic, (haemoglobin <8.0g/dL), body mass index (BMI) ≤17, or had signs of other chronic illnesses that were not consistent with tuberculosis. Those who had already initiated anti-TB treatment were also excluded from the study.

Postmortem tissue cohort

Informed consent, enrollment and autopsies of deceased individuals were performed according to the protocols outlined in Chapter 2, Section 2.3, by a collaborating research group led by Dr Stephen Cose based at the Medical Research Council/Uganda Virus Research Institute and London School of Hygiene & Tropical Medicine (MRC/UVRI & LSHTM) Uganda Research Unit.

Samples from deceased TB patients (n=10) and deceased individuals who were otherwise healthy but died due to trauma (n=10) were included in the study. Due to low numbers and the scarcity of available postmortem samples, there were no exclusion criteria based on age, sex, HIV status, or TB risk-associated habits (such as smoking and alcohol consumption). Deceased TB cases had pulmonary and/or extrapulmonary TB, clinically diagnosed by microscopy, culture test, Xpert MTB/RIF (Cepheid) and/or radiology. Deceased TB cases were not excluded if they had co-morbidities, such as hypertension and diabetes. Co-morbidity information was not available for healthy controls, although none had any evidence of lung disease or characteristics of ill health prior to injury and death, or during autopsy. To exclude possible cases of subclinical TB, only healthy controls with negative BAL MGIT liquid culture test results were included (this test was not performed for decedents in the TB cohort, as they were already clinically diagnosed). Trauma cases were excluded

if the cause of death was related to severe injury of the chest, such that thorax disfigurement prevented tissue sampling from the lungs, airways and/or hilar lymph nodes. The healthy control cohort was sub-classified according to evidence of immunological sensitization to *Mtb* antigens by performing the T-SPOT®.TB assay using PBMC isolated from blood collected postmortem, according to manufacturer's recommendations with minor modifications (methods described in Chapter 2, Section 2.4). Overall, decedents were divided into three cohorts based on clinical status and evidence for immunological sensitization to *Mtb* antigens: TB, $TSPOT^{+}$ and $TSPOT^{-}$.

Tonsil tissues (n=5) from living participants were donated by Dr Al Leslie at the Africa Health Research Institute (AHRI), South Africa. Recruited participants were clinically indicated for tonsillectomy, were HIV-uninfected, and excluded TB patients or suspected TB cases.

4.2.2 Tissue dissociation and single cell isolation

Postmortem tissue samples (including PBMC, lung tissue, hilar lymph nodes, BAL, and spleen) and tonsil tissues from living controls were processed and single cell suspensions were isolated according to the methods described in Chapter 2, Section 2.3.

4.2.3 Flow cytometry ICS and data acquisition

The T-SPOT®.TB test is a licenced, validated diagnostic kit, although its intended use is for freshly isolated PBMC sampled from living individuals. The reliability of the TSPOT assay in PBMC obtained and isolated postmortem is uncertain. As a secondary check to the TSPOT test performed by our collaborators in Uganda, a previously optimized SATVI in-house flow cytometry ICS assay was used to measure IFN-γ and TNF production by T cells upon stimulation with *Mtb* peptides (ESAT-6 and CFP-10). This IGRA therefore detects positive T cell responses to *Mtb* peptides as a measure of immunological sensitization to *Mtb.*

Cryopreserved PBMC from the living validation cohort and postmortem cohort were thawed and rested according to the flow cytometry ICS protocol described in Chapter 2, Section 2.5.1. Cells were stimulated with a pool of ESAT-6 and CFP-10 peptides at a final concentration of 1µg/mL in a total stimulation volume of 200µL containing $1x10^6$ PBMC. As positive control, $1x10^6$ PBMC were stimulated with 5µg/mL PHA (a mitogen to illustrate cell functionality) in a total volume of 200µL. An unstimulated fraction was used as a negative control. Cells were stimulated at 37°C in a humidified 5% CO_2 incubator for a total of 18 hours, adding brefeldin A (10µg/mL; Brefeldin A, Sigma Chemical Co.) at the beginning of stimulation.

Following stimulation, PBMC were stained with a panel of fluorochrome-labelled extracellular and intracellular antibodies using the flow cytometry ICS and data acquisition protocol described in Chapter 2, Section 2.5. The flow cytometry ICS panel for measuring T cell responses to *Mtb* peptides is described in Table 4.1.

Table 4.1: Flow cytometry ICS antibody panel for measuring T cell responses to ESAT-6 and CFP-10 peptides.

Marker	Fluorochrome/Dye	Rationale	Clone	Supplier
Extracellular (surface) markers				
Live/Dead	Fixable Near-IR Stain	Dead cell exclusion	N/A	ThermoFisher Scientific
CD3	BV785	T cells	SK7	BioLegend
HLA-DR	PE	T cell activation	L243	BD Biosciences
Intracellular (functional) markers				
IFN-γ	AF700	Function	B27	BD Biosciences
TNF	PE-Cy7	Function	Mab11	eBiocience

4.2.4 CyTOF antibody staining and data acquisition

All postmortem samples (cell suspensions of lung, BAL, hilar lymph nodes, spleen and PBMC) and control tonsil cells from living participants were stained with the full panel of

CyTOF antibodies (Chapter 2, Table 2.1) according to the protocol outlined in Chapter 2, Section 2.8.

4.2.5 Data analysis

All data presented in this chapter were analyzed by me, Carly Young-Bailie.

Flow cytometry ICS assay data analysis

Flow cytometry data were exported in FCS format and imported into FlowJo v10.7.1 software for gating. Gating to identify cytokine-producing T cell subsets was performed according to the gating strategy outlined in Figure 4.1. Briefly, antigen-specific T cells were identified as singlet, live, $CD3^{+}TNF^{+}IFN\text{-}\gamma^{+}$ cells (Figure 4.1). Frequencies and counts of cytokine-producing T cell data were exported in CSV format and imported into RStudio (R v4.2.1) for analysis and data visualization.

A responder, or individual displaying T cell responses to a pool of ESAT-6/CFP-10 peptides, indicating immunological sensitization to *Mtb* antigens, was characterized according to the definition described by Mpande and colleagues (Mpande et al., 2021). Briefly, positive responders were classified as having relative counts of antigen-specific $IFN\text{-}\gamma^{+}TNF^{+}$ T cells (stimulated with ESAT-6/CFP-10) that were significantly higher than the unstimulated condition (p-value <0.01 by Fisher's exact test), and with a fold-change of $IFN\text{-}\gamma^{+}TNF^{+}$ T cell frequencies of three or more above unstimulated T cells. For investigation of T cell HLA-DR expression, only samples with 10 or more $IFN\text{-}\gamma^{+}TNF^{+}$ co-expressing T cells were considered for further analysis.

To investigate antigen-specific responses between cohorts, background subtraction was achieved by subtracting the frequencies of cytokine-positive unstimulated cells (i.e., the

“background” value) from the frequencies of the induced cellular responses (i.e., the cytokine-producing responses in each stimulated conditions) (Chapter 3, Equation 1a). The distribution around zero was computed by calculating the 80% CI for all negative values after background subtraction. All values falling within the lower and upper bounds of the 80% CI distribution around zero were set to zero.

Statistical analysis to compare antigen-specific responses between cohorts were performed using unpaired Wilcoxon rank sum test, with the Holm-Bonferroni test to control for multiple comparisons (q-values). Correlations between cell viability and frequencies of antigen-specific T cell responses were performed using Spearman’s rank correlation coefficient.

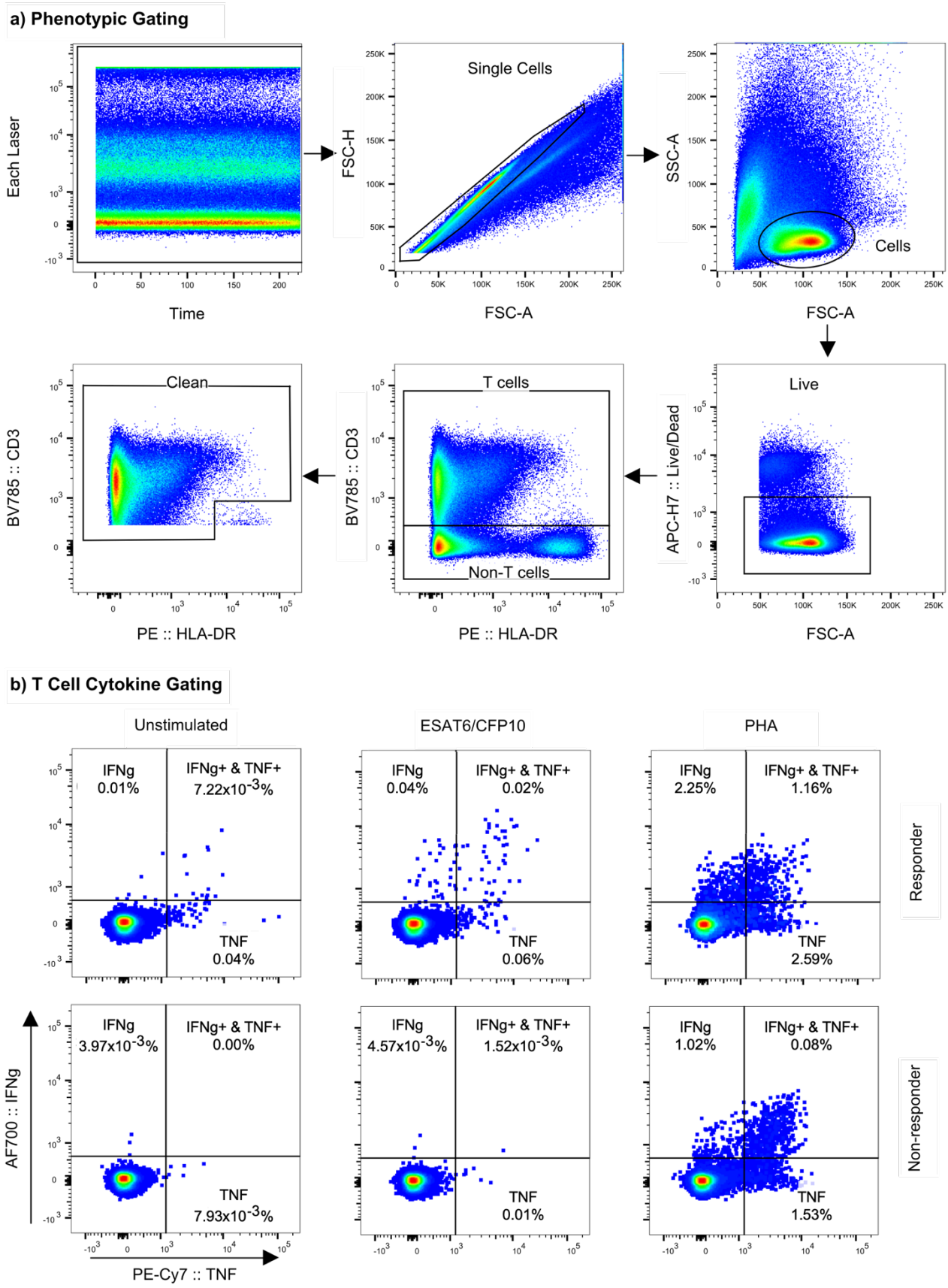

Figure 4.1: Gating strategy for flow cytometry ICS assay to quantify T cell responses to *Mtb* ESAT-6 and CFP-10 peptides. Flow charts describing the a) phenotypic gating strategy to identify T cells within PBMC from a representative donor. Live cells were identified after gating on time (time vs each laser) and single cells (FSC-H vs FSC-A and SSC-A vs FSC-A). T cells were identified by positive CD3 expression. Antigen-specific T cells were identified by b) IFN-γ and TNF cytokine gating. T cell cytokine expression by a representative responder and non-responder are shown.

CyTOF data analysis

For assessing the myeloid and lymphocyte immune subset composition across all tissues, total live, singlet cells were gated, and single FCS files were exported from FlowJo according to the strategy outlined in Chapter 2, Section 2.9 and Figure 2.2. The FCS files of total live cells were then imported into RStudio, and cells clustered using FAUST.

Thirteen lineage markers for assessing the composition of myeloid and lymphocyte subsets across tissue compartments were selected in a targeted approach to identify bulk populations of T cell subsets, myeloid cells, B cells and NK cells. The rationale for using a small subset of markers out of the large 44-marker panel was due to careful panel design to minimize signal spillover into channels containing subset-specific markers that are co-expressed, as discussed in Chapter 2, Section 2.6.1. Briefly, the CyTOF antibody panel was designed with the intent to maximize markers for NK and B cell phenotypic characterization, including several additional cell lineage markers for exclusion and/or analyses of the bulk immune tissue cell composition. Main lineage markers were assigned to channels with minimal spillover between one another to ensure that “pure” bulk populations could be reliably obtained. The remaining markers were assigned to NK and B cell-specific phenotyping markers that were intentionally and strategically allocated to only allow overlap between channels that are not co-expressed in NK and B cell subsets. Essentially, an NK-specific marker that, to the best of current knowledge, is not expressed on B cells was assigned to a channel that experienced spillover into or receiving from a B cell-specific marker, and vice versa. Due to this strategic design, the CyTOF panel was used to its maximum potential to fit the objectives of this study. However, with this approach to panel design, one should caution against running automated clustering algorithms using all markers within the full panel, as it is almost certain that technical artifacts exist in the data, potentially leading to false interpretations. Using knowledge of panel design and signal

spillover, myeloid and lymphoid immune cell populations across tissue compartments were investigated using a targeted selection of cell lineage and cytotoxic markers that experienced minimal to no spillover between one another, enabling reliable clustering.

To perform automated clustering and cell annotation using the FAUST algorithm, the depth score threshold was set to 0.075, selection quantile to 0.825 and the “nameOccuranceNum” parameter was set to 10. The “annotationsApproved” parameter was set to “TRUE” to instruct FAUST to run the method totally unsupervised. The FAUST algorithm was run using a selection of cell lineage markers and cytotoxic molecules (outlined in Table 4.2) as active channels for phenotypic annotation.

Table 4.2: CyTOF antibody panel for assessing the myeloid and lymphoid immune subset composition across tissue compartments.

Marker	Metal	Rationale	Clone	Antibody supplier
Extracellular (surface) markers				
CD3	*110Cd	T cells	UCHT1	BioLegend
CD4	*141Pr	T cells	RPA-T4	BioLegend
CD8a	*106Cd	T cells	RPA-T8	BioLegend
γδTCR	*151Eu	T cells	B1.1	BioLegend
CD33	*112Cd	Myeloid cells	WM53	BioLegend
CD11b	144Nd	Myeloid cells, NK maturation	ICRF44	Standard BioTools
CD14	151Eu	Monocytes	M5E2	Standard BioTools
CD16	209Bi	Monocytes, NK cells	3G8	Standard BioTools
CD56	149Sm	NK lineage	NCAM16.2	Standard BioTools
CD19	*164Dy	B cell lineage	HIB19	BioLegend
Intracellular (functional) markers				
Perforin	175Lu	Cytotoxic molecule	B-D48	Standard BioTools
Granzyme B	*168Er	Cytotoxic molecule	GB11	BioLegend
Granzyme K	*158Gd	Cytotoxic molecule	GM26E7	BioLegend

* In-house conjugated antibodies using Maxpar Antibody Labelling Kits (Standard BioTools).

The following markers were selected by FAUST to label cell phenotypes: CD3, CD4, CD8a, γδTCR, CD33, CD11b, CD14, CD56, CD19, perforin and granzyme B. Granzyme K and CD16 were not selected by FAUST as cell annotation markers, potentially due to relatively low expression levels across total cells and/or not being sufficiently bi- or multi-modal in distribution of expression on total live cells. Notably, clustering was performed on total live cells and $CD16^+$ granulocytes were not excluded prior. Using FAUST annotation, several cell subsets were investigated across tissues according to annotations described in Table 4.3. Frequencies of FAUST-clustered subsets were obtained by summing over counts for which cells shared common phenotypic annotations.

Table 4.3: Phenotypic definitions of immune cells in postmortem tissue compartments.

Cell Subset	Phenotypic Annotation
NK cells	$CD56^+CD19^-CD33^-CD14^-\gamma\delta TCR^-CD3^-$
B cells	$CD19^+CD33^-CD14^-\gamma\delta TCR^-CD3^-CD8a^-CD56^-$
Total T cells	$CD3^+CD19^-CD33^-$
CD4 T cells	$CD3^+CD4^+CD19^-CD33^-CD8a^-CD56^-CD14^-\gamma\delta TCR^-$
CD8 T cells	$CD3^+CD8a^+CD19^-CD33^-CD4^-CD56^-CD14^-\gamma\delta TCR^-$
NKT-like cells	$CD3^+CD56^+CD19^-CD33^-$
Tγδ cells*	$CD3^+\gamma\delta TCR^+CD14^+CD19^-CD33^-$
Myeloid cells	$CD33^+CD56^-CD19^-CD3^-$

* CD14 and γδTCR markers were included in the same channel for the CyTOF antibody panel and were therefore conjugated to the same metal isotope. This was done with the intent to maximize the number of markers included in the panel and is acceptable since CD14 and γδTCR are not co-expressed in a single cell subset. Therefore, the phenotypic annotation of Tγδ cells appearing to express $CD14^+$ is an intentional technical artifact. Monocytes and myeloid cells, typically expressing high levels of CD14, were accounted for by excluding CD33.

Expression values reported in this chapter are analogous to “median fluorescence intensity” (MFI) that are typically reported with flow cytometry. Since CyTOF does not measure fluorescence, a more appropriate term would be “median staining intensity” (MSI), which

reflects the relative expression levels of a given marker. Expression values for markers of interest were exported from expression matrices in R for FAUST-annotated subsets.

Statistical analysis to compare marker expression (MSI) and cell frequencies between cohorts was performed using unpaired Wilcoxon rank sum test for pair-wise comparisons with TB as the reference cohort, grouped by tissue compartment (i.e., PBMC, lung, hilar lymph node and spleen). Statistical comparisons were not performed for BAL samples, since there were too few datapoints in each cohort to reliably analyze. The Holm-Bonferroni test was used to control for multiple comparisons (q-values). Only results with q-values <0.25 are shown on graphs. No statistical comparisons were made between tissue compartments, only between cohorts (which were stratified by tissue type).

4.3 Results

4.3.1 Participant characteristics

Living participant validation cohort

Participant characteristics of living individuals in the PBMC flow cytometry ICS validation cohort have been detailed in Table 4.4, and are also available in the publication and accompanying online supplement for the 2021 study by Mpande and colleagues at SATVI (Mpande et al., 2021). Briefly, persistent QFT$^+$ participants (n=25) were HIV-uninfected male and female adolescents, between the ages of 14 and 16 years of age (median age was 15 years). Adult TB participants (n=25) were HIV-uninfected men and women between the ages of 21 and 42 years (median age of 32 years). Of the 25 persistent QFT$^+$ participants enrolled for the study, PBMC samples from 24 participants were analyzed due to exclusion of one participant who had low cell counts. Within the adult TB cohort, PBMC from 22 out of 25 enrolled participants were analyzed due to exclusion of three samples which had poor viability.

Table 4.4: Living participant validation cohort characteristics.

Cohort Definition	Persistent QFT$^+$	TB
Total participants enrolled, n	25	25
Age [range]	15 [14, 16]	32 [21, 42]
Sex, n (%)		
Female	12 (48%)	3 (12%)
Male	13 (52%)	22 (88%)
Ethnicity, n (%)		
Coloured	23 (92%)	14 (56%)
Black	2 (8%)	11 (44%)

Postmortem tissue cohort

Characteristics of decedents included in the postmortem cohort are detailed in Table 4.5. Deceased men and women were included in the study, with no exclusion criteria based on age, sex, or HIV status. Ethnicities of decedents remain unknown. Ten patients who succumbed to active TB disease were enrolled via consent by next-of-kin from the TB ward at the MNRH, Uganda. All TB patients had no known previous episodes of TB. Majority of TB cases were pulmonary TB: eight of ten decedents had active pulmonary TB disease, and two decedents had evidence of extrapulmonary TB. One pulmonary TB patient was also diagnosed with disseminated Kaposi's sarcoma (KS), associated with advanced HIV infection. This TB patient was not receiving TB treatment and had no information on record regarding antiretroviral (ARV) therapy. Kaposi's sarcoma is a condition characterized by multicentric neoplastic proliferation of vascular endothelial cells. Despite being infrequent worldwide, KS is the most common cancer in PLHIV in Africa (Dalla Pria et al., 2019). Two decedents were cases of extrapulmonary TB, one presenting with TB meningitis and one with abdominal TB. The patient with TB meningitis also had a hypertensive comorbidity, while the TB patient with abdominal TB had hypertension and diabetes comorbidities. Two pulmonary TB patients were hypertensive and one pulmonary TB patient had liver disease. Six TB patients had records of receiving anti-TB therapy for least 14 days prior to death. One pulmonary TB patient was not receiving TB treatment, and the deceased persons with extrapulmonary TB meningitis, abdominal TB, and pulmonary TB with HIV-associated disseminated KS were not on TB treatment prior to death.

Controls were otherwise healthy and died from trauma in the trauma/emergency units of the MNRH, Uganda. All healthy controls had negative BAL MGIT liquid culture test results (this test was not performed for decedents in the TB cohort). Healthy controls had no evidence of lung disease or characteristics of ill health prior to injury and death, or during autopsy.

The TSPOT assay was performed on PBMC from the 19 healthy controls, of which eight had a $TSPOT^+$ result and eight had a $TSPOT^-$ result. Three TSPOT results were indeterminate but were later classified as $TSPOT^-$ based on negative results from further investigation by an in-house flow cytometry ICS assay performed on cryopreserved postmortem PBMC (described in Section 4.3.2 below). The TSPOT assay was only performed in healthy controls and were not performed for the TB cohort.

There were no significant differences in age or sex between cohorts, although HIV status was skewed towards the TB cohort (6 of 7 HIV-infected individuals were TB decedents). This observation could be considered a feature of TB disease in PLHIV, since HIV infection is a known risk factor for advanced stages of TB disease and death (Bruchfeld et al., 2015). Five PLHIV had records of receiving antiretroviral therapy for a minimum of one month prior to death. However, two PLHIV had no information of ARV therapy on record, one of the decedents being the pulmonary TB case with HIV-associated disseminated KS, the other being classified as a $TSPOT^+$ control. All deceased persons within the $TSPOT^-$ cohort were HIV negative. Smoking ($p=5x10^{-3}$) and alcohol consumption ($p=3x10^{-3}$) were also skewed in the TB cohort, which are habits that have been associated as known risk factors for developing TB disease (Silva et al., 2018).

Autopsies were performed and single cell suspensions of tissue specimens were isolated on the same day as death (methods detailed in Chapter 2, Section 2.3). The postmortem interval (PMI) was measured as the time (in hours) from death to the time of counting cells immediately prior to cryopreservation. The median PMI for the $TSPOT^+$ cohort was 7 hours, was 6 hours for the $TSPOT^-$ cohort, and the TB cohort had a median PMI of 8.5 hours. The PMI in the TB cohort was significantly higher than healthy controls (Kruskal-Wallis rank sum test $p=0.02$; pairwise comparisons performed using Wilcoxon rank sum test: $TSPOT^-$ vs TB $p=0.01$; $TSPOT^+$ vs TB $p=0.03$; $TSPOT^-$ vs $TSPOT^+$ $p=0.76$).

Table 4.5: Postmortem tissue cohort characteristics.

Cohort Definition	TSPOT$^-$	TSPOT$^+$	TB	p-value[1]
Total decedents enrolled, n	11	8	10	-
Age [range]	39 [30, 55]	50 [39, 69]	40 [29, 45]	0.31
Post mortem interval (PMI, hours)[2] [range]	6 [5, 11]	7 [5, 9]	8.5 [6, 15]	0.02
Sex, n (%)				0.32
Female	5 (45%)	1 (12%)	3 (30%)	
Male	6 (55%)	7 (88%)	7 (70%)	
Smoking, n (%)				0.005
No	11 (100%)	8 (100%)	5 (50%)	
Yes	0 (0%)	0 (0%)	4 (40%)	
Unknown	0 (0%)	0 (0%)	1 (10%)	
Alcohol consumption, n (%)				0.003
No	11 (100%)	6 (75%)	3 (30%)	
Yes	0 (0%)	2 (25%)	4 (40%)	
Unknow	0 (0%)	0 (0%)	3 (30%)	
HIV status, n (%)				0.002
Negative	11 (100%)	7 (88%)	4 (40%)	
Positive	0 (0%)	1 (12%)	6 (60%)	
TSPOT result				
Negative	8 (73%)	8 (100%)	NA	
Positive	0 (0%)	0 (0%)	NA	
Indeterminate[3]	3 (27%)	0 (0%)	NA	
Cause of death in non-TB patients, n (%)				
Acute kidney injury	0 (0%)	1 (12%)	NA	
Abdominal injury	0 (0%)	1 (12%)	NA	
Head injury	9 (82%)	4 (50%)	NA	
Head injury with severe anaemia	1 (9.1%)	1 (12%)	NA	
Head and abdominal injury	1 (9.1%)	1 (12%)	NA	
TB status, n (%)				
Abdominal TB	NA	NA	1 (10%)	
TB meningitis	NA	NA	1 (10%)	
Pulmonary TB	NA	NA	7 (70%)	
Pulmonary TB with disseminated KS in HIV	NA	NA	1 (10%)	

Table 4.5 (continued): Postmortem tissue cohort characteristics.

Cohort Definition	TSPOT-	TSPOT+	TB	p-value[1]
TB treatment, n (%)				
2RHZE/4RH	NA	NA	4 (40%)	
BDQ-LZD-LFX-CFZ-CS	NA	NA	2 (20%)	
Not on medication	NA	NA	4 (40%)	
Duration of TB treatment[4], n (%)				
<1 month	NA	NA	3 (30%)	
>=2 months	NA	NA	3 (30%)	
No information/ not on medication	NA	NA	4 (40%)	
HIV treatment (ARV therapy), n (%)				
TDF-3TC-DTG	NA	0 (0%)	4 (40%)	
Atazanavir/ritonavir + lamivudine/zidovudine	NA	0 (0%)	1 (10%)	
No information	NA	1 (12%)	1 (10%)	
Duration of ARV therapy[5], n (%)				
<6 months	NA	0 (0%)	3 (30%)	
6 months-10 years	NA	0 (0%)	2 (20%)	
No information	NA	1 (12%)	1 (10%)	
Other co-morbidities, n (%)				
Hypertension	Unknown	Unknown	3 (30%)	
Hypertension and diabetes	Unknown	Unknown	1 (10%)	
Liver disease	Unknown	Unknown	1 (10%)	
Samples collected, n				
PBMC	11	8	10	
Lung (left upper lobe)	10	8	10	
Hilar lymph nodes	7	6	8	
BAL	7	2	4	
Spleen	7	6	8	

[1] Kruskal-Wallis rank sum test; Fisher's exact test.
[2] Postmortem interval (PMI) calculated from time of death to counting cells immediately prior to cryopreservation, measured in hours post-death.
[3] Indeterminate TSPOT results were classified as $TSPOT^-$ based on negative results from further investigation by a flow cytometry ICS assay performed on cryopreserved postmortem PBMC.
[4] Decedents of TB disease who were on treatment received drug therapy for least 14 days prior to death. One pulmonary TB patient was not receiving any TB treatment, and the deceased persons with TB meningitis, abdominal TB, and pulmonary TB with HIV-associated disseminated KS were not on TB treatment prior to succumbing to disease.
[5] Decedents who were HIV positive and on ARVs received drug therapy for at least 1 month prior to death. The HIV/TB patient with no ARV information was the pulmonary TB case of HIV-associated disseminated KS, and the other PLHIV with no ARV information being classified as a $TSPOT^+$ control.

Table 4.5 (continued): Postmortem tissue cohort characteristics.

Abbreviations:
HIV = human immunodeficiency virus
KS = Kaposi's sarcoma
ARV = antiretroviral
2RHZE/4RH = 2 months treatment with rifampin + isoniazid + pyrazinamide + ethambutol, followed by 4 months treatment with rifampin + isoniazid (standard 6 month drug-sensitive TB treatment regimen)
BDQ-LZD-LFX-CFZ-CS = bedaquiline + linezolid + levofloxacin + clofazimine + cycloserine
TDF-3TC-DTG = tenofovir + lamivudine + dolutegravir
PBMC = peripheral blood mononuclear cells
BAL = bronchoalveolar lavage

Control tonsils from living participants included HIV-uninfected individuals, four being female and one being male, who were clinically indicated for tonsillectomy. None of the participants were suspected TB cases or were diagnosed with TB. No information was provided regarding age, ethnicity, co-morbidities, and/or other clinical diagnoses.

4.3.2 T cell responses to *Mtb* peptides distinguishes between TSPOT^{-} and TSPOT^{+} in postmortem samples

A SATVI in-house flow cytometry ICS assay to detect T cell responses to *Mtb* peptides (ESAT-6 and CFP-10) (Mpande et al., 2021) was used as a secondary check for the TSPOT assay performed by our collaborating research group in Uganda. Results of TSPOT and flow cytometry ICS assays are detailed in Table 4.6.

Table 4.6: TSPOT and flow cytometry ICS results.

Group	TSPOT^{-} (n=11)	TSPOT^{+} (n=8)	TB (n=10)
Flow cytometry ICS result*			
Responders, n	0	4	2
Non-responders, n	11	4	8
TSPOT result			
Positive	0	8	NA
Negative	8	0	NA
Indeterminate	3	0	NA

* All participants had significant responses to the PHA positive control: the median fold-change of IFN-γ^{+}TNF^{+} T cell frequencies above unstimulated T cells was 800 (range 4-11674), and relative counts of antigen-specific IFN-γ^{+}TNF^{+} T cells (stimulated with PHA) were significantly higher than the unstimulated condition, with a median p-value of 2.58×10^{-263}.

The TSPOT assay yielded three indeterminate results, which were assigned to the TSPOT^{-} cohort based on negative results from the flow cytometry ICS assay (Table 4.6). Four participants within the TSPOT^{+} cohort were classified as non-responders according to the definition of *Mtb*-antigen responders by Mpande and colleagues (Mpande et al., 2021). Since the T-SPOT®.TB assay (Oxford Immunotec) is an FDA-approved, commercially available diagnostic test, it was decided that cohort classification would be based on TSPOT results, with the exception of the indeterminate TSPOT results for which the flow cytometry ICS data were used for classification. Interestingly, majority of participants with clinically diagnosed TB were classified as non-responders (eight of ten TB decedents were classified as non-responders, Table 4.6). All participants responded strongly to the PHA positive control: the median fold-change of IFN-γ+TNF+ T cell frequencies above unstimulated T cells was 800 (range 4-11674), and relative counts of antigen-specific IFN-γ+TNF+ T cells (stimulated with PHA) were significantly higher than the unstimulated condition, with a median p-value of 2.58×10^{-263}. Therefore, the PHA positive control in the flow cytometry ICS assay performed well and no results were classified as indeterminate.

The finding that half of the TSPOT$^+$ cohort and most TB decedents were classified as non-responders was surprising, since these groups had evidence of *Mtb*-immunological sensitization and clinical TB disease, respectively. Therefore, the magnitudes of *Mtb*-specific T cell responses measured using the flow cytometry ICS assay were investigated further (Figure 4.2). Firstly, PBMC obtained postmortem tended to have lower viabilities than what is usually reported from living individuals, which may affect functional responses. Thus, frequencies of antigen-specific IFN-γ^+TNF$^+$ T cells were correlated with frequencies of viable cells to assess whether there was a relationship between cytokine responses and cell death. Secondly, using publicly available data from the cohorts of QFT$^+$ participants and TB patients from Mpande et al., T cell antigen-specific responses were compared between living and postmortem samples to evaluate whether cellular functional responses were lower in PBMC harvested after death. Lastly, the 2021 study by Mpande and colleagues showed that *Mtb*-specific T cell functions measured by the flow cytometry ICS assay distinguished between QFT$^-$ and QFT$^+$ individuals, but not between QFT$^+$ and active TB. It was therefore hypothesized that frequencies of *Mtb*-specific IFN-γ^+TNF$^+$ T cells will differentiate between the TSPOT$^+$ and TSPOT$^-$ individuals in the postmortem cohort.

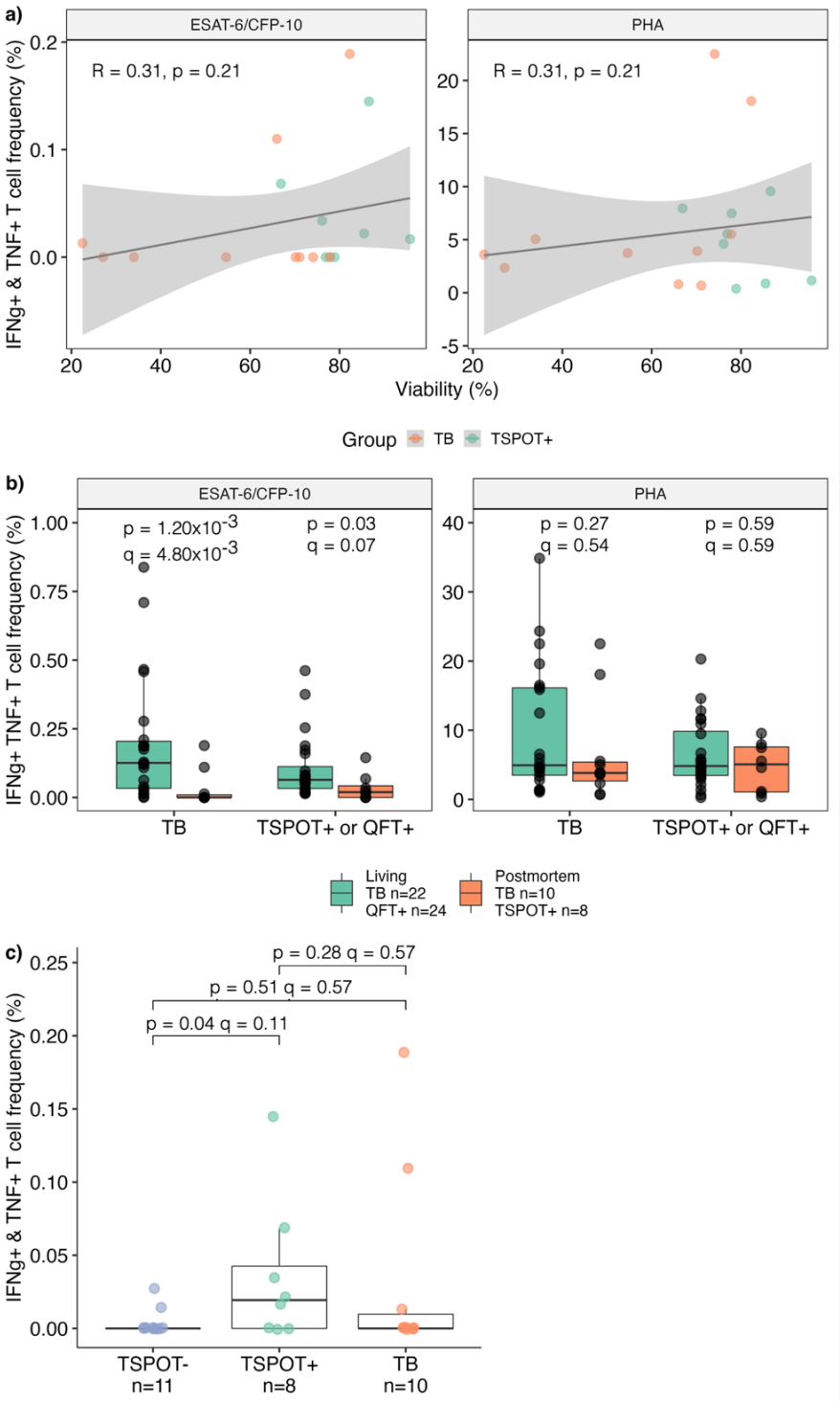

Figure 4.2: *Mtb*-specific T cell responses in PBMC obtained postmortem. a) Correlations between cell viability and frequencies of IFN-γ^{+}TNF^{+} T cells responding to ESAT-6 and CFP-10 peptides (left panel) and PHA mitogen (right panel). b) Frequencies of IFN-γ^{+}TNF^{+} T cells responding to ESAT-6 and CFP-10 peptides (left panel) and PHA mitogen (right panel) compared between living and postmortem cohorts, stratified according to clinical status: active TB disease, TSPOT^{+} (postmortem samples) and QFT^{+} (living cohort samples). c) Frequencies of IFN-γ^{+}TNF^{+} T cells responding to ESAT-6 and CFP-10 peptides, comparing *Mtb*-specific responses between cohorts in PBMC obtained postmortem. Statistical analysis in a) was performed using Spearman's rank correlation coefficient. Statistical analysis in a) and c) was performed using unpaired Wilcoxon rank sum test for pair-wise comparisons between living and postmortem cohorts (a) and pair-wise comparisons between TB and healthy cohorts (b) (p-values). The Holm-Bonferroni test was used to account for multiple comparisons (q-value). Each box represents median and interquartile range, whiskers indicate 1.5x IQR of the upper and lower quartiles.

T cell responses were not strongly correlated with cell viability (ESAT-6/CFP-10 R=0.31, p=21; PHA R=0.14, p=0.57; Figure 4.2a), suggesting that low *Mtb*-specific responses observed in $TSPOT^+$ and TB cohorts were not associated with degree of cell death. However, frequencies of IFN-γ^+TNF^+ T cells responding to ESAT-6 and CFP-10 peptides were significantly lower in postmortem samples relative to the living cohort (TB $p=1.20x10^{-3}$, $q=4.80x10^{-3}$; $TSPOT^+$ or QFT^+ p=0.03, q=0.07; Figure 4.2b). No significant differences were observed in PHA responses between postmortem and living cohorts. These data suggest that while postmortem T cells were responsive and functional, *Mtb*-specific responses may have been dampened postmortem. Additionally, the difference between T cell responses in postmortem TB versus living TB patients was more significant ($p=1.20x10^{-3}$, $q=4.80x10^{-3}$) compared to the difference observed between postmortem and living healthy controls (p=0.03, q=0.07; Figure 4.2b), and no differences were observed in PHA responses. Therefore, those who died with TB disease may have had hyporesponsive *Mtb*-specific T cells that may have become exhausted, which was not evident with living TB patients at baseline diagnosis or in healthy controls with evidence of immunological sensitization to *Mtb*. Despite the lower *Mtb*-specific T cell responses postmortem, frequencies of *Mtb*-specific T cells successfully distinguished between $TSPOT^-$ and $TSPOT^+$ (p=0.04, q=0.11), but not between $TSPOT^+$ or $TSPOT^-$ and TB (p>0.05; Figure 4.2c) in PBMC obtained postmortem, as hypothesized.

4.3.3 ΔHLA-DR MFI distinguishes between TB and $TSPOT^+$ in postmortem samples

Several publications have described a biomarker that measures the activation level of *Mtb*-specific T cells (by means of HLA-DR expression) that successfully distinguishes between TB patients and *Mtb*-sensitized controls (Adekambi et al., 2015; Wilkinson et al., 2016; Riou et al., 2017; Musvosvi et al., 2018; Riou et al., 2020; Mpande et al., 2021). Mpande and colleagues at SATVI also showed that *Mtb*-specific T cell ΔHLA-DR MFI distinguished

between remote and recent *Mtb* infection and was increased during progression to TB disease in a cohort of adolescents who progressed to active disease relative to non-progressing controls who were followed up over two years (Mpande et al., 2021). The ΔHLA-DR MFI biomarker was, therefore, proposed as a correlate of bacterial load (Mpande et al., 2021; Musvosvi et al., 2018; Riou et al., 2020). Based on our previous findings in living cohorts at SATVI, it was hypothesized that the ΔHLA-DR MFI biomarker on *Mtb*-specific IFN-γ^{+}TNF^{+} T cells will distinguish between postmortem TB and TSPOT^{+} samples (Figure 4.3).

Consistent with the biomarker definition by Mpande et al., ΔHLA-DR MFI on *Mtb*-specific IFN-γ^{+}TNF^{+} T cells successfully distinguished between TB and TSPOT^{+} in postmortem samples ($p=6.70x10^{-4}$; Figure 4.3a, right panel). Data from the living cohort of Mpande et al., 2021 were plotted for comparison (Figure 4.3a, left panel). The finding that no significant differences were observed between TB and TSPOT^{+} individuals for ΔHLA-DR MFI expression of T cells responding to PHA (Figure 4.3b), suggests that this biomarker is *Mtb*-specific and appropriate for use in living participants and samples obtained postmortem.

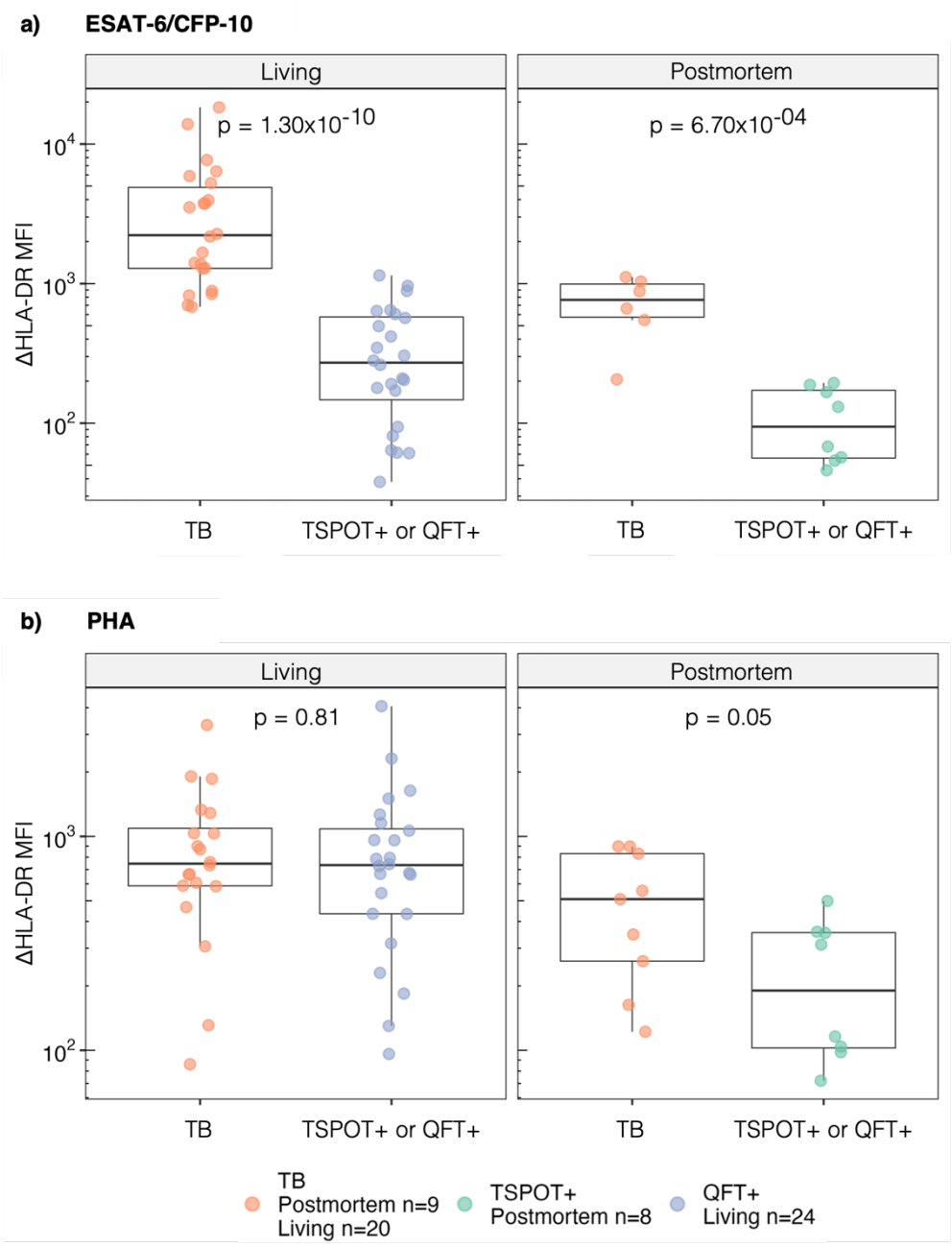

Figure 4.3: ΔHLA-DR MFI on *Mtb*-specific IFN-γ^+TNF$^+$ T distinguishes between TB and TSPOT$^+$ in PBMC obtained postmortem. Comparisons of the ΔHLA-DR MFI biomarker to distinguish between TB and TSPOT$^+$ in postmortem samples (right panels), and TB and QFT$^+$ in the living cohort (left panels), for T cells responding to a) *Mtb*-specific ESAT-6 and CFP-10 peptides, and b) the PHA mitogen. Statistical analyses were performed using unpaired Wilcoxon rank sum test to compare TB and healthy cohorts (p-value). Each box represents median and interquartile range (IQR), whiskers indicate 95% confidence intervals.

4.3.4 The myeloid and lymphocyte composition of postmortem tissue compartments

The immune cell composition of different tissue compartments was assessed by identifying cell subsets according to the phenotypic definitions described in Table 4.3. Since NK and B cells were the main subsets of investigation for the designed CyTOF panel, bulk NK and B cell populations were manually gated in FlowJo and imported into RStudio to perform further deep phenotypic analyses (Chapter 5). The rationale for manual gating of NK and B cell subsets was to obtain clean, bulk populations of the cells of interest, according to the current gold standard of cell annotation. Since frequencies of NK and B cells were available from manual gating, it was possible to validate frequencies of FAUST-annotated NK and B cells against manual gating (Figure 4.4).

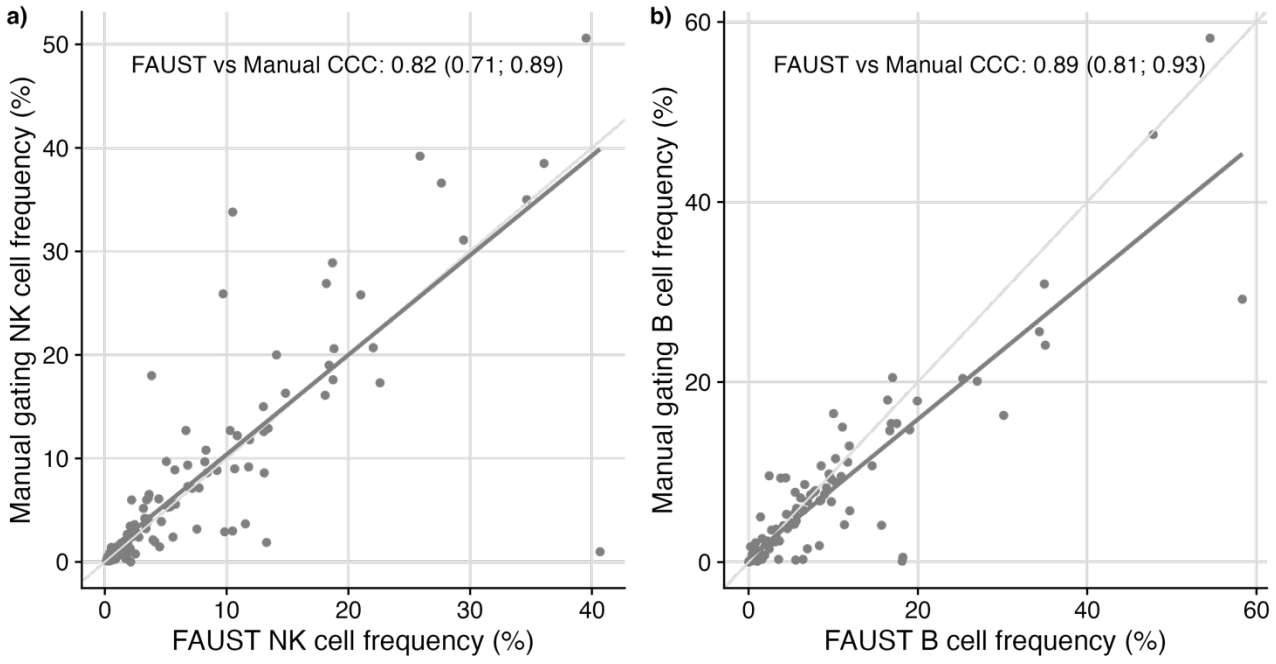

Figure 4.4: NK and B cell frequencies obtained by manual gating correlated against frequencies obtained using FAUST annotation. Manually gated a) NK cell and b) B cell frequencies were highly correlated with FAUST-annotated frequencies. Manually gated NK cells were phenotypically classified as $CD56^{+}CD19^{-}CD33^{-}CD21^{-}CD14^{-}\gamma\delta TCR^{-}CD3^{-}IgD^{-}$, FAUST-annotated NK cells were identified as $CD56^{+}CD19^{-}CD33^{-}CD14^{-}\gamma\delta TCR^{-}CD3^{-}$. Manually gated B cells were phenotypically classified as $CD19^{+}CD33^{-}CD14^{-}\gamma\delta TCR^{-}CD3^{-}CD8a^{-}CD56^{-}CD57^{-}$, FAUST-annotated B cells were identified as $CD19^{+}CD33^{-}CD14^{-}\gamma\delta TCR^{-}CD3^{-}CD8a^{-}CD56^{-}$. Numeric values correspond to the FASUT vs manual gating concordance correlation coefficients (CCC), values in brackets represent the 95% confidence intervals.

Frequencies of manually gated NK cells (CCC = 0.82) and B cells (CCC = 0.89) were highly correlated with frequencies of FAUST-annotated populations (Figure 4.4), giving confidence in the reliable annotation of cell subsets by unsupervised, automated clustering using the FAUST algorithm. Since not all cell populations were manually gated (such as T cell subsets and myeloid cells), it remains possible that some cell subsets may not have correlated well. However, FAUST performed extremely well to cluster NK and B cells which supports the belief that other cell phenotypes were also reliably annotated, unless the markers that define those subsets performed poorly (which is unlikely given the extensive efforts for optimal panel design and staining optimization). To further assess the performance of automated annotation by FAUST, the relative expression of phenotypic markers used to classify specific cell subsets were assessed by means of a heatmap (Figure 4.5).

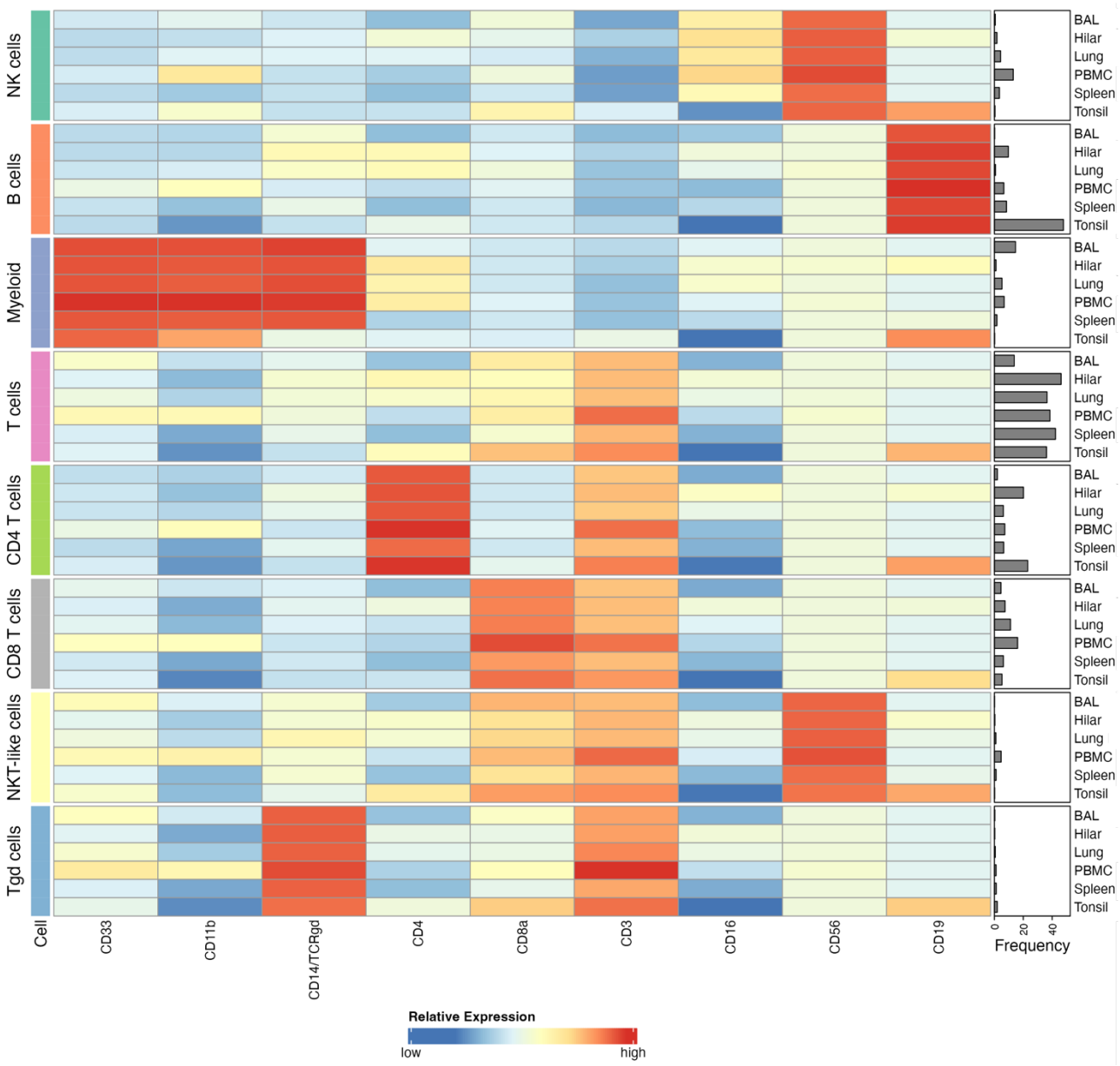

Figure 4.5: Relative expression heatmap of phenotypic markers to identify cells of the myeloid and lymphocyte immune cell composition across tissues. Relative expression (median staining intensity, MSI) values for each phenotypic marker (columns) of FAUST-annotated cell subsets (rows) across tissues (coloured group annotation left axis). Median frequencies of each subset within tissue compartments are displayed as the right-hand bar graph annotation.

Relative expression values (MSI) for each phenotypic marker of each cell subset corresponded to the definitions used to identify FAUST-annotated populations (Figure 4.5), again echoing the confidence with which results are reported using automated, unsupervised FAUST clustering. Frequencies of cell populations and subsets are detailed in Figure 4.6 and Table 4.7, to give an overview of the myeloid and lymphoid immune cell composition across human tissue compartments.

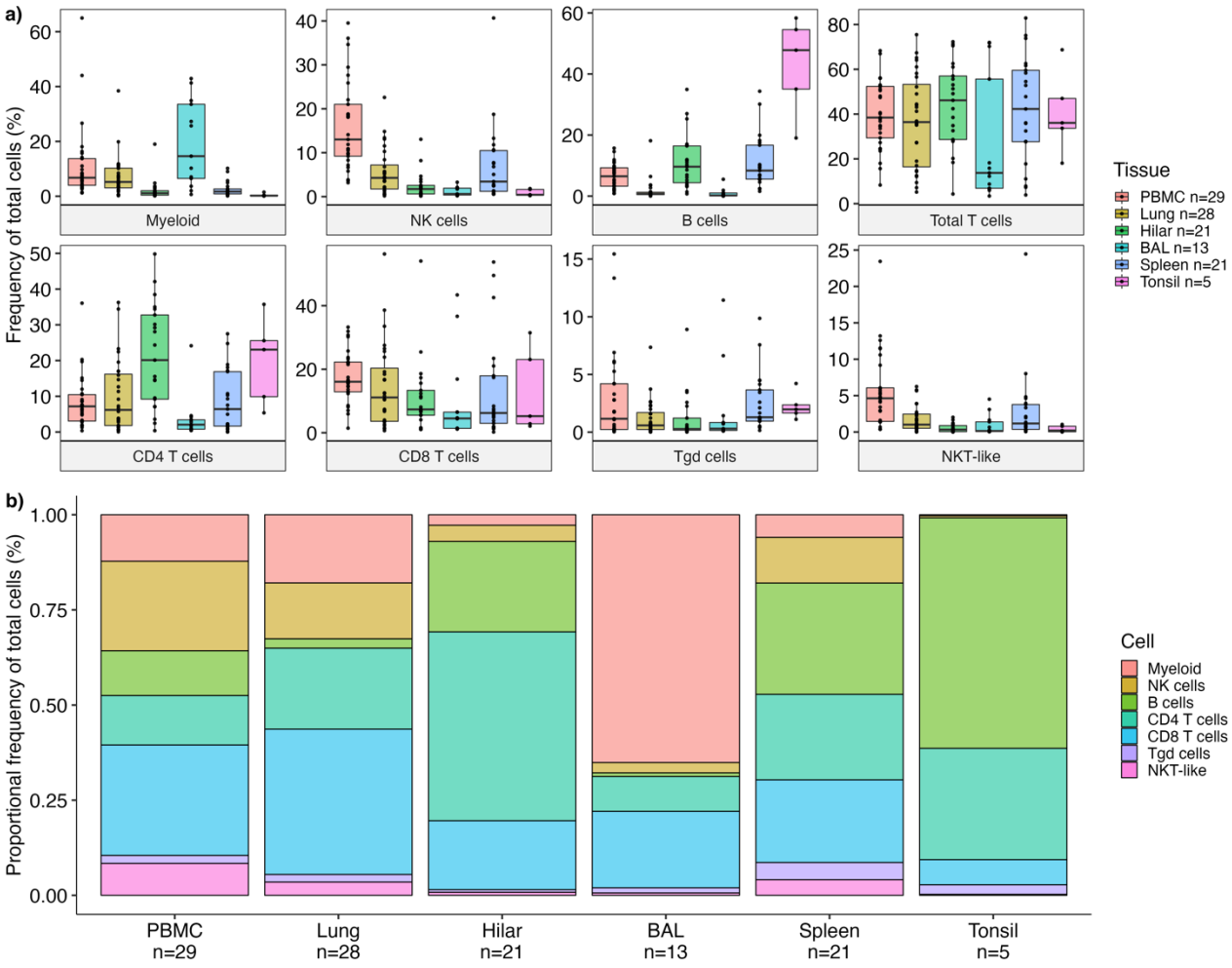

Figure 4.6: Frequencies of immune cell subsets across human tissue compartments. a) Absolute and b) proportional frequencies of immune cell populations, reported as a proportion of total live cells in the tissues. In boxplots, each box represents median and interquartile range (IQR), whiskers indicate 1.5x IQR of the upper and lower quartiles.

Table 4.7: Frequencies of immune cell subsets across human tissue compartments.

Cell subset	PBMC[1]	Lung[1]	Hilar Lymph Nodes[1]	BAL[1]	Spleen[1]	Tonsil[1, 2]
Myeloid cells	6.75 (4.00, 13.73)	5.22 (3.06, 10.25)	1.11 (0.39, 2.02)	14.62 (6.49, 33.55)	1.70 (0.85, 2.65)	0.20 (0.14, 0.38)
NK cells	13.02 (9.21, 21.02)	4.27 (1.73, 7.20)	1.73 (0.61, 2.56)	0.61 (0.36, 1.92)	3.43 (1.21, 10.49)	0.42 (0.35, 1.64)
B cells	6.50 (3.24, 9.28)	0.72 (0.49, 1.26)	9.63 (4.39, 16.43)	0.21 (0.09, 1.03)	8.35 (5.56, 16.69)	47.80 (35.06, 54.52)
Total T cells	38.44 (29.34, 52.38)	36.43 (16.43, 53.28)	46.15 (28.63, 57.02)	13.72 (6.88, 55.64)	42.29 (27.66, 59.56)	36.08 (33.67, 46.98)
CD4 T cells	7.18 (3.07, 10.46)	6.19 (1.81, 16.19)	20.12 (9.19, 32.76)	2.06 (0.79, 3.41)	6.42 (1.65, 16.90)	23.07 (9.90, 25.57)
CD8 T cells	16.05 (12.88, 22.26)	11.11 (3.60, 20.35)	7.35 (5.51, 13.35)	4.51 (1.38, 6.49)	6.21 (2.97, 17.93)	5.23 (2.84, 23.06)
T$\gamma\delta$ cells	1.16 (0.23, 4.19)	0.59 (0.23, 1.70)	0.27 (0.17, 1.22)	0.30 (0.15, 0.84)	1.29 (0.95, 3.66)	1.97 (1.66, 2.37)
NKT-like cells	4.63 (1.46, 6.07)	1.01 (0.52, 2.46)	0.33 (0.05, 0.88)	0.14 (0.08, 1.40)	1.17 (0.36, 3.78)	0.20 (0.03, 0.80)

[1] Frequency of total live cells (%): Median (IQR; interquartile range).

[2] Tonsil tissues were from living donors, while PBMC, lung, hilar lymph nodes, BAL and spleen were sampled postmortem.

The lung compartment was found to comprise mostly CD4 T cells (~6%), CD8 T cells (~11%) and myeloid cells (~5%), with a smaller yet substantial NK cell population (~4%). The hilar lymph nodes were comprised mainly of CD4 T cells (~20%), CD8 T cells (~7%) and B cells (~10%), while the BAL predominantly contained myeloid cells (~14%). The spleen had substantial populations of B cells (~8%), CD4 T cells (~6%), CD8 T cells (~6%) and NK cells (~3%). Tonsils from living participants were comprised almost exclusively of B cells (~48%) and CD4 T cells (~23%) (Figure 4.6). Frequencies and relative proportions of immune cell subsets reported for PBMC (Figure 4.6) were consistent with previously published literature, except for CD4 T cells which had lower frequencies. Total T cells were the most abundant cell population in the PBMC, as expected. However, results indicated that CD8 T cells (~16%) were the most abundant T cell subset in the peripheral blood, rather than CD4 T cells (~7%).

4.3.5 HIV-associated depletion of CD4 T cells occurs in peripheral blood and tissues

Since HIV infects and depletes CD4 T cells in the peripheral blood and tissue compartments, such as the lymph nodes, gastrointestinal tract, and BAL (Brenchley et al., 2004; Kalsdorf et al., 2009), it was hypothesized that HIV infection may be a confounding factor to the CD4 T cell populations reported in this postmortem study. Additionally, it has been documented that chronic infection and inflammatory diseases (including TB) alter myelopoiesis and lymphopoiesis, resulting in perturbations to peripheral cellular compartments during disease (Baldridge et al., 2010, 2011; Naranbhai et al., 2014; Scriba et al., 2017). It was therefore hypothesized that immune cell subsets, specifically T cell subsets, NK cells and B cells, are depleted in the peripheral blood during TB disease as a feature of infection and inflammation. The depletion of cell subsets in the peripheral blood was hypothesized to be accompanied by a significant increase in the frequencies of immune cells in the tissues, particularly the lung, as a feature of immune cell trafficking and homing to the tissues where

Mtb infection occurs. Figure 4.7 illustrates frequencies of CD4 T cells across postmortem tissue compartments stratified by HIV status.

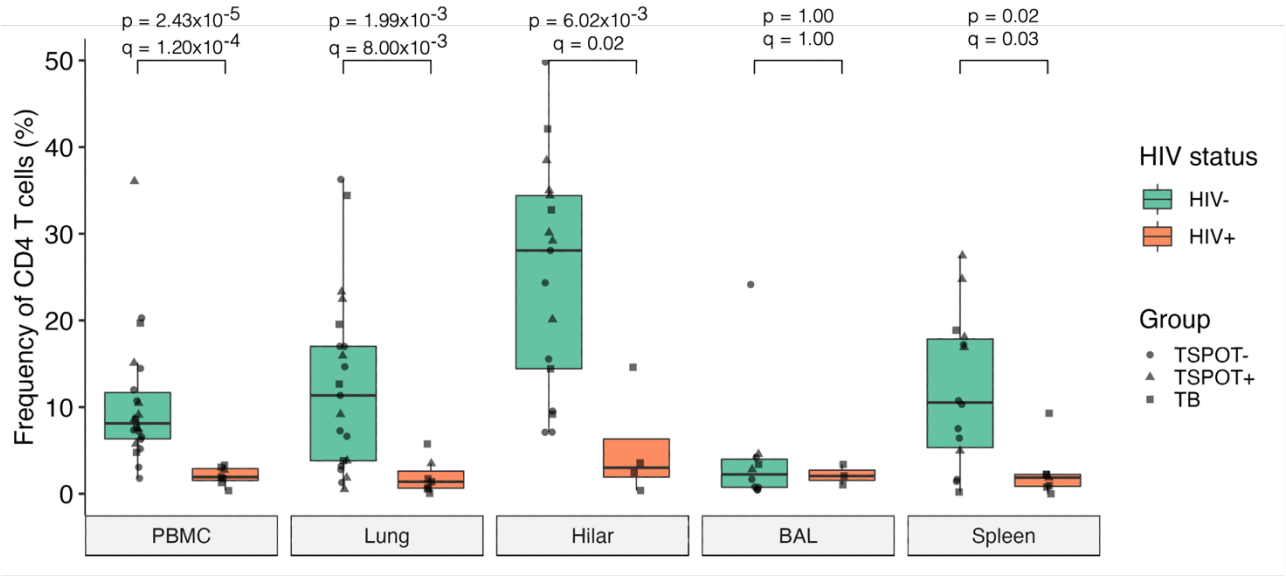

Figure 4.7: HIV-associated depletion of CD4 T cell frequencies across tissues. CD4 T cell frequencies across postmortem tissue compartments stratified according to HIV status. Statistical analysis was performed using unpaired Wilcoxon rank sum test for pair-wise comparisons between HIV groups (p-values). The Holm-Bonferroni test was used to account for multiple comparisons (q-value). In boxplots, each box represents median and interquartile range, whiskers in indicate 1.5x IQR of the upper and lower quartiles.

CD4 T cell frequencies were depleted in the peripheral blood, lungs, hilar lymph nodes and spleen of decedents with HIV infection relative to those who were HIV-uninfected (Figure 4.7). CD4 T cell frequencies in the BAL were not different between HIV^+ and HIV^- cohorts (Figure 4.7) and no other immune cell subsets (including total T cells, CD8 T cells, T$\gamma\delta$ cells, NKT-like cells, NK cells, B cells, and myeloid cells) had significantly different frequencies between HIV-infected and uninfected decedents (Figure 4.8). No immune cell subsets were significantly different between TB and healthy cohorts in peripheral blood or other tissue compartments (Figure 4.9).

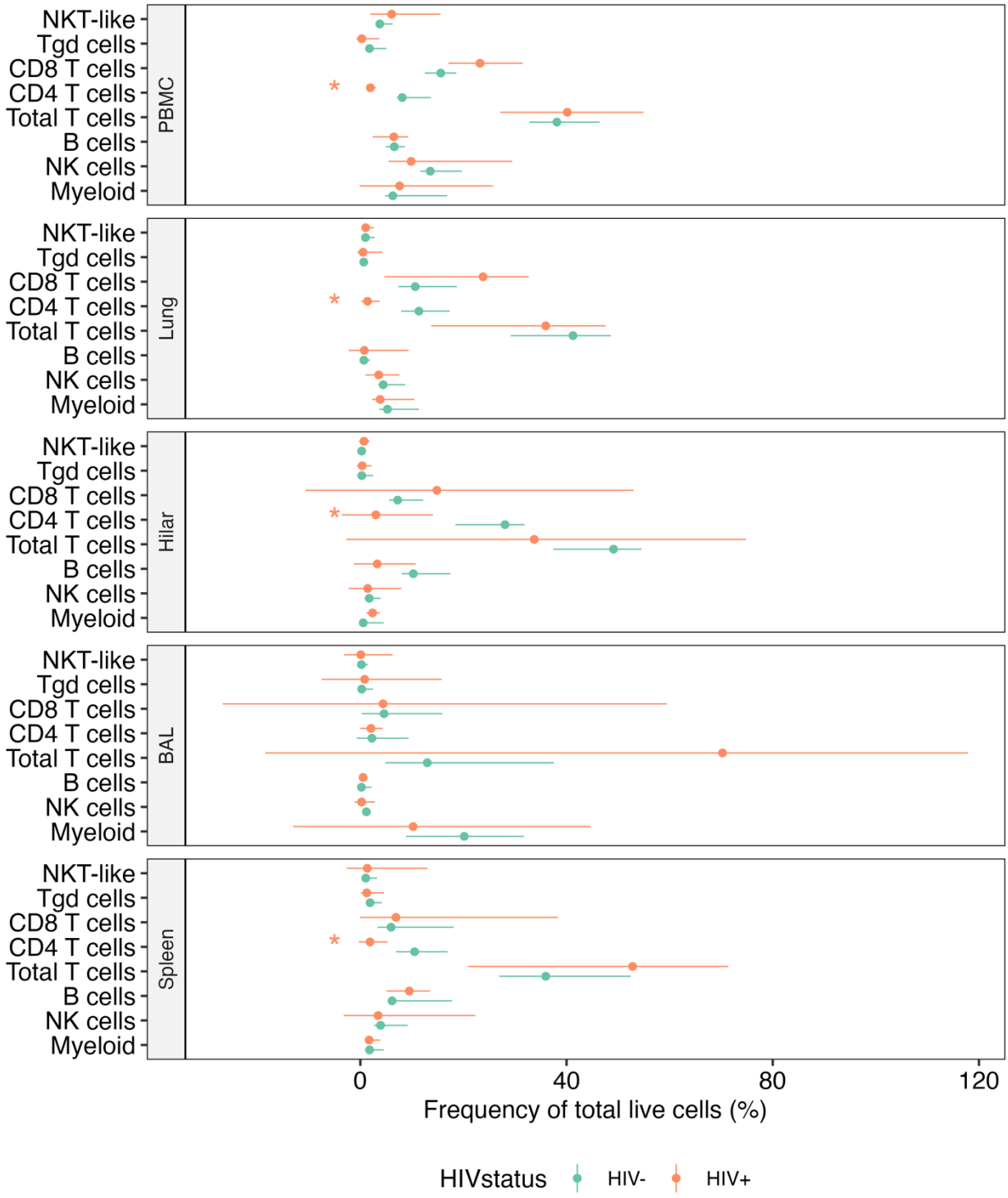

Figure 4.8: Frequencies of immune cell subsets stratified by HIV status across human tissue compartments. Frequencies obtained by summing over cell counts sharing common FASUT-annotated expressions according to Table 4.3. Statistical analysis was performed using unpaired Wilcoxon rank sum test for pair-wise comparisons between HIV^+ and HIV^- individuals (p-value), and the Holm-Bonferroni test to account for multiple comparisons (q-value). Each dot represents median frequency, whiskers indicate 95% confidence intervals. Stars (*) indicate statistically significant differences observed between HIV^- and HIV^+ individuals for CD4 T cells, detailed further in Figure 4.7.

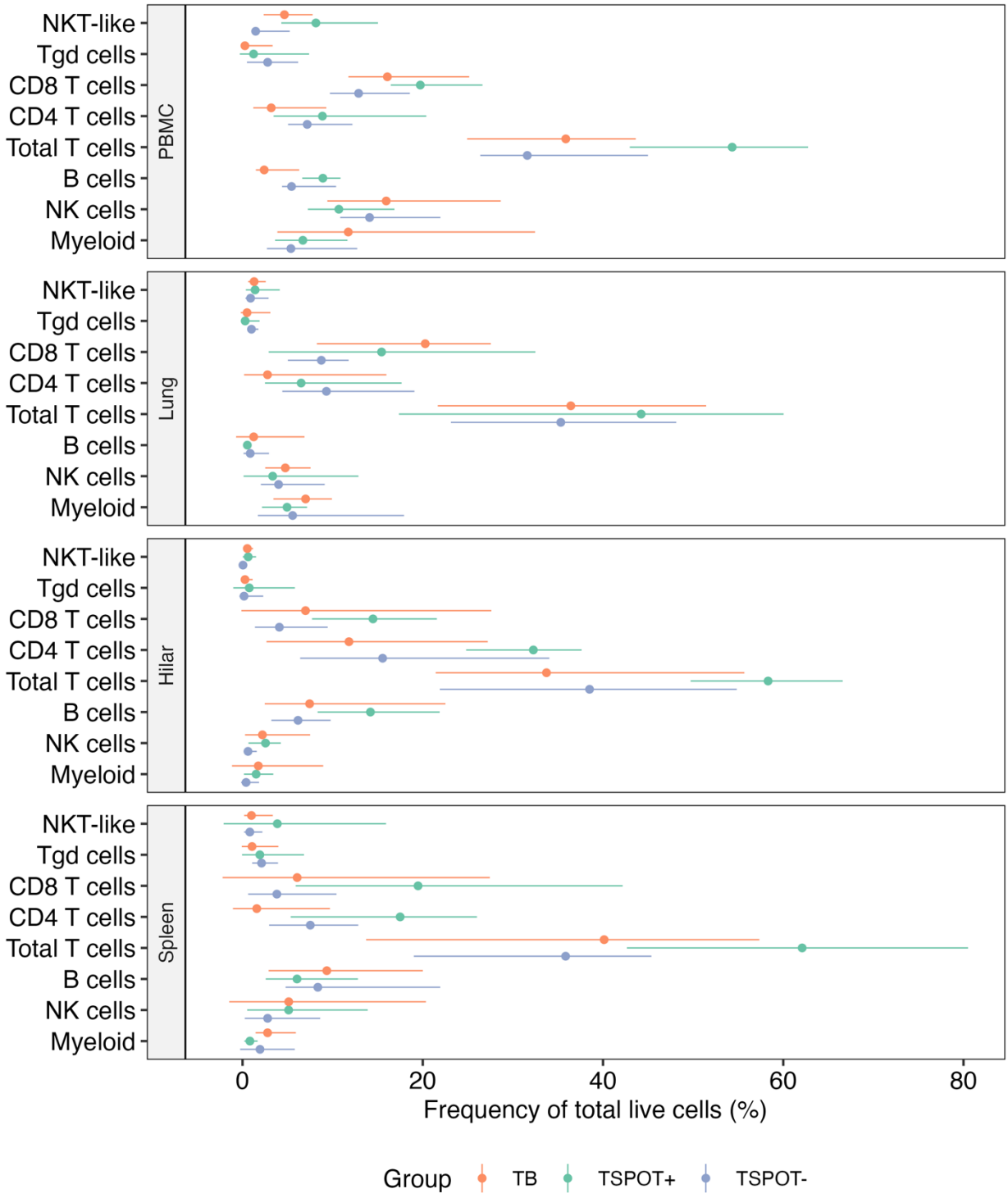

Figure 4.9: Frequencies of immune cell subsets stratified by TB disease and healthy cohorts across tissue compartments. Frequencies obtained by summing over cell counts sharing common FASUT-annotated expressions according to Table 4.3. Statistical analysis was performed using unpaired Wilcoxon rank sum test for pair-wise comparisons with TB as the reference group (p-value), and the Holm-Bonferroni test to account for multiple comparisons (q-value). Each dot represents median frequency, whiskers indicate 95% confidence intervals.

4.3.6 Cytotoxic marker-expressing cells are enriched in the hilar lymph nodes during TB

During *Mtb* infection, immune cells become activated and exert effector functions. It was hypothesized that during TB disease, immune cells expressing cytotoxic molecules are enriched in the peripheral blood and tissues as a possible reflection of immune activation. Previous literature has not clearly described the distribution of cytotoxic functions across the main cytotoxic immune cell subsets (including, NK cells, total T cells, CD4 T cells, CD8 T cells, NKT-like cells and T$\gamma\delta$ cells), and it is possible that TB disease alters cytotoxic functions in some but not all subsets. Hence, frequencies of total cytotoxic marker-expressing cells were assessed (Figure 4.10) by summing over total cells expressing one or both of perforin and/or granzyme B.

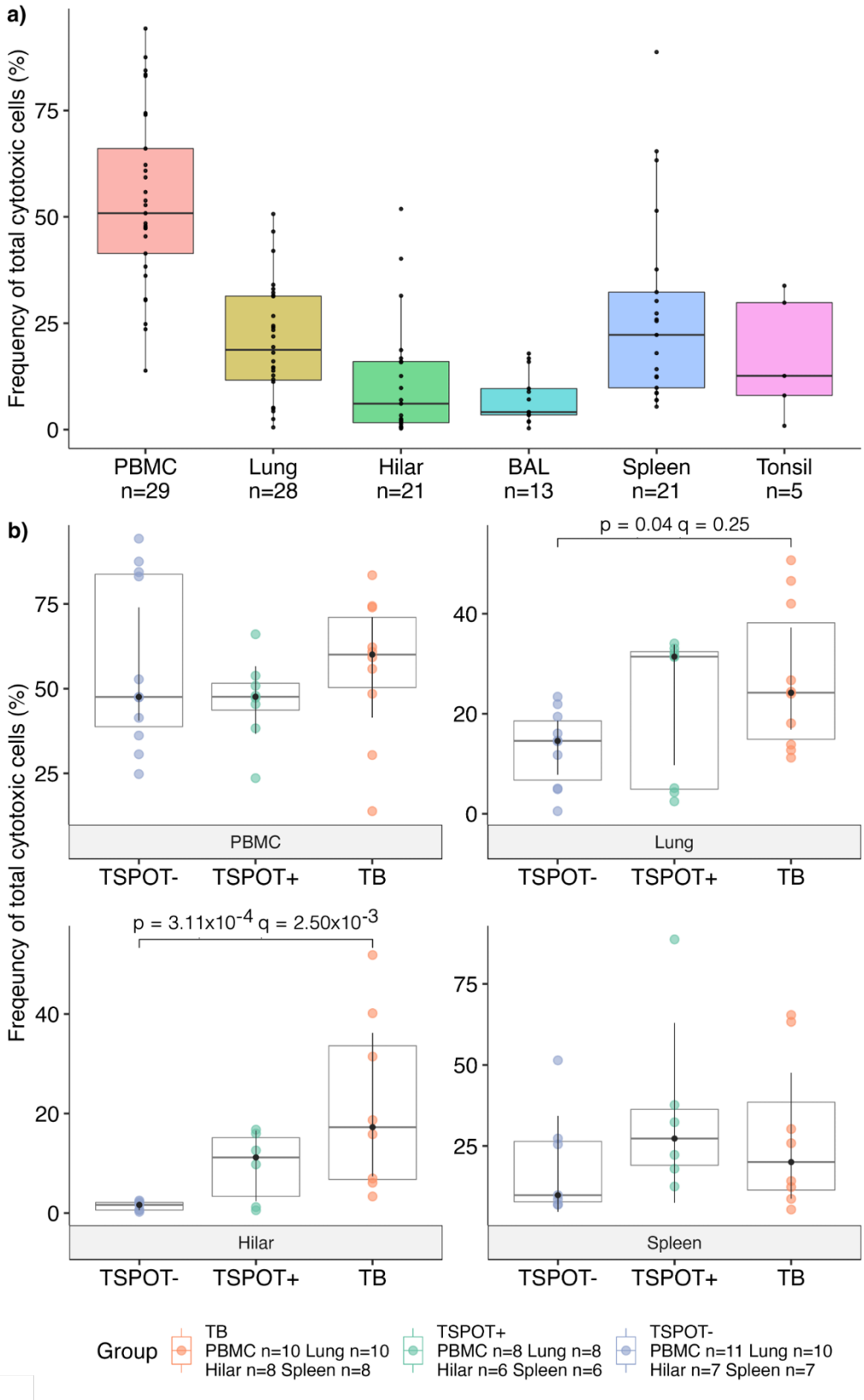

Figure 4.10: Frequencies of total cytotoxic marker-expressing cells across tissue compartments. a) Frequencies of total cytotoxic marker-expressing cells across tissue compartments, and b) frequencies of total cytotoxic marker-expressing cells in tissue compartments stratified according to cohort. Statistical analysis in b) was performed using unpaired Wilcoxon rank sum test for pair-wise comparisons with TB as the reference group (p-values), and the Holm-Bonferroni test was used to account for multiple comparisons (q-value). In boxplots, each box represents median and interquartile range (IQR). Whiskers in a) indicate 1.5x IQR of the upper and lower quartiles, and whiskers in b) indicate 95% confidence intervals.

Total cytotoxic marker-expressing cells were most abundant in the peripheral blood (~50%, Figure 4.10a) while only a small proportion of cytotoxic marker-expressing cells were present in tissue compartments (<25%, Figure 4.10a). Cytotoxic marker-expressing cells were enriched in the hilar lymph nodes of TB patients relative to $TSPOT^-$ controls ($p=3.11x10^{-4}$, $q=2.50x10^{-3}$), with the lungs also following a similar trend (p=0.04, q=0.25; Figure 4.10b). To further assess the subsets comprising the total cytotoxic marker-expressing population, lymphocyte subsets were phenotypically identified according to the definitions detailed in Table 4.3. Frequencies of lymphocyte subsets are reported as a proportion of the total cytotoxic marker-expressing population (Figure 4.11).

Total T cells comprised approximately 40-60% of the cytotoxic marker-expressing cells in peripheral blood and other tissues (Figure 4.11a). Of the total T cell population, CD8 T cells were the predominant subset expressing cytotoxic molecules. In the peripheral blood, CD8 T cells and NK cells comprised roughly equal proportions of the cytotoxic molecule-expressing population (~20% each, Figure 4.11b). The lung also had a substantial population of NK cells contributing to the total cytotoxic molecule-expressing population (>10%). There were no significant differences observed when each cytotoxic marker-expressing subset was compared in TB versus healthy control cohorts (data not shown), suggesting that the significant difference observed between TB and $TSPOT^-$ controls for total cytotoxic marker-expressing cells in the hilar lymph nodes (Figure 4.10b) may be driven by other immune cells (other than T cell subsets and NK cells) or could be due to a combined effect of all cytotoxic marker-expressing subsets.

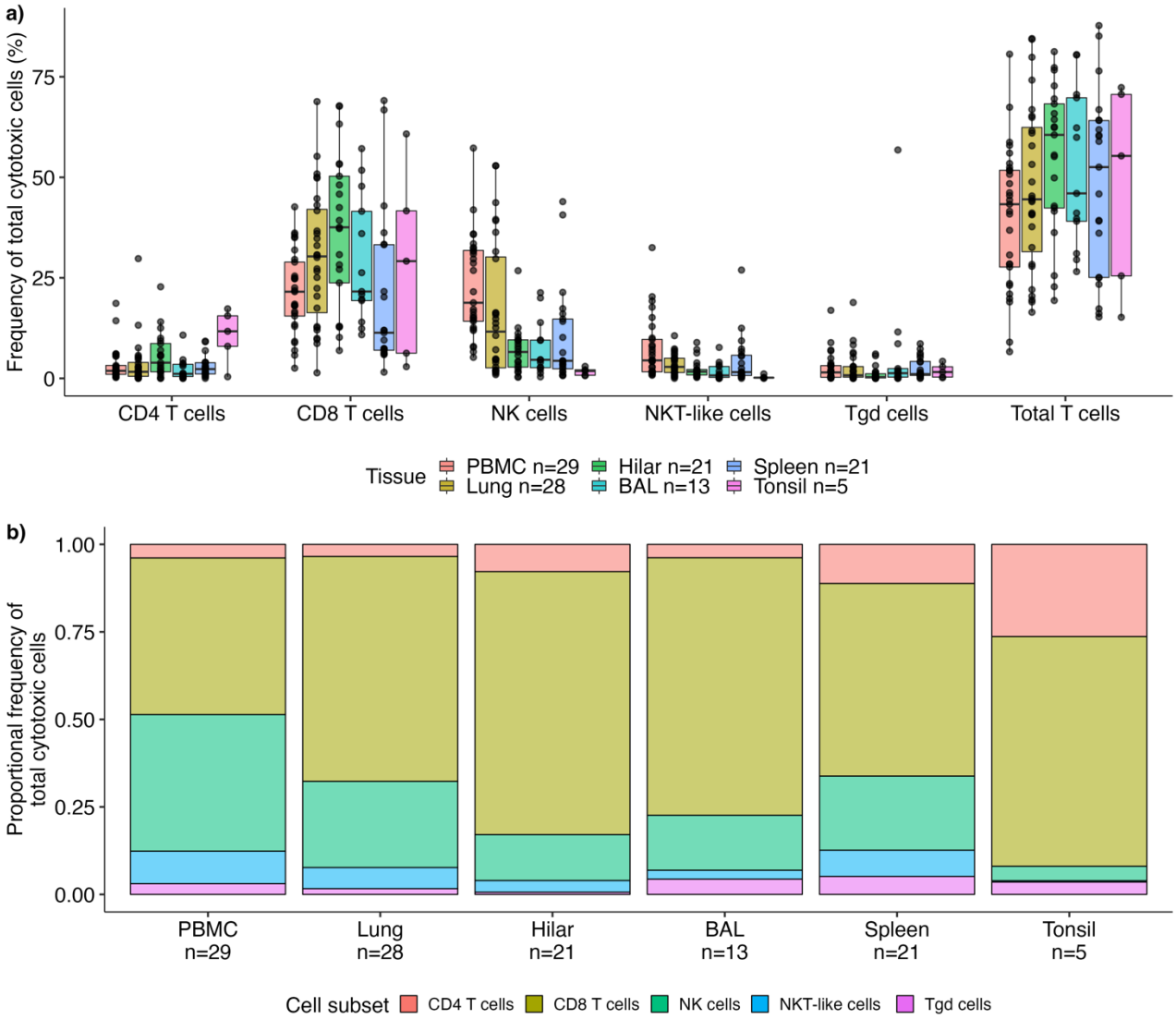

Figure 4.11: Frequencies of lymphocyte subsets comprising the total cytotoxic marker-expressing cell population across tissue compartments. a) Absolute frequencies and b) relative proportional frequencies of lymphocyte subsets, reported as a proportion of the total cytotoxic marker-expressing cell population in tissues. In boxplots, each box represents median and interquartile range (IQR), whiskers indicate 1.5x IQR of the upper and lower quartiles.

4.3.7 Granzyme B and granzyme K are upregulated in cytotoxic lymphocytes during TB

It was hypothesized that during TB, the expression of cytotoxic molecules is upregulated as a feature of immune activation during *Mtb* infection. The expression (MSI) of cytotoxic molecules (perforin, granzyme B and granzyme K) were assessed in the cytotoxic molecule-expressing lymphocyte subsets (Figure 4.12)

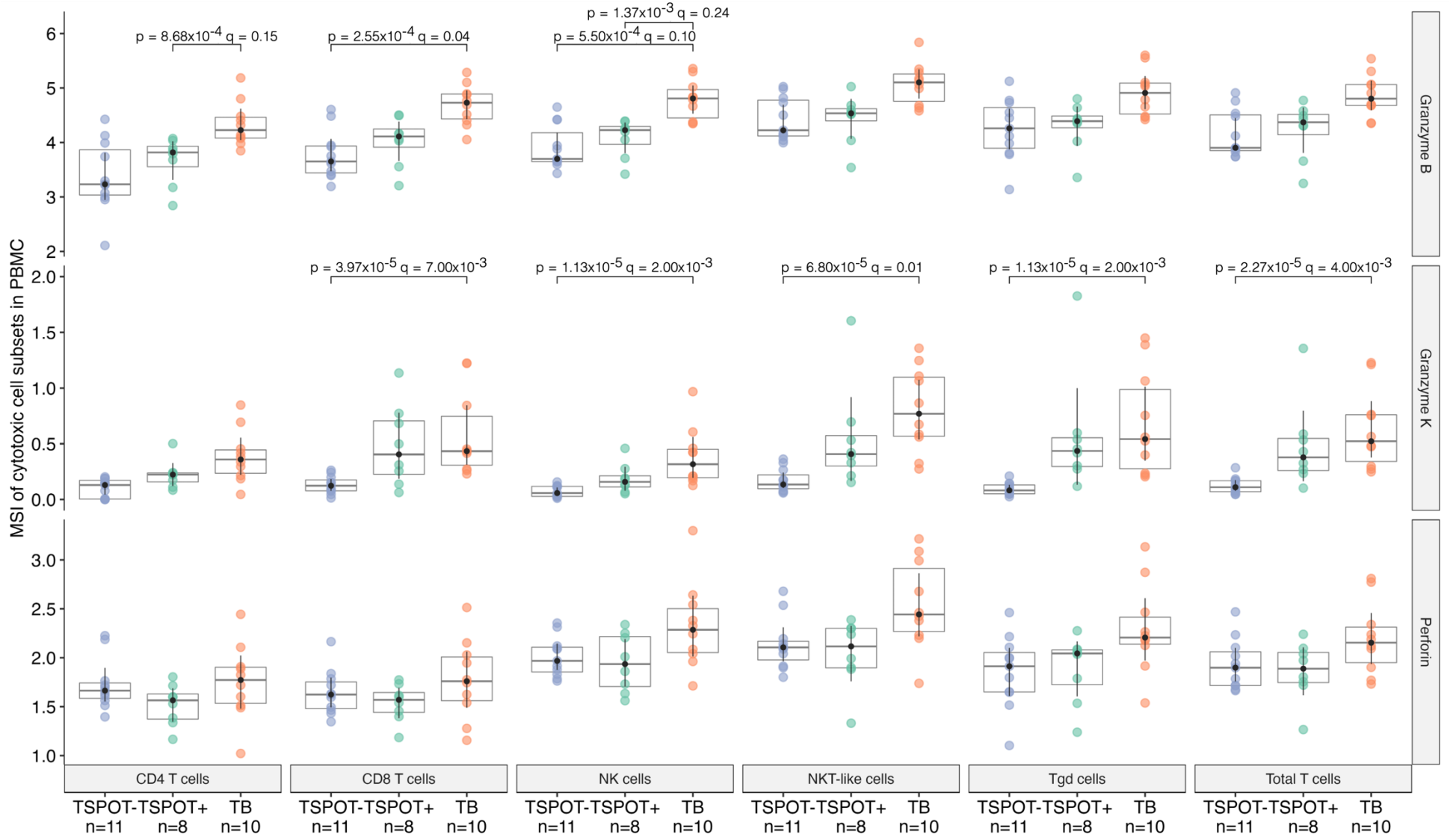

Figure 4.12: Expression of cytotoxic molecules within total cytotoxic marker-expressing lymphocytes in peripheral blood. Expression reported in the form of median staining intensity (MSI) for each marker in NK cells and T cell subsets. Statistical analysis was performed using unpaired Wilcoxon rank sum test for pair-wise comparisons with TB as the reference group (p-value), and the Holm-Bonferroni test to account for multiple comparisons (q-value). In boxplots, each box represents median and interquartile range, whiskers indicate 95% confidence intervals.

The expression of granzyme B was significantly higher in CD4 T cells ($TSPOT^+$ $p=8.68x10^{-4}$, $q=0.15$), CD8 T cells ($TSPOT^-$ $p=2.55x10^{-4}$, $q=0.04$), and NK cells ($TSPOT^+$ $p=1.37x10^{-3}$, $q=0.24$; $TSPOT^-$ $p=5.50x10^{-4}$, $q=0.10$) of TB patients relative to healthy controls (Figure 4.12). Although not statistically significant, potentially due to the small sample size, the expression of granzyme B in NKT-like cells, T$\gamma\delta$ cells, and total T cells appeared to be higher in the TB cohort relative to healthy controls. Granzyme K expression in CD8 T cells ($p=3.97x10^{-5}$, $q=7.00x10^{-3}$), NK cells ($p=1.13x10^{-5}$, $q=2.00x10^{-3}$), NKT-like cells ($p=6.80x10^{-5}$, $q=0.01$), T$\gamma\delta$ cells ($p=1.13x10^{-5}$, $q=2.00x10^{-3}$) and total T cells ($p=2.27x10^{-5}$, $q=4.00x10^{-3}$) was significantly higher in the TB cohort relative to $TSPOT^-$ controls (Figure 4.12). While CD4 T cells expressing granzyme K, and all lymphocytes expressing perforin were not significantly different between cohorts, there was a trend in the direction of upregulated expression in TB relative to controls. No significant findings or trends were observed when cytotoxic molecule expression was compared between cohorts within tissue compartments (data not shown).

To further subclassify cytotoxic marker-expressing immune cell subsets, immune cells were sub-classified according to co-expression patterns of perforin and granzyme B. It would be expected that double positive perforin$^+$granzyme B$^+$ cells co-expressed both markers at high levels, while perforin$^-$granzyme B$^+$ cells expressed low perforin and perforin$^+$granzyme B$^-$ cells expressed low granzyme B levels. It was also hypothesized that double-positive ("poly-cytotoxic") perforin$^+$granzyme B$^+$ cells expressed the highest levels of perforin and granzyme B, relative to the single-positive counterparts (perforin$^+$granzyme B$^-$ and perforin$^-$granzyme B$^+$, respectively). Additionally, it was hypothesized that granzyme K was co-expressed in granzyme B-expressing subsets and not in perforin-expressing subsets, based on previous literature (Bade et al., 2005; Bouwman et al., 2021; Bratke et al., 2005). Figure 4.13

illustrates the expression of perforin, granzyme B and granzyme K by total cells annotated according to perforin and granzyme B co-expression patterns.

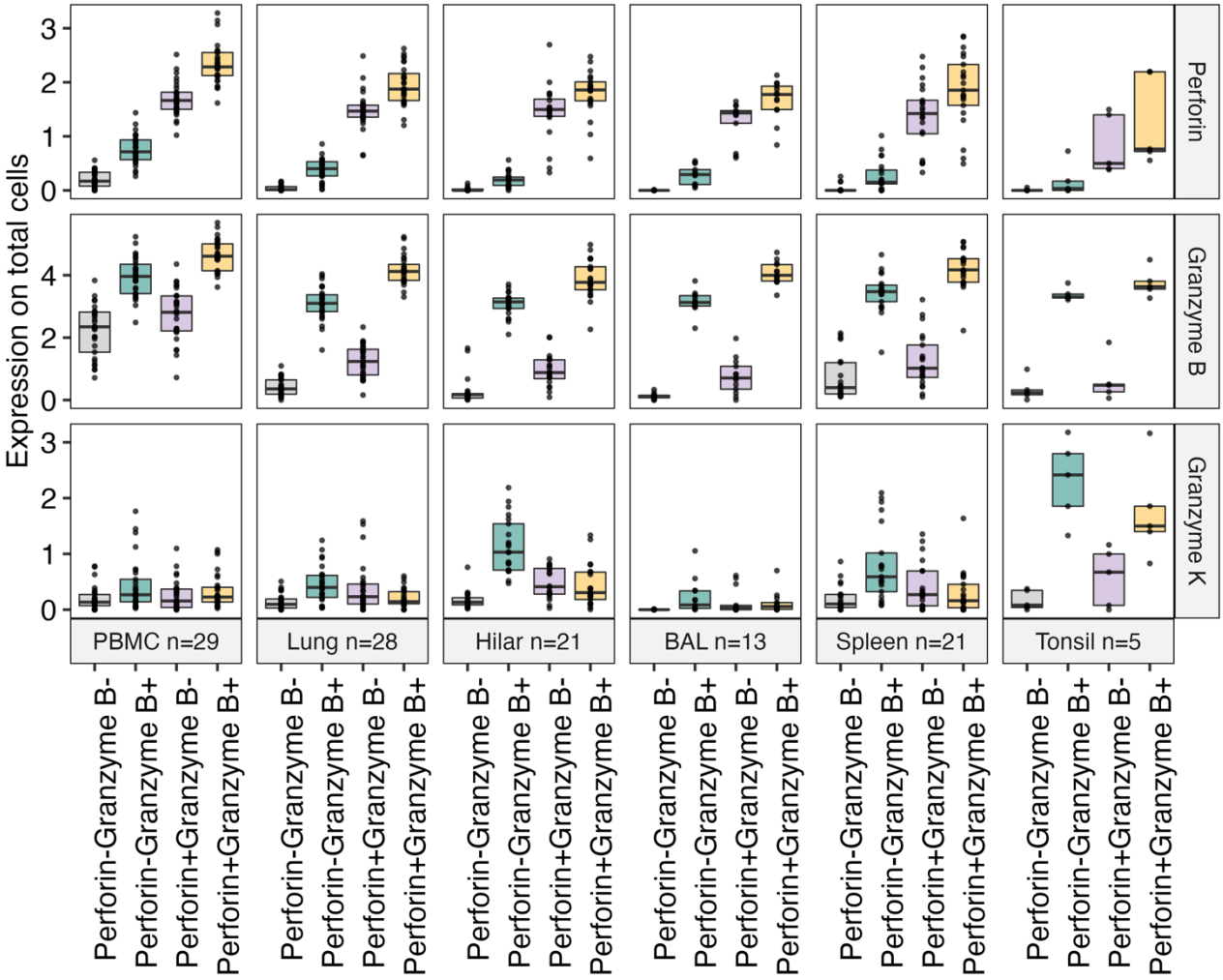

Figure 4.13: Expression of cytotoxic molecules in total live cells annotated according to perforin and granzyme B co-expression patterns. Expression reported in the form of median staining intensity (MSI) of each individual for each marker in total cells.

Double-positive perforin^{+}granzyme B^{+} cells co-expressed both markers at high levels, while perforin^{-}granzyme B^{+} cells expressed low perforin levels and perforin^{+}granzyme B^{-} cells expressed low granzyme B levels, as expected (Figure 4.13). Data also showed that double-positive perforin^{+}granzyme B^{+} cells expressed the highest levels of perforin and granzyme B, relative to the single-positive perforin^{+}granzyme B^{-} and perforin^{-}granzyme B^{+} cells, respectively. Therefore, poly-cytotoxic marker-expressing cells expressed higher levels of

cytotoxic markers relative to the mono-cytotoxic marker-expressing population, independently of cell type.

Granzyme K was expressed at relatively lower levels with no obvious bi- or multi-model distributions between subsets. Markers lacking bi- or multi-modal distributions of expression were not selected by FAUST as an annotation marker. However, in the hilar lymph nodes, spleen and tonsils, granzyme K appeared to exhibit higher expression in the perforin^{-} granzyme B^{+} subsets (Figure 4.13), which is consistent with previously published literature.

As a final subclassification of cytotoxic marker-expressing lymphocyte immune cells across tissue compartments, NK and T cell populations were subclassified within total cytotoxic marker-expressing cells. Figure 4.14 illustrates the frequencies of NK cells and T cell subsets classified according to perforin and granzyme B co-expression patterns, reported as a proportion of the total cytotoxic cells within tissue compartments.

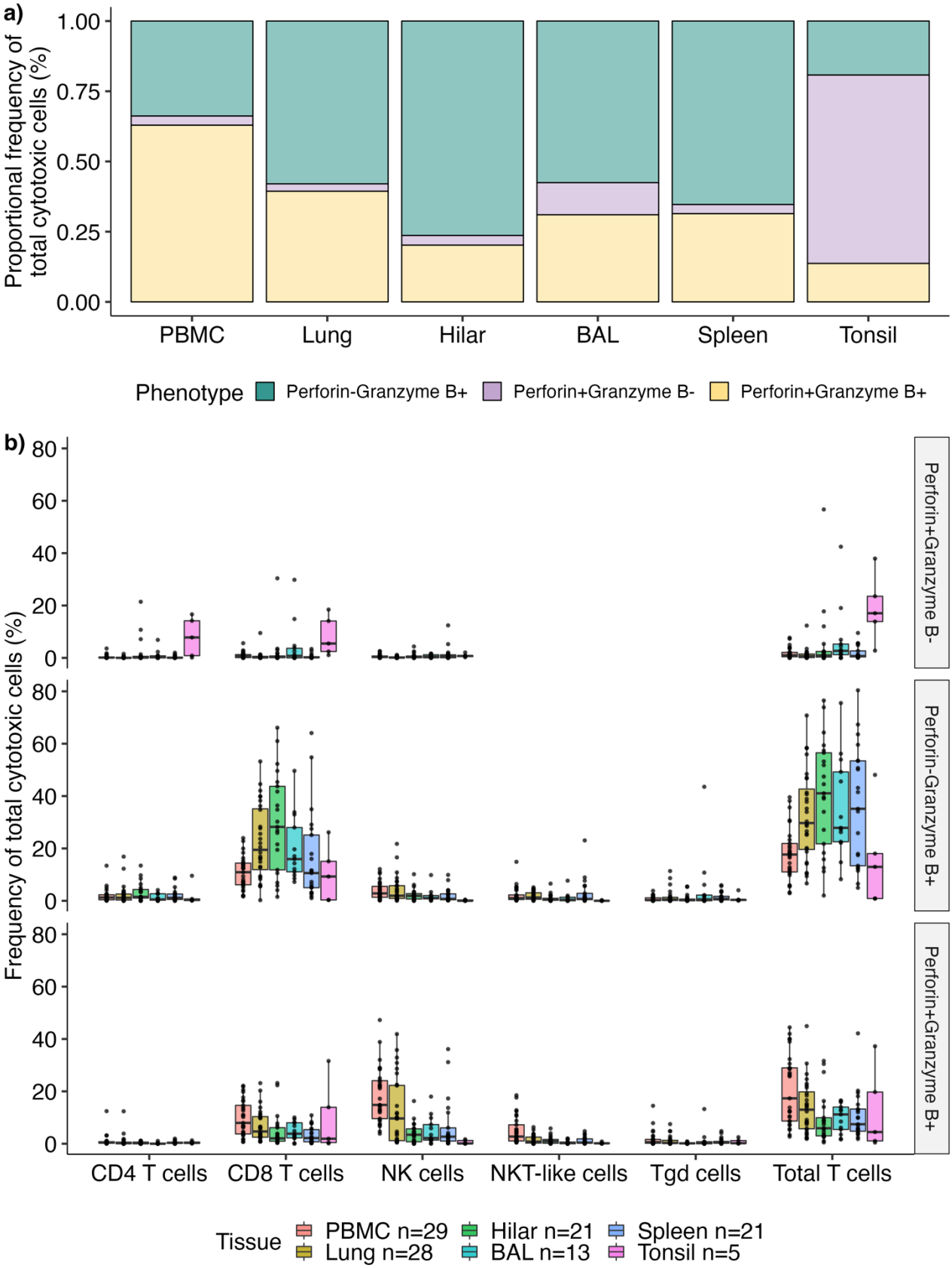

Figure 4.14: Frequencies of cytotoxic marker-expressing lymphocytes subclassified by perforin granzyme B co-expression in human tissues. a) Proportional frequencies of total cytotoxic marker-expressing cells, and b) frequencies of NK cells and T cell subsets comprising the total cytotoxic marker-expressing cell population, annotated according to perforin and granzyme B co-expression patterns. In boxplots, each box represents median and interquartile range (IQR), whiskers indicate 1.5x IQR of the upper and lower quartiles.

Cytotoxic marker-expressing cells in the peripheral blood were predominantly double-positive perforin^{+}granzyme B^{+}, while in the tissues (lung, hilar lymph nodes, BAL, and spleen) perforin^{-}granzyme B^{+} was the predominant subset. Control tonsil tissue from living participants predominantly displayed a perforin^{+}granzyme B^{-} phenotype (Figure 4.14a).

Frequencies of granzyme B^{-}perforin^{+} NK cells and T cell subsets were very low across all tissue compartments (namely PBMC, lung, hilar lymph nodes, BAL, and spleen), although the CD4 and CD8 T cells each comprised ~10% of the total cytotoxic marker-expressing population in the tonsil tissues (Figure 4.14b). In postmortem lung, hilar lymph nodes, BAL, and spleen, the total T cell population of perforin^{-}granzyme B^{+} cells comprised a large proportion (~30-40%) of total cytotoxic marker-expressing cells, which was substantially more than the double-positive perforin^{+}granzyme B^{+} population of T cells, which only comprised <10% of total cytotoxic marker-expressing cells in these tissues. Majority of the perforin^{-}granzyme B^{+} cells in the lung, hilar lymph nodes, BAL, and spleen were the CD8 T cell subset. Cytotoxic marker-expressing cells in the peripheral blood were mostly double-positive perforin^{+}granzyme B^{+} NK cells and total T cells, each having a frequency of ~15% of total cytotoxic marker-expressing cells in PBMC. Majority of the cytotoxic marker-expressing T cell population in the PBMC were perforin^{+}granzyme B^{+} CD8 T cells (~10%), with a smaller yet substantial population of double-positive NKT-like cells (~5%). Roughly 10% of total cytotoxic marker-expressing cells in the lungs were perforin^{+}granzyme B^{+} NK cells and ~5% were perforin^{+}granzyme B^{+} CD8 T cells.

4.4 Discussion and Conclusions

The TB field lacks a comprehensive understanding of proportions and frequencies of immune cell subsets and their functional roles against *Mtb* and infection-associated pathology within tissue compartments throughout the human body. Uncovering functional and mechanistic pathways that are implicated in the cause and/or consequence of progression to TB disease holds the potential to inform development of new intervention strategies. Functional and mechanistic studies in human tissues are needed to inform rational design of clinical applications. However, the field of modern human TB tissue immunology is still in its infancy. Therefore, evaluating the leukocyte composition of various human tissues in TB patients and healthy controls offers a good starting point to identify cell subsets of interest for further investigation into functional and mechanistic properties. To address this gap, the data presented in this chapter provides a comprehensive overview of the myeloid and lymphoid immune composition within various tissues obtained from TB patients and healthy controls and offers insights into the cytotoxic potential of cytotoxic lymphocytes in the different tissue compartments.

4.4.1 Potential biomarkers for *Mtb* infection and TB disease in postmortem PBMC

To compare immune response features between clinical groups, it was important to classify healthy controls according to evidence of immunological sensitization to *Mtb*. The FDA-approved TSPOT test was performed using freshly isolated PBMC from peripheral blood obtained postmortem. However, the TSPOT assay is intended for use in living individuals and has not been validated for postmortem samples. As a secondary test to confirm the findings of the TSPOT test performed by our collaborators in Uganda, a standardized SATVI in-house flow cytometry ICS assay was performed on cryopreserved postmortem PBMC in

the same decedents. The ICS assay is an IGRA test, measuring T cell functional responses to *Mtb* peptides (ESAT-6 and CFP-10).

Using the flow cytometry ICS assay, four of the eight TSPOT^{+} individuals and eight of the ten TB patients were classified as non-responders. This was an interesting finding since TB patients had clinical evidence of disease and consequently of *Mtb* infection, which was expected to be reflected by identifying *Mtb*-specific T cells. While frequencies of *Mtb*-specific IFN-γ^{+}TNF^{+} T cells were significantly lower in TB and TSPOT^{+} postmortem samples relative to samples from living participants, there were no differences in the magnitude of T cell responses to the PHA positive control between living and postmortem cohorts. It is possible that PBMC obtained postmortem had reduced functionality after cryopreservation, although T cell responses to the PHA positive control confirmed that their functional ability to respond to mitogenic stimulation was not obviously impeded. Additionally, reduced functionality was not associated with increased cell death since *Mtb*-specific T cell responses to ESAT-6 and CFP-10 were not correlated with cell viability. Perhaps T cell responses to *Mtb* peptides via TCR binding (which are highly specific) are sensitive to even slight postmortem changes in cell viability and function. In contrast, PHA induces activation via lectin proteins binding to TCR glycans resulting in receptor cross-linking. Therefore, PHA responses induce strong T cell responses that are less specific than peptide activation, which requires precise conformations between the MHC-peptide-TCR complex to induce immune responses. As an alternative hypothesis, perhaps differences in disease severity between living and postmortem cohorts may play a role. Conceivably, the postmortem cohort of TB patients represents a more severe end of the TB spectrum, where the immune system likely failed to control infection and individuals succumbed to disease and/or excessive inflammation-associated complications. On the other hand, TB patients in the living cohort from the Mpande et al. study were mostly classified as responders to *Mtb* peptides (19 of 22 TB patients [~86%] were classified as positive responders; data not shown), and were recruited

at baseline diagnosis, before initiating anti-TB treatment (Mpande et al., 2021). Notably, TB patients in the living cohort were not screened or selected for *Mtb* responses prior to inclusion in the study. Living TB patients who self-presented to clinics with symptoms of disease were likely at earlier stages of disease when the immune system was activated and responsive to high antigen load. In contrast, it may be hypothesized that low *Mtb*-specific responses in postmortem cases were possibly due to hyporesponsive T cell functions towards *Mtb,* where immune cells were likely exhausted after extensive activation by *Mtb* antigens, which may have contributed towards immune failure to control the infection. It should also be noted that it is not necessarily true that all individuals who had active TB and died were those who succumbed to the most severe forms of end-stage disease. While this may be true in some cases, it remains possible that TB patients without very severe disease could have been hospitalized and succumbed to complications due to blood clots (such as stroke, heart attack, pulmonary embolism, etc.) or haemorrhage. Unfortunately, these details were not available for the cohort in this study, but for the most part, information that were received indicated that all decedents in the postmortem TB cohort had confirmed TB disease and were hospitalized due to severe illness.

Another hypothesis, although less likely, is that T cell responses are damped by TB treatment. There are published data to show that TB therapy decreases IFN-γ responses to *Mtb* antigens within the QFT assay (Chang et al., 2017; Petruccioli et al., 2018; Riou et al., 2020; Chee et al., 2010). However, four out of ten TB patients (40%) in the postmortem cohort were not receiving anti-TB treatment, and only three of the six patients (50%) that were receiving treatment had been taking antibiotics for two months or longer. Therefore, it is unlikely that the dampened T cell responses in the postmortem TB cohort were due to anti-TB therapy.

Differences in sensitivity between assay techniques may offer another explanation for discordance between TSPOT results and ICS results for some individuals in the TSPOT^{+} cohort who classified as non-responders. The TSPOT test is an ELISpot-based assay, which has been shown to be the most sensitive readout system and is most appropriate for detection of low-level responses (Karlsson et al., 2003; Tischer et al., 2014). Studies have also shown that ELISpot assays were more sensitive than flow cytometry ICS assays for quantifying antigen-specific cells (Meierhoff et al., 2002; Tassignon et al., 2005). Since TSPOT is an FDA-approved test and the technique is considered the most sensitive readout, the TSPOT result was used as the classification criterion to divide healthy decedents into groups of *Mtb*-sensitized or non-*Mtb*-sensitized controls (except for the three TSPOT indeterminate results, for which the flow cytometry ICS assay was used for classification).

It should also be noted that our standardized in-house ICS assay for measuring T cell responses to *Mtb* peptides, was developed in a living cohort and was therefore, not fully optimized for postmortem samples. The observation that *Mtb*-specific T cell responses were lower in postmortem samples may indicate that further optimization might be required for a more proficient definition of responder status. When using the flow cytometry ICS assay in future studies to characterize T cell responses to *Mtb* peptides in PBMC that are isolated and cryopreserved postmortem, two points should be considered: 1) decreasing the fold-change threshold, and 2) slightly increase the p-value cut-off. Alternatively, the stimulation time could be increased to maximize detection of cytokines produced, although careful evaluation of cell viability is required for lengthily stimulation times. Overall, further studies are required to evaluate the threshold parameters and stimulation times for responder characterization using the flow cytometry ICS assay with PBMC obtained postmortem.

The current *Mtb* immunodiagnostic tools (including TST and IGRA) are limited to indicating immunological sensitization to *Mtb* antigens and do not distinguish between different stages

of the TB spectrum, ranging from asymptomatic *Mtb*-infection to active disease. Consistent with this limitation, Mpande and colleagues showed that measuring the magnitude of *Mtb*-specific T cell responses by flow cytometry ICS distinguished between QFT^- and QFT^+ individuals, but not between QFT^+ participants and TB patients (Mpande et al., 2021). Accordingly, the postmortem data presented in this chapter showed that frequencies of *Mtb*-specific T cells successfully distinguished between $TSPOT^-$ and $TSPOT^+$, but not between $TSPOT^+$ and TB.

HLA-DR is a molecule typically constitutively expressed by APCs and is associated with antigen presentation. However, HLA-DR is expressed on T cells upon activation, although why and how activated T cells express HLA-DR remains to be fully understood. More recently, the ΔHLA-DR MFI biomarker on *Mtb*-specific IFN-$\gamma^+$$TNF^+$ T cells has shown to successfully distinguish between active TB and *Mtb*-sensitized controls (Adekambi et al., 2015; Wilkinson et al., 2016; Riou et al., 2017; Musvosvi et al., 2018; Riou et al., 2020; Mpande et al., 2021). Amongst the QFT^+ population in the 2021 study by Mpande and colleagues, the T cell activation ΔHLA-DR MFI biomarker was also able to discriminate between those with recent QFT conversion, disease progression or active disease and persistent QFT^+ non-progressors (Mpande et al., 2021). The underlying hypothesis is that the ΔHLA-DR MFI biomarker reflects *Mtb* antigen load, where *Mtb*-specific T cells are exposed to higher levels of antigen, which is higher during TB progression and in active TB compared to controlled infection, and that successful treatment effectively reduces this *Mtb* load (Mpande et al., 2021; Musvosvi et al., 2018; Riou et al., 2020). A biomarker that reflects *Mtb* antigen load is a significant advance over current *Mtb* immunodiagnostics which do not distinguish between different stages of *Mtb* infection, nor identify risk of disease progression. The implications of this biomarker present an opportunity to identify groups of asymptomatic individuals who are at high risk of developing TB disease and may, in particular benefit from TPT, with relevance in high incidence settings. The postmortem data presented in this

chapter illustrated that the ΔHLA-DR MFI biomarker also offers an *Mtb*-specific tool to distinguish between TB and $TSPOT^+$ in postmortem samples. While the immunodiagnostic implications of the postmortem ΔHLA-DR MFI biomarker would not directly benefit individuals who have died, this tool may prove useful to aid in retrospective estimation of antigen load and classification of decedents into appropriate cohorts according to different stages of *Mtb* infection and progression. Most importantly, it would be of interest to further study the ΔHLA-DR MFI biomarker in the blood of postmortem TB cases and associate the data with bacterial load in the tissues to confirm whether ΔHLA-DR MFI is indeed a correlate of bacterial burden, which cannot be demonstrated in living humans and has not yet been demonstrated in animal models. Data from such an investigation holds the potential to address a major gap in the TB biomarker field, with important implications for preventative therapies in high-risk individuals.

4.4.2 Frequencies and proportions of myeloid and lymphocyte subsets across postmortem tissue compartments

The primary aim of this chapter was to provide a comprehensive overview of the myeloid and lymphoid immune subset composition of various tissues obtained postmortem in TB patients and healthy controls. Using the FAUST clustering algorithm, the following cell populations were identified across tissue compartments: total NK cells, B cells, myeloid cells, and T cells; including T cell subsets: CD4 T cells, CD8 T cells, NKT-like cells and $T\gamma\delta$ cells. Frequencies of FAUST-annotated NK and B cells were also highly correlated with the same subsets identified by gold standard manual gating, validating the FAUST clustering method.

The lung compartment for the postmortem study presented in this thesis was sampled from the left upper lobe and comprised mostly CD4 T cells, CD8 T cells and myeloid cells, with a

substantial NK cell population. There were very few B cells, NKT-like cells and Tγδ cells in the lungs. Within the cellular component of the BAL (representing the luminal side of the peripheral airways), myeloid cells were the largest population (most likely alveolar macrophages, although this not certain since the antibody panel lacked alveolar macrophage-specific markers, such as CD206), with smaller populations of CD4 and CD8 T cells. Frequencies of myeloid cells reported in the lungs and BAL were lower than expected (~90% of the BAL were expected to be myeloid cells), although it should be noted that single cell suspensions of tissue cells required extensive filtering steps to remove debris and clumps to maintain cell quality and prevent blockage during data acquisition. Cells were filtered using 35μm filters, which may have removed larger macrophage populations. Additionally, frequencies of myeloid and lymphocyte populations were reported as a frequency of total live $CD45^+$ cells. However, there were many other cell types that could not be evaluated based on the selection of the markers in the designed panel, which was centered around NK and B cell phenotypic markers. In addition to immune subsets, the tissues are also comprised of epithelial and endothelial tissue, blood vessels, connective tissues, adipose tissue, and other hematopoietic cells (e.g., megakaryocytes, Langerhans cells, mast cells, eosinophils, neutrophils, basophils) that fall beyond the scope of investigation for this thesis, thus the panel did not include markers to identify these subsets. Therefore, it is likely that many cell subsets were overlooked and could not be evaluated with the current panel.

The hilar lymph nodes were comprised mainly of CD4 T cells, CD8 T cells and B cells, which is consistent with the established dogma that lymph nodes are major immune sights housing B cells and T cells (specifically CD4 T cells). Similar to the hilar lymph nodes, tonsil tissue from living participants were comprised almost exclusively of B cells and T cells, primarily of the CD4 T cell subset. Postmortem spleen samples had large populations of B cells, CD4 T cells and CD8 T cells in roughly equal proportions and a smaller, yet substantial population

of NK cells. Overall, these findings are consistent with published literature, giving confidence with which data are reported, and providing a proof-of-concept for the use of postmortem samples to investigate immune subsets in the tissues. By reporting frequency estimates and relative abundances of immune subsets across tissue compartments, these data also offer valuable insights for investigators who may be looking to design future tissue immunology studies.

Frequencies and relative proportions of immune cell subsets reported for PBMC were consistent with previously published literature (Autissier et al., 2010; Kleiveland, 2015), except for CD4 T cells which had lower frequencies than what has been previously reported. Since HIV infection was not an exclusion criterion for this study, low frequencies of CD4 T cells observed in the peripheral blood may have been confounded by HIV status of participating decedents, which was investigated further. HIV is known to infect and deplete CD4 T cells in the blood. It has also been shown that HIV infection is associated with CD4 T cell depletion in the lymph nodes, gastrointestinal tract, and BAL (Brenchley et al., 2004; Kalsdorf et al., 2009). More specifically in the BAL, the depletion of CD4 T cells in HIV infected persons was also associated with impaired BCG-specific CD4 T cells responses, possibly contributing the HIV-associated elevated risk for developing TB disease (Kalsdorf et al., 2009). It was therefore hypothesized that HIV infection would be associated with depleted CD4 T cell frequencies in the peripheral blood and tissues. Indeed, results showed that CD4 T cells in HIV^+ individuals were significantly depleted relative to uninfected decedents in the PBMC, lung, hilar lymph nodes and spleen. However, unlike the Kalsdorf, et al. study in 2009 (Kalsdorf et al., 2009), HIV infection was not associated with depletion of CD4 T cells in the BAL compartment. HIV infection did not appear to be associated with alterations to other immune cell populations including total T cells, CD8 T cells, T$\gamma\delta$ cells, NKT-like cells, NK cells, B cells, and myeloid cells. However, it remains possible that HIV-

associated changes may have occurred within smaller subsets of the bulk populations and/or may have affected functionality, which requires further investigation.

It has been well documented that chronic infection and inflammatory diseases, including TB, alter myelopoiesis and lymphopoiesis, resulting in differences to peripheral cellular compartments during health and disease (Baldridge et al., 2010, 2011; Chowdhury et al., 2018; Naranbhai et al., 2014; Scriba et al., 2017). It was therefore hypothesized that immune cell subsets (specifically T cell subsets, NK cells and B cells) were depleted in the peripheral blood during TB disease. Additionally, it has been proposed that during TB disease, immune cells are activated and trafficked to the site of *Mtb* infection (Masopust & Schenkel, 2013; Portevin et al., 2012; Junqueira-Kipnis et al., 2003b). Therefore, the depletion of cell subsets in the peripheral blood were hypothesized to be accompanied by enrichment of immune cells in the tissues, particularly the lung where primary *Mtb* infection occurs. However, no significant differences were observed between TB and healthy cohorts in the peripheral blood or other tissue compartments. Despite no changes to bulk lymphocyte populations in the peripheral blood and tissues during TB disease, it remains possible that their subsets and functional characteristics (such as cytokine production and cytotoxic capacity) may be altered, which requires further investigation in the tissues.

4.4.3 The composition of cytotoxic marker-expressing lymphocytes across tissue compartments

Cytotoxic lymphocytes play a role in the host immune response to *Mtb* infection by secreting cytokines, chemokines and cytotoxins that aid in cytolytic killing of *Mtb*-infected cells. In this chapter, several cytotoxic marker-expressing subsets were investigated in the peripheral blood and tissues including, CD4 T cells, CD8 T cells, NKT-like cells, T$\gamma\delta$ cells, and NK cells. Results showed that majority of the cytotoxic marker-expressing population in the peripheral

blood, lung, hilar lymph nodes, BAL, spleen, and tonsils were T cells, specifically of the CD8 T cell subset. Agreeably, confocal microscopy data in a 2007 study by Andersson and colleagues also showed that CD8 T cells were the main producers of cytolytic effector molecules in TB lesions of lung biopsies (Andersson et al., 2007), although other tissues (such as lymph nodes and spleen) were not investigated in this study. Results presented in this chapter showed that NK cells also contributed a substantial proportion of total cytotoxic marker-expressing lymphocytes in the peripheral blood and lungs, which highlights NK cells as potentially important cytolytic players in the during lung disease. A deeper investigation into tissue NK cell phenotypes and cytotoxic potential is presented in Chapter 5.

During infection and disease, immune cells become activated and upregulate expression of cytotoxic molecules to exert effector functions and undergo cytotoxic killing of target cells (Chávez-Galán et al., 2019; Serbina et al., 2000; Nisha Rajeswari et al., 2006), which rationalized the hypothesis that cytotoxic marker-expressing lymphocytes were enriched in the peripheral blood and tissues during TB. There were no differences in the frequencies of cytotoxic marker-expressing NK cells or T cell subsets between cohorts in any tissue. A recent study also showed that expression of cytotoxic molecules (perforin and granzyme B) and a degranulation marker (CD107a) by CD4 T cells, CD8 T cells and NK cells in the lymph nodes were not different between clinical cohorts of culture-positive versus lymph node culture-negative TB patients (Kathamuthu et al., 2022). It is likely that cytotoxic cells in the tissues have tightly controlled homeostatic mechanisms to mediate excessive expression of cytotoxic molecules that may induce tissue pathology.

Interestingly, frequencies of total cytotoxic marker-expressing cells (irrespective of NK or T cell sub-classification) were enriched in postmortem hilar lymph nodes and lungs of TB decedents. These findings possibly indicate that cytotoxic marker-expressing lymphocytes trafficked to the lung and hilar lymph nodes during TB disease or that the cells upregulated

these cytotoxic markers. Another study reported increased perforin-expressing lymphocytes in the organs of *Mtb*-infected mice, specifically the lungs, liver, and spleen, which were not detected in organs of uninfected mice (Serbina et al., 2000). These findings were based on immunohistochemistry staining of tissues that could not distinguish between different lymphocytic populations to pinpoint the predominant perforin-expressing subsets. Additionally, the lymph nodes were not included in the study. However, these data do support the finding that TB disease is associated with increased cytotoxic potential of lymphocytes in the tissues.

Altogether, the data presented in this chapter suggest that TB disease is associated with increased cytotoxic potential of immune cells in the lungs and lymph nodes. However, this effect was not driven by a single NK cell or T cell subset in particular. Rather, the effect was likely due to an additive/combined effect. More specifically, slightly increased frequencies of cytotoxic marker-expressing subsets during TB could have produced a significant effect when considered as a collective population in the tissues; but were not different when investigated in isolation. This is plausible since it is well understood that immune cells do not act in isolation, but rather function as an orchestrated system with many individual components acting in tandem. Alternatively, increased frequencies of the total cytotoxic marker-expressing population may have been driven by other cytotoxic marker-expressing subsets such as DCs (Jahrsdörfer et al., 2010, 2014), mast cells (Strik et al., 2007), neutrophils (C. Wagner et al., 2004), and basophils (Tschopp et al., 2006). However, these cells could not be delineated based on the antibody panel, which lacked markers to identify these cell subsets.

The cytotoxic potential of cytotoxic lymphocyte populations in the peripheral blood and tissues were investigated further by evaluating the expression levels (MSI) of cytotoxic molecules in NK cells and T cell subsets and comparisons were made between cohorts.

Data showed that the expression of granzyme B, granzyme K and perforin were higher in peripheral blood NK cells and total T cells, including subsets of CD4 T cells, CD8 T cells, NKT-like cells, and T$\gamma\delta$ cells. These findings illustrate that cytotoxic molecules in lymphocytes within the peripheral blood were upregulated during active disease, suggesting heightened immune activation or differentiation. Agreeably, a 2019 study by Chávez-Galán and colleagues also showed that CD8 T cells in the peripheral blood had higher cytotoxicity in TB patients relative to healthy controls, which was mediated by HLA class I molecules on autologous monocytes in the presence of mycobacterial antigens (Chávez-Galán et al., 2019).

Results presented in this chapter also showed that only <25% of cells in the tissues expressed cytotoxic molecules, while >50% of total cells in the peripheral blood expressed cytotoxic molecules. Together, these data suggest that cells within the tissues may be predominantly hypo-cytotoxic and do not express cytotoxic molecules at high levels. This may be a protective feature of tissue immunology to limit inflammation-induced tissue pathology that may occur in response to the myriad of potential immunogens that are inhaled, specifically referring to the lungs, BAL, and lung-draining hilar lymph nodes. Alternatively, it is also possible that some cytotoxic lymphocytes in the tissues may have been depleted of their cytotoxic molecules following a killing event when cytotoxic cells degranulate to release their cytotoxic molecules and initiate target cell killing. It is also likely that tissue specimens may have been sampled from regions of the lung or other tissues where *Mtb* were not present, therefore not fully reflecting the cytotoxic immune cell composition in the granuloma or *Mtb*-enriched tissues. An *in situ* imaging study by Andersson and colleagues in 2007 demonstrated that CD8 and CD4 T cells were enriched in pulmonary lesions of patients with chronic TB compared to distal lung parenchyma with normal tissue pathology and uninfected control lungs. There were also significant reductions in the frequency of macrophages in the TB lesions compared to distal lung parenchyma and

uninfected control tissues (Andersson et al., 2007). Together, these data demonstrate that regions of the *Mtb*-infected lung in humans can have different cellular compositions (and perhaps functional characteristics) compared unaffected areas within the same lung. This emphasizes the importance of targeted sampling when performing human tissue immunology studies. Notably, the pathologist performing the autopsies for the postmortem study in this thesis obtained samples from the left upper lobe of all decedents and did not perform targeted sampling of pathological TB lesions. Therefore, not all samples may accurately reflect immunological composition and cytotoxic potential of *Mtb*-infected lesions in the TB lung (which is discussed further in the limitations section below; Section 4.4.4).

Cytotoxic marker-expressing cells were further investigated according to their co-expression patterns of perforin and granzyme B. It was hypothesized that double-positive perforin^{+}granzyme B^{+} cells had the highest expression of perforin and granzyme B relative to their single-positive perforin^{+}granzyme B^{-} and perforin^{-}granzyme B^{+} counterparts, respectively. The rationale for this hypothesis was based on T cell data that showed polyfunctional T cells (i.e., T cells expressing more than one cytokine) expressed higher levels of cytokines relative to single cytokine-producing T cells (Hersperger et al., 2012; Boyd et al., 2015; Burel et al., 2017). In support of the hypothesis, postmortem data in peripheral blood and tissues, and tonsils from living participants, had the highest expression of perforin and granzyme B in the double positive perforin^{+}granzyme B^{+} population relative to single positive subsets. It was also shown that cytotoxic marker-expressing subsets in the PBMC were predominantly double-positive perforin^{+}granzyme B^{+} subsets, while the postmortem tissues were comprised mostly of the single-positive perforin^{-}granzyme B^{+} population. It should be noted that granzyme B requires perforin-induced holes to enter the target cell membrane where granzyme B induces apoptosis by activating the caspase cascade (Voskoboinik et al., 2015). Therefore, granzyme B expression in the absence of co-expressed perforin is unlikely to induce a potent cytotoxic response. Together, these data

provide further evidence that cells within the tissue compartments have a lower cytotoxic potential than in the peripheral blood, which is a likely homeostatic mechanism to prevent inflammation-induced pathology in the tissues.

Within the cytotoxic marker-expressing immune cells in the tissues, the predominant perforin$^-$granzyme B$^+$ subset was comprised almost exclusively of T cells, specifically CD8 T cells. The peripheral blood, and the lungs to a lesser extent, contained the highest proportions of perforin$^+$granzyme B$^+$ cells which were comprised largely of NK cells and a smaller population of CD8 T cells. Therefore, the data suggest that peripheral blood cells had the highest cytotoxic potential, mostly attributed to NK cells and CD8 T cells. In contrast, tissue compartments had a low cytotoxic potential relative to the peripheral blood and comprised mostly of granzyme B-expressing CD8 T cells. A 2020 study by Kathamuthu and colleagues showed that patients with tuberculous lymphadenitis had lower frequencies of cytotoxic marker-expressing CD8 T cells and NK cells (*ex vivo* and stimulated with *Mtb*-specific antigens) in the lymph nodes compared to peripheral blood of the same participants. Together, these data support the finding that peripheral blood lymphocytes have a higher cytotoxic potential than their tissue counterparts (Kathamuthu et al., 2020). However, further investigation is needed to fully evaluate the killing capabilities of mono-cytotoxic marker-expressing CD8 T cells in postmortem tissues and their role during *Mtb* infection.

Although granzyme K was not selected as marker for cell annotation using FAUST, the relative expression levels of granzyme K were evaluated on cytotoxic marker-expressing subsets. It was hypothesized, based on previous literature (Bade et al., 2005; Bratke et al., 2005; Bouwman et al., 2021), that granzyme K was co-expressed in cell subsets with granzyme B but not perforin. Therefore, granzyme K was expected to be expressed at highest levels in perforin$^-$granzyme B$^+$ subsets. Findings suggested that in the hilar lymph nodes and tonsil (and in the spleen and lung to a lesser extent), granzyme K was indeed

co-expressed with granzyme B in the perforin^{-}granzyme B^{+} population. Granzyme K was expressed at relatively low levels in the BAL and peripheral blood. Interestingly, granzyme K has been shown to have extracellular targets for cleavage and activation (such as protease activated receptors – PAR) that induce cytokine production upon activation (D. M. Cooper et al., 2011; Kaiserman et al., 2022; Sharma et al., 2016; Wensink et al., 2014). It would be useful to further investigate the cytotoxic and immunoregulatory roles of granzyme K in the tissues during TB disease.

4.4.4 Limitations

This postmortem study presents a novel and unique dataset, including TB patients who succumbed to disease and controls who were otherwise healthy but died due to trauma. Adding to the novelty of this study was the sampling from various tissues, allowing characterization of immune cell subsets from different anatomical compartments throughout the human body. Overall, the size of the total postmortem sample set was substantial: PBMC n=29, lung n=28, hilar lymph nodes n=21, spleen n=21, BAL n=13. Experts in the cytometry field would appreciate the extensive efforts required to design and optimize an antibody panel of such high dimensionality, as well as time required to acquire a dataset of 112 samples using a CyTOF instrument. However, despite having a relatively large sample set, when stratifying decedents according to clinical status, the number of individuals per group for each tissue compartment was relatively small. As a result of the small sample size per cohort, there was limited statistical power for performing comparisons between groups, possibly contributing to the lack of differences observed, especially after adjusting for multiple comparisons. As such, many of the observations reported in this chapter require more datapoints to fully evaluate the strength of the findings.

Another point of limitation for this study was the confounding variable of HIV status, whereby HIV-positive individuals mostly occurred in the TB group. This is not entirely surprising since HIV is a known risk factor for advanced stages of TB disease and death. However, this does pose a problem when performing comparisons between cohorts. Due to the relatively low sample size per cohort and the rather extreme skewing of HIV in the TB cohort, the use of complex mathematical models and statistical tests to account for the HIV confounder were cautioned against. As such, basic non-parametric statistical tests were used and the potential effect of HIV on the observations reported in this study cannot be fully excluded. Similarly, smoking and alcohol consumption are known risk factors for developing TB disease (Silva et al., 2018), and were also disproportionally prevalent in the TB cohort. Acquisition of more datapoints to balance and match decedents with confounding variables in each cohort would prove useful to evaluate and/or account for the effects of HIV, smoking and alcohol consumption.

It should be noted that the lung is a particularly large organ, and the pulmonary immune system is composed of multiple different interacting compartments. Therefore, the immune composition of the lung can appear different depending on the sampling region. Since all lung tissue sections were sampled from the left upper lobe; it is likely that not all TB decedents had *Mtb*-containing lesions from the sampled site. Therefore, the regions of sampled lung tissues may not have contained activated cells responding to *Mtb* infection in the TB cohort, possibly explaining the lack of differences observed between cohorts. The same argument may be applied to the cellular fraction of the BAL, which does not sample the entire lung airway, rather an area within the bronchial space which was most accessible to the pathologist. Sampling from the hilar lymph nodes and spleen was performed by isolating single cell suspensions from the entire organs, resulting in a mixture of all lymph node and spleen compartments in a single sample. As previously discussed (in Section 4.1), the lymph nodes and spleen are highly organized structures that contain sub-

compartmentalized regions that carry out specific functions. In this study, the structural architecture of the lymph nodes and spleen were not retained, and the entire organs were sampled as a single cell suspension. In future studies, it would be valuable to investigate such organs in a manner that maintains structural integrity, which may reveal points of immunological differences and the composition of immune populations between health and TB disease. Finally, NHP models have shown that not all lymph nodes are equal in their ability to control infection, demonstrating within-host variability of bacterial killing in different lymph nodes (Ganchua et al., 2018). The lymph node data presented in this thesis were derived from mixing multiple hilar lymph nodes as a single cell suspension. Therefore, some lymph nodes may have carried high *Mtb* loads while others not, and potential differences that were present in a hilar lymph node in isolation may have been averaged out by including of other lymph nodes that represented more normal pathology. Future investigations should investigate within-host variability of human lymph nodes regarding their capacities for bacterial killing and pathogen clearance.

The cytotoxic potential of immune cells was evaluated by means of relative expression levels of cytotoxic molecules. To evaluate the true cytolytic capacity of immune cells, a functional assay is required to demonstrate the active killing of immune cells against target cells. Reporting relative expression of cytotoxic molecules can be considered a reflection of the cytotoxic potential at the immediate point upon staining. However, intracellular staining of cytotoxic molecules cannot detect a recent degranulation event that may have occurred prior to staining. For example, immune cell subsets that are highly cytotoxic and functionally active *in vivo* may have degranulated to release their cytotoxic molecules from the cell and induce target cell killing, in which case cytotoxic molecules within the cell would not be stained. This concept is further complicated by the compartment under investigation. More specifically, one would not expect immune cells in the peripheral blood to readily degranulate and release their cytotoxic molecules into circulation (unless under extenuating

circumstances where infection has spread to the bloodstream). Therefore, measuring relative levels of cytotoxic molecule expression may be a reliable indicator of cytotoxic potential for peripheral blood cytotoxic immune cell subsets. On the other hand, immune cells in the tissues, specifically at the site of *Mtb* infection and TB disease, are expected to be functionally active and exert effector functions, possibly being reflected as degranulated cells with low cytotoxic molecule expression. However, in this thesis it was not confirmed whether tissues were sampled directly from *Mtb*-containing lesions. Overall, reports of cytotoxic potential reported in this thesis are reported with acknowledgement of these limitations and have been discussed with discretion, also considering other points of evidence and contextual information.

The PMI variable was measured as the time from death to the point of counting cells immediately before cryopreservation. Since there was a significant difference between TB and healthy cohorts, the PMI variable has the potential to be a confounding factor in the results. However, the PMIs across all cohorts were very low considering the immense tasks of performing postmortem consenting, autopsies, tissue harvesting and cell isolation within the same day. It may be argued that the statistical significance observed for the 1.5 to 2.5-hour PMI time difference between groups may not be logistically significant or greatly impact that phenotypic and/or functional characteristics of isolated cells.

Finally, the nature of this postmortem investigation required tissue samples to be resected during autopsy shortly after death. Naturally, peripheral blood poses as a contamination source of immune cells around and within the sampled organs. Blood-borne cell contamination of tissues has the potential to confound identification and purification of leukocytes that truly participate in local immunological processes within the tissues (Anderson et al., 2014). Measures were taken to minimize cross contamination with peripheral blood, such as gently rinsing resected organs with medium prior to further mincing

of the tissue. However, organs themselves are highly vascularized and may have still experienced mixing with peripheral immune cells. In animal studies, a common solution involves putative removal of blood leukocytes by perfusing tissues with cell-free solution postmortem, although this technique has been shown to have unintended consequences (such as leaving behind vascular-bound lymphocytes and unintentionally depleting leukocyte populations within tissue compartments that may be of interest) (Anderson et al., 2014). As an alternative workaround, intravascular staining is a useful tool to discriminate vascular and tissue leukocytes (Anderson et al., 2012, 2014; Mortlock et al., 2022; Potter et al., 2021). Briefly, an intravascular antibody is administered to stain >99% of peripheral blood immune cells, thereby allowing one to identify lymphocytes that were in circulation and those within the tissues. Although certainly useful, this technique was not adopted in this study, but may be considered for additional postmortem studies that are planned for the near future. Despite the possibility of peripheral blood immune cell contamination across tissue compartments, it could be counterargued that the extent was likely minimal since frequencies and phenotypes of immune cells observed in peripheral blood and tissues were distinct. This is particularly true for NK cell subsets which displayed vastly differing phenotypic characteristics and cytotoxic marker expression patterns between peripheral blood and tissues, which is discussed further in Chapter 5.

4.4.5 Conclusions

Further functional and mechanistic studies in human tissue compartments are needed to develop clinical TB interventions. However, the findings presented in this chapter provides a good starting point by offering valuable information to inform rational design of future tissue immunology studies. By providing a proof-of-concept for potential blood-based biomarkers in postmortem samples and providing a comprehensive overview of the myeloid, lymphoid,

and cytotoxic immune cell composition across tissue compartments during health and TB disease, it is hoped that these findings may pave the way for novel discoveries in the field.

Chapter 5: Characterization of human NK cells across tissue compartments in TB and controls.

"Innovation is the key to the future, but basic research is the key to future innovation."

- Jerome Isaac Friedman

5.1 Introduction

In the previous chapter, postmortem tissues were investigated to provide an overview of the myeloid and lymphoid composition across different compartments throughout the body and identify differences in proportions and cytotoxic potential that occur during health and TB disease. Since the primary focus of this thesis was surrounding NK cell determinants of immunity to *Mtb* in humans, this chapter now delves deeper into the NK-specific hypotheses in the field of TB tissue immunology.

Many studies investigating TB immunology have been limited to investigating peripheral cells, as blood is the most accessible compartment that can be sampled with little risk to the study participant, at relatively low cost. As such, NK cell studies in the context of TB have mostly demonstrated perturbations in NK cell populations and/or functional responses to *Mtb* in the peripheral blood (Bozzano et al., 2009; Cai et al., 2020; Chowdhury et al., 2018; Feinberg et al., 2004; Gerosa et al., 2002; L. D. Harris et al., 2020; Scriba et al., 2017; Suliman et al., 2016). However, there is evidence to support the important role of NK cells within tissue microenvironments (Cong & Wei, 2019; Culley, 2009; Hervier et al., 2019b), which may not reflect observations in the peripheral blood, since circulating cells only represent a small subset of the total immune landscape within the body.

Animal models, enabling site-of-disease studies, have demonstrated a potential role for NK cells in the response to *Mtb* infection in mice (Feng et al., 2006; Junqueira-Kipnis et al., 2003b) and NHPs (Esaulova et al., 2021). These animal studies suggested that NK cells play a protective role against *Mtb* infection in the lungs through cytokine production and memory-like recall responses to repeated exposure to *Mtb* antigens. In the few studies performed using human tissues, NK cells were thought to be recruited to the lung during TB disease where they play a dynamic role in modulating the immune response to *Mtb* (Portevin

et al., 2012; Schierloh, Yokobori, et al., 2005). However, these data were generated from participants for whom medical interventions were indicated due to severe immunopathology and did not include appropriate control cohorts, such as healthy individuals with or without evidence of *Mtb* immunological sensitization.

To get a more comprehensive understanding of the role of NK cells in TB disease, studies are required to investigate NK subsets in different tissue compartments in both TB patients and healthy controls. In doing so, differences observed in tissue NK cell phenotypes, frequencies and/or functions during health and disease may reveal interesting avenues for further investigations, that in turn, may uncover novel targets for TB drugs, host-directed therapies, and vaccine design. In the cancer field for instance, NK cell-mediated immunotherapies have shown promising anti-tumor effects in preclinical studies using strategies such as adoptive transfer of activated NK cells that are expanded *ex vivo,* chimeric antigen receptor (CAR)-NK cells, and NK cell extracellular vesicles targeting tumor cells (reviewed by Hu et al., 2019). Perhaps techniques used in the cancer field may be repurposed for developing NK-targeted tools that modulate their cytokine-producing and cytotoxic abilities to favour *Mtb* clearance in the tissues and at the site of disease.

The study presented in this chapter characterizes NK cell phenotypes and cytotoxic potential across human tissue compartments in TB cases and controls, offering novel contributions to the TB tissue immunology field.

5.2 Methods and Materials

5.2.1 Study decedents

In this chapter, results are presented from the same postmortem tissue cohort described in Chapter 4, Section 4.2.1. Briefly, ten TB patients who succumbed to disease and 19 controls, who were otherwise healthy but died due to trauma, were identified via next of kin, who were approached for consent to include tissues from the deceased person prior to autopsy. Informed consent and enrollment were performed at the Mulago National Referral Hospital (MNRH), Uganda by a trained counselor from a collaborating research group led by Dr Stephen Cose based at the Medical Research Council/Uganda Virus Research Institute and London School of Hygiene & Tropical Medicine (MRC/UVRI & LSHTM) Uganda Research Unit. Next of kin were re-consented two weeks following initial consenting. Autopsies and tissue sampling were performed by a pathologist at the MNRH, Uganda. There were no exclusion criteria based on age, sex, HIV status, other co-morbidities, or TB risk-associated habits (such as smoking and alcohol consumption). TB cases were clinically diagnosed with active disease and were admitted to the TB ward at MNRH prior to death.

Controls were admitted to the trauma/emergency unit at the MNRH and were identified as otherwise healthy individuals who died due to trauma and/or accidental injury. Healthy controls had no evidence of lung disease or characteristics of ill health prior to death or during autopsy and were excluded if they had a positive BAL MGIT liquid culture test result (indicating potential subclinical or undiagnosed TB). Healthy controls were subclassified into two groups based on evidence of *Mtb* immunological sensitization using the T-SPOT®.TB assay (Oxford Immunotec), or a standardized flow cytometry ICS assay routinely used at SATVI (the latter was used for classification in cases of indeterminate TSPOT results).

Tonsil tissues from living participants were included as a control and were kindly donated by Dr Al Leslie at the Africa Health Research Institute (AHRI), South Africa. Participants were HIV-uninfected individuals who were clinically indicated for tonsillectomy and excluded TB patients or suspected TB cases.

5.2.2 Tissue dissociation and single cell isolation

Postmortem tissue samples (including PBMC, lung tissue, hilar lymph nodes, BAL, and spleen) and tonsil tissues from living controls were processed and single cell suspensions were isolated by Dr Stephen Cose's research group, according to the methods described in Chapter 2, Section 2.3. Single cell suspensions of tissue samples were then shipped to SATVI, South Africa for CyTOF antibody staining and data acquisition.

5.2.3 CyTOF antibody staining and data acquisition

All postmortem samples and tonsil cells from living participants were stained with the full panel of CyTOF antibodies (Chapter 2, Table 2.1) and data were acquired on the CyTOF2 instrument according to the protocol outlined in Chapter 2, Section 2.8. For ease of reference, a comprehensive list of antibody targets of specific interest in the context of NK cells are outlined in Table 5.1.

Table 5.1: CyTOF NK cell antibody panel

Marker	Metal	Rationale	Clone	Antibody supplier
Extracellular (surface) markers				
CD49a	*162Dy	Tissue-residency	TS2/7	BioLegend
CD103	*145Nd	Tissue-residency	Ber-ACT8	BioLegend
CCR6	*147Sm	Tissue-residency	G034E3	BioLegend
CXCR3	*113Cd	Tissue-residency	G025H7	BioLegend
CD56	149Sm	NK lineage	NCAM16.2	Standard BioTools
CD16	209Bi	Maturation	3G8	Standard BioTools
CD57	172Yb	Maturation	HCD57	Standard BioTools
CD38	167Er	Maturation	HIT2	Standard BioTools
CD27	*146Nd	Maturation/memory	O323	BioLegend
CD11b	144Nd	Maturation	ICRF44	Standard BioTools
NKp46	*163Dy	Activating receptor	9E2	BioLegend
DNAM1	*155Gd	Activating receptor	DX11	BD Biosciences
NKG2D	166Er	Activating receptor	ON72	Standard BioTools
NKG2A	169Tm	Inhibiting receptor	Z199	Standard BioTools
KIR	*156Gd	Inhibiting receptor	DX27	BioLegend
CD69	*165Ho	Activation marker	FN50	BioLegend
HLA-DR	170Er	Activation marker	L243	Standard BioTools
PD1	*153Eu	Checkpoint protein	EH12.2H7	BioLegend
PDL1	*150Nd	Checkpoint protein	29E.2A3	BioLegend
TACTILE	*165Ho	Checkpoint protein	NK92.39	BioLegend
TIGIT	154Sm	Checkpoint protein	MBSA43	Standard BioTools
Fas-L	*148Nd	Cytotoxic mediator	NOK-1	BioLegend
Intracellular (functional) markers				
Perforin	175Lu	Cytotoxic molecule	B-D48	Standard BioTools
Granzyme B	*168Er	Cytotoxic molecule	GB11	BioLegend
Granzyme K	*158Gd	Cytotoxic molecule	GM26E7	BioLegend

* In-house conjugated antibodies using Maxpar Antibody Labeling Kits (Standard BioTools).

5.2.4 Data analysis

Bulk NK cells were exported from FlowJo and imported into R Studio for phenotypic analysis, according to the strategy outlined in Chapter 2, Section 2.9 and Figure 2.2. To perform phenotyping of NK cells, the FAUST algorithm was run using all NK cell-specific markers of interest (outlined in Table 5.1) as active channels for phenotypic annotation. From the full NK cell panel, the following subset of markers from the NK cell antibody panel were selected by FAUST to label cell phenotypes: CD56, CD16, CD57, CD103, CD49a, CXCR3, CD38, CD7, Fas-L, NKG2A, NKG2D, perforin and granzyme B. Notably, regulatory checks and extensive optimization confirmed that all markers within the panel were staining cells adequately. However, the FAUST algorithm only selected markers with bi- or multi-modal distribution patterns of expression to place “cut points” for cell clustering and annotation. For other FAUST parameters, the depth score threshold was set to 0.05, selection quantile to 0.9 and the “nameOccuranceNum” parameter was set to 2. The experimental unit was set to the tissue type (i.e., PBMC, lung, hilar lymph node, BAL, spleen, and tonsil) to specify the unit of analysis of samples contained in the gating set for clustering. The “annotationsApproved” parameter was set to “TRUE” to instruct FAUST to run the method totally unsupervised. Frequencies of clustered NK subsets were obtained by summing over counts for which cells shared common annotation expressions.

As previously discussed in Chapter 4, the term “median staining intensity” (MSI) was used throughout to describe the relative expression level of a given marker. Expression values for markers of interest were exported from expression matrices in R for total NK cells and FAUST-annotated subsets. Statistical analysis to compare marker expression (MSI) and cell frequencies between cohorts was performed using unpaired Wilcoxon rank sum test for pair-wise comparisons with TB as the reference cohort, grouped by tissue compartment (i.e., PBMC, lung, hilar lymph node and spleen). Statistical comparisons were not performed

between cohorts for BAL samples, since there were too few datapoints in each cohort to reliably analyze. The Holm-Bonferroni test was used to control for multiple comparisons (q-values). Only results with q-values <0.25 are shown on graphs. No statistical comparisons were made between tissue compartments, only between cohorts (which were stratified by tissue type).

5.3 Results

5.3.1 Decedent characteristics

Results are presented from the same postmortem cohort described in Chapter 4, Table 4.5. Briefly, decedents included men and women between the ages of 29 and 69 years. The postmortem TB cohort (n=10) included eight cases of pulmonary TB and two extrapulmonary TB cases. Seven decedents were HIV co-infected (n=7; six of which were TB cases). Five of the seven HIV-infected decedents were receiving ARV therapy for at least one month prior to death, while two had no information regarding treatment. Five of ten TB cases had co-morbidities of hypertension (n=3), hypertension with diabetes (n=1) and liver disease (n=1). Six of ten TB cases were receiving anti-TB therapy for at least two weeks prior to death, while four had no record of receiving treatment. Trauma cases were healthy controls who had no known evidence of illness prior to death or during autopsy (n=19) and were classified into two cohorts based on evidence of *Mtb* sensitization: $TSPOT^-$ (n=11) and $TSPOT^+$ (n=8). During autopsy, specimens were collected from different compartments: PBMC ($TSPOT^-$ n=11, $TSPOT^+$ n=8, TB n=10), lung (left upper lobe; $TSPOT^-$ n=10, $TSPOT^+$ n=8, TB n=10), hilar lymph nodes ($TSPOT^-$ n=7, $TSPOT^+$ n=6, TB n=8), BAL ($TSPOT^-$ n=7, $TSPOT^+$ n=2, TB n=4), and spleen ($TSPOT^-$ n=7, $TSPOT^+$ n=6, TB n=8).

5.3.2 Tissue-resident NK cells are enriched in the lungs of TB cases

A series of tissue-resident markers were included in the CyTOF antibody panel to investigate tissue homing in postmortem samples, including CD103, CD49a, CCR6 and CXCR3. It was hypothesized that tissue-resident markers were upregulated on NK cells in the tissues compared to the peripheral blood cells. During TB, NK cells actively migrate to the site of disease to perform functional roles such as cytotoxic and cytokine-producing mediators of infection (Portevin et al., 2012; Esaulova et al., 2021; Feng et al., 2006; Junqueira-Kipnis et al., 2003b). It was hypothesized that tissue-resident NK subsets would be depleted in the periphery and enriched in the lungs of TB decedents relative to controls, possibly reflecting NK homing to affected tissues during active disease. Notably, “tissue-resident NK cells” were defined as the population of NK cells expressing one or more markers of tissue residency, according to published literature (Franklin et al., 2022; Hashemi & Malarkannan, 2020). Frequencies of total tissue-resident NK cells were obtained by summing over $CD103^+$, $CD49a^+$ and/or $CXCR3^+$ NK cells annotated by the unsupervised clustering (i.e., cells annotated as positively expressing one or more tissue-resident marker).

Tissue-resident markers CD103, CD49a, CCR6 and CXCR3 were expressed at low levels on NK cells in peripheral blood (Figure 5.1a and b) and frequencies of tissue-resident marker-expressing NK cells occurred almost exclusively in the tissues and very few occurred in the peripheral blood, as expected (Figure 5.1c). CCR6 and CD103 were expressed at relatively low levels on NK cells across all tissue compartments (Figure 5.1a and b). CD49a was abundantly expressed on lung NK cells (Figure 5.1a and b), while CXCR3 was expressed at high levels on NK cells in all tissues and was the predominant NK cell tissue resident marker in the hilar lymph nodes, BAL, and spleen (Figure 5.1b).

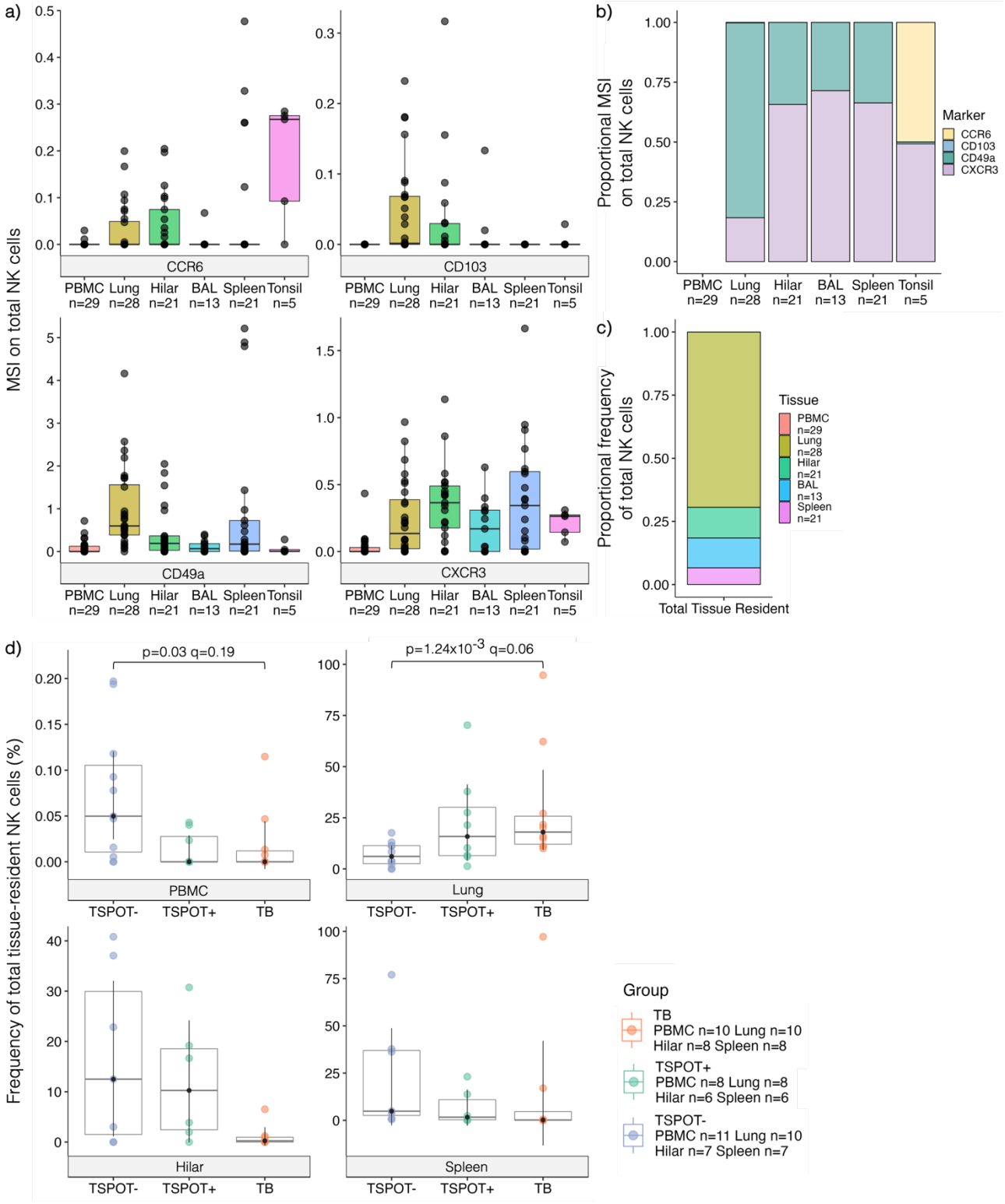

Figure 5.1: Tissue-resident NK cells in postmortem tissues and peripheral blood. a) Absolute values and b) proportional expression of tissue-resident markers across total tissue and peripheral blood NK cells. Expression reported in the form of median staining intensity (MSI) for each marker in total NK cells. Frequencies of tissue-resident marker-expressing NK cells shown as c) proportions across tissue samples and d) stratified according to cohort. Statistical analysis in d) was performed using unpaired Wilcoxon rank sum test for pair-wise comparisons with TB as the reference group (p-value), and the Holm-Bonferroni test to account for multiple comparisons (q-value). In boxplots, each box represents median and interquartile range (IQR). Whiskers in a) represent 1.5x IQR of the upper and lower quartiles, and whiskers in d) indicate 95% confidence intervals.

Tissue-resident NK cells from TB decedents had lower frequencies in the peripheral blood ($p=0.03$, $q=0.19$) and higher frequencies in the lung ($p=7.24x10^{-3}$, $q=0.06$) relative to $TSPOT^-$ controls (Figure 5.1d). However, the p-value fell below the cut-off for statistical significance upon correction for multiple comparisons. No significant differences in tissue-resident NK cell frequencies were observed between cohorts in the spleen and hilar lymph nodes (Figure 5.1d).

CCR6 was expressed at low levels on NK cells across all postmortem tissue compartments (Figure 5.1a and b). To demonstrate that low expression levels on NK cells in the postmortem tissues was not due to poor performance of the antibody, the expression of tissue-resident markers was investigated in control tonsil samples from living individuals. Data from tonsil tissues showed that CCR6 and CXCR3 were expressed at high levels on NK cells with similar expression levels, while CD103 and CD49a were expressed at low levels (Figure 5.1a and b).

5.3.3 NK cells in the tissues are predominantly phenotypically immature subsets

The diversity of tissue-resident and circulating NK cells was further assessed by sub-classification according to traditional NK cell phenotyping using CD56 and CD16 co-expression patterns. Importantly, the terms “tissue-resident” and “circulating” do not infer tissue localization but are standard terms to describe phenotypic characteristics of NK cell subsets that either express markers of tissue residency or lack expression of tissue-resident markers, respectively. Therefore, NK cells in the tissues and peripheral blood may include both tissue-resident and circulating subsets. Based on published literature, it was hypothesized that NK cells in the peripheral blood and lung tissue are mostly $CD16^{hi}$ cells that lack expression of tissue-resident markers (Hervier et al., 2019a; Marquardt et al., 2017b), while and NK cells in the secondary lymphoid organs are predominantly

$CD56^{hi}CD16^{lo}$ cells (Björkström et al., 2016; Marquardt et al., 2015; Sharkey et al., 2015) that also lack expression of tissue-resident markers (i.e., “circulating” NK cells) (Figure 5.2).

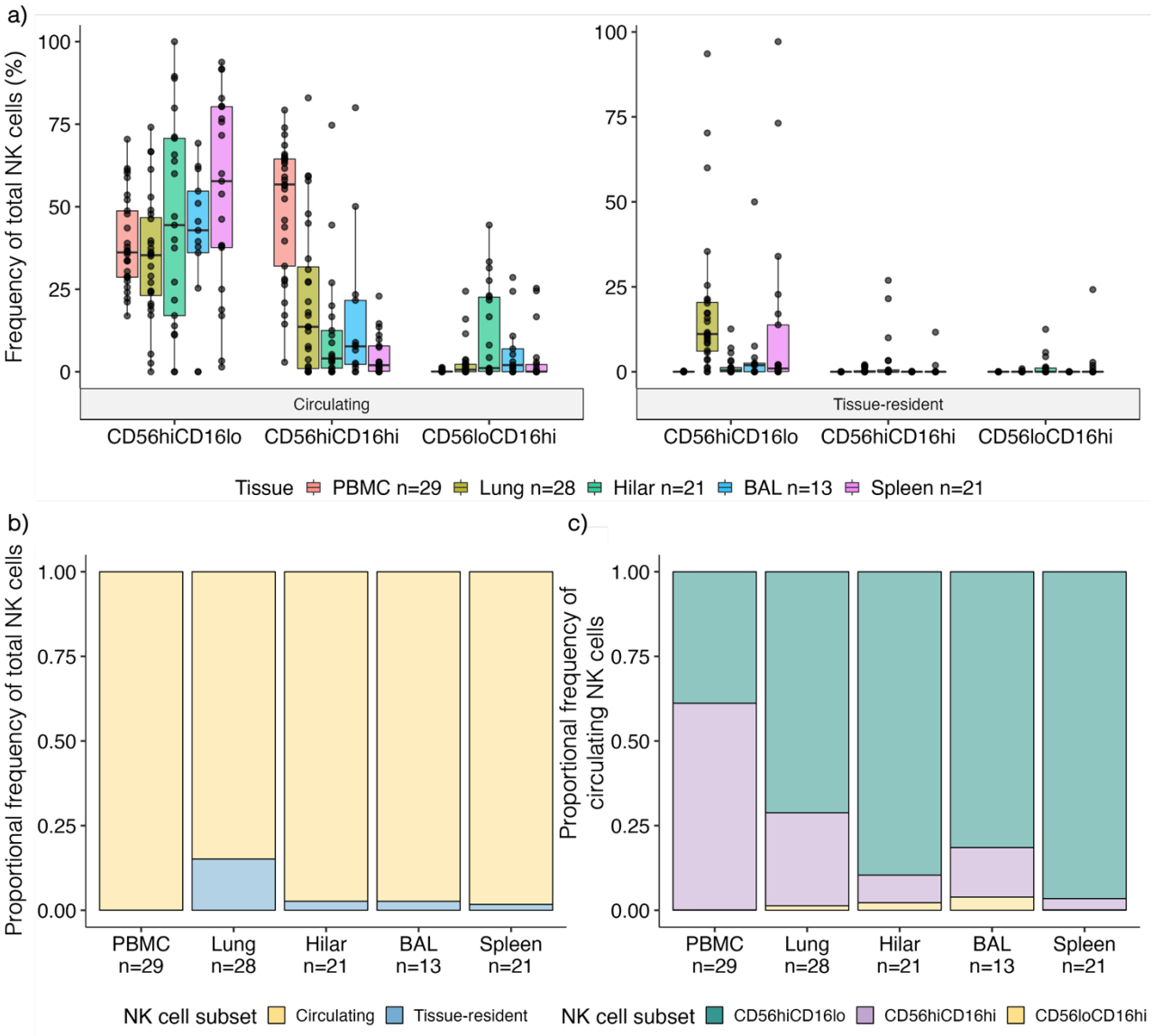

Figure 5.2: Circulating and tissue-resident NK cell subsets across tissues. a) Frequencies of circulating and tissue-resident NK cells, subclassified according to CD56 and CD16 co-expression patterns. b) Relative proportions of total circulating and tissue-resident NK cell frequencies across tissues. c) Proportional frequencies of circulating NK cell subsets subclassified according to CD56 and CD16 co-expression patterns. In boxplots, each box represents median and interquartile range (IQR), whiskers indicate 1.5x IQR of the upper and lower quartiles.

As hypothesized, circulating NK cells were predominant in the peripheral blood and tissues; comprising >90% of the total NK cell population in the peripheral blood, hilar lymph nodes, BAL, and spleen, and ~80% of the lung tissue (Figure 5.2a and b). Tissue-resident NK cells

comprised ~15-20% of the lung tissue and were phenotypically classified as immature $CD56^{hi}CD16^{lo}$ $NK_{regulatory}$ cells (Figure 5.2a and b). Circulating NK cells in the peripheral blood were mostly mature, $CD16^{hi}$ NK cells (Figure 5.2a and c), while NK cells in the lung, hilar lymph nodes, spleen and BAL compartments were mainly of the immature $CD56^{hi}CD16^{lo}$ phenotype (Figure 5.2a and c).

5.3.4 NK cells lacking expression of cytotoxic markers are enriched in the TB lung

Published literature (Kathamuthu et al., 2020) and data presented in Chapter 4 (Figure 4.11a) showed that frequencies of cytotoxic marker-expressing NK cells were highest in the peripheral blood compared to the tissue compartment. To confirm that the cytotoxic potential of NK cells in peripheral blood was higher than tissue compartments, it was hypothesized that relative expression of perforin, granzyme B and granzyme K would be higher in peripheral blood NK cells relative to tissue (Figure 5.3).

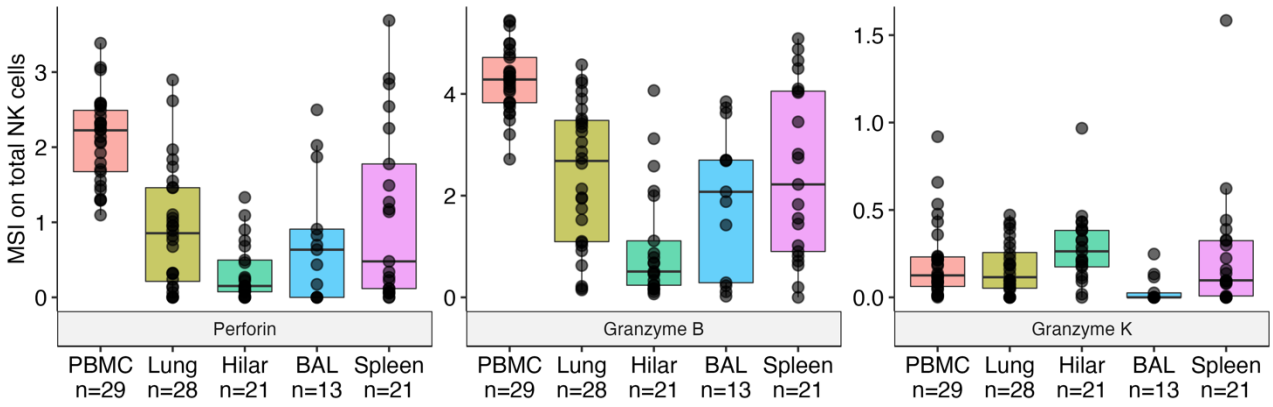

Figure 5.3: Expression of cytotoxic molecules in NK cell subsets across compartments. Expression reported in the form of median staining intensity (MSI) for each marker in NK cell subsets. In boxplots, each box represents median and interquartile range (IQR), whiskers indicate 1.5x IQR of the upper and lower quartiles.

Peripheral blood NK cells expressed more perforin and granzyme B relative to NK cells in tissue compartments (Figure 5.3a), as hypothesized. However, granzyme K was expressed at low levels across all tissue compartments and was mostly expressed by NK cells in the

hilar lymph nodes. To further characterize NK populations across peripheral blood and tissue compartments, the expression of cytotoxic molecules (perforin, granzyme B and granzyme K) was evaluated across NK cell subsets, subclassified according to CD56 and CD16 co-expression patterns. NK cell subsets in the peripheral blood have been extensively studied and are well-characterized (Angelo et al., 2015; Del Zotto et al., 2020; S. L. Smith et al., 2020). Based on the current understanding of NK cell biology, which was mostly derived from evidence in human peripheral blood studies, it was hypothesized that mature $CD16^{hi}$ NK cells expressed cytotoxic markers at high levels, in contrast to their immature $CD56^{hi}CD16^{lo}$ counterparts which expressed perforin and granzyme B at low levels (Béziat et al., 2011; Björkström, Ljunggren, et al., 2010b; Björkström, Riese, et al., 2010). The $CD56^{hi}$ subset was hypothesized to be the granzyme K-expressing subset, based on published literature (Bade et al., 2005; Bouwman et al., 2021; Bratke et al., 2005).

Results confirmed that perforin and granzyme B expression were higher in the $CD16^{hi}$ NK cells, while $CD56^{hi}CD16^{lo}$ NK cells had lower expression of these cytotoxic markers in peripheral blood (Figure 5.4a). However, in the tissue compartments, perforin and granzyme B expression was highest in the $CD56^{hi}CD16^{hi}$ subset, and lowest in the $CD56^{hi}CD16^{lo}$ and $CD56^{lo}CD16^{hi}$ subsets (Figure 5.4a). Therefore, terminally differentiated $CD56^{lo}CD16^{hi}$ NK cells in tissues were either hypo-cytotoxic or had degranulated and released their cytotoxic molecules into the surrounding microenvironment. Granzyme K was expressed at low levels across all NK cell subsets in all compartments, displaying no clear pattern of dominant expression in any specific NK subset (Figure 5.4a).

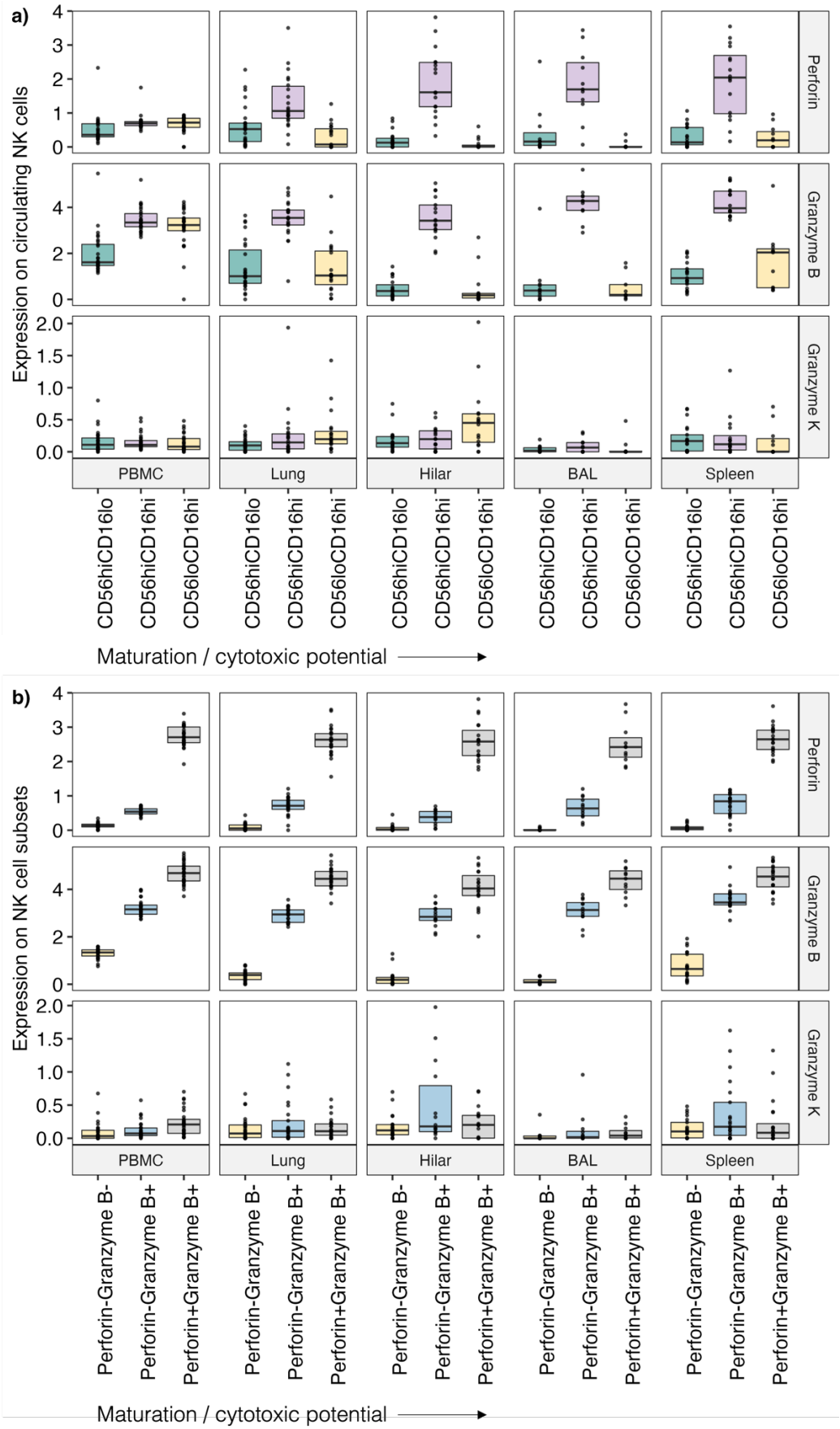

Figure 5.4: Cytotoxic marker expression in NK cell subsets across tissue compartments. a) NK cell subsets classified according to CD56 and CD16 co-expression patterns, and b) NK cell subsets classified according to FASUT annotation using perforin and granzyme B co-expression in various tissue compartments. Expression reported in the form of median staining intensity (MSI) for each marker in NK cell subsets.

Since peripheral and tissue NK cell subsets appeared to have different phenotypes and cytotoxic potential, the expression of cytotoxic molecules was compared between NK subsets annotated according to expression of perforin and/or granzyme B. It was hypothesized that double-positive perforin^{+}granzyme B^{+} ("poly-cytotoxic") NK cells had the highest expression of cytotoxic molecules relative to their single-positive perforin^{-}granzyme B^{+} ("mono-cytotoxic") counterparts. This hypothesis was also investigated in Chapter 4 within total cytotoxic marker-expressing cells (not delineated according to lymphocyte subsets). The rationale of this hypothesis was based on published data showing that polyfunctional T cells co-expressing more than one cytokine expressed higher levels of cytokines relative to single cytokine-producing T cells (Hersperger et al., 2012; Boyd et al., 2015; Burel et al., 2017).

Accordingly, expression levels of perforin and granzyme B followed a stepwise increase from the annotated double-negative to mono-cytotoxic to poly-cytotoxic NK cell subsets (Figure 5.4b). Notably, subsets of single-positive perforin^{+}granzyme B^{-} cells were not identified. In the granzyme B-positive subsets (i.e., perforin^{-}granzyme B^{+} and perforin^{+}granzyme B^{+}), the double-positive population had the highest expression levels of granzyme B (Figure 5.4b), suggesting a higher cytotoxic potential of the double-positive population relative to phenotypically single-positive NK cells. Additionally, the perforin^{-} granzyme B^{-} and perforin^{-}granzyme B^{+} populations were annotated as perforin negative, due to low perforin expression relative to double-positive perforin^{+}granzyme B^{+} NK cells (Figure 5.4b). However, the single-positive perforin^{-}granzyme B^{+} population expressed slightly higher perforin levels relative to double-negative perforin^{-}granzyme B^{-} NK cells, suggesting that these "mono-cytotoxic" cells were phenotypically perforin^{lo}granzyme B^{+} rather than perforin^{-}granzyme B^{+}. This observation was a likely artifact from automated, bi-modal annotation using the FAUST algorithm. Overall, classification of NK cell maturation

and terminal differentiation follows a spectrum of increasing cytotoxic potential from double-negative, mono-cytotoxic to poly-cytotoxic NK cell subsets.

The cytotoxic potential of NK cell subsets was then compared between cohorts. It was hypothesized, based on findings reported in Chapter 3 and Chapter 4, that NK cells in TB patients had higher cytotoxic potential relative to controls, possibly reflecting a state of immune activation and effector cell responses due to higher *Mtb* antigen load. The expression of cytotoxic molecules (perforin, granzyme B and granzyme K) on total NK cells and frequencies of cytotoxic marker-expressing subsets were compared between cohorts. Granzyme K was not used as an annotation marker, therefore granzyme K expression (MSI) was investigated in subsets expressing perforin and/or granzyme B (Figure 5.5).

In support of the hypothesis, peripheral blood NK cells in TB decedents had significantly higher expression levels of perforin ($TSPOT^-$ $p=7.88x10^{-4}$, $q=0.02$), granzyme B ($TSPOT^-$ $p=1.70x10^{-4}$, $q=3.90x10^{-3}$) and granzyme K ($TSPOT^-$ $p=3.97x10^{-5}$, $q=9.50x10^{-4}$) relative to $TSPOT^-$ controls (Figure 5.5a). Granzyme B expression in peripheral NK cells was also significantly higher in TB decedents relative to $TSPOT^+$ controls ($TSPOT^+$ $p=1.37x10^{-3}$, $q=0.03$). Although expression levels of perforin and granzyme K were not significantly different between TB and $TSPOT^+$ controls, there was an apparent trend suggesting higher expression in NK cells of TB decedents relative to controls (Figure 5.5a). No trends or significant findings were observed for cytotoxic molecule expression in the tissues, which was generally low across all compartments (Figure 5.6).

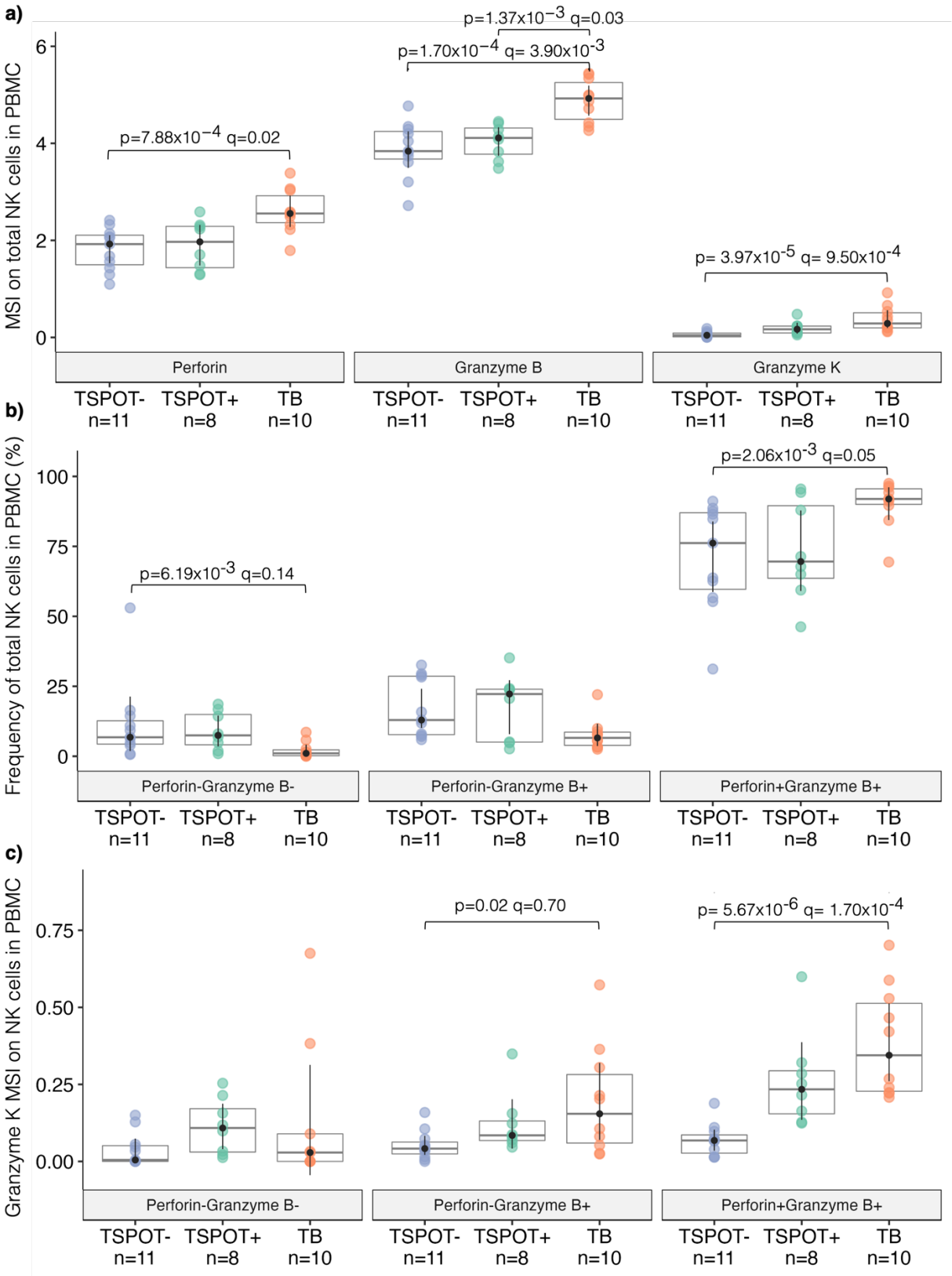

Figure 5.5: Relative expression and frequencies of cytotoxic marker-expressing NK cell subsets in TB and healthy controls. a) Comparison of cytotoxic molecule expression in peripheral NK cells between cohorts. b) Frequencies of cytotoxic marker-expressing NK cell subsets compared between cohorts. c) Comparison of granzyme K expression between cohorts in peripheral NK cells subclassified according to perforin and granzyme B co-expression. Marker expression reported in the form of median staining intensity (MSI). Statistical analysis in a), b) and c) was performed using unpaired Wilcoxon rank sum test for pair-wise comparisons with TB as the reference group (p-value), and the Holm-Bonferroni test to account for multiple comparisons (q-value). In boxplots, each box represents median and interquartile range, whiskers indicate 95% confidence intervals.

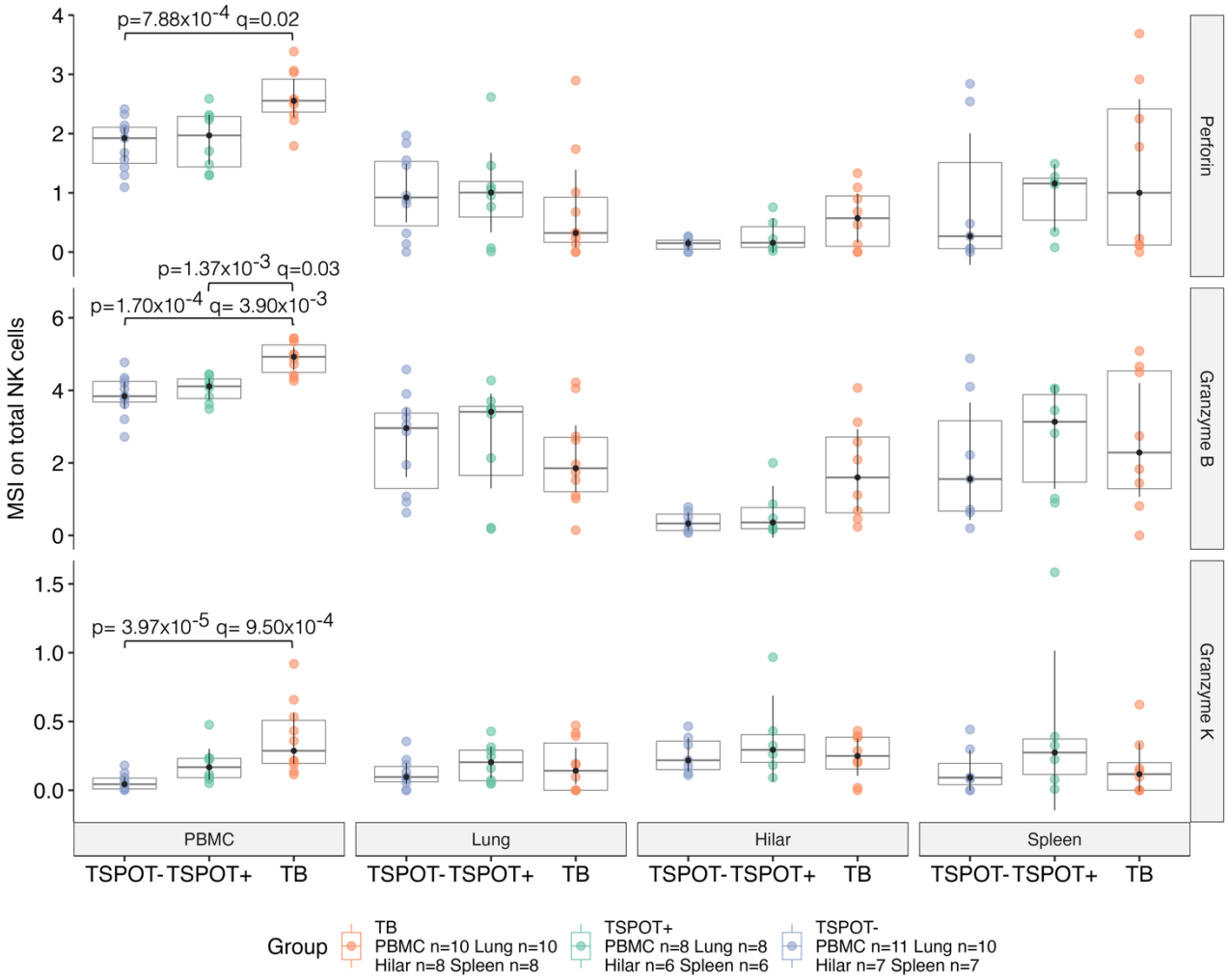

Figure 5.6: Cytotoxic marker expression in total NK cells from postmortem tissue compartments. Expression reported in the form of median staining intensity (MSI) for each marker in total NK cells. Statistical analysis was performed using unpaired Wilcoxon rank sum test for pair-wise comparisons with TB as the reference group (p-value), and the Holm-Bonferroni test to account for multiple comparisons (q-value). In boxplots, each box represents median and interquartile range, whiskers indicate 95% confidence intervals.

Frequencies of cytotoxic marker-expressing subsets were compared between cohorts. Peripheral blood perforin$^-$granzyme B$^-$ NK cells were depleted ($p=6.19x10^{-3}$, $q=0.14$) and perforin$^+$granzyme B$^+$ NK cells were significantly increased ($p=2.06x10^{-3}$, $q=0.05$) in the TB cohort compared to TSPOT$^-$ controls (Figure 5.5b), indicating that NK cells with high cytotoxic potential were enriched in the periphery of TB decedents. No significant differences in frequencies of cytotoxic marker-expressing subsets were observed in tissues (Figure 5.7).

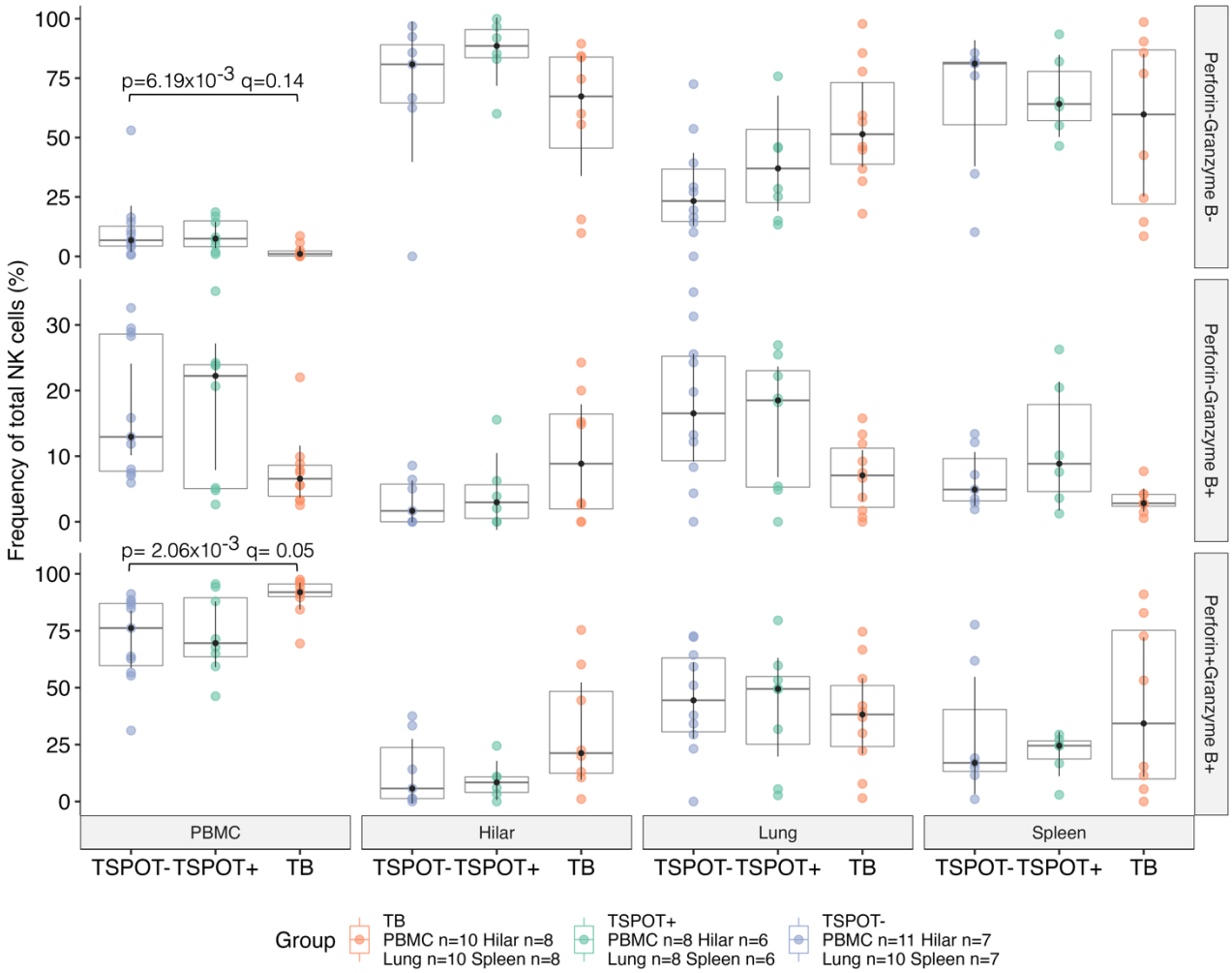

Figure 5.7: Frequencies of cytotoxic marker-expressing NK cells from postmortem tissue compartments. Statistical analysis was performed using unpaired Wilcoxon rank sum test for pair-wise comparisons with TB as the reference group (p-value), and the Holm-Bonferroni test to account for multiple comparisons (q-value). In boxplots, each box represents median and interquartile range, whiskers indicate 95% confidence intervals.

Since granzyme K was not used as an annotation marker by FAUST, expression of granzyme K was compared between cohorts in perforin- and/or granzyme B-expressing NK populations. The TB cohort expressed higher levels of granzyme K relative to $TSPOT^-$ in $perforin^-granzyme\ B^+$ ($p=5.67x10^{-6}$, $q=1.40x10^{-4}$) and $perforin^+granzyme\ B^+$ ($p=0.02$, $q=0.56$) subsets (Figure 5.5c).

NK cell cytotoxic potential was further investigated in the context of the gold standard NK subset classification based on CD56 and CD16 co-expression patterns (Figure 5.8).

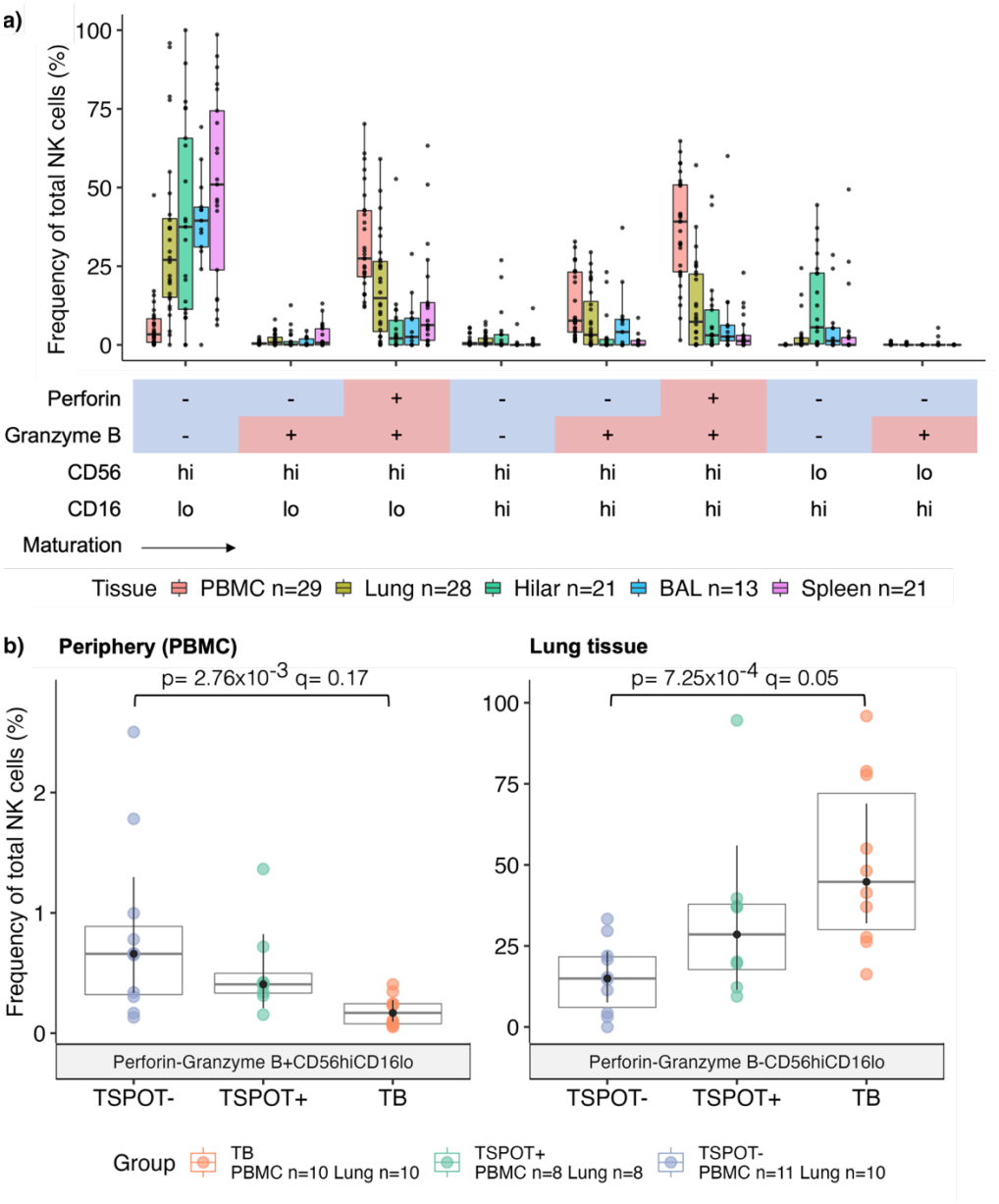

Figure 5.8: Frequencies of cytotoxic NK cell subsets, subclassified according to CD56 and CD16 co-expression patterns, across compartments and cohorts. a) Frequencies of NK cell subsets classified according to expression of cytotoxic molecules and CD56/CD16 co-expression across tissue compartments. b) Frequencies of peripheral blood and lung NK cells compared between cohorts, subclassified according to perforin, granzyme B, CD56 and CD16 co-expression. Statistical analysis in b) was performed using unpaired Wilcoxon rank sum test for pair-wise comparisons with TB as the reference group (p-value), and the Holm-Bonferroni test to account for multiple comparisons (q-value). In boxplots, each box represents median and interquartile range (IQR). Whiskers in a) indicate 1.5x IQR of the upper and lower quartiles, and whiskers in b) indicate 95% confidence interval.

Majority of peripheral NK cells were comprised of the $CD56^{hi}CD16^{hi}$ subset and were further subclassified as being mono- ($perforin^{-}granzyme\ B^{+}$) and poly-cytotoxic ($perforin^{+}granzyme\ B^{+}$). The phenotypically immature $CD56^{hi}CD16^{lo}$ subset of peripheral NK cells were poly-

cytotoxic for perforin and granzyme B expression (Figure 5.8a). NK cells from hilar lymph nodes, BAL and spleen were mainly immature $CD56^{hi}CD16^{lo}$ cells that were double-negative for perforin and granzyme B expression (Figure 5.8a). Lung NK cells had a large proportion of $CD56^{hi}CD16^{lo}$ cells that were double-negative for perforin and granzyme B and a smaller proportion that were poly-cytotoxic ($perforin^{+}granzyme\ B^{+}$). The smaller population of $CD56^{hi}CD16^{hi}$ NK cells in the lungs were either mono- or poly-cytotoxic subsets (Figure 5.10a). Overall, the $CD16^{hi}$ NK cells in peripheral blood had high cytotoxic potential, and even immature $CD56^{hi}CD16^{lo}$ NK cells in the peripheral blood were poly-cytotoxic. Therefore, peripheral blood contained NK cells with high cytotoxic potential, while hilar lymph nodes, BAL and spleen had mainly immature, double-negative ($perforin^{-}granzyme\ B^{-}$) NK subsets. NK cells within the lung compartment had a mixture of double-negative, mono- and poly-cytotoxic subsets, predominantly of the immature $CD56^{hi}CD16^{lo}$ phenotype.

Comparisons between cohorts revealed fewer mono-cytotoxic ($perforin^{-}granzyme\ B^{+}$), immature $CD56^{hi}CD16^{lo}$ NK cells in the peripheral blood of TB decedents relative to $TSPOT^{-}$ controls ($p=2.76x10^{-3}$, q=0.17; Figure 5.8b). Lung tissue in TB was enriched with $perforin^{-}$ $granzyme\ B^{-}$ immature $CD56^{hi}CD16^{lo}$ NK cells relative to $TSPOT^{-}$ controls ($p=7.25x10^{-4}$, q=0.05; Figure 5.8b). No significant differences were observed with other NK cell subsets within peripheral blood and tissues (Figure 5.9). Again, these findings may indicate that NK cells in the lungs of TB patients who succumbed to disease were either hypo-cytotoxic or had degranulated to release cytotoxic molecules into the surrounding microenvironment.

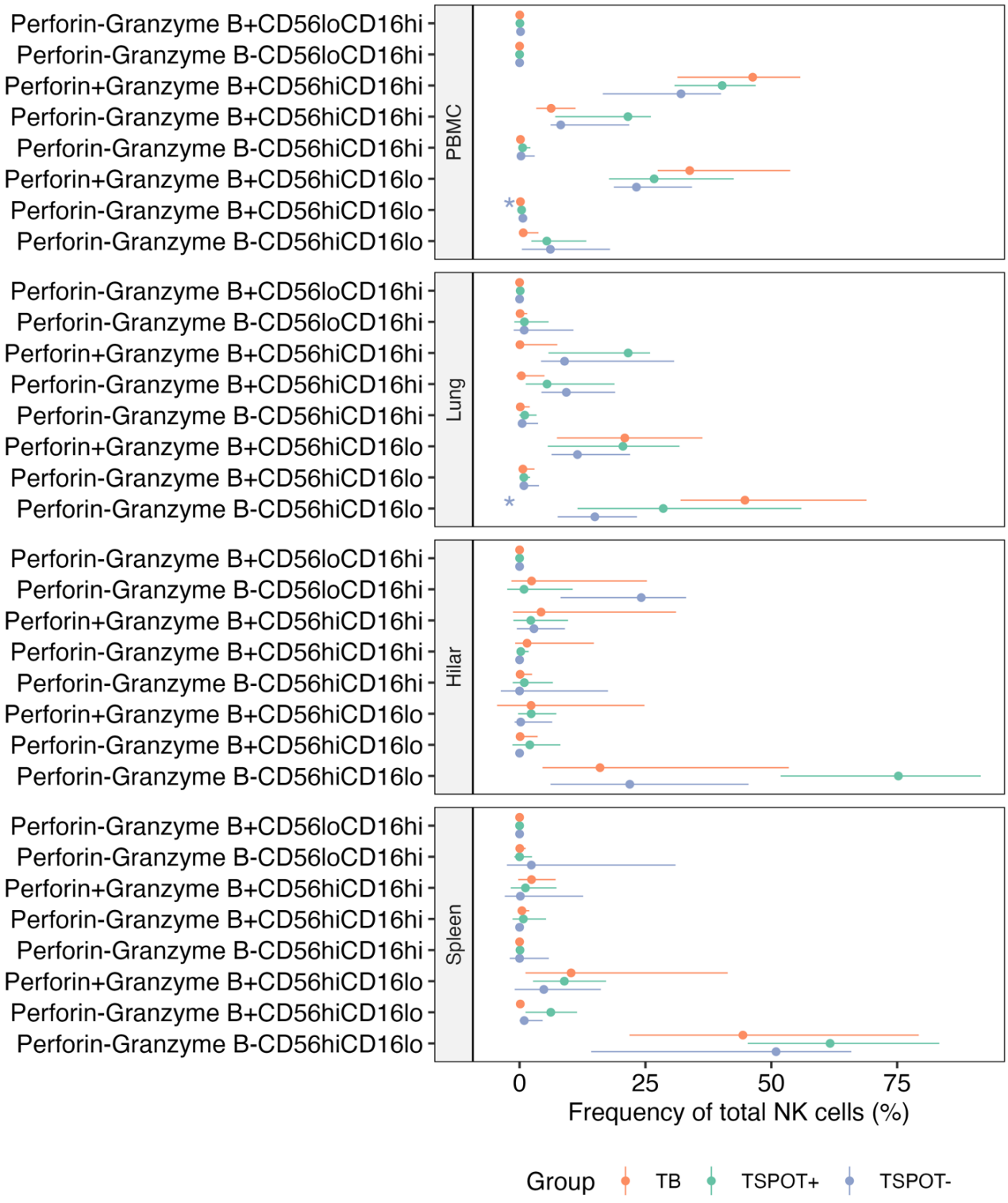

Figure 5.9: Frequencies of cytotoxic marker-expressing NK cells from postmortem tissue compartments, subclassified according to CD56 and CD16 co-expression. Statistical analysis was performed using unpaired Wilcoxon rank sum test for pair-wise comparisons with TB as the reference group (p-value), and the Holm-Bonferroni test to account for multiple comparisons (q-value). Each dot represents median frequency, whiskers indicate 95% confidence intervals. Stars (*) indicate statistically significant differences observed between cohorts, detailed further in Figure 5.8.

5.3.5 Immature NK cells are depleted in the peripheral blood and enriched in the TB lung

Although NK cells are traditionally classified according to the CD56/CD16 phenotypic characterization, NK cells also express a variety of receptors that reflect their maturation status. The expression of maturation markers; CD38, CD57, CD11b and CD27, was investigated across compartments and between cohorts to further characterize NK cells within tissues. It was hypothesized that NK cells in TB patients express maturation markers at high levels, possibly reflecting a state of immune activation and NK maturation towards more terminally differentiated effector phenotypes during disease.

NK cells in the peripheral blood and all tissues expressed CD38, CD57 and CD11b, while CD27 was expressed almost exclusively on NK cells of the hilar lymph nodes (Figure 5.10a). As a control, expression patterns of NK cell maturation markers in tonsil tissues from living individuals showed that CD38 and CD11b were expressed at high levels on tonsil NK cells, while CD57 and CD27 were expressed at low levels (Figure 5.10a).

Comparisons between cohorts revealed that CD38 expression on NK cells in the peripheral blood was significantly upregulated in TB relative to $TSPOT^{+}$ ($p=1.37x10^{-3}$, $q=0.04$) and $TSPOT^{-}$ ($p=1.13x10^{-5}$, $q=3.40x10^{-4}$) controls (Figure 5.10b). In contrast, CD57 was significantly downregulated in PBMC ($p=1.52x10^{-3}$, $q=0.04$) and lung ($p=3.89x10^{-3}$, $q=0.10$) of TB decedents relative to $TSPOT^{-}$ controls. The inverse relationship between CD38 and CD57 in the peripheral blood may reflect a switch in the maturation phenotype of NK cells during TB, either as a cause or a consequence of disease. No other trends were noted for CD11b and CD27, or CD38 and CD57 in other tissue compartments (Figure 5.11).

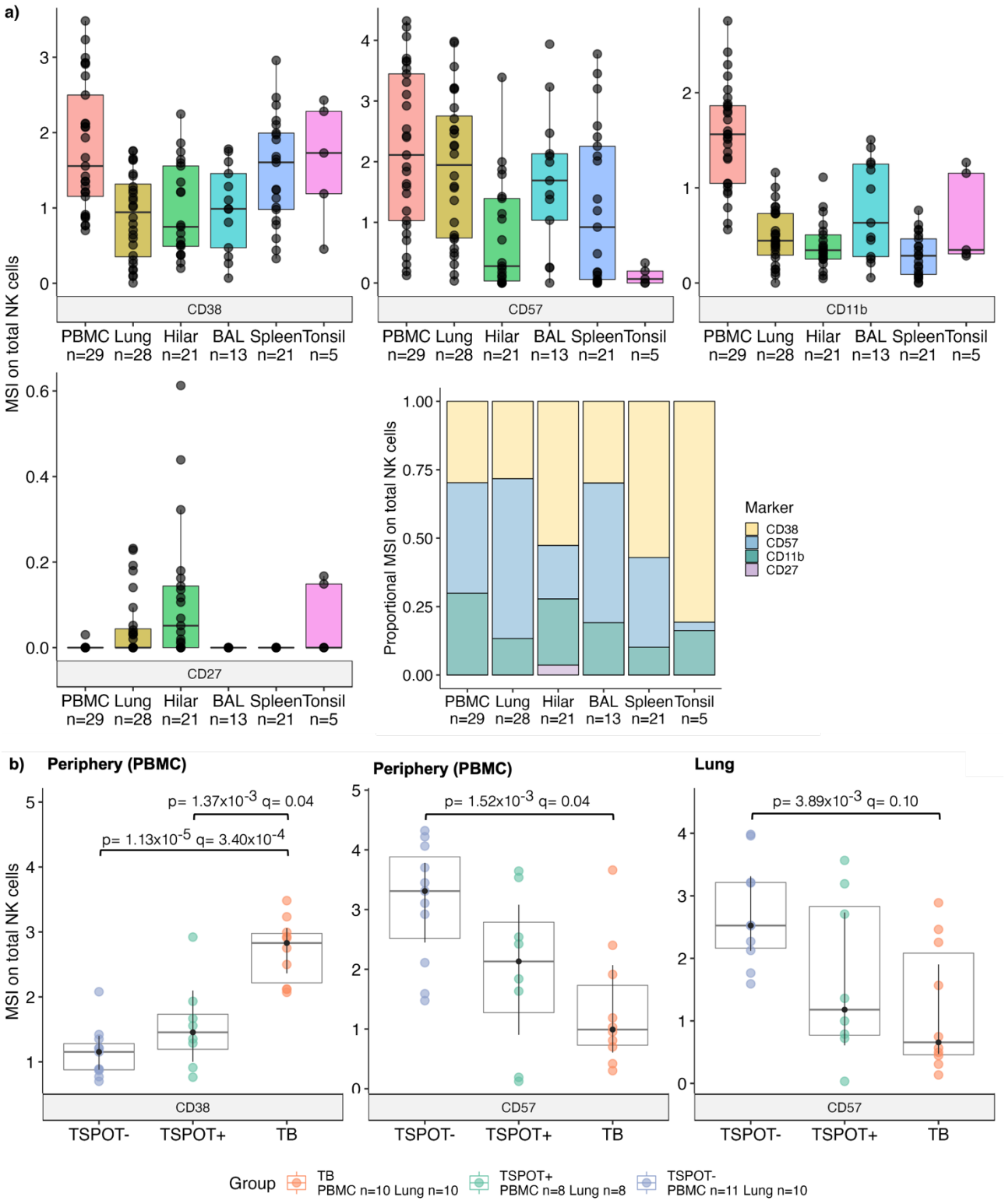

Figure 5.10: Expression of NK cell maturation markers across tissue compartments and cohorts. a) NK cell maturation marker expression and relative proportional expression across tissue compartments, and b) comparison of activation marker expression in peripheral NK cells between cohorts. Expression reported in the form of median staining intensity (MSI) for each marker on total NK cells. Statistical analysis in b) was performed using unpaired Wilcoxon rank sum test for pair-wise comparisons with TB as the reference group (p-value), and the Holm-Bonferroni test to account for multiple comparisons (q-value). In boxplots, each box represents median and interquartile range (IQR). Whiskers in a) indicate 1.5x IQR of the upper and lower quartiles, and whiskers in b) indicate 95% confidence intervals.

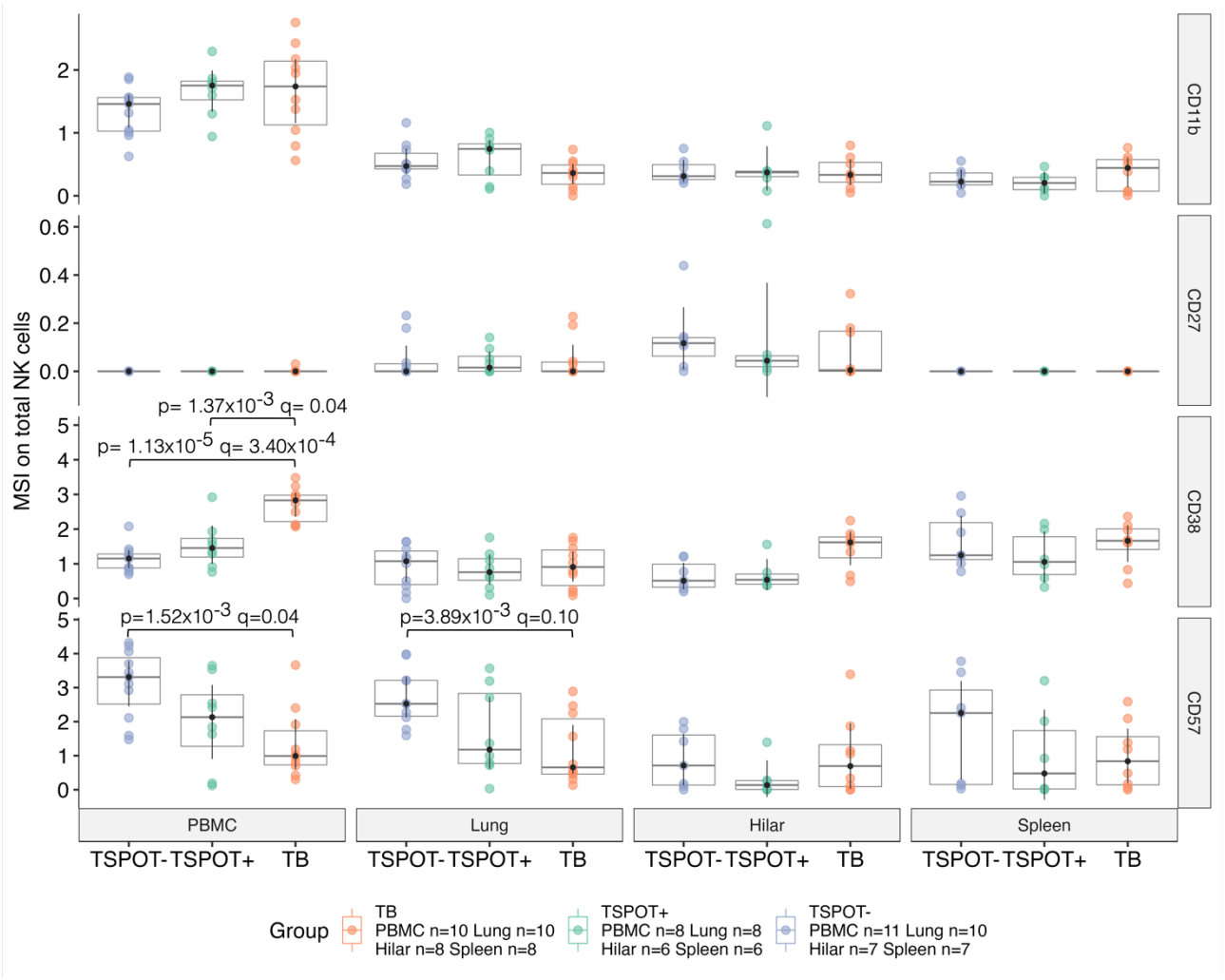

Figure 5.11: Expression of maturation markers on total NK cells from postmortem tissue compartments. Expression reported in the form of median staining intensity (MSI) for each marker in total NK cells. Statistical analysis was performed using unpaired Wilcoxon rank sum test for pair-wise comparisons with TB as the reference group (p-value), and the Holm-Bonferroni test to account for multiple comparisons (q-value). In boxplots, each box represents median and interquartile range, whiskers indicate 95% confidence intervals.

NK cells were annotated according to CD57 and CD38 co-expression. It was hypothesized that NK cells in the peripheral blood are $CD57^+$ and/or $CD38^+$, suggesting a more mature phenotype and that $CD57^+$ and/or $CD38^+$ NK cells are enriched during TB when immune activation and expansion of maturation marker-expressing NK cells are expected to occur.

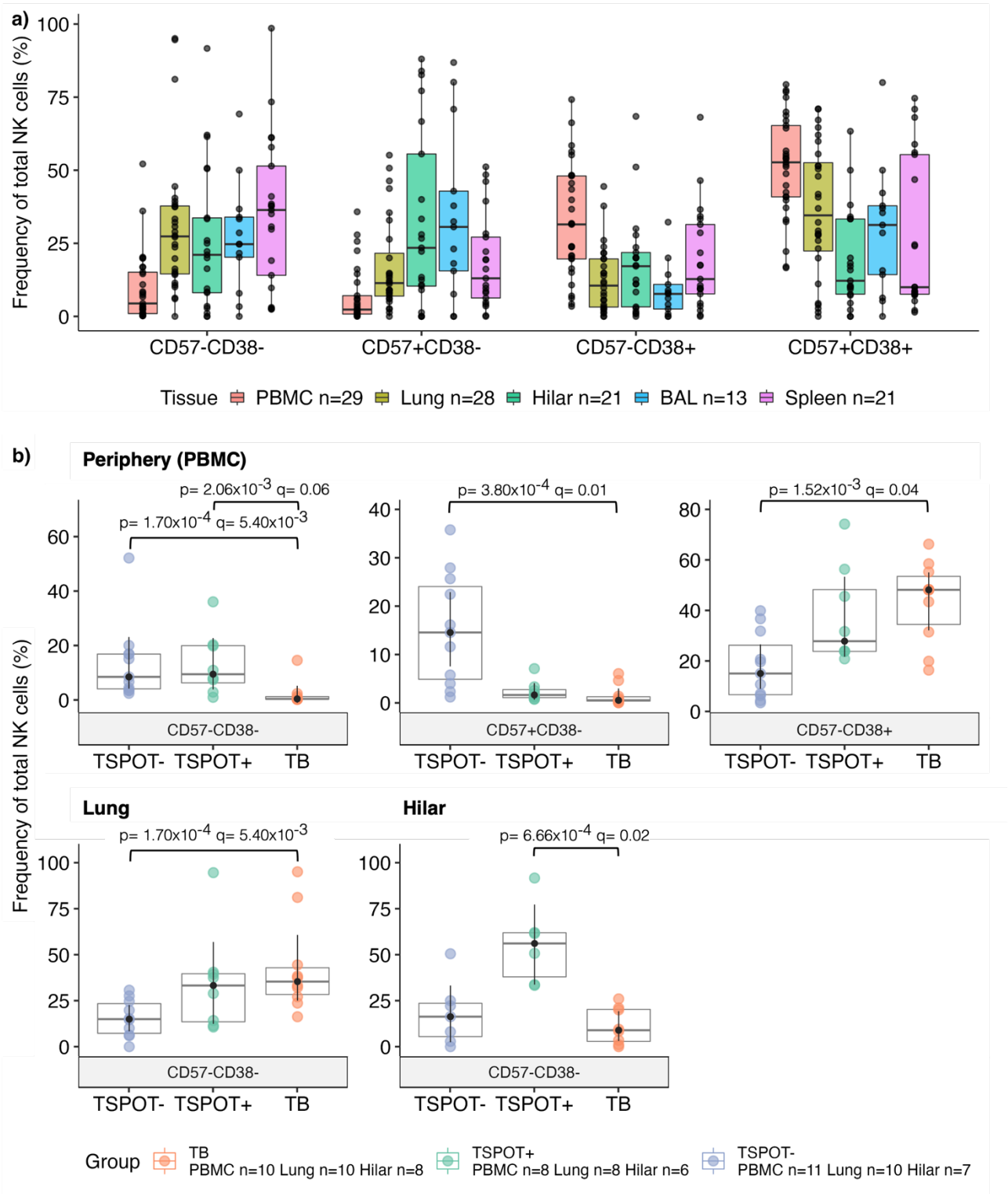

Figure 5.12: Frequencies of maturation marker-expressing NK cells across tissue compartments and cohorts. a) Maturation marker-expressing NK cell frequencies across tissue compartments, and b) comparison of maturation marker-expressing NK cells between cohorts. Statistical analysis in b) was performed using unpaired Wilcoxon rank sum test for pair-wise comparisons with TB as the reference group (p-value), and the Holm-Bonferroni test to account for multiple comparisons (q-value). In boxplots, each box represents median and interquartile range (IQR). Whiskers in a) indicate 1.5x IQR of the upper and lower quartiles, and whiskers in b) indicate 95% confidence intervals.

As hypothesized, NK cells in the peripheral blood were predominantly phenotypically mature subsets, while NK cells in the lung were comprised of both $CD57^{-}CD38^{-}$ and $CD57^{+}CD38^{+}$ subsets (Figure 5.12a). Frequencies of CD57-expressing NK cells in TB were lower ($p=3.80x10^{-4}$, q=0.01) while frequencies of CD38-expressing NK cells were enriched ($p=1.52x10^{-3}$, q=0.04) in the peripheral blood relative to $TSPOT^{-}$ controls (Figure 5.12b). Together, NK maturation data show that peripheral blood NK cells had lower MSI of CD57 (i.e., fewer markers on the NK cell surface; Figure 5.10) and had lower frequencies of $CD57^{+}$ NK cells (Figure 5.12), while CD38 was upregulated (i.e., higher expression per cell) and had higher frequencies of $CD38^{+}$ NK cells in TB compared to controls.

Interestingly, CD57 and CD38 double-negative cells in TB decedents were depleted in PBMC relative to $TSPOT^{+}$ ($p=2.06x10^{-3}$, q=0.06) and $TSPOT^{-}$ controls ($p=1.70x10^{-4}$, $q=5.40x10^{-3}$, Figure 5.12b), perhaps indicating a switch of peripheral blood NK cells towards a more mature CD38-expressing phenotype. However, the same $CD57^{-}CD37^{-}$ NK population was enriched in the TB lung relative to $TSPOT^{-}$ controls ($p=1.05x10^{-3}$, q=0.03, Figure 5.12), possibly suggesting migration of this subset from the peripheral blood to the lung during TB disease, or downregulation of these markers. In the hilar lymph nodes, TB decedents had significantly lower levels of $CD57^{-}CD37^{-}$ NK cells relative to $TSPOT^{+}$ controls ($p=6.66x10^{-4}$, q=0.02, Figure 5.12). No other significant differences or trends were reported for other CD38/CD57-expressing subsets across tissues (Figure 5.13).

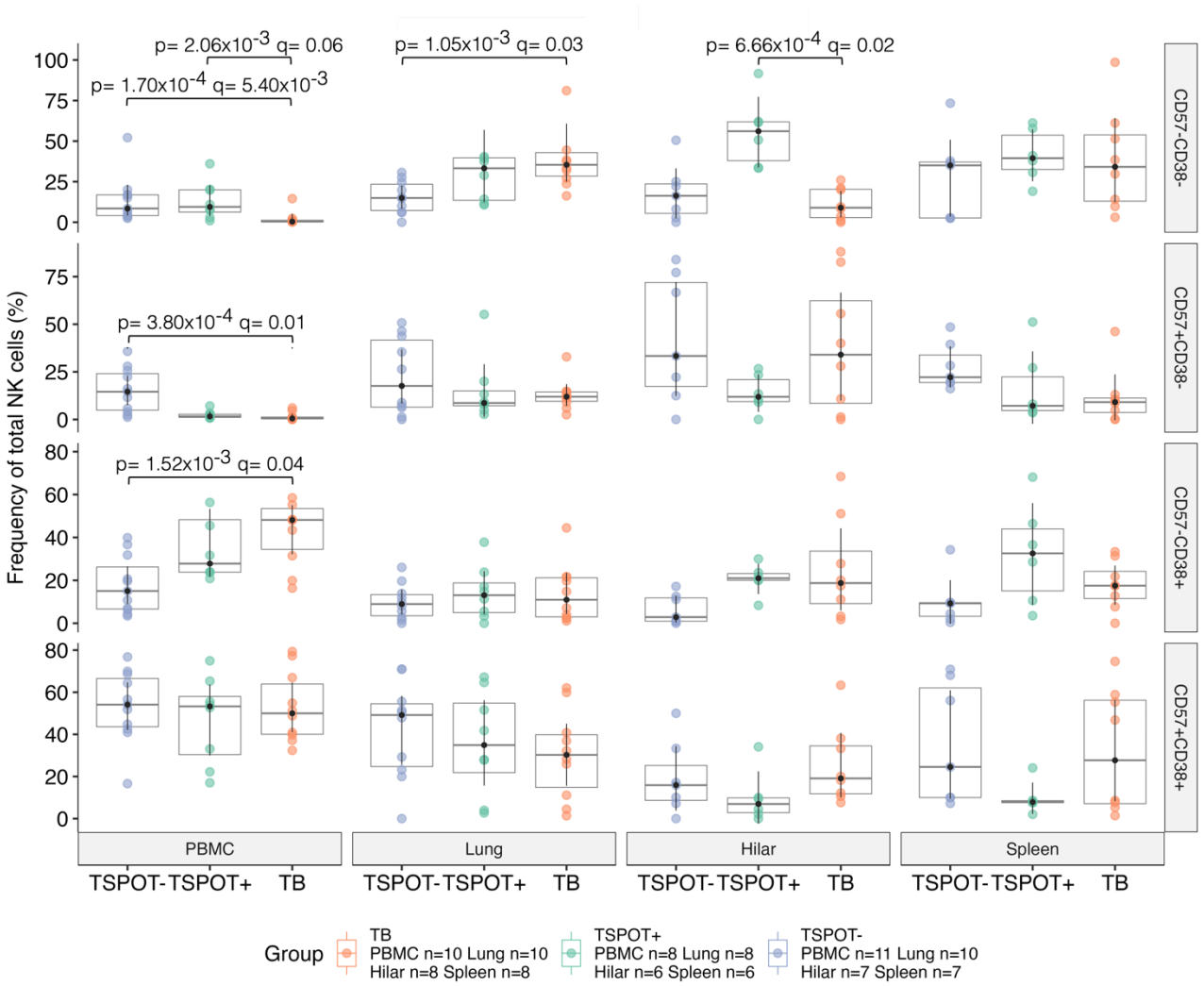

Figure 5.13: Frequencies of maturation marker-expressing NK cells from postmortem tissue compartments. Statistical analysis was performed using unpaired Wilcoxon rank sum test for pair-wise comparisons with TB as the reference group (p-value), and the Holm-Bonferroni test to account for multiple comparisons (q-value). In boxplots, each box represents median and interquartile range, whiskers indicate 95% confidence intervals.

5.3.6 Peripheral blood NK cells in TB express more inhibiting than activating receptors

NK cells can express multiple activating and inhibiting molecules at a given time, and NK cells can also up- or down-regulate the expression of these receptors in response to factors within the local microenvironment (such as cytokines, IL-2, IL-15 and IL-21) (Han et al., 2018; Huenecke et al., 2010; Lenart et al., 2021). NK cell activation is governed by the fine balance between activating and inhibiting signals transduced in different proportions by ligands binding NK receptors. It was hypothesized that during TB, NK cells upregulated

expression of activating receptors as a feature of inflammation in response to immune sensing of *Mtb*, resulting in a cascade of immune cell activation (Figure 5.14).

Activating receptors NKp46, DNAM1 and NKG2D, and inhibiting receptor NKG2A were expressed at high levels in peripheral blood NK cells (Figure 5.14a). Expression of inhibiting KIR was upregulated in the lung (Figure 5.14a), which is consistent with published literature to suggest that lung NK cells are KIR-expressing (Marquardt et al., 2017b). As a control, expression patterns of NK cell activating and inhibiting receptors in tonsil tissues from living individuals showed that tonsil NK cells expressed relatively high levels of activating NKp46, DNAM1, and NKG2D, and inhibiting NKG2A, while inhibiting receptor KIR was not expressed (median MSI of 0). Together, these data show that NK cells in across tissue compartments express vastly different patterns of inhibiting and activating molecules to regulate NK cell function. Peripheral blood NK cells in TB expressed significantly higher levels of activating DNAM1 ($TSPOT^-$ $p=1.05x10^{-3}$, $q=0.04$) and NKG2D ($TSPOT^+$ $p=1.37x10^{-3}$, $q=0.05$; $TSPOT^-$ $p=1.13x10^{-5}$, $q=4.50x10^{-4}$), and inhibiting KIR ($TSPOT^-$ $p=1.26x10^{-3}$, $q=0.05$) above those of controls (Figure 5.14b). No significant differences were observed for the expression of NK activating and inhibiting receptors between cohorts in tissue compartments (Figure 5.15). Therefore, peripheral NK cells in TB decedents expressed both activating and inhibiting receptors at higher levels relative to controls.

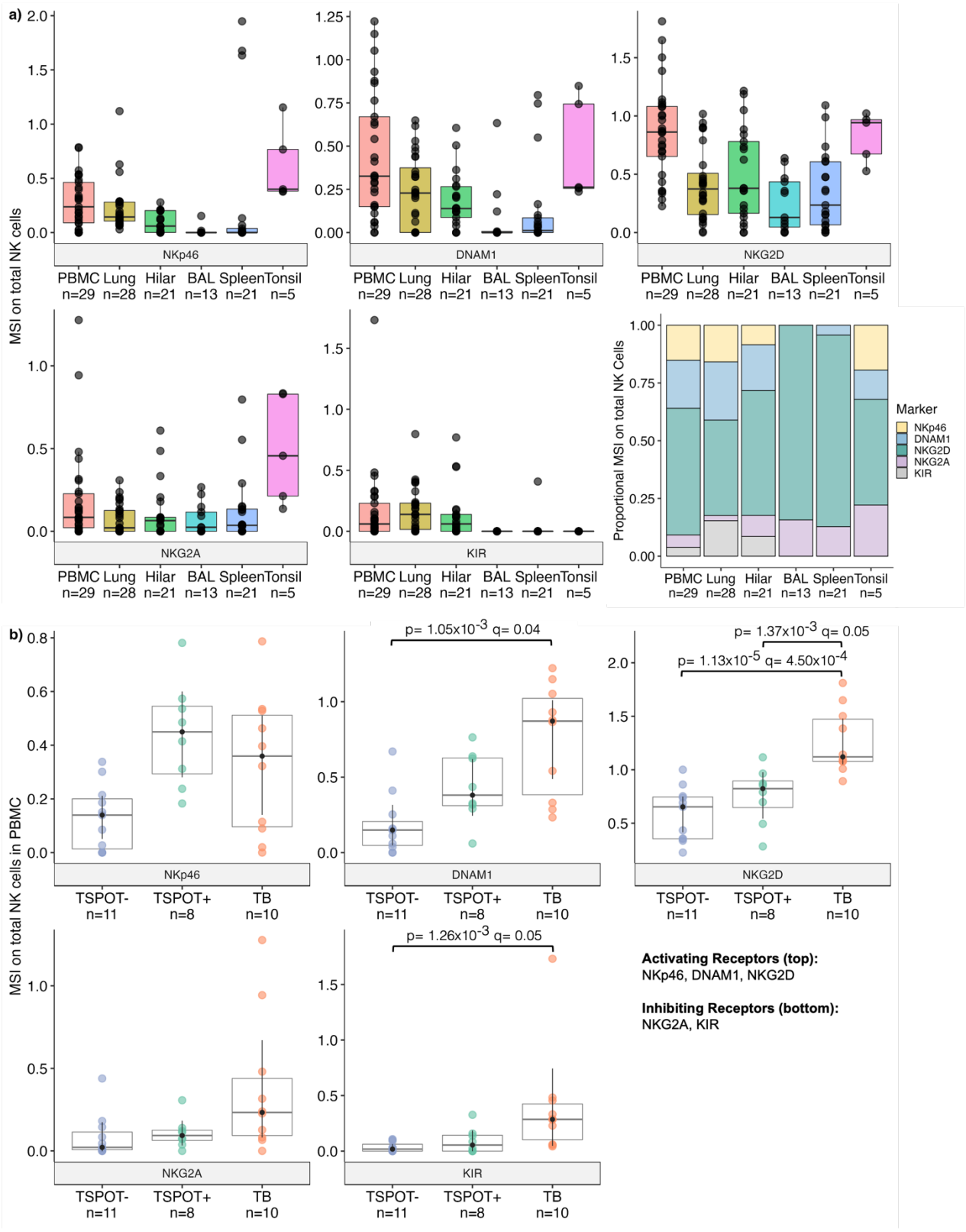

Figure 5.14: Expression of NK cell activating and inhibiting receptors across tissue compartments and cohorts. a) NK cell activating (NKp46, DNAM1, NKG2D) and inhibiting receptor (NKG2A, KIR) expression and relative proportional expression across tissue compartments, and b) comparison of activating and inhibiting receptor expression in peripheral NK cells between cohorts. Expression levels reported in the form of median staining intensity (MSI) for each marker on total NK cells. Statistical analysis in b) was performed using unpaired Wilcoxon rank sum test for pair-wise comparisons with TB as the reference group (p-value), and the Holm-Bonferroni test to account for multiple comparisons (q-value). In boxplots, each box represents median and interquartile range (IQR). Whiskers in a) indicate 1.5x IQR of the upper and lower quartiles, and whiskers in b) indicate 95% confidence intervals.

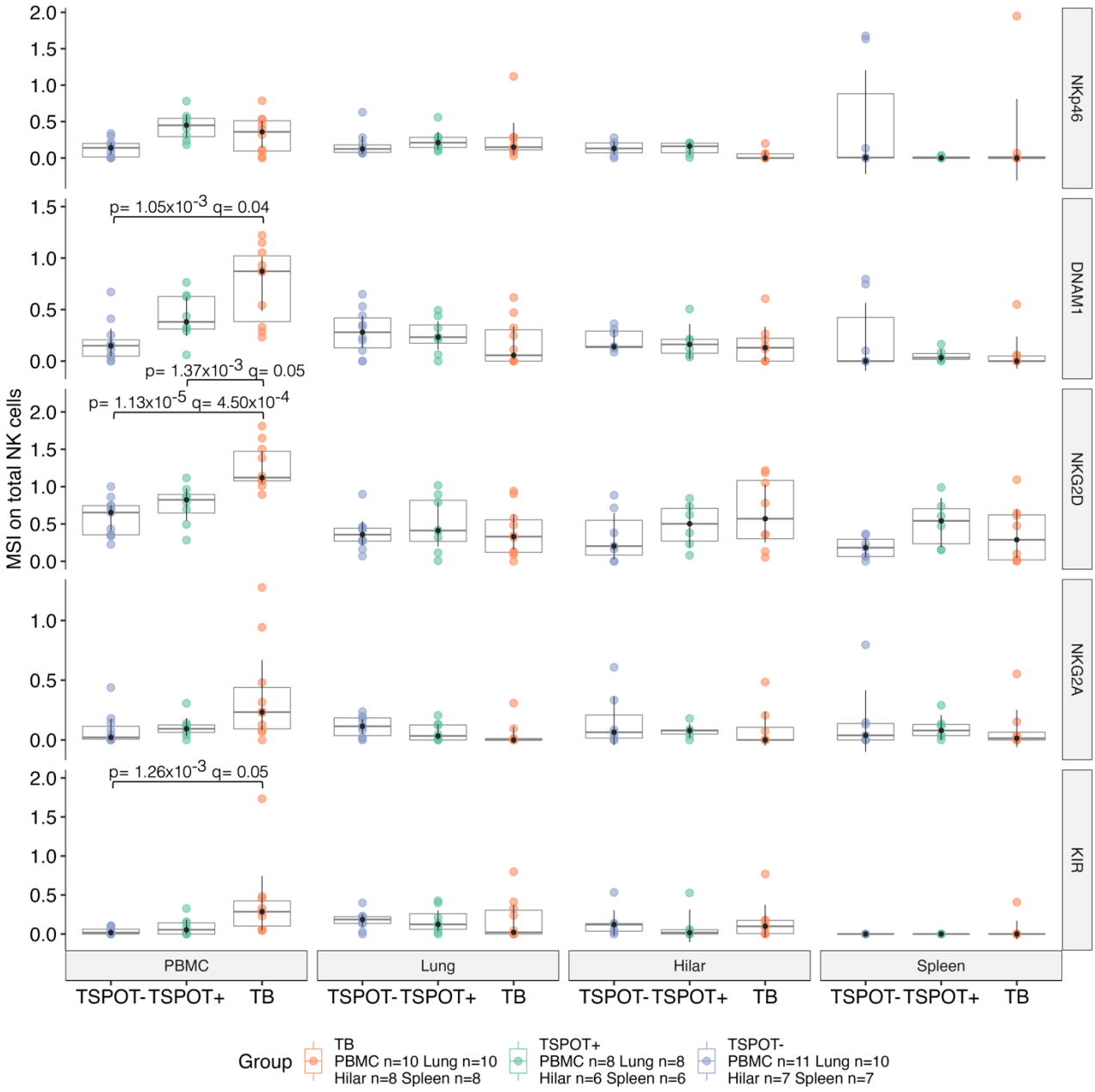

Figure 5.15: Expression of activating and inhibiting receptors on total NK cells from postmortem tissue compartments. Activating receptors include NKp46, DNAM1, NKG2D. Inhibiting receptors include NKG2A and KIR. Expression reported in the form of median staining intensity (MSI) for each marker in total NK cells. Statistical analysis was performed using unpaired Wilcoxon rank sum test for pair-wise comparisons with TB as the reference group (p-value), and the Holm-Bonferroni test to account for multiple comparisons (q-value). In boxplots, each box represents median and interquartile range, whiskers indicate 95% confidence intervals.

Activating NKG2D and inhibiting NKG2A markers were used for cell cluster annotation. The frequencies of NKG2D- and/or NKG2A-expressing NK cells were evaluated across tissue compartments and between cohorts (Figure 5.16).

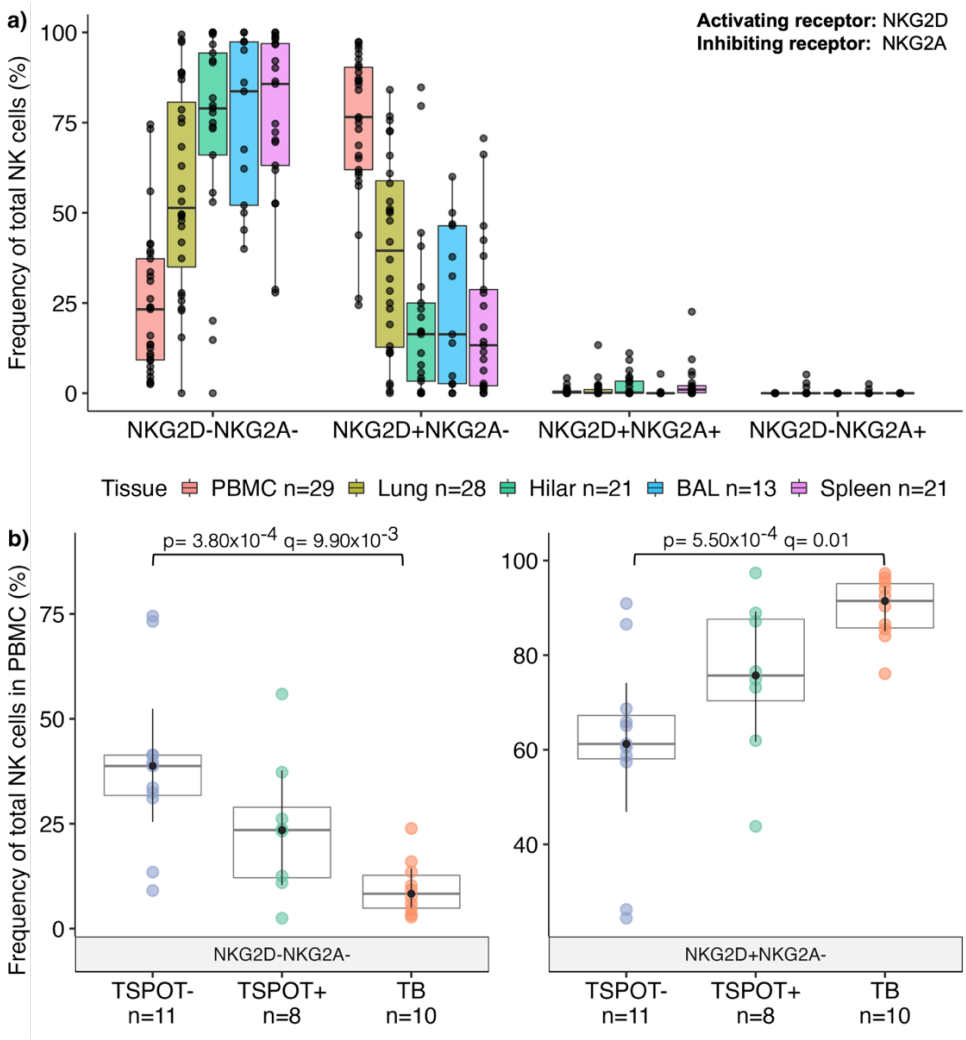

Figure 5.16: Frequencies of activating NKG2D- and inhibiting NKG2A-expressing NK cells across tissue compartments and cohorts. a) Activating and inhibiting receptor expressing NK cell frequencies across tissue compartments, and b) comparison of activating and inhibiting receptor expressing peripheral NK cells between cohorts. Statistical analysis in b) was performed using unpaired Wilcoxon rank sum test for pair-wise comparisons with TB as the reference group (p-value), and the Holm-Bonferroni test to account for multiple comparisons (q-value). In boxplots, each box represents median and interquartile range (IQR). Whiskers in a) indicate 1.5x IQR of the upper and lower quartiles, and whiskers in b) indicate 95% confidence intervals.

NK cells in peripheral blood were mostly of the NKG2D^{+}NKG2A^{-} phenotype. In contrast, tissue NK cells were predominantly NKG2D^{-}NKG2A^{-}, with smaller proportions of the NKG2D^{+}NKG2A^{-} subset (Figure 5.16a). Peripheral NK cells with the NKG2D^{-}NKG2A^{-} phenotype were depleted in TB decedents relative to TSPOT^{-} controls ($p=3.80\times10^{-4}$, $q=9.90\times10^{-3}$), while the NKG2D^{+}NKG2A^{-} subset was enriched in TB compared to TSPOT^{-} ($p=5.50\times10^{-4}$, $q=0.01$) (Figure 5.16b). No differences in NKG2A- and/or NKG2D-expressing NK cells were observed in the tissue compartments (Figure 5.17).

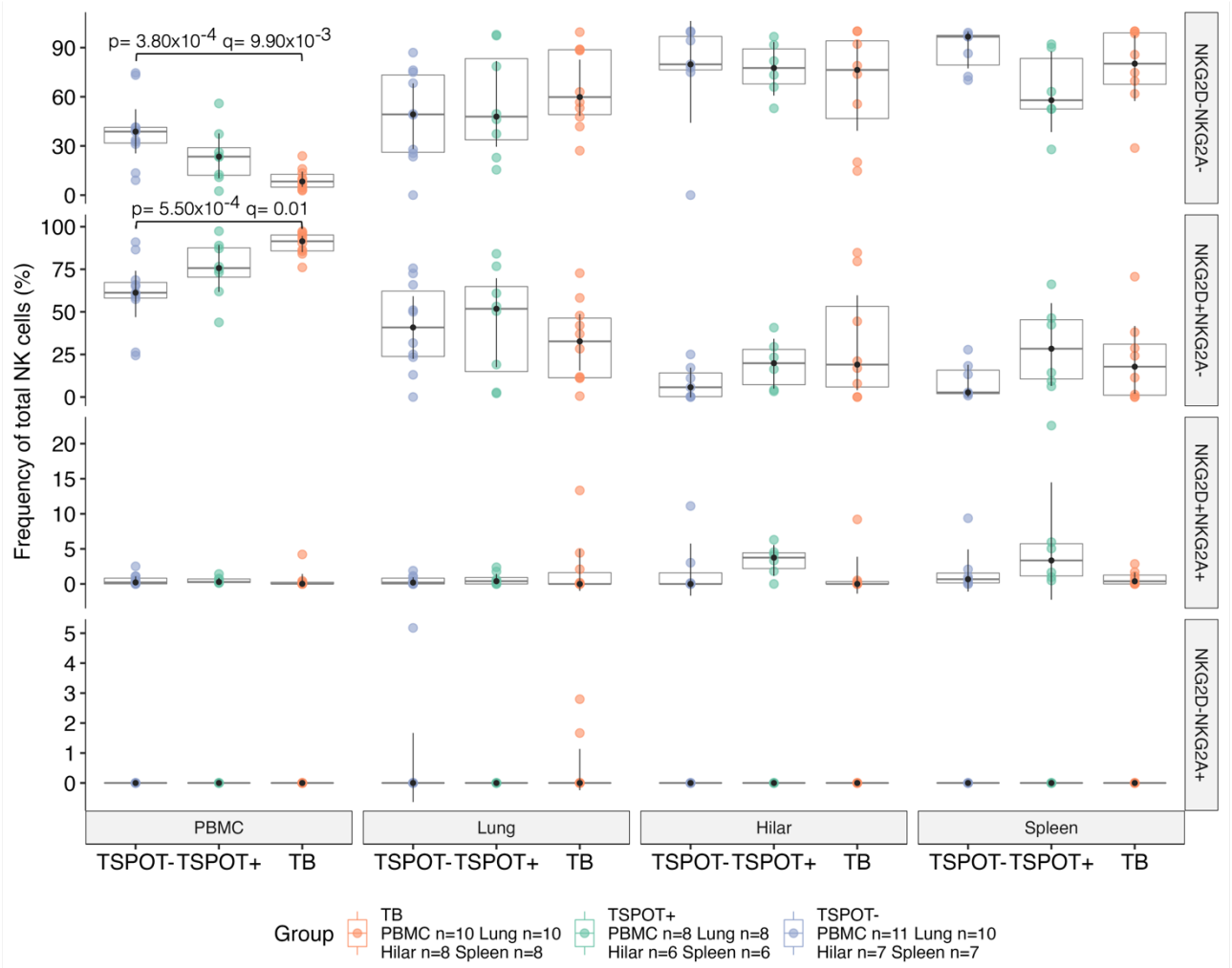

Figure 5.17: Frequencies of activating (NKG2D) and inhibiting (NKG2A) receptor-expressing NK cells from postmortem tissue compartments. Statistical analysis was performed using unpaired Wilcoxon rank sum test for pair-wise comparisons with TB as the reference group (p-value), and the Holm-Bonferroni test to account for multiple comparisons (q-value). In boxplots, each box represents median and interquartile range, whiskers indicate 95% confidence intervals.

NK cell function is governed via signal transduction pathways that are initiated by ligation with multiple activating and inhibiting receptors in different proportions and combinations. To investigate the relative proportions of potential activating and inhibiting signals delivered to NK cells, the ratios of inhibiting to activating receptor expression on NK cells was compared between cohorts (Figure 5.18). I formulated an equation to obtain the inhibiting/activating receptor expression ratio, whereby average expression values of all inhibiting receptors (NKG2A and KIR) were divided by average expression of all activating receptors (NKp46, DNAM1, and NKG2D) (Equation 3). Based on expression data and enrichment of activating receptor-expressing ($NKG2D^{+}NKG2A^{-}$) NK cells in TB relative to

healthy controls, it was hypothesized that the overall inhibiting/activating receptor ratio would be lower in TB relative to controls, possibly indicating a less inhibitory, more activated phenotype during TB disease.

$$\text{Inhibiting/activating receptor ratio} = \frac{(\text{NKG2A+KIR})/2}{(\text{NKp46+DNAM1+NKG2D})/3}$$

Equation 3: Mathematical procedures to determine the NK cell inhibiting/activating receptor expression ratio. Expression reported in terms of median staining intensity (MSI).

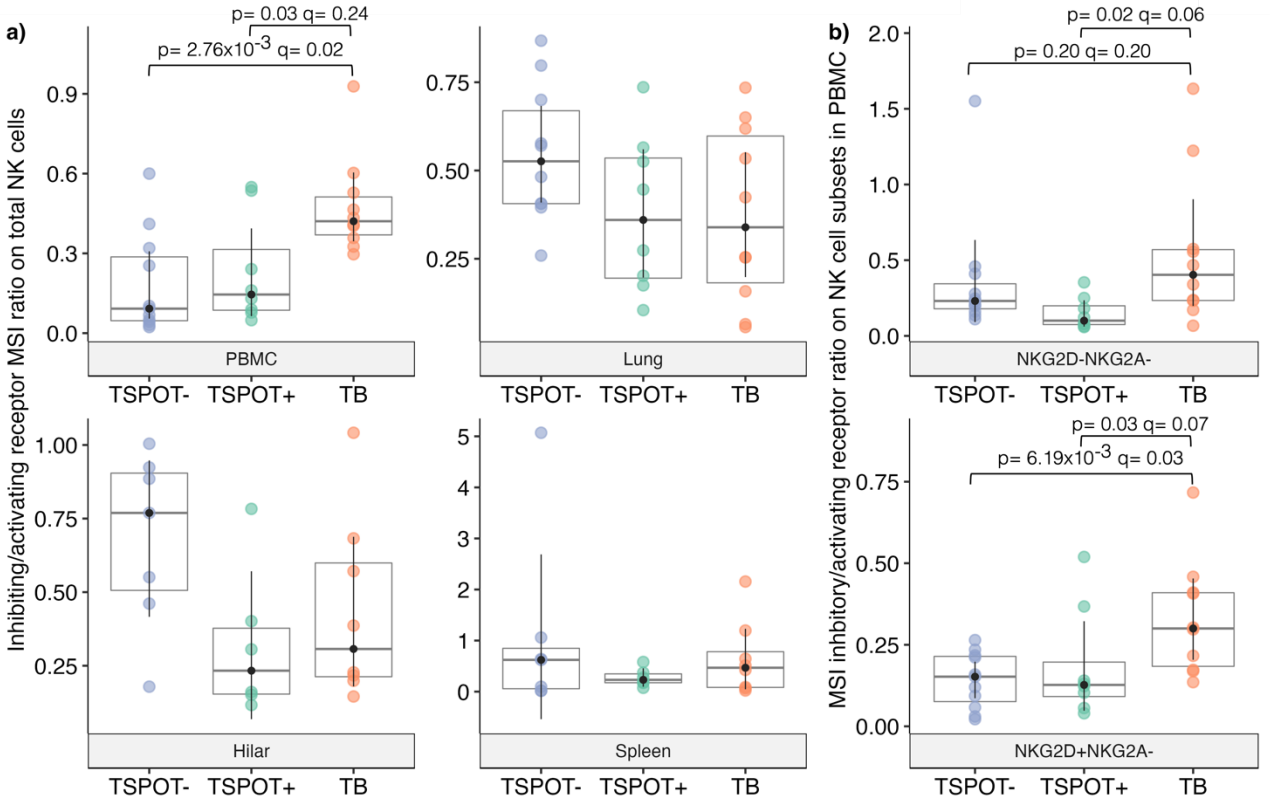

Figure 5.18: Ratios of inhibiting to activating receptor expression on NK cells. a) Inhibiting/activating receptor expression ratio of total NK cells compared across cohorts in different tissue compartments. b) Comparisons of inhibiting/activating receptor expression ratio between cohorts in peripheral NK subsets, subclassified according to NKG2D (activating receptor) and NKG2A (inhibiting receptor) co-expression patterns. Expression reported in the form of median staining intensity (MSI). Statistical analysis in a) and b) was performed using unpaired Wilcoxon rank sum test for pair-wise comparisons with TB as the reference group (p-value), and the Holm-Bonferroni test to account for multiple comparisons (q-value). In boxplots, each box represents median and interquartile range, whiskers indicate 95% confidence intervals.

Contrary to the hypothesis, results showed that the ratio of inhibiting/activating receptor expression was significantly higher in peripheral NK cells of TB decedents relative to controls ($TSPOT^+$ p=0.03, q=0.24; $TSPOT^-$ $p=2.75x10^{-3}$, q=0.02; Figure 5.18a). No differences or trends in the inhibiting/activating receptor expression ratio were observed in total NK cells of the tissue compartments (Figure 5.18a). The inhibiting/activating receptor expression ratio was also investigated in $NKG2D^-NKG2A^-$ and $NKG2D^+NKG2A^-$ subsets in PBMC to confirm whether the predominant peripheral blood subsets were following the same trend. In both peripheral blood $NKG2D^-NKG2A^-$ ($TSPOT^+$ p=0.02, q=0.06; $TSPOT^-$ p=0.20, q=0.20) and $NKG2D^+NKG2A^-$ subsets ($TSPOT^+$ p=0.03, q=0.07; $TSPOT^-$ $p=6.19x10^{-3}$, q=0.03), TB cases had a higher ratio of inhibiting to activating expression levels relative to control cohorts (Figure 5.18b). Therefore, despite TB decedents having higher frequencies of activating receptor-expressing $NKG2D^+NKG2A^-$ cells, the overall expression ratio of inhibiting receptors outweighed the expression of activating receptors relative to cases who were otherwise healthy.

5.3.7 NK cell activation and immunoregulation

In addition to activating and inhibiting receptors (Section 5.3.5), NK cells also express markers that reflect the current state of NK cell activation and/or immunoregulation. More specifically, expression of CD69 and HLA-DR by NK cells reflects a state of activation in the peripheral blood (i.e., activation markers indicating currently active NK cells, but are not directly involved in regulating signal transduction pathways for NK cell activation) (Borrego et al., 1999; Clausen et al., 2003; Erokhina et al., 2021; Moretta et al., 1991). Additionally, NK cells also express immune checkpoint proteins (PD1, PDL1, TACTILE, and TIGIT) and markers involved in apoptosis/cytotoxicity (Fas-L; with a different killing mechanism than cytotoxic molecules). The expression of activation and immunoregulatory markers was investigated across tissue compartments (Figure 5.19) and compared between cohorts

(Figure 5.20). It was hypothesized that expression of activation markers (CD69 and HLA-DR) and Fas-L (a cytotoxic mediator) would be upregulated in TB relative to healthy controls, possibly reflecting immune activation in response to *Mtb* infection and disease. In contrast, immune checkpoint proteins were hypothesized to be downregulated on NK cells during TB relative to healthy controls to allow better activation and enhanced functional capacity in response to high *Mtb* antigen load.

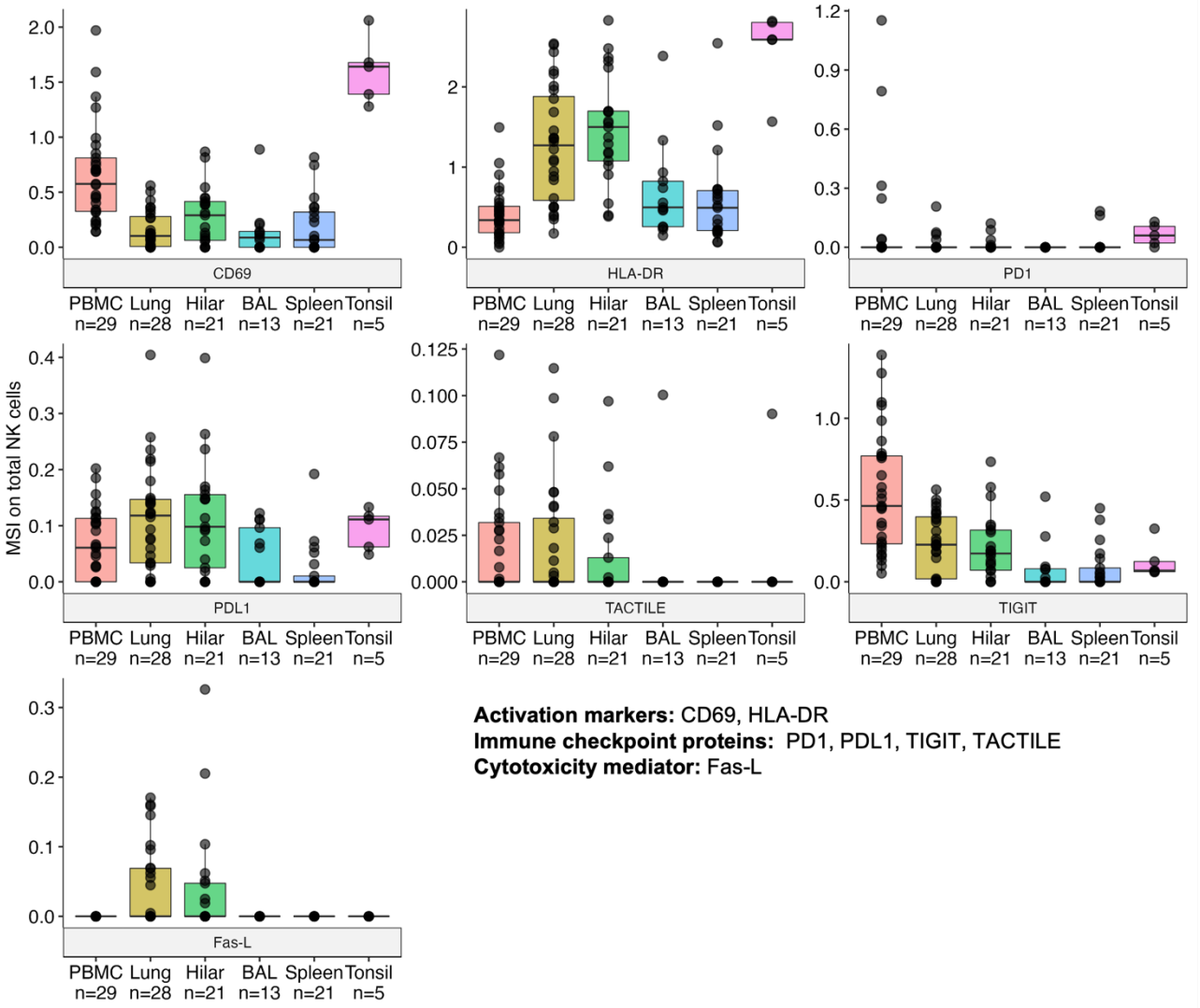

Figure 5.19: Expression of NK cell markers of activation and immunoregulation across tissue compartments. Expression reported in the form of median staining intensity (MSI) for each marker per decedent in total NK cells. In boxplots, each box represents median and interquartile range, whiskers in indicate 1.5x IQR of the upper and lower quartiles.

TACTILE, PD1 and Fas-L were expressed at low levels in all compartments (median level expression of 0; Figure 5.19). PDL1 and TIGIT were expressed in PBMC, lung and hilar lymph node, while being expressed at low levels in BAL and spleen. Peripheral NK cells had highest expression of CD69 and TIGIT relative to tissues, while lung and hilar lymph nodes had higher levels of HLA-DR and PDL1 relative to other compartments (Figure 5.19).

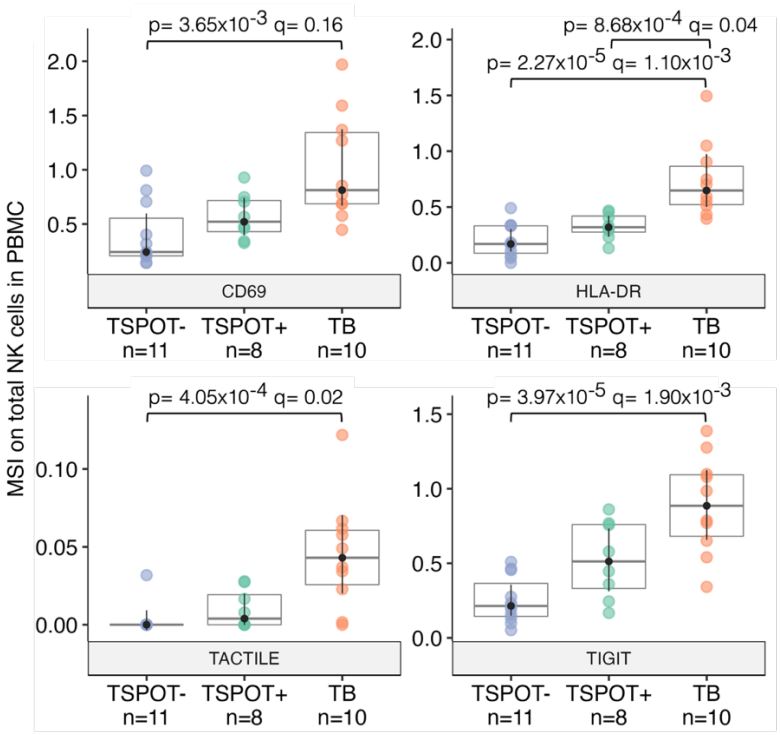

Figure 5.20: Expression of NK cell markers of activation and immunoregulation in TB and controls. Comparison of activation and immunoregulatory marker expression in peripheral NK cells between cohorts. Expression reported in the form of median staining intensity (MSI) for each marker on total NK cells. Statistical analysis was performed using unpaired Wilcoxon rank sum test for pair-wise comparisons with TB as the reference group (p-value), and the Holm-Bonferroni test to account for multiple comparisons (q-value). In boxplots, each box represents median and interquartile range, whiskers indicate 95% confidence intervals.

Expression of CD69 ($TSPOT^-$ $p=3.65x10^{-3}$, $q=0.16$), HLA-DR ($TSPOT^-$ $p=2.27x10^{-5}$, $q=1.10x10^{-3}$), TACTILE ($TSPOT^-$ $p=4.05x10^{-4}$, $q=0.02$) and TIGIT ($TSPOT^-$ $p=3.97x10^{-5}$, $q=1.90x10^{-3}$) on total peripheral NK cells was significantly higher in TB relative to $TSPOT^-$ controls. HLA-DR expression in TB was also significantly higher than $TSPOT^+$ controls ($TSPOT^+$ $p=8.68x10^{-4}$, $q=0.04$; Figure 5.20). No significant differences were observed for expression of these molecules in NK cells within tissue compartments (Figure 5.21).

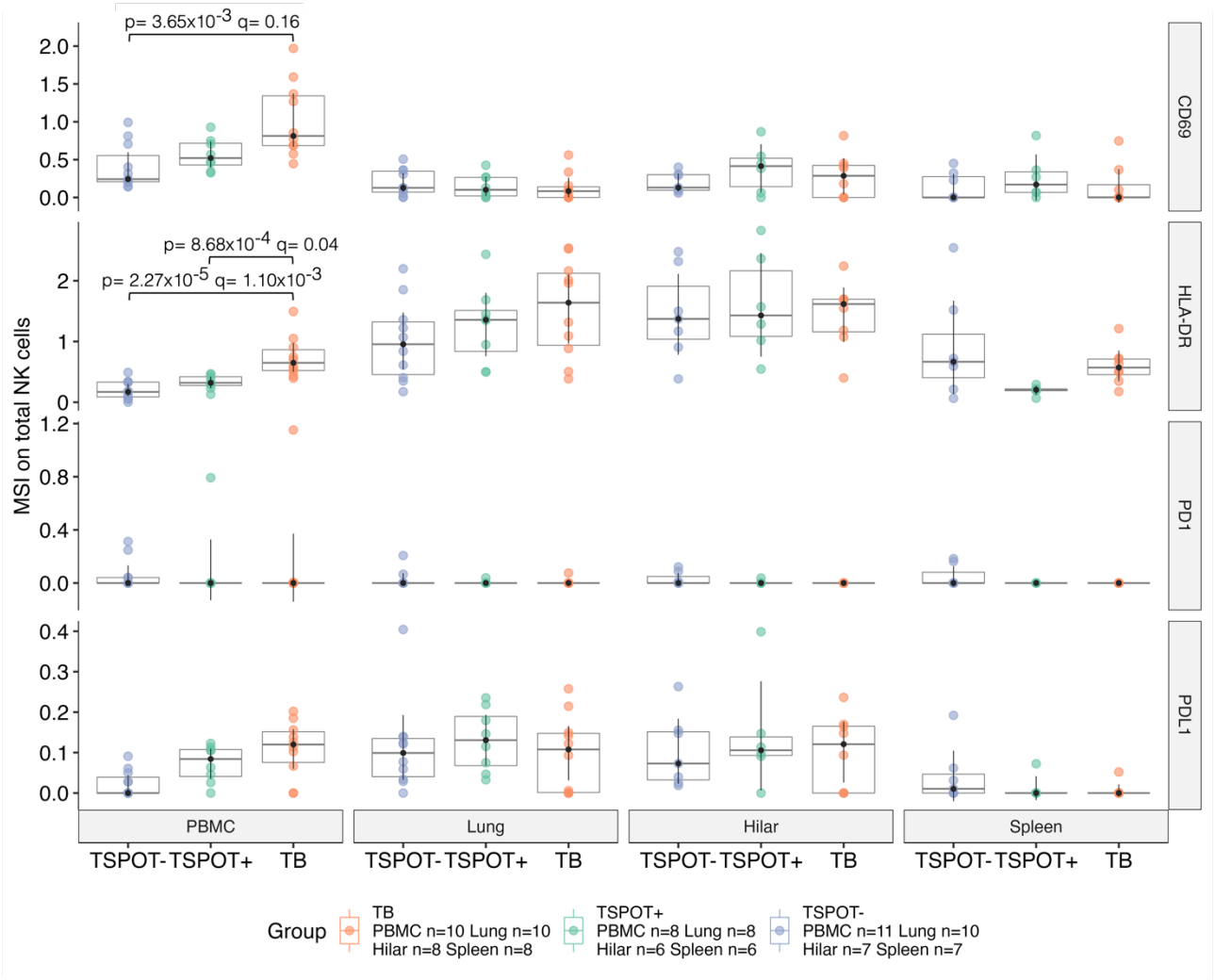

Figure 5.21: Expression of activation markers, immune checkpoint proteins and cytotoxic mediators on total NK cells from postmortem tissue compartments. Activation markers include CD69 and HLA-DR. Immune checkpoint proteins include PD1, PDL1, TIGIT and TACTILE. Fas-L includes a mediator of cytotoxic activity. Expression reported in the form of median staining intensity for each marker in total NK cells. Statistical analysis was performed using unpaired Wilcoxon rank sum test for pair-wise comparisons with TB as the reference group (p-value), and the Holm-Bonferroni test to account for multiple comparisons (q-value). In boxplots, each box represents median and interquartile range, whiskers indicate 95% confidence intervals.

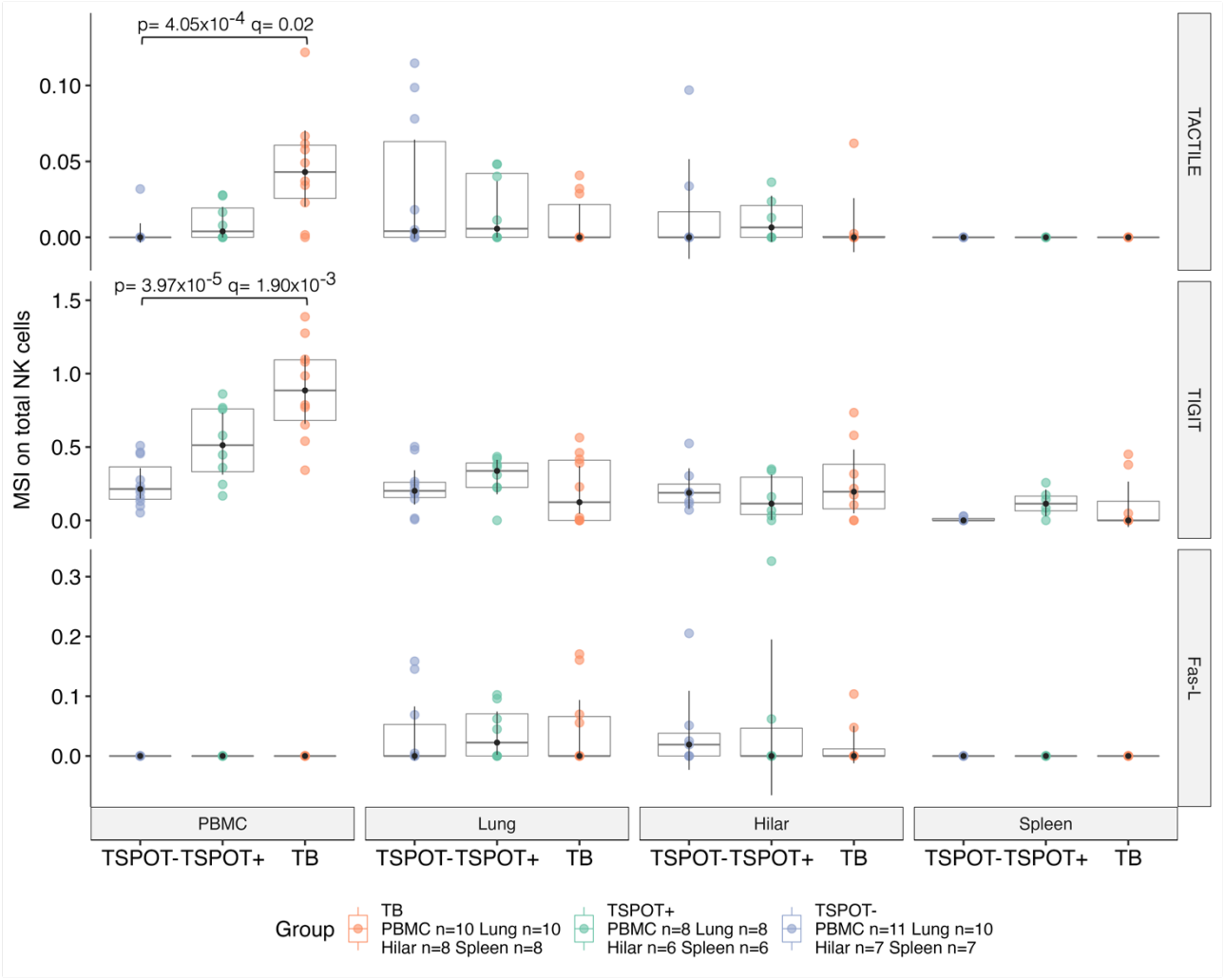

Figure 5.21 (continued): Expression of activation markers, immune checkpoint proteins and cytotoxic mediators on total NK cells from postmortem tissue compartments. Activation markers include CD69 and HLA-DR. Immune checkpoint proteins include PD1, PDL1, TIGIT and TACTILE. Fas-L includes a mediator of cytotoxic activity. Expression reported in the form of median staining intensity for each marker in total NK cells. Statistical analysis was performed using unpaired Wilcoxon rank sum test for pair-wise comparisons with TB as the reference group (p-value), and the Holm-Bonferroni test to account for multiple comparisons (q-value). In boxplots, each box represents median and interquartile range, whiskers indicate 95% confidence intervals.

Although FAUST selected Fas-L as a cell annotation marker, frequencies of Fas-L-expressing NK cells were not evaluated between compartments and cohorts, since Fas-L-expressing NK cells in lung, hilar lymph nodes, BAL and spleen did not survive filtering. More specifically, Fas-L^{+} NK cells had a median frequency of 0%, with less than 25% of individuals having frequencies above 0% in all compartments.

5.4 Discussion and Conclusions

The postmortem study presented in this chapter provides a phenotypic characterization of human NK cell phenotypes and cytotoxic potential across various tissue compartments; and includes comparisons between TB cases and controls. For this discussion, the characteristics of NK cell subsets in postmortem peripheral blood and tissues are discussed first, followed by a discussion on NK cell features in TB and controls.

5.4.1 Characterizing NK cell subsets in postmortem peripheral blood and tissues

The lung is the primary site of *Mtb* infection and pulmonary TB is the most common form of TB disease. Therefore, to explore NK biology in the lung a series of lung-associated NK cell tissue-resident markers were selected to investigate tissue homing. As expected, tissue-resident markers were upregulated in tissue NK cells, with little to no expression in peripheral blood NK cells. Also, frequencies of total tissue-resident marker-expressing NK cells ($CD103^+$, $CD49a^+$, and/or $CXCR3^+$) were most abundant the lung compartment. The hallmark tissue-residency markers in NK cell biology include CD103 and CD49a (Marquardt et al., 2019; Franklin et al., 2022). Agreeably, CD49a was abundantly expressed in the lungs, although CD103 was expressed at relatively low levels in the lungs and other tissue compartments. Despite its relatively low expression, CD103 was sufficiently bimodal in its distribution to be used as an annotation marker by automated FAUST clustering. CXCR3 is not the most widely used marker for NK cells tissue residency, although CXCR3 has also been shown to play an important role in the accumulation of NK cells in the lungs and airways during pulmonary fibrosis (Jiang et al., 2004), viral (Carlin et al., 2018) and bacterial (Jiang et al., 2004) infections. Data presented in this chapter demonstrates that CXCR3 was expressed at high levels on NK cells in the lungs, hilar lymph nodes, BAL, spleen, and tonsils, indicating that CXCR3 may be a good tissue-residency marker for most tissues and

is not necessarily lung-specific. In the context of TB disease, CXCR3-expressing NK cells were found to migrate into tuberculous pleural fluid, where they have been suggested to play a role against *Mtb* infection (Fu et al., 2013). However, little has been shown regarding the role of CXCR3-expressing NK cells directly in the tissues during *Mtb* infection, offering an interesting avenue to be explored further.

CCR6 has been implicated as an important chemokine receptor that is involved in the recruitment of cells to epithelial and mucosal sites in the lung and gut (Ito et al., 2011). CCR6 is most widely expressed on T cells, B cells, DC, although there is evidence to suggest populations of CCR6-expressing NK cells (Berahovich et al., 2006), which rationalized inclusion for the analyses. CCR6 was expressed at low levels on NK cells in postmortem tissues (lung, spleen, and hilar lymph nodes), but was expressed at high levels in control tonsils from living individuals, demonstrating that the lack of CCR6 in postmortem tissues was not due to technical artifacts related to poor performance or staining capacity of the marker. Given that the CCR6 antibody was detected relatively high expression levels in living tonsil tissue, the low expression patterns in postmortem samples could be ascribed to two explanations. Firstly, it is possible that NK cells in PBMC, lung, hilar lymph nodes and spleen simply do not express high levels of CCR6 (in contrast to abundant expression in the tonsils). Secondly, low levels of CCR6 expression in postmortem tissue specimens may be due to postmortem decay of the protein. For example, a marker may be affected or downregulated by signaling and/or cell death pathways that are initiated after death. Tonsil tissues were included in the FAUST analysis of NK cells (alongside postmortem samples) and CCR6 was also not chosen as an annotation marker for tonsils. Therefore, it seems plausible that CCR6 expression was not sufficiently bi- or multi-modal in its distribution pattern across all tissues for FAUST annotation and/or was simply expressed at low levels in PBMC, lung, BAL, hilar lymph nodes and spleen. However, the influence of the postmortem process cannot be excluded. The same arguments are applicable to all markers

within the panel that were expressed at low levels and/or not selected by FAUST for phenotypic annotation.

Previous data has shown that roughly 20% of lung NK cells express tissue residency markers and are referred to as “tissue-resident” NK cells, which are phenotypically immature ($CD56^{hi}CD16^{lo}$) (G. E. Cooper et al., 2018; Dogra et al., 2020). Consistent with previous literature, postmortem tissue-resident NK cells comprised ~15-20% of the total lung NK population and were almost exclusively of the immature $CD56^{hi}CD16^{lo}$ phenotype. According to published literature, most peripheral and lung NK cells do not express tissue-residency markers and are classified as “circulating” NK cells (comprising roughly 80% of the total NK population in lung tissue) (G. E. Cooper et al., 2018). Consistent with this, data from the postmortem study presented in this thesis showed that NK cells in the peripheral blood and tissues were predominantly circulating NK cells (lacking expression of CD103, CD49a and CXCR3 by automated annotation). More specifically, circulating NK cells comprised ~100% of the total PBMC NK population, while the hilar lymph nodes, BAL and spleen were >90% circulating NK cells. Consistent with published literature, ~85% of lung NK cells expressed markers consistent with a circulating cell phenotype.

Circulating NK cells in the peripheral blood and lung have been reported as “mature”, with a predominant $CD56^{lo}CD16^{hi}$ phenotype (Hervier et al., 2019a; Marquardt et al., 2017b; Dogra et al., 2020). Consistent with the literature, majority of NK cells in PBMC (~65%) were phenotypically mature, $CD16^{hi}$. To further confirm the mature phenotype of peripheral NK cells, the expression of CD38 and CD57 maturation markers were investigated among NK subsets. The postmortem data suggest that NK cells in PBMC co-expressed CD38 and/or CD57 maturation markers in $CD56^{lo}CD16^{hi}$ (totaling ~65% of peripheral blood NK cells) and $CD56^{hi}CD16^{lo}$ (totaling ~35% peripheral blood NK cells) subsets. Agreeably, the recent study by Dogra and colleagues also showed that the most predominant NK phenotype in

the blood is $CD56^{dim}CD16^{+}CD57^{+}$ NK cells. Therefore, our phenotypic classification of NK subsets within postmortem PBMC are consistent with published literature.

Circulating NK cells in the lungs, hilar lymph node, BAL, spleen, and tonsils were comprised mainly of the $CD56^{hi}CD16^{lo}$ subset, suggesting a more immature phenotype. This finding is partially consistent with results described by Dogra and colleagues in 2020, who showed that NK cells in the lymph nodes and tonsils were predominantly $CD56^{bright}CD16^{-}$ NK cells (Dogra et al., 2020). However, Dogra et al., showed that NK cells in the spleen and lung were mainly $CD56^{dim}CD16^{+}$ NK cells (Dogra et al., 2020), and other published data investigating lung NK cells also reported most lung NK cells expressed the mature $CD56^{lo}CD16^{hi}$ phenotype (Hervier et al., 2019a; Marquardt et al., 2017b; Dogra et al., 2020). Notably, these published data were not investigated within the TB context. These studies included normal human lung tissue, sampled as far as possible from pathological lesions in resected lung lobes from postmortem tissue donors or individuals undergoing lobectomy. Upon further investigation using additional maturation markers (CD38 and CD57), it was confirmed that most NK cells in postmortem hilar lymph nodes, BAL, and spleen were double-negative for both CD38 and CD57. In the lung there was a smaller, yet substantial proportion of NK cells that were $CD57^{+}CD38^{+}$. Therefore, NK cells within the hilar lymph nodes, BAL and spleen are predominantly immature by means of phenotypic classification, while some NK cells in the lung expressed maturation markers, possibly indicating a more differentiated phenotype. It is unlikely that conflicting data in predominant NK cell phenotype in the lungs and spleen reported in this chapter are due to technical artifacts, although it is possible that highly vascularized organs (such as the lungs and spleen) may have resulted in cross-contamination between the blood and tissue compartments. However, since the major NK cell phenotypes in the tissues were distinct from the blood, it is unlikely that results presented in this thesis are subject to excessive cross-contamination.

Most circulating NK cells are in a resting state, yet they contain pre-formed cytotoxic granules that are ready to be released upon activation. Therefore, it is not uncommon to detect perforin and granzymes in unstimulated, NK cells *ex vivo.* In fact, the expression of cytotoxic molecules may reflect the maturation status of an NK subset, thereby enabling further classification based on cytotoxic potential. To sub-classify NK cells based on cytotoxic potential, NK cells were clustered according to perforin and granzyme B expression. Notably, granzyme K was not selected as an annotation marker, presumably due to low expression level and lack of marker bimodality across all compartments. Three main NK cell subsets were identified and classified according to relative perforin and granzyme B expression levels: 1) perforin^{-}granzyme B^{-}, here forth referred to as cytotoxic double-negative NK cells; 2) perforin^{-}granzyme B^{+}, dubbed mono-cytotoxic NK cells; and 3) perforin^{+}granzyme B^{+}, poly-cytotoxic NK cells. Notably, mono-cytotoxic perforin^{-}granzyme B^{+} NK cells are unlikely to induce potent cytotoxic killing responses since granzyme B requires co-expression with perforin to enter a target cell and cleave caspase molecules through perforin-induced holes in the target cell membrane. Results showed that poly-cytotoxic NK cells had the highest overall expression of perforin and granzyme B relative to mono-cytotoxic NK cells. Mono-cytotoxic cells were in turn more cytotoxic than double-negative NK cells. These findings suggest a spectrum of NK cell maturation with increasing cytotoxic potential from double-negative to mono- and poly-cytotoxic NK cells in both PBMC and tissue compartments. It was also hypothesized that granzyme K was co-expressed in granzyme B-expressing subsets and not in perforin-expressing subsets, based on previous literature (Bade et al., 2005; Bouwman et al., 2021; Bratke et al., 2005). NK cell results showed that granzyme K expression was generally low across all NK cell subsets but was slightly higher in the perforin^{-}granzyme B^{+} subset.

Peripheral blood NK cells were predominantly poly-cytotoxic in both CD56^{hi}CD16^{lo} and CD16^{hi} subsets. However, mainstream understanding suggests that CD56^{hi}CD16^{lo} NK cells

in peripheral blood are phenotypically immature with low cytolytic activity, while $CD16^{hi}$ NK cells are terminally differentiated and demonstrate high capacity for cytotoxic killing of target cells (Béziat et al., 2011; Björkström, Ljunggren, et al., 2010b; Björkström, Riese, et al., 2010). At a glance, our results may seem contradictory to current definitions. However, upon further investigation findings were consistent with published literature. Since overall expression levels of perforin and granzyme B were higher in peripheral blood NK cells relative to the tissues, most NK cell subsets in the peripheral blood are likely to be annotated as cells expressing cytotoxic markers. It is certainly probable that all peripheral blood NK cell subsets express granzyme B and perforin. However, when considering relative levels of expression, the immature $CD56^{hi}CD16^{lo}$ NK cells in the peripheral blood indeed expressed lower levels of perforin and granzyme B relative to the mature $CD16^{hi}$ subset(s). Together, these findings are consistent with the current understanding that most peripheral blood NK cells are terminally differentiated ($CD16^{+/hi}$) with high cytotoxic potential, while $CD56^{hi}CD16^{lo}$ NK cells are less common in the periphery and have lower cytotoxic potential (relative to their mature $CD16^{+/hi}$ counterparts).

Circulating NK cells in the periphery may be thought of as “loaded guns” that survey the body with readiness to degranulate and kill compromised cells when the trigger is pulled. The NK cell “trigger” is the tightly controlled balance of activating and inhibiting signals delivered via NK surface receptors (described in more detail at a later stage). Using *in vitro* culturing and stimulation, peripheral blood NK cells can degranulate and induce cytolytic killing, but this is not a typical process that occurs in the periphery *in vivo.* Rather, NK cells would be recruited to the site of disease, where they are activated and exert their effector functions in the tissues. Once recruited to the tissues, it is possible that NK cells adopt very different phenotypic and functional characteristics compared to their peripheral blood counterparts. The tissues, particularly the lung in the context of *Mtb* infection, are where NK cells are expected to degranulate and exert their cytolytic effector functions. It is, therefore,

possible that NK cells in the tissues that express cytotoxic molecules at low levels may have recently degranulated and released cytotoxic molecules to induce target cell killing within the local microenvironment. This scenario is possible since postmortem samples were thawed and stained directly ex-cryopreservation. Therefore, low expression of cytotoxic molecules may reflect recent NK cell degranulation that occurred prior to antibody staining and fixation, which may be a feature of the immune response to *Mtb* infection. Quantifying extracellular expression of CD107a is often used to measure NK cell degranulation. However, the CD107a assay for measuring NK cell degranulation requires *in vitro* culturing with stimulatory antigens, which was infeasible with the current study design that aimed to phenotype NK cells *ex vivo.* The mechanisms and infeasibility of measuring CD107a as a degranulation marker in this thesis is discussed further in-depth in Chapter 6. Alternatively, low expression of cytotoxic molecules may be interpreted as a hypo-cytotoxic state, in which cytotoxic molecules were not expressed or were downmodulated. Overall, interpreting the relative expression levels of cytotoxic molecules in tissue NK cells remains challenging and it is impossible to state with certainty whether a cytotoxic degranulation event has occurred in the current dataset. For the most part, this chapter reports the cytotoxic potential of NK cells based on the expression of cytotoxic molecules, which could be thought of as the immediate readiness of a cell to degranulate at the exact time of fixing. No interpretations of the true cytolytic nature could be made, although speculations may be constructed based on other evidence for NK cell maturation/activation status. Functional killing assays would provide clarity to further characterize the true cytotoxic capacity of NK cells in the peripheral blood and tissues.

The 2017 study by Marquardt and colleagues (Marquardt et al., 2017b), suggested that human lung NK cells were mainly of the differentiated $CD56^{lo}CD16^{hi}$ phenotype, but this subset in the lungs was “hypofunctional” by demonstrating decreased capacity for degranulation towards target cells relative to the highly cytotoxic $CD56^{lo}CD16^{hi}$ NK cells in

the peripheral blood (Marquardt et al., 2017b). Since tissue-resident cells only comprised a small population in the lung and were virtually absent in other tissues, the expression of cytotoxic markers in circulating NK cells was investigated across subsets. As previously discussed, $CD56^{hi}CD16^{lo}$ NK cells in the peripheral blood expressed perforin and granzyme B at low levels, while $CD16^{hi}$ populations expressed cytotoxic molecules at high levels (consistent with previous literature). However, in tissue compartments (lung, hilar lymph node, BAL, and spleen), immature $CD56^{hi}CD16^{lo}$ and terminally differentiated $CD56^{lo}CD16^{hi}$ subsets expressed perforin and granzyme B at low levels. The $CD56^{hi}CD16^{hi}$ subset in tissue compartments was the cytotoxic marker-expressing subset. Lower expression of cytotoxic molecules in NK cells may suggest downregulated expression, perhaps supporting published data showing hypo-functionality of the $CD56^{lo}CD16^{hi}$ population. However, lower expression of perforin and granzyme B in mature $CD56^{lo}CD16^{hi}$ in the tissues may also result from recent NK degranulation and target cell killing.

Together with the information on maturation markers and cytotoxic molecules, the expression data for activating and inhibiting receptors provides extra clues about the overall activation status of NK cells across compartments. The expression of activating (NKp46, DNAM1 and NKG2D) and inhibiting (NKG2A and KIR) receptors on the NK cell surface was investigated. Notably, some KIRs are considered activating, while others are classified as inhibiting (Blunt & Khakoo, 2020). The KIR antibody used in the CyTOF panel was clone DX27, which binds KIR2DL2, characterized as an inhibiting receptor. Inhibiting receptor KIR was mainly expressed on NK cells in the lung, which is consistent with published literature suggesting that lung NK cells were KIR-expressing (Marquardt et al., 2017b). NKG2D and NKG2A were used as cell annotation markers to identify NK cell subsets. Majority of NK cells in the PBMC were activating receptor-expressing $NKG2D^{+}NKG2A^{-}$ cells, while most NK cells in the hilar lymph nodes, BAL and spleen were $NKG2D^{-}NKG2A^{-}$. NK cells in the lung were mostly $NKG2D^{-}NKG2A^{-}$ (~50%), but also had a substantial proportion of

NKG2D^{+}NKG2A^{-} NK cells (~35-40%). Therefore, activating receptor-expressing NK cells predominating in the peripheral blood, with a large proportion in the lung, have high potential to be activated via the “induced self” pathway.

CD69 is a differentiation antigen that is expressed shortly following activation of NK cells and functions to sustain NK cell activation and mediate cytotoxic activity (Borrego et al., 1999; Clausen et al., 2003; Lanier, Buck, et al., 1988; Moretta et al., 1991), although CD69 has also been considered an NK cell tissue-resident marker in some published data (Bankovich et al., 2010; Hashemi & Malarkannan, 2020; Marquardt et al., 2017b; Sathaliyawala et al., 2013; Shiow et al., 2006). In the context of TB, CD69 has been recognized for its role in sustaining NK cell activation in response to *Mtb* infection (Pokkali et al., 2009; Borrego et al., 1999). CD69 was not used to annotate cells, therefore analyses were limited to evaluating CD69 expression levels (MSI). Results indicated that CD69 was expressed at high levels in the peripheral blood relative to tissue compartments, supporting the classification of CD69 as an activation marker in peripheral NK cells rather than a marker of tissue residency.

In a review by Erokhina and colleagues (2020), evidence was provided to suggest that HLA-DR-expressing NK cells participate in the first-line defense and crosstalk with the adaptive immune system by producing IFN-γ, having high proliferative activity and participating in the cytotoxic response (Erokhina et al., 2021). Evidence was also discussed regarding the possible role of HLA-DR in antigen processing and MHC-II presentation on the NK cell surface but for the most part, HLA-DR expression on NK cells is most associated with a state of activation. Results presented in this chapter showed that HLA-DR was expressed at high levels on NK cells in the lungs and hilar lymph node, which may be related to the high degree of antigen presentation that occurs in the lung due to multitudes of inhaled environmental and autologous antigens. However, the concept of HLA-DR playing a role in

NK cell antigen presentation is relatively novel and requires much more detailed investigation by the field.

In addition to inhibiting and activating receptors, NK cells also express proteins that function as immune checkpoints (such as PD1, PDL1, TACTILE and TIGIT) and cytotoxicity mediators (such as Fas-L). Inhibiting receptors on the surface of NK cells regulate activation and prevent NK-mediated damage to healthy tissue. However, additional receptors acting as inhibitory checkpoints also contribute towards maintaining immune homeostasis. Some NK cell checkpoint regulators include PD1, TIGIT and TACTILE (CD96). PD1 and TIGIT are expressed in NK cells and act as gatekeeps of the immune response. The interaction of PD1 and TIGIT with their ligands (PDL1 and CD155, respectively) downregulate NK cell functions (Harjunpää & Guillerey, 2020; Pesce et al., 2019; Sivori et al., 2019b). Additionally, TACTILE is also considered an immune checkpoint protein and shares its ligand (CD155) with TIGIT. Upon binding its ligand, TACTILE acts as a negative regulator of cytokine production (Chan et al., 2014; Minton, 2014; Sivori et al., 2019b). Besides degranulation and secretion of cytolytic molecules for target cell killing, NK cells may also use the Fas-L pathway to mediate cytotoxicity. When Fas-L on the surface of NK cells binds the Fas receptor expressed on a target cells, the caspase cascade is initiated to induce apoptosis of the target cell (Chua et al., 2004; Eischen & Leibson, 1997; Montel et al., 1995). Expression data revealed that TACTILE, PD1 and Fas-L were expressed at very low levels in all compartments (median level expression of 0). Notably, Fas-L can occur in membrane-bound form, or as a secreted, soluble molecule. Only the membrane bound form of Fas-L was investigated on NK cells in this postmortem study, which was shown to be expressed at low levels across all tissue compartments. However, the role of soluble Fas-L in tissue NK cells may be an interesting avenue to explore further.

Expression of PDL1 on the surface of immune cells serves a receptor which initiates a “halt” signal for the immune response and acts as an immune checkpoint when bound to its receptor, PD1. Since NK cells in the lungs and hilar lymph nodes expressed relatively high levels of PDL1 but hardly expressed PD1, it may be possible that tissue NK cells themselves act as important regulators of the local immune response, particularly in the lung and the lung-draining hilar lymph nodes. It is likely that this occurs when other immune cells (such as T cells) express PD1 that is recognized by PDL1 on NK cells, which in turn, serves to regulate T cell activation and cytokine expression, thereby mediating detrimental inflammation and pathology (Kauffman et al., 2021). Therefore, NK cells may be important regulators of inflammation in the lung.

To align all the data for phenotypic characterization of NK cells, Figure 5.22 provides a comprehensive summary of the predominant NK cells populations across tissue compartments using FAUST annotation data, including CD56 and CD16 phenotyping, cytotoxic potential (perforin and granzyme B), maturation markers (CD57 and CD38) and activating (NKG2D) and inhibiting (NKG2A) receptors. NK cells in the peripheral blood were predominantly $CD16^{hi}$, with a smaller proportion of $CD56^{hi}CD16^{lo}$ NK cells. Both subsets in the peripheral blood were phenotypically classified as $perforin^{+}granzyme\ B^{+}NKG2D^{+}NKG2A^{-}CD38^{+}CD57^{+/-}$. However, the $CD56^{hi}CD16^{lo}$ subset was shown to express lower levels of perforin and granzyme B relative to $CD16^{hi}$ cells, consistent with literature suggesting that $CD56^{hi}CD16^{lo}$ are immature and hypo-cytotoxic. Majority of NK cells in the lungs, hilar lymph nodes, BAL, spleen, and tonsils were phenotypically immature ($CD56^{hi}CD16^{lo}$) and lacked expression of cytotoxic molecules, maturation markers and activating and inhibiting receptors, confirming their immature status. Therefore, NK cells in the tissues are predominantly immature with low cytotoxic potential. There was a smaller (yet substantial) subset of $CD56^{hi}CD16^{lo}perforin^{+}granzyme\ B^{+}NKG2D^{+}NKG2A^{-}$

$CD38^{+}CD57^{+}$ NK cells in the lungs that appeared to have a more mature-like phenotype and high cytotoxic potential, potentially undergoing terminal differentiation.

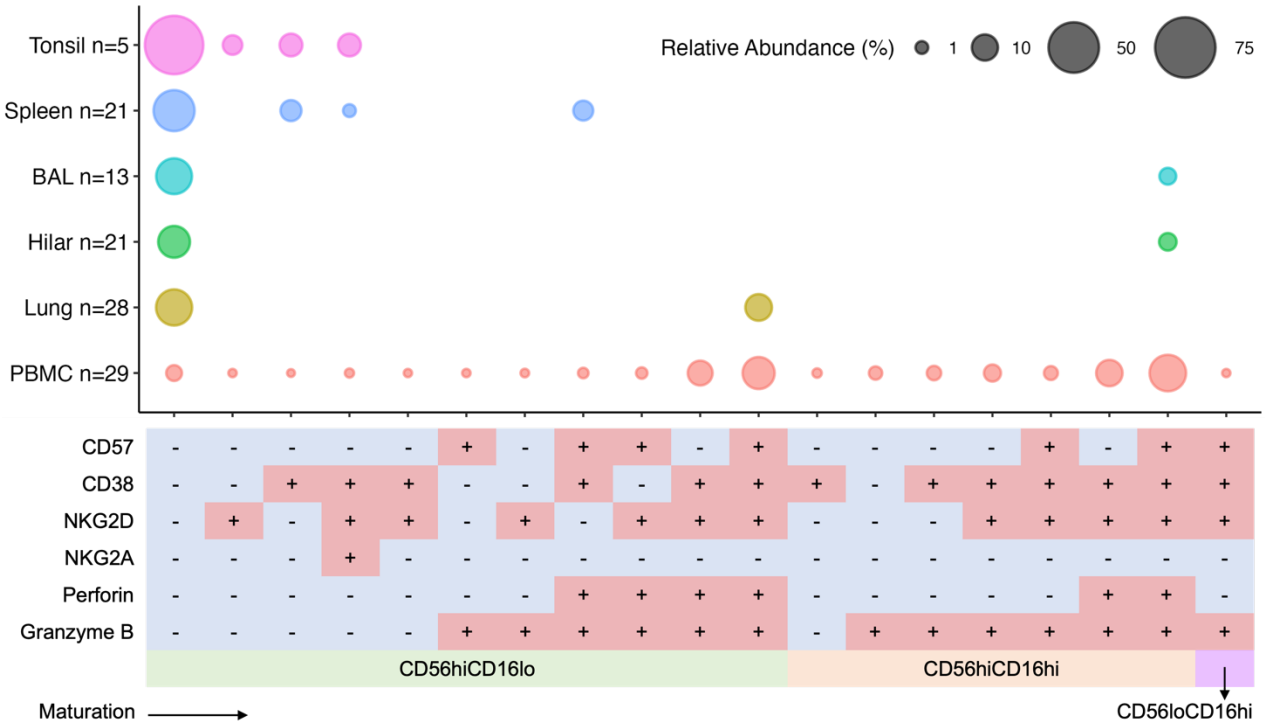

Figure 5.22: Relative abundance of NK cell subsets across compartments. Subsets classified according to co-expression patterns of CD56, CD16, cytotoxic molecules (perforin, granzyme B and granzyme K), maturation markers (CD38 and CD57), and activating (NKG2D) and inhibiting (NKG2A) receptors. NK cell subsets were filtered to include only populations for which at least 75% of the cohort had a frequency of above 0% (i.e., q25>0).

5.4.2 NK cell features in TB and controls

In the previous section, NK cells in the peripheral blood, lungs, hilar lymph nodes, BAL, and spleen were characterized. However, one of the main objectives of this tissue immunology study was to evaluate whether features of NK cell tissue homing, cytotoxicity, maturation, and activation status differ in TB cases and controls.

During infection and disease, immune cells are activated to exert their effector functions. As previously discussed, NK cells are potent killers of pathogen-infected cells, primarily by degranulating to secrete cytotoxic molecules that induce apoptosis of the target cell. Data

reported in Chapter 3 and 4 showed that peripheral NK cells in living TB patients and peripheral lymphocytes in TB decedents, respectively, had higher cytotoxic potential than healthy controls. It was therefore hypothesized that peripheral NK cells would have higher cytotoxic potential in TB relative to healthy controls in the postmortem cohort, possibly reflecting NK cell activation during *Mtb* infection. In support of these findings, total NK cells in the peripheral blood of TB decedents expressed more perforin, granzyme B and granzyme K relative to controls; and frequencies of double-positive perforin and granzyme B-expressing (poly-cytotoxic) NK cells were predominant in PBMC and were enriched in the peripheral blood of TB decedents relative to controls. Granzyme K expression in the poly-cytotoxic (perforin^{+}granzyme B^{+}) and mono-cytotoxic (perforin^{-}granzyme B^{+}) NK cells was also higher in TB decedents relative to controls. Interestingly, frequencies of double-negative (perf^{-}granzyme B^{-}) NK cells were depleted in the peripheral blood in TB decedent relative to controls. Using further subclassification based on CD56 and CD16 co-expression patterns, supporting data showed that double-positive (perforin^{+}granzyme B^{+}) NK cells of CD56^{hi}CD16^{lo} and CD56^{hi}CD16^{hi} phenotypes were trending towards enrichment in PBMC of TB decedents relative to controls. Together, these data suggest that peripheral NK cells may be undergoing differentiation towards a more cytotoxic phenotype during TB.

Other lines of evidence were generated to support the finding that NK cells in the peripheral blood were more mature and activated during TB disease. Firstly, it was shown that the expression of activation markers CD69 and HLA-DR (not necessarily directly involved in NK cell activation but are expressed as a feature of prior activation) were upregulated in TB decedents relative to healthy controls. These findings were consistent with published literature which has shown upregulated expression of activation markers CD69 and HLA-DR on NK cells during TB disease relative to controls in the peripheral blood (Kust et al., 2021; Schierloh, Alemán, et al., 2005) and pleural fluid (Pokkali et al., 2009) of humans, and in the lungs of *Mtb*-infected mice (Junqueira-Kipnis et al., 2003b). Therefore, upregulated

expression of CD69 and HLA-DR on NK cells during TB disease reflect immune activation and may play a role in sustaining NK cell activation (Pokkali et al., 2009; Borrego et al., 1999).

As a second line of evidence to support the finding that NK cells in the peripheral blood of TB patients were more activated and mature compared to healthy controls, CD57 and CD38 were investigated as NK cell maturation markers. NK cells in the peripheral blood of TB decedents expressed significantly higher levels of CD38 in TB relative to healthy controls, while CD57 was downregulated in TB. Frequencies of CD57 and/or CD38-expressing cells also indicated an inverse relationship between CD57 and CD38 during TB disease. More specifically, TB decedents had higher frequencies of $CD57^{-}CD38^{+}$ NK cells and depletion of the $CD57^{+}CD38^{-}$ subset in the peripheral blood relative to controls. There is currently little data to support or rationalize why CD57 and CD38 expression may exhibit an inverse relationship on NK cells during infection and disease. Perhaps these markers have distinct expression patterns along the spectrum of NK cell differentiation, although there is little information describing expression patterns and/or role of these markers during NK cell maturation. Further investigation into the role of CD57 and CD38 expression on NK cells during *Mtb* infection may uncover key mechanistic differences that occur during TB disease.

Expression of activating and inhibiting receptors was previously discussed as potentially important indicators of the overall activation state of NK cells (Section 5.4.1). Peripheral blood NK cells in TB decedents revealed higher expression levels of activating DNAM1 and NKG2D and inhibiting KIR receptors, with elevated frequencies of $NKG2D^{+}NKG2A^{-}$ NK cells in TB relative to controls. The $NKG2D^{-}NKG2A^{-}$ subset of peripheral blood NK cells was depleted in TB relative to controls, suggesting a switch in NK cell phenotype towards an activated NKG2D-expressing phenotype during TB. This is consistent with previous literature where *in vitro* exposure of NK cells to *Mtb* induced upregulated expression of

NKG2D and NKp46 which in turn, increased expression of granulysin and perforin through the MAP kinase signaling pathway (C.-C. Lu et al., 2014). Gene expression studies have also shown an association of increased inhibiting KIR expression amongst patients with active TB relative to healthy controls (Mahfouz et al., 2011; Méndez et al., 2006; Pydi et al., 2013; Salie et al., 2015), which is consistent with the data reported in this chapter. Overall, the data suggest that NK cells upregulate both inhibiting and activating receptors during TB disease. It is tempting to assume that upregulated expression of activating receptors would imply NK activation, while upregulated expression of inhibiting receptors would result in NK hypo-functionality. However, the reality is likely more complex. NK cell function is governed by complex signal transduction pathways delivered by multiple activating and inhibiting receptors on the cell surface at different proportions and combinations. Therefore, the ratio of inhibiting and activating receptor expression may reveal information regarding the overall activation state of NK cells. The inhibiting/activating ratio of receptor expression was higher in total peripheral blood NK cells, and within the $NKG2D^{+}NKG2A^{-}$ and $NKG2D^{-}NKG2A^{-}$ subsets in TB decedents relative to controls. Therefore, despite having enrichment of activating-receptor phenotype ($NKG2D^{+}NKG2A^{-}$), NK cells in the peripheral blood expressed higher proportions of inhibiting receptors during TB. Additionally, immune checkpoint proteins TACTILE and TIGIT were upregulated in TB decedents relative to controls who were otherwise healthy. The immune checkpoint receptor TIGIT inhibits NK cytotoxicity directly through ITIM and counter inhibits NK-mediated cytotoxicity by providing an “alternative self” mechanism for MHC-I inhibition (Stanietsky et al., 2009). TACTILE acts as a negative regulator of cytokine production (Chan et al., 2014; Minton, 2014; Sivori et al., 2019b). Therefore, NK cells in the peripheral blood during TB upregulate immune checkpoint proteins and express an overall “inhibitory” phenotype.

To summarize, NK cells in the peripheral blood of TB decedents expressed more cytotoxic molecules (perforin, granzyme B and granzyme K), activating receptors (DNAM1 and

NKG2D) and activation markers (CD69 and HLA-DR) relative to healthy controls, possibly as a feature of *Mtb* infection and immune activation. However, peripheral blood NK cells in TB decedents also had increased expression of immune checkpoints (TIGIT and TACTILE) relative to healthy controls, and an overall inhibiting phenotype, classified according to a higher ratio of inhibiting to activating receptor expression. These data may be argued as a potential cause of disease, whereby NK cells expressing inhibiting receptors in TB patients are hypo-functional and are thus implicated in the progression to end-stage disease. Although this argument is plausible, a more likely explanation of this phenotype during TB disease lies in NK cell licensing/education via the "rheostat model". These concepts are explored further below.

As previously described, NK cells express many different inhibiting receptors that bind self MHC-I molecules with different affinities. Therefore, NK cells are exposed to different degrees of inhibition, depending on the inhibiting receptor repertoire and the MHC-I molecules expressed in the local microenvironment (Held & Kunz, 1998; Parham, 2006). The concept of NK cell licensing has been reported in both mouse model (Kim et al., 2005a) and human studies (Anfossi et al., 2006b; Kim et al., 2008; Yawata et al., 2008), which suggest that NK cells expressing more, and multiple different inhibiting receptors that bind self MHC-I are most responsive and have enhanced functional activity by secreting IFN-γ and cytolytic granules. In contrast, as the number of inhibiting receptors decreases, NK cells become less responsive. The engagement of inhibiting receptors by host MHC-I are the most widely investigated molecules in the context of NK cell licensing and education. However, NK cells also express inhibitory receptors for non-MHC-I ligands, including immune checkpoint proteins, such as TIGIT (He & Tian, 2017). Despite the role of immune checkpoints for down-modulating NK responses, there are also data to suggest that engagement of immune checkpoints are necessary for optimal NK cell licensing and functional responses (He et al., 2017). Therefore, NK cell responses appear to be fine-tuned

through integration of multiple inhibiting and activating signals (Béziat et al., 2013; Fauriat et al., 2010; Yu et al., 2007), which is often referred to as the “rheostat” model. The rheostat model has been proposed as an explanation for differences observed in the magnitude of NK cell responses, which cannot be rationalized by the oversimplified responsive/hypo-responsive states linked to phenotypic characterization (Goodson-Gregg et al., 2020; Brodin et al., 2009; Joncker et al., 2009). The rheostat analogy considers that NK cell function is opposed by inhibitory receptors but also proposes that the lytic potential and the threshold of activation should be considered together: as the resistance to activation increases, the stored capacity of cytotoxic molecules increases, resulting in enhanced capacity for target cell killing (Goodson-Gregg et al., 2020; Prager et al., 2019). Therefore, the NK cell activation and function can be viewed as an on/off switch that is controlled and fine-tuned by NK receptors that act as a rheostat. Therefore, NK cells in the peripheral blood of TB patients were phenotypically activated and mature, with high cytotoxic potential, but NK cells were also “inhibitory” by expressing a higher ratio of inhibiting to activating receptors and immune checkpoints. These findings compliment the hypothesis that NK cells were activated during TB disease, since the NK cells were likely licensed and had a higher functional potential, according to the rheostat model. Perhaps the rheostat model is particularly important for NK cells circulating in the peripheral blood during TB disease, where they are activated, mature, and licensed, but remain inhibited until they reach a site of infection. It could be argued that inhibitory receptors and immune checkpoint molecules that are expressed on the NK cell surface could serve a purpose to prevent degranulation and inflammatory cytokine expression of activated NK cells in the peripheral blood and tissues where non-specific triggering of cell killing is undesirable. It is presumed that NK cell function and lysis of target cells occur mostly at the site of disease, where infection with *Mtb* occurs mainly in the tissues.

During TB disease, activated immune cells are recruited to the site of *Mtb* infection where they carry out their effector functions (Portevin et al., 2012; Esaulova et al., 2021; Feng et al., 2006; Junqueira-Kipnis et al., 2003b). It was therefore hypothesized that frequencies of tissue-resident NK cells would be higher in TB relative to controls. In support of the hypothesis, frequencies of total tissue-resident NK cells were depleted in the periphery and enriched in the lung of TB decedents compared to controls, possibly suggesting NK cell migration and lung homing. Tissue homing is a known feature of NK cells during infection and disease which was demonstrated by a 2003 study by Junqueira-Kipnis and colleagues showing that NK cells were recruited to the murine lung during *Mtb* infection, where they produced IFN-γ and perforin (Junqueira-Kipnis et al., 2003b). Currently, there is little data to disentangle whether the migration of NK cells to the lungs during TB disease in humans results in functional responses to aid in *Mtb*-killing that may be favourable and/or detrimental to the host. In fact, there are very little data in the tissue immunology field that characterize NK phenotypic and functional differences that occur during health and TB disease. To partially address this gap, tissue NK cell characteristics were compared between health and TB disease to highlight potential differences in maturation and/or activation status, as well as cytotoxic potential.

Immature, $CD56^{hi}CD16^{lo}$perforin^{-}granyme $B^{-}CD57^{-}CD38^{-}$ NK cells were enriched in the TB lung, with the same subset being depleted in the peripheral blood during TB. These data may suggest active migration of immature NK cells from the periphery towards lung tissue during active disease, when *Mtb* burden in the lung is thought to be high. Perhaps the enrichment of immature, hypo-cytotoxic NK cells in the lung tissue were implicated in the cause or a potential consequence of progression to disease. It has been proposed that the hypo-cytotoxic nature of NK cells in the lungs plays a role in homeostasis to prevent inflammation-induced tissue pathology in response to the myriad of inhaled environmental antigens (Cong & Wei, 2019; Robinson et al., 1984). Although requiring further investigation,

hypo-cytotoxic NK cells in the lung may be a double-edged sword that may play a role in the immunosuppressive microenvironment that could be implicated in disease progression. Alternatively, enrichment of phenotypically "hypo-cytotoxic", immature NK cells may indicate recent degranulation of cytotoxic molecules. However, based on the overall phenotype of this subset, it is most likely that low expression of cytotoxic molecules is a characteristic feature of immature $NK_{regulatory}$ cells. The $NK_{regulatory}$ subset are phenotypically classified as $CD56^{hi}CD16^{lo}$ and are considered hypo-cytotoxic with high cytokine-secreting capabilities. Rather than acting as cytolytic mediators to kill pathogen-infected cells in the tissues, perhaps NK cells in the tissues act as cytokine-producers that fine-tune responses by other immune cells, such as macrophages. Unfortunately, the functionality of NK cells by means of cytokine-production was not measured in postmortem tissues during this study. An exciting avenue for further investigation would be to characterize the cytokine-producing capabilities of $CD56^{hi}CD16^{lo}$ cells that are enriched in the TB lung and determine how NK cytokine responses modulate *Mtb* clearance by phagocytes. These data may potentially highlight an important role of $NK_{regulatory}$ cells as mediators or regulators of the local inflammatory milieu in the lung during TB.

5.4.3 Limitations

The limitations described in Chapter 4, Section 4.4.4 remain largely applicable for this chapter. Briefly, the small sample sizes and low statistical power did not allow potential confounders (HIV status, smoking and alcohol consumption) to be accounted for. It was also not confirmed whether tissues were sampled directly from *Mtb*-containing lesions. Reports of cytotoxic potential in this thesis were limited to evaluating expression of perforin, granzyme B and granzyme K, and further functional killing assays are required to confirm cytotoxic killing abilities.

Chapter 4, Section 4.4.4 also discussed potential cross-contamination of tissue cells with peripheral blood immune cells, having the potential to confound identification and purification of leukocytes truly participating in local tissue immune responses. Although certainly possible, peripheral blood immune cell contamination was likely minimal, specifically since the NK cell data presented in this chapter were vastly different in phenotypic characteristics and cytotoxic potential between NK subsets within the peripheral blood and tissues. Further investigation for this dataset may consider modeling techniques to predict the degree of cross-contamination from blood-borne leukocytes (for example, by regressing frequencies of immune cell subsets in the tissues with frequencies in the peripheral blood). Perhaps a more useful technique for future studies may be the use of intravascular staining to distinguish vascular and tissue leukocytes, as discussed in Chapter 4 (Anderson et al., 2012, 2014; Mortlock et al., 2022; Potter et al., 2021).

In the tissue dataset, it was also observed that MSI and frequency data had more variability in the tissues relative to the blood. This observation may be one of the reasons, among others discussed previously, why there were relatively few differences observed between cohorts in the tissues. Further investigation is required to determine whether there is a biological underpinning to this observation or whether it may be due to technical variability, such as the postmortem interval. Nevertheless, this observation suggests that a more thorough investigation would require a much larger sample size.

Another limitation was the final numbers of total, viable NK cells that were obtained for analysis from individual samples and donors, which were frequently relatively low. There were four major points of cell loss that occurred at different stages of sample processing and acquisition. Firstly, the use of postmortem samples posed its own challenges to optimize tissue harvesting and cell isolation (performed by the collaborating Ugandan research group) and thawing and staining of delicate specimens. Secondly, single cell suspensions

of tissue samples were prone to dying, based on the high percentage of Trypan blue-stained cells after thawing and cisplatin^{+} cells following acquisition. Despite extensive efforts to maximize and maintain cell viability and acquire the highest number of high-quality cells for each sample, cell viability was generally low (particularly for tissue samples – PBMC appeared to have more viable cells that were less prone to dying). Thirdly, mass cytometry is known for its low sampling efficiency. More specifically, flow cytometry has a higher sampling efficiency, enabling >95% of cells to be acquired, as opposed to CyTOF which only allows for 30% sampling efficiency. Mass cytometry therefore suffers substantial loss of cells once injected into the instrument, enabling only a smaller proportion to be recorded. Finally, data analysis included steps to further exclude acquired events that were characteristic of cell debris, fragments and dead cells, further diminishing the total number of analyzable events per sample. The resulting number of total NK cells was relatively low, shown in Table 5.2.

Table 5.2: Counts of total, live NK cells per compartment.

Tissue	Total sample number (n) = 117[1]
BAL (n=13)	160 [16, 5 125]
Hilar lymph nodes (n=21)	778 [15, 5 837]
Lung (n=28)	1 204 [2, 8 335]
PBMC (n=29)	28 783 [2 043, 106 410]
Spleen (n=21)	1 903 [88, 24 057]

[1]NK cell counts: Median [Range]
Minimum number of cells for inclusion in analysis was 15 cells.

Despite the limitation of low sampling efficiency and low cell numbers acquired by mass cytometry, CyTOF technology was immensely useful for the purpose of this investigation. More specifically, the autofluorescent nature of lung, lung-draining hilar lymph nodes and BAL samples was presumably due to carbon build-up within resident phagocytes within the

lung that stems from exposure to smoke and/or air pollution (Kulkarni et al., 2005; Phipps et al., 2010; Demling, 2008; Young et al., 2019). Acquiring data from autofluorescent samples using conventional flow cytometry poses a substantial challenge due to high autofluorescence signal in multiple channels spilling over and contaminating signal in other channels, making resolution of the true signal almost impossible to resolve (Young et al., 2019). This spillover further reduces the number of available channels for detection in an already-limited panel (typically between 8 and 18 markers in standard flow cytometers). Although newer technologies, such as spectral flow cytometry, are advancing to allow resolution of autofluorescence from real signal and increase the size of antibody panels, CyTOF has been demonstrated in this thesis as a fit-for-purpose tool to acquire high dimensional data (more than 45 markers) and perform phenotypic analysis of cells from autofluorescent samples.

Lastly, NK cells are not only potent killers of pathogen-infected and neoplastic cells but are also important producers of cytokines. More specifically, NK cells produce IFN-γ (the hallmark cytokine in TB), TNF and IL-22, all of which have relevance in the context of TB (Allen et al., 2015; Biron et al., 1999; Choreño Parra et al., 2017; P. Kumar et al., 2013; van den Bosch et al., 1995; Warren et al., 1995; Xu et al., 2014). Therefore, a major functional role for NK cells during TB disease was not included in this study. Future studies are planned to investigate NK cell functional characteristics within postmortem tissue compartments in TB decedents and controls, for which optimization is currently underway.

5.4.4 Conclusions

Despite several limitations, this study successfully characterized NK cells across tissue compartments in TB and healthy controls. Perhaps most importantly, this study demonstrated the feasibility of performing human immunology studies using postmortem

tissues. By describing the methodology and framework for high-dimensional analysis of tissue data, it is hoped that this thesis will pave the way for novel studies that inform mechanistic targets (which may or may not involve NK cell biology), with relevance for developing novel clinical interventions.

Chapter 6: Concluding Remarks.

“There is no real ending. It’s just the place where you stop the story.”

- Frank Herbert

NK cells have been highlighted as potentially important innate responders during *Mtb* infection, although their precise role during TB pathogenesis remains uncertain (Allen et al., 2015; Choreño Parra et al., 2017; Sia et al., 2015). The main objective of this study was to gain a better understanding of NK cell function and phenotype in the peripheral blood and human tissues, adding insights about various stages of the TB spectrum. To achieve this objective, NK cell cytokine production was quantified to determine functional changes that occur longitudinally in peripheral blood with time to TB diagnosis in adolescent progressors versus controllers. Next, a cytokine neutralization assay was designed to investigate bystander activation of peripheral NK cells and quantify changes in cytokine production and cytotoxic potential that occur when T cell and myeloid cytokine-mediated pathways were blocked in adult TB patients and healthy controls. Finally, to characterize NK cell subsets across human tissues, postmortem samples from blood, lung, hilar lymph nodes, BAL, and spleen were acquired from a cohort of adult TB patients who succumbed to disease and controls who were otherwise healthy but died due to trauma. These data provide a steppingstone for NK cells in the TB field, delivering insights into NK cell function and tissue immunology that may be further investigated as potential targets for modulation in preventative or therapeutic strategies, which are further discussed here.

The TB spectrum (Figure 6.1) includes different stages ranging from asymptomatic infection to active disease (Barry et al., 2009; Drain et al., 2018; Esmail et al., 2014). During exposure, inhalation of aerosolized bacilli may result in *Mtb* infection. In some cases, the host immune response may effectively clear the infection, while in other cases, controlled/remote infection may occur when *Mtb* bacilli are not fully cleared. Individuals with recent *Mtb* infection are most at risk for developing active disease and would benefit most from TPT (Menzies et al., 2021; Reichler et al., 2018; Vynnycky & Fine, 1997b). In contrast, remote infection (when an individual was infected many years prior) is typically not transmissible and may persist for many years, in which case the remaining lifetime risk for developing active disease is

substantially lower, yet possible (Behr et al., 2018). The precise immunological mechanisms governing whether an individual progresses to active disease or controls *Mtb* infection remain unknown and are influenced by many factors. Subclinical and active, symptomatic TB disease may be actively transmissible states, during which *Mtb* bacilli may be spread in the community, although some subclinical and symptomatic TB cases may not be infectious. In those with active TB disease, initiation of anti-TB treatment successfully clears the infection in most cases, and a patient is typically considered cured after completing the full antibiotic regimen and returning to full health. However, some cured patients may experience relapse, which is characterized by recurrence of the disease and/or the signs and symptoms following a period of improvement. Relapse occurs when bacilli have not been fully cleared by anti-TB treatment and recurrence occurs with the same infecting *Mtb* strain. Alternatively, recurrent TB may occur if an individual has been reinfected with a different strain than what had occurred at primary disease, which happens more often in endemic regions where there is high infection pressure. Individuals may progress or revert between different stages of TB disease along the spectrum, but the precise causes and/or consequences of *Mtb* clearance, progression or reversion remain poorly defined. In some cases, especially in the absence of treatment, a TB patient may succumb to active disease and die. Most human immunology studies in the TB field have been performed using samples from living TB patients and controls at various stages along the TB spectrum. More specifically, these studies have mostly been limited to investigating perturbations, immunological mechanisms, and pathways occurring in peripheral blood immune cells in humans (which only represent a subset of the immune landscape in the body). Overall, human tissue studies in the context of TB immunology remain few and far between, and the mechanisms governing the progression from active disease to death remain understudied; which are major gaps in the field that my thesis aimed to address.

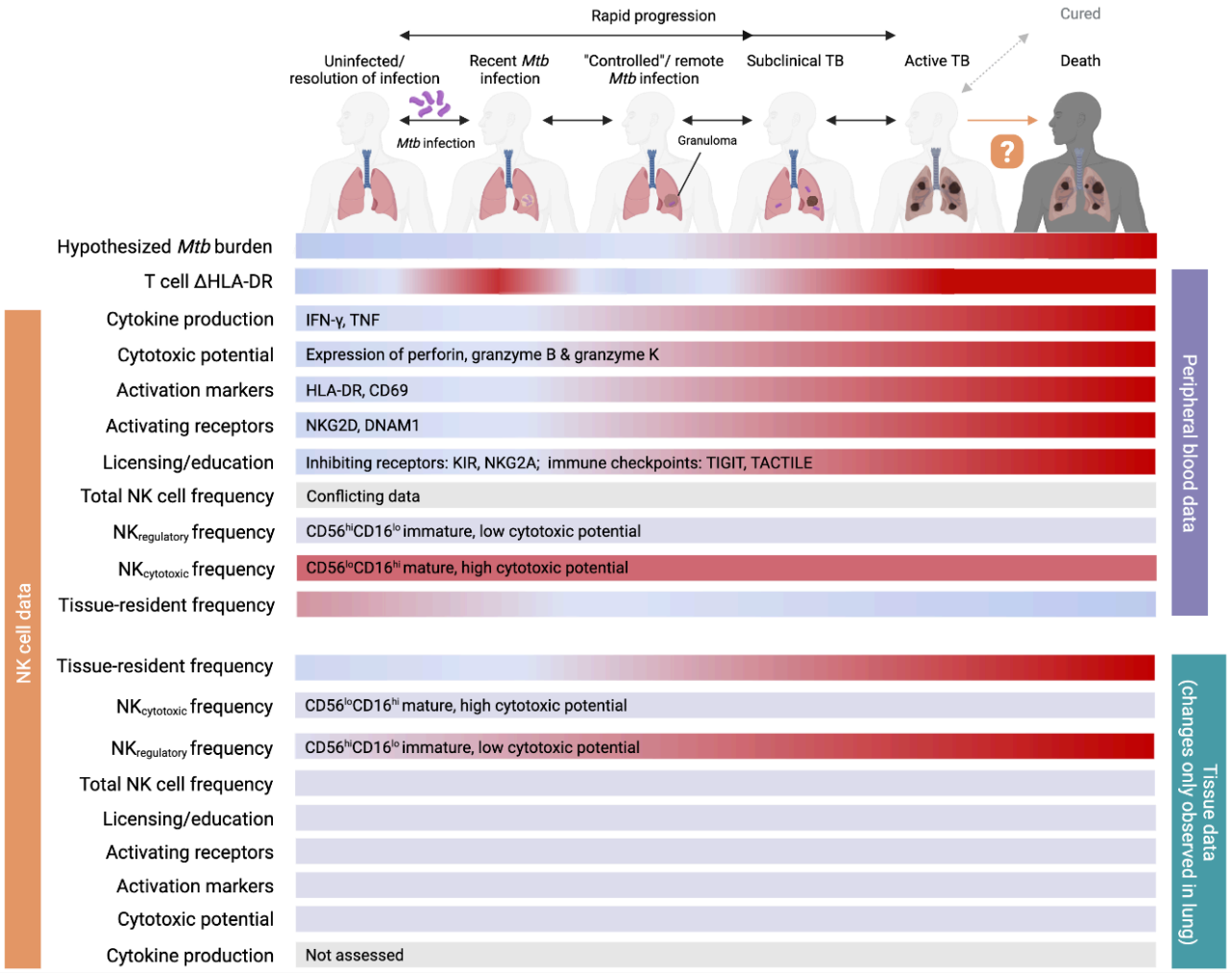

Figure 6.1: NK cell kinetics across the TB spectrum. Visual illustration of hypothesized *Mtb* burden, antigen-specific T cell HLA-DR expression, and NK cell kinetics during the full spectrum of TB, following exposure to *Mtb,* progression to disease, and cure or death. NK cell characteristics were investigated in the blood and tissues, including subset frequencies, cytokine production, cytotoxic potential, activation markers, activating receptors, and licensing/education. Gradient between blue and red denote the direction in response along the TB spectrum, with red representing high and blue low outcomes. *Mtb* infection induces T cell activation, detected as *Mtb*-specific T cell ΔHLA-DR levels that are highest during recent *Mtb* exposure, subclinical and active disease, and are also detectable at high levels after death. T cell ΔHLA-DR levels are lower during "controlled'/remote *Mtb* infection and after cure. While there are conflicting data in the field, frequencies of total NK cells, $NK_{regulatory}$ (least predominant subset) and $NK_{cytotoxic}$ (most predominant subset) were not different in the peripheral blood between stages of the TB spectrum. However, in the tissues (including postmortem lung, BAL, hilar lymph nodes, spleen, and in control tonsils from living participatns), $NK_{cytotoxic}$ were the least predominant subset, while $NK_{regulatory}$ were most predominant subset that had increasing frequencies detected along the TB spectrum towards death in active disease cases. Frequencies of NK cells expressing tissue-resident markers (dubbed "tissue-resident NK cells") were depleted in the peripheral blood and increased in the lungs, suggesting NK cell tissue migration along the TB spectrum towards death in cases with active TB. Kinetics of NK cell cytokine production, cytotoxic potential, and phenotypic evidence of NK activation and licensing/education were highest towards death of TB cases in peripheral blood, while no changes were observed in tissue data.

Mtb burden is hypothesized to be dynamic and fluctuate along the TB spectrum where bacterial load increases from *Mtb* infection, through subclinical and active, symptomatic TB disease (Figure 6.1). In the case of cured TB, which occurs in ~86% of patients who adhere to the recommended anti-TB treatment regimens (WHO, 2022), *in vivo* bacterial burden in the tissues is hypothesized to subside and *Mtb* is thought to be cleared completely or may persist at a low level. In contrast, when individuals succumb to TB disease, *Mtb* burden is hypothesized to be highest as uncontrolled infection and a failed immune response led to the highest state of bacterial load and most severe forms of TB disease. Of course, this is not always true, as some individuals with TB disease succumb to other complications, such as haemorrhage, stroke, heart attack or pulmonary embolism (Gupta et al., 2017; Huang et al., 2020). Notably, TB-associated thrombosis occurs via various mechanisms such as local invasion, venous compression/obstruction (Gogna et al., 1999), or by producing a transitory hypercoagulable state (Naithani et al., 2007; Turken et al., 2002). These complications remain rare and are mostly associated with more advanced stages in the TB spectrum (Kouismi et al., 2013) and therefore, represent cases with unfavourable/failed immune responses in controlling *Mtb* infection. Unfortunately, the true bacterial burden in the TB cohort of this thesis remains unknown and a study is currently underway which aims to address this gap by quantifying *Mtb* burden in postmortem tissues. It is possible that *Mtb* burden is highest at death in those with TB disease due to uncontrolled infection and a failed immune response. This may be expected in those with newly diagnosed disease prior or soon after to initiating anti-TB treatment. Alternatively, bacterial burden at death may be low in some patients who mostly clear *Mtb,* but who rather succumb to inflammation-induced pathology (i.e., excessive, pathological immune responses). Data from the *Mtb* quantification study may provide insight about the range in *Mtb* burden at death in TB patients. Although it should also be forewarned that failure to detect *Mtb* burden in a particular tissue sample does not necessarily mean that bacterial load in the entire organ or

tissue is nil or low. A negative result for *Mtb* quantification may be due to sampling of paucibacillary or non-infected tissue lesions, which is a limitation that is discussed at a later point in this chapter. Therefore, optimal experimental design and careful consideration are required to successfully disentangle the relationships between *Mtb* burden and death in those with active TB disease.

The Global Plan to End TB (Stop TB Partnership, 2022) has highlighted the development of TB biomarkers as an important step towards reaching our goal to end TB by 2030. Towards this objective, several studies (Adekambi et al., 2015; Musvosvi et al., 2018; Riou et al., 2017, 2020; Wilkinson et al., 2016) showed that activation of *Mtb*-specific T cells, measured as HLA-DR, CD38 or Ki67 expression, was increased in patients with TB disease relative to healthy controls. A recent study by Mpande and colleagues at SATVI (Mpande et al., 2021), showed that HLA-DR expression on *Mtb*-specific T cell as a marker of activation status was also upregulated in early *Mtb* infection. These findings suggest that *Mtb*-specific T cell activation could be used as a biomarker of *in vivo Mtb* burden, as the biomarker was able to distinguish between recent *Mtb* infection, controlled/remote *Mtb* infection and active disease, which are disease states with elevated *Mtb* burden (Mpande et al., 2021). However, this hypothesis is yet to be fully validated, as *Mtb* burden in the lungs and infected tissues has never been associated with peripheral blood T cell ΔHLA-DR data in a head-to-head comparison in the same individuals. To partially address this knowledge gap, the data presented in my thesis offers a proof-of-concept that T cell function and HLA-DR levels measured postmortem can distinguish between individuals with and without *Mtb*-immunological sensitization and TB disease in PBMC samples that were obtained after death. These findings serve as the foundation for which future studies may evaluate the hypothesis that HLA-DR expression on antigen-specific T cells may be a biomarker for bacterial load in human tissues. To achieve this, bacterial load may be quantified directly in the tissues and at the site of disease (by targeted biopsies at tuberculous lesions in the

tissues) using culturing methods or quantitative PCR techniques, such as droplet digital PCR (DD-PCR) (Fan et al., 2022) or quantitative real-time PCR (qRT-PCR) (Barletta et al., 2014), which may then be associated directly with T cell functionality and HLA-DR expression data in the PBMC of the same individual. Although tissue samples cannot easily be obtained in living individuals, due to ethical considerations that would submit a patient to invasive medical procedures for biopsy, it is possible that bacterial load could be quantified in the sputum as a means for evaluating whether the T cell ΔHLA-DR biomarker fits the hypothesis of being a proxy for bacterial load in the respiratory tract in a living cohort. However, this approach is subject to major limitations since not all individuals can produce a suitable sputum sample, and stages of recent and remote *Mtb* infection and subclinical TB are often paucibacillary or undetectable (Khan et al., 2007; Sakundarno et al., 2009). Most importantly, a culture negative sputum sample does not represent the absence of *Mtb* in the lung parenchyma and/or lymph nodes and sputum does not represent the bacterial load directly in the tissues and at the site of disease. Therefore, quantifying bacterial load in a living cohort is challenging. In postmortem cohorts bacilli can be sampled and quantified directly from the site of disease, offering a feasible approach to determine if the PBMC antigen-specific T cell ΔHLA-DR biomarker is associated with tissue pathology (by means of radiological data, such as x-ray or PET-CT) in TB patients and healthy controls. To develop this technique, a postmortem cohort would also be useful to determine whether the ΔHLA-DR biomarker is a suitable proxy for extent of disease (i.e., tissue pathology) and bacterial load in the tissues. The hypothesis would be that patients with more advanced stages of TB disease have increased bacterial load and more severe pathological lesions in the tissues, which is associated with T cell activation in the blood. The approach proposed here with postmortem data would serve as a cornerstone for further development of the T cell ΔHLA-DR biomarker (or any other TB biomarker for that matter, including the many transcriptomic signatures that have been reported), to identify living individuals with high

bacterial load and tissue pathology who are at risk of developing active disease and may benefit from TPT or anti-TB therapy.

Perturbations in peripheral cell frequencies have been proposed as potential biomarkers for diagnostics and/or predicting those who are at risk for developing active disease (reviewed by Goletti et al., 2016). In the context of NK cells, changes observed in peripheral blood have been contradictory, with some publications reporting increased (Schierloh, Alemán, et al., 2005), decreased (Cai et al., 2020; Chowdhury et al., 2018; Scriba et al., 2017), or no change (Nirmala et al., 2001; Vankayalapati et al., 2002) in NK cells frequencies. In this thesis, data showed that NK cell frequencies were not different between active TB and healthy controls in living and postmortem cohorts. Altogether, NK cell frequencies are an unlikely candidate for the TB biomarker field due to the high degree of heterogeneity and conflicting data between study populations. One of the likely reasons for this contradictory data is linked to differences in the inflammatory status of the host. There are extensive data in the field to show that haematopoiesis is altered during inflammatory diseases, including TB, leading to changes in lymphocyte subsets (such as NK cells) in the peripheral blood (Baldridge et al., 2010, 2011; Naranbhai et al., 2014; Scriba et al., 2017). Therefore, differences in inflammatory status of the host greatly influences frequencies and functions of immune cells in the peripheral blood, which in turn, can modulate the outcome of *Mtb* infection, persistence, progression and/or reversion on the TB spectrum. Additionally, the inflammatory status of the host is altered during *Mtb* infection, clearance and/or re-inflection, which occur at different rates and frequencies in high and low endemic areas. Partly for these reasons, the field has struggled to classify different stages of the TB spectrum and identify robust biomarkers.

In addition to immune cell frequencies, it has been proposed that functions of NK cells may serve as TB biomarkers of disease state (Goletti et al., 2016). Like frequencies of immune

subsets, the functional responses of immune cells are also influenced by the inflammatory status of the host (Baldridge et al., 2010, 2011; Naranbhai et al., 2014; Scriba et al., 2017). In my thesis, functional data from the adolescent progressors and controllers showed that cytokine production in peripheral blood NK cells was significantly associated with progression to TB. More specifically, low NK cell cytokine responses occurred at timepoints further from TB diagnosis, which steadily increased to significantly higher levels at timepoints closer to TB diagnosis in progressors relative to controllers. However, it is unlikely that NK cell function would serve as a useful TB biomarker since NK cells are rapid responders to bystander activation and their responses can be modulated via signals produced by accessory cells within the local microenvironment and the overall inflammatory status of the host. To demonstrate the plasticity of NK cell function during inflammatory disease, we showed that cytokine producing NK cells that were associated with TB progression occurred in response to PBMC stimulation with *Mtb* peptides (for which NK cells do not possess receptors) and these NK cell responses where significantly associated with IL-2 production by CD4 T cells. Therefore, NK cell cytokine production was likely occurring in response to cytokines produced by other immune cells in the inflammatory milieu during TB disease. Additionally, decreased NK cell cytotoxic potential was more pronounced in TB patients relative to controls when T cell-associated IL-2 was blocked in PBMC stimulated with *Mtb* peptides and lysate, suggesting that T cells play an important role in NK cell activation and cytotoxic potential during TB. Finally, expression of NK cell cytotoxic molecules, activation markers, activating receptors and evidence of NK cell licensing and education were higher in TB cases relative to their healthy controls, which is also a likely reflection of ongoing inflammatory responses that heighten NK cell function during disease. An interesting avenue for further investigation would be to evaluate whether the promising T cell ΔHLA-DR biomarker is associated with these indicators of NK cell activation and function during TB disease. These data are available to address this research question and

will be performed in upcoming analyses as part of a sub-study. Based on the principles of bystander activation and the data presented in this thesis, it is hypothesized that *Mtb* burden in the tissues is strongly associated with the T cell ΔHLA-DR activation biomarker that in turn, is also associated with NK cell activation and function during inflammatory disease.

In a meta-analysis of the therapeutic effects of rhIL-2 as an adjunctive immunotherapy against TB, IL-2 was concluded to promote CD4 T cell and NK cell proliferation and improve sputum culture and smear conversion in TB patients (R. Zhang et al., 2018; Young et al., 2020). Therefore, rhIL-2 may be a promising immunotherapy to enhance NK cell function via bystander activation and promote bacterial clearance in the tissues during *Mtb* infection and TB disease; although large scale, multicentre clinical trials are still needed. Other immunotherapeutic HDTs are currently being investigated in the cancer field which may also enhance NK cell killing of *Mtb* infected cells at the site of disease. More specifically, NK cell-mediated immunotherapies have demonstrated enhanced tumour killing using adoptive transfer of activated NK cells that are expanded *ex vivo* (using stimulants such as cytokines and antibodies). Additionally, CAR-NK cells and NK cell extracellular vesicles have shown promising anti-tumor effects in pre-clinical studies (Hu et al., 2019). Therefore, the adoption of such therapies in the TB field may serve as promising tools to improve TB prognosis by enhancing NK cell functions to promote clearance of *Mtb*-infected immune cells. However, the cost and practicality of implementing such strategies remain a far reach for the TB field. It is well known that TB is endemic in some low- to middle-income countries (WHO, 2022), where low-cost strategies are essential for enabling rollout. Even in endemic countries, where low-cost antibiotic therapies are free, there is limited reach in many communities due to social challenges faced by individuals. Amongst the several socio-economic determinants of TB is delayed or missing diagnosis and treatment due to healthcare not always being accessible in communities of low-income countries (Duarte et al., 2018; Hargreaves et al., 2011; Wingfield et al., 2018), including South Africa. Therefore, high-cost HDTs that require

highly specialized medical laboratories and frequent follow-up visits are not likely to be effective strategies for endemic settings. However, with the advancement of technologies and further investigation into streamlining such therapies for increased accessibility and community reach, the field should not be too quick to discard these approaches.

Rather than HDTs, development of new TB vaccines may be more achievable in the near future. New TB vaccines have been highlighted as one of the main priorities for the Global Plan to End TB (Stop TB Partnership, 2022), with the following characteristics: safe, efficacious, effective, available, durable, accessible, and affordable. Several of the most promising TB vaccines that have advanced to clinical trials were designed with the intent to induce polyfunctional CD4 Th1 cell responses that are associated with a protective immune response against *Mtb* infection (reviewed extensively by Lewinsohn et al., 2017; Morgan et al., 2021). However, no new TB vaccines have been licensed in almost a century. Nevertheless, the published data from vaccine trials have revealed that polyfunctional T cell responses are successfully induced by vaccines, including BCG (Scriba et al., 2011; M. Tameris et al., 2014; Tait et al., 2019), and that NK cell functions are also induced by vaccination (Penn-Nicholson et al., 2015), presumably via the process of bystander activation and/or trained immunity (Kleinnijenhuis et al., 2014b; M. Murphy et al., 2023; Penn-Nicholson et al., 2015). Importantly, NK cell activation in these studies were observed shortly after vaccination, reflecting immune activation. However, there is evidence to suggest that longer-term outcomes of vaccination may reflect immunological memory, such as durable BCG-boosted memory NK cell responses that were observed for up to one year in a BCG re-vaccination study by Suliman and colleagues in 2016 (Suliman et al., 2016). Data in this thesis demonstrated that T cell-mediated IL-2 bystander activation is important for NK cell cytotoxic potential in response to *Mtb* antigens in TB patients. As a clinical translation of these data, it may be possible to design vaccines that induce T cell-mediated bystander activation pathways, such that T cell cytokines (such as IL-2) produced in

response to a vaccine would enhance NK cell cytotoxicity and functional killing of *Mtb*-infected cells to promote bacterial clearance in the tissues. Although this is what most vaccines already do, perhaps the concept of increased NK cell function via T cell-mediated bystander activation could be enhanced even further with more optimization and perhaps induce more long-term NK cell memory-like responses. With further development, vaccines may be designed to develop and maintain memory T cell responses that produce NK cell-activating and cytotoxic responses upon exposure to *Mtb.* Furthermore, vaccines may also be designed to directly target NK cell trained immunity, such that epigenetic programming enables NK cells to respond with greater magnitude upon subsequent heterologous exposure (Netea et al., 2016). Finally, in most clinical trials of new TB vaccine candidates, T cell responses are often included as an endpoint to measure immunogenicity outcomes in participants. It is well known that immunogenicity does not imply protection, although it does give an indication of a vaccine-induced immune response and the potential for long-lived immunological memory. I propose that the TB vaccine field is missing an important endpoint, which is the analysis of NK cell responses in clinical trial data, including cytokine production and cytotoxicity, and perhaps evidence of durable, long-lived memory-like NK cell responses.

NK cell biology has mostly been studied in the peripheral blood, which only represents a subset of the immune landscape throughout the body and does not necessarily reflect immune cell biology that occurs in the tissues (Brighenti & Andersson, 2012; Farber, 2021; Saris et al., 2021). Tissue data showed that tissue-resident NK cells (i.e., NK cells expressing markers of tissue residency) and $NK_{regulatory}$ cells with an immature, $CD56^{hi}CD16^{lo}$ phenotype and low cytotoxic potential were enriched in the lungs of TB cases who succumbed to disease relative to healthy controls. These data confirm findings from human and animal models demonstrating tissue migration to the lungs during active disease (Esaulova et al., 2021; Feng et al., 2006; Junqueira-Kipnis et al., 2003b; Portevin et al.,

2012), which would represent a state of immune activation and recruitment of immune cells towards the site of infection to assist with clearing bacilli. However, $NK_{regulatory}$ cells are traditionally classified as the hypo-cytotoxic subset that do not directly participate in killing of *Mtb*-infected cells. Rather, this subset is primarily responsible for secreting cytokines and can mature into terminally differentiated cytotoxic cells (Béziat et al., 2011; Björkström, Ljunggren, et al., 2010a; Yu et al., 2010). Therefore, immature $NK_{regulatory}$ cells that are enriched in the postmortem TB lung may represent migration of a key subset of cytokine-producing immune cells that may participate in shaping the immune response at the site of infection and disease. Alternatively, there may have been selective depletion of the $NK_{cytotoxic}$ subset, perhaps due to exhaustion and/or cell death, or $NK_{cytotoxic}$ cells in the lung may have undergone de-differentiation towards the cytokine-producing subset that can modulate other immune cells at the site of disease. Unfortunately, NK cell functional responses were not measured in the tissues and these hypotheses could not be fully evaluated. However, the data in this thesis lays a foundation to support the need for further NK cell tissue immunology studies in the TB field by providing evidence to suggest that $NK_{regulatory}$ cells are potentially interesting cells to be studied in the lungs of TB cases. Investigating the role of cytokine producing $NK_{regulatory}$ cells at the site of disease in postmortem samples may reveal an important subset that either contributes towards the cause and/or consequence of TB disease. Most importantly, this thesis demonstrated the feasibility of performing immunology studies in postmortem human tissues that are not traditionally accessible in living cohorts. This study successfully described the necessary methodology and developed the framework for data analysis that will be applied in future studies to address the most pertinent questions regarding the role of NK cells (and other immune cell subsets) in TB immunopathology. The following supplementary text box describes some practical lessons learned from this human postmortem tissue immunology study, which summarizes some useful points to consider in the context of study design and troubleshooting.

Text Box: Practical lessons learned from a human postmortem tissue immunology study.

→ Tissue immunology studies in a postmortem cohort are feasible!

→ Larger tissue sections could be sampled to increase the number of cells isolated into cell suspensions, thereby increasing the chances of analyzing more rare immune cell subsets in the tissues (including NK cells).

→ For *ex vivo* antibody staining, cells should be rested for a maximum of 1 hour in complete medium (RMPI + 10% FCS) supplemented with 6000U/mL DNase I to prevent clumping and obtain maximal viability after thawing. The individual performing the antibody staining should work with haste to maintain maximal viability of cell suspensions prior to fixation.

→ Tissue cell suspensions that were isolated and cryopreserved within a postmortem interval of 5-15 hours are viable (>70%) upon thawing. Therefore, with further optimization, cryopreserved tissue cell suspensions may be suitable for culturing and *in vitro* stimulation.

→ Future postmortem tissue studies investigating immune cell functions should optimize resting and stimulation times to maximize cell viability during *in vitro* culturing. Shorter stimulation times are likely to yield the highest quality data as tissue cell suspensions tend to die more rapidly than cells isolated from peripheral blood.

→ Tissue specimens sampled from the lungs and lung-draining lymph nodes are black in colour and autofluorescent due to intracellular carbon build up (presumably due to smoking and/or air pollution), making non-fluorescence-based cytometry techniques (such as CyTOF) favourable over traditional, fluorescence-based flow cytometry.

→ Iodine contamination of cell suspensions interferes with CyTOF data acquisition. Iodine contamination in a sample may lead to excessive signal that deteriorates the mass cytometer detector at a higher rate than usual. Excessive iodine contamination necessitates dilution of the sample to reduce the signal burden on the detector at a given time. However, dilution substantially increase acquisition time and costs. Therefore, iodine-containing compounds and reagents should be avoided at every step in the tissue harvesting and processing stages; including reagents used to sterilize surfaces and/or dissection tools.

→ Barium contamination of cell suspensions interferes with CyTOF data acquisition. All CyTOF reagents should be purchased as CyTOF-grade quality, and only stored in single-use plastic containers in which they are received. Reagents should not be made up or stored in glassware that has been washed using municipal tap water and/or detergents, as these may contain barium compounds. Barium contamination of a sample (like iodine) will create excessive signal that deteriorated the mass cytometer detector and necessitates dilution of the sample, thereby increasing run time and running costs.

→ At least low levels of barium contamination occur in most lung and lung-draining samples. It is believed that air pollution is also a source of barium contamination, which is unavoidably inhaled in most settings. Panel design is therefore, crucial to avoid the assignment of antibodies into any channel that may experience signal spillover (-1, +1 and +16 mass units) from any of the several barium channels. Unfortunately, barium contamination that occurs in lung and lung-draining samples reduces the number of potential markers in the panel, but it is necessary to avoid spillover artifacts that may lead to incorrect interpretation of the data.

→ Panel optimization is crucial! To avoid artifacts in the data, markers should be assigned to channels such that those experiencing signal spillover from another channel are not co-expressed on the same cell. Antibody titrations will also aid in optimizing concentrations to reduce spillover between channels.

→ Panel size may be increased by assigning two markers to the same channel which are not co-expressed on the same cell subsets (e.g., CD14 and $\gamma\delta$TCR, or CD3 and CD19, could be assigned to the same channel).

The vast variability and plasticity of functional potential within the spectrum of NK cell subsets puts these cells in good stead as important responders to pathogenic threats. Data in this thesis certainly demonstrated functional differences in NK cell cytokine responses between health and disease in peripheral blood. However, no significant differences were observed between TB decedents and healthy controls when assessing cytotoxic molecules, activation markers, activating receptors and markers of NK cell licensing and education in tissue NK cells. Considering the highly variable levels obtained from the dataset, the sample size of this study was too small. By increasing the sample size per cohort, it is also likely that certain comparisons that did not reach statistical significance in this thesis due to limited sample size may be better powered to detect differences. Additionally, sampling only took place at the left upper lobes of the lung tissue and airways in all participants, and not specifically targeting tuberculous lesions or granulomas where *Mtb* burden is likely to be highest during TB and therefore, most likely to demonstrate activated phenotypes and functional responses. Additionally, there were little evidence to suggest NK cell differentiation and activation in the tissues, which may be a true representation of homeostatic tissue immunology as a means of preventing inflammation-induced tissue pathology, where it would be undesirable to have continuous cytokine production and cytolytic killing in response to the many immunogens that are inhaled in the airways and lungs and transported to the lymph nodes and spleen. Although relatively little has been published regarding the precise role of NK cells in the TB granuloma, older reports have suggested that NK cells play an immunosuppressive, regulatory role in granulomatous inflammation (Epstein et al., 1989; Hashimoto et al., 1990). Therefore, the characterization of NK cell cytotoxic potential, activation and licensing and education in postmortem tissues presented in this thesis are likely to have been representative of granulomatous and/or non-*Mtb*-containing lesions that display a homeostatic, regulatory state of NK cell phenotypes. To improve this approach, when performing NK cell functional assays and quantifying *Mtb*

burden in the tissues, it is recommended that pathological lesions are investigated alongside non-pathological specimens in TB cases, while also including specimens from healthy individuals as a control cohort.

This thesis was also subject to several assay-specific and technical limitations, which have been discussed extensively in the respective chapters. Towards the overarching limitations, the overall sample size per cohort (including the ACS cohort, the adult cohort for NK cell functional assays, and the postmortem cohort) were suboptimal and require inclusion of more individuals to increase statistical power. Cytokine production by NK cells was only evaluated in the ACS progressors and controllers cohort, and the adult cohort for NK cell functional assays using PBMC, but not in the tissue samples from the postmortem cohort. In future tissue immunology studies, it would be of high priority to investigate cytokine production by NK subsets, which may reveal key differences in NK cell function in the tissues during health and disease.

In addition to cytokine production, NK cells are potent cytolytic killers of pathogen-infected cells, that have been highlighted as potentially important role players during *Mtb* infection and TB disease. For this reason, it is of interest to investigate the cytotoxic functions of NK cells. In this thesis, evaluation of NK cell cytotoxic function was limited to reporting cytotoxic potential (in terms of MFI/MSI), which only reflects the relative abundance of cytotoxic molecules within the NK cell subsets. Together with other phenotypic data, measuring the expression of cytotoxic molecules was useful for evaluating the likely activating, inhibiting, and licensing/education status of NK cell subsets in postmortem tissue specimens. However, expression of cytotoxic markers is not an established proxy for NK cell cytolytic killing. To compliment cytotoxic molecule expression data, it is also possible to measure the expression of CD107a using cytometry techniques, which is thought to provide evidence of NK degranulation. Unlike cytokines, cytotoxic molecules are pre-formed and stored in

intracellular, cytotoxic granules containing lysosomal-associated membrane glycoproteins (LAMPs), such as CD107a (LAMP-1), in their lipid bilayer. The expression of CD107a becomes temporarily detectable on the cell surface when intracellular vesicles are transported and fuse with the cell membrane to release cytotoxic molecules into the surrounding microenvironment. Therefore, extracellular expression of CD107a is considered a marker for NK cell degranulation and a proxy for cytotoxic potential (Alter et al., 2004; Betts & Koup, 2004). In conjunction with measuring cytotoxic molecules, inclusion of CD107a in this thesis would have certainly been useful to evaluate whether an NK cell had undergone degranulation, which would have added valuable data to these investigations. Although CD107a was considered for the cytometry panels, it was decided against for the main reason of requiring addition to a cell culture upon *in vitro* antigen stimulation. As already discussed, this thesis only assessed postmortem tissue data *ex vivo*. Therefore, CD107a was not a suitable candidate for the mass cytometry panel. Once processing of postmortem tissue samples has been optimized to obtain suitable cell viability for stimulation and culturing, inclusion of CD107a in the panel may be considered. Although CD107a could have been used for the flow cytometry NK cell functional assay in PBMC, it was also decided against since staining requires a high titer to be added prior to stimulation that may have interfered with the addition of neutralization antibodies that were added at the same time. With further optimization, it is certainly possible that CD107a staining for NK cell degranulation may be included in the cytokine neutralization assay, which is an avenue for consideration in future studies. Nevertheless, the expression of neither cytotoxic molecules nor CD107a directly imply cytolytic killing by NK cells. Therefore, future studies require functional killing assays as the gold-standard to evaluate the true cytolytic activity of NK cell subsets in the tissues by measuring NK killing against target cells, such as *Mtb*-infected immune cells, *in vitro*.

Another major limitation for the postmortem study was the loss of structural integrity of tissue specimens that were sampled from the lungs, hilar lymph nodes and spleen. It is well established that *Mtb* infection in the tissues is characterized by an orchestrated migration of immune cells to the site of infection, such that secondary immune structures and granulomas are formed allow interaction of immune cells with one another and bacilli (Esaulova et al., 2021; McCaffrey et al., 2022). However, the generation of tissue cell suspensions to perform single cell cytometry assays did not permit evaluation of geographical interactions between immune cell subsets and bacilli. Therefore, the data presented in this thesis may represent a mixture of healthy and pathological tissue regions and cannot disentangle the immunological dynamics of the tissue landscape. Using high-dimensional imagine techniques, such as microscopy (Kang et al., 2020), mesoscopy (Francis et al., 2020), MIBI-TOF (Keren et al., 2019) or spatial transcriptomic techniques (Longo et al., 2021; C. G. Williams et al., 2022), the structural integrity of tissue specimens may be maintained and the structural organization of interacting immune cells and bacilli may be directly observed and quantified. A study with this objective is currently underway at SATVI, using a human postmortem cohort of TB cases and controls, which is likely to uncover new knowledge in the TB tissue immunology field.

Several other projects have also stemmed from this postmortem study, which allows for other avenues to be explored from the data generated in this thesis. Due to limited time and in the interest of maintaining the NK cell focus of this study, these data were not included in my thesis. Firstly, it was discussed in Chapter 2: Methods and Materials, that the mass cytometry panel for the postmortem tissue study was designed to include NK and B cell-specific markers. However, the B cell component of the analysis was not included in this thesis as it fell beyond the primary scope of the NK cell focal point. I have analyzed the data related to B cell phenotypes which are readily available and are being prepared for a publication later this year. In recent years, B cells have moved to the forefront of interest

with data to suggest that B cells and plasma cells may play important roles in the immune response to *Mtb* infection (Kozakiewicz et al., 2013; Loxton, 2019; Lyashchenko et al., 2020; Maglione & Chan, 2009; Rijnink et al., 2021; Swanson et al., 2023). Therefore, the B cell sub-study is hoped to shed some light on their phenotypic characterization in the field of TB tissue immunology.

Secondly, included in the mass cytometry panel are markers for investigating several T cell subsets, including CD4 T cells, CD8 T cells, γδ T cells, and NKT-like cells. Frequencies and cytotoxic potential of these T cell subsets were reported in Chapter 4. However, the acquired dataset holds much more potential for further investigations into T cell tissue immunology in TB. For example, the role of Th_{17} cells have piqued the interest of the TB field for their potentially protective role against *Mtb* infection and TB disease. *Mtb*-specific CD4 T cells that produce IL-17 are known as Th_{17} cells, which are heterogenous and may co-express IFN-γ or IL-10, depending on the type of infection (Zielinski et al., 2012). Cells co-expressing IFN-γ and IL-17 are referred to as $Th_{1/17}$ cells that are identified phenotypically by co-expression of CCR6 and CXCR3 (Acosta-Rodriguez et al., 2007; Becattini et al., 2015). One of the most prevalent *Mtb*-specific CD4 T cell subsets include $Th_{1/17}$ $CXCR3^+CCR6^+$ cells that outnumber Th_1 $CXCR3^+CCR6^-$ cells in most cases (Arlehamn et al., 2013; Nikitina et al., 2018; Strickland et al., 2017). In animal models, infection and vaccine-induced IL-17-producing CD4 T cells are associated with rapid pathogen clearance via recruitment of Th_1 immune cells (A. M. Cooper & Khader, 2008; Dijkman et al., 2019; Khader et al., 2007; Sia & Rengarajan, 2019). In a more recent NHP study, recruitment of $CXCR3^+CCR6^+$ Th_1 and Th_{17} subsets to the airways and lungs of macaques likely contributed to immune control of *Mtb* burden (Shanmugasundaram et al., 2020). In human studies, data suggest that higher levels of circulating IL-17^+ CD4 T cells occur in healthy *Mtb*-sensitized controls relative to patients with active TB disease (Scriba et al., 2008). However, other human studies have shown that there is a correlation between IL-17- and IFN-γ-producing CD4 T

cells and disease severity (Jurado et al., 2012). The current hypothesis is that IL-17-producing T cells are important role players in the anti-mycobacterial immune response at early stages of *Mtb* infection, although persistent *Mtb* infection and continued $Th_{1/17}$ responses are associated with inflammation-induced tissue pathology and increasing bacterial burden (Cruz et al., 2010; Lyadova & Panteleev, 2015; Torrado & Cooper, 2010). Overall, pre-clinical vaccine data suggest a protective role of Th_{17} and Th_1 cells against early stages of *Mtb* infection (Darrah et al., 2020; Dijkman et al., 2019). Acquired data in the postmortem cohort will allow for phenotypic identification of $CXCR3^+CCR6^+$ $Th_{1/17}$-like cells, which is planned as another sub-study stemming from this thesis. Although *Mtb*-specific cytokine responses could not be identified in this subset, the available data may still provide valuable insights into the phenotypic characterization and relative abundances that occur across tissue compartments during health and TB disease. These data may act as a steppingstone for further functional and mechanistic investigations into the precise role of $Th_{1/17}$ cells in human tissues.

In conclusion, the data presented in this thesis provides compelling evidence that NK cells may be important role players in the tissue response to *Mtb* infection. Overall, this thesis offers a foundation from which several other avenues of research will stem to hopefully identify functional and mechanistic targets for clinical interventions (such as TB vaccines and/or HDTs) that may curb the TB epidemic. Paul A.M. Dirac once wrote, “The measure of greatness in a scientific idea is the extent to which it stimulates thought and opens up new lines of research.”. If what Dirac says is true, then this thesis certainly fits the bill as a steppingstone towards achieving SATVI’s vision: A World Without TB.

References

Abbas, A. K., Lichtman, A. H., & Pillai, S. (2014). *Cellular and Molecular Immunology E-Book*. Elsevier Health Sciences.

Abdullah, M., Chai, P.-S., Chong, M.-Y., Tohit, E. R. M., Ramasamy, R., Pei, C. P., & Vidyadaran, S. (2012). Gender effect on in vitro lymphocyte subset levels of healthy individuals. *Cellular Immunology*, *272*(2), 214–219. https://doi.org/10.1016/j.cellimm.2011.10.009

Abubakar, I., Pimpin, L., Ariti, C., Beynon, R., Mangtani, P., Sterne, J. a. C., Fine, P. E. M., Smith, P. G., Lipman, M., Elliman, D., Watson, J. M., Drumright, L. N., Whiting, P. F., Vynnycky, E., & Rodrigues, L. C. (2013). Systematic review and meta-analysis of the current evidence on the duration of protection by bacillus Calmette-Guérin vaccination against tuberculosis. *Health Technology Assessment (Winchester, England)*, *17*(37), 1–372, v–vi. https://doi.org/10.3310/hta17370

Abu-Raddad, L. J., Sabatelli, L., Achterberg, J. T., Sugimoto, J. D., Longini, I. M., Dye, C., & Halloran, M. E. (2009). Epidemiological benefits of more-effective tuberculosis vaccines, drugs, and diagnostics. *Proceedings of the National Academy of Sciences of the United States of America*, *106*(33), 13980–13985. https://doi.org/10.1073/pnas.0901720106

Acosta-Rodriguez, E. V., Rivino, L., Geginat, J., Jarrossay, D., Gattorno, M., Lanzavecchia, A., Sallusto, F., & Napolitani, G. (2007). Surface phenotype and antigenic specificity of human interleukin 17-producing T helper memory cells. *Nature Immunology*, *8*(6), 639–646. https://doi.org/10.1038/ni1467

Adekambi, T., Ibegbu, C. C., Cagle, S., Kalokhe, A. S., Wang, Y. F., Hu, Y., Day, C. L., Ray, S. M., & Rengarajan, J. (2015). Biomarkers on patient T cells diagnose active tuberculosis and monitor treatment response. *The Journal of Clinical Investigation*, *125*(5), 1827–1838. https://doi.org/10.1172/JCI77990

Al-Attar, A., Presnell, S. R., Peterson, C. A., Thomas, D. T., & Lutz, C. T. (2016). Data correlations between gender, cytomegalovirus infection and T cells, NK cells, and soluble immune mediators in elderly humans. *Data in Brief*, *8*, 536–544. https://doi.org/10.1016/j.dib.2016.06.006

Algood, H. M. S., Lin, P. L., & Flynn, J. L. (2005). Tumor necrosis factor and chemokine interactions in the formation and maintenance of granulomas in tuberculosis. *Clinical Infectious Diseases: An Official Publication of the Infectious Diseases Society of America*, *41 Suppl 3*, S189-193. https://doi.org/10.1086/429994

Allen, M., Bailey, C., Cahatol, I., Dodge, L., Yim, J., Kassissa, C., Luong, J., Kasko, S., Pandya, S., & Venketaraman, V. (2015). Mechanisms of Control of Mycobacterium tuberculosis by NK Cells: Role of Glutathione. *Frontiers in Immunology*, *6*. https://doi.org/10.3389/fimmu.2015.00508

Alter, G., Malenfant, J. M., & Altfeld, M. (2004). CD107a as a functional marker for the identification of natural killer cell activity. *Journal of Immunological Methods*, *294*(1–2), 15–22. https://doi.org/10.1016/j.jim.2004.08.008

Andersen, P., Munk, M. E., Pollock, J. M., & Doherty, T. M. (2000). Specific immune-based diagnosis of tuberculosis. *Lancet (London, England)*, *356*(9235), 1099–1104. https://doi.org/10.1016/s0140-6736(00)02742-2

Anderson, K. G., Mayer-Barber, K., Sung, H., Beura, L., James, B. R., Taylor, J. J., Qunaj, L., Griffith, T. S., Vezys, V., Barber, D. L., & Masopust, D. (2014). Intravascular staining for discrimination of vascular and tissue leukocytes. *Nature Protocols*, *9*(1), 209–222. https://doi.org/10.1038/nprot.2014.005

Anderson, K. G., Sung, H., Skon, C. N., Lefrancois, L., Deisinger, A., Vezys, V., & Masopust, D. (2012). Cutting edge: Intravascular staining redefines lung CD8 T cell responses. *Journal of Immunology (Baltimore, Md.: 1950)*, *189*(6), 2702–2706. https://doi.org/10.4049/jimmunol.1201682

Andersson, J., Samarina, A., Fink, J., Rahman, S., & Grundström, S. (2007). Impaired Expression of Perforin and Granulysin in CD8+ T Cells at the Site of Infection in Human Chronic Pulmonary Tuberculosis. *Infection and Immunity*, *75*(11), 5210–5222. https://doi.org/10.1128/IAI.00624-07

Anfossi, N., André, P., Guia, S., Falk, C. S., Roetynck, S., Stewart, C. A., Breso, V., Frassati, C., Reviron, D., Middleton, D., Romagné, F., Ugolini, S., & Vivier, E. (2006a). Human NK Cell Education by Inhibitory Receptors for MHC Class I. *Immunity*, *25*(2), 331–342. https://doi.org/10.1016/j.immuni.2006.06.013

Anfossi, N., André, P., Guia, S., Falk, C. S., Roetynck, S., Stewart, C. A., Breso, V., Frassati, C., Reviron, D., Middleton, D., Romagné, F., Ugolini, S., & Vivier, E. (2006b). Human NK Cell Education by Inhibitory Receptors for MHC Class I. *Immunity*, *25*(2), 331–342. https://doi.org/10.1016/j.immuni.2006.06.013

Angelo, L. S., Banerjee, P. P., Monaco-Shawver, L., Rosen, J. B., Makedonas, G., Forbes, L. R., Mace, E. M., & Orange, J. S. (2015). Practical NK cell phenotyping and variability in healthy adults. *Immunologic Research*, *62*(3), 341–356. https://doi.org/10.1007/s12026-015-8664-y

Apt, A., & Kramnik, I. (2009). Man and mouse TB: Contradictions and solutions. *Tuberculosis (Edinburgh, Scotland)*, *89*(3), 195–198. https://doi.org/10.1016/j.tube.2009.02.002

Arambula, A., Brown, J. R., & Neff, L. (2021). Anatomy and physiology of the palatine tonsils, adenoids, and lingual tonsils. *World Journal of Otorhinolaryngology - Head and Neck Surgery*, *7*(3), 155–160. https://doi.org/10.1016/j.wjorl.2021.04.003

Arlehamn, C. S. L., Gerasimova, A., Mele, F., Henderson, R., Swann, J., Greenbaum, J. A., Kim, Y., Sidney, J., James, E. A., Taplitz, R., McKinney, D. M., Kwok, W. W., Grey, H., Sallusto, F., Peters, B., & Sette, A. (2013). Memory T Cells in Latent Mycobacterium tuberculosis Infection Are Directed against Three Antigenic Islands and Largely Contained in a CXCR3+CCR6+ Th1 Subset. *PLOS Pathogens*, *9*(1), e1003130. https://doi.org/10.1371/journal.ppat.1003130

Arruvito, L., Giulianelli, S., Flores, A. C., Paladino, N., Barboza, M., Lanari, C., & Fainboim, L. (2008). NK cells expressing a progesterone receptor are susceptible to progesterone-induced apoptosis. *Journal of Immunology (Baltimore, Md.: 1950)*, *180*(8), 5746–5753. https://doi.org/10.4049/jimmunol.180.8.5746

Arshad, T., Mansur, F., Palek, R., Manzoor, S., & Liska, V. (2020). A Double Edged Sword Role of Interleukin-22 in Wound Healing and Tissue Regeneration. *Frontiers in Immunology*, *11*, 2148. https://doi.org/10.3389/fimmu.2020.02148

Assmann, N., O'Brien, K. L., Donnelly, R. P., Dyck, L., Zaiatz-Bittencourt, V., Loftus, R. M., Heinrich, P., Oefner, P. J., Lynch, L., Gardiner, C. M., Dettmer, K., & Finlay, D. K. (2017). Srebp-controlled glucose metabolism is essential for NK cell functional responses. *Nature Immunology*, *18*(11), Article 11. https://doi.org/10.1038/ni.3838

Autissier, P., Soulas, C., Burdo, T. H., & Williams, K. C. (2010). Evaluation of a 12-color flow cytometry panel to study lymphocyte, monocyte, and dendritic cell subsets in humans. *Cytometry Part A: The Journal of the International Society for Advancement of Cytometry*, *77*(5), 410–419.

Bade, B., Boettcher, H. E., Lohrmann, J., Hink-Schauer, C., Bratke, K., Jenne, D. E., Virchow, J. C., & Luttmann, W. (2005). Differential expression of the granzymes A, K and M and perforin in human peripheral blood lymphocytes. *International Immunology*, *17*(11), 1419–1428. https://doi.org/10.1093/intimm/dxh320

Baena, A., & Porcelli, S. A. (2009). Evasion and subversion of antigen presentation by Mycobacterium tuberculosis. *Tissue Antigens*, *74*(3), 189–204. https://doi.org/10.1111/j.1399-0039.2009.01301.x

Baldridge, M. T., King, K. Y., Boles, N. C., Weksberg, D. C., & Goodell, M. A. (2010). Quiescent haematopoietic stem cells are activated by IFN-gamma in response to chronic infection. *Nature*, *465*(7299), 793–797. https://doi.org/10.1038/nature09135

Baldridge, M. T., King, K. Y., & Goodell, M. A. (2011). Inflammatory signals regulate hematopoietic stem cells. *Trends in Immunology*, *32*(2), 57–65. https://doi.org/10.1016/j.it.2010.12.003

Balsamo, M., Manzini, C., Pietra, G., Raggi, F., Blengio, F., Mingari, M. C., Varesio, L., Moretta, L., Bosco, M. C., & Vitale, M. (2013). Hypoxia downregulates the expression of activating receptors involved in NK-cell-mediated target cell killing without affecting ADCC. *European Journal of Immunology*, *43*(10), 2756–2764. https://doi.org/10.1002/eji.201343448

Bankovich, A. J., Shiow, L. R., & Cyster, J. G. (2010). CD69 suppresses sphingosine 1-phosophate receptor-1 (S1P1) function through interaction with membrane helix 4. *The Journal of Biological Chemistry*, *285*(29), 22328–22337. https://doi.org/10.1074/jbc.M110.123299

Barletta, F., Vandelannoote, K., Collantes, J., Evans, C. A., Arévalo, J., & Rigouts, L. (2014). Standardization of a TaqMan-Based Real-Time PCR for the Detection of Mycobacterium tuberculosis-Complex in Human Sputum. *The American Journal of Tropical Medicine and Hygiene*, *91*(4), 709–714. https://doi.org/10.4269/ajtmh.13-0603

Barry, C. E., Boshoff, H. I., Dartois, V., Dick, T., Ehrt, S., Flynn, J., Schnappinger, D., Wilkinson, R. J., & Young, D. (2009). The spectrum of latent tuberculosis: Rethinking the biology and intervention strategies. *Nature Reviews. Microbiology*, *7*(12), 845–855. https://doi.org/10.1038/nrmicro2236

Bastian, M., Braun, T., Bruns, H., Röllinghoff, M., & Stenger, S. (2008). Mycobacterial lipopeptides elicit CD4+ CTLs in Mycobacterium tuberculosis-infected humans. *Journal of Immunology (Baltimore, Md.: 1950)*, *180*(5), 3436–3446. https://doi.org/10.4049/jimmunol.180.5.3436

Bates, M. N., Khalakdina, A., Pai, M., Chang, L., Lessa, F., & Smith, K. R. (2007). Risk of tuberculosis from exposure to tobacco smoke: A systematic review and meta-analysis. *Archives of Internal Medicine*, *167*(4), 335–342. https://doi.org/10.1001/archinte.167.4.335

Batoni, G., Esin, S., Favilli, F., Pardini, M., Bottai, D., Maisetta, G., Florio, W., & Campa, M. (2005). Human CD56bright and CD56dim natural killer cell subsets respond differentially to direct stimulation with Mycobacterium bovis bacillus Calmette-Guérin. *Scandinavian Journal of Immunology*, *62*(6), 498–506. https://doi.org/10.1111/j.1365-3083.2005.01692.x

Bauer, S., Groh, V., Wu, J., Steinle, A., Phillips, J. H., Lanier, L. L., & Spies, T. (1999). Activation of NK Cells and T Cells by NKG2D, a Receptor for Stress-Inducible MICA. *Science*, *285*(5428), 727–729. https://doi.org/10.1126/science.285.5428.727

Becattini, S., Latorre, D., Mele, F., Foglierini, M., De Gregorio, C., Cassotta, A., Fernandez, B., Kelderman, S., Schumacher, T. N., Corti, D., Lanzavecchia, A., & Sallusto, F. (2015). T cell immunity. Functional heterogeneity of human memory $CD4^+$ T cell clones primed by pathogens or vaccines. *Science (New York, N.Y.)*, *347*(6220), 400–406. https://doi.org/10.1126/science.1260668

Becker, I., Salaiza, N., Aguirre, M., Delgado, J., Carrillo-Carrasco, N., Kobeh, L. G., Ruiz, A., Cervantes, R., Torres, A. P., Cabrera, N., González, A., Maldonado, C., & Isibasi, A. (2003). Leishmania lipophosphoglycan (LPG) activates NK cells through toll-like receptor-2. *Molecular and Biochemical Parasitology*, *130*(2), 65–74. https://doi.org/10.1016/s0166-6851(03)00160-9

Becknell, B., & Caligiuri, M. A. (2005). Interleukin-2, interleukin-15, and their roles in human natural killer cells. *Advances in Immunology*, *86*, 209–239. https://doi.org/10.1016/S0065-2776(04)86006-1

Behr, M. A., Edelstein, P. H., & Ramakrishnan, L. (2018). Revisiting the timetable of tuberculosis. *The BMJ*, *362*, k2738. https://doi.org/10.1136/bmj.k2738

Berahovich, R. D., Lai, N. L., Wei, Z., Lanier, L. L., & Schall, T. J. (2006). Evidence for NK cell subsets based on chemokine receptor expression. *Journal of Immunology (Baltimore, Md.: 1950)*, *177*(11), 7833–7840. https://doi.org/10.4049/jimmunol.177.11.7833

Berhani, O., Glasner, A., Kahlon, S., Duev-Cohen, A., Yamin, R., Horwitz, E., Enk, J., Moshel, O., Varvak, A., Porgador, A., Jonjic, S., & Mandelboim, O. (2019). Human anti-NKp46 antibody for studies of NKp46-dependent NK cell function and its applications for type 1 diabetes and cancer research. *European Journal of Immunology*, *49*(2), 228–241. https://doi.org/10.1002/eji.201847611

Betts, M. R., & Koup, R. A. (2004). Detection of T-cell degranulation: CD107a and b. *Methods in Cell Biology*, *75*, 497–512. https://doi.org/10.1016/s0091-679x(04)75020-7

Béziat, V., Dalgard, O., Asselah, T., Halfon, P., Bedossa, P., Boudifa, A., Hervier, B., Theodorou, I., Martinot, M., Debré, P., Björkström, N. K., Malmberg, K.-J., Marcellin, P., & Vieillard, V. (2012). CMV drives clonal expansion of NKG2C+ NK cells expressing self-specific KIRs in chronic hepatitis patients. *European Journal of Immunology*, *42*(2), 447–457. https://doi.org/10.1002/eji.201141826

Béziat, V., Duffy, D., Quoc, S. N., Garff-Tavernier, M. L., Decocq, J., Combadière, B., Debré, P., & Vieillard, V. (2011). CD56brightCD16+ NK Cells: A Functional Intermediate Stage of NK Cell Differentiation. *The Journal of Immunology*, *186*(12), 6753–6761. https://doi.org/10.4049/jimmunol.1100330

Béziat, V., Traherne, J. A., Liu, L. L., Jayaraman, J., Enqvist, M., Larsson, S., Trowsdale, J., & Malmberg, K.-J. (2013). Influence of KIR gene copy number on natural killer cell education. *Blood*, *121*(23), 4703–4707. https://doi.org/10.1182/blood-2012-10-461442

Bhatt, K., Verma, S., Ellner, J. J., & Salgame, P. (2015). Quest for correlates of protection against tuberculosis. *Clinical and Vaccine Immunology: CVI*, *22*(3), 258–266. https://doi.org/10.1128/CVI.00721-14

Bhuju, S., Aranday-Cortes, E., Villarreal-Ramos, B., Xing, Z., Singh, M., & Vordermeier, H. M. (2012). Global Gene Transcriptome Analysis in Vaccinated Cattle Revealed a Dominant Role of IL-22 for Protection against Bovine Tuberculosis. *PLOS Pathogens*, *8*(12), e1003077. https://doi.org/10.1371/journal.ppat.1003077

Bienenstock, J. (1982). Gut and bronchus associated lymphoid tissue: An overview. *Advances in Experimental Medicine and Biology*, *149*, 471–477. https://doi.org/10.1007/978-1-4684-9066-4_66

Bird, C. H., Sutton, V. R., Sun, J., Hirst, C. E., Novak, A., Kumar, S., Trapani, J. A., & Bird, P. I. (1998). Selective Regulation of Apoptosis: The Cytotoxic Lymphocyte Serpin Proteinase Inhibitor 9 Protects against Granzyme B-Mediated Apoptosis without Perturbing the Fas Cell Death Pathway. *Molecular and Cellular Biology*, *18*(11), 6387–6398.

Biron, C. A., Byron, K. S., & Sullivan, J. L. (1989). Severe herpesvirus infections in an adolescent without natural killer cells. *The New England Journal of Medicine*, *320*(26), 1731–1735. https://doi.org/10.1056/NEJM198906293202605

Biron, C. A., Nguyen, K. B., Pien, G. C., Cousens, L. P., & Salazar-Mather, T. P. (1999). Natural Killer Cells in Antiviral Defense: Function and Regulation by Innate Cytokines. *Annual Review of Immunology*, *17*(1), 189–220. https://doi.org/10.1146/annurev.immunol.17.1.189

Björkström, N. K., Ljunggren, H.-G., & Michaëlsson, J. (2016). Emerging insights into natural killer cells in human peripheral tissues. *Nature Reviews. Immunology*, *16*(5), 310–320. https://doi.org/10.1038/nri.2016.34

Björkström, N. K., Ljunggren, H.-G., & Sandberg, J. K. (2010a). CD56 negative NK cells: Origin, function, and role in chronic viral disease. *Trends in Immunology*, *31*(11), 401–406. https://doi.org/10.1016/j.it.2010.08.003

Björkström, N. K., Ljunggren, H.-G., & Sandberg, J. K. (2010b). CD56 negative NK cells: Origin, function, and role in chronic viral disease. *Trends in Immunology*, *31*(11), 401–406. https://doi.org/10.1016/j.it.2010.08.003

Björkström, N. K., Riese, P., Heuts, F., Andersson, S., Fauriat, C., Ivarsson, M. A., Björklund, A. T., Flodström-Tullberg, M., Michaëlsson, J., Rottenberg, M. E., Guzmán, C. A., Ljunggren, H.-G., & Malmberg, K.-J. (2010). Expression patterns of NKG2A, KIR, and CD57 define a process of CD56dim NK-cell differentiation uncoupled from NK-cell education. *Blood*, *116*(19), 3853–3864. https://doi.org/10.1182/blood-2010-04-281675

Björkström, N. K., Strunz, B., & Ljunggren, H.-G. (2021). Natural killer cells in antiviral immunity. *Nature Reviews Immunology*, 1–12. https://doi.org/10.1038/s41577-021-00558-3

Blunt, M. D., & Khakoo, S. I. (2020). Activating killer cell immunoglobulin-like receptors: Detection, function and therapeutic use. *International Journal of Immunogenetics*, *47*(1), 1–12. https://doi.org/10.1111/iji.12461

Boehme, C. C., Nabeta, P., Hillemann, D., Nicol, M. P., Shenai, S., Krapp, F., Allen, J., Tahirli, R., Blakemore, R., Rustomjee, R., Milovic, A., Jones, M., O'Brien, S. M., Persing, D. H., Ruesch-Gerdes, S., Gotuzzo, E., Rodrigues, C., Alland, D., & Perkins, M. D. (2010). Rapid molecular detection of tuberculosis and rifampin resistance. *The New England Journal of Medicine*, *363*(11), 1005–1015. https://doi.org/10.1056/NEJMoa0907847

Boehme, C. C., Nicol, M. P., Nabeta, P., Michael, J. S., Gotuzzo, E., Tahirli, R., Gler, M. T., Blakemore, R., Worodria, W., Gray, C., Huang, L., Caceres, T., Mehdiyev, R., Raymond, L., Whitelaw, A., Sagadevan, K., Alexander, H., Albert, H., Cobelens, F., … Perkins, M. D. (2011). Feasibility, diagnostic accuracy, and effectiveness of decentralised use of the Xpert MTB/RIF test for diagnosis of tuberculosis and multidrug resistance: A multicentre implementation study. *Lancet (London, England)*, *377*(9776), 1495–1505. https://doi.org/10.1016/S0140-6736(11)60438-8

Boivin, W. A., Cooper, D. M., Hiebert, P. R., & Granville, D. J. (2009). Intracellular versus extracellular granzyme B in immunity and disease: Challenging the dogma. *Laboratory Investigation*, *89*(11), Article 11. https://doi.org/10.1038/labinvest.2009.91

Borrego, F., Robertson, M. J., Ritz, J., Peña, J., & Solana, R. (1999). CD69 is a stimulatory receptor for natural killer cell and its cytotoxic effect is blocked by CD94 inhibitory receptor. *Immunology*, *97*(1), 159–165. https://doi.org/10.1046/j.1365-2567.1999.00738.x

Bouman, A., Heineman, M. J., & Faas, M. M. (2005). Sex hormones and the immune response in humans. *Human Reproduction Update*, *11*(4), 411–423. https://doi.org/10.1093/humupd/dmi008

Bouwman, A. C., van Daalen, K. R., Crnko, S., ten Broeke, T., & Bovenschen, N. (2021). Intracellular and Extracellular Roles of Granzyme K. *Frontiers in Immunology*, *12*. https://www.frontiersin.org/articles/10.3389/fimmu.2021.677707

Boyaka, P. N., Wright, P. F., Marinaro, M., Kiyono, H., Johnson, J. E., Gonzales, R. A., Ikizler, M. R., Werkhaven, J. A., Jackson, R. J., Fujihashi, K., Di Fabio, S., Staats, H. F., & McGhee, J. R. (2000). Human Nasopharyngeal-Associated Lymphoreticular Tissues. *The American Journal of Pathology*, *157*(6), 2023–2035.

Boyd, A., Almeida, J. R., Darrah, P. A., Sauce, D., Seder, R. A., Appay, V., Gorochov, G., & Larsen, M. (2015). Pathogen-Specific T Cell Polyfunctionality Is a Correlate of T Cell Efficacy and Immune Protection. *PLoS ONE*, *10*(6), e0128714. https://doi.org/10.1371/journal.pone.0128714

Bozzano, F., Costa, P., Passalacqua, G., Dodi, F., Ravera, S., Pagano, G., Canonica, G. W., Moretta, L., & De Maria, A. (2009). Functionally relevant decreases in activatory receptor expression on NK cells are associated with pulmonary tuberculosis in vivo and persist after successful treatment. *International Immunology*, *21*(7), 779–791. https://doi.org/10.1093/intimm/dxp046

Brandstadter, J. D., & Yang, Y. (2011). Natural Killer Cell Responses to Viral Infection. *Journal of Innate Immunity*, *3*(3), 274–279. https://doi.org/10.1159/000324176

Bratke, K., Kuepper, M., Bade, B., Virchow Jr., J. C., & Luttmann, W. (2005). Differential expression of human granzymes A, B, and K in natural killer cells and during CD8+ T cell differentiation in peripheral blood. *European Journal of Immunology*, *35*(9), 2608–2616. https://doi.org/10.1002/eji.200526122

Brenchley, J. M., Schacker, T. W., Ruff, L. E., Price, D. A., Taylor, J. H., Beilman, G. J., Nguyen, P. L., Khoruts, A., Larson, M., Haase, A. T., & Douek, D. C. (2004). CD4+ T Cell Depletion during all Stages of HIV Disease Occurs Predominantly in the Gastrointestinal Tract. *The Journal of Experimental Medicine*, *200*(6), 749–759. https://doi.org/10.1084/jem.20040874

Brighenti, S., & Andersson, J. (2012). Local Immune Responses in Human Tuberculosis: Learning From the Site of Infection. *The Journal of Infectious Diseases*, *205*(suppl_2), S316–S324. https://doi.org/10.1093/infdis/jis043

Brigl, M., & Brenner, M. B. (2004). CD1: Antigen Presentation and T Cell Function. *Annual Review of Immunology*, *22*(1), 817–890. https://doi.org/10.1146/annurev.immunol.22.012703.104608

Brodin, P., Kärre, K., & Höglund, P. (2009). NK cell education: Not an on-off switch but a tunable rheostat. *Trends in Immunology*, *30*(4), 143–149. https://doi.org/10.1016/j.it.2009.01.006

Bronte, V., & Pittet, M. J. (2013). The spleen in local and systemic regulation of immunity. *Immunity*, *39*(5), 806–818. https://doi.org/10.1016/j.immuni.2013.10.010

Bruchfeld, J., Correia-Neves, M., & Källenius, G. (2015). Tuberculosis and HIV Coinfection. *Cold Spring Harbor Perspectives in Medicine*, *5*(7), a017871. https://doi.org/10.1101/cshperspect.a017871

Burel, J. G., Apte, S. H., Groves, P. L., McCarthy, J. S., & Doolan, D. L. (2017). Polyfunctional and IFN-γ monofunctional human CD4+ T cell populations are molecularly distinct. *JCI Insight*, *2*(3), e87499. https://doi.org/10.1172/jci.insight.87499

Cai, Y., Dai, Y., Wang, Y., Yang, Q., Guo, J., Wei, C., Chen, W., Huang, H., Zhu, J., Zhang, C., Zheng, W., Wen, Z., Liu, H., Zhang, M., Xing, S., Jin, Q., Feng, C. G., & Chen, X. (2020). Single-cell transcriptomics of blood reveals a natural killer cell subset depletion in tuberculosis. *EBioMedicine*, *53*, 102686. https://doi.org/10.1016/j.ebiom.2020.102686

Caligiuri, M. A. (2008). Human natural killer cells. *Blood*, *112*(3), 461–469. https://doi.org/10.1182/blood-2007-09-077438

Cao, Y., Wang, X., Jin, T., Tian, Y., Dai, C., Widarma, C., Song, R., & Xu, F. (2020). Immune checkpoint molecules in natural killer cells as potential targets for cancer immunotherapy. *Signal Transduction and Targeted Therapy*, *5*(1), 1–19. https://doi.org/10.1038/s41392-020-00348-8

Carbone, E., Ruggiero, G., Terrazzano, G., Palomba, C., Manzo, C., Fontana, S., Spits, H., Kärre, K., & Zappacosta, S. (1997). A New Mechanism of NK Cell Cytotoxicity Activation: The CD40–CD40 Ligand Interaction. *Journal of Experimental Medicine*, *185*(12), 2053–2060. https://doi.org/10.1084/jem.185.12.2053

Carlin, L. E., Hemann, E. A., Zacharias, Z. R., Heusel, J. W., & Legge, K. L. (2018). Natural Killer Cell Recruitment to the Lung During Influenza A Virus Infection Is Dependent on CXCR3, CCR5, and Virus Exposure Dose. *Frontiers in Immunology*, *9*, 781. https://doi.org/10.3389/fimmu.2018.00781

Carson, W. E., Fehniger, T. A., & Caligiuri, M. A. (1997). CD56bright natural killer cell subsets: Characterization of distinct functional responses to interleukin-2 and the c-kit ligand. *European Journal of Immunology*, *27*(2), 354–360. https://doi.org/10.1002/eji.1830270203

Carson, W. E., Giri, J. G., Lindemann, M. J., Linett, M. L., Ahdieh, M., Paxton, R., Anderson, D., Eisenmann, J., Grabstein, K., & Caligiuri, M. A. (1994). Interleukin (IL) 15 is a novel cytokine that activates human natural killer cells via components of the IL-2 receptor. *The Journal of Experimental Medicine*, *180*(4), 1395–1403. https://doi.org/10.1084/jem.180.4.1395

Caruso, A. M., Serbina, N., Klein, E., Triebold, K., Bloom, B. R., & Flynn, J. L. (1999). Mice Deficient in CD4 T Cells Have Only Transiently Diminished Levels of IFN-γ, Yet Succumb to Tuberculosis. *The Journal of Immunology*, *162*(9), 5407–5416.

Casanova, J.-L., Holland, S. M., & Notarangelo, L. D. (2012). Inborn Errors of Human JAKs and STATs. *Immunity*, *36*(4), 515–528. https://doi.org/10.1016/j.immuni.2012.03.016

Cerwenka, A., Baron, J. L., & Lanier, L. L. (2001). Ectopic expression of retinoic acid early inducible-1 gene (RAE-1) permits natural killer cell-mediated rejection of a MHC class I-bearing tumor in vivo. *Proceedings of the National Academy of Sciences of the United States of America*, *98*(20), 11521–11526. https://doi.org/10.1073/pnas.201238598

Chalifour, A., Jeannin, P., Gauchat, J.-F., Blaecke, A., Malissard, M., N'Guyen, T., Thieblemont, N., & Delneste, Y. (2004). Direct bacterial protein PAMP recognition by human NK cells involves TLRs and triggers α-defensin production. *Blood*, *104*(6), 1778–1783. https://doi.org/10.1182/blood-2003-08-2820

Chan, C. J., Martinet, L., Gilfillan, S., Souza-Fonseca-Guimaraes, F., Chow, M. T., Town, L., Ritchie, D. S., Colonna, M., Andrews, D. M., & Smyth, M. J. (2014). The receptors CD96 and CD226 oppose each other in the regulation of natural killer cell functions. *Nature Immunology*, *15*(5), Article 5. https://doi.org/10.1038/ni.2850

Chang, P.-C., Wang, P.-H., & Chen, K.-T. (2017). Use of the QuantiFERON-TB Gold In-Tube Test in the Diagnosis and Monitoring of Treatment Efficacy in Active Pulmonary Tuberculosis. *International Journal of Environmental Research and Public Health*, *14*(3), Article 3. https://doi.org/10.3390/ijerph14030236

Chávez-Galán, L., Illescas-Eugenio, J., Alvarez-Sekely, M., Baez-Saldaña, R., Chávez, R., & Lascurain, R. (2019). Tuberculosis patients display a high proportion of CD8+ T cells with a high cytotoxic potential. *Microbiology and Immunology*, *63*(8), 316–327. https://doi.org/10.1111/1348-0421.12724

Chee, C. B. E., Khinmar, K. W., Gan, S. H., Barkham, T. M., Koh, C. K., Shen, L., & Wang, Y. T. (2010). Tuberculosis treatment effect on T-cell interferon-γ responses to Mycobacterium tuberculosis-specific antigens. *European Respiratory Journal*, *36*(2), 355–361. https://doi.org/10.1183/09031936.00151309

Chevrier, S., Crowell, H. L., Zanotelli, V. R. T., Engler, S., Robinson, M. D., & Bodenmiller, B. (2018). Compensation of Signal Spillover in Suspension and Imaging Mass Cytometry. *Cell Systems*, *6*(5), 612-620.e5. https://doi.org/10.1016/j.cels.2018.02.010

Chng, W. J., Tan, G. B., & Kuperan, P. (2004). Establishment of Adult Peripheral Blood Lymphocyte Subset Reference Range for an Asian Population by Single-Platform Flow Cytometry: Influence of Age, Sex, and Race and Comparison with Other Published Studies. *Clinical and Vaccine Immunology*, *11*(1), 168–173. https://doi.org/10.1128/CDLI.11.1.168-173.2004

Cho, S., Mehra, V., Thoma-Uszynski, S., Stenger, S., Serbina, N., Mazzaccaro, R. J., Flynn, J. L., Barnes, P. F., Southwood, S., Celis, E., Bloom, B. R., Modlin, R. L., & Sette, A. (2000). Antimicrobial activity of MHC class I-restricted CD8+ T cells in human tuberculosis. *Proceedings of the National Academy of Sciences*, *97*(22), 12210–12215. https://doi.org/10.1073/pnas.210391497

Choi, Y. H., Lim, E. J., Kim, S. W., Moon, Y. W., Park, K. S., & An, H.-J. (2019). IL-27 enhances IL-15/IL-18-mediated activation of human natural killer cells. *Journal for ImmunoTherapy of Cancer*, *7*(1), 168. https://doi.org/10.1186/s40425-019-0652-7

Choreño Parra, J. A., Martínez Zúñiga, N., Jiménez Zamudio, L. A., Jiménez Álvarez, L. A., Salinas Lara, C., & Zúñiga, J. (2017). Memory of Natural Killer Cells: A New Chance against Mycobacterium tuberculosis? *Frontiers in Immunology*, *8*. https://doi.org/10.3389/fimmu.2017.00967

Chowdhury, R. R., Vallania, F., Yang, Q., Lopez Angel, C. J., Darboe, F., Penn-Nicholson, A., Rozot, V., Nemes, E., Malherbe, S. T., Ronacher, K., Walzl, G., Hanekom, W., Davis, M. M., Winter, J., Chen, X., Scriba, T. J., Khatri, P., & Chien, Y. (2018). A multi-cohort study of the immune factors associated with M. tuberculosis infection outcomes. *Nature*, *560*(7720), Article 7720. https://doi.org/10.1038/s41586-018-0439-x

Chua, H. L., Serov, Y., & Brahmi, Z. (2004). Regulation of FasL expression in natural killer cells. *Human Immunology*, *65*(4), 317–327. https://doi.org/10.1016/j.humimm.2004.01.004

Churchyard, G., Kim, P., Shah, N. S., Rustomjee, R., Gandhi, N., Mathema, B., Dowdy, D., Kasmar, A., & Cardenas, V. (2017). What We Know About Tuberculosis Transmission: An Overview. *The Journal of Infectious Diseases*, *216*(suppl_6), S629–S635. https://doi.org/10.1093/infdis/jix362

Clark, R., & Kupper, T. (2005). Old Meets New: The Interaction Between Innate and Adaptive Immunity. *Journal of Investigative Dermatology*, *125*(4), 629–637. https://doi.org/10.1111/j.0022-202X.2005.23856.x

Clausen, J., Vergeiner, B., Enk, M., Petzer, A. L., Gastl, G., & Gunsilius, E. (2003). Functional significance of the activation-associated receptors CD25 and CD69 on human NK-cells and NK-like T-cells. *Immunobiology*, *207*(2), 85–93. https://doi.org/10.1078/0171-2985-00219

Colditz, G. A., Brewer, T. F., Berkey, C. S., Wilson, M. E., Burdick, E., Fineberg, H. V., & Mosteller, F. (1994). Efficacy of BCG vaccine in the prevention of tuberculosis. Meta-analysis of the published literature. *JAMA*, *271*(9), 698–702.

Collins, A. M., Rylance, J., Wootton, D. G., Wright, A. D., Wright, A. K. A., Fullerton, D. G., & Gordon, S. B. (2014). Bronchoalveolar Lavage (BAL) for Research; Obtaining Adequate Sample Yield. *Journal of Visualized Experiments : JoVE*, *85*, 4345. https://doi.org/10.3791/4345

Cong, J., Wang, X., Zheng, X., Wang, D., Fu, B., Sun, R., Tian, Z., & Wei, H. (2018). Dysfunction of Natural Killer Cells by FBP1-Induced Inhibition of Glycolysis during Lung Cancer Progression. *Cell Metabolism*, *28*(2), 243-255.e5. https://doi.org/10.1016/j.cmet.2018.06.021

Cong, J., & Wei, H. (2019). Natural Killer Cells in the Lungs. *Frontiers in Immunology*, *10*. https://doi.org/10.3389/fimmu.2019.01416

Cooper, A. M., & Khader, S. A. (2008). The role of cytokines in the initiation, expansion, and control of cellular immunity to tuberculosis. *Immunological Reviews*, *226*, 191–204. https://doi.org/10.1111/j.1600-065X.2008.00702.x

Cooper, A. M., Mayer-Barber, K. D., & Sher, A. (2011). Role of innate cytokines in mycobacterial infection. *Mucosal Immunology*, *4*(3), 252–260. https://doi.org/10.1038/mi.2011.13

Cooper, D. M., Pechkovsky, D. V., Hackett, T. L., Knight, D. A., & Granville, D. J. (2011). Granzyme K Activates Protease-Activated Receptor-1. *PLoS ONE*, *6*(6), e21484. https://doi.org/10.1371/journal.pone.0021484

Cooper, G. E., Ostridge, K., Khakoo, S. I., Wilkinson, T. M. A., & Staples, K. J. (2018). Human CD49a+ Lung Natural Killer Cell Cytotoxicity in Response to Influenza A Virus. *Frontiers in Immunology*, *9*, 1671. https://doi.org/10.3389/fimmu.2018.01671

Cooper, M. A., Fehniger, T. A., & Caligiuri, M. A. (2001). The biology of human natural killer-cell subsets. *Trends in Immunology*, *22*(11), 633–640. https://doi.org/10.1016/s1471-4906(01)02060-9

Cosman, D., Müllberg, J., Sutherland, C. L., Chin, W., Armitage, R., Fanslow, W., Kubin, M., & Chalupny, N. J. (2001). ULBPs, novel MHC class I-related molecules, bind to CMV glycoprotein UL16 and stimulate NK cytotoxicity through the NKG2D receptor. *Immunity*, *14*(2), 123–133. https://doi.org/10.1016/s1074-7613(01)00095-4

Cruciani, M., Scarparo, C., Malena, M., Bosco, O., Serpelloni, G., & Mengoli, C. (2004). Meta-Analysis of BACTEC MGIT 960 and BACTEC 460 TB, with or without Solid Media, for Detection of Mycobacteria. *Journal of Clinical Microbiology*, *42*(5), 2321–2325. https://doi.org/10.1128/JCM.42.5.2321-2325.2004

Cruz, A., Fraga, A. G., Fountain, J. J., Rangel-Moreno, J., Torrado, E., Saraiva, M., Pereira, D. R., Randall, T. D., Pedrosa, J., Cooper, A. M., & Castro, A. G. (2010). Pathological role of interleukin 17 in mice subjected to repeated BCG vaccination after infection with Mycobacterium tuberculosis. *The Journal of Experimental Medicine*, *207*(8), 1609–1616. https://doi.org/10.1084/jem.20100265

Culley, F. J. (2009). Natural killer cells in infection and inflammation of the lung. *Immunology*, *128*(2), 151–163. https://doi.org/10.1111/j.1365-2567.2009.03167.x

Dalla Pria, A., Pinato, D. J., Bracchi, M., & Bower, M. (2019). Recent advances in HIV-associated Kaposi sarcoma. *F1000Research*, *8*, F1000 Faculty Rev-970. https://doi.org/10.12688/f1000research.17401.1

Daniel, T. M. (2006). The history of tuberculosis. *Respiratory Medicine*, *100*(11), 1862–1870. https://doi.org/10.1016/j.rmed.2006.08.006

Darrah, P. A., Zeppa, J. J., Maiello, P., Hackney, J. A., Wadsworth, M. H., Hughes, T. K., Pokkali, S., Swanson, P. A., Grant, N. L., Rodgers, M. A., Kamath, M., Causgrove, C. M., Laddy, D. J., Bonavia, A., Casimiro, D., Lin, P. L., Klein, E., White, A. G., Scanga, C. A., … Seder, R. A. (2020). Prevention of tuberculosis in macaques after intravenous BCG immunization. *Nature*, *577*(7788), Article 7788. https://doi.org/10.1038/s41586-019-1817-8

Del Zotto, G., Antonini, F., Pesce, S., Moretta, F., Moretta, L., & Marcenaro, E. (2020). Comprehensive Phenotyping of Human PB NK Cells by Flow Cytometry. *Cytometry Part A*, *97*(9), 891–899. https://doi.org/10.1002/cyto.a.24001

Demling, R. H. (2008). Smoke Inhalation Lung Injury: An Update. *Eplasty*, *8*, e27.

Deretic, V. (2014). Autophagy in Tuberculosis. *Cold Spring Harbor Perspectives in Medicine*, *4*(11), a018481. https://doi.org/10.1101/cshperspect.a018481

Detjen, A. K., DiNardo, A. R., Leyden, J., Steingart, K. R., Menzies, D., Schiller, I., Dendukuri, N., & Mandalakas, A. M. (2015). Xpert MTB/RIF assay for the diagnosis of pulmonary tuberculosis in children: A systematic review and meta-analysis. *The Lancet. Respiratory Medicine*, *3*(6), 451–461. https://doi.org/10.1016/S2213-2600(15)00095-8

Dheda, K., Barry, C. E., & Maartens, G. (2016). Tuberculosis. *Lancet (London, England)*, *387*(10024), 1211–1226. https://doi.org/10.1016/S0140-6736(15)00151-8

Dheda, K., Gumbo, T., Gandhi, N. R., Murray, M., Theron, G., Udwadia, Z., Migliori, G. B., & Warren, R. (2014). Global control of tuberculosis: From extensively drug-resistant to untreatable tuberculosis. *The Lancet. Respiratory Medicine*, *2*(4), 321–338. https://doi.org/10.1016/S2213-2600(14)70031-1

Dhiman, R., Indramohan, M., Barnes, P. F., Nayak, R. C., Paidipally, P., Rao, L. V. M., & Vankayalapati, R. (2009). IL-22 Produced by Human NK Cells Inhibits Growth of Mycobacterium tuberculosis by Enhancing Phagolysosomal Fusion. *The Journal of Immunology*, *183*(10), 6639–6645. https://doi.org/10.4049/jimmunol.0902587

Diefenbach, A., Jensen, E. R., Jamieson, A. M., & Raulet, D. H. (2001). Rae1 and H60 ligands of the NKG2D receptor stimulate tumour immunity. *Nature*, *413*(6852), 165–171. https://doi.org/10.1038/35093109

Dieli, F., Troye-Blomberg, M., Ivanyi, J., Fournié, J. J., Krensky, A. M., Bonneville, M., Peyrat, M. A., Caccamo, N., Sireci, G., & Salerno, A. (2001). Granulysin-dependent killing of intracellular and extracellular Mycobacterium tuberculosis by Vgamma9/Vdelta2 T lymphocytes. *The Journal of Infectious Diseases*, *184*(8), 1082–1085. https://doi.org/10.1086/323600

Diggins, K. E., Ferrell, P. B., & Irish, J. M. (2015). Methods for discovery and characterization of cell subsets in high dimensional mass cytometry data. *Methods (San Diego, Calif.)*, *82*, 55–63. https://doi.org/10.1016/j.ymeth.2015.05.008

Dijkman, K., Sombroek, C. C., Vervenne, R. A. W., Hofman, S. O., Boot, C., Remarque, E. J., Kocken, C. H. M., Ottenhoff, T. H. M., Kondova, I., Khayum, M. A., Haanstra, K. G., Vierboom, M. P. M., & Verreck, F. A. W. (2019). Prevention of tuberculosis infection and

disease by local BCG in repeatedly exposed rhesus macaques. *Nature Medicine*, *25*(2), 255–262. https://doi.org/10.1038/s41591-018-0319-9

Dogra, P., Rancan, C., Ma, W., Toth, M., Senda, T., Carpenter, D. J., Kubota, M., Matsumoto, R., Thapa, P., Szabo, P. A., Li Poon, M. M., Li, J., Arakawa-Hoyt, J., Shen, Y., Fong, L., Lanier, L. L., & Farber, D. L. (2020). Tissue Determinants of Human NK Cell Development, Function, and Residence. *Cell*, *180*(4), 749-763.e13. https://doi.org/10.1016/j.cell.2020.01.022

Donaldson, J. G., Lippincott-Schwartz, J., & Klausner, R. D. (1991). Guanine nucleotides modulate the effects of brefeldin A in semipermeable cells: Regulation of the association of a 110-kD peripheral membrane protein with the Golgi apparatus. *The Journal of Cell Biology*, *112*(4), 579–588.

Donnelly, R. P., Loftus, R. M., Keating, S. E., Liou, K. T., Biron, C. A., Gardiner, C. M., & Finlay, D. K. (2014). MTORC1-Dependent Metabolic Reprogramming Is a Prerequisite for NK Cell Effector Function. *The Journal of Immunology*, *193*(9), 4477–4484. https://doi.org/10.4049/jimmunol.1401558

Dowdy, D. W., Basu, S., & Andrews, J. R. (2013). Is passive diagnosis enough? The impact of subclinical disease on diagnostic strategies for tuberculosis. *American Journal of Respiratory and Critical Care Medicine*, *187*(5), 543–551. https://doi.org/10.1164/rccm.201207-1217OC

Drain, P. K., Bajema, K. L., Dowdy, D., Dheda, K., Naidoo, K., Schumacher, S. G., Ma, S., Meermeier, E., Lewinsohn, D. M., & Sherman, D. R. (2018). Incipient and Subclinical Tuberculosis: A Clinical Review of Early Stages and Progression of Infection. *Clinical Microbiology Reviews*, *31*(4), e00021-18. https://doi.org/10.1128/CMR.00021-18

Duarte, R., Lönnroth, K., Carvalho, C., Lima, F., Carvalho, A. C. C., Muñoz-Torrico, M., & Centis, R. (2018). Tuberculosis, social determinants and co-morbidities (including HIV). *Pulmonology*, *24*(2), 115–119. https://doi.org/10.1016/j.rppnen.2017.11.003

Dudakov, J. A., Hanash, A. M., & van den Brink, M. R. M. (2015). Interleukin-22: Immunobiology and pathology. *Annual Review of Immunology*, *33*, 747–785. https://doi.org/10.1146/annurev-immunol-032414-112123

Ehlers, S., & Schaible, U. E. (2012). The granuloma in tuberculosis: Dynamics of a host-pathogen collusion. *Frontiers in Immunology*, *3*, 411. https://doi.org/10.3389/fimmu.2012.00411

Eischen, C. M., & Leibson, P. J. (1997). Role for NK-cell-associated Fas ligand in cell-mediated cytotoxicity and apoptosis. *Research in Immunology*, *148*(3), 164–169. https://doi.org/10.1016/S0923-2494(97)84219-8

Elkington, P., Lerm, M., Kapoor, N., Mahon, R., Pienaar, E., Huh, D., Kaushal, D., & Schlesinger, L. S. (2019). In Vitro Granuloma Models of Tuberculosis: Potential and Challenges. *The Journal of Infectious Diseases*, *219*(12), 1858–1866. https://doi.org/10.1093/infdis/jiz020

Ellis, T. M., McKenzie, R. S., Simms, P. E., Helfrich, B. A., & Fisher, R. I. (1989). Induction of human lymphokine-activated killer cells by IFN-alpha and IFN-gamma. *Journal of Immunology (Baltimore, Md.: 1950)*, *143*(12), 4282–4286.

Epstein, W. L., Hashimoto, A., Pincelli, C., & Fukuyama, K. (1989). Possible role of natural killer cells in granulomatous inflammation. *Sarcoidosis*, *6 Suppl 1*, 8–9.

Eriksson, M., Meadows, S. K., Basu, S., Mselle, T. F., Wira, C. R., & Sentman, C. L. (2006). TLRs mediate IFN-gamma production by human uterine NK cells in endometrium. *Journal of Immunology (Baltimore, Md.: 1950)*, *176*(10), 6219–6224. https://doi.org/10.4049/jimmunol.176.10.6219

Erkens, C. G. M., Slump, E., Verhagen, M., Schimmel, H., Cobelens, F., & van den Hof, S. (2016). Risk of developing tuberculosis disease among persons diagnosed with latent tuberculosis infection in the Netherlands. *The European Respiratory Journal*, *48*(5), 1420–1428. https://doi.org/10.1183/13993003.01157-2016

Erokhina, S. A., Streltsova, M. A., Kanevskiy, L. M., Grechikhina, M. V., Sapozhnikov, A. M., & Kovalenko, E. I. (2021). HLA-DR-expressing NK cells: Effective killers suspected for antigen presentation. *Journal of Leukocyte Biology*, *109*(2), 327–337. https://doi.org/10.1002/JLB.3RU0420-668RR

Esaulova, E., Das, S., Singh, D. K., Choreño-Parra, J. A., Swain, A., Arthur, L., Rangel-Moreno, J., Ahmed, M., Singh, B., Gupta, A., Fernández-López, L. A., Garcia-Hernandez, M. de la L., Bucsan, A., Moodley, C., Mehra, S., García-Latorre, E., Zuniga, J., Atkinson, J., Kaushal, D., … Khader, S. A. (2021). The immune landscape in tuberculosis reveals populations linked to disease and latency. *Cell Host & Microbe*, *29*(2), 165-178.e8. https://doi.org/10.1016/j.chom.2020.11.013

Esin, S., & Batoni, G. (2015). Natural Killer Cells: A Coherent Model for Their Functional Role in Mycobacterium tuberculosis Infection. *Journal of Innate Immunity*, *7*(1), 11–24. https://doi.org/10.1159/000363321

Esin, S., Batoni, G., Pardini, M., Favilli, F., Bottai, D., Maisetta, G., Florio, W., Vanacore, R., Wigzell, H., & Campa, M. (2004). Functional characterization of human natural killer cells responding to Mycobacterium bovis bacille Calmette-Guérin. *Immunology*, *112*(1), 143–152. https://doi.org/10.1111/j.1365-2567.2004.01858.x

Esin, S., Counoupas, C., Aulicino, A., Brancatisano, F. L., Maisetta, G., Bottai, D., Di Luca, M., Florio, W., Campa, M., & Batoni, G. (2013a). Interaction of Mycobacterium tuberculosis Cell Wall Components with the Human Natural Killer Cell Receptors NKp44 and Toll-Like Receptor 2. *Scandinavian Journal of Immunology*, *77*(6), 460–469. https://doi.org/10.1111/sji.12052

Esin, S., Counoupas, C., Aulicino, A., Brancatisano, F. L., Maisetta, G., Bottai, D., Di Luca, M., Florio, W., Campa, M., & Batoni, G. (2013b). Interaction of Mycobacterium tuberculosis cell wall components with the human natural killer cell receptors NKp44 and Toll-like receptor 2. *Scandinavian Journal of Immunology*, *77*(6), 460–469. https://doi.org/10.1111/sji.12052

Esmail, H., Barry, C. E., Young, D. B., & Wilkinson, R. J. (2014). The ongoing challenge of latent tuberculosis. *Philosophical Transactions of the Royal Society of London. Series B, Biological Sciences*, *369*(1645), 20130437. https://doi.org/10.1098/rstb.2013.0437

Esmail, H., Lai, R. P., Lesosky, M., Wilkinson, K. A., Graham, C. M., Coussens, A. K., Oni, T., Warwick, J. M., Said-Hartley, Q., Koegelenberg, C. F., Walzl, G., Flynn, J. L., Young, D. B., Barry Iii, C. E., O'Garra, A., & Wilkinson, R. J. (2016). Characterization of progressive HIV-associated tuberculosis using 2-deoxy-2-[18F]fluoro-D-glucose positron emission and computed tomography. *Nature Medicine*, *22*(10), 1090–1093. https://doi.org/10.1038/nm.4161

Fan, Y., Chen, J., Liu, M., Xu, X., Zhang, Y., Yue, P., Cao, W., Ji, Z., Su, X., Wen, S., Kong, J., Zhou, G., Li, B., Dong, Y., Liu, A., & Bao, F. (2022). Application of Droplet Digital PCR to Detection of Mycobacterium tuberculosis and Mycobacterium leprae Infections: A Narrative Review. *Infection and Drug Resistance*, *15*, 1067–1076. https://doi.org/10.2147/IDR.S349607

Farber, D. L. (2021). Tissues, not blood, are where immune cells function. *Nature*, *593*(7860), 506–509. https://doi.org/10.1038/d41586-021-01396-y

Farhat, M., Greenaway, C., Pai, M., & Menzies, D. (2006). False-positive tuberculin skin tests: What is the absolute effect of BCG and non-tuberculous mycobacteria? *The International Journal of Tuberculosis and Lung Disease: The Official Journal of the International Union Against Tuberculosis and Lung Disease*, *10*(11), 1192–1204.

Fauriat, C., Ivarsson, M. A., Ljunggren, H.-G., Malmberg, K.-J., & Michaëlsson, J. (2010). Education of human natural killer cells by activating killer cell immunoglobulin-like receptors. *Blood*, *115*(6), 1166–1174. https://doi.org/10.1182/blood-2009-09-245746

Fehniger, T. A., Cooper, M. A., Nuovo, G. J., Cella, M., Facchetti, F., Colonna, M., & Caligiuri, M. A. (2003). CD56bright natural killer cells are present in human lymph nodes and are activated by T cell–derived IL-2: A potential new link between adaptive and innate immunity. *Blood*, *101*(8), 3052–3057. https://doi.org/10.1182/blood-2002-09-2876

Feinberg, J., Fieschi, C., Doffinger, R., Feinberg, M., Leclerc, T., Boisson-Dupuis, S., Picard, C., Bustamante, J., Chapgier, A., Filipe-Santos, O., Ku, C.-L., Beaucoudrey, L. de, Reichenbach, J., Antoni, G., Baldé, R., Alcaïs, A., & Casanova, J.-L. (2004). Bacillus Calmette Guérin triggers the IL-12/IFN-γ axis by an IRAK-4- and NEMO-dependent, non-cognate interaction between monocytes, NK, and T lymphocytes. *European Journal of Immunology*, *34*(11), 3276–3284. https://doi.org/10.1002/eji.200425221

Feng, C. G., Kaviratne, M., Rothfuchs, A. G., Cheever, A., Hieny, S., Young, H. A., Wynn, T. A., & Sher, A. (2006). NK Cell-Derived IFN-γ Differentially Regulates Innate Resistance and Neutrophil Response in T Cell-Deficient Hosts Infected with Mycobacterium tuberculosis. *The Journal of Immunology*, *177*(10), 7086–7093. https://doi.org/10.4049/jimmunol.177.10.7086

Fernandez, N. C., Treiner, E., Vance, R. E., Jamieson, A. M., Lemieux, S., & Raulet, D. H. (2005). A subset of natural killer cells achieves self-tolerance without expressing inhibitory receptors specific for self-MHC molecules. *Blood*, *105*(11), 4416–4423. https://doi.org/10.1182/blood-2004-08-3156

Finck, R., Simonds, E. F., Jager, A., Krishnaswamy, S., Sachs, K., Fantl, W., Pe'er, D., Nolan, G. P., & Bendall, S. C. (2013). Normalization of mass cytometry data with bead standards. *Cytometry. Part A : The Journal of the International Society for Analytical Cytology*, *83*(5), 483–494. https://doi.org/10.1002/cyto.a.22271

Flynn, J. L., Chan, J., & Lin, P. L. (2011). Macrophages and control of granulomatous inflammation in tuberculosis. *Mucosal Immunology*, *4*(3), 271–278. https://doi.org/10.1038/mi.2011.14

Flynn, J. L., Gideon, H. P., Mattila, J. T., & Lin, P. L. (2015). Immunology studies in non-human primate models of tuberculosis. *Immunological Reviews*, *264*(1), 60–73. https://doi.org/10.1111/imr.12258

Francis, R. J., Robb, G., McCann, L., Khatri, B., Keeble, J., Dagg, B., Amos, B., Salguero, F. J., Ho, M. M., Bullen, A., McConnell, G., & MacLellan-Gibson, K. (2020). Three-dimensional in situ morphometrics of Mycobacterium tuberculosis infection within lesions by optical mesoscopy and novel acid-fast staining. *Scientific Reports*, *10*, 21774. https://doi.org/10.1038/s41598-020-78640-4

Franklin, M., Connolly, E., & Hussell, T. (2022). Recruited and Tissue-Resident Natural Killer Cells in the Lung During Infection and Cancer. *Frontiers in Immunology*, *13*, 887503. https://doi.org/10.3389/fimmu.2022.887503

Frascella, B., Richards, A. S., Sossen, B., Emery, J. C., Odone, A., Law, I., Onozaki, I., Esmail, H., & Houben, R. M. G. J. (2021). Subclinical Tuberculosis Disease-A Review and Analysis of Prevalence Surveys to Inform Definitions, Burden, Associations, and Screening Methodology. *Clinical Infectious Diseases: An Official Publication of the Infectious Diseases Society of America*, *73*(3), e830–e841. https://doi.org/10.1093/cid/ciaa1402

Freud, A. G., Mundy-Bosse, B. L., Yu, J., & Caligiuri, M. A. (2017). The broad spectrum of human natural killer cell diversity. *Immunity*, *47*(5), 820–833. https://doi.org/10.1016/j.immuni.2017.10.008

Fu, X., Yang, B., Lao, S., Fan, Y., & Wu, C. (2013). Human memory-like NK cells migrating to tuberculous pleural fluid via IP-10/CXCR3 and SDF-1/CXCR4 axis produce IFN-γ in response to Bacille Calmette Guerin. *Clinical Immunology (Orlando, Fla.)*, *148*(1), 113–123. https://doi.org/10.1016/j.clim.2013.04.003

Fu, X., Yu, S., Yang, B., Lao, S., Li, B., & Wu, C. (2016). Memory-Like Antigen-Specific Human NK Cells from TB Pleural Fluids Produced IL-22 in Response to IL-15 or Mycobacterium tuberculosis Antigens. *PLOS ONE*, *11*(3), e0151721. https://doi.org/10.1371/journal.pone.0151721

Ganchua, S. K. C., Cadena, A. M., Maiello, P., Gideon, H. P., Myers, A. J., Junecko, B. F., Klein, E. C., Lin, P. L., Mattila, J. T., & Flynn, J. L. (2018). Lymph nodes are sites of prolonged bacterial persistence during Mycobacterium tuberculosis infection in macaques. *PLoS Pathogens*, *14*(11), e1007337. https://doi.org/10.1371/journal.ppat.1007337

Ganchua, S. K. C., White, A. G., Klein, E. C., & Flynn, J. L. (2020). Lymph nodes—The neglected battlefield in tuberculosis. *PLoS Pathogens*, *16*(8), e1008632. https://doi.org/10.1371/journal.ppat.1008632

Geginat, J., Paroni, M., Facciotti, F., Gruarin, P., Kastirr, I., Caprioli, F., Pagani, M., & Abrignani, S. (2013). The CD4-centered universe of human T cell subsets. *Seminars in Immunology*, *25*(4), 252–262. https://doi.org/10.1016/j.smim.2013.10.012

Gerosa, F., Baldani-Guerra, B., Nisii, C., Marchesini, V., Carra, G., & Trinchieri, G. (2002). Reciprocal Activating Interaction between Natural Killer Cells and Dendritic Cells. *The Journal of Experimental Medicine*, *195*(3), 327–333. https://doi.org/10.1084/jem.20010938

Getahun, H., Gunneberg, C., Granich, R., & Nunn, P. (2010). HIV Infection—Associated Tuberculosis: The Epidemiology and the Response. *Clinical Infectious Diseases*, *50*(Supplement_3), S201–S207. https://doi.org/10.1086/651492

Gillard, G. O., Bivas-Benita, M., Hovav, A.-H., Grandpre, L. E., Panas, M. W., Seaman, M. S., Haynes, B. F., & Letvin, N. L. (2011). Thy1+ NK [corrected] cells from vaccinia virus-primed mice confer protection against vaccinia virus challenge in the absence of adaptive lymphocytes. *PLoS Pathogens*, *7*(8), e1002141. https://doi.org/10.1371/journal.ppat.1002141

Godfrey, D. I., Uldrich, A. P., McCluskey, J., Rossjohn, J., & Moody, D. B. (2015). The burgeoning family of unconventional T cells. *Nature Immunology*, *16*(11), Article 11. https://doi.org/10.1038/ni.3298

Gogna, A., Pradhan, G. R., Sinha, R. S., & Gupta, B. (1999). Tuberculosis presenting as deep vein thrombosis. *Postgraduate Medical Journal*, *75*(880), 104–105. https://doi.org/10.1136/pgmj.75.880.104

Goletti, D., Petruccioli, E., Joosten, S. A., & Ottenhoff, T. H. M. (2016). Tuberculosis Biomarkers: From Diagnosis to Protection. *Infectious Disease Reports*, *8*(2), 6568. https://doi.org/10.4081/idr.2016.6568

Goodson-Gregg, F. J., Krepel, S. A., & Anderson, S. K. (2020). Tuning of human NK cells by endogenous HLA-C expression. *Immunogenetics*, *72*(4), 205–215. https://doi.org/10.1007/s00251-020-01161-x

Greene, E., Finak, G., D'Amico, L. A., Bhardwaj, N., Church, C. D., Morishima, C., Ramchurren, N., Taube, J. M., Nghiem, P. T., Cheever, M. A., Fling, S. P., & Gottardo, R. (2021). New interpretable machine-learning method for single-cell data reveals correlates of clinical response to cancer immunotherapy. *Patterns*, *2*(12), 100372. https://doi.org/10.1016/j.patter.2021.100372

Grégoire, C., Chasson, L., Luci, C., Tomasello, E., Geissmann, F., Vivier, E., & Walzer, T. (2007). The trafficking of natural killer cells. *Immunological Reviews*, *220*(1), 169–182. https://doi.org/10.1111/j.1600-065X.2007.00563.x

Griffiths, G. M., & Isaaz, S. (1993). Granzymes A and B are targeted to the lytic granules of lymphocytes by the mannose-6-phosphate receptor. *Journal of Cell Biology*, *120*(4), 885–896. https://doi.org/10.1083/jcb.120.4.885

Grossman, W. J., Verbsky, J. W., Tollefsen, B. L., Kemper, C., Atkinson, J. P., & Ley, T. J. (2004). Differential expression of granzymes A and B in human cytotoxic lymphocyte subsets and T regulatory cells. *Blood*, *104*(9), 2840–2848. https://doi.org/10.1182/blood-2004-03-0859

Guo, H., & Topham, D. J. (2010). Interleukin-22 (IL-22) Production by Pulmonary Natural Killer Cells and the Potential Role of IL-22 during Primary Influenza Virus Infection. *Journal of Virology*, *84*(15), 7750–7759. https://doi.org/10.1128/JVI.00187-10

Guo, J., Zhang, X., Chen, X., & Cai, Y. (2022). Proteomics in Biomarker Discovery for Tuberculosis: Current Status and Future Perspectives. *Frontiers in Microbiology*, *13*, 845229. https://doi.org/10.3389/fmicb.2022.845229

Gupta, A., Mrigpuri, P., Faye, A., Bandyopadhyay, D., & Singla, R. (2017). Pulmonary tuberculosis - An emerging risk factor for venous thromboembolism: A case series and review of literature. *Lung India : Official Organ of Indian Chest Society*, *34*(1), 65–69. https://doi.org/10.4103/0970-2113.197110

Gutierrez-Arcelus, M., Teslovich, N., Mola, A. R., Polidoro, R. B., Nathan, A., Kim, H., Hannes, S., Slowikowski, K., Watts, G. F. M., Korsunsky, I., Brenner, M. B., Raychaudhuri, S., & Brennan, P. J. (2019). Lymphocyte innateness defined by transcriptional states reflects a balance between proliferation and effector functions. *Nature Communications*, *10*(1), Article 1. https://doi.org/10.1038/s41467-019-08604-4

Hammer, Q., Rückert, T., & Romagnani, C. (2018). Natural killer cell specificity for viral infections. *Nature Immunology*, *19*(8), 800–808. https://doi.org/10.1038/s41590-018-0163-6

Han, B., Mao, F., Zhao, Y., Lv, Y., Teng, Y., Duan, M., Chen, W., Cheng, P., Wang, T., Liang, Z., Zhang, J., Liu, Y., Guo, G., Zou, Q., Zhuang, Y., & Peng, L. (2018). Altered NKp30, NKp46, NKG2D, and DNAM-1 Expression on Circulating NK Cells Is Associated with Tumor Progression in Human Gastric Cancer. *Journal of Immunology Research*, *2018*, e6248590. https://doi.org/10.1155/2018/6248590

Hao, S., Zhao, J., Zhou, J., Zhao, S., Hu, Y., & Hou, Y. (2007). Modulation of 17beta-estradiol on the number and cytotoxicity of NK cells in vivo related to MCM and activating receptors. *International Immunopharmacology*, *7*(13), 1765–1775. https://doi.org/10.1016/j.intimp.2007.09.017

Hargreaves, J. R., Boccia, D., Evans, C. A., Adato, M., Petticrew, M., & Porter, J. D. H. (2011). The Social Determinants of Tuberculosis: From Evidence to Action. *American Journal of Public Health*, *101*(4), 654–662. https://doi.org/10.2105/AJPH.2010.199505

Harjunpää, H., & Guillerey, C. (2020). TIGIT as an emerging immune checkpoint. *Clinical and Experimental Immunology*, *200*(2), 108–119. https://doi.org/10.1111/cei.13407

Harris, L. D., Khayumbi, J., Ongalo, J., Sasser, L. E., Tonui, J., Campbell, A., Odhiambo, F. H., Ouma, S. G., Alter, G., Gandhi, N. R., & Day, C. L. (2020). Distinct Human NK Cell Phenotypes and Functional Responses to Mycobacterium tuberculosis in Adults From TB Endemic and Non-endemic Regions. *Frontiers in Cellular and Infection Microbiology*, *10*. https://doi.org/10.3389/fcimb.2020.00120

Harris, R. C., Sumner, T., Knight, G. M., Zhang, H., & White, R. G. (2020). Potential impact of tuberculosis vaccines in China, South Africa, and India. *Science Translational Medicine*, *12*(564), eaax4607. https://doi.org/10.1126/scitranslmed.aax4607

Hashemi, E., & Malarkannan, S. (2020). Tissue-Resident NK Cells: Development, Maturation, and Clinical Relevance. *Cancers*, *12*(6), Article 6. https://doi.org/10.3390/cancers12061553

Hashimoto, A., Pincelli, C., Fujioka, A., Fukuyama, K., & Epstein, W. L. (1990). Relationship between NK cells and granulomatous inflammation in mice. *Journal of Clinical & Laboratory Immunology*, *33*(1), 41–47.

Havlir, D. V., Getahun, H., Sanne, I., & Nunn, P. (2008). Opportunities and challenges for HIV care in overlapping HIV and TB epidemics. *JAMA*, *300*(4), 423–430. https://doi.org/10.1001/jama.300.4.423

Hayakawa, Y., Huntington, N. D., Nutt, S. L., & Smyth, M. J. (2006). Functional subsets of mouse natural killer cells. *Immunological Reviews*, *214*(1), 47–55. https://doi.org/10.1111/j.1600-065X.2006.00454.x

Hayakawa, Y., & Smyth, M. J. (2006). CD27 Dissects Mature NK Cells into Two Subsets with Distinct Responsiveness and Migratory Capacity. *The Journal of Immunology*, *176*(3), 1517–1524. https://doi.org/10.4049/jimmunol.176.3.1517

He, Y., Peng, H., Sun, R., Wei, H., Ljunggren, H.-G., Yokoyama, W. M., & Tian, Z. (2017). Contribution of inhibitory receptor TIGIT to NK cell education. *Journal of Autoimmunity*, *81*, 1–12. https://doi.org/10.1016/j.jaut.2017.04.001

He, Y., & Tian, Z. (2017). NK cell education via nonclassical MHC and non-MHC ligands. *Cellular & Molecular Immunology*, *14*(4), Article 4. https://doi.org/10.1038/cmi.2016.26

Held, W., & Kunz, B. (1998). An allele-specific, stochastic gene expression process controls the expression of multiple Ly49family genes and generates a diverse, MHC-specific NK cell receptor repertoire. *European Journal of Immunology*, *28*(8), 2407–2416. https://doi.org/10.1002/(SICI)1521-4141(199808)28:08<2407::AID-IMMU2407>3.0.CO;2-D

Hermans, S. M., Zinyakatira, N., Caldwell, J., Cobelens, F. G. J., Boulle, A., & Wood, R. (2021). High Rates of Recurrent Tuberculosis Disease: A Population-level Cohort Study. *Clinical Infectious Diseases: An Official Publication of the Infectious Diseases Society of America*, *72*(11), 1919–1926. https://doi.org/10.1093/cid/ciaa470

Herndler-Brandstetter, D., Shan, L., Yao, Y., Stecher, C., Plajer, V., Lietzenmayer, M., Strowig, T., de Zoete, M. R., Palm, N. W., Chen, J., Blish, C. A., Frleta, D., Gurer, C., Macdonald, L. E., Murphy, A. J., Yancopoulos, G. D., Montgomery, R. R., & Flavell, R. A. (2017). Humanized mouse model supports development, function, and tissue residency of human natural killer cells. *Proceedings of the National Academy of Sciences of the United States of America*, *114*(45), E9626–E9634. https://doi.org/10.1073/pnas.1705301114

Heron, M., Grutters, J. C., ten Dam-Molenkamp, K. M., Hijdra, D., van Heugten-Roeling, A., Claessen, A. M. E., Ruven, H. J. T., van den Bosch, J. M. M., & van Velzen-Blad, H. (2012). Bronchoalveolar lavage cell pattern from healthy human lung. *Clinical and Experimental Immunology*, *167*(3), 523–531. https://doi.org/10.1111/j.1365-2249.2011.04529.x

Herrera, M. T., Guzmán-Beltrán, S., Bobadilla, K., Santos-Mendoza, T., Flores-Valdez, M. A., Gutiérrez-González, L. H., & González, Y. (2022). Human Pulmonary Tuberculosis: Understanding the Immune Response in the Bronchoalveolar System. *Biomolecules*, *12*(8), Article 8. https://doi.org/10.3390/biom12081148

Hersperger, A. R., Makedonas, G., & Betts, M. R. (2008). Flow cytometric detection of perforin upregulation in human CD8 T cells. *Cytometry Part A*, *73A*(11), 1050–1057. https://doi.org/10.1002/cyto.a.20596

Hersperger, A. R., Siciliano, N. A., & Eisenlohr, L. C. (2012). Comparable polyfunctionality of ectromelia virus- and vaccinia virus-specific murine T cells despite markedly different in vivo replication and pathogenicity. *Journal of Virology*, *86*(13), 7298–7309. https://doi.org/10.1128/JVI.00038-12

Hervier, B., Russick, J., Cremer, I., & Vieillard, V. (2019a). NK Cells in the Human Lungs. *Frontiers in Immunology*, *10*, 1263. https://doi.org/10.3389/fimmu.2019.01263

Hervier, B., Russick, J., Cremer, I., & Vieillard, V. (2019b). NK Cells in the Human Lungs. *Frontiers in Immunology*, *10*, 1263. https://doi.org/10.3389/fimmu.2019.01263

Hirokawa, K., Utsuyama, M., Hayashi, Y., Kitagawa, M., Makinodan, T., & Fulop, T. (2013). Slower immune system aging in women versus men in the Japanese population. *Immunity & Ageing*, *10*(1), 19. https://doi.org/10.1186/1742-4933-10-19

Hoebe, K., Janssen, E., & Beutler, B. (2004). The interface between innate and adaptive immunity. *Nature Immunology*, *5*(10), Article 10. https://doi.org/10.1038/ni1004-971

Horowitz, A., Behrens, R. H., Okell, L., Fooks, A. R., & Riley, E. M. (2010a). NK Cells as Effectors of Acquired Immune Responses: Effector CD4+ T Cell-Dependent Activation of NK Cells Following Vaccination. *The Journal of Immunology*, *185*(5), 2808–2818. https://doi.org/10.4049/jimmunol.1000844

Horowitz, A., Behrens, R. H., Okell, L., Fooks, A. R., & Riley, E. M. (2010b). NK Cells as Effectors of Acquired Immune Responses: Effector CD4+ T Cell-Dependent Activation of NK Cells Following Vaccination. *The Journal of Immunology*, *185*(5), 2808–2818. https://doi.org/10.4049/jimmunol.1000844

Horowitz, A., Stegmann, K., & Riley, E. M. (2012). Activation of Natural Killer cells during microbial infections. *Frontiers in Immunology*, *0*. https://doi.org/10.3389/fimmu.2011.00088

Horowitz, A., Strauss-Albee, D. M., Leipold, M., Kubo, J., Nemat-Gorgani, N., Dogan, O. C., Dekker, C. L., Mackey, S., Maecker, H., Swan, G. E., Davis, M. M., Norman, P. J., Guethlein, L. A., Desai, M., Parham, P., & Blish, C. A. (2013). Genetic and environmental determinants of human NK cell diversity revealed by mass cytometry. *Science Translational Medicine*, *5*(208), 208ra145. https://doi.org/10.1126/scitranslmed.3006702

Houben, D., Demangel, C., van Ingen, J., Perez, J., Baldeón, L., Abdallah, A. M., Caleechurn, L., Bottai, D., van Zon, M., de Punder, K., van der Laan, T., Kant, A., Bossers-de Vries, R., Willemsen, P., Bitter, W., van Soolingen, D., Brosch, R., van der Wel, N., & Peters, P. J. (2012). ESX-1-mediated translocation to the cytosol controls virulence of mycobacteria. *Cellular Microbiology*, *14*(8), 1287–1298. https://doi.org/10.1111/j.1462-5822.2012.01799.x

Houben, R. M. G. J., & Dodd, P. J. (2016). The Global Burden of Latent Tuberculosis Infection: A Re-estimation Using Mathematical Modelling. *PLOS Medicine*, *13*(10), e1002152. https://doi.org/10.1371/journal.pmed.1002152

House, I. G., House, C. M., Brennan, A. J., Gilan, O., Dawson, M. A., Whisstock, J. C., Law, R. H., Trapani, J. A., & Voskoboinik, I. (2017). Regulation of perforin activation and pre-synaptic toxicity through C-terminal glycosylation. *EMBO Reports*, *18*(10), 1775–1785. https://doi.org/10.15252/embr.201744351

Hu, W., Wang, G., Huang, D., Sui, M., & Xu, Y. (2019). Cancer Immunotherapy Based on Natural Killer Cells: Current Progress and New Opportunities. *Frontiers in Immunology*, *10*. https://www.frontiersin.org/articles/10.3389/fimmu.2019.01205

Huang, L., Yin, C., Gu, X., Tang, X., Zhang, X., Hu, C., & Chen, W. (2020). Severe pulmonary tuberculosis complicated with insidious pulmonary thromboembolism: A case report and literature review. *Journal of Thrombosis and Thrombolysis*, *49*(4), 644–650. https://doi.org/10.1007/s11239-019-01967-x

Hudspeth, K., Pontarini, E., Tentorio, P., Cimino, M., Donadon, M., Torzilli, G., Lugli, E., Della Bella, S., Gershwin, M. E., & Mavilio, D. (2013). The role of natural killer cells in autoimmune liver

disease: A comprehensive review. *Journal of Autoimmunity*, *46*, 55–65. https://doi.org/10.1016/j.jaut.2013.07.003

Huenecke, S., Zimmermann, S. Y., Kloess, S., Esser, R., Brinkmann, A., Tramsen, L., Koenig, M., Erben, S., Seidl, C., Tonn, T., Eggert, A., Schramm, A., Bader, P., Klingebiel, T., Lehrnbecher, T., Passweg, J. R., Soerensen, J., Schwabe, D., & Koehl, U. (2010). IL-2-driven regulation of NK cell receptors with regard to the distribution of CD16+ and CD16- subpopulations and in vivo influence after haploidentical NK cell infusion. *Journal of Immunotherapy (Hagerstown, Md.: 1997)*, *33*(2), 200–210. https://doi.org/10.1097/CJI.0b013e3181bb46f7

Ikawa, T., Hirose, S., Masuda, K., Kakugawa, K., Satoh, R., Shibano-Satoh, A., Kominami, R., Katsura, Y., & Kawamoto, H. (2010). An Essential Developmental Checkpoint for Production of the T Cell Lineage. *Science*, *329*(5987), 93–96. https://doi.org/10.1126/science.1188995

Inngjerdingen, M., Kveberg, L., Naper, C., & Vaage, J. T. (2011). Natural killer cell subsets in man and rodents. *Tissue Antigens*, *78*(2), 81–88. https://doi.org/10.1111/j.1399-0039.2011.01714.x

Islam, R., Pupovac, A., Evtimov, V., Boyd, N., Shu, R., Boyd, R., & Trounson, A. (2021). Enhancing a Natural Killer: Modification of NK Cells for Cancer Immunotherapy. *Cells*, *10*(5), Article 5. https://doi.org/10.3390/cells10051058

Ito, T., Carson, W. F., Cavassani, K. A., Connett, J. M., & Kunkel, S. L. (2011). CCR6 as a mediator of immunity in the lung and gut. *Experimental Cell Research*, *317*(5), 613–619. https://doi.org/10.1016/j.yexcr.2010.12.018

Jahrsdörfer, B., Beyer, T., Schrezenmeier, H., Debatin, K.-M., & Fabricius, D. (2014). Granzyme B Is a Key Regulator of Plasmacytoid Dendritic Cell Immunogenicity. *Blood*, *124*(21), 4127. https://doi.org/10.1182/blood.V124.21.4127.4127

Jahrsdörfer, B., Vollmer, A., Blackwell, S. E., Maier, J., Sontheimer, K., Beyer, T., Mandel, B., Lunov, O., Tron, K., Nienhaus, G. U., Simmet, T., Debatin, K.-M., Weiner, G. J., & Fabricius, D. (2010). Granzyme B produced by human plasmacytoid dendritic cells suppresses T-cell expansion. *Blood*, *115*(6), 1156–1165. https://doi.org/10.1182/blood-2009-07-235382

Jeon, C. Y., & Murray, M. B. (2008). Diabetes mellitus increases the risk of active tuberculosis: A systematic review of 13 observational studies. *PLoS Medicine*, *5*(7), e152. https://doi.org/10.1371/journal.pmed.0050152

Jewett, A., & Bonavida, B. (1995). Interferon-alpha activates cytotoxic function but inhibits interleukin-2-mediated proliferation and tumor necrosis factor-alpha secretion by immature human natural killer cells. *Journal of Clinical Immunology*, *15*(1), 35–44. https://doi.org/10.1007/BF01489488

Jiang, D., Liang, J., Hodge, J., Lu, B., Zhu, Z., Yu, S., Fan, J., Gao, Y., Yin, Z., Homer, R., Gerard, C., & Noble, P. W. (2004). Regulation of pulmonary fibrosis by chemokine receptor CXCR3. *Journal of Clinical Investigation*, *114*(2), 291–299. https://doi.org/10.1172/JCI200416861

Johansson, S., Johansson, M., Rosmaraki, E., Vahlne, G., Mehr, R., Salmon-Divon, M., Lemonnier, F., Kärre, K., & Höglund, P. (2005). Natural killer cell education in mice with single or multiple

major histocompatibility complex class I molecules. *Journal of Experimental Medicine*, *201*(7), 1145–1155. https://doi.org/10.1084/jem.20050167

Joncker, N. T., Fernandez, N. C., Treiner, E., Vivier, E., & Raulet, D. H. (2009). NK Cell Responsiveness Is Tuned Commensurate with the Number of Inhibitory Receptors for Self-MHC Class I: The Rheostat Model 1. *The Journal of Immunology*, *182*(8), 4572–4580. https://doi.org/10.4049/jimmunol.0803900

Judge, S. J., Darrow, M. A., Thorpe, S. W., Gingrich, A. A., O'Donnell, E. F., Bellini, A. R., Sturgill, I. R., Vick, L. V., Dunai, C., Stoffel, K. M., Lyu, Y., Chen, S., Cho, M., Rebhun, R. B., Monjazeb, A. M., Murphy, W. J., & Canter, R. J. (2020). Analysis of tumor-infiltrating NK and T cells highlights IL-15 stimulation and TIGIT blockade as a combination immunotherapy strategy for soft tissue sarcomas. *Journal for ImmunoTherapy of Cancer*, *8*(2), e001355. https://doi.org/10.1136/jitc-2020-001355

Junqueira-Kipnis, A. P., Kipnis, A., Jamieson, A., Juarrero, M. G., Diefenbach, A., Raulet, D. H., Turner, J., & Orme, I. M. (2003a). NK cells respond to pulmonary infection with Mycobacterium tuberculosis, but play a minimal role in protection. *Journal of Immunology (Baltimore, Md.: 1950)*, *171*(11), 6039–6045. https://doi.org/10.4049/jimmunol.171.11.6039

Junqueira-Kipnis, A. P., Kipnis, A., Jamieson, A., Juarrero, M. G., Diefenbach, A., Raulet, D. H., Turner, J., & Orme, I. M. (2003b). NK Cells Respond to Pulmonary Infection with Mycobacterium tuberculosis, but Play a Minimal Role in Protection 1. *The Journal of Immunology*, *171*(11), 6039–6045. https://doi.org/10.4049/jimmunol.171.11.6039

Jurado, J. O., Pasquinelli, V., Alvarez, I. B., Peña, D., Rovetta, A. I., Tateosian, N. L., Romeo, H. E., Musella, R. M., Palmero, D., Chuluyán, H. E., & García, V. E. (2012). IL-17 and IFN-γ expression in lymphocytes from patients with active tuberculosis correlates with the severity of the disease. *Journal of Leukocyte Biology*, *91*(6), 991–1002. https://doi.org/10.1189/jlb.1211619

Kaiserman, D., Zhao, P., Rowe, C. L., Leong, A., Barlow, N., Joeckel, L. T., Hitchen, C., Stewart, S. E., Hollenberg, M. D., Bunnett, N., Suhrbier, A., & Bird, P. I. (2022). Granzyme K initiates IL-6 and IL-8 release from epithelial cells by activating protease-activated receptor 2. *PLOS ONE*, *17*(7), e0270584. https://doi.org/10.1371/journal.pone.0270584

Kalsdorf, B., Scriba, T. J., Wood, K., Day, C. L., Dheda, K., Dawson, R., Hanekom, W. A., Lange, C., & Wilkinson, R. J. (2009). HIV-1 Infection Impairs the Bronchoalveolar T-Cell Response to Mycobacteria. *American Journal of Respiratory and Critical Care Medicine*, *180*(12), 1262–1270. https://doi.org/10.1164/rccm.200907-1011OC

Kamath, A. B., Woodworth, J., Xiong, X., Taylor, C., Weng, Y., & Behar, S. M. (2004). Cytolytic CD8+ T Cells Recognizing CFP10 Are Recruited to the Lung after Mycobacterium tuberculosis Infection. *Journal of Experimental Medicine*, *200*(11), 1479–1489. https://doi.org/10.1084/jem.20041690

Kang, G.-Y., Rhyu, H.-J., Choi, H.-H., Shin, S. J., & Hyun, Y.-M. (2020). 3D Imaging of the Transparent Mycobacterium tuberculosis-Infected Lung Verifies the Localization of Innate Immune Cells With Granuloma. *Frontiers in Cellular and Infection Microbiology*, *10*. https://www.frontiersin.org/articles/10.3389/fcimb.2020.00226

Kara, E. E., Comerford, I., Fenix, K. A., Bastow, C. R., Gregor, C. E., McKenzie, D. R., & McColl, S. R. (2014). Tailored Immune Responses: Novel Effector Helper T Cell Subsets in Protective Immunity. *PLOS Pathogens*, *10*(2), e1003905. https://doi.org/10.1371/journal.ppat.1003905

Karlsson, A. C., Martin, J. N., Younger, S. R., Bredt, B. M., Epling, L., Ronquillo, R., Varma, A., Deeks, S. G., McCune, J. M., Nixon, D. F., & Sinclair, E. (2003). Comparison of the ELISPOT and cytokine flow cytometry assays for the enumeration of antigen-specific T cells. *Journal of Immunological Methods*, *283*(1–2), 141–153. https://doi.org/10.1016/j.jim.2003.09.001

Kärre, K., Ljunggren, H. G., Piontek, G., & Kiessling, R. (1986). Selective rejection of H–2-deficient lymphoma variants suggests alternative immune defence strategy. *Nature*, *319*(6055), Article 6055. https://doi.org/10.1038/319675a0

Kathamuthu, G. R., Moideen, K., Sridhar, R., Baskaran, D., & Babu, S. (2020). Diminished Frequencies of Cytotoxic Marker Expressing T- and NK Cells at the Site of Mycobacterium tuberculosis Infection. *Frontiers in Immunology*, *11*. https://www.frontiersin.org/articles/10.3389/fimmu.2020.585293

Kathamuthu, G. R., Sridhar, R., Baskaran, D., & Babu, S. (2022). Dominant expansion of CD4+, CD8+ T and NK cells expressing Th1/Tc1/Type 1 cytokines in culture-positive lymph node tuberculosis. *PLOS ONE*, *17*(5), e0269109. https://doi.org/10.1371/journal.pone.0269109

Kauffman, K. D., Sakai, S., Lora, N. E., Namasivayam, S., Baker, P. J., Kamenyeva, O., Foreman, T. W., Nelson, C. E., Oliveira-de-Souza, D., Vinhaes, C. L., Yaniv, Z., Lindestam Arleham, C. S., Sette, A., Freeman, G. J., Moore, R., NIAID/DIR Tuberculosis Imaging Program, Sher, A., Mayer-Barber, K. D., Andrade, B. B., … Barber, D. L. (2021). PD-1 blockade exacerbates Mycobacterium tuberculosis infection in rhesus macaques. *Science Immunology*, *6*(55), eabf3861. https://doi.org/10.1126/sciimmunol.abf3861

Kaufmann, S. H. (2001). How can immunology contribute to the control of tuberculosis? *Nature Reviews. Immunology*, *1*(1), 20–30. https://doi.org/10.1038/35095558

Keating, S. E., Zaiatz-Bittencourt, V., Loftus, R. M., Keane, C., Brennan, K., Finlay, D. K., & Gardiner, C. M. (2016). Metabolic Reprogramming Supports IFN-γ Production by CD56bright NK Cells. *The Journal of Immunology*, *196*(6), 2552–2560. https://doi.org/10.4049/jimmunol.1501783

Keppel, M. P., Saucier, N., Mah, A. Y., Vogel, T. P., & Cooper, M. A. (2015). Activation-Specific Metabolic Requirements for NK Cell IFN-γ Production. *The Journal of Immunology*, *194*(4), 1954–1962. https://doi.org/10.4049/jimmunol.1402099

Keren, L., Bosse, M., Thompson, S., Risom, T., Vijayaragavan, K., McCaffrey, E., Marquez, D., Angoshtari, R., Greenwald, N. F., Fienberg, H., Wang, J., Kambham, N., Kirkwood, D., Nolan, G., Montine, T. J., Galli, S. J., West, R., Bendall, S. C., & Angelo, M. (2019). MIBI-TOF: A multiplexed imaging platform relates cellular phenotypes and tissue structure. *Science Advances*, *5*(10), eaax5851. https://doi.org/10.1126/sciadv.aax5851

Khader, S. A., Bell, G. K., Pearl, J. E., Fountain, J. J., Rangel-Moreno, J., Cilley, G. E., Shen, F., Eaton, S. M., Gaffen, S. L., Swain, S. L., Locksley, R. M., Haynes, L., Randall, T. D., & Cooper, A. M. (2007). IL-23 and IL-17 in the establishment of protective pulmonary CD4+ T cell responses after vaccination and during Mycobacterium tuberculosis challenge. *Nature Immunology*, *8*(4), 369–377. https://doi.org/10.1038/ni1449

Khan, M. S., Dar, O., Sismanidis, C., Shah, K., & Godfrey-Faussett, P. (2007). Improvement of tuberculosis case detection and reduction of discrepancies between men and women by simple sputum-submission instructions: A pragmatic randomised controlled trial. *The Lancet*, *369*(9577), 1955–1960. https://doi.org/10.1016/S0140-6736(07)60916-7

Kim, S., Poursine-Laurent, J., Truscott, S. M., Lybarger, L., Song, Y.-J., Yang, L., French, A. R., Sunwoo, J. B., Lemieux, S., Hansen, T. H., & Yokoyama, W. M. (2005a). Licensing of natural killer cells by host major histocompatibility complex class I molecules. *Nature*, *436*(7051), Article 7051. https://doi.org/10.1038/nature03847

Kim, S., Poursine-Laurent, J., Truscott, S. M., Lybarger, L., Song, Y.-J., Yang, L., French, A. R., Sunwoo, J. B., Lemieux, S., Hansen, T. H., & Yokoyama, W. M. (2005b). Licensing of natural killer cells by host major histocompatibility complex class I molecules. *Nature*, *436*(7051), 709–713. https://doi.org/10.1038/nature03847

Kim, S., Sunwoo, J. B., Yang, L., Choi, T., Song, Y.-J., French, A. R., Vlahiotis, A., Piccirillo, J. F., Cella, M., Colonna, M., Mohanakumar, T., Hsu, K. C., Dupont, B., & Yokoyama, W. M. (2008). HLA alleles determine differences in human natural killer cell responsiveness and potency. *Proceedings of the National Academy of Sciences*, *105*(8), 3053–3058. https://doi.org/10.1073/pnas.0712229105

Klausner, R. D., Donaldson, J. G., & Lippincott-Schwartz, J. (1992). Brefeldin A: Insights into the control of membrane traffic and organelle structure. *The Journal of Cell Biology*, *116*(5), 1071–1080. https://doi.org/10.1083/jcb.116.5.1071

Klein, S. L., & Flanagan, K. L. (2016). Sex differences in immune responses. *Nature Reviews Immunology*, *16*(10), Article 10. https://doi.org/10.1038/nri.2016.90

Kleinnijenhuis, J., Quintin, J., Preijers, F., Joosten, L. A. B., Jacobs, C., Xavier, R. J., van der Meer, J. W. M., van Crevel, R., & Netea, M. G. (2014a). BCG-induced trained immunity in NK cells: Role for non-specific protection to infection. *Clinical Immunology (Orlando, Fla.)*, *155*(2), 213–219. https://doi.org/10.1016/j.clim.2014.10.005

Kleinnijenhuis, J., Quintin, J., Preijers, F., Joosten, L. A. B., Jacobs, C., Xavier, R. J., van der Meer, J. W. M., van Crevel, R., & Netea, M. G. (2014b). BCG-induced trained immunity in NK cells: Role for non-specific protection to infection. *Clinical Immunology (Orlando, Fla.)*, *155*(2), 213–219. https://doi.org/10.1016/j.clim.2014.10.005

Kleiveland, C. R. (2015). Peripheral Blood Mononuclear Cells. In K. Verhoeckx, P. Cotter, I. López-Expósito, C. Kleiveland, T. Lea, A. Mackie, T. Requena, D. Swiatecka, & H. Wichers (Eds.), *The Impact of Food Bioactives on Health: In vitro and ex vivo models* (pp. 161–167). Springer International Publishing. https://doi.org/10.1007/978-3-319-16104-4_15

Kondo, M., Weissman, I. L., & Akashi, K. (1997). Identification of clonogenic common lymphoid progenitors in mouse bone marrow. *Cell*, *91*(5), 661–672. https://doi.org/10.1016/s0092-8674(00)80453-5

Konjević, G., Vuletić, A., & Džodić, K. M. M. and R. (2017). The Role of Activating and Inhibitory NK Cell Receptors in Antitumor Immune Response. In *Natural Killer Cells*. IntechOpen. https://doi.org/10.5772/intechopen.69729

Kouismi, H., Laine, M., Bourkadi, J.-E., & Iraqi, G. (2013). Association of deep venous thrombosis with pulmonary tuberculosis. *Egyptian Journal of Chest Diseases and Tuberculosis*, *62*(3), 541–543. https://doi.org/10.1016/j.ejcdt.2013.06.001

Kozakiewicz, L., Phuah, J., Flynn, J., & Chan, J. (2013). The Role of B Cells and Humoral Immunity in Mycobacterium tuberculosis Infection. *Advances in Experimental Medicine and Biology*, *783*, 225–250. https://doi.org/10.1007/978-1-4614-6111-1_12

Krensky, A. M., & Clayberger, C. (2005). Granulysin: A Novel Host Defense Molecule. *American Journal of Transplantation*, *5*(8), 1789–1792. https://doi.org/10.1111/j.1600-6143.2005.00970.x

Kulkarni, N. S., Prudon, B., Panditi, S. L., Abebe, Y., & Grigg, J. (2005). Carbon loading of alveolar macrophages in adults and children exposed to biomass smoke particles. *Science of The Total Environment*, *345*(1), 23–30. https://doi.org/10.1016/j.scitotenv.2004.10.016

Kumar, P., Thakar, M. S., Ouyang, W., & Malarkannan, S. (2013). IL-22 from conventional NK cells is epithelial regenerative and inflammation protective during influenza infection. *Mucosal Immunology*, *6*(1), 69–82.

Kumar, S. (2018). Natural killer cell cytotoxicity and its regulation by inhibitory receptors. *Immunology*, *154*(3), 383–393. https://doi.org/10.1111/imm.12921

Kumar, V. (2020). Pulmonary Innate Immune Response Determines the Outcome of Inflammation During Pneumonia and Sepsis-Associated Acute Lung Injury. *Frontiers in Immunology*, *11*. https://www.frontiersin.org/articles/10.3389/fimmu.2020.01722

Kust, S. A., Streltsova, M. A., Panteleev, A. V., Karpina, N. L., Lyadova, I. V., Sapozhnikov, A. M., & Kovalenko, E. I. (2021). HLA-DR-Positive NK Cells Expand in Response to Mycobacterium Tuberculosis Antigens and Mediate Mycobacteria-Induced T Cell Activation. *Frontiers in Immunology*, *12*. https://www.frontiersin.org/articles/10.3389/fimmu.2021.662128

Lai, L., Yeo, J. G., & Albani, S. (2017). Singlet gating in mass cytometry. *Cytometry Part A*, *91*(2), 170–172. https://doi.org/10.1002/cyto.a.23034

Lam, A., Prabhu, R., Gross, C. M., Riesenberg, L. A., Singh, V., & Aggarwal, S. (2017). Role of apoptosis and autophagy in tuberculosis. *American Journal of Physiology - Lung Cellular and Molecular Physiology*, *313*(2), L218–L229. https://doi.org/10.1152/ajplung.00162.2017

Lanier, L. L. (2005). NK cell recognition. *Annual Review of Immunology*, *23*, 225–274. https://doi.org/10.1146/annurev.immunol.23.021704.115526

Lanier, L. L., Buck, D. W., Rhodes, L., Ding, A., Evans, E., Barney, C., & Phillips, J. H. (1988). Interleukin 2 activation of natural killer cells rapidly induces the expression and phosphorylation of the Leu-23 activation antigen. *The Journal of Experimental Medicine*, *167*(5), 1572–1585. https://doi.org/10.1084/jem.167.5.1572

Lanier, L. L., Chang, C., Azuma, M., Ruitenberg, J. J., Hemperly, J. J., & Phillips, J. H. (1991). Molecular and functional analysis of human natural killer cell-associated neural cell adhesion molecule (N-CAM/CD56). *Journal of Immunology (Baltimore, Md.: 1950)*, *146*(12), 4421–4426.

Lanier, L. L., Ruitenberg, J. J., & Phillips, J. H. (1988). Functional and biochemical analysis of CD16 antigen on natural killer cells and granulocytes. *The Journal of Immunology*, *141*(10), 3478–3485.

Lanier, L. L., Testi, R., Bindl, J., & Phillips, J. H. (1989). Identity of Leu-19 (CD56) leukocyte differentiation antigen and neural cell adhesion molecule. *The Journal of Experimental Medicine*, *169*(6), 2233–2238. https://doi.org/10.1084/jem.169.6.2233

Lee, B.-W., Yap, H.-K., Chew, F.-T., Quah, T.-C., Prabhakaran, K., Chan, G. S. H., Wong, S.-C., & Seah, C.-C. (1996). Age- and sex-related changes in lymphocyte subpopulations of healthy Asian subjects: From birth to adulthood. *Cytometry*, *26*(1), 8–15. https://doi.org/10.1002/(SICI)1097-0320(19960315)26:1<8::AID-CYTO2>3.0.CO;2-E

Lehmann, C., Zeis, M., & Uharek, L. (2001). Activation of natural killer cells with interleukin 2 (IL-2) and IL-12 increases perforin binding and subsequent lysis of tumour cells. *British Journal of Haematology*, *114*(3), 660–665. https://doi.org/10.1046/j.1365-2141.2001.02995.x

Leipold, M. D., Newell, E. W., & Maecker, H. T. (2015). Multiparameter phenotyping of human PBMCs using mass cytometry. *Methods in Molecular Biology*, *1343*, 81–95.

Lenart, M., Kluczewska, A., Szaflarska, A., Rutkowska-Zapała, M., Wąsik, M., Ziemiańska-Pięta, A., Kobylarz, K., Pituch-Noworolska, A., & Siedlar, M. (2021). Selective downregulation of natural killer activating receptors on NK cells and upregulation of PD-1 expression on T cells in children with severe and/or recurrent Herpes simplex virus infections. *Immunobiology*, *226*(3), 152097. https://doi.org/10.1016/j.imbio.2021.152097

Lewinsohn, D. A., Lewinsohn, D. M., & Scriba, T. J. (2017). Polyfunctional CD4+ T Cells As Targets for Tuberculosis Vaccination. *Frontiers in Immunology*, *8*, 1262. https://doi.org/10.3389/fimmu.2017.01262

Li, L., Leid, M., & Rothenberg, E. V. (2010). An Early T Cell Lineage Commitment Checkpoint Dependent on the Transcription Factor Bcl11b. *Science*, *329*(5987), 89–93. https://doi.org/10.1126/science.1188989

Li, P., Burke, S., Wang, J., Chen, X., Ortiz, M., Lee, S.-C., Lu, D., Campos, L., Goulding, D., Ng, B. L., Dougan, G., Huntly, B., Gottgens, B., Jenkins, N. A., Copeland, N. G., Colucci, F., & Liu, P. (2010). Reprogramming of T Cells to Natural Killer–Like Cells upon Bcl11b Deletion. *Science*, *329*(5987), 85–89. https://doi.org/10.1126/science.1188063

Li, S., Wang, D., Wei, P., Liu, R., Guo, J., Yang, B., Zhang, H., Lu, J., Gao, M., & Pang, Y. (2021). Elevated Natural Killer Cell-Mediated Cytotoxicity Is Associated with Cavity Formation in Pulmonary Tuberculosis Patients. *Journal of Immunology Research*, *2021*, e7925903. https://doi.org/10.1155/2021/7925903

Liao, S., & Padera, T. P. (2013). Lymphatic Function and Immune Regulation in Health and Disease. *Lymphatic Research and Biology*, *11*(3), 136–143. https://doi.org/10.1089/lrb.2013.0012

Lieberman, J. (2003). The ABCs of granule-mediated cytotoxicity: New weapons in the arsenal. *Nature Reviews Immunology*, *3*(5), Article 5. https://doi.org/10.1038/nri1083

Lin, L., Finak, G., Ushey, K., Seshadri, C., Hawn, T. R., Frahm, N., Scriba, T. J., Mahomed, H., Hanekom, W., Bart, P.-A., Pantaleo, G., Tomaras, G. D., Rerks-Ngarm, S., Kaewkungwal,

J., Nitayaphan, S., Pitisuttithum, P., Michael, N. L., Kim, J. H., Robb, M. L., … Gottardo, R. (2015). COMPASS identifies T-cell subsets correlated with clinical outcomes. *Nature Biotechnology*, *33*(6), Article 6. https://doi.org/10.1038/nbt.3187

Lin, P. L., Ford, C. B., Coleman, M. T., Myers, A. J., Gawande, R., Ioerger, T., Sacchettini, J., Fortune, S. M., & Flynn, J. L. (2014). Sterilization of granulomas is common in active and latent tuberculosis despite within-host variability in bacterial killing. *Nature Medicine*, *20*(1), 75–79. https://doi.org/10.1038/nm.3412

Liu, C. H., Liu, H., & Ge, B. (2017). Innate immunity in tuberculosis: Host defense vs pathogen evasion. *Cellular & Molecular Immunology*, *14*(12), Article 12. https://doi.org/10.1038/cmi.2017.88

Liu, M., Liang, S., & Zhang, C. (2021). NK Cells in Autoimmune Diseases: Protective or Pathogenic? *Frontiers in Immunology*, *12*, 701. https://doi.org/10.3389/fimmu.2021.624687

Liu, Y., Ou, Q., Liu, Q., Gao, Y., Wu, J., Zhang, B., Weng, X., Shao, L., & Zhang, W. (2017). The expressions and roles of different forms of IL-22 in Mycobacterium tuberculosis infection. *Tuberculosis*, *107*, 95–103. https://doi.org/10.1016/j.tube.2017.08.009

Liu, Y., Zhao, S., Li, Y., Song, W., Yu, C., Gao, L., Ran, J., He, D., & Li, H. (2021). Effect of ambient air pollution on tuberculosis risks and mortality in Shandong, China: A multi-city modeling study of the short- and long-term effects of pollutants. *Environmental Science and Pollution Research International*, *28*(22), 27757–27768. https://doi.org/10.1007/s11356-021-12621-6

Loftus, R. M., Assmann, N., Kedia-Mehta, N., O'Brien, K. L., Garcia, A., Gillespie, C., Hukelmann, J. L., Oefner, P. J., Lamond, A. I., Gardiner, C. M., Dettmer, K., Cantrell, D. A., Sinclair, L. V., & Finlay, D. K. (2018). Amino acid-dependent cMyc expression is essential for NK cell metabolic and functional responses in mice. *Nature Communications*, *9*(1), Article 1. https://doi.org/10.1038/s41467-018-04719-2

Longo, S. K., Guo, M. G., Ji, A. L., & Khavari, P. A. (2021). Integrating single-cell and spatial transcriptomics to elucidate intercellular tissue dynamics. *Nature Reviews Genetics*, *22*(10), Article 10. https://doi.org/10.1038/s41576-021-00370-8

Lopez, J. A., Susanto, O., Jenkins, M. R., Lukoyanova, N., Sutton, V. R., Law, R. H. P., Johnston, A., Bird, C. H., Bird, P. I., Whisstock, J. C., Trapani, J. A., Saibil, H. R., & Voskoboinik, I. (2013). Perforin forms transient pores on the target cell plasma membrane to facilitate rapid access of granzymes during killer cell attack. *Blood*, *121*(14), 2659–2668. https://doi.org/10.1182/blood-2012-07-446146

Lopez-Vergès, S., Milush, J. M., Schwartz, B. S., Pando, M. J., Jarjoura, J., York, V. A., Houchins, J. P., Miller, S., Kang, S.-M., Norris, P. J., Nixon, D. F., & Lanier, L. L. (2011). Expansion of a unique $CD57^{+}$NKG2Chi natural killer cell subset during acute human cytomegalovirus infection. *Proceedings of the National Academy of Sciences of the United States of America*, *108*(36), 14725–14732. https://doi.org/10.1073/pnas.1110900108

Loxton, A. G. (2019). Bcells and their regulatory functions during Tuberculosis: Latency and active disease. *Molecular Immunology*, *111*, 145–151. https://doi.org/10.1016/j.molimm.2019.04.012

Lu, C.-C., Wu, T.-S., Hsu, Y.-J., Chang, C.-J., Lin, C.-S., Chia, J.-H., Wu, T.-L., Huang, T.-T., Martel, J., Ojcius, D. M., Young, J. D., & Lai, H.-C. (2014). NK cells kill mycobacteria directly by releasing perforin and granulysin. *Journal of Leukocyte Biology*, *96*(6), 1119–1129. https://doi.org/10.1189/jlb.4A0713-363RR

Lu, Y.-J., Barreira-Silva, P., Boyce, S., Powers, J., Cavallo, K., & Behar, S. M. (2021). CD4 T cell help prevents CD8 T cell exhaustion and promotes control of Mycobacterium tuberculosis infection. *Cell Reports*, *36*(11). https://doi.org/10.1016/j.celrep.2021.109696

Lunemann, S., Langeneckert, A. E., Martrus, G., Hess, L. U., Salzberger, W., Ziegler, A. E., Löbl, S. M., Poch, T., Ravichandran, G., Sauter, J., Schmidt, A. H., Schramm, C., Oldhafer, K. J., Altfeld, M., & Körner, C. (2019). Human liver-derived CXCR6+ NK cells are predominantly educated through NKG2A and show reduced cytokine production. *Journal of Leukocyte Biology*, *105*(6), 1331–1340. https://doi.org/10.1002/JLB.1MA1118-428R

Lutz, C. T., Al-Attar, A., Presnell, S. R., Peterson, C. A., & Thomas, D. T. (2016). The effect of sex on immune cells in healthy aging: Elderly women have more robust natural killer (NK) lymphocytes than do elderly men. *The Journal of Immunology*, *196*(1 Supplement), 204.2-204.2.

Lyadova, I. V., & Panteleev, A. V. (2015). Th1 and Th17 Cells in Tuberculosis: Protection, Pathology, and Biomarkers. *Mediators of Inflammation*, *2015*, 854507. https://doi.org/10.1155/2015/854507

Lyashchenko, K. P., Vordermeier, H. M., & Waters, W. R. (2020). Memory B cells and tuberculosis. *Veterinary Immunology and Immunopathology*, *221*, 110016. https://doi.org/10.1016/j.vetimm.2020.110016

Ma, A., Koka, R., & Burkett, P. (2006). Diverse functions of IL-2, IL-15, and IL-7 in lymphoid homeostasis. *Annual Review of Immunology*, *24*, 657–679. https://doi.org/10.1146/annurev.immunol.24.021605.090727

Ma, J., Zhao, S., Gao, X., Wang, R., Liu, J., Zhou, X., & Zhou, Y. (2021). The Roles of Inflammasomes in Host Defense against Mycobacterium tuberculosis. *Pathogens*, *10*(2), 120. https://doi.org/10.3390/pathogens10020120

Maglione, P. J., & Chan, J. (2009). How B cells shape the immune response against Mycobacterium tuberculosis. *European Journal of Immunology*, *39*(3), 676–686. https://doi.org/10.1002/eji.200839148

Mahfouz, R., Halas, H., Hoteit, R., Saadeh, M., Shamseddeen, W., Charafeddine, K., Itani, L., & Araj, G. F. (2011). Study of KIR genes in Lebanese patients with tuberculosis. *The International Journal of Tuberculosis and Lung Disease*, *15*(12), 1688–1691. https://doi.org/10.5588/ijtld.11.0138

Majewska-Szczepanik, M., Paust, S., von Andrian, U. H., Askenase, P. W., & Szczepanik, M. (2013). Natural killer cell-mediated contact sensitivity develops rapidly and depends on interferon-α, interferon-γ and interleukin-12. *Immunology*, *140*(1), 98–110. https://doi.org/10.1111/imm.12120

Makino, Y., Kanno, R., Ito, T., Higashino, K., & Taniguchi, M. (1995). Predominant expression of invariant Vα14+ TCR α chain in NK1.1+ T cell populations. *International Immunology*, *7*(7), 1157–1161. https://doi.org/10.1093/intimm/7.7.1157

Malnati, M. S., Lusso, P., Ciccone, E., Moretta, A., Moretta, L., & Long, E. O. (1993). Recognition of virus-infected cells by natural killer cell clones is controlled by polymorphic target cell elements. *Journal of Experimental Medicine*, *178*(3), 961–969. https://doi.org/10.1084/jem.178.3.961

Mandal, A., & Viswanathan, C. (2015). Natural killer cells: In health and disease. *Hematology/Oncology and Stem Cell Therapy*, *8*(2), 47–55. https://doi.org/10.1016/j.hemonc.2014.11.006

Mangtani, P., Abubakar, I., Ariti, C., Beynon, R., Pimpin, L., Fine, P. E. M., Rodrigues, L. C., Smith, P. G., Lipman, M., Whiting, P. F., & Sterne, J. A. (2014). Protection by BCG vaccine against tuberculosis: A systematic review of randomized controlled trials. *Clinical Infectious Diseases: An Official Publication of the Infectious Diseases Society of America*, *58*(4), 470–480. https://doi.org/10.1093/cid/cit790

Marquardt, N., Béziat, V., Nyström, S., Hengst, J., Ivarsson, M. A., Kekäläinen, E., Johansson, H., Mjösberg, J., Westgren, M., Lankisch, T. O., Wedemeyer, H., Ellis, E. C., Ljunggren, H.-G., Michaëlsson, J., & Björkström, N. K. (2015). Cutting edge: Identification and characterization of human intrahepatic CD49a+ NK cells. *Journal of Immunology (Baltimore, Md.: 1950)*, *194*(6), 2467–2471. https://doi.org/10.4049/jimmunol.1402756

Marquardt, N., Kekäläinen, E., Chen, P., Kvedaraite, E., Wilson, J. N., Ivarsson, M. A., Mjösberg, J., Berglin, L., Säfholm, J., Manson, M. L., Adner, M., Al-Ameri, M., Bergman, P., Orre, A.-C., Svensson, M., Dahlén, B., Dahlén, S.-E., Ljunggren, H.-G., & Michaëlsson, J. (2017a). Human lung natural killer cells are predominantly comprised of highly differentiated hypofunctional CD69-CD56dim cells. *The Journal of Allergy and Clinical Immunology*, *139*(4), 1321-1330.e4. https://doi.org/10.1016/j.jaci.2016.07.043

Marquardt, N., Kekäläinen, E., Chen, P., Kvedaraite, E., Wilson, J. N., Ivarsson, M. A., Mjösberg, J., Berglin, L., Säfholm, J., Manson, M. L., Adner, M., Al-Ameri, M., Bergman, P., Orre, A.-C., Svensson, M., Dahlén, B., Dahlén, S.-E., Ljunggren, H.-G., & Michaëlsson, J. (2017b). Human lung natural killer cells are predominantly comprised of highly differentiated hypofunctional CD69−CD56dim cells. *Journal of Allergy and Clinical Immunology*, *139*(4), 1321-1330.e4. https://doi.org/10.1016/j.jaci.2016.07.043

Marquardt, N., Kekäläinen, E., Chen, P., Lourda, M., Wilson, J. N., Scharenberg, M., Bergman, P., Al-Ameri, M., Hård, J., Mold, J. E., Ljunggren, H.-G., & Michaëlsson, J. (2019). Unique transcriptional and protein-expression signature in human lung tissue-resident NK cells. *Nature Communications*, *10*(1), Article 1. https://doi.org/10.1038/s41467-019-11632-9

Martínez-Lostao, L., Anel, A., & Pardo, J. (2015). How Do Cytotoxic Lymphocytes Kill Cancer Cells? *Clinical Cancer Research: An Official Journal of the American Association for Cancer Research*, *21*(22), 5047–5056. https://doi.org/10.1158/1078-0432.CCR-15-0685

Masopust, D., & Schenkel, J. M. (2013). The integration of T cell migration, differentiation and function. *Nature Reviews Immunology*, *13*(5), Article 5. https://doi.org/10.1038/nri3442

Mathema, B., Andrews, J. R., Cohen, T., Borgdorff, M. W., Behr, M., Glynn, J. R., Rustomjee, R., Silk, B. J., & Wood, R. (2017). Drivers of Tuberculosis Transmission. *The Journal of Infectious Diseases*, *216*(suppl_6), S644–S653. https://doi.org/10.1093/infdis/jix354

Matthews, K., Wilkinson, K. A., Kalsdorf, B., Roberts, T., Diacon, A., Walzl, G., Wolske, J., Ntsekhe, M., Syed, F., Russell, J., Mayosi, B. M., Dawson, R., Dheda, K., Wilkinson, R. J., Hanekom, W. A., & Scriba, T. J. (2011). Predominance of interleukin-22 over interleukin-17 at the site of disease in human tuberculosis. *Tuberculosis (Edinburgh, Scotland)*, *91*(6), 587–593. https://doi.org/10.1016/j.tube.2011.06.009

McCaffrey, E. F., Donato, M., Keren, L., Chen, Z., Delmastro, A., Fitzpatrick, M. B., Gupta, S., Greenwald, N. F., Baranski, A., Graf, W., Kumar, R., Bosse, M., Fullaway, C. C., Ramdial, P. K., Forgó, E., Jojic, V., Van Valen, D., Mehra, S., Khader, S. A., … Angelo, M. (2022). The immunoregulatory landscape of human tuberculosis granulomas. *Nature Immunology*, *23*(2), Article 2. https://doi.org/10.1038/s41590-021-01121-x

Mebius, R. E., & Kraal, G. (2005). Structure and function of the spleen. *Nature Reviews. Immunology*, *5*(8), 606–616. https://doi.org/10.1038/nri1669

Meierhoff, G., Ott, P. A., Lehmann, P. V., & Schloot, N. C. (2002). Cytokine detection by ELISPOT: Relevance for immunological studies in type 1 diabetes. *Diabetes/Metabolism Research and Reviews*, *18*(5), 367.

Méndez, A., Granda, H., Meenagh, A., Contreras, S., Zavaleta, R., Mendoza, M. F., Izquierdo, L., Sarmiento, M. E., Acosta, A., & Middleton, D. (2006). Study of KIR genes in tuberculosis patients. *Tissue Antigens*, *68*(5), 386–389. https://doi.org/10.1111/j.1399-0039.2006.00685.x

Menzies, N. A., Swartwood, N., Testa, C., Malyuta, Y., Hill, A. N., Marks, S. M., Cohen, T., & Salomon, J. A. (2021). Time Since Infection and Risks of Future Disease for Individuals with Mycobacterium tuberculosis Infection in the United States. *Epidemiology (Cambridge, Mass.)*, *32*(1), 70–78. https://doi.org/10.1097/EDE.0000000000001271

Meraviglia, S., El Daker, S., Dieli, F., Martini, F., & Martino, A. (2011). Γδ T cells cross-link innate and adaptive immunity in Mycobacterium tuberculosis infection. *Clinical & Developmental Immunology*, *2011*, 587315. https://doi.org/10.1155/2011/587315

Meskas, J., Yokosawa, D., Wang, S., Segat, G. C., & Brinkman, R. R. (2022). flowCut: An R package for automated removal of outlier events and flagging of files based on time versus fluorescence analysis. *Cytometry Part A*, *n/a*(n/a). https://doi.org/10.1002/cyto.a.24670

Minton, K. (2014). A TACTILE restraint. *Nature Reviews Immunology*, *14*(5), Article 5. https://doi.org/10.1038/nri3664

Mølhave, M., & Wejse, C. (2020). Historical review of studies on the effect of treating latent tuberculosis. *International Journal of Infectious Diseases: IJID: Official Publication of the International Society for Infectious Diseases*, *92S*, S31–S36. https://doi.org/10.1016/j.ijid.2020.03.011

Mollenhauer, H. H., Morré, D. J., & Rowe, L. D. (1990). Alteration of intracellular traffic by monensin; mechanism, specificity and relationship to toxicity. *Biochimica Et Biophysica Acta*, *1031*(2), 225–246. https://doi.org/10.1016/0304-4157(90)90008-z

Montel, A. H., Bochan, M. R., Hobbs, J. A., Lynch, D. H., & Brahmi, Z. (1995). Fas involvement in cytotoxicity mediated by human NK cells. *Cellular Immunology*, *166*(2), 236–246. https://doi.org/10.1006/cimm.1995.9974

Montoya, C. J., Cataño, J. C., Ramirez, Z., Rugeles, M. T., Wilson, S. B., & Landay, A. L. (2008). Invariant NKT cells from HIV-1 or Mycobacterium tuberculosis-infected patients express an activated phenotype. *Clinical Immunology*, *127*(1), 1–6. https://doi.org/10.1016/j.clim.2007.12.006

Morán-Mendoza, O., Marion, S. A., Elwood, K., Patrick, D., & FitzGerald, J. M. (2010). Risk factors for developing tuberculosis: A 12-year follow-up of contacts of tuberculosis cases. *The International Journal of Tuberculosis and Lung Disease: The Official Journal of the International Union Against Tuberculosis and Lung Disease*, *14*(9), 1112–1119.

Moretta, A., Poggi, A., Pende, D., Tripodi, G., Orengo, A. M., Pella, N., Augugliaro, R., Bottino, C., Ciccone, E., & Moretta, L. (1991). CD69-mediated pathway of lymphocyte activation: Anti-CD69 monoclonal antibodies trigger the cytolytic activity of different lymphoid effector cells with the exception of cytolytic T lymphocytes expressing T cell receptor alpha/beta. *The Journal of Experimental Medicine*, *174*(6), 1393–1398. https://doi.org/10.1084/jem.174.6.1393

Morgan, J., Muskat, K., Tippalagama, R., Sette, A., Burel, J., & Lindestam Arlehamn, C. S. (2021). Classical CD4 T cells as the cornerstone of antimycobacterial immunity. *Immunological Reviews*, *301*(1), 10–29. https://doi.org/10.1111/imr.12963

Morikawa, F., Nakano, A., Nakano, H., Oseko, F., & Morikawa, S. (1989). Enhanced Natural Killer Cell Activity in Patients with Pulmonary Tuberculosis. *Japanese Journal of Medicine*, *28*(3), 316–322. https://doi.org/10.2169/internalmedicine1962.28.316

Mortlock, R. D., Wu, C., Potter, E. L., Abraham, D. M., Allan, D. S. J., Hong, S. G., Roederer, M., & Dunbar, C. E. (2022). Tissue Trafficking Kinetics of Rhesus Macaque Natural Killer Cells Measured by Serial Intravascular Staining. *Frontiers in Immunology*, *12*. https://www.frontiersin.org/articles/10.3389/fimmu.2021.772332

Mpande, C. A. M., Musvosvi, M., Rozot, V., Mosito, B., Reid, T. D., Schreuder, C., Lloyd, T., Bilek, N., Huang, H., Obermoser, G., Davis, M. M., Ruhwald, M., Hatherill, M., Scriba, T. J., Nemes, E., Mahomed, H., Hanekom, W. A., Kafaar, F., Workman, L., … Hussey, G. (2021). Antigen-Specific T-Cell Activation Distinguishes between Recent and Remote Tuberculosis Infection. *American Journal of Respiratory and Critical Care Medicine*, *203*(12), 1556–1565. https://doi.org/10.1164/rccm.202007-2686OC

Murphy, K., & Weaver, C. (2016). *Janeway's Immunobiology*. Garland Science.

Murphy, M., Suliman, S., Briel, L., Veldtsman, H., Khomba, N., Africa, H., Steyn, M., Snyders, C. I., Rensburg, I. C. van, Walzl, G., Chegou, N. N., Hatherill, M., Hanekom, W. A., Scriba, T. J., & Nemes, E. (2023). Newborn BCG vaccination induces robust infant IFN γ -expressing NK cell responses to mycobacteria. *International Journal of Infectious Diseases*, *0*(0). https://doi.org/10.1016/j.ijid.2023.02.018

Musvosvi, M., Duffy, D., Filander, E., Africa, H., Mabwe, S., Jaxa, L., Bilek, N., Llibre, A., Rouilly, V., Hatherill, M., Albert, M., Scriba, T. J., & Nemes, E. (2018). T-cell biomarkers for diagnosis of tuberculosis: Candidate evaluation by a simple whole blood assay for clinical translation. *European Respiratory Journal*, *51*(3). https://doi.org/10.1183/13993003.00153-2018

Naithani, R., Agrawal, N., & Choudhary, V. P. (2007). Deep venous thrombosis associated with tuberculosis. *Blood Coagulation & Fibrinolysis: An International Journal in Haemostasis and Thrombosis*, *18*(4), 377–380. https://doi.org/10.1097/MBC.0b013e3280d942b4

Naranbhai, V., Hill, A. V. S., Abdool Karim, S. S., Naidoo, K., Abdool Karim, Q., Warimwe, G. M., McShane, H., & Fletcher, H. (2014). Ratio of monocytes to lymphocytes in peripheral blood identifies adults at risk of incident tuberculosis among HIV-infected adults initiating antiretroviral therapy. *The Journal of Infectious Diseases*, *209*(4), 500–509. https://doi.org/10.1093/infdis/jit494

Ndlovu, H., & Marakalala, M. J. (2016). Granulomas and Inflammation: Host-Directed Therapies for Tuberculosis. *Frontiers in Immunology*, *7*, 434. https://doi.org/10.3389/fimmu.2016.00434

Nebenführ, A., Ritzenthaler, C., & Robinson, D. G. (2002). Brefeldin A: deciphering an enigmatic inhibitor of secretion. *Plant Physiology*, *130*(3), 1102–1108.

Netea, M. G., Joosten, L. A. B., Latz, E., Mills, K. H. G., Natoli, G., Stunnenberg, H. G., O'Neill, L. A. J., & Xavier, R. J. (2016). Trained immunity: A program of innate immune memory in health and disease. *Science (New York, N.Y.)*, *352*(6284), aaf1098. https://doi.org/10.1126/science.aaf1098

Newman, K. C., & Riley, E. M. (2007). Whatever turns you on: Accessory-cell-dependent activation of NK cells by pathogens. *Nature Reviews Immunology*, *7*(4), 279–291. https://doi.org/10.1038/nri2057

Nicholas, K. J., Greenplate, A. R., Flaherty, D. K., Matlock, B. K., Juan, J. S., Smith, R. M., Irish, J. M., & Kalams, S. A. (2016). Multiparameter analysis of stimulated human peripheral blood mononuclear cells: A comparison of mass and fluorescence cytometry. *Cytometry Part A*, *89*(3), 271–280. https://doi.org/10.1002/cyto.a.22799

Nicol, M. P., Schumacher, S. G., Workman, L., Broger, T., Baard, C., Prins, M., Bateman, L., du Toit, E., van Heerden, J., Szekely, R., Zar, H. J., & Denkinger, C. M. (2021). Accuracy of a Novel Urine Test, Fujifilm SILVAMP Tuberculosis Lipoarabinomannan, for the Diagnosis of Pulmonary Tuberculosis in Children. *Clinical Infectious Diseases: An Official Publication of the Infectious Diseases Society of America*, *72*(9), e280–e288. https://doi.org/10.1093/cid/ciaa1052

Nicol, M. P., & Zar, H. J. (2020). Advances in the diagnosis of pulmonary tuberculosis in children. *Paediatric Respiratory Reviews*, *36*, 52–56. https://doi.org/10.1016/j.prrv.2020.05.003

Nigro, C. L., Macagno, M., Sangiolo, D., Bertolaccini, L., Aglietta, M., & Merlano, M. C. (2019). NK-mediated antibody-dependent cell-mediated cytotoxicity in solid tumors: Biological evidence and clinical perspectives. *Annals of Translational Medicine*, *7*(5), Article 5. https://doi.org/10.21037/atm.2019.01.42

Nikitina, I. Y., Panteleev, A. V., Kosmiadi, G. A., Serdyuk, Y. V., Nenasheva, T. A., Nikolaev, A. A., Gorelova, L. A., Radaeva, T. V., Kiseleva, Y. Y., Bozhenko, V. K., & Lyadova, I. V. (2018). Th1, Th17, and Th1Th17 Lymphocytes during Tuberculosis: Th1 Lymphocytes Predominate and Appear as Low-Differentiated CXCR3+CCR6+ Cells in the Blood and Highly Differentiated CXCR3+/-CCR6- Cells in the Lungs. *Journal of Immunology (Baltimore, Md.: 1950)*, *200*(6), 2090–2103. https://doi.org/10.4049/jimmunol.1701424

Nikzad, R., Angelo, L. S., Aviles-Padilla, K., Le, D. T., Singh, V. K., Bimler, L., Vukmanovic-Stejic, M., Vendrame, E., Ranganath, T., Simpson, L., Haigwood, N. L., Blish, C. A., Akbar, A. N., & Paust, S. (2019). Human natural killer cells mediate adaptive immunity to viral antigens. *Science Immunology*, *4*(35). https://doi.org/10.1126/sciimmunol.aat8116

Nirmala, R., Narayanan, P. R., Mathew, R., Maran, M., & Deivanayagam, C. N. (2001). Reduced NK activity in pulmonary tuberculosis patients with/without HIV infection: Identifying the defective stage and studying the effect of interleukins on NK activity. *Tuberculosis (Edinburgh, Scotland)*, *81*(5–6), 343–352. https://doi.org/10.1054/tube.2001.0309

Nisha Rajeswari, D., Selvaraj, P., Jawahar, M. S., Adhilakshmi, A. R., Vidyarani, M., & Narayanan, P. R. (2006). Elevated percentage of perforin positive cells in active pulmonary tuberculosis. *The Indian Journal of Medical Research*, *123*(5), 687–690.

Nogusa, S., Murasko, D. M., & Gardner, E. M. (2012). Differential Effects of Stimulatory Factors on Natural Killer Cell Activities of Young and Aged Mice. *The Journals of Gerontology: Series A*, *67*(9), 947–954. https://doi.org/10.1093/gerona/gls079

Ogongo, P., Steyn, A. J., Karim, F., Dullabh, K. J., Awala, I., Madansein, R., Leslie, A., & Behar, S. M. (2020). Differential skewing of donor-unrestricted and γδ T cell repertoires in tuberculosis-infected human lungs. *The Journal of Clinical Investigation*, *130*(1), 214–230. https://doi.org/10.1172/JCI130711

O'Leary, J. G., Goodarzi, M., Drayton, D. L., & von Andrian, U. H. (2006). T cell- and B cell-independent adaptive immunity mediated by natural killer cells. *Nature Immunology*, *7*(5), 507–516. https://doi.org/10.1038/ni1332

Orange, J. S. (2002). Human natural killer cell deficiencies and susceptibility to infection. *Microbes and Infection*, *4*(15), 1545–1558. https://doi.org/10.1016/s1286-4579(02)00038-2

Orcl, L., Tagaya, M., Amherdt, M., Perrelet, A., Donaldson, J. G., Lippincott-Schwartz, J., Klausner, R. D., & Rothman, J. E. (1991). Brefeldin A, a drug that blocks secretion, prevents the assembly of non-clathrin-coated buds on Golgi cisternae. *Cell*, *64*(6), 1183–1195.

Ordonez, A. A., Tasneen, R., Pokkali, S., Xu, Z., Converse, P. J., Klunk, M. H., Mollura, D. J., Nuermberger, E. L., & Jain, S. K. (2016). Mouse model of pulmonary cavitary tuberculosis and expression of matrix metalloproteinase-9. *Disease Models & Mechanisms*, *9*(7), 779–788. https://doi.org/10.1242/dmm.025643

Ordway, D. J., Pinto, L., Costa, L., Martins, M., Leandro, C., Viveiros, M., Amaral, L., Arroz, M. J., Ventura, F. A., & Dockrell, H. M. (2005). Gamma delta T cell responses associated with the development of tuberculosis in health care workers. *FEMS Immunology and Medical Microbiology*, *43*(3), 339–350. https://doi.org/10.1016/j.femsim.2004.09.005

Orme, I. M. (1988). A mouse model of the recrudescence of latent tuberculosis in the elderly. *The American Review of Respiratory Disease*, *137*(3), 716–718. https://doi.org/10.1164/ajrccm/137.3.716

Pabst, R., & Tschernig, T. (1995). Lymphocytes in the lung: An often neglected cell. *Anatomy and Embryology*, *192*(4), 293–299. https://doi.org/10.1007/BF00710098

Pagán, A. J., & Ramakrishnan, L. (2014). Immunity and Immunopathology in the Tuberculous Granuloma. *Cold Spring Harbor Perspectives in Medicine*, *5*(9), a018499. https://doi.org/10.1101/cshperspect.a018499

Pai, M., Behr, M. A., Dowdy, D., Dheda, K., Divangahi, M., Boehme, C. C., Ginsberg, A., Swaminathan, S., Spigelman, M., Getahun, H., Menzies, D., & Raviglione, M. (2016). Tuberculosis. *Nature Reviews. Disease Primers*, *2*, 16076. https://doi.org/10.1038/nrdp.2016.76

Pai, M., Denkinger, C. M., Kik, S. V., Rangaka, M. X., Zwerling, A., Oxlade, O., Metcalfe, J. Z., Cattamanchi, A., Dowdy, D. W., Dheda, K., & Banaei, N. (2014). Gamma interferon release assays for detection of Mycobacterium tuberculosis infection. *Clinical Microbiology Reviews*, *27*(1), 3–20. https://doi.org/10.1128/CMR.00034-13

Pai, M., Nicol, M. P., & Boehme, C. C. (2016). Tuberculosis Diagnostics: State of the Art and Future Directions. *Microbiology Spectrum*, *4*(5), 4.5.16. https://doi.org/10.1128/microbiolspec.TBTB2-0019-2016

Pande, T., Pai, M., Khan, F. A., & Denkinger, C. M. (2015). Use of chest radiography in the 22 highest tuberculosis burden countries. *The European Respiratory Journal*, *46*(6), 1816–1819. https://doi.org/10.1183/13993003.01064-2015

Pardo, J., Balkow, S., Anel, A., & Simon, M. M. (2002). Granzymes are essential for natural killer cell-mediated and perf-facilitated tumor control. *European Journal of Immunology*, *32*(10), 2881–2887. https://doi.org/10.1002/1521-4141(2002010)32:10<2881::AID-IMMU2881>3.0.CO;2-K

Parham, P. (2006). Taking license with natural killer cell maturation and repertoire development. *Immunological Reviews*, *214*(1), 155–160. https://doi.org/10.1111/j.1600-065X.2006.00462.x

Paul, S., & Lal, G. (2017). The Molecular Mechanism of Natural Killer Cells Function and Its Importance in Cancer Immunotherapy. *Frontiers in Immunology*, *0*. https://doi.org/10.3389/fimmu.2017.01124

Peng, M. Y., Wang, Z. H., Yao, C. Y., Jiang, L. N., Jin, Q. L., Wang, J., & Li, B. Q. (2008). Interleukin 17-producing gamma delta T cells increased in patients with active pulmonary tuberculosis. *Cellular & Molecular Immunology*, *5*(3), 203–208. https://doi.org/10.1038/cmi.2008.25

Penn-Nicholson, A., Geldenhuys, H., Burny, W., van der Most, R., Day, C. L., Jongert, E., Moris, P., Hatherill, M., Ofori-Anyinam, O., & Hanekom, W. (2015). Safety and immunogenicity of candidate vaccine M72/AS01E in adolescents in a TB endemic setting. *Vaccine*, *33*(32), 4025–4034. https://doi.org/10.1016/j.vaccine.2015.05.088

Pesce, S., Greppi, M., Grossi, F., Del Zotto, G., Moretta, L., Sivori, S., Genova, C., & Marcenaro, E. (2019). PD/1-PD-Ls Checkpoint: Insight on the Potential Role of NK Cells. *Frontiers in Immunology*, *10*. https://www.frontiersin.org/articles/10.3389/fimmu.2019.01242

Peter, J. G., Zijenah, L. S., Chanda, D., Clowes, P., Lesosky, M., Gina, P., Mehta, N., Calligaro, G., Lombard, C. J., Kadzirange, G., Bandason, T., Chansa, A., Liusha, N., Mangu, C., Mtafya, B., Msila, H., Rachow, A., Hoelscher, M., Mwaba, P., … Dheda, K. (2016). Effect on mortality of point-of-care, urine-based lipoarabinomannan testing to guide tuberculosis treatment

initiation in HIV-positive hospital inpatients: A pragmatic, parallel-group, multicountry, open-label, randomised controlled trial. *Lancet (London, England)*, *387*(10024), 1187–1197. https://doi.org/10.1016/S0140-6736(15)01092-2

Petruccioli, E., Chiacchio, T., Vanini, V., Cuzzi, G., Codecasa, L. R., Ferrarese, M., Schininà, V., Palmieri, F., Ippolito, G., & Goletti, D. (2018). Effect of therapy on Quantiferon-Plus response in patients with active and latent tuberculosis infection. *Scientific Reports*, *8*, 15626. https://doi.org/10.1038/s41598-018-33825-w

Phan, M.-T., Chun, S., Kim, S.-H., Ali, A. K., Lee, S.-H., Kim, S., Kim, S.-H., & Cho, D. (2017). Natural killer cell subsets and receptor expression in peripheral blood mononuclear cells of a healthy Korean population: Reference range, influence of age and sex, and correlation between NK cell receptors and cytotoxicity. *Human Immunology*, *78*(2), 103–112. https://doi.org/10.1016/j.humimm.2016.11.006

Phipps, J. C., Aronoff, D. M., Curtis, J. L., Goel, D., O'Brien, E., & Mancuso, P. (2010). Cigarette Smoke Exposure Impairs Pulmonary Bacterial Clearance and Alveolar Macrophage Complement-Mediated Phagocytosis of Streptococcus pneumoniae. *Infection and Immunity*, *78*(3), 1214–1220. https://doi.org/10.1128/IAI.00963-09

Poccia, F., Malkovsky, M., Pollak, A., Colizzi, V., Sireci, G., Salerno, A., & Dieli, F. (1999). In vivo gammadelta T cell priming to mycobacterial antigens by primary Mycobacterium tuberculosis infection and exposure to nonpeptidic ligands. *Molecular Medicine (Cambridge, Mass.)*, *5*(7), 471–476.

Pokkali, S., Das, S. D., & Selvaraj, A. (2009). Differential upregulation of chemokine receptors on CD56+ NK cells and their transmigration to the site of infection in tuberculous pleurisy. *FEMS Immunology & Medical Microbiology*, *55*(3), 352–360. https://doi.org/10.1111/j.1574-695X.2008.00520.x

Portevin, D., Via, L. E., Eum, S., & Young, D. (2012). Natural killer cells are recruited during pulmonary tuberculosis and their ex vivo responses to mycobacteria vary between healthy human donors in association with KIR haplotype. *Cellular Microbiology*, *14*(11), 1734–1744. https://doi.org/10.1111/j.1462-5822.2012.01834.x

Potter, E. L., Gideon, H. P., Tkachev, V., Fabozzi, G., Chassiakos, A., Petrovas, C., Darrah, P. A., Lin, P. L., Foulds, K. E., Kean, L. S., Flynn, J. L., & Roederer, M. (2021). Measurement of leukocyte trafficking kinetics in macaques by serial intravascular staining. *Science Translational Medicine*, *13*(576), eabb4582. https://doi.org/10.1126/scitranslmed.abb4582

Poznanski, S. M., & Ashkar, A. A. (2019). What Defines NK Cell Functional Fate: Phenotype or Metabolism? *Frontiers in Immunology*, *10*. https://doi.org/10.3389/fimmu.2019.01414

Poznanski, S. M., Nham, T., Chew, M. V., Lee, A. J., Hammill, J. A., Fan, I. Y., Butcher, M., Bramson, J. L., Lee, D. A., Hirte, H. W., & Ashkar, A. A. (2018). Expanded CD56superbrightCD16+ NK Cells from Ovarian Cancer Patients Are Cytotoxic against Autologous Tumor in a Patient-Derived Xenograft Murine Model. *Cancer Immunology Research*, *6*(10), 1174–1185. https://doi.org/10.1158/2326-6066.CIR-18-0144

Prager, I., Liesche, C., van Ooijen, H., Urlaub, D., Verron, Q., Sandström, N., Fasbender, F., Claus, M., Eils, R., Beaudouin, J., Önfelt, B., & Watzl, C. (2019). NK cells switch from granzyme B to death receptor–mediated cytotoxicity during serial killing. *Journal of Experimental Medicine*, *216*(9), 2113–2127. https://doi.org/10.1084/jem.20181454

Prager, I., & Watzl, C. (2019). Mechanisms of natural killer cell-mediated cellular cytotoxicity. *Journal of Leukocyte Biology*, *105*(6), 1319–1329. https://doi.org/10.1002/JLB.MR0718-269R

Prakash, M. D., Bird, C. H., & Bird, P. I. (2009). Active and zymogen forms of granzyme B are constitutively released from cytotoxic lymphocytes in the absence of target cell engagement. *Immunology & Cell Biology*, *87*(3), 249–254. https://doi.org/10.1038/icb.2008.98

Pydi, S. S., Sunder, S. R., Venkatasubramanian, S., Kovvali, S., Jonnalagada, S., & Valluri, V. L. (2013). Killer cell immunoglobulin like receptor gene association with tuberculosis. *Human Immunology*, *74*(1), 85–92. https://doi.org/10.1016/j.humimm.2012.10.006

Qiu, F., Maniar, A., Diaz, M. Q., Chapoval, A. I., & Medvedev, A. E. (2011). Activation of cytokine-producing and antitumor activities of natural killer cells and macrophages by engagement of Toll-like and NOD-like receptors. *Innate Immunity*, *17*(4), 375–387. https://doi.org/10.1177/1753425910372000

Ramakrishnan, L. (2012). Revisiting the role of the granuloma in tuberculosis. *Nature Reviews. Immunology*, *12*(5), 352–366. https://doi.org/10.1038/nri3211

Raulet, D. H. (2004). Interplay of natural killer cells and their receptors with the adaptive immune response. *Nature Immunology*, *5*(10), 996–1002. https://doi.org/10.1038/ni1114

Reeves, R. K., Li, H., Jost, S., Blass, E., Li, H., Schafer, J. L., Varner, V., Manickam, C., Eslamizar, L., Altfeld, M., von Andrian, U. H., & Barouch, D. H. (2015). Antigen-specific NK cell memory in rhesus macaques. *Nature Immunology*, *16*(9), 927–932. https://doi.org/10.1038/ni.3227

Rehm, J., Samokhvalov, A. V., Neuman, M. G., Room, R., Parry, C., Lönnroth, K., Patra, J., Poznyak, V., & Popova, S. (2009). The association between alcohol use, alcohol use disorders and tuberculosis (TB). A systematic review. *BMC Public Health*, *9*, 450. https://doi.org/10.1186/1471-2458-9-450

Reichler, M. R., Khan, A., Sterling, T. R., Zhao, H., Chen, B., Yuan, Y., Moran, J., McAuley, J., Mangura, B., & Tuberculosis Epidemiologic Studies Consortium Task Order 2 Team. (2020). Risk Factors for Tuberculosis and Effect of Preventive Therapy Among Close Contacts of Persons With Infectious Tuberculosis. *Clinical Infectious Diseases: An Official Publication of the Infectious Diseases Society of America*, *70*(8), 1562–1572. https://doi.org/10.1093/cid/ciz438

Reichler, M. R., Khan, A., Sterling, T. R., Zhao, H., Moran, J., McAuley, J., Bessler, P., & Mangura, B. (2018). Risk and Timing of Tuberculosis Among Close Contacts of Persons with Infectious Tuberculosis. *The Journal of Infectious Diseases*, *218*(6), 1000–1008. https://doi.org/10.1093/infdis/jiy265

Restrepo, L. M., Barrera, L. F., & Garcia, L. F. (1990). Natural killer cell activity in patients with pulmonary tuberculosis and in healthy controls. *Tubercle*, *71*(2), 95–102. https://doi.org/10.1016/0041-3879(90)90003-q

Ribot, J. C., Lopes, N., & Silva-Santos, B. (2021). Γδ T cells in tissue physiology and surveillance. *Nature Reviews Immunology*, *21*(4), Article 4. https://doi.org/10.1038/s41577-020-00452-4

Richmond, I., Pritchard, G. E., Ashcroft, T., Avery, A., Corris, P. A., & Walters, E. H. (1993). Bronchus associated lymphoid tissue (BALT) in human lung: Its distribution in smokers and non-smokers. *Thorax*, *48*(11), 1130–1134. https://doi.org/10.1136/thx.48.11.1130

Rijnink, W. F., Ottenhoff, T. H. M., & Joosten, S. A. (2021). B-Cells and Antibodies as Contributors to Effector Immune Responses in Tuberculosis. *Frontiers in Immunology*, *12*. https://doi.org/10.3389/fimmu.2021.640168

Riou, C., Berkowitz, N., Goliath, R., Burgers, W. A., & Wilkinson, R. J. (2017). Analysis of the Phenotype of Mycobacterium tuberculosis-Specific CD4+ T Cells to Discriminate Latent from Active Tuberculosis in HIV-Uninfected and HIV-Infected Individuals. *Frontiers in Immunology*, *8*. https://www.frontiersin.org/articles/10.3389/fimmu.2017.00968

Riou, C., Du Bruyn, E., Ruzive, S., Goliath, R. T., Lindestam Arlehamn, C. S., Sette, A., Sher, A., Barber, D. L., & Wilkinson, R. J. (2020). Disease extent and anti-tubercular treatment response correlates with Mycobacterium tuberculosis-specific CD4 T-cell phenotype regardless of HIV-1 status. *Clinical & Translational Immunology*, *9*(9), e1176. https://doi.org/10.1002/cti2.1176

Robinson, B. W., Pinkston, P., & Crystal, R. G. (1984). Natural killer cells are present in the normal human lung but are functionally impotent. *The Journal of Clinical Investigation*, *74*(3), 942–950. https://doi.org/10.1172/JCI111513

Roy, A., Eisenhut, M., Harris, R. J., Rodrigues, L. C., Sridhar, S., Habermann, S., Snell, L., Mangtani, P., Adetifa, I., Lalvani, A., & Abubakar, I. (2014). Effect of BCG vaccination against Mycobacterium tuberculosis infection in children: Systematic review and meta-analysis. *BMJ (Clinical Research Ed.)*, *349*, g4643. https://doi.org/10.1136/bmj.g4643

Rozot, V., Nemes, E., Geldenhuys, H., Musvosvi, M., Toefy, A., Rantangee, F., Makhethe, L., Erasmus, M., Bilek, N., Mabwe, S., Finak, G., Fulp, W., Ginsberg, A. M., Hokey, D. A., Shey, M., Gurunathan, S., DiazGranados, C., Bekker, L.-G., Hatherill, M., & Scriba, T. J. (2020). Multidimensional analyses reveal modulation of adaptive and innate immune subsets by tuberculosis vaccines. *Communications Biology*, *3*. https://doi.org/10.1038/s42003-020-01288-3

Ruibal, P., Voogd, L., Joosten, S. A., & Ottenhoff, T. H. M. (2021). The role of donor-unrestricted T-cells, innate lymphoid cells, and NK cells in anti-mycobacterial immunity. *Immunological Reviews*, *301*(1), 30–47. https://doi.org/10.1111/imr.12948

Russell, D. G. (2011). Mycobacterium tuberculosis and the intimate discourse of a chronic infection. *Immunological Reviews*, *240*(1), 252–268. https://doi.org/10.1111/j.1600-065X.2010.00984.x

Sakai, S., Kauffman, K. D., Sallin, M. A., Sharpe, A. H., Young, H. A., Ganusov, V. V., & Barber, D. L. (2016). CD4 T Cell-Derived IFN-γ Plays a Minimal Role in Control of Pulmonary Mycobacterium tuberculosis Infection and Must Be Actively Repressed by PD-1 to Prevent Lethal Disease. *PLOS Pathogens*, *12*(5), e1005667. https://doi.org/10.1371/journal.ppat.1005667

Sakundarno, M., Nurjazuli, N., Jati, S. P., Sariningdyah, R., Purwadi, S., Alisjahbana, B., & van der Werf, M. J. (2009). Insufficient quality of sputum submitted for tuberculosis diagnosis and associated factors, in Klaten district, Indonesia. *BMC Pulmonary Medicine*, *9*(1), 16. https://doi.org/10.1186/1471-2466-9-16

Salie, M., Daya, M., Möller, M., & Hoal, E. G. (2015). Activating KIRs alter susceptibility to pulmonary tuberculosis in a South African population. *Tuberculosis*, *95*(6), 817–821. https://doi.org/10.1016/j.tube.2015.09.003

Salzberger, W., Martrus, G., Bachmann, K., Goebels, H., Heß, L., Koch, M., Langeneckert, A., Lunemann, S., Oldhafer, K. J., Pfeifer, C., Poch, T., Richert, L., Schramm, C., Wahib, R., Bunders, M. J., & Altfeld, M. (2018). Tissue-resident NK cells differ in their expression profile of the nutrient transporters Glut1, CD98 and CD71. *PLOS ONE*, *13*(7), e0201170. https://doi.org/10.1371/journal.pone.0201170

Saris, A., Reijnders, T. D. Y., Nossent, E. J., Schuurman, A. R., Verhoeff, J., Asten, S. van, Bontkes, H., Blok, S., Duitman, J., Bogaard, H.-J., Heunks, L., Lutter, R., Poll, T. van der, & Vallejo, J. J. G. (2021). Distinct cellular immune profiles in the airways and blood of critically ill patients with COVID-19. *Thorax*, *76*(10), 1010–1019. https://doi.org/10.1136/thoraxjnl-2020-216256

Sathaliyawala, T., Kubota, M., Yudanin, N., Turner, D., Camp, P., Thome, J. J. C., Bickham, K. L., Lerner, H., Goldstein, M., Sykes, M., Kato, T., & Farber, D. L. (2013). Distribution and compartmentalization of human circulating and tissue-resident memory T cell subsets. *Immunity*, *38*(1), 187–197. https://doi.org/10.1016/j.immuni.2012.09.020

Scanga, C. A., Mohan, V. P., Yu, K., Joseph, H., Tanaka, K., Chan, J., & Flynn, J. L. (2000). Depletion of Cd4+ T Cells Causes Reactivation of Murine Persistent Tuberculosis despite Continued Expression of Interferon γ and Nitric Oxide Synthase 2. *The Journal of Experimental Medicine*, *192*(3), 347–358.

Schierloh, P., Alemán, M., Yokobori, N., Alves, L., Roldán, N., Abbate, E., Sasiain, M. del C., & De La Barrera, S. (2005). NK cell activity in tuberculosis is associated with impaired CD11a and ICAM-1 expression: A regulatory role of monocytes in NK activation. *Immunology*, *116*(4), 541–552. https://doi.org/10.1111/j.1365-2567.2005.02259.x

Schierloh, P., Yokobori, N., Alemán, M., Musella, R. M., Beigier-Bompadre, M., Saab, M. A., Alves, L., Abbate, E., de la Barrera, S. S., & Sasiain, M. C. (2005). Increased Susceptibility to Apoptosis of CD56 ^{dim} CD16 $^{+}$ NK Cells Induces the Enrichment of IFN-γ-Producing CD56 ^{bright} Cells in Tuberculous Pleurisy. *The Journal of Immunology*, *175*(10), 6852–6860. https://doi.org/10.4049/jimmunol.175.10.6852

Scriba, T. J., Kalsdorf, B., Abrahams, D.-A., Isaacs, F., Hofmeister, J., Black, G., Hassan, H. Y., Wilkinson, R. J., Walzl, G., Gelderbloem, S. J., Mahomed, H., Hussey, G. D., & Hanekom, W. A. (2008). Distinct, specific IL-17- and IL-22-producing CD4+ T cell subsets contribute to the human anti-mycobacterial immune response. *Journal of Immunology (Baltimore, Md.: 1950)*, *180*(3), 1962–1970. https://doi.org/10.4049/jimmunol.180.3.1962

Scriba, T. J., Penn-Nicholson, A., Shankar, S., Hraha, T., Thompson, E. G., Sterling, D., Nemes, E., Darboe, F., Suliman, S., Amon, L. M., Mahomed, H., Erasmus, M., Whatney, W., Johnson, J. L., Boom, W. H., Hatherill, M., Valvo, J., Groote, M. A. D., Ochsner, U. A., … Team, other members of the A. cohort study. (2017). Sequential inflammatory processes define human progression from M. tuberculosis infection to tuberculosis disease. *PLOS Pathogens*, *13*(11), e1006687. https://doi.org/10.1371/journal.ppat.1006687

Scriba, T. J., Tameris, M., Mansoor, N., Smit, E., van der Merwe, L., Mauff, K., Hughes, E. J., Moyo, S., Brittain, N., Lawrie, A., Mulenga, H., de Kock, M., Gelderbloem, S., Veldsman, A., Hatherill, M., Geldenhuys, H., Hill, A. V. S., Hussey, G. D., Mahomed, H., … McShane, H. (2011). Dose-Finding Study of the Novel Tuberculosis Vaccine, MVA85A, in Healthy BCG-

Vaccinated Infants. *The Journal of Infectious Diseases*, *203*(12), 1832–1843. https://doi.org/10.1093/infdis/jir195

Segerberg, F., Lundtoft, C., Reid, S., Hjorton, K., Leonard, D., Nordmark, G., Carlsten, M., & Hagberg, N. (2019). Autoantibodies to Killer Cell Immunoglobulin-Like Receptors in Patients With Systemic Lupus Erythematosus Induce Natural Killer Cell Hyporesponsiveness. *Frontiers in Immunology*, *10*, 2164. https://doi.org/10.3389/fimmu.2019.02164

Semple, P. L., Watkins, M., Davids, V., Krensky, A. M., Hanekom, W. A., Kaplan, G., & Ress, S. (2010). Induction of Granulysin and Perforin Cytolytic Mediator Expression in 10-Week-Old Infants Vaccinated with BCG at Birth. *Journal of Immunology Research*, *2011*, e438463. https://doi.org/10.1155/2011/438463

Senju, H., Kumagai, A., Nakamura, Y., Yamaguchi, H., Nakatomi, K., Fukami, S., Shiraishi, K., Harada, Y., Nakamura, M., Okamura, H., Tanaka, Y., & Mukae, H. (2018). Effect of IL-18 on the Expansion and Phenotype of Human Natural Killer Cells: Application to Cancer Immunotherapy. *International Journal of Biological Sciences*, *14*(3), 331–340. https://doi.org/10.7150/ijbs.22809

Serbina, N. V., Lazarevic, V., & Flynn, J. L. (2001). CD4(+) T cells are required for the development of cytotoxic CD8(+) T cells during Mycobacterium tuberculosis infection. *Journal of Immunology (Baltimore, Md.: 1950)*, *167*(12), 6991–7000. https://doi.org/10.4049/jimmunol.167.12.6991

Serbina, N. V., Liu, C.-C., Scanga, C. A., & Flynn, J. L. (2000). CD8+ CTL from Lungs of Mycobacterium tuberculosis-Infected Mice Express Perforin In Vivo and Lyse Infected Macrophages1. *The Journal of Immunology*, *165*(1), 353–363. https://doi.org/10.4049/jimmunol.165.1.353

Sester, M., Sotgiu, G., Lange, C., Giehl, C., Girardi, E., Migliori, G. B., Bossink, A., Dheda, K., Diel, R., Dominguez, J., Lipman, M., Nemeth, J., Ravn, P., Winkler, S., Huitric, E., Sandgren, A., & Manissero, D. (2011). Interferon-γ release assays for the diagnosis of active tuberculosis: A systematic review and meta-analysis. *The European Respiratory Journal*, *37*(1), 100–111. https://doi.org/10.1183/09031936.00114810

Shanmugasundaram, U., Bucsan, A. N., Ganatra, S. R., Ibegbu, C., Quezada, M., Blair, R. V., Alvarez, X., Velu, V., Kaushal, D., & Rengarajan, J. (2020). Pulmonary Mycobacterium tuberculosis control associates with CXCR3- and CCR6-expressing antigen-specific Th1 and Th17 cell recruitment. *JCI Insight*, *5*(14), e137858, 137858. https://doi.org/10.1172/jci.insight.137858

Sharkey, A. M., Xiong, S., Kennedy, P. R., Gardner, L., Farrell, L. E., Chazara, O., Ivarsson, M. A., Hiby, S. E., Colucci, F., & Moffett, A. (2015). Tissue-Specific Education of Decidual NK Cells. *The Journal of Immunology Author Choice*, *195*(7), 3026–3032. https://doi.org/10.4049/jimmunol.1501229

Sharma, M., Merkulova, Y., Raithatha, S., Parkinson, L. G., Shen, Y., Cooper, D., & Granville, D. J. (2016). Extracellular granzyme K mediates endothelial activation through the cleavage of protease-activated receptor-1. *The FEBS Journal*, *283*(9), 1734–1747. https://doi.org/10.1111/febs.13699

Shiow, L. R., Rosen, D. B., Brdicková, N., Xu, Y., An, J., Lanier, L. L., Cyster, J. G., & Matloubian, M. (2006). CD69 acts downstream of interferon-alpha/beta to inhibit S1P1 and lymphocyte

egress from lymphoid organs. *Nature*, *440*(7083), 540–544. https://doi.org/10.1038/nature04606

Sia, J. K., Georgieva, M., & Rengarajan, J. (2015). Innate Immune Defenses in Human Tuberculosis: An Overview of the Interactions between *Mycobacterium tuberculosis* and Innate Immune Cells. *Journal of Immunology Research*, *2015*, e747543. https://doi.org/10.1155/2015/747543

Sia, J. K., & Rengarajan, J. (2019). Immunology of Mycobacterium tuberculosis infections. *Microbiology Spectrum*, *7*(4), 10.1128/microbiolspec.GPP3-0022–2018. https://doi.org/10.1128/microbiolspec.GPP3-0022-2018

Silva, D. R., Muñoz-Torrico, M., Duarte, R., Galvão, T., Bonini, E. H., Arbex, F. F., Arbex, M. A., Augusto, V. M., Rabahi, M. F., & Mello, F. C. de Q. (2018). Risk factors for tuberculosis: Diabetes, smoking, alcohol use, and the use of other drugs. *Jornal Brasileiro de Pneumologia*, *44*(2), 145–152. https://doi.org/10.1590/S1806-37562017000000443

Singh, A. K., & Gupta, U. D. (2018). Animal models of tuberculosis: Lesson learnt. *The Indian Journal of Medical Research*, *147*(5), 456–463. https://doi.org/10.4103/ijmr.IJMR_554_18

Sinha, P., Lönnroth, K., Bhargava, A., Heysell, S. K., Sarkar, S., Salgame, P., Rudgard, W., Boccia, D., Aartsen, D. V., & Hochberg, N. S. (2021). Food for thought: Addressing undernutrition to end tuberculosis. *The Lancet Infectious Diseases*, *21*(10), e318–e325. https://doi.org/10.1016/S1473-3099(20)30792-1

Sivori, S., Carlomagno, S., Pesce, S., Moretta, A., Vitale, M., & Marcenaro, E. (2014). TLR/NCR/KIR: Which One to Use and When? *Frontiers in Immunology*, *0*. https://doi.org/10.3389/fimmu.2014.00105

Sivori, S., Vacca, P., Del Zotto, G., Munari, E., Mingari, M. C., & Moretta, L. (2019a). Human NK cells: Surface receptors, inhibitory checkpoints, and translational applications. *Cellular & Molecular Immunology*, *16*(5), 430–441. https://doi.org/10.1038/s41423-019-0206-4

Sivori, S., Vacca, P., Del Zotto, G., Munari, E., Mingari, M. C., & Moretta, L. (2019b). Human NK cells: Surface receptors, inhibitory checkpoints, and translational applications. *Cellular and Molecular Immunology*, *16*(5), 430–441. https://doi.org/10.1038/s41423-019-0206-4

Smith, C. M., Wilson, N. S., Waithman, J., Villadangos, J. A., Carbone, F. R., Heath, W. R., & Belz, G. T. (2004). Cognate CD4+ T cell licensing of dendritic cells in CD8+ T cell immunity. *Nature Immunology*, *5*(11), Article 11. https://doi.org/10.1038/ni1129

Smith, S. L., Kennedy, P. R., Stacey, K. B., Worboys, J. D., Yarwood, A., Seo, S., Solloa, E. H., Mistretta, B., Chatterjee, S. S., Gunaratne, P., Allette, K., Wang, Y.-C., Smith, M. L., Sebra, R., Mace, E. M., Horowitz, A., Thomson, W., Martin, P., Eyre, S., & Davis, D. M. (2020). Diversity of peripheral blood human NK cells identified by single-cell RNA sequencing. *Blood Advances*, *4*(7), 1388–1406. https://doi.org/10.1182/bloodadvances.2019000699

Smyth, M. J., Cretney, E., Kelly, J. M., Westwood, J. A., Street, S. E. A., Yagita, H., Takeda, K., Dommelen, S. L. H. van, Degli-Esposti, M. A., & Hayakawa, Y. (2005). Activation of NK cell cytotoxicity. *Molecular Immunology*, *42*(4), 501–510. https://doi.org/10.1016/j.molimm.2004.07.034

Sørensen, A. L., Nagai, S., Houen, G., Andersen, P., & Andersen, A. B. (1995). Purification and characterization of a low-molecular-mass T-cell antigen secreted by Mycobacterium tuberculosis. *Infection and Immunity*, *63*(5), 1710–1717.

Souza-Fonseca-Guimaraes, F., Parlato, M., Fitting, C., Cavaillon, J.-M., & Adib-Conquy, M. (2012). NK cell tolerance to TLR agonists mediated by regulatory T cells after polymicrobial sepsis. *Journal of Immunology (Baltimore, Md.: 1950)*, *188*(12), 5850–5858. https://doi.org/10.4049/jimmunol.1103616

Souza-Fonseca-Guimaraes, F., Parlato, M., Philippart, F., Misset, B., Cavaillon, J.-M., Adib-Conquy, M., & Captain study group. (2012). Toll-like receptors expression and interferon-γ production by NK cells in human sepsis. *Critical Care (London, England)*, *16*(5), R206. https://doi.org/10.1186/cc11838

Stanietsky, N., Simic, H., Arapovic, J., Toporik, A., Levy, O., Novik, A., Levine, Z., Beiman, M., Dassa, L., Achdout, H., Stern-Ginossar, N., Tsukerman, P., Jonjic, S., & Mandelboim, O. (2009). The interaction of TIGIT with PVR and PVRL2 inhibits human NK cell cytotoxicity. *Proceedings of the National Academy of Sciences of the United States of America*, *106*(42), 17858–17863. https://doi.org/10.1073/pnas.0903474106

Stanzel, F. (2012). Bronchoalveolar Lavage. *Principles and Practice of Interventional Pulmonology*, 165–176. https://doi.org/10.1007/978-1-4614-4292-9_16

Steingart, K. R., Henry, M., Ng, V., Hopewell, P. C., Ramsay, A., Cunningham, J., Urbanczik, R., Perkins, M., Aziz, M. A., & Pai, M. (2006). Fluorescence versus conventional sputum smear microscopy for tuberculosis: A systematic review. *The Lancet. Infectious Diseases*, *6*(9), 570–581. https://doi.org/10.1016/S1473-3099(06)70578-3

Steingart, K. R., Ng, V., Henry, M., Hopewell, P. C., Ramsay, A., Cunningham, J., Urbanczik, R., Perkins, M. D., Aziz, M. A., & Pai, M. (2006). Sputum processing methods to improve the sensitivity of smear microscopy for tuberculosis: A systematic review. *The Lancet Infectious Diseases*, *6*(10), 664–674. https://doi.org/10.1016/S1473-3099(06)70602-8

Steingart, K. R., Schiller, I., Horne, D. J., Pai, M., Boehme, C. C., & Dendukuri, N. (2014). Xpert® MTB/RIF assay for pulmonary tuberculosis and rifampicin resistance in adults. *The Cochrane Database of Systematic Reviews*, *1*, CD009593. https://doi.org/10.1002/14651858.CD009593.pub3

Stenger, S., Hanson, D. A., Teitelbaum, R., Dewan, P., Niazi, K. R., Froelich, C. J., Ganz, T., Thoma-Uszynski, S., Melián, A., Bogdan, C., Porcelli, S. A., Bloom, B. R., Krensky, A. M., & Modlin, R. L. (1998). An Antimicrobial Activity of Cytolytic T Cells Mediated by Granulysin. *Science*, *282*(5386), 121–125. https://doi.org/10.1126/science.282.5386.121

Stop TB Partnership. (2022). *The Global Plan to End TB*. https://omnibook.com/view/dc664b3a-14b4-4cc0-8042-ea8f27e902a6

Strickland, N., Müller, T. L., Berkowitz, N., Goliath, R., Carrington, M. N., Wilkinson, R. J., Burgers, W. A., & Riou, C. (2017). Characterization of Mycobacterium tuberculosis-specific cells using MHC class II tetramers reveals phenotypic differences related to HIV infection and TB disease. *Journal of Immunology (Baltimore, Md.: 1950)*, ji1700849. https://doi.org/10.4049/jimmunol.1700849

Strik, M. C. M., de Koning, P. J. A., Kleijmeer, M. J., Bladergroen, B. A., Wolbink, A. M., Griffith, J. M., Wouters, D., Fukuoka, Y., Schwartz, L. B., Hack, C. E., van Ham, S. M., & Kummer, J. A. (2007). Human mast cells produce and release the cytotoxic lymphocyte associated protease granzyme B upon activation. *Molecular Immunology*, *44*(14), 3462–3472. https://doi.org/10.1016/j.molimm.2007.03.024

Strober, W. (1997). Trypan blue exclusion test of cell viability. *Current Protocols in Immunology*, *21*(1), A. 3B. 1-A. 3B. 2.

Suliman, S., Geldenhuys, H., Johnson, J. L., Hughes, J. E., Smit, E., Murphy, M., Toefy, A., Lerumo, L., Hopley, C., Pienaar, B., Chheng, P., Nemes, E., Hoft, D. F., Hanekom, W. A., Boom, W. H., Hatherill, M., & Scriba, T. J. (2016). Bacillus Calmette–Guérin (BCG) Revaccination of Adults with Latent Mycobacterium tuberculosis Infection Induces Long-Lived BCG-Reactive NK Cell Responses. *The Journal of Immunology*, *197*(4), 1100–1110. https://doi.org/10.4049/jimmunol.1501996

Sun, J., Bird, C. H., Sutton, V., McDonald, L., Coughlin, P. B., De Jong, T. A., Trapani, J. A., & Bird, P. I. (1996). A cytosolic granzyme B inhibitor related to the viral apoptotic regulator cytokine response modifier A is present in cytotoxic lymphocytes. *The Journal of Biological Chemistry*, *271*(44), 27802–27809. https://doi.org/10.1074/jbc.271.44.27802

Sun, J. C., & Lanier, L. L. (2009). Natural killer cells remember: An evolutionary bridge between innate and adaptive immunity? *European Journal of Immunology*, *39*(8), 2059–2064. https://doi.org/10.1002/eji.200939435

Sun, J. C., Lopez-Verges, S., Kim, C. C., DeRisi, J. L., & Lanier, L. L. (2011). NK Cells and Immune "Memory." *The Journal of Immunology*, *186*(4), 1891–1897. https://doi.org/10.4049/jimmunol.1003035

Sun, J. C., Ma, A., & Lanier, L. L. (2009). Cutting Edge: IL-15-independent NK cell response to mouse cytomegalovirus infection. *Journal of Immunology (Baltimore, Md.: 1950)*, *183*(5), 2911–2914. https://doi.org/10.4049/jimmunol.0901872

Suttles, J., & Stout, R. D. (2009). Macrophage CD40 signaling: A pivotal regulator of disease protection and pathogenesis. *Seminars in Immunology*, *21*(5), 257–264. https://doi.org/10.1016/j.smim.2009.05.011

Swanson, R. V., Gupta, A., Foreman, T. W., Lu, L., Choreno-Parra, J. A., Mbandi, S. K., Rosa, B. A., Akter, S., Das, S., Ahmed, M., Garcia-Hernandez, M. de la L., Singh, D. K., Esaulova, E., Artyomov, M. N., Gommerman, J., Mehra, S., Zuniga, J., Mitreva, M., Scriba, T. J., … Khader, S. A. (2023). Antigen-specific B cells direct T follicular-like helper cells into lymphoid follicles to mediate Mycobacterium tuberculosis control. *Nature Immunology*, 1–14. https://doi.org/10.1038/s41590-023-01476-3

Tait, D. R., Hatherill, M., Van Der Meeren, O., Ginsberg, A. M., Van Brakel, E., Salaun, B., Scriba, T. J., Akite, E. J., Ayles, H. M., Bollaerts, A., Demoitié, M.-A., Diacon, A., Evans, T. G., Gillard, P., Hellström, E., Innes, J. C., Lempicki, M., Malahleha, M., Martinson, N., … Roman, F. (2019). Final Analysis of a Trial of M72/AS01E Vaccine to Prevent Tuberculosis. *New England Journal of Medicine*, *381*(25), 2429–2439. https://doi.org/10.1056/NEJMoa1909953

Takahashi, C., Au-Yeung, A., Fuh, F., Ramirez-Montagut, T., Bolen, C., Mathews, W., & O'Gorman, W. E. (2017). Mass cytometry panel optimization through the designed distribution of signal interference. *Cytometry Part A*, *91*(1), 39–47. https://doi.org/10.1002/cyto.a.22977

Takeuchi, A., & Saito, T. (2017). CD4 CTL, a Cytotoxic Subset of CD4+ T Cells, Their Differentiation and Function. *Frontiers in Immunology*, *8*. https://www.frontiersin.org/articles/10.3389/fimmu.2017.00194

Tameris, M. D., Hatherill, M., Landry, B. S., Scriba, T. J., Snowden, M. A., Lockhart, S., Shea, J. E., McClain, J. B., Hussey, G. D., Hanekom, W. A., Mahomed, H., & McShane, H. (2013). Safety and efficacy of MVA85A, a new tuberculosis vaccine, in infants previously vaccinated with BCG: A randomised, placebo-controlled phase 2b trial. *The Lancet*, *381*(9871), 1021–1028. https://doi.org/10.1016/S0140-6736(13)60177-4

Tameris, M., Geldenhuys, H., Luabeya, A. K., Smit, E., Hughes, J. E., Vermaak, S., Hanekom, W. A., Hatherill, M., Mahomed, H., McShane, H., & Scriba, T. J. (2014). The Candidate TB Vaccine, MVA85A, Induces Highly Durable Th1 Responses. *PLOS ONE*, *9*(2), e87340. https://doi.org/10.1371/journal.pone.0087340

Tan, J. S., Canaday, D. H., Boom, W. H., Balaji, K. N., Schwander, S. K., & Rich, E. A. (1997). Human alveolar T lymphocyte responses to Mycobacterium tuberculosis antigens: Role for CD4+ and CD8+ cytotoxic T cells and relative resistance of alveolar macrophages to lysis. *Journal of Immunology (Baltimore, Md.: 1950)*, *159*(1), 290–297.

Tassignon, J., Burny, W., Dahmani, S., Zhou, L., Stordeur, P., Byl, B., & De Groote, D. (2005). Monitoring of cellular responses after vaccination against tetanus toxoid: Comparison of the measurement of IFN-gamma production by ELISA, ELISPOT, flow cytometry and real-time PCR. *Journal of Immunological Methods*, *305*(2), 188–198. https://doi.org/10.1016/j.jim.2005.07.014

Thiel, B. A., Worodria, W., Nalukwago, S., Nsereko, M., Sanyu, I., Rejani, L., Zawedde, J., Canaday, D. H., Stein, C. M., Chervenak, K. A., Malone, L. L., Kiyemba, R., Silver, R. F., Johnson, J. L., Mayanja-Kizza, H., & Boom, W. H. (2021). Immune cells in bronchoalveolar lavage fluid of Ugandan adults who resist versus those who develop latent Mycobacterium tuberculosis infection. *PLoS ONE*, *16*(4), e0249477. https://doi.org/10.1371/journal.pone.0249477

Tischer, S., Dieks, D., Sukdolak, C., Bunse, C., Figueiredo, C., Immenschuh, S., Borchers, S., Stripecke, R., Maecker-Kolhoff, B., Blasczyk, R., & Eiz-Vesper, B. (2014). Evaluation of suitable target antigens and immunoassays for high-accuracy immune monitoring of cytomegalovirus and Epstein-Barr virus-specific T cells as targets of interest in immunotherapeutic approaches. *Journal of Immunological Methods*, *408*, 101–113. https://doi.org/10.1016/j.jim.2014.05.011

Tomescu, C., Chehimi, J., Maino, V. C., & Montaner, L. J. (2007). NK cell lysis of HIV-1-infected autologous CD4 primary T cells: Requirement for IFN-mediated NK activation by plasmacytoid dendritic cells. *Journal of Immunology (Baltimore, Md.: 1950)*, *179*(4), 2097–2104. https://doi.org/10.4049/jimmunol.179.4.2097

Tomescu, C., Mavilio, D., & Montaner, L. J. (2015). Lysis of HIV-1-infected autologous CD4+ primary T cells by interferon-alpha-activated NK cells requires NKp46 and NKG2D. *AIDS (London, England)*, *29*(14), 1767–1773. https://doi.org/10.1097/QAD.0000000000000777

Topham, N. J., & Hewitt, E. W. (2009). Natural killer cell cytotoxicity: How do they pull the trigger? *Immunology*, *128*(1), 7–15. https://doi.org/10.1111/j.1365-2567.2009.03123.x

Torrado, E., & Cooper, A. M. (2010). IL-17 and Th17 cells in tuberculosis. *Cytokine & Growth Factor Reviews*, *21*(6), 455–462. https://doi.org/10.1016/j.cytogfr.2010.10.004

Trapani, J. A. (2001). Granzymes: A family of lymphocyte granule serine proteases. *Genome Biology*, *2*(12), reviews3014.1. https://doi.org/10.1186/gb-2001-2-12-reviews3014

Tripathy, S. K., Keyel, P. A., Yang, L., Pingel, J. T., Cheng, T. P., Schneeberger, A., & Yokoyama, W. M. (2008). Continuous engagement of a self-specific activation receptor induces NK cell tolerance. *Journal of Experimental Medicine*, *205*(8), 1829–1841. https://doi.org/10.1084/jem.20072446

Trunz, B. B., Fine, P., & Dye, C. (2006). Effect of BCG vaccination on childhood tuberculous meningitis and miliary tuberculosis worldwide: A meta-analysis and assessment of cost-effectiveness. *Lancet (London, England)*, *367*(9517), 1173–1180. https://doi.org/10.1016/S0140-6736(06)68507-3

Tschopp, C. M., Spiegl, N., Didichenko, S., Lutmann, W., Julius, P., Virchow, J. C., Hack, C. E., & Dahinden, C. A. (2006). Granzyme B, a novel mediator of allergic inflammation: Its induction and release in blood basophils and human asthma. *Blood*, *108*(7), 2290–2299. https://doi.org/10.1182/blood-2006-03-010348

Tupin, E., Kinjo, Y., & Kronenberg, M. (2007). The unique role of natural killer T cells in the response to microorganisms. *Nature Reviews Microbiology*, *5*(6), Article 6. https://doi.org/10.1038/nrmicro1657

Turken, O., Kunter, E., Sezer, M., Solmazgul, E., Cerrahoglu, K., Bozkanat, E., Ozturk, A., & Ilvan, A. (2002). Hemostatic changes in active pulmonary tuberculosis. *The International Journal of Tuberculosis and Lung Disease: The Official Journal of the International Union Against Tuberculosis and Lung Disease*, *6*(10), 927–932.

Udwadia, Z. F. (2012). MDR, XDR, TDR tuberculosis: Ominous progression. *Thorax*, *67*(4), 286–288. https://doi.org/10.1136/thoraxjnl-2012-201663

van den Bosch, G., Preijers, F., Vreugdenhil, A., Hendriks, J., Maas, F., & De Witte, T. (1995). Granulocyte-macrophage colony-stimulating factor (GM-CSF) counteracts the inhibiting effect of monocytes on natural killer (NK) cells. *Clinical and Experimental Immunology*, *101*(3), 515–520.

van Rensburg, I. C., & Loxton, A. G. (2015). Transcriptomics: The key to biomarker discovery during tuberculosis? *Biomarkers in Medicine*, *9*(5), 483–495. https://doi.org/10.2217/bmm.15.16

Vankayalapati, R., Garg, A., Porgador, A., Griffith, D. E., Klucar, P., Safi, H., Girard, W. M., Cosman, D., Spies, T., & Barnes, P. F. (2005). Role of NK cell-activating receptors and their ligands in the lysis of mononuclear phagocytes infected with an intracellular bacterium. *Journal of Immunology (Baltimore, Md.: 1950)*, *175*(7), 4611–4617. https://doi.org/10.4049/jimmunol.175.7.4611

Vankayalapati, R., Wizel, B., Weis, S. E., Safi, H., Lakey, D. L., Mandelboim, O., Samten, B., Porgador, A., & Barnes, P. F. (2002). The NKp46 Receptor Contributes to NK Cell Lysis of Mononuclear Phagocytes Infected with an Intracellular Bacterium. *The Journal of Immunology*, *168*(7), 3451–3457. https://doi.org/10.4049/jimmunol.168.7.3451

Veenstra, H., Baumann, R., Carroll, N. M., Lukey, P. T., Kidd, M., Beyers, N., Bolliger, C. T., Van Helden, P. D., & Walzl, G. (2006). Changes in leucocyte and lymphocyte subsets during tuberculosis treatment; prominence of CD3dimCD56+ natural killer T cells in fast treatment

responders. *Clinical and Experimental Immunology*, *145*(2), 252–260. https://doi.org/10.1111/j.1365-2249.2006.03144.x

Venkatasubramanian, S., Cheekatla, S., Paidipally, P., Tripathi, D., Welch, E., Tvinnereim, A. R., Nurieva, R., & Vankayalapati, R. (2017). IL-21-dependent expansion of memory-like NK cells enhances protective immune responses against Mycobacterium tuberculosis. *Mucosal Immunology*, *10*(4), 1031–1042. https://doi.org/10.1038/mi.2016.105

Vivier, E., Raulet, D. H., Moretta, A., Caligiuri, M. A., Zitvogel, L., Lanier, L. L., Yokoyama, W. M., & Ugolini, S. (2011). Innate or adaptive immunity? The example of natural killer cells. *Science (New York, N.Y.)*, *331*(6013), 44–49. https://doi.org/10.1126/science.1198687

Voskoboinik, I., Whisstock, J. C., & Trapani, J. A. (2015). Perforin and granzymes: Function, dysfunction and human pathology. *Nature Reviews Immunology*, *15*(6), Article 6. https://doi.org/10.1038/nri3839

Vynnycky, E., & Fine, P. E. (1997a). The natural history of tuberculosis: The implications of age-dependent risks of disease and the role of reinfection. *Epidemiology and Infection*, *119*(2), 183–201. https://doi.org/10.1017/s0950268897007917

Vynnycky, E., & Fine, P. E. (1997b). The natural history of tuberculosis: The implications of age-dependent risks of disease and the role of reinfection. *Epidemiology and Infection*, *119*(2), 183–201.

Wagner, C., Iking-Konert, C., Denefleh, B., Stegmaier, S., Hug, F., & Hänsch, G. M. (2004). Granzyme B and perforin: Constitutive expression in human polymorphonuclear neutrophils. *Blood*, *103*(3), 1099–1104. https://doi.org/10.1182/blood-2003-04-1069

Wagner, J. A., Rosario, M., Romee, R., Berrien-Elliott, M. M., Schneider, S. E., Leong, J. W., Sullivan, R. P., Jewell, B. A., Becker-Hapak, M., Schappe, T., Abdel-Latif, S., Ireland, A. R., Jaishankar, D., King, J. A., Vij, R., Clement, D., Goodridge, J., Malmberg, K.-J., Wong, H. C., & Fehniger, T. A. (2017). CD56bright NK cells exhibit potent antitumor responses following IL-15 priming. *The Journal of Clinical Investigation*, *127*(11), 4042–4058. https://doi.org/10.1172/JCI90387

Walzl, G., Ronacher, K., Hanekom, W., Scriba, T. J., & Zumla, A. (2011). Immunological biomarkers of tuberculosis. *Nature Reviews Immunology*, *11*(5), Article 5. https://doi.org/10.1038/nri2960

Wang, K. S., Ritz, J., & Frank, D. A. (1999). IL-2 Induces STAT4 Activation in Primary NK Cells and NK Cell Lines, But Not in T Cells. *The Journal of Immunology*, *162*(1), 299–304.

Wang, W., Erbe, A. K., Hank, J. A., Morris, Z. S., & Sondel, P. M. (2015). NK Cell-Mediated Antibody-Dependent Cellular Cytotoxicity in Cancer Immunotherapy. *Frontiers in Immunology*, *6*. https://doi.org/10.3389/fimmu.2015.00368

Warren, H. S., Kinnear, B. F., Phillips, J. H., & Lanier, L. L. (1995). Production of IL-5 by human NK cells and regulation of IL-5 secretion by IL-4, IL-10, and IL-12. *The Journal of Immunology*, *154*(10), 5144–5152.

Wawrocki, S., & Druszczynska, M. (2017). Inflammasomes in Mycobacterium tuberculosis-Driven Immunity. *The Canadian Journal of Infectious Diseases & Medical Microbiology = Journal*

Canadien Des Maladies Infectieuses et de La Microbiologie Médicale, *2017*, 2309478. https://doi.org/10.1155/2017/2309478

Wensink, A. C., Kemp, V., Fermie, J., García Laorden, M. I., van der Poll, T., Hack, C. E., & Bovenschen, N. (2014). Granzyme K synergistically potentiates LPS-induced cytokine responses in human monocytes. *Proceedings of the National Academy of Sciences*, *111*(16), 5974–5979. https://doi.org/10.1073/pnas.1317347111

WHO. (2008). *Stop TB policy paper: Contributing to health system strengthening: Guiding principles for national tuberculosis programmes*. World Health Organization.

WHO. (2013). *Systematic Screening for Active Tuberculosis: Principles and Recommendations*. World Health Organization. http://www.ncbi.nlm.nih.gov/books/NBK294083/

WHO. (2022). *Global Tuberculosis Report*.

Wilharm, E., Parry, M. A. A., Friebel, R., Tschesche, H., Matschiner, G., Sommerhoff, C. P., & Jenne, D. E. (1999). Generation of Catalytically Active Granzyme K from Escherichia coli Inclusion Bodies and Identification of Efficient Granzyme K Inhibitors in Human Plasma *. *Journal of Biological Chemistry*, *274*(38), 27331–27337. https://doi.org/10.1074/jbc.274.38.27331

Wilkinson, K. A., Oni, T., Gideon, H. P., Goliath, R., Wilkinson, R. J., & Riou, C. (2016). Activation Profile of Mycobacterium tuberculosis-Specific CD4(+) T Cells Reflects Disease Activity Irrespective of HIV Status. *American Journal of Respiratory and Critical Care Medicine*, *193*(11), 1307–1310. https://doi.org/10.1164/rccm.201601-0116LE

Willard-Mack, C. L. (2006). Normal Structure, Function, and Histology of Lymph Nodes. *Toxicologic Pathology*, *34*(5), 409–424. https://doi.org/10.1080/01926230600867727

Williams, C. G., Lee, H. J., Asatsuma, T., Vento-Tormo, R., & Haque, A. (2022). An introduction to spatial transcriptomics for biomedical research. *Genome Medicine*, *14*(1), 68. https://doi.org/10.1186/s13073-022-01075-1

Williams, M. A., & Bevan, M. J. (2007). Effector and memory CTL differentiation. *Annual Review of Immunology*, *25*, 171–192. https://doi.org/10.1146/annurev.immunol.25.022106.141548

Wingfield, T., Tovar, M. A., Datta, S., Saunders, M. J., & Evans, C. A. (2018). Addressing social determinants to end tuberculosis. *The Lancet*, *391*(10126), 1129–1132. https://doi.org/10.1016/S0140-6736(18)30484-7

Wolter, F., Glässner, A., Krämer, B., Kokordelis, P., Finnemann, C., Kaczmarek, D. J., Goeser, F., Lutz, P., Nischalke, H. D., Strassburg, C. P., Spengler, U., & Nattermann, J. (2015). Hypoxia impairs anti-viral activity of natural killer (NK) cells but has little effect on anti-fibrotic NK cell functions in hepatitis C virus infection. *Journal of Hepatology*, *63*(6), 1334–1344. https://doi.org/10.1016/j.jhep.2015.08.008

Wu, L., & Van Kaer, L. (2011). Natural killer T cells in health and disease. *Frontiers in Bioscience (Scholar Edition)*, *3*, 236–251.

Xu, X., Weiss, I. D., Zhang, H., Singh, S. P., Wynn, T. A., Wilson, M. S., & Farber, J. M. (2014). Conventional NK cells can produce IL-22 and promote host defense in K. pneumoniae

pneumonia. *Journal of Immunology (Baltimore, Md.: 1950)*, *192*(4), 1778–1786. https://doi.org/10.4049/jimmunol.1300039

Yawata, M., Yawata, N., Draghi, M., Partheniou, F., Little, A.-M., & Parham, P. (2008). MHC class I–specific inhibitory receptors and their ligands structure diverse human NK-cell repertoires toward a balance of missing self-response. *Blood*, *112*(6), 2369–2380. https://doi.org/10.1182/blood-2008-03-143727

Yokoyama, W. M., Kim, S., & French, A. R. (2004). The dynamic life of natural killer cells. *Annual Review of Immunology*, *22*, 405–429. https://doi.org/10.1146/annurev.immunol.22.012703.104711

Yoneda, T., Kasai, M., Ishibashi, J., Nishikawa, K., Tokunaga, T., & Mikami, R. (1983). NK cell activity in pulmonary tuberculosis. *British Journal of Diseases of the Chest*, *77*(2), 185–188. https://doi.org/10.1016/0007-0971(83)90026-8

Yong, Y. K., Tan, H. Y., Saeidi, A., Wong, W. F., Vignesh, R., Velu, V., Eri, R., Larsson, M., & Shankar, E. M. (2019). Immune Biomarkers for Diagnosis and Treatment Monitoring of Tuberculosis: Current Developments and Future Prospects. *Frontiers in Microbiology*, *10*. https://www.frontiersin.org/articles/10.3389/fmicb.2019.02789

Young, C., Ahlers, P., Hiemstra, A. M., Loxton, A. G., Gutschmidt, A., Malherbe, S. T., Walzl, G., Du Plessis, N., Koegelenberg, C. F. N., Kleynhans, L., Ronacher, K., Shaw, J. A., Simon, D., McAnda, S., Swartz, K. C., & the SU-IRG consortium. (2019). Performance and immune characteristics of bronchoalveolar lavage by research bronchoscopy in pulmonary tuberculosis and other lung diseases in the Western Cape, South Africa. *Translational Medicine Communications*, *4*(1), 7. https://doi.org/10.1186/s41231-019-0039-2

Young, C., Walzl, G., & Du Plessis, N. (2020). Therapeutic host-directed strategies to improve outcome in tuberculosis. *Mucosal Immunology*, *13*(2), Article 2. https://doi.org/10.1038/s41385-019-0226-5

Yu, J., Freud, A. G., & Caligiuri, M. A. (2013). Location and cellular stages of NK cell development. *Trends in Immunology*, *34*(12), 10.1016/j.it.2013.07.005. https://doi.org/10.1016/j.it.2013.07.005

Yu, J., Heller, G., Chewning, J., Kim, S., Yokoyama, W. M., & Hsu, K. C. (2007). Hierarchy of the Human Natural Killer Cell Response Is Determined by Class and Quantity of Inhibitory Receptors for Self-HLA-B and HLA-C Ligands1. *The Journal of Immunology*, *179*(9), 5977–5989. https://doi.org/10.4049/jimmunol.179.9.5977

Yu, J., Mao, H. C., Wei, M., Hughes, T., Zhang, J., Park, I., Liu, S., McClory, S., Marcucci, G., Trotta, R., & Caligiuri, M. A. (2010). CD94 surface density identifies a functional intermediary between the CD56bright and CD56dim human NK-cell subsets. *Blood*, *115*(2), 274–281. https://doi.org/10.1182/blood-2009-04-215491

Zaiatz-Bittencourt, V., Finlay, D. K., & Gardiner, C. M. (2018). Canonical TGF-β Signaling Pathway Represses Human NK Cell Metabolism. *The Journal of Immunology*, *200*(12), 3934–3941. https://doi.org/10.4049/jimmunol.1701461

Zak, D. E., Penn-Nicholson, A., Scriba, T. J., Thompson, E., Suliman, S., Amon, L. M., Mahomed, H., Erasmus, M., Whatney, W., Hussey, G. D., Abrahams, D., Kafaar, F., Hawkridge, T.,

Verver, S., Hughes, E. J., Ota, M., Sutherland, J., Howe, R., Dockrell, H. M., … ACS and GC6-74 cohort study groups. (2016). A blood RNA signature for tuberculosis disease risk: A prospective cohort study. *Lancet (London, England)*, *387*(10035), 2312–2322. https://doi.org/10.1016/S0140-6736(15)01316-1

Zenewicz, L. A., & Flavell, R. A. (2011). Recent advances in IL-22 biology. *International Immunology*, *23*(3), 159–163. https://doi.org/10.1093/intimm/dxr001

Zhai, W., Wu, F., Zhang, Y., Fu, Y., & Liu, Z. (2019). The Immune Escape Mechanisms of Mycobacterium Tuberculosis. *International Journal of Molecular Sciences*, *20*(2), 340. https://doi.org/10.3390/ijms20020340

Zhang, R., Xi, X., Wang, C., Pan, Y., Ge, C., Zhang, L., Zhang, S., & Liu, H. (2018). Therapeutic effects of recombinant human interleukin 2 as adjunctive immunotherapy against tuberculosis: A systematic review and meta-analysis. *PLoS ONE*, *13*(7), e0201025. https://doi.org/10.1371/journal.pone.0201025

Zhang, Y., Wallace, D. L., de Lara, C. M., Ghattas, H., Asquith, B., Worth, A., Griffin, G. E., Taylor, G. P., Tough, D. F., Beverley, P. C. L., & Macallan, D. C. (2007). In vivo kinetics of human natural killer cells: The effects of ageing and acute and chronic viral infection. *Immunology*, *121*(2), 258–265. https://doi.org/10.1111/j.1365-2567.2007.02573.x

Zhu, J., Yamane, H., & Paul, W. E. (2010). Differentiation of effector CD4 T cell populations (*). *Annual Review of Immunology*, *28*, 445–489. https://doi.org/10.1146/annurev-immunol-030409-101212

Zielinski, C. E., Mele, F., Aschenbrenner, D., Jarrossay, D., Ronchi, F., Gattorno, M., Monticelli, S., Lanzavecchia, A., & Sallusto, F. (2012). Pathogen-induced human TH17 cells produce IFN-γ or IL-10 and are regulated by IL-1β. *Nature*, *484*(7395), 514–518. https://doi.org/10.1038/nature10957

Zunder, E. R., Finck, R., Behbehani, G. K., Amir, E.-A. D., Krishnaswamy, S., Gonzalez, V. D., Lorang, C. G., Bjornson, Z., Spitzer, M. H., Bodenmiller, B., Fantl, W. J., Pe'er, D., & Nolan, G. P. (2015). Palladium-based mass tag cell barcoding with a doublet-filtering scheme and single-cell deconvolution algorithm. *Nature Protocols*, *10*(2), 316–333. https://doi.org/10.1038/nprot.2015.020

Zwirner, N. W., & Domaica, C. I. (2010). Cytokine regulation of natural killer cell effector functions. *BioFactors (Oxford, England)*, *36*(4), 274–288. https://doi.org/10.1002/biof.107